

A Reproduced Copy
OF

N72 - 28901

Reproduced for NASA
by the
NASA Scientific and Technical Information Facility

145

NASA TECHNICAL MEMORANDUM

NASA TM X - 64669

VIBRATION MANUAL

(NASA-TM-X-64669) VIBRATION MANUAL C.
Green (NASA) 1 Dec. 1971 592 p CSCL 20K

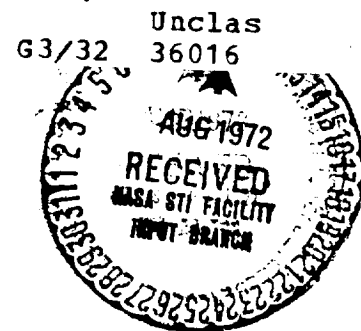
N72-28901

Astronautics Laboratory

December 1, 1971

NASA

*George C. Marshall Space Flight Center
Marshall Space Flight Center, Alabama*



1. REPORT NO. TM X- 64669		2. GOVERNMENT ACCESSION NO.		3. RECIPIENT'S CATALOG NO. N72-28941	
4. TITLE AND SUBTITLE Vibration Manual				5. REPORT DATE December 1, 1971	
				6. PERFORMING ORGANIZATION CODE	
7. AUTHOR(S) Claude Green, Editor				8. PERFORMING ORGANIZATION REPORT NO.	
9. PERFORMING ORGANIZATION NAME AND ADDRESS George C. Marshall Space Flight Center Marshall Space Flight Center, Alabama 35812				10. WORK UNIT NO.	
				11. CONTRACT OR GRANT NO.	
12. SPONSORING AGENCY NAME AND ADDRESS National Aeronautics And Space Administration Washington, D. C. 20546				13. TYPE OF REPORT & PERIOD COVERED Technical Memorandum	
				14. SPONSORING AGENCY CODE	
15. SUPPLEMENTARY NOTES Prepared by Astronautics Laboratory, Science and Engineering					
16. ABSTRACT <p>This document provides guidelines of the methods and applications used in vibration technology at MSFC. Its purpose is to provide a practical tool for coordination and understanding between industry and government groups concerned with vibration of systems and equipments. Topics covered include measuring, reducing, analyzing, and methods for obtaining simulated environments and formulating vibration specifications. Other sections cover methods for vibration and shock testing, theoretical aspects of data processing, vibration response analysis, and techniques of designing for vibration.</p>					
17. KEY WORDS			18. DISTRIBUTION STATEMENT		
19. SECURITY CLASSIF. (of this report) Unclassified		20. SECURITY CLASSIF. (of this page) Unclassified		21. NO. OF PAGES 592	
				22. PRICE \$ 30 31.75	

December 1, 1971

TM X-64669

APPROVAL

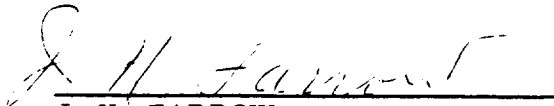
VIBRATION MANUAL

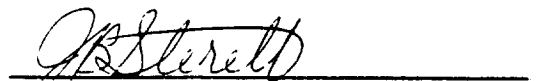
By

Claude Green, Editor

The information in this report has been reviewed for security classification. Review of any information concerning Department of Defense or Atomic Energy Commission programs has been made by the MSFC Security Classification Officer. This report, in its entirety, has been determined to be unclassified.

This document has also been reviewed and approved for technical accuracy.


J. H. FARROW
Chief, Dynamics Analysis Branch


J. B. STERETT
Chief, Analytical Mechanics Division

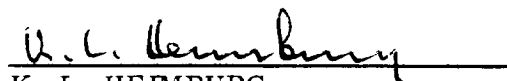

K. L. HEIMBURG
Director, Astronautics Laboratory

TABLE OF CONTENTS

	Page
INTRODUCTION	1
SECTION I. SOURCES OF VIBRATION	2
A. Sources and Causes of Vibration.....	2
B. Complete Vibration Environment.....	4
SECTION II. ACCELEROMETERS.....	7
A. Accelerometer Considerations	7
B. General Accelerometer Principles	8
C. Piezoelectric (Crystal) Accelerometers ...	9
D. Strain Bridge Accelerometers	12
E. Piezoresistive Accelerometers.....	17
F. Force Balance (Servo) Accelerometers....	17
G. Potentiometer Accelerometers.....	19
H. Accelerometer Comparison	20
I. General Accelerometer Selection Characteristics	20
SECTION III. MICROPHONES.....	22
A. Condenser Microphones.....	22
B. Piezoelectric Microphones.....	24
C. Tuned Circuit Microphone	26
D. Microphone Selection	28
SECTION IV. MOUNTING OF VIBRATION TRANSDUCERS AND MICROPHONES	32
A. Vibration Transducer Mounting.....	32
B. Microphone Mounting	34
C. Associated Factors — Transducer Mounting.....	35
SECTION V. CALIBRATION.....	39
A. General	39
B. The Nature of Dynamic Data.....	40

TABLE OF CONTENTS (Continued)

	Page
C. Transducer Subsystem Calibration	42
D. Data-Transmission and Data-Recording Subsystems Calibration	52
SECTION VI. DATA TRANSMISSION.	56
A. Basic Telemetry System	56
B. Telemetry Systems Used for Vibration Data.	59
C. Direct Data Transmission	69
D. System Accuracy	73
SECTION VII. DATA RECORDING.	74
A. Magnetic Tape Recorders	74
B. Oscillographs	78
C. Oscillograph — Magnetic Tape System	80
D. X-Y Plotters	80
E. Direct Writing Recorders	82
F. Oscilloscope and Camera.	82
SECTION VIII. DATA REDUCTION.	83
A. Basic Characteristics of Vibration Data	83
B. Basic Descriptions of Vibration Data	89
C. General Techniques for Periodic Data Reduction	103
D. General Techniques for Random Data Reduction	111
E. Determination of Noise Bandwidth	140
F. Practical Considerations for Power Spectra Measurements	149
G. Multiple Filter Analyzers	152
H. A Method of Calibrating a Swept Filter Analyzer or a Multiple Filter Analyzer for Power Spectral Density Analysis	154

TABLE OF CONTENTS (Continued)

	Page
SECTION IX. INTERPRETATION AND EVALUATION OF DATA.	156
A. Evaluation of Randomness	156
B. Verification of Stationarity.	170
C. Determination of Data Equivalence	182
D. Interpretation and Application of Amplitude Probability Density Functions	201
E. Interpretation and Application of Correlation Functions	217
SECTION X. ACOUSTIC, VIBRATION, AND SHOCK TESTS. . . .	267
A. Acoustic Tests.	267
B. Shock and Vibration Tests	271
SECTION XI. VIBRATION AND ENVIRONMENTS AND TEST SPECIFICATIONS.	281
A. Stage and Vehicle Vibration and Shock Criteria	281
B. Payload Vibration and Shock Criteria.	289
SECTION XII. THEORETICAL CONSIDERATIONS	292
A. Vibration Terms — Their Meanings and Uses	292
B. Random Process and Probability Distribution	296
C. Random Processes in Vibration Analysis	307
D. Amplitude and Frequency Distribution in Random Noise	311
E. Vibration Excitation Sources	318
F. Digital Vibration Analysis	345

TABLE OF CONTENTS (Concluded)

	Page
SECTION XIII. VIBRATION RESPONSE ANALYSIS	389
A. Review of Fundamentals	389
B. Equation of Motion — Steady State	397
C. Equations of Motion — Transients	427
D. Equations of Motion — Acoustic Impinge- ment	431
E. Application and Examples — Direct Steady State Forcing.	443
F. Equivalent Systems.	465
G. Non-Linear Vibrations	472
H. Supporting Mathematics.	486
SECTION XIV. DESIGNING FOR VIBRATION	507
A. Vibration Load Analysis Procedure	507
B. Use of Vibration Loads in Strength Analyses ..	532
C. Vibration Damage.	536
D. The MSFC Environment Documents	541
E. Useful Relationships	548
APPENDIX. DEFINITION OF TERMS	553
REFERENCES	565
BIBLIOGRAPHY	573

LIST OF ILLUSTRATIONS

Figure	Title	Page
1.	Schematic of a mass-spring type vibration transducer . . .	9
2.	Frequency response curves for various values of critical damping (C/C_c) of a linear second order mass-spring system (sinusoidal input)	10
3.	Schematic of a typical compression-type piezoelectric accelerometer	11
4.	Electrical and mechanical schematic of a typical strain-bridge accelerometer	16
5.	Block diagram of a force balance (servo) accelerometer	18
6.	Schematic of a typical potentiometer accelerometer	20
7.	Condenser microphone	23
8.	Piezoelectric microphone	25
9.	Piezoelectric microphone	25
10.	Vibration compensating piezoelectric microphone	26
11.	Tuned circuit microphone	27
12.	Vibration response of general microphone types	29
13.	Sensitivity ranges of general microphone types	30
14.	Direct mounting of transducer	33
15.	Multiple mounting of transducers	33
16.	Transducers mounted on odd-shape structure	33

LIST OF ILLUSTRATIONS (Continued)

Figure	Title	Page
17.	Static test microphone mounting	36
18.	Typical flight vehicle microphone mountings	37
19.	Wheatstone-Bridge circuit	47
20.	Shunt calibration system	49
21.	Inflight calibration signals	54
22.	Basic telemetry system.	57
23.	Direct data transmission system.	57
24.	FM/FM channel spacing	63
25.	FM/FM telemetry	65
26.	SS/FM channel unit.	67
27.	SS/FM telemetry and ground station	68
28.	Impedance matching devices.	71
29.	Basic electromagnetic tape head	75
30.	Oscillograph optical elements.	79
31.	Oscillograph-magnetic tape system	81
32.	Computation of mean values	86
33.	Computation of mean square values	87
34.	Computation of autocorrelation values	88
35.	Typical discrete frequency spectrum	92

LIST OF ILLUSTRATIONS (Continued)

Figure	Title	Page
36.	Typical probability density plot.	93
37.	Typical autocorrelation plot.	95
38.	Typical power spectrum	97
39.	Typical joint probability density plot	98
40.	Typical cross correlation plot	100
41.	Typical cross-power spectrum	102
42.	Functional block diagram for multiple filter type spectrum analyzer	105
43.	Functional block diagram for single filter type spectrum analyzer	106
44.	Properly resolved frequency spectrum for periodic data	109
45.	Functional block diagram for amplitude probability density analyzer.	114
46.	Estimation uncertainty versus WBT product	116
47.	Functional block diagram for autocorrelation analyzer . . .	121
48.	Estimation uncertainty versus BT product	123
49.	Functional block diagram for power spectral density analyzer	128
50.	Functional block diagram for joint amplitude probability density analyzer.	134
51.	Functional block diagram for cross-correlation analyzer	138

LIST OF ILLUSTRATIONS (Continued)

Figure	Title	Page
52.	Functional block diagram for cross-power spectral density analyzer.	141
53.	Test setup for filter noise bandwidth calibration	145
54.	Magnitude response function for bandpass filter.	146
55.	Multiple filter analyzer.	153
56.	Actual power spectra plots.	158
57.	Actual probability density plots.	160
58.	Typical autocorrelation plots	161
59.	Analysis of continuous mean square value measurements.	164
60.	Acceptance regions for randomness test	167
61.	Acceptance regions for randomness and stationarity test	175
62.	Illustration of typical autocorrelation functions	221
63.	Autocorrelation function for sine wave plus noise.	225
64.	Transmission path determination example	226
65.	Possible normalized cross-correlation function for transmission path example.	227
66.	Idealized structure with motion excitation.	233
67.	Gain and phase factors for frequency response functions.	237
68.	Real and imaginary parts for frequency response functions.	239

LIST OF ILLUSTRATIONS (Continued)

Figure	Title	Page
69.	Simple idealized structure with force excitation.	239
70.	Response power spectrum for simple structure	248
71.	Data for frequency response function measurement confidence.	265
72.	Mode test setup for saturn vehicle.	273
73.	Drop-test shock machine	274
74.	Hydraulic - pneumatic shock machine	276
75.	Electromagnetic vibration shaker	276
76.	Armature behavior over usable frequency range	277
77.	Functional block diagram of sinusoidal sweep generating system	279
78.	Functional diagram of a random vibration generating system	280
79.	Flow chart for determining the vibration environment of a new vehicle structure	287
80.	Sinusoidal function $x = A \sin \omega t$	293
81.	Record of a random experiment with a die	296
82.	Probability distribution of a discrete random variable . . .	298
83.	Probability distribution for a discrete random variable. . .	300
84.	Probability distribution function for continuous random variable	300

LIST OF ILLUSTRATIONS (Continued)

Figure	Title	Page
85.	Ensemble of sample functions.	301
86.	Ensemble of continuous random processes as a function of time	308
87.	Sample of response of a panel to random noise excitation	313
88.	Normal and Rayleigh probability distribution functions . . .	314
89.	Ensemble of measured time histories of force.	322
90.	Time record of a nonstationary random force function . . .	327
91.	Amplitude sampling of $F(t)$ at even intervals of time	329
92.	Block diagrams of electronic analog CCTS for computing statistical averages	331
93.	Typical filter characteristic.	335
94.	Bar graph of the amplitude of filtered discrete frequency components	336
95.	Finite isolated pulses and their Fourier transforms	339
96.	Bar graph of the mean square amplitudes of discrete frequency components	342
97.	The correlation function $C_F(\tau)$ of a sinusoid is the absolute value of a cosinusoid $C_F(\tau) = \cos \omega \tau $	345
98.	Illustration of folding about the nyquist cutoff frequency f_c	346
99.	Illustration of quantization error.	347

LIST OF ILLUSTRATIONS (Continued)

Figure	Title	Page
100.	Two-dimensional histogram representing $f(x,y)$. (Number in each square represents observed frequency.)	368
101.	Typical equiprobability ellipses	371
102.	Functions to be computed for two records.	373
103.	Joint probability functions for two records	373
104.	Generalized model: one-degree-of-freedom system.	398
105.	Magnification factor versus frequency ratio	403
106.	Phase angle versus frequency ratio	403
107.	Bode plot (κ versus r)	405
108.	Bode plot (ϕ versus r)	405
109.	Nyquist plot.	406
110.	Potential energy in a spring	406
111.	Simple supported beam with two loads	416
112.	Two-degree-of-freedom system	423
113.	Thin plate with small deflection	424
114.	Plate element free body	425
115.	Panel structure	436
116.	Beam element, free body section	447
117.	Cylinder geometry and displacement field.	453

LIST OF ILLUSTRATIONS (Concluded)

Figure	Title	Page
118.	Lines of constant energy in the phase plane for the hard spring, $K > 0$	476
119.	Lines of constant energy in the phase plane for the soft spring, $K < 0$	476
120.	Response curves for the hard spring	480
121.	Response curves for the soft spring.	481
122.	Response curves for the non-linear spring with damping.	483
123.	Jump phenomenon or hysteresis resonance for the non-linear spring with damping.	483
124.	Panel damping	510
125.	Cold helium feeder duct installation.	530

LIST OF TABLES

Table	Title	Page
1.	Accelerometer Characteristics and Comparison	13
2.	Microphone Comparison	31
3.	Subcarrier Bands (± 7.5 -Percent Deviations).	61
4.	Subcarrier Bands (± 15 -Percent Deviations)	62
5.	FM Carrier Record Reproduce System Frequency Response	78
6.	Run Test for Stationarity	181
7.	Vibration Data Layout for Two-Way Analysis of Variance.	188
8.	Two-Way Analysis of Variance Table.	192
9.	Experimental Results	197
10.	Results.	200
11.	Optimum Numbered Class Intervals k as a Function of the Sample Size N	350
12.	Values of c^2 for Equiprobability Ellipses	371
13.	Time Estimates for Digital Vibration Program	381

ACKNOWLEDGMENTS

This report is the result of a combined effort of several Marshall Space Flight Center laboratories. Principal contributions were from Computation Laboratory and Astronautics Laboratory. Since most sections of this report are the consensus of several inputs, no author credits are given. However, significant technical and editorial contributions were made by Technical Products Company, The Boeing Company, Julius S. Bendat, Loren D. Enochson, and Allen G. Piersol.

FOREWORD

This report was originally published in 1963 by the MSFC Vibration Committee, edited by Jack A. Jones, and was revised in 1968 by the Astronautics Laboratory. The revision was published as Internal Note, IN-P&VE-S-68-1, dated July 31, 1968.

The purpose of this report is to provide a tool for practical use in vibration engineering for Marshall Space Flight Center and contractor personnel.

VIBRATION MANUAL

INTRODUCTION

The vibration engineer is mainly concerned with keeping the vibrations of a space vehicle to a level which is not detrimental to the man or the machine and designing the machine to survive the environment. The main source of mechanical vibrations in vehicles is the rocket engines which generate vibration and acoustic energy over a wide range of frequencies. The resulting vibration environment can be severe with respect to airframe fatigue and damage to equipment.

To ensure the structural and functional integrity of the vehicle systems, it is necessary to determine the vibration environment of a vehicle or component. This environment can be approximated by analytical methods, or it can be predicted by comparison to the known vibration levels of a similar vehicle. If the vehicle is available, the environment can be determined by static firings and flight tests.

The known vibration environment can then be approximately reproduced or simulated in the laboratory to improve the design or to prove adequacy of the vehicle or components. Static firings and flight tests can be considered as methods to obtain the vibration environment and also as environmental tests of the vehicle.

This report describes how analysis and evaluation of data from static firings and flight tests yield the information necessary for writing vibration specifications in environmental testing.

This report is intended to help to correlate the terms, ideas, and methods of the groups concerned with vibrations, and to promote better understanding and coordination between all groups by serving as a guide in the vibration field.

SECTION I. SOURCES OF VIBRATION

To understand the problems of space vehicle vibrations, it is necessary to have a general background in the various sources of these vibrations. This section provides some general information regarding these sources and their causes. A more detailed discussion of these sources of vibration is beyond the scope of this section and will not be included. Additional considerations on sources of vibration excitation are presented in Section XIV while Reference 1, 2, and 3 provide comprehensive coverage of this subject.

A. Sources and Causes of Vibration

A space vehicle may have many different causes of vibration, but each one can be characterized by one of the following sources:

1. Acoustic.
2. Aerodynamic.
3. Mechanical.

These sources of vibration vary in predominance depending upon the design of the vehicle, the design of the launch pad, the phase of the vehicle flight, and the total mission of the vehicle.

1. ACOUSTIC

Sound fields provide the excitation energy for acoustically induced vibrations. Acoustic fields may be generated in many ways. The sound field of the rocket engine itself is caused by the acoustic energy generated in the rocket engine because of moving parts, fuel flow, and fuel combustion.

The sound field of the turbulent exhaust from the rocket engine has its origin downstream from the plane of the engine exhaust. This exhaust turbulence produces a more severe sound field in the vehicle than does the engine itself, and is considered to be the most predominant cause of vehicle vibration while the vehicle is in the atmosphere at speeds below Mach 1.

The sound field of the turbulent wake generated by the engine exhaust induces structural vibration. Structures susceptible to acoustic (also aerodynamic) pressures are skin panels, skin stiffeners, and bulkheads [1].

The extent of this vibration is dependent upon the frequency spectrum, amplitude, and space correlation of the sound field plus the mechanical impedance of the structure [2].

2. AERODYNAMIC

Several aerodynamic phenomena exist that are associated with high-speed flight in the atmosphere which supply excitation energy that induces vehicle vibration. Some of the aerodynamic effects that cause vehicle vibration are as follows:

- a. Pressure fluctuations in the turbulent boundary layer around the vehicle.
- b. Flutter of a fin or panel in the airstream due to dynamic instability.
- c. Turbulent wakes generated by air flow past vehicle projections in atmospheric flight.
- d. Flow over recesses and cavities.
- e. Oscillating shock waves that may be attached to the vehicle surface.
- f. Buffet flow separation, which occurs when the air in the boundary layer is forced to flow around sharp corners.
- g. High-velocity flow through pipes.

Aerodynamically induced excitation normally reaches maximum values in the vicinity of Mach 1 and maximum dynamic pressure ($\max q$).

3. MECHANICAL

Mechanical sources of vibration originate from direct mechanical excitation. The main mechanical source of vibration usually comes from the engines and related equipment, such as pumps, motors, compressors, and generators.

These vibration sources originate in the acceleration of moving parts and in the periodic variations of gas, electrical, and other energy forces.

These mechanical vibration forces act both as forces within the equipment and as external forces [3]. In outer space, when airborne sources of excitation have ceased to exist, rocket engine operation will continue to induce mechanically coupled vibration. This type of vibration will be most severe at positions near the engine and diminish at more remote locations because of the damping and impedance mismatch inherent in the vehicle structure.

High magnitude transient vibration levels, caused by rapid pressure changes at engine ignition and cutoff, cause a transient excitation of the structure. These transients are short in duration and are measured in milliseconds.

Other mechanical sources of vibration are as follows:

- a. Transportation of the vehicle from one site to another.
- b. Mechanical release of the vehicle from the launch pad by explosive bolts or some quick-release device.
- c. Engine gimbaling.
- d. Variable thrust because of rough combustion.
- e. Separation of the stages by mechanical means, such as explosive charges, retro rockets, and ullage rockets.
- f. Landing impact of a recoverable vehicle.
- g. Propellant sloshing.

Mechanical vibrations that are high in magnitude and of long duration can cause wear in contact surfaces, equipment malfunction, crew discomfort, and, most important, structural fatigue.

B. Complete Vibration Environment

The complete vibration environment of a vehicle includes all vibration experienced from manufacture to the completion of a mission.

The vehicle must first be transported from the manufacturing site to a place suitable for static firing. The vibration environment during transport

may be severe, depending upon the mode of transportation and the carriage system. The vibration experienced during this period may be very different from the flight environment for which the vehicle was designed.

After the vehicle has reached the test site, one or more static firings are conducted to check the vehicle systems before delivery to the launch site. Often, one of the most severe vibration environments is caused by exhaust turbulence during static firing. This exhaust turbulence vibration level is generally developed in the first few seconds after ignition and continues throughout the static firing. The vehicle is also subjected to local mechanical vibration, gimbaling effects, and ground handling prior to and subsequent to static firing.

After completing these static firings, the vehicle is again subjected to transport vibration when it is taken to its permanent base, launch site, or temporary site (in the case of a mobile launch vehicle). When the vehicle reaches its launch site, it may again be static fired for a short duration to perform a systems check. After the systems check is complete, the vehicle is ready for its flight objective.

When the booster engines develop thrust while still on the launch pad, turbulence of the exhaust stream is again a principal vibration source. All evidence to date indicates this turbulence to be the most severe vibration excitation source. Not only does the most severe source of vibration occur before liftoff, but the position of the vehicle on the launch pad and the presence of other structures in the launch vicinity provide means of reflecting the sound field or changing the radiation pattern of the sound field. Ground reflection, which increases the sound pressure level of the vehicle, is evident up to an altitude of at least 50 nozzle exit diameters and diminishes at higher altitudes. As the vehicle is in motion and its forward velocity increases, the noise environment is reduced [2]. Some of the reasons for this decrease are as follows:

- a. Decrease of pressure with altitude.
- b. Increase of time required for noise to travel forward from source in flow behind missile.
- c. Decrease in relative velocity between the jet flow and the atmosphere.

The acoustic field is usually hemispherical until the vehicle is airborne, and then slowly changes to spherical as the reflection from the launch area is diminished by the gain in altitude. The sound pressure level on the launch pad is dependent upon the type of exhaust deflection of the exhaust tunnel, or muffler effect. This engine exhaust noise continues to affect the vibration levels, with diminishing intensity, until the vehicle exceeds the speed of sound or leaves the atmosphere.

While the vehicle is still in the atmosphere, other aerodynamic effects such as flutter, pressure fluctuations, and buffeting may develop and upon exceeding the speed of sound, oscillating shock waves are generated that can cause high-level vibration transients.

After the vehicle has passed the speed of sound, the acoustical source from the exhaust no longer affects vehicle vibration, and once out of the atmosphere neither the acoustic nor the external aerodynamic sources are present. Under these conditions, only the mechanical sources remain to cause vibration. Re-entering the atmosphere produces aerodynamic shock waves which can induce high-level transient vibrations, and again the vehicle is subjected to aerodynamic pressure, turbulence, buffeting, and flutter. Finally, vibration and shock which the vehicle experiences caused by landing impact, must be considered in analysis of complete vehicle vibration environment.

SECTION II. ACCELEROMETERS

The purpose of this section is to provide general knowledge of the principles, characteristics, and applications of accelerometers used by the Marshall Space Flight Center for the measurement of vibration and shock. This section will aid in the selection of a general type of accelerometer for the measurement of a specific environment; however, it is not intended to be a guide for the selection of specific accelerometers. References are given at the end of this report for more detailed information on vibration and shock measurement and accelerometer theory. For more information about or selection of specific accelerometers, literature and specifications of accelerometer manufactures, and laboratory test results should be consulted, some of which are given in References 4, 5, 6, 7, 8, and 9.

A. Accelerometer Considerations

An accelerometer is a transducer which converts the acceleration input that it experiences into a proportional output quantity. Accelerometers are available in many forms for widely varied applications. They are used in aircraft and missile navigation systems as well as for the measurement of vibration and shock. The requirements for an accelerometer vary from the extremely sensitive low-frequency types used in vehicle navigational systems to those used in vibration and shock studies, which must be capable of sensing motion over a very wide range of frequency and magnitude.

Virtually all accelerometers used for shock and vibration measurement are electromechanical transducers (sensors or pickups); i. e., the instrument output quantity is an electrical signal. Motion is converted into an electrical signal because the electrical signal may be transmitted over considerable distances (Section VI), and the electrical signal may be used as the input to amplifiers, filters, analyzers, and recorders for data recording and reduction purposes (Sections VII and VIII). The time history of the electrical signal may then be used to provide information concerning the frequency and waveform of the vibration as well as its magnitude (Section IX).

Many different types of transducers have been developed for the purpose of converting mechanical motions into equivalent electrical signals. These include piezoelectric, strain gage, piezoresistive, force balance (servo), potentiometer, variable inductance, electrokinetic, magnetostrictive, variable capacitance, and permanent magnet self-generating instruments.

The first five of these transducers are the most commonly used accelerometers at MSFC. These transducers are used for structural response measurements and will be discussed in the following paragraphs.

B. General Accelerometer Principles

All accelerometers to be discussed involve one basic mechanical principle; i.e., the response of a mass-spring system. The base of a mass-spring system (seismic instrument) or its equivalent is attached to the point where shock or vibration is to be measured, and the acceleration force is sensed by the transducing element from the motion of the mass (seismic mass) relative to the base. An accelerometer operates below the natural frequency of the mass-spring system. When the frequency of the point to be measured is above the natural frequency of the mass-spring system, the transducer can become either a displacement or a velocity transducer, depending on whether the sensor measures displacement or velocity. The mass-spring transducer shown schematically in Figure 1 consists of a mass suspended from the transducer case by a spring. The motion of the mass within the case may be damped by a viscous fluid, electric current, or other device symbolized by a dashpot.

The ratio of the relative displacement amplitude of the mass-spring system between the mass and transducer case to the acceleration amplitude of the case is shown in Figure 2 as a function of frequency for various values of critical damping ratio. This frequency response curve shows that the acceleration amplitude is directly proportional to relative displacement for frequencies well below the natural frequency of the system. Thus, this transducer is used as an accelerometer when the vibration frequency is below the natural frequency of the system and within the flat portion of the response curve. If the transducer is undamped, the response curve is substantially flat below approximately 20 percent of the natural frequency. Consequently, an undamped accelerometer can be used for the measurement of acceleration when the vibration frequency does not exceed approximately 20 percent of the natural frequency of the accelerometer. The range of measurable frequency increases as the damping of the accelerometer is increased, up to an optimum value of damping. When the fraction of critical damping is approximately 0.65, an accelerometer gives reasonably accurate results to frequencies of approximately 60 percent of the natural frequency of the accelerometer. Thus, it can be seen that the useful frequency range of an accelerometer increases as its natural frequency increases.

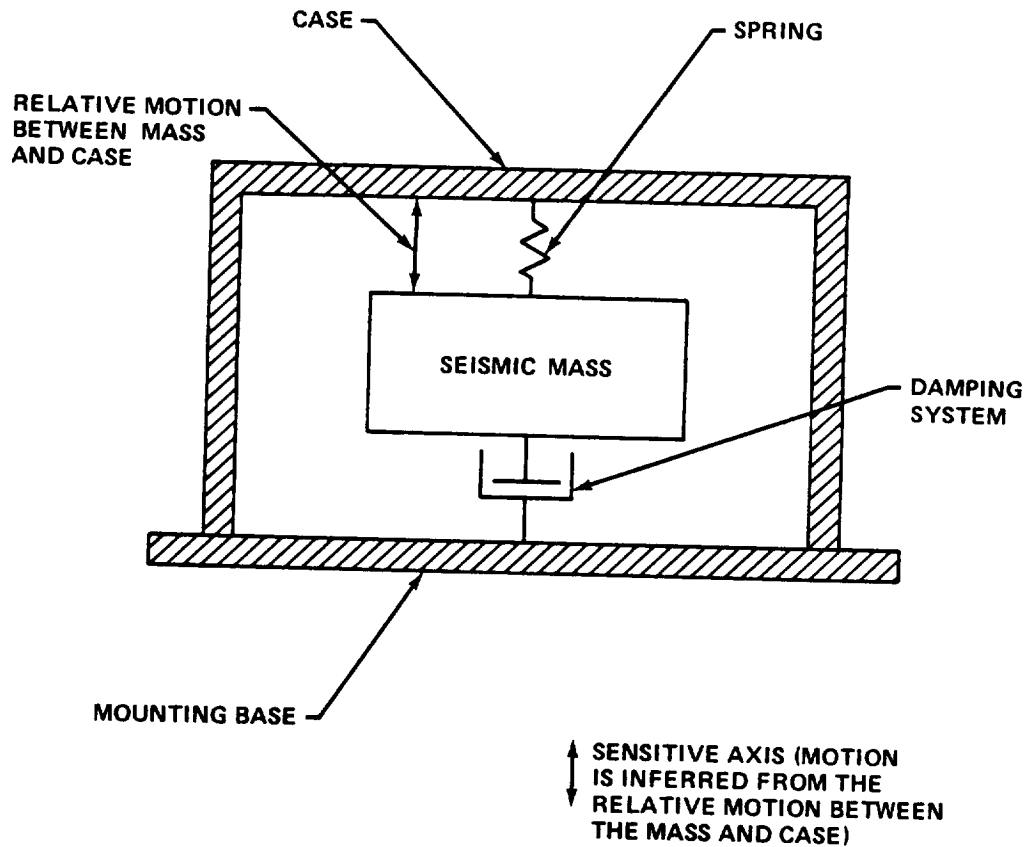


Figure 1. Schematic of a mass-spring type vibration transducer.

For a constant acceleration, the output sensitivity of an accelerometer is dependent of the sensing parameter. If the sensing parameter employs mass deflection, the electrical signal of the transducer may be very small at high frequencies since the deflection of the spring is inversely proportional to the square of the natural frequency. However, a piezoelectric accelerometer has as one of its advantages the ability to sense acceleration directly and the electrical signal remains relatively constant with frequency.

C. Piezoelectric (Crystal) Accelerometers

Figure 3 shows schematically a self-generating accelerometer requiring no external power in which the transducing element is a small disc of piezoelectric (crystal) material. Piezoelectric materials generate an

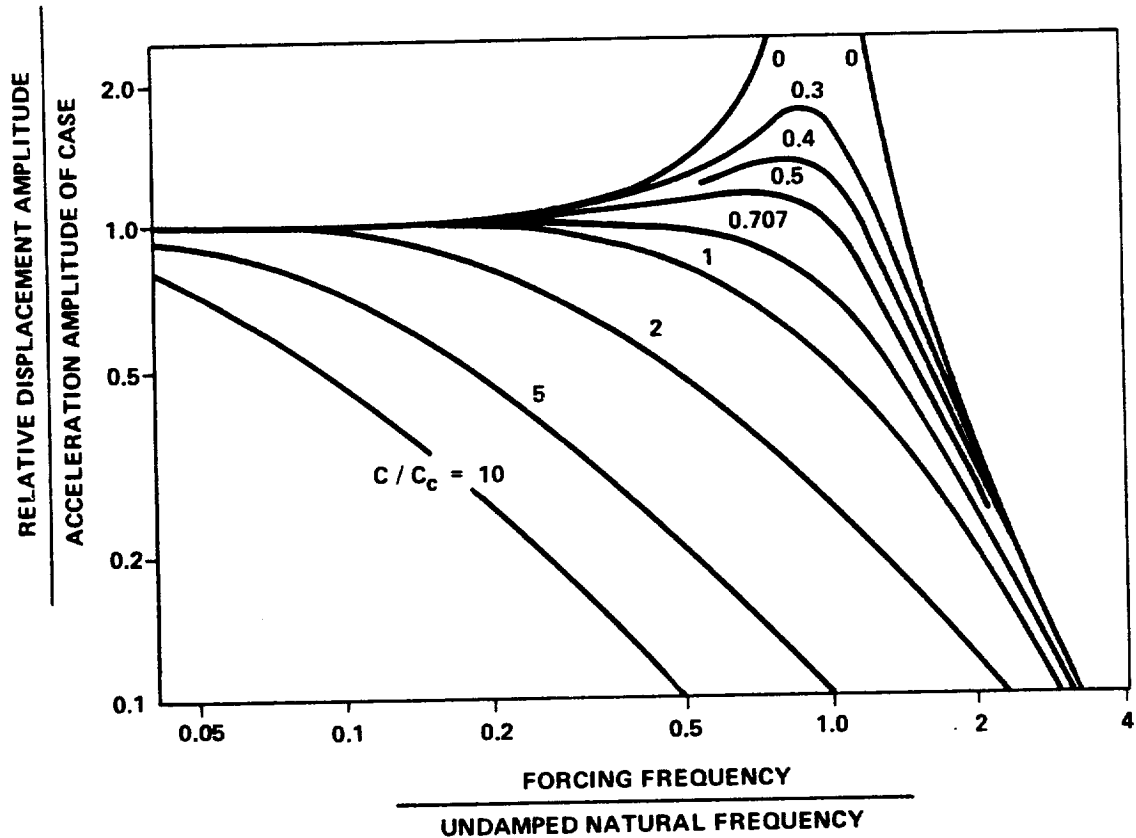


Figure 2. Frequency response curves for various values of critical damping (C/C_c) of a linear second order mass-spring system (sinusoidal input).

electrical charge when subjected to mechanical strain. The piezoelectric element may be either a natural or synthetic crystal or a ceramic material, such as barium titanate. The piezoelectric materials contain crystal domains oriented either by nature or artificial polarization, and the slight relative motion of these domains, resulting when a load is applied, causes an electrical charge to be generated. Materials of this type generally exhibit high elastic stiffness and usually act as a part of the spring in the mass-spring system. The type shown is of compression design and consists of a seismic mass compressed between a spring and wafer of piezoelectric material. The inertial force experienced by the mass causes a proportional change in strain within the crystal. This change in strain causes an electrical charge to be developed by the crystal. If the change in strain is within the linear elastic

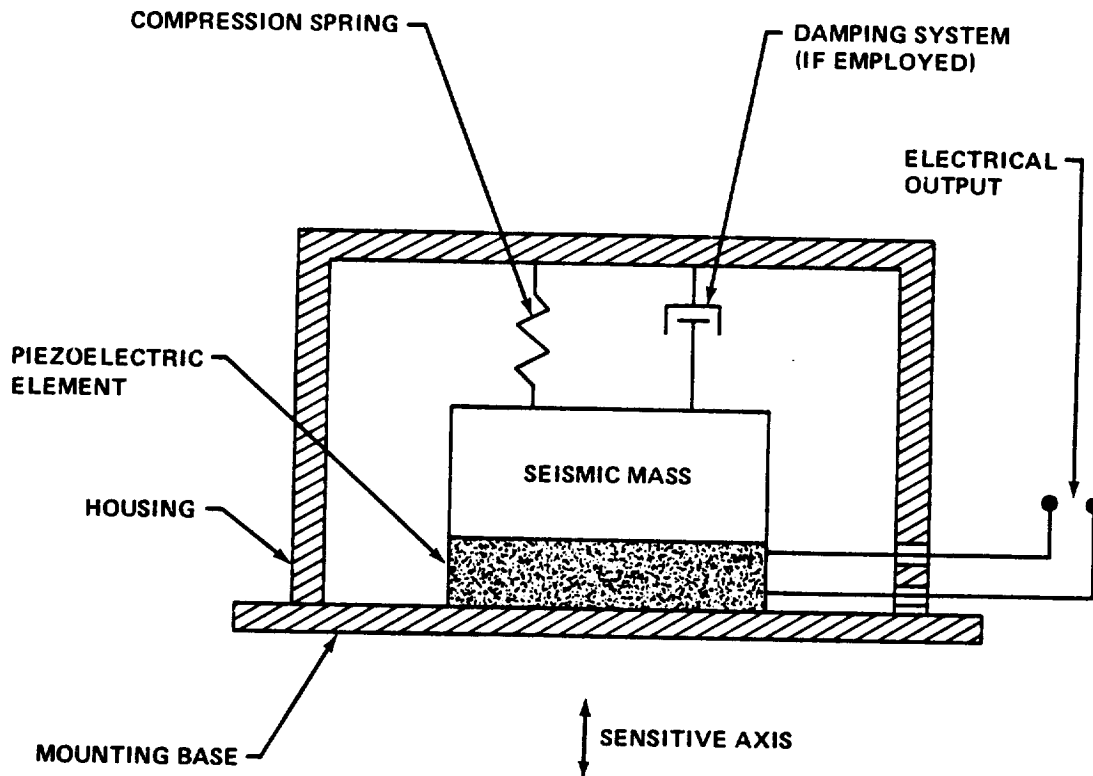


Figure 3. Schematic of a typical compression-type piezoelectric accelerometer.

range, the charge will be in proportion to the inertial force or acceleration experienced by the mass. The compression spring is preloaded such that the crystal wafer is always maintained in compression. The resulting mechanical system exhibits virtually no damping and a high resonant frequency (usually between 25 and 75 kHz).

There are various basic designs of piezoelectric accelerometers in which the crystal element is subject to different kinds of stress. These include the basic compression design, shear design, bender design, and different arrangements of these basic types. Modern design of these configurations mechanically isolates the crystal element from the instrument case to minimize or avoid the effects of case distortion on sensitivity.

To avoid electrical difficulties known as "ground loops," electrical insulation between the accelerometer and ground should be provided. Some crystal accelerometers have their active elements electrically insulated

from the case. Others are non-isolated electrically, and an electrically insulating stud or washer is used.

The piezoelectric accelerometer behaves as a charge generator, with the generated charge proportional to acceleration. It is not capable of measurement down to zero frequency, and its low-frequency response is dependent upon the electronics of the accelerometer cable and coupling amplifier combination. The traditional way to improve the low-frequency response has been to use intermediate impedance matching amplifiers (cathode or source followers) that have higher input impedance but low output impedance so that long cables may be used to remote readout instruments without affecting sensitivity. Charge amplifiers are often used for the same purpose. A discussion of impedance matching electronics, amplifiers, and connecting cables (along with the problem of cable noise) used with piezoelectric accelerometers is given in Section VI.

Due to the high resonant frequency (usually between 25 and 75 kHz), size, and ruggedness of crystal accelerometers, they are widely used for the measurement of both vibration and shock. There is a great variety of instruments available with a wide range of frequency response and acceleration range characteristics. Since damping is low, instrumentation for shock measurement should include low-pass filters to avoid falsification of data by accelerometer "ringing" at resonant frequencies. Also, a wide variety of operating temperature ranges is available with crystal accelerometers. For more details of piezoelectric accelerometer characteristics and a comparison with other accelerometers, refer to Table 1.

Recent innovations in crystal accelerometer design include the improvement of damping characteristics of certain models. This tends to eliminate undesirable resonant ringing under shock application and extends the useful frequency range. Also, progress is being made in decreasing the extremely high output impedance characteristic of these instruments. In some cases, source followers are incorporated directly inside the instrument case without a significant increase in size or weight.

D. Strain Bridge Accelerometers

The electrical resistance of a wire is proportional to the applied strain, increasing when it is stretched and decreasing when compressed axially or when initial tension is relieved. Strain bridge accelerometers are based on this principle. The transducing element is one or more fine strain

TABLE 1. ACCELEROMETER CHARACTERISTICS AND COMPARISON

Characteristic	Type of Accelerometer			
	Piezoelectric	Strain Bridge	Piezoresistive	Force Balance (Servo)
Size	Small 0.6 in. dia \times 0.8 in. to approx. 0.2 \times 0.3 in.	Small 1 in. ³	Small 0.6 in. dia \times 0.8 in.	Medium 1.0 in. dia \times 2.0 in. or 1.4 \times 1.5 \times 3.0 in.
Weight (oz)	Light-Very Light 0.03 to 2.0	Light 3 to 5	Light 1.25	Medium 3 to 8
Overall Accuracy (%)	1 to 5	0.5 to 2	1 to 4	0.1 to 1
Ruggedness	Very good	Good	Good-Fair	Good
Price (dollars)	50 to 500	250 to 400	300 to 500	450 to 1000
Frequency Response ($\pm 5\%$)	Very high From 2 Hz (when used with source follower) to as high as 22 kHz.	High dc to as high as 2 kHz	Very high dc to as high as 20 kHz	Medium-Low dc to 300 Hz
Acceleration Range	0 to 2000 g for vibration; 10 000 to 20 000 g for shock	± 5 to ± 50 g	± 10 000 g for vibration to 50 000 g full scale for shock	± 0.5 to ± 50 g
Temperature Range	-300° to +500° F, some to 1100° F, some to 2000° F with fluid cooling, some to cryo- genic temp.	-65° to +250° F	-65° to +250° F	-40° to +212° F
Cross-Axis Sensitivity (%)	5 max.	1	3 max.	0.2
				Potentiometer
				Large
				Heavy 8 to 32
				1 to 3
				Fair
				65 to 250
				Low dc to 10 Hz
				± 0.5 to ± 30 g
				—
				—

TABLE 1. (Concluded)

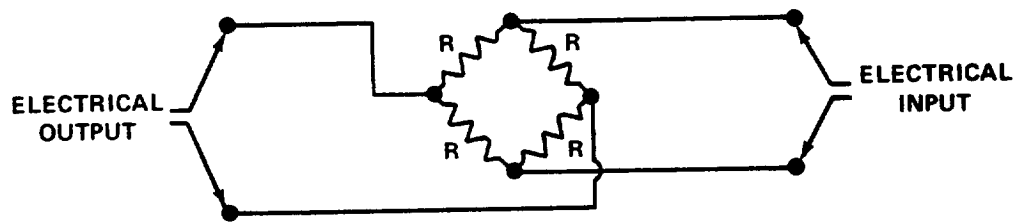
Characteristic	Type of Accelerometer				
	Piezoelectric	Strain Bridge	Piezoresistive	Force Balance (Servo)	Potentiometer
Output Level	Low 5 to 72 mV/g	Low to 50 mV Full Scale	High ±250 mV Full Scale	High ±5 to ±10V Full Scale	High up to 20 V/g
Excitation	None	Regulated ac or dc	Regulated ac or dc	Unregulated dc	Regulated ac or dc
Additional Equipment Required	AC amplifier Demodulator if dc output required	Low-level amplifier Demodulator if dc output required	Low-level amplifier Demodulator if dc output required	None if dc output required	Voltage regulator
General Disadvantages	1. No static response 2. Poor low frequency response 3. Low signal output	1. Requires regulated input source 2. Low signal output	1. Requires regulated input source 2. Some are susceptible to damage	1. Limited frequency range 2. Some are sensitive to angular acceleration	1. Poor resolution 2. Size and weight 3. Limited frequency range
General Advantages	1. Self-generating 2. High frequency response 3. Small size 4. Rugged	1. Good linearity 2. Static response 3. Relative small size	1. Static response 2. High frequency response 3. High signal output	1. Good linearity 2. Static response 3. Unregulated power source 4. Large signal output	1. Good linearity 2. Static response 3. Large signal output
Applications	Vibration and shock measurement on structural components	Bending mode studies and structural vibration measurements	Vibration and shock measurement on structural components	Bending mode and POGO effect studies	Bending mode and POGO effect studies

wires arranged so an applied strain changes their resistance in response to the relative displacement between a seismic mass and the instrument case.

A typical schematic illustration of a strain bridge accelerometer (Fig. 4) consists of a mass suspended by unbonded strain wire and employs a viscous damping fluid. The mass is free to move in the direction of the sensitive axis but is restrained against other motion. The inertial force experienced by the mass when it is accelerated causes a change in the strain of the supporting wires and a proportional change in their resistances. In Figure 4, the strain wires act as the spring portion of the mass-spring system. To increase sensitivity, the strain wires are arranged electrically to form the elements of a Wheatstone-Bridge circuit, with one or more active legs. An electrical schematic is shown at top of Figure 4. This change in strain in the wires create bridge-resistive unbalance, and in the appropriate circuit an output voltage appears proportional to the acceleration.

The bridge is balanced externally and may be excited with either a dc or ac source. The bridge can be excited by an ac carrier signal, if desired, at some frequency well above the highest test frequency (see Section VI for discussion of carrier frequencies). If ac excitation is used, the ac excitation frequency should be at least five times higher than the highest data frequency expected. However, ac excitation frequencies above approximately 3 kHz should not be attempted on long cable runs because phase balancing problems may appear. Care should be taken not to exceed the rated excitation voltage of the transducer to avoid burning the strain wires.

Strain-bridge accelerometers can be used for measurements down to zero frequency and have sensitivities up to 50 mV (rms) for full-scale output, even with acceleration inputs of 1 g or less. Natural frequencies can be as high as 5000 Hz, although natural frequencies of a few hundred Hz are more common. The damping is usually about 0.7 of critical at room temperature. Since the damping fluids generally used change viscosity with temperature, the damping and the resonant frequency will be temperature sensitive. However, temperature-compensated instruments are available, and improvements in damping have been made. Newer fluid damping systems utilize viscous oil shearing. Low-viscosity oil is used, permitting exceptionally small viscosity changes in low- and high-temperature applications. This, in turn, minimizes damping changes. These units should be inspected frequently for damping fluid leaks. Also, some newer model strain accelerometers incorporate gas damping in which the movement of the seismic mass pumps a gas from a chamber through a porous plug. This system has the advantage of lower damping



ELECTRICAL SCHEMATIC

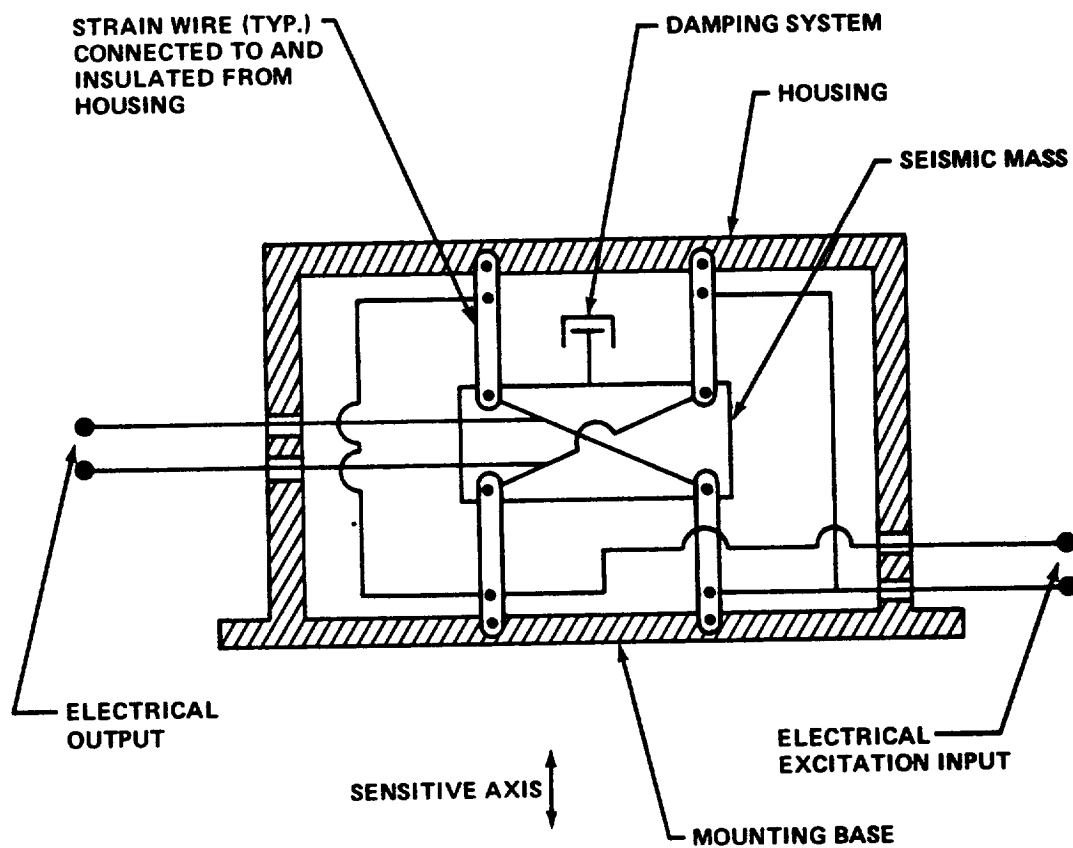


Figure 4. Electrical and mechanical schematic of a typical strain-bridge accelerometer.

change with temperature than previously used damping mediums. Newer models also show a trend away from pendulous suspension to minimize cross-axis sensitivity and sensitivity to angular accelerations. Table 1 should be referred to for more details of strain-bridge accelerometers and a comparison with other accelerometers.

E. Piezoresistive Accelerometers

Piezoresistive strain-gage accelerometers are similar in principal to wire strain-gage units and are based on the principle of the semiconductor strain gage. In place of wires, small chips of semiconductor crystal are used and arranged electrically to form the elements of a Wheatstone Bridge. These provide greater electrical output than conventional strain wire sensing elements.

The piezoresistive accelerometer combines several advantages of the strain-bridge accelerometer and the crystal accelerometer. While it is capable of measuring response down to zero frequency, its high-frequency limits and acceleration ranges are comparable to piezoelectric accelerometers. For example, one model has a range of ± 2500 g (peak) and develops ± 250 mV (peak) with an excitation voltage of 10 Vdc. Damping is 0.06 critical at a resonant frequency of 30 kHz. Therefore, the range of linear frequency response (± 5 percent) is given as 0 to 6000 Hz. A newer model for high g measurement offers a full-scale shock range of 50 000 g and frequency capabilities extending from dc to a resonant frequency of better than 100 kHz. Table 1 should be referred to for more details of piezoresistive accelerometers and a comparison with other accelerometers.

As compared to piezoelectric accelerometers, piezoresistive accelerometers are just slightly larger and are excellent for shock measurements (within the acceleration limit) because of their low-frequency capabilities. They are less rugged than piezoelectric accelerometers; in earlier models, a drop of a few inches onto a hard surface can cause considerable damage. However, ruggedness has been improved. This type of accelerometer is still in the developmental stage, and one problem has been in obtaining wider temperature compensation.

F. Force Balance (Servo) Accelerometers

The force balance accelerometer, more popularly known as the servo accelerometer, is basically an electromechanical feedback system which is actuated by a seismic mass. The essential components of the instrument are illustrated in Figure 5. When the instrument is excited along its sensitive

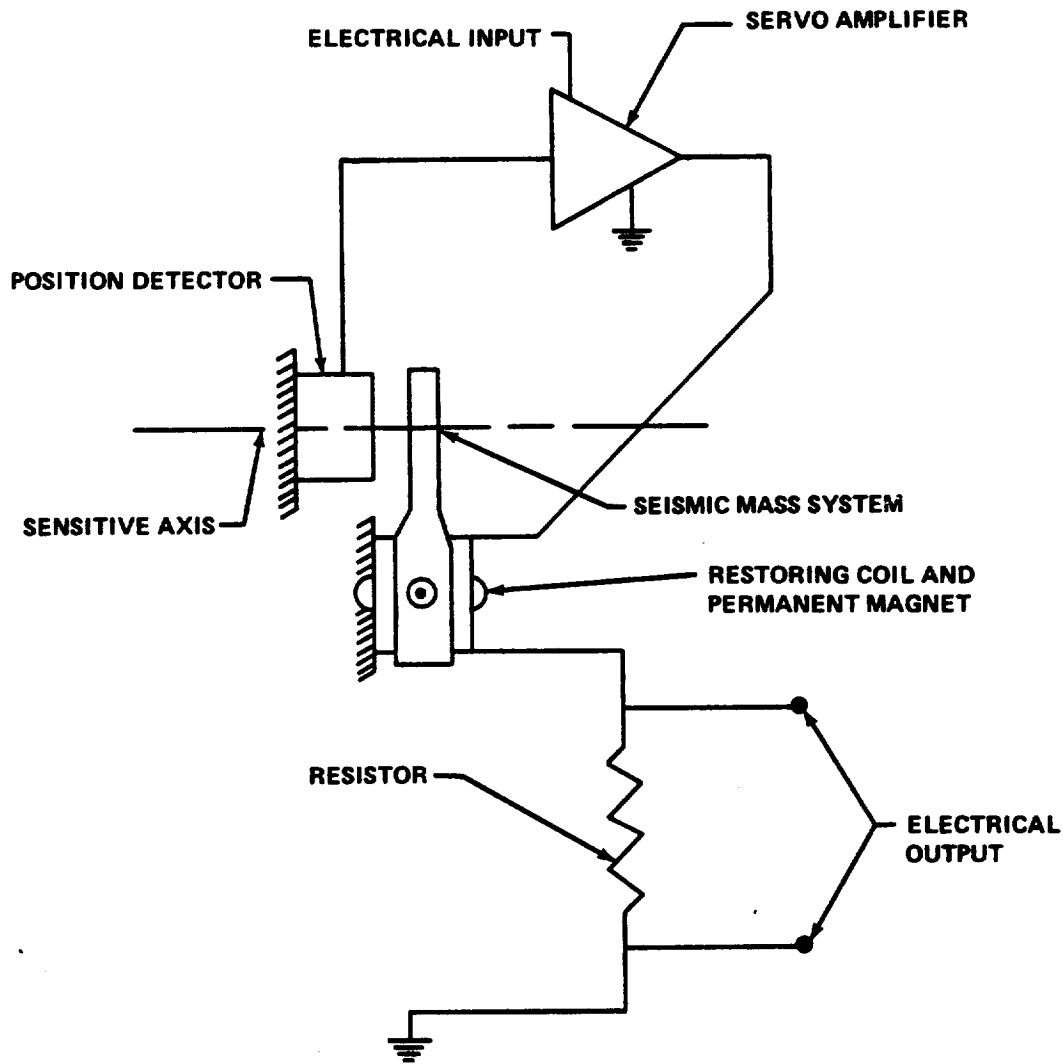


Figure 5. Block diagram of a force balance (servo) accelerometer.

axis by an input acceleration, the seismic mass tends to move. A position detector, which consists of an inductive type pickoff coil in an oscillator circuit, converts the amount of deflection of the mass relative to the case into a proportional electrical signal. This causes a change in the output current of a small servoamplifier. The output current is fed back to a restoring coil located within a permanent magnetic field which develops a restoring force (or torque) equal and opposite to the original inertia force experienced by the mass. Thus, the complete servocircuit acts like a stiff mechanical spring. The acceleration is now measured as a voltage drop across a resistor

which is in series with the output of the servoamplifier, since the restoring current (proportional to restoring force) is a measure of the initial acceleration.

There are two classes of servoforce balance accelerometers; a pendulous type, having an unbalanced pivoting mass with angular displacement, and a nonpendulous type, having a mass which is displaced rectilinearly. In pendulous types, small rotations approximate linear motion and movement is considered to be linear along a fixed axis of sensitivity. Because of this, angular types are often sensitive to angular acceleration.

The force balance accelerometer offers much higher accuracy than other types of accelerometers and is used extensively in inertial guidance systems for missiles and rockets. However, since low natural frequency and high damping are characteristic of the force balance accelerometer, its use in measuring vibration environments is generally limited to measuring low level accelerations at low frequencies. Force balance accelerometers may be damped either electrically or by a viscous fluid, and have high sensitivities. A typical instrument might be calibrated for a range of ± 10 g with a sensitivity of 0.8 V/g. Table 1 should be referred to for more details of force balance accelerometers and a comparison with other accelerometers.

G. Potentiometer Accelerometers

The potentiometer accelerometer consists of a mass-spring-damper system and a potentiometer circuit, shown schematically in Figure 6. The potentiometer wiper is connected to the seismic mass, and a constant voltage is maintained across the resistance element of the potentiometer. When the instrument experiences acceleration, the mass is displaced relative to the base, causing a change in the output voltage of the potentiometer circuit.

A typical unit is fluid, air, or magnetically damped from 70 to 140 percent critical and is relatively heavy. This type of instrument is used mainly for measuring very low accelerations at low frequencies and most have natural frequencies below 30 Hz. One of their main disadvantages is that their resolution is limited by the diameter of the resistance wire in the potentiometer, thereby requiring a relatively large displacement to produce a usable signal. Their principle advantage is their high output and their flat response from half of their natural frequency down to zero frequency. Table 1 should be referred to for more details of potentiometer accelerometers and a comparison with other accelerometers.

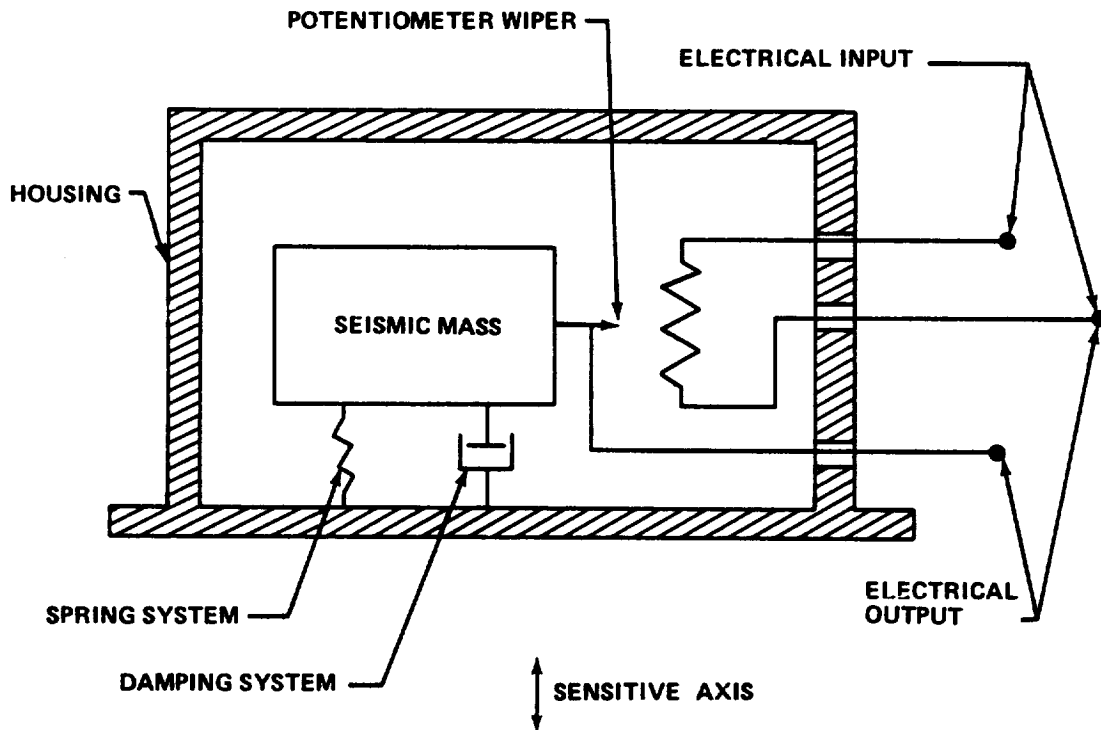


Figure 6. Schematic of a typical potentiometer accelerometer.

H. Accelerometer Comparison

Table 1 gives a comparison of various basic accelerometer characteristics for the accelerometers previously discussed. The various values presented here do not represent any specific accelerometers but represent an approximate general range of the types available. It should be noted that these accelerometers are being continuously improved and that the values given in this chart may change with further developments and new products.

I. General Accelerometer Selection Characteristics

Certain important characteristics to consider when selecting an accelerometer are basic and will be treated here. For specific information or more detailed analysis, specific manufacturer specifications and literature on accelerometers should be consulted.

When considering an accelerometer for a given application, both environmental and operational parameters must be given attention. Two basic questions must be answered:

1. Will the accelerometer measure the environment? Consider:
 - a. Acceleration range of accelerometer.
 - b. Frequency response of accelerometer.
 - c. Frequency and amplitude ranges of the complete data acquisition and display system.
 - d. Temperature effect on sensitivity.
 - e. Cross-axis sensitivity.
 - f. Acoustic sensitivity.
 - g. Sensitivity of accelerometer.
2. Will the accelerometer survive the environment? Consider:
 - a. Temperature limits.
 - b. Shock and vibration damage thresholds.
 - c. The possibility of destructive excitement of the accelerometer at or near its resonant frequency.
 - d. Possible excitation of associated electronics at destructive levels.
 - e. Protection of transducer system from physical damage by either mechanical or human factors.

SECTION III. MICROPHONES

The purpose of this section is to provide a basic knowledge on the general types of microphones used for acoustic measurements. This section is not intended to be a guide for the selection of a specific microphone.

The three most commonly used types of microphones at MSFC are discussed in sufficient detail to ensure an understanding of the basics of microphone operation. The three general types of microphones are:

- a. Condenser microphone.
- b. Piezoelectric microphone.
- c. Tuned circuit microphone.

Diagrams are presented to aid in the discussion of these general types. A comparison of the characteristics of the three types of microphones is made to give further information on the application of each general type of microphone. A discussion on the selection of a general type of microphone is made in the last paragraph of this section.

A. Condenser Microphones

In basic terms, the condenser microphone is analogous to an electrical circuit containing a variable capacitor. The primary parts of this microphone are the metal housing, a thin metal diaphragm, and a backplate. The backplate and metal diaphragm are separated by an air gap and these elements constitute the electrodes of the variable capacitor. Figure 7 illustrates the basic construction of this type of microphone.

The capacitor (diaphragm and backplate) is energized by a dc voltage source. Sound waves impinging on the diaphragm causes a displacement of the diaphragm. This movement will change the capacitance of the diaphragm-backplate capacitor. A change in capacitance of the circuit changes the circuit output voltage. The magnitude of the output voltage is proportional to the pressure level of the sound wave.

To maintain static pressure equilibrium, the air gap between the electrodes of the capacitor is vented. This venting to the atmosphere causes

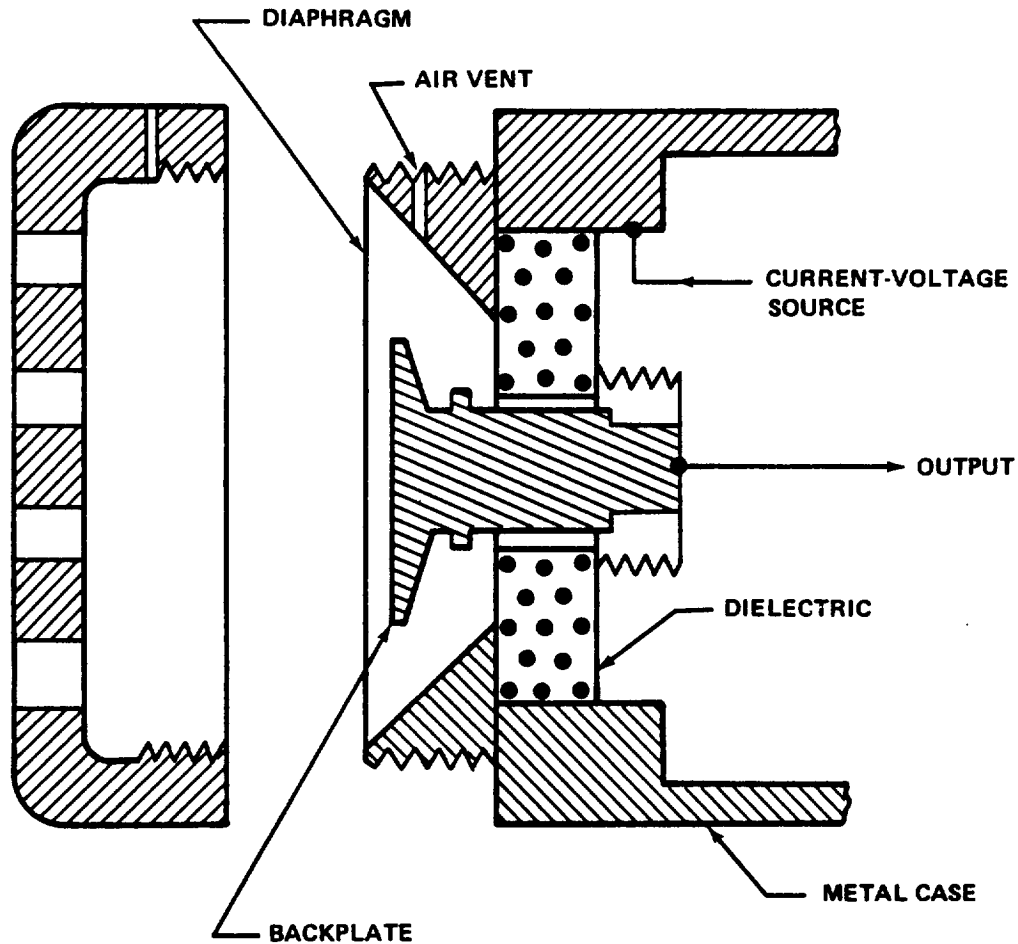


Figure 7. Condenser microphone.

causes the major limitation of this type of microphone. When large amounts of water vapor are present in the atmosphere, the dielectric constant of the air between the two electrodes of the capacitor becomes very low, allowing a direct current to flow, blocking the operation of the instrument. This same adverse effect is caused by condensation brought about by rapid temperature changes. Another limitation to the use of this type of microphone is the high output impedance of the instrument, particularly at low frequencies. Because of this high output impedance, a cathode follower, mounted close to the microphone, is required. High output impedance also increases the susceptibility to electrical leakage in atmospheres or high humidity. One advantage of this type of microphone is the small mass of the diaphragm which makes this type less sensitive to vibration than many piezoelectric microphones. From the disadvantages stated previously it is obvious that this type of microphone is not suited for flight test measurements.

B. Piezoelectric Microphones

The piezoelectric microphone is a self-generating transducer which uses piezoelectric sensing elements to generate a voltage when subjected to a physical strain. The fundamental principles of this general type of microphone have been discussed in Section II under piezoelectric accelerometers. Since the operation of piezoelectric elements has already been discussed, this section will deal with the manner by which the change in strain is created in the piezoelectric element.

Two different types of construction are available for the piezoelectric microphone. The first of these is similar in construction to the condenser microphone. This type consists of a diaphragm and a rigid backplate with the piezoelectric element located between them. Sound waves impinging on the diaphragm cause it to be displaced, thus causing a change in strain on the piezoelectric element. This change of strain causes a generation of voltage across the element. The second type of construction is similar but does not use a diaphragm. Sound waves physically excite the piezoelectric element. The sound waves hitting the element cause the change of strain, thereby causing a generation of voltage across the element. Figures 8 and 9 show these types of microphones.

The operating characteristics, frequency response and sensitivity, of piezoelectric microphones are dependent on the kind of material which is used as the sensing element. Elements which are most generally used in piezoelectric microphones are Rochelle salt, barium titanite, ammonium dihydrogen phosphate, and lead zirconium titanate. Piezoelectric microphones are well suited for measuring noise levels under adverse environmental conditions. This general type of microphone can be sealed such that changes in atmospheric conditions will not adversely affect the operation of the instrument. Up to this point only the simple type of piezoelectric microphone has been discussed and it has one major disadvantage in that it is susceptible to vibration. The movement of the microphone diaphragm by mechanical vibration causes a change of strain on the piezoelectric element, thereby giving an erroneous indication of the sound pressure level. Therefore, this type of microphone cannot be used in a vibration environment without proper isolation. Modifications on the simple microphone have been made to eliminate this disadvantage. This modified type uses two identical sensing elements. The first element measures the acoustic level while the second element is reversed in the electrical circuit to compensate for any mechanical vibration which might be present. As with the other piezoelectric microphones this type can be sealed

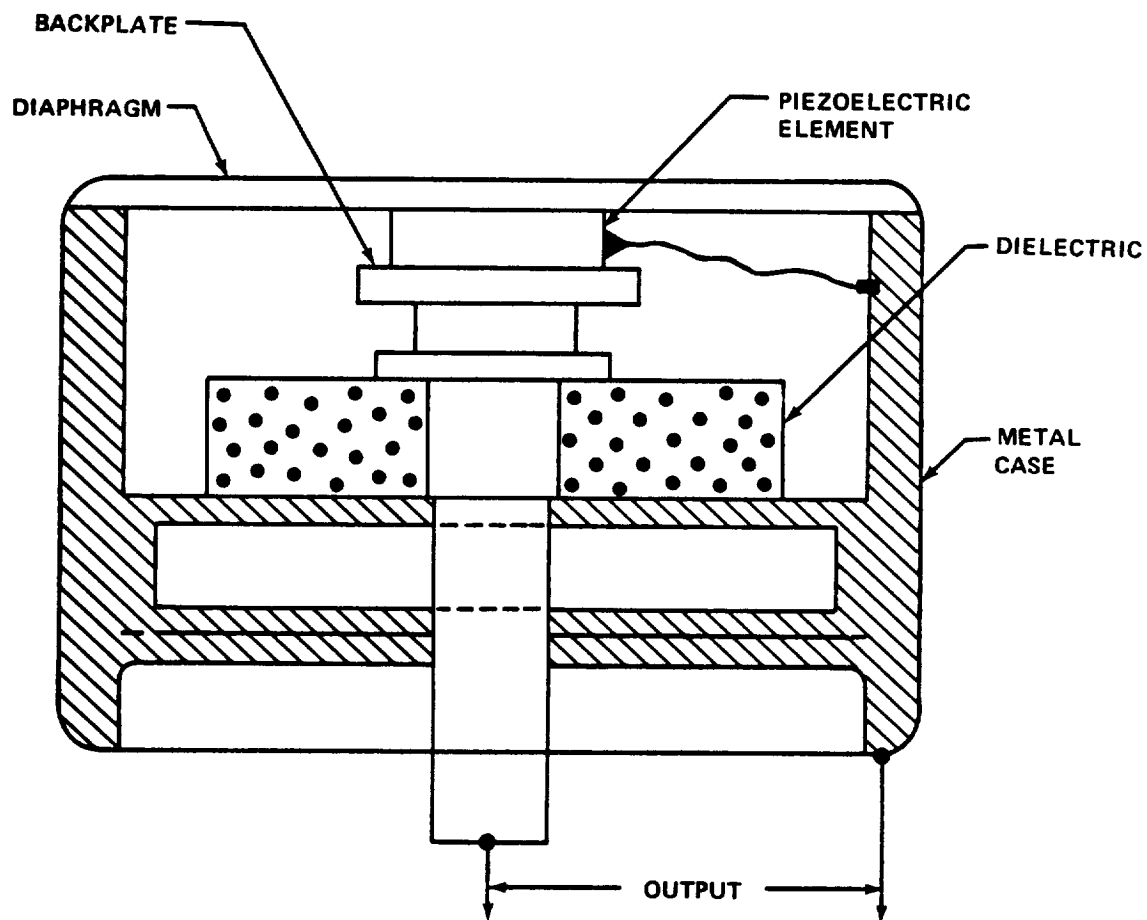


Figure 8. Piezoelectric microphone.

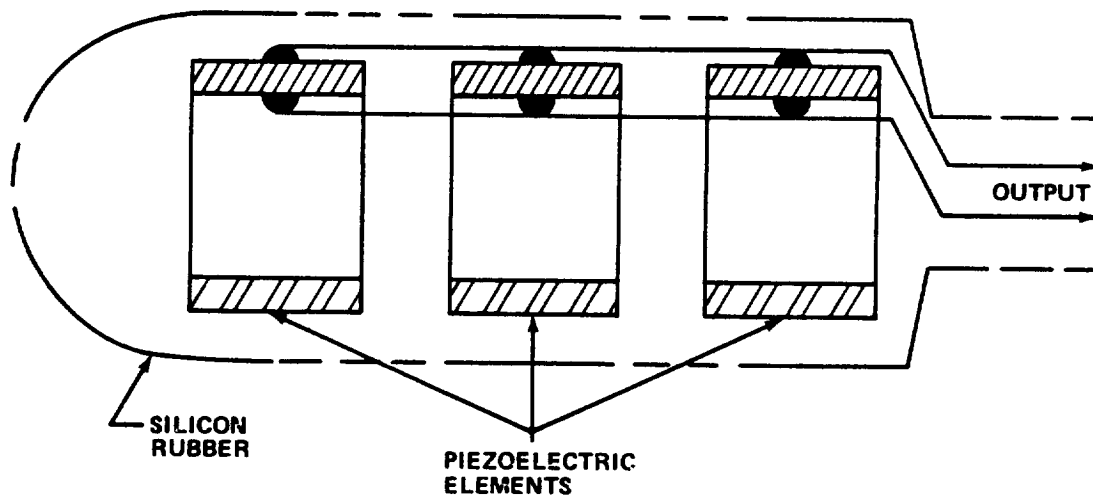


Figure 9. Piezoelectric microphone.

so that changes in atmospheric conditions will not effect the microphone operation. This type is shown in Figure 10. This modification makes this type of microphone useful for mounting on flight vehicles and other vibrating structures.

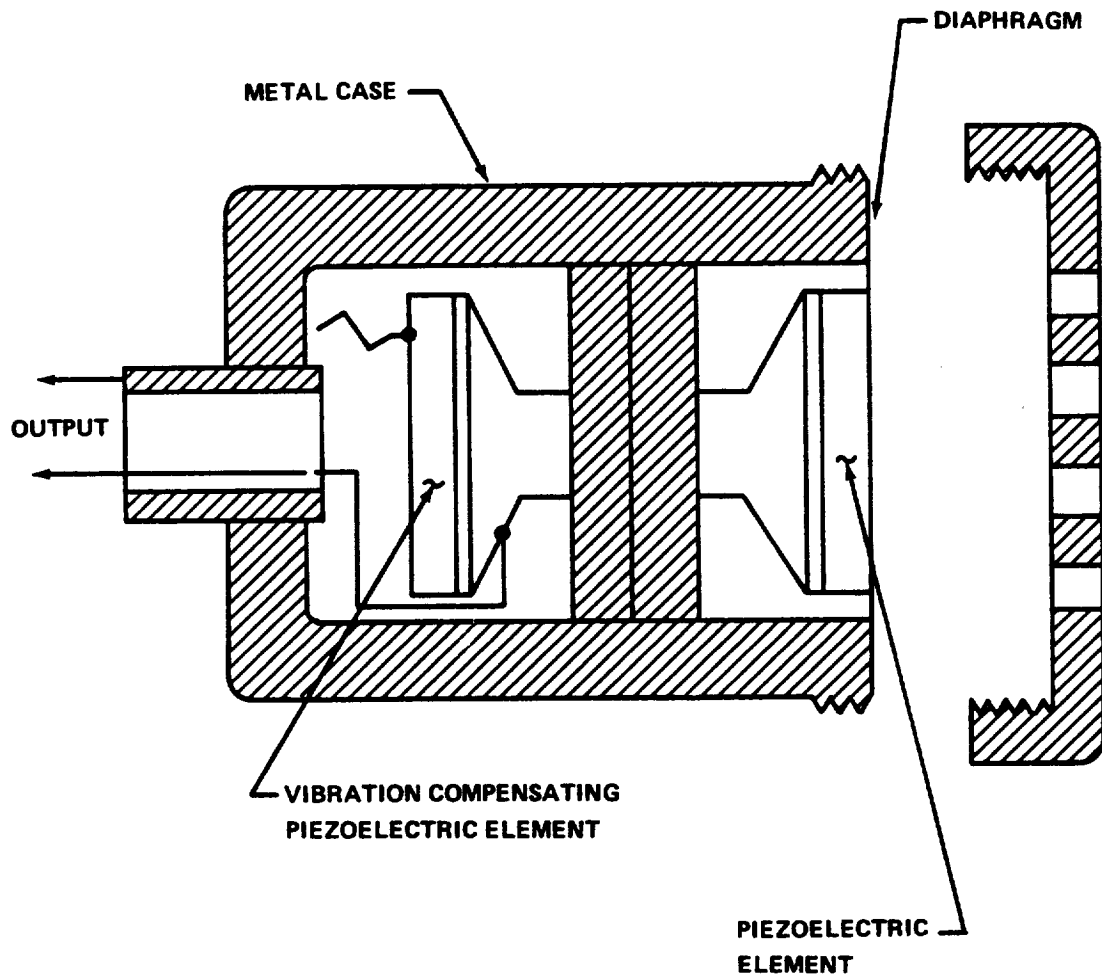


Figure 10. Vibration compensating piezoelectric microphone.

C. Tuned Circuit Microphone

In tuned circuit microphones, as in the previous microphones, diaphragm movement caused by impinging sound waves describes the basic operation of this microphone. In this type, the diaphragm is coupled in an electrical circuit with a variable condenser or inductance coil. These elements make up

a tuned electrical circuit and any movement of the diaphragm will cause a change in the resonant frequency of the circuit. This change can be related to the displacement of the diaphragm and thereby to the pressure level of the sound wave. Figure 11 shows the major elements of this microphone.

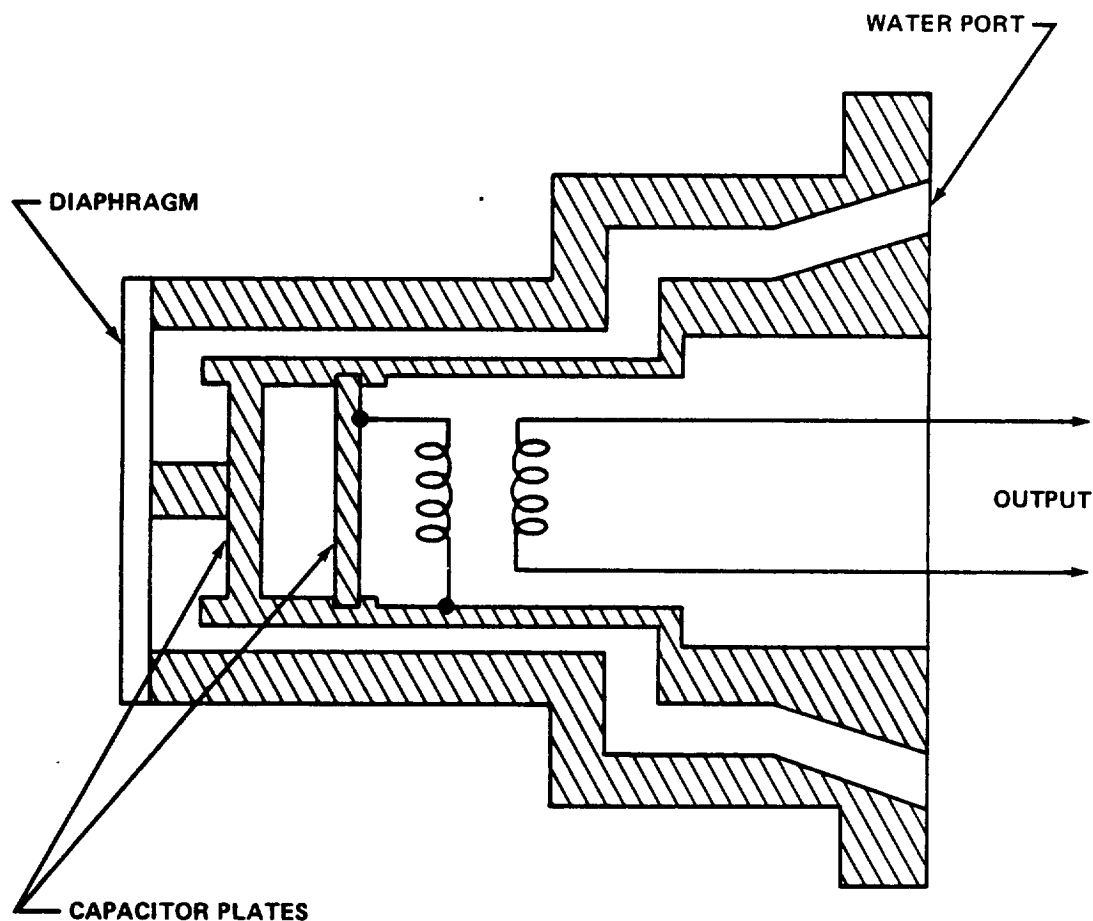


Figure 11. Tuned circuit microphone.

The major advantage of a tuned circuit microphone is that it is available with facilities for complete water cooling. This cooling system makes this type of microphone very useful in regions of extreme temperatures.

The massive diaphragm used in this instrument makes it very susceptible to mechanical vibration, in a way similar to that discussed previously

under piezoelectric microphones. Because of this disadvantage, this type of microphone cannot be used in a vibration environment without proper isolation.

D. Microphone Selection

The choice of the type of microphone to be used for a specified measurement is dependent upon the predicted environment in which the microphone will be required to operate. Microphones mounted on board flight vehicles are required to measure the magnitude of the acoustic field produced by the rocket during flight. The microphone mounted on board must be able to endure the vibrations caused by flight and atmospheric pressure and temperature changes caused by changing altitudes.

Vibration environments are critical to the operation of the microphone and limit the selection of the equipment to be used. Therefore, response of the microphone to vibration is a major consideration in microphone selection. Figure 12 shows the vibration responses for the general types of microphones. The piezoelectric microphones shown are not those which have vibration compensating elements. Microphones that are not located on board the vehicle may not require vibration or altitude compensation but may require temperature and humidity compensation.

The expected pressure level of the sound wave influences the selection of the microphone. Figure 13 gives an indication of the sensitivity ranges of the general types of microphones. This figure indicates the voltage output per microbar of pressure for the general types of microphones. As can be seen, the piezoelectric microphone has the lowest range of sensitivity.

All types of microphones, with the exception of the water-cooled tuned circuit device, will respond to rapid heat rate changes and constant heat flux fields; therefore, the temperature environment is another item to be considered.

It is difficult to compensate for temperature effects, vibration effects, etc. by proper calibration; therefore, the choice of a specific microphone should be made so that these effects are minimized. Table 2 is presented to give a indication of the relative merits of the above-mentioned general types of microphones. The information given are ranges for the general types; the specification sheet on the microphone should be consulted for specific microphones.

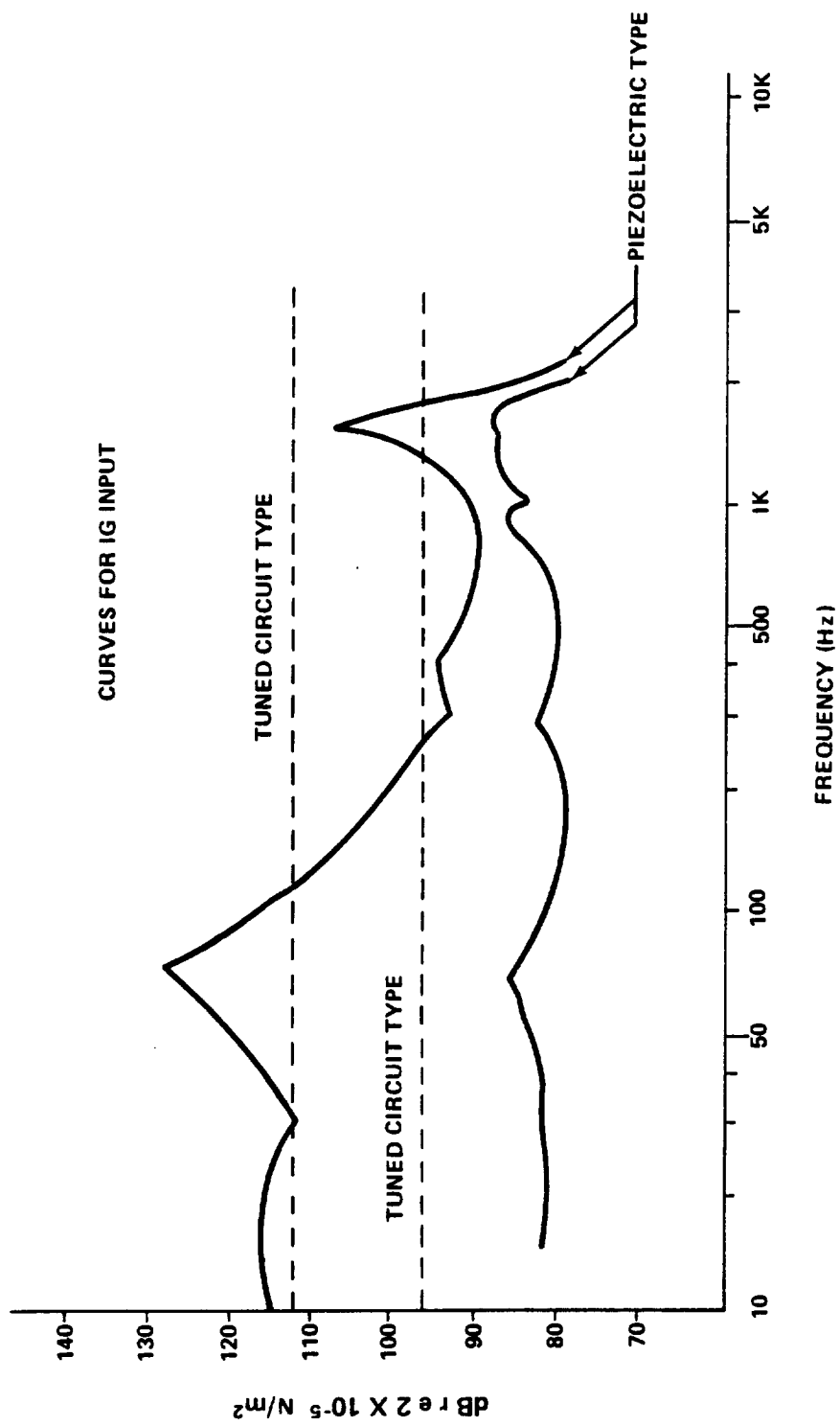


Figure 12. Vibration response of general microphone types.

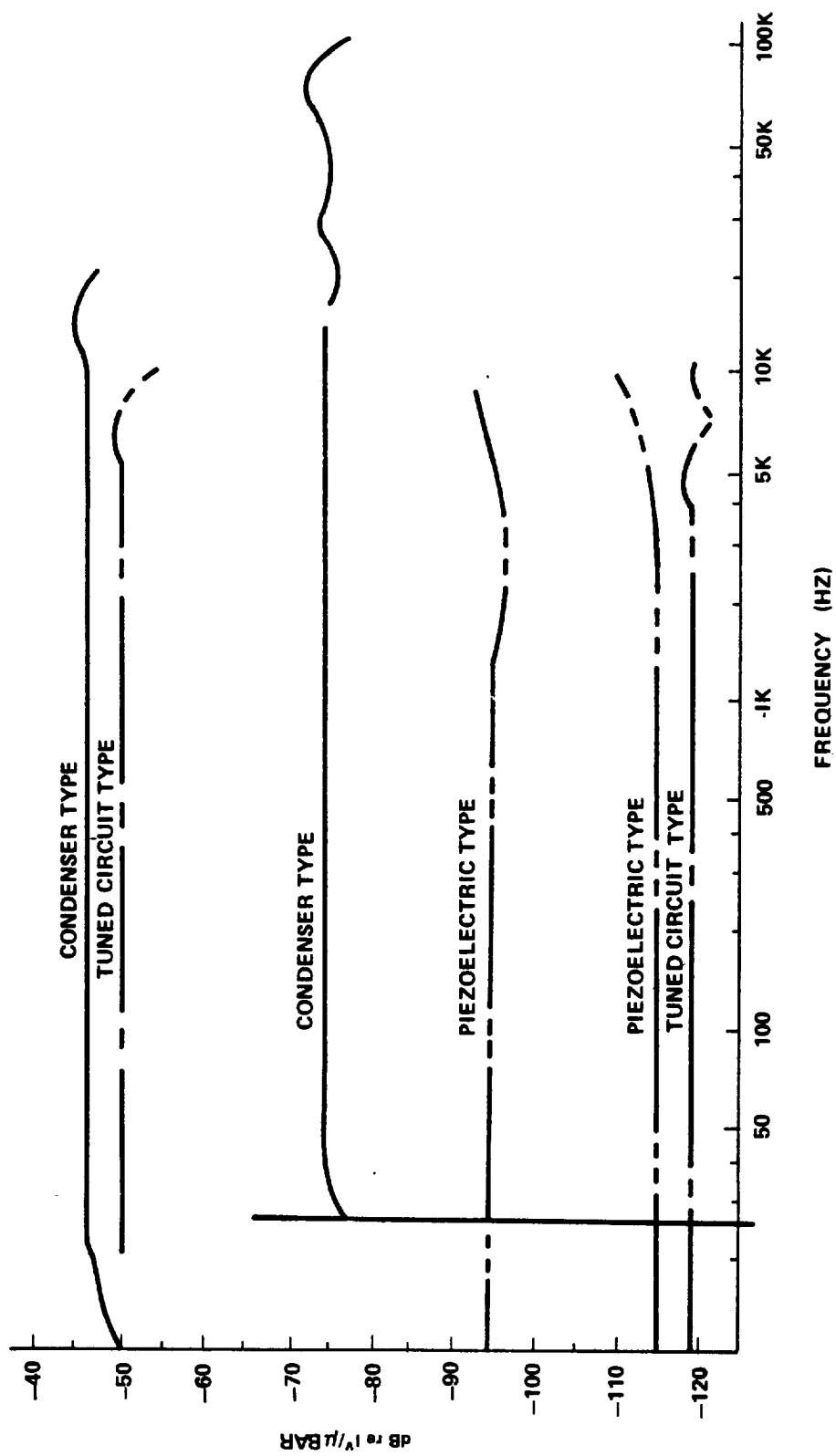


Figure 13. Sensitivity ranges of general microphone types.

TABLE 2. MICROPHONE COMPARISON

Characteristic	Condenser Microphone	Piezoelectric Microphone	Tuned Circuit Microphone
Size	0.43 to 2.54 cm in dia.	1.0 to 1.8 cm in dia.	.48 to 2.54 cm in dia.
Weight	—	20 to 198 g	10 to 256 g
Frequency Response	Linear to 6 kHz	Linear to 3 kHz	Linear to 4 kHz
Directional Sensitivity	omni to 4 kHz	omni to 3 kHz	—
Temperature Range	-50 to 100° C	-60° to 260° C	-75° to 1000° C
Output Level	.020 to .104 Volts/bar	.003 to 1000 Volts/bar	.002 to .080 Volts/bar
Excitation (Input Power Required)	dc	None	dc
Additional Equipment Required	Cathode Follower	Heat Shield in Severe Temperatures	Oscillator and Detector
General Disadvantages	<ol style="list-style-type: none"> 1. Sensitive to environments of high humidity 2. Sensitive to rapid temperature changes 3. Need dc power supply 	<ol style="list-style-type: none"> 1. Basic type sensitive to vibrations 2. Low output 3. Heat shield required at high temperatures 	<ol style="list-style-type: none"> 1. Sensitive to vibration
General Advantages	<ol style="list-style-type: none"> 1. Sensitivity to vibration is slight 	<ol style="list-style-type: none"> 1. Self-generating 2. Can be sealed and therefore used in environment of changing atmospheric conditions 3. Modified types available to compensate for vibrations 	<ol style="list-style-type: none"> 1. Water cooled to operate at high temperatures

SECTION IV. MOUNTING OF VIBRATION TRANSDUCERS AND MICROPHONES

This section presents basic considerations in the mounting of vibration transducers and microphones. Methods of mounting and associated problems are discussed for those types of mountings most commonly used at MSFC. Also, refer to References 10, 11, and 12 for further discussions.

A. Vibration Transducer Mounting

Transducer mounting is one of the most important considerations in the design of a vibration measurement system. Basically, a mounting must couple the transducer to the structure or component experiencing vibration such that the transducer accurately follows the motion of the surface to which the mounting is attached.

The method selected in mounting a transducer depends on the transducer type, the frequency and acceleration range to be measured, and the geometry of the mounting surface. If the surface-mounting conditions permit, the most desirable method is to attach the transducer directly to the structure. This eliminates spring mass system effects inherent in some types of mountings and, consequently, the transducer has an undistorted response to a higher frequency range. This type of mounting is illustrated in Figure 14.

1. MOUNTING BLOCKS

Usually, the transducer is attached to the structure or component by means of special mounting block or bracket. Odd shaped surfaces, the need to align the transducer in a particular direction, or the mounting of multiple transducers necessitates the use of adapters or blocks. Figure 15 illustrates a typical transducer-mounting block configuration where two transducers have been mounted to measure motion in more than one direction. Figure 16 shows a transducer-mounting block arrangement where the transducer is mounted on an odd-shaped structure requiring a block to align the transducer sensitive axis in a particular direction.

Since the mounting block and transducer combination acts as a spring-mass system it has its own resonant frequency and also an attenuation frequency range. The lowest resonant frequency of the mounting block with the transducer attached must be well above the highest frequency of interest so that the magnitude and phase of motion are undistorted in the required frequency range. In general, mounting blocks or brackets should be as rigid

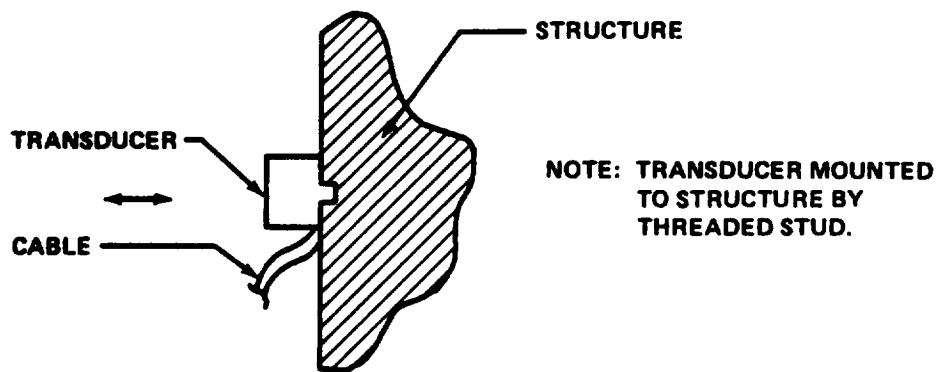


Figure 14. Direct mounting of transducer.

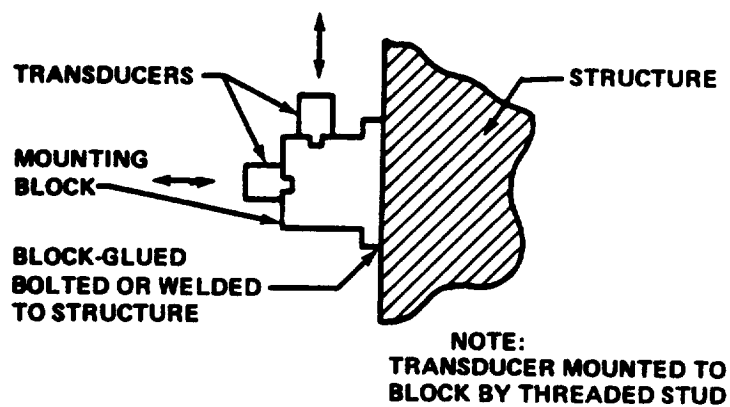


Figure 15. Multiple mounting of transducers.

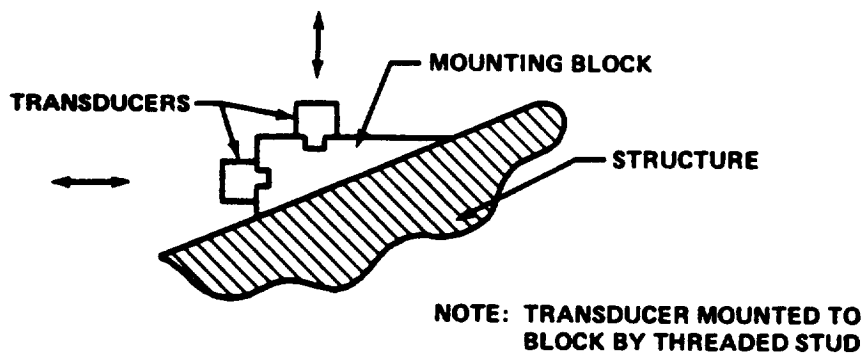


Figure 16. Transducers mounted on odd-shape structure.

and light as possible. Rigidity is important; otherwise, the mounting system will attempt to increase the motion of the structure to be measured by the transducer. Heavy mounting blocks affect the weight and frequency of the structure or component being vibrated and should be avoided. The mounting block-transducer combination must be tested on a vibration shaker at a constant g level through the required frequency range to indicate the linearity of the system.

2. ADHESIVE BONDING

If the transducer or mounting block cannot be welded or bolted to the structure, adhesive bonding may be used. Adhesives employed include double-backed tape and various types of cements (epoxies, dental cements, etc.). If the double-back tape is used, test frequencies should be kept below 2000 Hz [10] since above this frequency the transducer will not accurately follow the structural motion. Acceleration for a tape-mounted assembly should be restricted to less than 3 g since the tape may break loose at higher levels. If cements are used to secure the mounting to the test specimen, the transducer readings are not usually reliable above 5000 Hz. The use of adhesives should be avoided in cryogenic environments since they experience elasticity changes and loss of adhesion at low temperature resulting in a loss of reliability for the measurement.

A problem with cemented assemblies is their deceptively sturdy appearance. The strength of a cemented mounting cannot necessarily be judged by hand pressure. Since a calibration by vibration cannot be performed on flight vehicles after the assembly is cemented in place, the actual quality of the mounting cannot be verified. The integrity of the mount must be ensured by laboratory evaluation of the various cements and careful mounting techniques.

B. Microphone Mounting

Since the primary function of a microphone is to obtain a meaningful measurement of an acoustic field, the microphone mounting must be designed to this objective. Microphone directivity and the acoustic geometry of the test area must be considered when selecting microphone locations. Microphone elements are usually sensitive to vibration and must be isolated from support vibration. In general, there are two methods of vibration isolation employed: mechanical isolation and electrical isolation. The choice of isolation technique is governed by the environment to which the microphone will be subjected.

1. MECHANICALLY ISOLATED MICROPHONES

Mechanically isolated microphones are frequently employed for field measurements but are not generally used for either static testing or flight testing. Commercially available vibration isolators may be used to mount the microphone, but they must be used with caution. If the isolator microphone natural frequencies are within the acoustic frequency range of interest, a true reading cannot be obtained from the microphone. This problem makes it difficult to properly isolate microphones located on flight vehicles by mechanical methods. However, for mid- and far-field measurements, microphones can be mounted directly to concrete or similar massive type structures. Massive structures effectively isolate the microphone from mechanical vibration within the acoustic frequency range of interest. Other techniques for field measurements support the microphones by suspension systems that isolate the transducer from support vibrations. Figure 17 illustrates a method for obtaining microphone measurements at various altitudes while isolating the microphones from vibration by suspension from balloons.

2. ELECTRICALLY ISOLATED MICROPHONES

Flight and static test vehicles usually employ rigidly mounted microphones that are electrically isolated from vibration. The piezoelectric types described in Section III are ideally suited for flight measurements. Mounting techniques for this microphone type are generally the same as discussed previously for vibration transducers. Special mounting considerations are necessary for flight measurements caused by the acoustic environment. The external skin of the flight vehicle is subjected to acoustic noise from several sources (see Section I) and Figure 18 illustrates a mounting designed to measure this external sound level. One of the microphones shown in Figure 18 is flush mounted to permit measurement of the boundary layer acoustic noise and other external noise without disturbing the aerodynamic shape of the vehicle. Figure 18 also shows an electrically isolated microphone mounted on a ring frame to measure the vehicle internal noise level.

C. Associated Factors – Transducer Mounting

In addition to the method of attachment, there are many other factors to consider in the mounting of transducers. The following paragraphs outline some factors associated with the mounting of accelerometers and microphones.

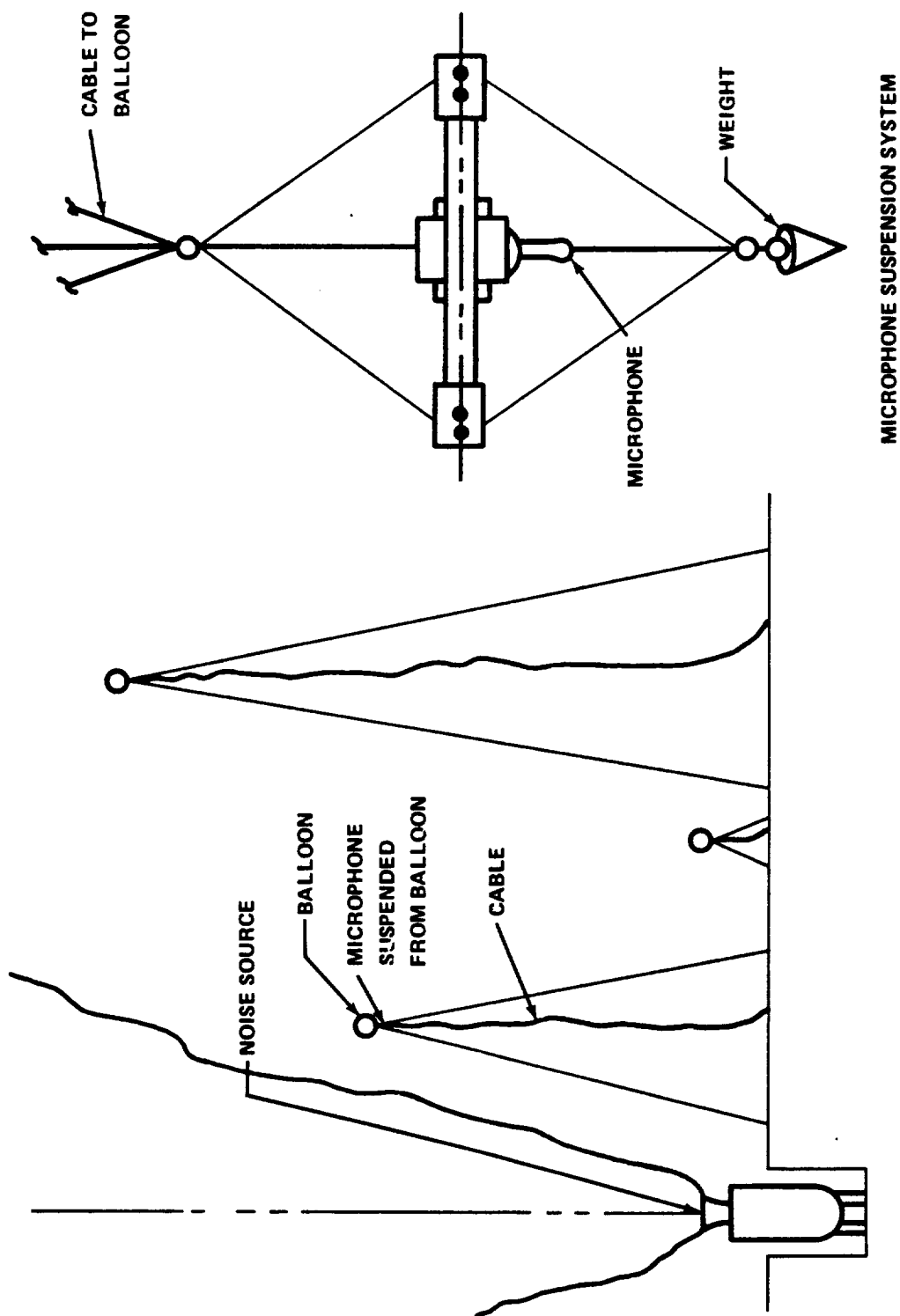


Figure 17. Static test microphone mounting.

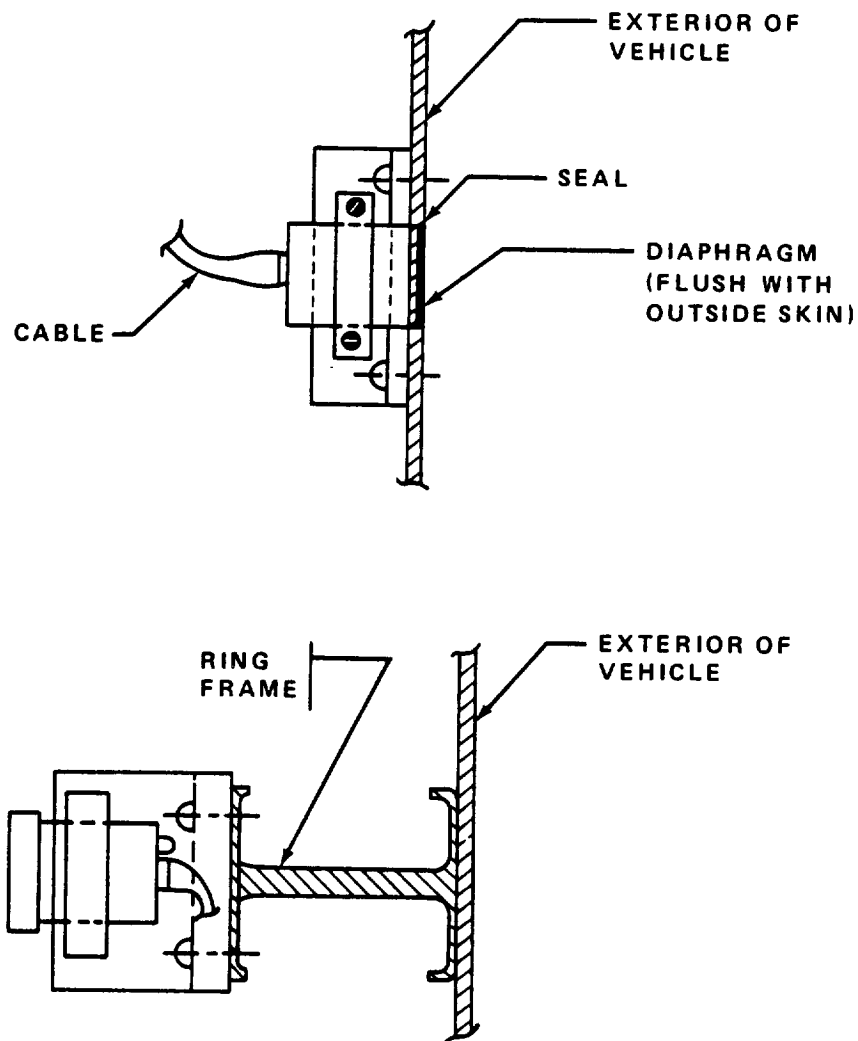


Figure 18. Typical flight vehicle microphone mountings.

1. TEMPERATURE EFFECTS

Some transducers exhibit high sensitivity to rate-of-change of temperature, called pyroelectric effect. The pyroelectric effect should not be confused with ordinary ambient temperature effect. Some transducers suddenly cooled or heated during a test react violently in the output response.

2. ELECTRICAL ISOLATION

A transducer should be isolated electrically from the ground to decrease the influence of ground loops. When threaded holes can be used, electrically isolated mounting studs are commercially available. However, these cannot be used on some hardware such as tubing, cameras, solar cells, etc., and other methods of isolation are required. A practical method useful for many applications is to cement the transducer in place with insulating material in between. The minimum amount of insulating material should be used to decrease the spring-mass effect in the vibration environment.

3. CABLE ROUTING

Transducer cable termination and routing can become important for some applications. Routings should be carefully considered to minimize the danger of physical damage and triboelectric effects. Too much slack in the cable often results in spurious signals. Movement of the cable, either jerking or steady state vibration, is an important source of noise.

4. MAGNETIC FIELDS

There are instances where transducers have to work in the presences of strong magnetic forces. Interference might develop at either the transducer or the connecting cables. The center conductor of many cables is paramagnetic and is a possible interference source. Auxiliary cable vibrations which could interfere with case-sensitive transducers might be caused by ac magnetic fields.

5. TRANSDUCER LOCATIONS

All transducer locations should be accurately identified and the mounting described by photographs or drawings. The orientation of the transducer sensitive axis on the test specimen or flight vehicle must be completely defined to permit proper data evaluation. This is extremely important in the evaluation of all vibration and acoustic data.

SECTION V. CALIBRATION

This section defines calibration procedures and problems associated with the dynamic instrumentation of launch vehicles. The material presented is general and deals with basic considerations related to any vibration or acoustic data acquisition system calibration. The nature of dynamic data is discussed and basic relationships used in sinusoidal calibration techniques are derived. Calibration procedures are discussed for transducers, data transmission, and data recording systems. The dynamic systems discussed are those for measuring vibration, acoustic, and shock environments, and are characterized by high-frequency response requirements. For further discussions, refer to References 13, 14, and 15.

A. General

The purpose of calibration is to determine the relationship between the final observed value of data and the true value of the environment at the sensing instrument location. When this relationship is known, the observed values may be properly interpreted. The calibration techniques which are most directly applicable to a particular instrumentation system will depend on the components of the system, system location and use, and the type of measurement.

Regardless of the method used in calibration, certain principles must be followed whenever possible. These principles are listed below:

1. The calibration should cover the expected range of environmental conditions. This means that the effect of frequency, amplitude, temperature, and other variables should be determined and accounted for in the calibration procedure when applicable.
2. Reference standards must be reliable. The accuracy of the calibration is, at best, no better than that of the reference.
3. Repeatability of calibration measurements should be established within limits to determine reliability of data. This requires several tests in which the same reference is applied repeatedly and the resulting indications are observed and recorded. The variation in these results indicates probable errors because of system characteristics, as determined by statistical analysis.

The most desirable calibration procedure for vehicular vibration and acoustic measurements would be a complete end-to-end stimulation; i.e., excitation of the transducer with a known environment equivalent to the expected environment and observation of the resultant output from the data reduction system. However, in most cases, this procedure is unrealistic because of its complexity. Therefore, it is usually necessary to calibrate the transducer subsystem independently of the data transmission and data recording subsystems.

B. The Nature of Dynamic Data

Dynamic data are usually broad-band random waveshapes which can be described by three parameters:

1. The magnitude of the measured quantity; e.g., power spectral density, sound pressure level, etc.
2. The variation of magnitude with respect to frequency; i.e., spectral characteristics.
3. The time history of magnitude at any particular frequency or band of frequencies.

These random data are analyzed by statistical methods in terms of mean-square values, probability density functions, power spectral density, etc. Other statistical methods may use correlation techniques to isolate periodic functions that are superimposed on random functions. Although random data are most commonly encountered in practice, it can be shown that sinusoidal calibration is applicable.

1. SINUSOIDAL CALIBRATION AND MATHEMATICAL RELATIONS

Instruments used to acquire high-frequency random wave data are often calibrated by application of a sinusoidal waveform. This is true whether the environment is simulated mechanically or electrically. A major advantage of sinusoidal calibration is the ability to calculate exactly the parameters that describe the waveform or environment. The following relationships are presented since they are commonly employed in sinusoidal calibration.

Sinusoidal vibration may be described by the equation of displacement

$$X = X_0 \sin \omega t$$

where

- X = instantaneous displacement
- X_0 = peak displacement
- t = time
- ω = angular frequency.

Differentiating yields the linear velocity

$$\dot{X} = X_0 \omega \sin \omega t$$

Differentiating again gives instantaneous acceleration

$$\ddot{X} = -X_0 \omega^2 \cos \omega t$$

Now, since angular frequency (ω) is related to cyclic frequency (f) by the equation

$$\omega = 2\pi f$$

and acceleration may be expressed in terms of g-level as

$$g = \frac{\ddot{X}}{K_g}$$
$$g = \frac{-4X_0 \pi^2 f^2 \cos \omega t}{K_g}$$

where K_g = gravitational constant.

Peak acceleration is obtained by setting $\cos \omega t$ to ± 1 , its maximum possible values.

$$G_p = \pm \frac{4X_0 \pi^2 f^2}{K_g}$$

Acceleration levels are commonly discussed in terms of peak-to-peak values which represent the "double amplitude" values, or twice the peak values although in flight measurements the range is specified in $\pm G_p$, which is a peak value

$$G_{p-p} = 2 G_p$$

The acceleration level which is considered representative of the vibratory energy level is the root-mean-square value, or rms level. This is the common measure of random vibration data and is represented mathematically as

$$G_{rms} = \frac{1}{T} \int_0^T g^2 dt$$

where T is the time of integration. This indicates that the rms level is the square root of the sum of the squared mean instantaneous values. For a sinusoidal function,

$$G_{rms} = \frac{G_p}{\sqrt{2}}$$

Similar derivations for random Gaussian motion are found in Reference 10. However, in random waveforms, it is not possible to relate rms or average values to peak values exactly. The rms-to-mean ratio is defined as the form factor of a wave. The form factor of a sine wave is 1.11 while the form factor of a random Gaussian noise is 1.26. Consequently, when an averaging meter which has been calibrated with a sine wave to indicate rms is used with random noise, the reading must be corrected by multiplying by the ratio 1.26/1.11 or 1.14.

C. Transducer Subsystem Calibration

The calibration of vibration and acoustic measuring transducers consists of determining their sensitivity or simply the ratio of output to input.

The specific information required for transducer calibration depends on the instrument type and intended use. Flight measurements, field measurements, laboratory measurements, etc., require different approaches to the problem of calibration.

The output-to-input ratio must be known for all frequencies that the transducer will experience. Variations in environmental conditions may necessitate the determination of the effects of temperature, supply voltage variations, radiation, acoustic noise, electromagnetic field, altitude, and humidity upon the transducer. The linearity of the transducer should be checked over the full range of magnitude of vibration or sound pressure level.

1. ACCELEROMETER SUBSYSTEM CALIBRATION

Calibration of accelerometers is performed by excitation under controlled laboratory conditions. At the beginning of laboratory calibration, the accelerometer subsystem gain should be adjusted such that the subsystem output is equivalent to that of the signal preconditioning circuit voltage. This adjustment should be made while vibrating the accelerometer at a nominal frequency and at the full-scale acceleration level within the capabilities of the excitation source.

To obtain frequency response the output of the accelerometer should be measured over the full frequency spectrum of the anticipated environment. The acceleration level should be selected so that the excitation amplitude limitations are not exceeded during the calibration procedure.

Linearity can be checked by setting the transducer acceleration level at a percentage of the desired full-scale acceleration level and recording the system output. This process is repeated at higher percentages up to 100 percent full-scale and the data plotted to check linearity. Normal increments are 20 or 25 percent with a return to the lowest percentage point after reaching full-scale to determine hysteresis characteristics. The accelerometer should be vibrated at a nominal frequency during this check, or, if a resonant beam is required, the resonant frequency of the beam should be used.

a. Gravity Methods

Some types of accelerometers can be calibrated under static conditions by means of earth gravity and centrifuge devices. These instruments generally have response at zero frequency and include the following types:

1. Wire strain bridge.
2. Servo (force-balance) .
3. Piezoresistive.
4. Potentiometer.

The 2-g or "Flip" calibration method takes advantage of the zero frequency or static response of an accelerometer. If an accelerometer is mounted with its sensitive axis in a vertical position, it senses the 1-g acceleration of the earth's gravitational field. If the accelerometer is turned 90 degrees so that its sensitive axis is parallel to the local horizontal, the instrument senses zero acceleration. If it is turned 90 degrees again, it is 180 degrees from its original position, and it senses the earth's gravitational field in the opposite direction. It could be said to go from a positive 1-g to a negative 1-g level, a total excursion of 2 g.

This calibration procedure has inherent accuracy. It is important to use good leveling techniques and to measure the 90-degree angle changes accurately. A spirit level and square are usually sufficient for the accuracy desired in field measurements.

Again, it is important to have the same transducer input voltage level for both calibration and data acquisition.

This method is only useful for accelerometers whose operating range is low enough for the 2-g calibration signal to be a significant portion of the expected data levels.

b. Centrifuge Method

A calibration method similar to the earth gravity technique is the centrifuge method. In this method, a centrifuge is used to apply constant acceleration to the vibration transducer. The centrifuge is usually a balanced table that rotates about a vertical axis. Cable leads from the transducer and power supply are usually brought to the table through low noise sliprings and brushes. Centrifuges are commercially available that provide acceleration levels up to 100 g and special machines are available that produce much higher levels. Accelerometers that have a frequency range down to zero Hz and have negligible sensitivity to rotation may be calibrated on a centrifuge or rotating table. The general accelerometer types listed in Paragraph a. above can usually be calibrated by the centrifuge method.

In the calibration procedure, the transducer must be mounted on the rotating table such that its sensitive axis is exactly aligned along a radius of the circle of rotation. The acceleration acting on the transducer is calculated from the equation:

$$A = \omega^2 R$$

where

A = acceleration

ω = angular velocity

R = distance from the axis of rotation to the center of gravity of the movable mass element inside the transducer.

c. Electrodynamic Shakers

Sinusoidal motion for the calibration of vibration transducers is usually generated by means of an electrodynamic shaker. The electrodynamic shakers directly convert electrical energy into sinusoidal motion. Transducers are subjected to sinusoidal motion such that the transducer produces an electrical signal which can be accurately measured and the ratio of electrical output to mechanical input evaluated.

d. Comparison Method

A frequently used method of calibrating a vibration transducer is by direct comparison of the output voltage to that of a secondary standard accelerometer. The secondary standard accelerometer has been checked with a primary acceleration standard and is used for laboratory calibration only. The accelerometer to be calibrated is mounted on the shaker table or a centrifuge table back-to-back with the secondary standard such that the two accelerometers experience the same vibration environment. This is done by locating the accelerometers so that their sensitive axes are directly in line with each other and with the direction of applied acceleration. This often results in the bases of the accelerometers being turned toward each other, hence the back-to-back term.

The secondary standard accelerometer has an accuracy of 3 percent traceable to the National Bureau of Standards. The readout system is accurate to 1 percent. The maximum difference observed when secondary standard systems are checked against each other has been 5 percent.

e. Piezoelectric Accelerometer Calibration Techniques

Since the frequency response of piezoelectric accelerometers does not extend down to zero Hz, they are not calibrated under static conditions. However, the characteristics of piezoelectric accelerometers (see Section II) permit calibration by the application of sinusoidal motion to the transducer. The accelerometer may be calibrated by the comparison method or by an absolute calibration method using an electrodynamic shaker as a motion generator.

A crystal accelerometer can be visualized as a charge generator combined with a small and discrete amount of capacitance. The crystal accelerometer normally requires impedance-matching devices which are sensitive to cable length. However, if the accelerometer signal is fed into a charge sensing amplifier, these limitations no longer apply.

A charge amplifier is a high-gain-voltage amplifier with a negative capacity feedback. This system possesses a complex input impedance including a dynamic capacitance portion, which is so large that any change of cable capacitance represents an insignificant portion of the total. Therefore, large variations of cable length have no overall effect on system sensitivity.

Many charge amplifiers contain an internal calibration source and a dial for insertion of the individual transducer sensitivity into the amplifier. Systems of this type require only proper setting of sensitivity, selection of the range to be used, and recording of the internal calibration signal. No calculations are required.

Another technique is the electrical simulation of a crystal accelerometer by placing a capacitor in series with a voltage generator. If the transducer sensitivity and the value of the capacitance are known, the voltage can be calculated by the equation:

$$E = \frac{Q}{C}$$

where

- E = output voltage of the simulated accelerometer
- C = capacitance of the simulated accelerometer
- Q = charge of the accelerometer calculated by multiplying the sensitivity (coulombs/g) by the simulated g-level.

The voltage, E, should be set to correspond to the proper acceleration level and the charge amplifier gain set to output this voltage.

f. Strain-Gage Accelerometer Calibration

To understand strain-gage accelerometer calibration methods, the electrical characteristics of this transducer must be understood.

All strain transducers are based on variations of the Wheatstone-Bridge circuit, which consists of four resistances arranged as shown in Figure 19. These strain-sensing resistors are constructed so that their resistances change when a physical stimulus (in this case, acceleration) is applied to the transducer. If the beam on which a strain-sensing resistor is located goes into tension, the resistance increases; if it goes into compression, the resistance decreases. The instrument output voltage, E_o , appears when $R_1 \neq R_2$ or $R_3 \neq R_4$, or both. The circuit characteristic is such that the resistances in adjacent legs are subject to algebraic subtraction, and the resistances in opposite legs add. The transducer may be constructed with one, two, or four active arms. An active arm is one whose resistance varies with the physical stimulus on the transducer. When the bridge circuit has less than four active arms, fixed resistors are used to complete the circuit.

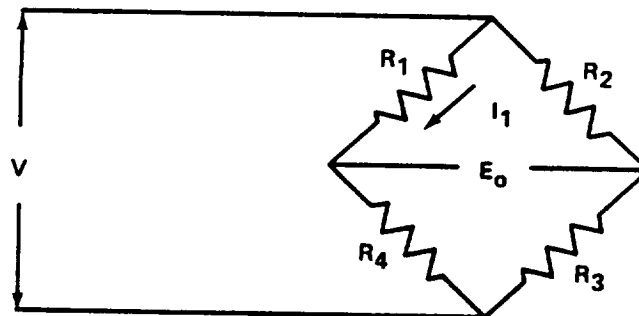


Figure 19. Wheatstone-Bridge circuit.

Referring to Figure 19, if the input voltage V is applied to the circuit and the resistance of R_1 is changed by the amount ΔR , we have:

$$R'_1 = R_1 - \Delta R \quad (\text{if the change is a decrease in resistance}).$$

If I_1 is the current through R_1 , then

$$I_1 = \frac{V}{R'_1 + R_4}$$

and the bridge output voltage,

$$E_o = \frac{V}{2} - I_1 R'_1$$

now by substitution,

$$E_o = V \frac{R_1 - R'_1}{2(R_1 + R'_1)}$$

or

$$E_o = V \frac{\Delta R}{2(2R_1 - \Delta R)}.$$

Since ΔR is small, the denominator can be simplified, and the term becomes

$$E_o = V \frac{\Delta R}{4R_1}.$$

From the preceding equations, it may be seen that the transducer output is always directly proportional to the input voltage. Where shunt calibration techniques are not used, care must be taken to insure that the input voltage level is the same during data acquisition as that used for calibration.

Since the electrical output of a strain-bridge accelerometer is induced by a resistance change caused by acceleration, the acceleration may be simulated electrically by placing a calibration resistor parallel to one leg of the Wheatstone Bridge. This technique is known as shunt calibration. In Figure 20, the resistance value of the parallel combination, R_c and R_1 , is

$$R' = \frac{R_c R_1}{R_c + R_1} \quad .$$

The circuit cannot tell whether the resistance change across the resistor, R_1 , is caused by acceleration or by the insertion of the calibration resistor, R_c .

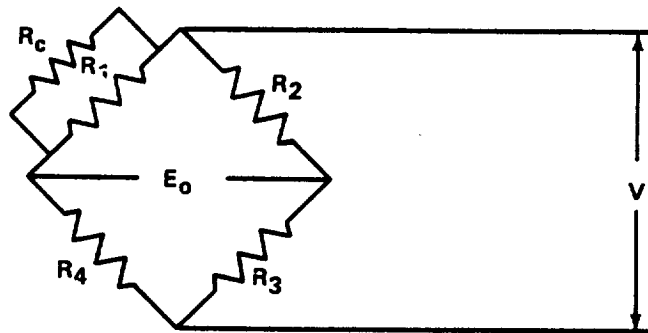


Figure 20. Shunt calibration system.

The sensitivity of a strain-gage accelerometer is expressed in $mV/V/g$. This means that if a given magnitude of accelerative force is imposed on the transducer, the output voltage will be a certain number of millivolts for each input volt applied to the transducer. Since the input voltage is always known, an output versus acceleration curve may be plotted for the transducer. The output voltage induced by a given calibrate resistor for the input voltage level may also be easily calculated. The calibrate resistor may then be set equal to an acceleration level. Note that once this is done, a specific calibrate resistor value is always equal to a specific acceleration level, regardless of input level. Two conditions must always be satisfied when applying the calibrate resistor: (1) it must always be applied to the same leg of the bridge, and (2) it must always be applied at the same electrical lead distance from the transducer.

Although the methods described may be used with fair accuracy, it is preferable to apply acceleration to the transducer and plot output versus

acceleration level. It is also preferable to read the output voltage produced by direct application of the calibrate resistor. Calibrate resistors are normally in the range of 20 000 to 150 000 ohms. They should be precision resistors of 0.1 percent tolerance.

2. MICROPHONE CALIBRATION

In general, the calibration requirements for microphones closely parallel those previously discussed for accelerometers. There should be a complete set of calibration curves available on each microphone. The environments in which the microphone will be operated should be determined for each application, and the response of the microphone to these environments should be defined. In the case of new microphones, the manufacturer's curves and specifications may partially fulfill these requirements. However, as the microphone is used, it must be calibrated periodically to ensure its continued satisfactory operation. The period between calibrations depends upon the frequency of microphone usage. All microphones should be calibrated a minimum of once every 6 months with a National Bureau of Standards calibrated reference standard. Each microphone should be calibrated prior to (pre-cal) and after (post-cal) each test application to determine possible alteration of the microphone response as a result of the test environments.

Microphones may be calibrated by several methods depending largely upon the particular microphone and the type of calibration required. The three basic microphone calibration systems most commonly used at MSFC are:

- a. High-intensity pistonphone system.
- b. Plane wave tube system.
- c. High-intensity calibration system.

a. Pistonphone System

The pistonphone system utilized a pistonphone, high-impedance pre-amplifier, voltmeter, counter, and associated power supplies. The pistonphone consists of two electrically driven pistons of different size operating in a known volume. The cyclic motion of the piston generates a sinusoidal pressure whose sound pressure level (SPL) value has been predetermined from volume and displacement calculations from previous measurements. SPL is a common acoustic term that can be described by the equation [14]

$$SPL = 20 \log_{10} \frac{P_{rms}}{P_o}$$

where

- SPL = sound pressure level in decibels
 P_{rms} = root mean square pressure value in microbars
 P_o = reference pressure (at MSFC, 0.0002 microbar).

The two pistons operate in the same volume since the chamber can be moved from one to the other. Since the pistons are of different size, their displacements are different and so are the SPL values they generate. By utilizing this characteristic and changing volume size in several discrete steps, a typical pistonphone system can generate SPL values from 110 to 170 dB in 10 dB increments. A typical frequency range is from 1 to 200 Hz. This type of calibration system is used primarily for certification of near- and far-field microphones at regular intervals. Both sensitivity and frequency response should be checked and records kept for the performance of each microphone.

To use the pistonphone system to check a microphone's sensitivity in the calibrator frequency range, the microphone is inserted in the chamber such that its diaphragm face is flush with the chamber wall, thereby not affecting the chamber volume. The microphone output is then connected to the preamplifier whose output is in turn connected to the voltmeter. The motor that drives the piston is then started and set to the desired speed (frequency) and the microphone output read from the voltmeter. Since the SPL value in the chamber is known and the microphone output at the SPL value is known, the sensitivity of the microphone can now be calculated. Checks of the complete calibration system may be made using a standard reference microphone in the system.

b. Plane Wave Tube

The plane wave tube system uses the calibration techniques of the comparison method. A standard reference microphone is excited by a pistonphone and the output recorded. The microphone is placed in the plane wave tube and the tube excited until the microphone output is identical to that generated by the pistonphone. This simulates the same sound pressure level in the plane wave tube as existed in the pistonphone. The microphone to be tested may be calibrated by mounting it side by side with the reference standard microphone in the plane wave tube and recording the output voltages for comparison.

c. High Intensity Calibration System

This system is designed to calibrate microphones in the frequency range from 5 Hz to 10 kHz at SPL levels from 110 to 190 dB. This system

is still in the development stage and several problems have been encountered. However, MSFC test engineers are improving the system and it promises to be a useful method for the calibration of high-intensity microphones.

d. Far-Field Techniques

At MSFC, acoustic monitors in remote far-field locations are calibrated by an acoustic calibrator and a voltage insertion technique. Microphones are acoustically calibrated by a portable calibrator. The gain is adjusted to a predetermined level and the voltage at the amplifier output is noted. The calibrator is removed and the monitoring station's self-contained reference oscillator is turned on. This amplitude stable oscillator inserts a voltage in series with the microphone and the gain is adjusted until the output at the amplifier is the same as that read during the acoustic calibration. The reference oscillator may be controlled from a central monitoring station to eliminate the necessity of an acoustic calibrate for every test.

e. Midfield Techniques

A voltage insertion method is generally used for calibration of the piezoelectric microphones used for midfield data acquisition. An open-circuit sensitivity for each microphone is obtained from the laboratory calibration, and a voltage representing the desired SPL for calibration at a given location is inserted into the system in place of the microphone. The output signal is recorded on magnetic tape before test data recording and serves as a pre-determined SPL reference. These calibrations should be made as close to test time as possible.

D. Data-Transmission and Data-Recording Subsystems Calibration

At MSFC, the calibration of the data-transmission and data-recording subsystem involves the sending of a simulated or actual transducer subsystem output signal through the entire system of cables, telemetry, and data recorders. A signal representing a known percentage of full-scale is injected into the front end of the data-transmission subsystem, and the data-recording subsystem is referenced to this signal.

1. FLIGHT TESTING

The calibration signal input to the telemetry system should represent full-scale peak-to-peak amplitude in all cases, except where the single-sideband

telemetry system (SS/FM) is involved. Full-scale calibration is required because it defines the data limits directly through all subsystems of the data-transmission and data-recording equipment, and its significance is easily understood. Time-history records of an event should include a calibration signal to be used as a reference by the data analysis personnel.

A typical inflight calibration procedure is schematically represented in Figure 21 for the Saturn V telemetry system. Inflight calibration for six FM/FM assemblies and three SS/FM assemblies is accomplished over a 4.5-sec time interval. The calibrator impresses a series of six (0 to 5 V) staircase signals to the FM/FM assemblies and a 1700 Hz, 1-V peak-to-peak signal to the SS/FM assemblies. These calibrate signals are transmitted and recorded during flight to calibrate the end-to-end system from telemeter to data-recording equipment.

Preflight calibration of FM/FM telemetry systems consists of impressing a 0 to 5 V step calibrate signal on the systems. The SS/FM system has a 0 to 3000 Hz sweep signal impressed on it for calibration. This SS/FM calibrate signal sweeps in a logarithmic manner with the rate of frequency change proportional to frequency.

2. STATIC TESTING

If the data from the transducers are to be directly recorded during static testing, the piezoelectric channels are calibrated by substituting an equivalent signal voltage at the signal conditioner input terminals or by exciting the transducer. A static test data transmission system using telemetry techniques is calibrated by the methods discussed in Subparagraph 1. above.

The accelerometer may be excited by a shaker if only a few measurements are required. Portable fixed-frequency shakers are available for such purposes. One such unit produces acceleration levels adjustable up to 20 g-rms at a frequency of 120 Hz, with distortion of less than 1 percent and accuracy of better than 98 percent. Units are also available with a fixed frequency of 240 Hz. These signals when carried through the data transmission and data recording system serve as a calibrated reference point for data evaluation.

When many measurements are required, shaking the accelerometers becomes impractical and a voltage substitution method of calibration is required. This technique involves simulation of accelerometer output by impressing a voltage on the accelerometer channel and measuring the overall

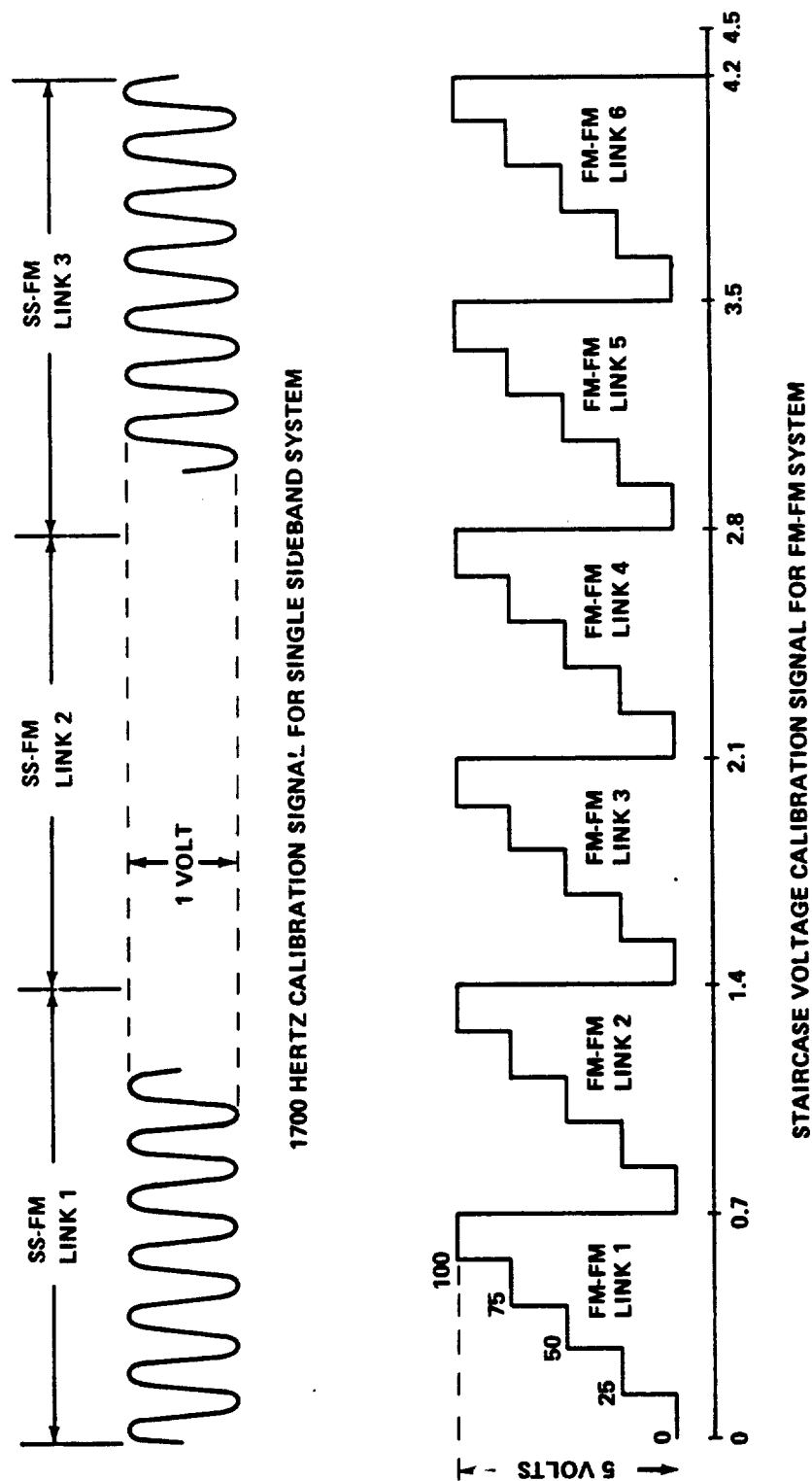


Figure 21. Inflight calibration signals.

sensitivity. A simulated voltage should be inserted at the signal conditioner input terminals according to the following relationship:

$$E_{ins} = E_{cal} \frac{C_{cal}}{C_{total}}$$

where

E_{ins} = insertion voltage, mV/g

E_{cal} = manufacturer's calibration value, mV/g

C_{cal} = capacitance of accelerometer and short cable furnished by manufacturer

C_{total} = total capacitance of accelerometer, short cable, and cable to signal conditioner input terminals, all in parallel.

Up to 14 accelerometer channels may be calibrated simultaneously by using a millivoltmeter. However, one channel is normally reserved for voice communication. The millivoltmeter supplies 14 separately adjustable voltages from 1 to 1000 mV at frequencies from 100 to 5000 Hz with accuracies from 98 to 99 percent of the amplitude. Single-channel millivolters are also available.

After calibration, but before vehicle test, each accelerometer is tested by tapping with a small tool on the nearby structure. The channel is monitored on an oscilloscope to determine if the transient signal comes through. This is commonly referred to as a "tap test" or "peck check."

SECTION VI. DATA TRANSMISSION

The purpose of this section is to familiarize the reader with data transmission systems in general. Emphasis is given to systems that have direct application to vibration data transmission. This section is divided into four main areas: a basic telemetry system and its components, the different types of telemetry systems used for vibration data, direct data transmission, and system accuracy.

If a more rigorous mathematical discussion of the data systems is desired, refer to References 16, 17, 18, and 19.

Data transmission may be accomplished by three methods: Radio telemetry, hardwire telemetry, and direct (or hardwire) transmission. A radio telemetry system processes electrical signals representing physical measurements at a remote location, and transmits these electrical signals by radiation to a chosen location for display and recording. Hardwire telemetry uses the same processes as radio telemetry, but in hardwire telemetry the radio link signals are transmitted by metallic conduction rather than by radiation (Fig. 22). Direct data transmission (hardwire) does not involve radiation of data signals (Fig. 23). The cable is a metallic conductor between the transducer and the signal conditioning, display, and recording equipment. Direct transmission is inherently more accurate than telemetering because fewer operations are performed on the data signal.

A. Basic Telemetry System

The basic telemetry system consists of a transducer, a data transmission system, and a display or storage device. Figure 22 illustrates a basic radio telemetering system. The signal from the transducer is fed through the data transmission system and applied to the display or storage device. A remote signal processor, a transmitter, a receiver, and a local signal processor form the basic transmission system. Essential differences between various telemetry systems lie in the form of modulation.

1. REMOTE SIGNAL PROCESSOR

In some cases the transducer output can be used to modulate the transmitter carrier directly, but then separate radio frequency transmitters would be required for each measurement. To avoid this waste of the available frequency spectrum, techniques have been developed which permit many

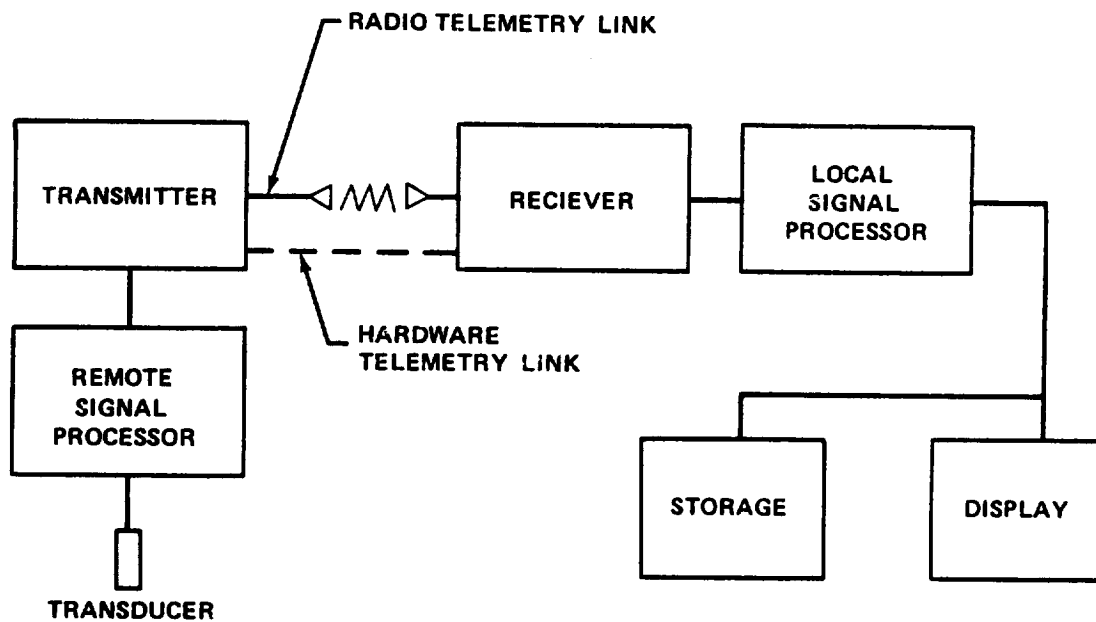


Figure 22. Basic telemetry system.

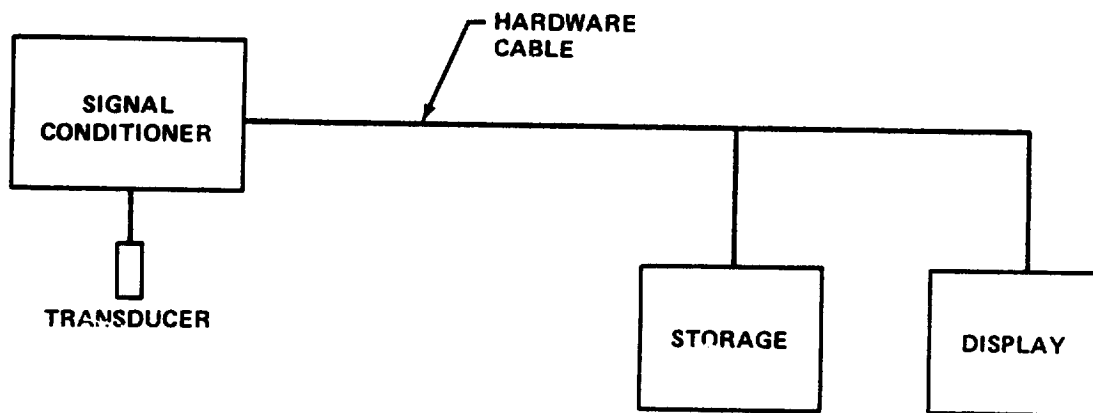


Figure 23. Direct data transmission system.

measurements to be transmitted on one transmitter. These techniques employ either frequency separation or time sharing. Both techniques are known as "multiplexing," which means to transmit two or more separate signals over one communication channel.

Frequency separation employs separate subcarrier frequency channels for each measurement channel. The subcarrier frequencies are spaced so that each channel remains separate from the others.

In time sharing, a specific time is allotted for each measurement so that each measurement is sequentially transmitted over a common data channel.

In addition to multiplexing, the remote signal processor performs any necessary data signal conditioning. Signals may be amplified or attenuated to make them compatible with other signals being multiplexed, and unwanted frequencies are filtered out to prevent crosstalk. In time-multiplexed systems, the data signal is encoded with the appropriate pulse modulation and synchronization pulses are generated.

2. TRANSMITTER AND RECEIVER

The radio telemetry transmitter and receiver employ conventional techniques. Telemetry systems are predominantly frequency modulated (FM) because of the inherent immunity of FM to amplitude effects on the signals caused by noise. Frequency modulation is modulation in which the instantaneous frequency is the sum of the carrier center frequency and a frequency which is a function of the modulating, (or data) signal. In mathematical terms, frequency modulation for a sinusoidal modulating signal is:

$$e = E_o \sin (\omega_c t + m \sin \omega_s t)$$

where

e = instantaneous amplitude
 E_o = peak amplitude
 ω_c = carrier angular frequency
 t = time
 ω_s = modulating signal angular frequency
 m = modulation index (modulation index is carrier frequency deviation divided by the modulating frequency).

The equation here is expressed as a sine function whereas Reference 16 employs a cosine function. The two forms are equivalent, one merely is 90 degrees out of phase with the other.

In the United States, standards have been established by the Inter-Range Instrumentation Group (IRIG) specifying the characteristics of telemetry systems [17]. These standards establish a total of 44 telemetry channels in

the very high frequency (VHF) range between 225 and 260 MHz. Each channel is assigned a minimum bandwidth of 500 kHz and a maximum deviation of ± 125 kHz. The channel specification is such that harmonic interference between channels is prevented. Since the Bessel function of the first kind and n^{th} order [16], with argument m shows that a frequency modulated wave is composed of sidebands spaced by the modulation frequency, the modulation index (m) must be limited to 1.64 to prevent important sidebands of the 125 kHz deviation occurring outside the assigned 500 kHz channel. Therefore, the data bandwidth (or maximum frequency of the data is:

$$f_d = \frac{\text{frequency deviation}}{\text{modulation index}} = \frac{125 \text{ kHz}}{1.64} = 76.3 \text{ kHz} \quad .$$

This data bandwidth limitation is basic and applies to all telemetry systems that use double FM systems. This includes the Single Sideband (SS/FM) system, which will be treated in detail later.

The IRIG standards for telemetry receivers require that the receivers operate on all telemetry frequencies between 216 and 260 MHz without design modification [17]. The receiver is designed to have a maximum bandwidth of 600 kHz between 60 dB points and a stability of 0.005 percent. These requirements are imposed on the receiver to ensure flexibility of operation and a high degree of rejection of unwanted adjacent channel and spurious signals.

3. LOCAL SIGNAL PROCESSING

The local signal processor performs the inverse function of the remote unit. Its exact form is dictated by the remote unit multiplexing technique. It demultiplexes the data into a form suitable for display or recording.

B. Telemetry Systems Used For Vibration Data

The preceding text has been a general discussion of telemetry. The following paragraphs are a more detailed discussion of specific systems used in the acquisition of structural vibration data.

1. FM/FM

A standard IRIG FM/FM telemetry system employs 18 subcarrier oscillators frequency modulated by transducers. These oscillators in turn frequency modulate a radio frequency (RF) carrier. This RF carrier is transmitted to a ground station where the composite FM signal is separated back into the original 18 subcarrier frequencies. The subcarrier signals are passed through discriminators whose outputs correspond to the original transducer signal. When each

measurement is continuous, each subcarrier channel data from only one transducer. The system capacity is then only 18 measurements.

The instantaneous frequency of each subcarrier oscillator is proportional to the instantaneous amplitude of the analog voltage from its transducer. The rate of frequency change of the subcarrier is proportional to the instantaneous frequency of the transducer output. The center frequency and bandwidth of each subcarrier channel conforms to standards established by IRIG. As stated previously, the equation for the frequency modulated signal is:

$$e = E_o \sin (\omega_c t + m \sin \omega_d t) ,$$

where $\sin \omega_c t$ represents the carrier signal and $\sin \omega_d t$ represents the data signal. Expanding this equation gives:

$$e = E_o \left\{ J_0(m) \sin \omega_c t + J_1(m) \left[\sin (\omega_c + \omega_d) t - \sin (\omega_c - \omega_d) t \right] \right. \\ \left. + J_2(m) \left[\sin (\omega_c + 2\omega_d) t + \sin (\omega_c - 2\omega_d) t \right] + \dots \right\}$$

where

e	= instantaneous amplitude
E_o	= peak amplitude
$J_n(m)$	= Bessel function of the 1st kind of order n with argument m
m	= modulation index (carrier frequency deviation divided by modulating frequency)
ω_c	= carrier angular frequency
ω_d	= data angular frequency
t	= time.

Here, the first term is the carrier component, the second term is the first-order upper sideband, and the third term is the first-order lower sideband. The fourth and fifth terms are second-order sideband components. It may be seen that each modulated subcarrier signal is composed of center frequency plus sidebands spaced at the data frequency whose amplitudes are proportional to the modulation index.

Multiplexing the 18 subcarriers is done by assigning different center frequencies to each of the oscillators and limiting their data bandwidth to prevent channel crosstalk. The maximum deviation of each subcarrier oscillator is limited to ± 7.5 percent of its center frequency. Table 3 lists all 18 subcarrier bands assigned by IRIG with their center frequencies, upper and lower maximum frequency deviations, and their data frequency response. In this table the index

TABLE 3. SUBCARRIER BANDS (± 7.5 -PERCENT DEVIATION)

Band	Center Freq (Hz)	Lower Limit (Hz)	Upper Limit (Hz)	Freq ^a Response (Hz)
1	400	370	430	6.0
2	560	518	602	8.4
3	730	675	785	11.0
4	960	888	1 032	14.0
5	1 300	1 202	1 399	20.0
6	1 700	1 572	1 828	25.0
7	2 300	2 127	2 473	35.0
8	3 000	2 775	3 225	45.0
9	3 900	3 607	4 193	59.0
10	5 400	4 995	5 805	81.0
11	7 350	6 799	7 901	110.0
12	10 500	9 712	11 288	160.0
13	14 500	13 412	15 588	220.0
14	22 000	20 350	23 650	330.0
15	30 000	27 750	32 250	450.0
16	40 000	37 000	43 000	600.0
17	52 500	48 562	56 438	790.0
18	70 000	64 750	75 250	1 050.0

a. For ± 7.5 -percent deviation.

of modulation is five. Figure 24 shows the frequency spectra of the equation up to the eighth sideband pair for the four highest frequency channels with sinusoidal modulation. The modulation frequency for each channel is the highest allowed by IRIG standards. If the data frequency were doubled, the spacing between sidebands and center frequency would be doubled so that cross-talk between channels would occur.

For special broadband data applications, the subcarrier deviation can be increased to 15 percent with the frequency excursion and data bandwidth shown in Table 4. The 15-percent channels are designated by letters rather than Arabic numerals. The problem of sidebands becomes severe with these expanded channels, so only every other channel can be used.

TABLE 4. SUBCARRIER BANDS (± 15 -PERCENT DEVIATION)

Band	Center Freq (Hz)	Lower Limit (Hz)	Upper Limit (Hz)	Freq ^a Response (Hz)
A	22 000	18 700	25 300	660.0
B	30 000	25 500	34 500	900.
C	40 000	34 000	46 000	1 200.
D	52 500	44 625	60 375	1 600.
E	70 000	59 500	80 500	2 100.
Band Used		Omit Bands (Table 3)		
A		13, 15, and B		
B		14, 16, A and C		
C		15, 17, B and D		
D		16, 18, C and E		
E		17 and D		

a. For ± 15 percent deviation

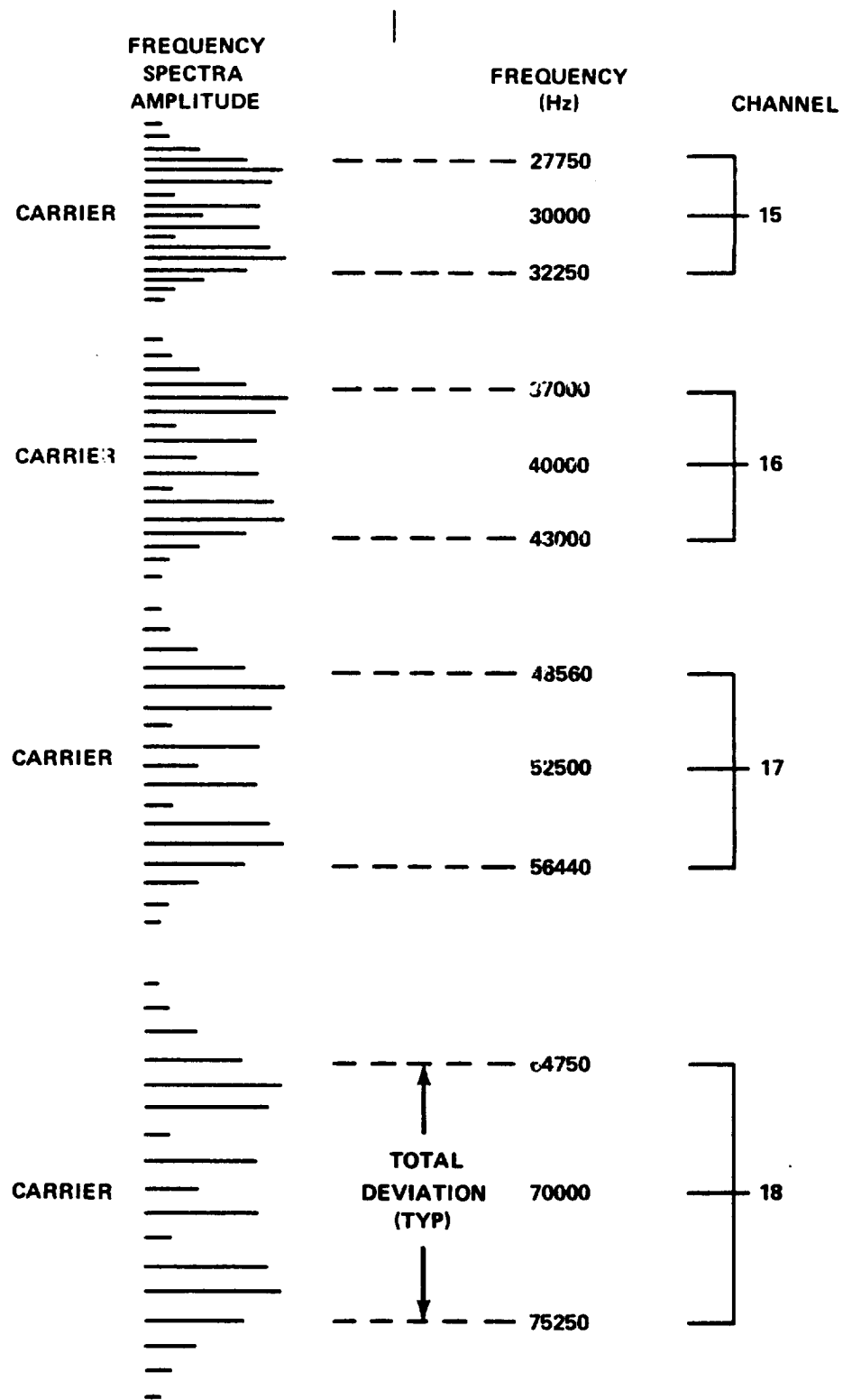


Figure 24. FM/FM channel spacing.

Although the complete IRIG FM/FM system contains 18 subcarrier channels, only channels 2 through 18 are used. Channel 1 is omitted because its center frequency coincides with the vehicle primary power supply frequency of 400 Hz.

The graduated frequency response of the various channels results in limitations on the use of certain channels for vibration data and requires the use of the higher channels for the majority of this data. Since vibration data are generally broadband data, channels 17 and 18 are normally used. Exceptions are bending mode and POGO data, which are relatively low frequency and may be transmitted on the lower channels.

The inputs from all 17 of the modulated channels are linearly mixed and used to frequency modulate the VHF oscillator in the transmitter. The signal at the output of the receiver in Figure 25 is identical to the multiplexed linear output. The data signals for each of the channels are recovered from their composite signal by proper discriminators and filtered for display and analysis.

2. FM/FM/FM

Triple FM is employed to subdivide the standard channels into multiple low response data channels. FM/FM/FM is a technique for trading data bandwidth and accuracy for additional channels. Each of the high-frequency subcarriers can be modulated by several low-frequency subcarriers that are modulated by their individual transducers. For example, channel 17 of link 1 in the Saturn V Instrument Unit is submultiplexed with IRIG channels 2 through 8. All other channels are standard. The data bandwidth of channels 2 through 8 is 158 Hz, instead of the normal channel 17 bandwidth of 790 Hz, for a channel efficiency of 20 percent with a maximum channel frequency response of 45 Hz. Since each FM/FM/FM channel uses two stages of modulation and the modulation index in the second channel is limited to one or less, the data accuracy suffers.

3. SS/FM

The standard FM/FM telemetry system has a serious shortcoming in its bandwidth utilization efficiency. Utilized to its maximum capacity, the total data bandwidth of an FM/FM system operating with a deviation ratio of 5 is 4008 Hz. Because the highest subcarrier frequency required to transmit these data is 76.3 kHz, the subcarrier data frequency utilization is less than 6 percent. Because of this poor utilization, the highest frequency response obtainable on a standard channel is 1050 Hz, and this response is obtainable only on one channel. An FM/FM telemetry system is incapable of handling the large quantities of wideband dynamic data required at MSFC on present and future vehicles.

The SS/FM telemetry system was designed and developed at MSFC as a complement to the FM system, primarily for high-frequency dynamic measurements. The system has a capacity of 15 channels with frequency responses of approximately 3 kHz. The maximum frequency to be accommodated on the RF link is 75.8 kHz. The total data bandwidth is 45kHz, which is 10 times that available with an FM/FM system. The frequency utilization efficiency is approximately 60 percent. Figures 26 and 27 illustrate the SS/FM system.

The SS/FM telemetry system, like the FM/FM system, uses frequency division multiplexing techniques to transmit multiple data channels on a common FM carrier. Unlike the FM/FM system, each SS/FM channel has a 30 Hz to 3 kHz data frequency response. The analog voltage from each transducer modulates a 455 kHz channel carrier signal. The output of the first modulator has the lower sideband removed by a filter, and is transposed in frequency by a second modulator to its assigned position in the multiplexed spectrum. The multiplexer output in the form of 15 data channels, each transposed to a different frequency, frequency modulates a UHF FM transmitter. In addition to the multiplexed channels modulating the transmitter, a reference signal derived from the same master signal as the channel carriers is provided. Since frequency synchronization is required in single sideband transmission, the reference tone provides synchronization between transmitter and receiver. The reference tone also provides an amplitude reference for both multiplexer and demultiplexer so that rms values of the composite signal remain relatively constant.

The receiving portion of the single sideband system reverses the process of the transmitting portion. The receiver output of a standard FM receiver is fed through a demultiplexer, which uses the reference tone for synchronization. Each channel is transposed from its assigned position in the spectrum to its original frequency. The data from each channel are then amplified and fed to appropriate readout devices.

Both the sending and receiving portions of the system employ equipment common to all channels, along with components designed for each individual channel. The common equipment handles the composite signal from all channels and generates the carrier frequencies required for the channel frequency transpositions. Unlike FM/FM where channel equipment is suitable for only one specific channel, all channel equipment in the present SS/FM system is identical and interchangeable. The necessary frequency differences between channels for multiplexing are generated and supplied by the common equipment.

4. TIME SHARING

Time sharing is a special application of FM/FM and SS/FM telemetry primarily used in vibration and acoustic data acquisition. Time sharing is a

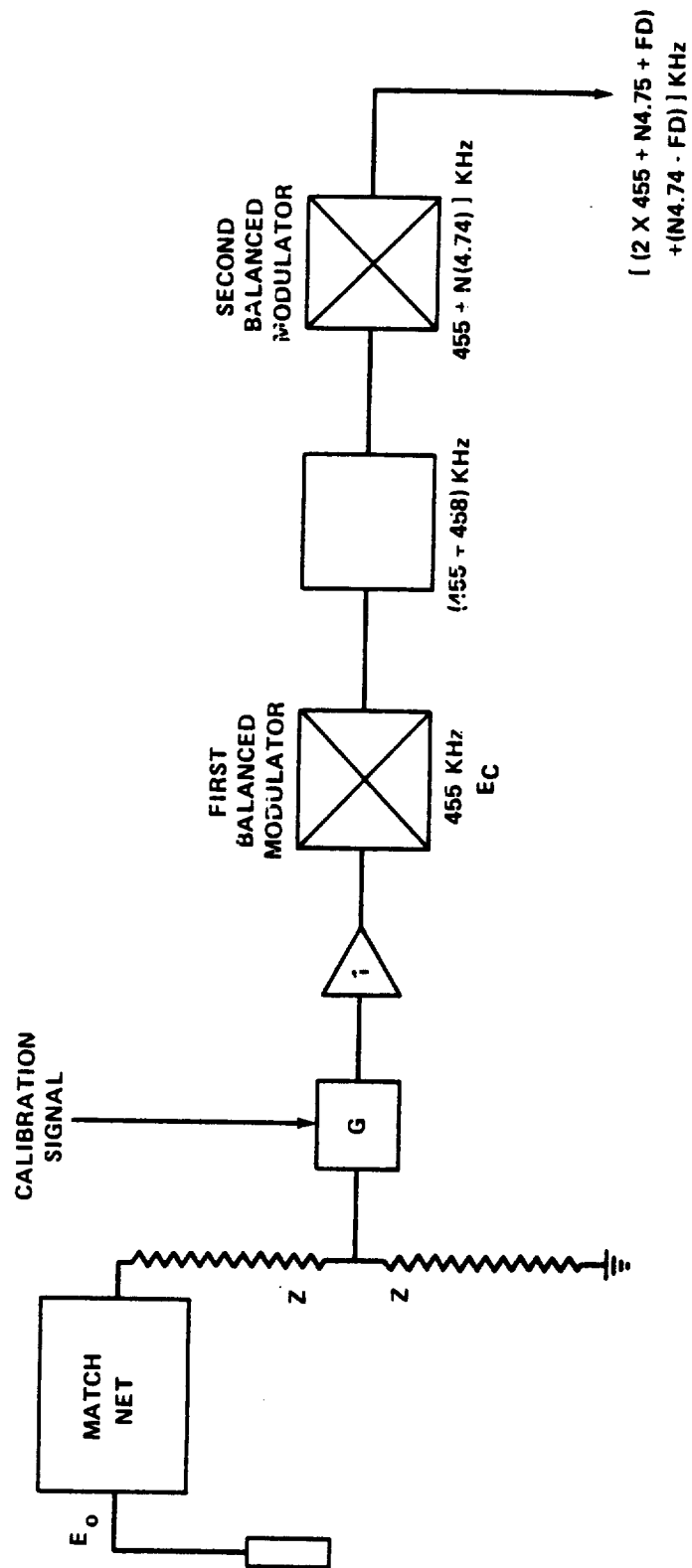


Figure 26. SS/FM channel unit.

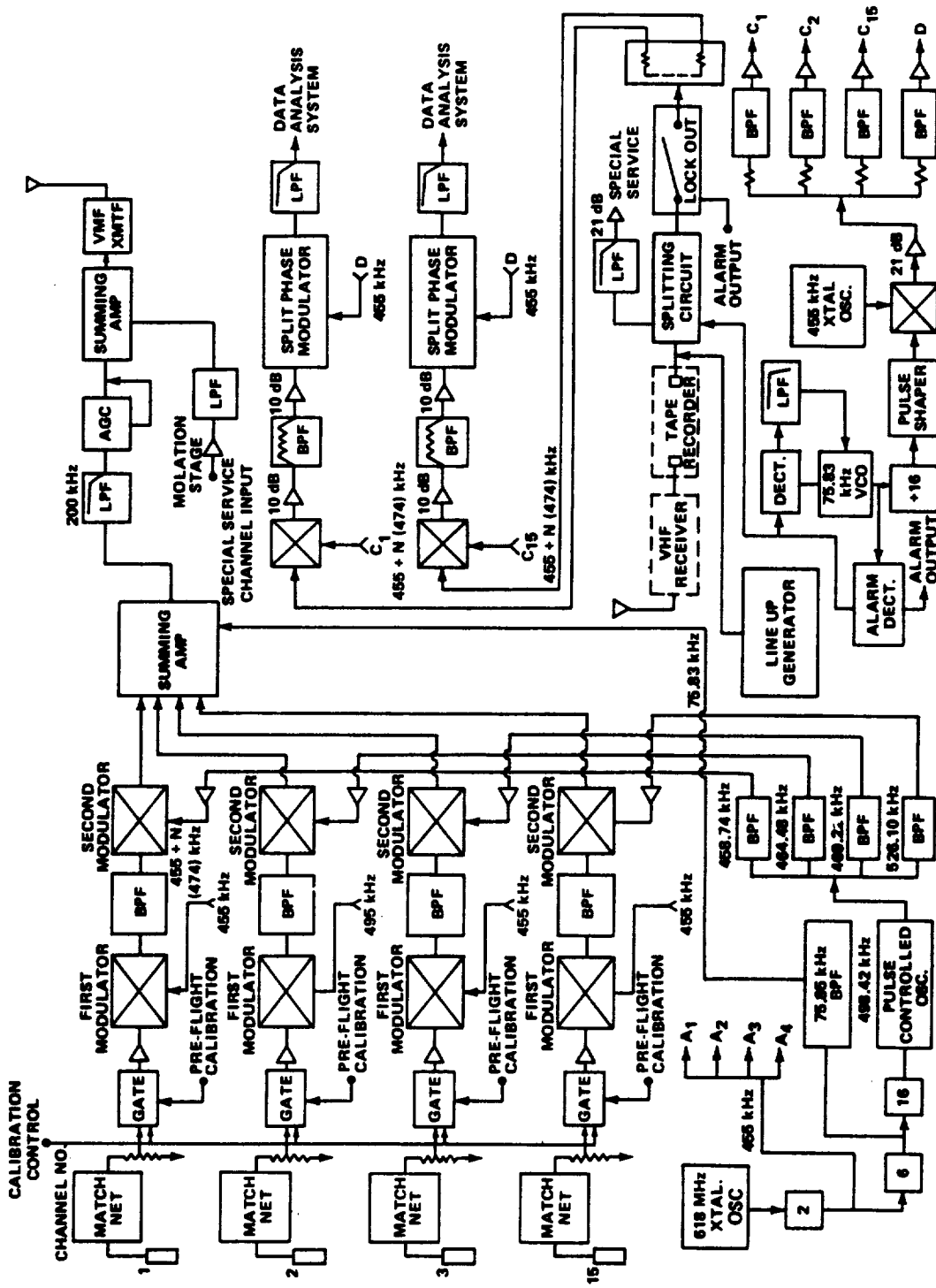


Figure 27. SS/FM telemetry and ground station.

technique for using a single subcarrier channel to sequentially carry two or more transducer outputs, each for a finite period of time. Two- and four-segment time sharing commutators are employed. Since both complete a cycle of all segments in 12 seconds, the two segment commutator transmits each measurement for 6 seconds while the four segment commutator transmits each measurement for three seconds.

C. Direct Data Transmission

A direct data transmission system consists of a transducer, signal conditioning circuits, recorder or display unit or both, and connecting cables (Fig. 23). In cases where the output impedance of the transducer is greatly different from that of the cable, an impedance matching device may be required. The direct system is potentially more accurate than telemetered data because frequency translation or conversion is not usually involved. The accuracy actually obtained is dependent on the components and measurement techniques used.

1. TRANSDUCERS

Two of the most commonly used types of transducers are piezoelectric and strain bridge, as discussed in Section II. These will be the only types considered in this section.

Strain bridge accelerometers require four conductor cables. These cables may be either in the form of two twisted pairs or separately shielded cabled pairs. Strain bridge accelerometers have a frequency response of 0 to 2000 Hz. This means that the response of the cable will not limit the overall system characteristics.

Piezoelectric accelerometers are inherently wide dynamic response devices and require a wide dynamic range for the transmission and readout system. As a general rule, an accelerometer selected for a specific measurement should have a resonant frequency five times greater than the highest data frequency expected.

Piezoelectric accelerometers have characteristic capacitance ranges of 200 to 2000 pF. If the capacitance of the cable is large with respect to the accelerometer, the cable will "load" the accelerometer and serious degradation of the signal will result. Cable capacitance is dependent on the type of cable used and is directly proportional to the length of cable used. Obviously, as cable length increases, a point will be reached when signal attenuation is no longer acceptable. It is obvious that an accelerometer with a large characteristic capacitance will tolerate more capacitive loading than a transducer with low capacitance.

A solution to this problem is to isolate the accelerometer from long lengths of cable by inserting an impedance matching element in the line near the accelerometer.

2. IMPEDANCE MATCHING

Since piezoelectric accelerometer output impedance can be high in relation to cable characteristic impedance, a matching circuit, or signal conditioner, is needed to match the accelerometer to the transmission cable. The matching circuit is usually a vacuum tube cathode follower (Fig. 28), or an emitter follower if transistors are used. These circuits have high input impedance to match the accelerometer output impedance and a low output impedance to match the cable input impedance. Output impedance of the matching circuit should be 30 to 100 ohms when used with open circuit cable of lengths up to 914.4 m (3000 feet). Impedance values outside this range will result in introduction of transients, and possible signal waveform distortion and attenuation.

3. TRANSMISSION CABLES

Careful consideration must be given to the type of cable used in data transmission. Three basic types of cable are normally used: coaxial, twisted pair-shielded, and quad-shielded.

Coaxial cable is inherently unbalanced and is a natural selection to connect an unbalanced amplifier output to the unbalanced magnetic tape recorder input. The coaxial cable shield is sometimes erroneously believed to provide shielding at audio frequencies. At audio frequencies, in contrast to radio frequencies, current penetrates the braid shielding and provides a means for undesired electromagnetic coupling to other circuits.

Twisted pair-shielded and quad-shielded cable can be used where one of the conductors is grounded at the recorder end only. This type of cable may be generally used where high impedance circuits are not required. This circuit is less susceptible to noise pickup than the coaxial type by a margin of 30 to 40 decibels. However, the grounded pair is not suitable for lengths of more than about 914.4 m (3000 feet), because the frequency response cannot be made flat enough over the required bandwidth. For long lengths, 914.4 m (3000 feet) or more, the shielded pair with balanced coupling transformer offers the best choice for low noise pickup and side frequency response. It is better than coaxial cable by a margin of 40 to 50 decibels. However, the introduction of such a transformer may degrade low frequency response and completely eliminate any very low frequency data.

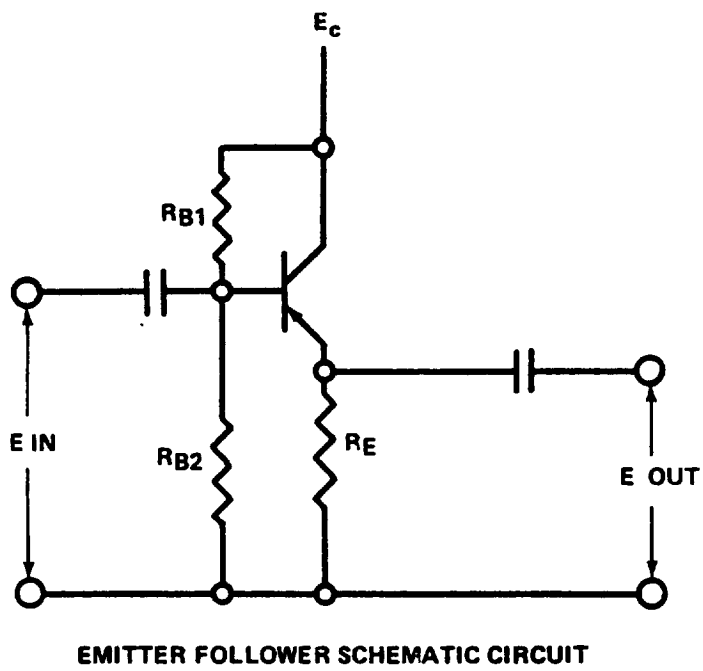
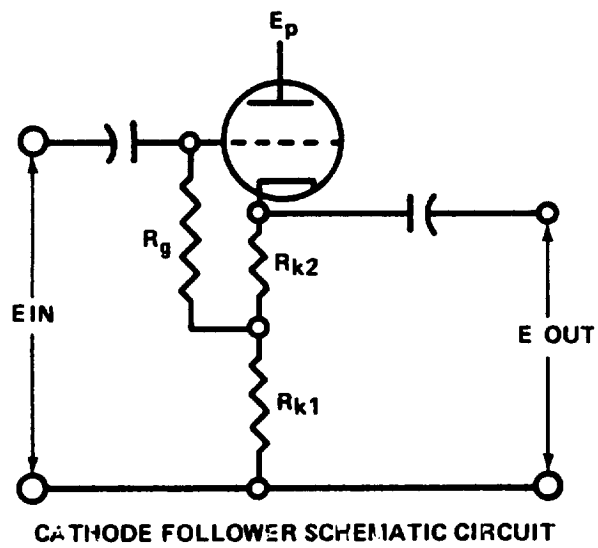


Figure 28. Impedance matching devices.

Shielded cables are subject to the triboelectric effect (voltage generated as a result of vibration of the cable insulation). An example of the triboelectric effect is presented in Reference 18. This effect may be avoided by special construction which consists of providing a drainage path for the triboelectric voltages. This consideration is especially important in selecting the cable between the accelerometer and the impedance matching device because this section of cable will be in a vibrational and acoustical environment. Normally the cable furnished with the accelerometer is of low noise construction, and should be used where possible.

Ground-loop problems in cables can be avoided by grounding cable shields at only one location. This location is normally where the readout and recording systems are located. This means that the circuit common lead is above ground potential all the way from the isolated circuit common of the accelerometer to the recorder. Each cathode follower and amplifier used at MSFC for field vibration measurements has an individual power supply which provides a high degree of isolation from other channels and reduces the possibility of interference between channels through the common capacitance of the power line.

In very low frequency systems, the cable usually is equivalent to a simple metallic conduction link. In this case, the cable series impedance is so low and the shunt impedance is so high that the transducer sees essentially the signal conditioning input impedance.

4. OVERALL SYSTEM FREQUENCY RESPONSE

If the frequency response characteristics of the components of a system are not considered, it is possible for abnormally high voltages to enter the recording electronics, resulting in unintelligible records. Undamped transducer resonant peaks at the frequency of the FM magnetic tape carrier frequency would cause high voltages at the recorder input if the peaks coincided with a resonant peak caused by an improperly terminated cable driven by a low impedance amplifier. This would result in a frequency interference effect. A beat frequency would be recorded and would result in misleading data.

The lowest signal level that can be handled by a system is set by the residual noise level of the system. The upper value is set by the overload or overdrive capabilities of the amplifier which, to a great extent at higher frequencies, is controlled by the capacitance load on the amplifier. The higher the frequency, the greater the attenuation, transients, and signal distortion.

D. System Accuracy

The following paragraphs provide some general considerations relative to system accuracy. No attempt is made in this paragraph to completely specify the accuracy of any particular system because systems are varied and may contain different combination of components.

The accuracy of a system is a function of the accuracies of all the individual components in the system. If a component of 95 percent accuracy is functionally in series with other component of 95 percent accuracy, then the system accuracy becomes $.95 \times .95$ or approximately 90 percent overall. Thus, it is seen that the accuracy of a system may be substantially lowered by including one inaccurate component.

Frequency response of individual components in a system must also be considered. A system that is quite accurate at one data frequency may possess poor accuracy at another frequency.

Direct recording offers the highest system accuracy because fewer components and operations on the data are necessary. FM/FM telemetry systems are generally considered to have a working accuracy under ideal conditions of about 95 percent. The SS/FM system accuracy is much lower than that of the FM/FM system.

One of the most important factors in determining system accuracy is the calibration of the components. Section V of this manual discusses the calibration procedures used in data transmission systems.

SECTION VII. DATA RECORDING

This section provides basic information on data recording systems and examines in some detail the systems used extensively for vibration and acoustic data recording. Magnetic tape recorders are discussed since the majority of vibration and acoustic data are stored on magnetic tape. Other means of data recording such as X-Y plotters and oscillographs are also discussed.

A. Magnetic Tape Recorders

Magnetic tape recorders are used as a means of recording and storing data for later analysis and evaluation. The data are recorded as an electrical signal which can represent an unlimited variety of physical or scientific phenomena. These physical or scientific phenomena are converted to an electrical signal by the measuring instrument (transducer).

Tape recording systems usually fall into one of two categories: analog or digital. Analog systems record electrical signals as a continuous function of the input signal. Digital systems translate the electrical signal into a series of bits or pulses (generally in the binary code) which are required in the handling of the data by digital computers and other digital processing systems.

1. THE MAGNETIC RECORDING SYSTEM

The magnetic recording system consists of three basic subsystems: the electronics, the record and reproduce head assemblies, and the tape transport subsystem. The electronics part of the system supplies the input data in proper form to the record head and recovers the data from the reproduce head. The head assembly has both a record and reproduce section. The record section impresses the input data onto the magnetic tape as variations in local magnetization; the reproduce section reconverts these variations into electrical signals. The tape transport drives the magnetic tape past the head assembly at constant speed.

The magnetic tape, while not an integral part of the recording system, is nevertheless extremely important in overall system operation. In some instances it is the tape which imposes the limitations on performance. Care in selecting tape to match recording requirements is well justified.

a. Record and Reproduce Heads

The recording heads are electromagnets which have a small gap in the core across which the tape is moved as shown in Figure 29. As the tape crosses this gap in the core, it acts as a magnetic shunt across the gap. When the tape is in motion, that part which leaves the edge of the gap is left permanently magnetized in the direction of head magnetization at that instant. The intensity of magnetization is proportional to the instantaneous signal current in the head at the instant that portion of the tape left the gap.

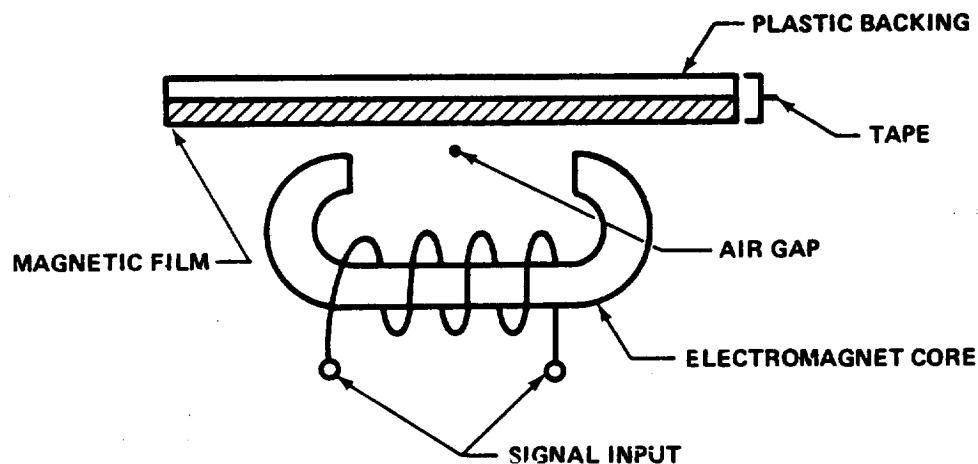


Figure 29. Basic electromagnetic tape head.

The reproduce head is an electromagnet similar to the record head. When the magnetized tape particles are shunted across its gap, a magnetic flux is developed in the core. As the tape moves, the variations in flux induce a voltage in the head winding proportional to the rate of change of the magnetic field in the gap. This voltage, with appropriate processing by the reproduce electronics, re-creates the original input signal.

There are several important differences between the reproduction process and the recording process. One difference is that the intensity of magnetization of the tape corresponds to the signal current used in recording. The tape is magnetized regardless of its speed past the tape head. It is important that the tape speed selected be compatible to the rate of change, or frequency, of the information to be recorded so that well-defined changes are recorded on tape. The reproduce head does not respond directly to the magnetic intensity of the tape, but to the rate of change of magnetic intensity. The flux in the reproduce head is representative of the average magnetization of the region bridging the head gap, but no voltage is induced across the reproduce head winding unless the flux density changes. This value can only

change when the tape moves. The magnitude of this induced voltage is proportional to the rate of flux density change and the number of turns contained in the reproduce head coil winding. From basic electrical concepts we have the formula

$$e = N \frac{d\phi}{dt}$$

where

e = magnitude of the induced voltage

N = number of coil turns

ϕ = flux density.

b. Tape Transports

The tape transports commonly used for data recording handle tapes of either 1.27-cm (1/2-inch) or 2.54-cm (1-inch) width. The 1.27-cm (1/2-inch) tape transport is capable of recording seven information channels spaced side by side on the tape. The 2.54-cm (1-inch) tape transport can record 14 channels of information. However, the full transport capacity can seldom be used for data. A channel may be required for voice annotation in addition to speed reference channels such as "speedlock" or some other wow and flutter compensation system.

Tape transports are divided into two general types: the reel transport and the loop transport. Initial recording of data on magnetic tape is accomplished on a reel transport tape machine. This transport moves the tape from a storage reel, across the heads, and onto a take-up reel. The recorded information may be played back or monitored if the machine is equipped with both record and reproduce heads.

The tape loop transport operates with a continuous loop of magnetic tape. This feature may be used to capture a certain time segment of data in order to produce a quasi-repetitive segment. This mechanism may also be used as a time delay device.

2. RECORDING METHODS

The two primary systems used in magnetic tape recording are amplitude modulation (AM) or direct recording and frequency modulation (FM) recording. The direct system is less complicated and requires fewer electronic operations than FM recording, but it has poor low-frequency response characteristics. The FM method has the distinct advantage of operating at frequencies down to zero Hz.

a. Direct Recording

The direct recording system contains an amplifier which conditions the input signal and generates a bias voltage and frequency. This compensates for nonlinearities in head characteristics and magnetic tape oxide coating. Direct reproduce amplifiers consist of an input preamplifier, a frequency equalizer network, and an output amplifier. The frequency equalizer network characteristics must be different for different tape speeds. For this reason, the equalizer network is normally a "plug-in" type unit and may be quickly changed when a change in tape speed is desired.

The frequency equalizer network is used to compensate for system nonlinearities in order to attain a system frequency response of ± 3 dB from 300 Hz to 300 kHz at a tape speed of 152.4 cm/sec (60 in./sec). System frequency response decreases as the tape speed is reduced. For example, at 4.76 cm/sec (1-7/8 in./sec) tape speed, a tape recorder would have a response of ± 3 dB from 50 Hz to 10 kHz. This decrease in system frequency response is attributable to tape saturation, tape wow and flutter, and head gap effects.

b. FM Recording

The greatest advantage of FM recording is low-frequency response. At 152.4 cm/sec (60 in./sec) tape speed, a system response of 0 to 20 000 Hz may be attained. This technique involves frequency modulating a carrier with the input signal and recording the frequency modulated signal at the tape saturation level. The record amplifier consists of an input amplifier and buffer, a voltage-controlled oscillator, and an output amplifier.

The FM reproduce system consists of a preamplifier, limiter (or clipper), discriminator, and output filter. The output filter is changed with tape speed. Table 5 gives FM system response at the various standard tape speeds. Values given are for a response of $\pm 1/2$ dB.

TABLE 5. FM CARRIER RECORD REPRODUCE SYSTEM
FREQUENCY RESPONSE

Tape Speed, cm/sec (in./sec)	System Bandwidth with Standard Output Filter (Hz)
52.4 (60)	0 to 20 000
76.2 (30)	0 to 10 000
38.1 (15)	0 to 5 000
19.05 (7-1/2)	0 to 2 500
9.52 (3-3/4)	0 to 1 250
4.76 (1-7/8)	0 to 625

For economy and ease of operation, the tape speed selected should be no higher than necessary to capture the highest frequency components of the data expected. The filtering characteristics of FM tape systems may be used to eliminate undesired high frequency noise and transients.

3. MAGNETIC TAPE HANDLING

Magnetic tape must be handled and stored with care. New tape should always be degaussed before use. Tape not in use should be kept in protective cans and stored in a cool place. Tape should never be allowed near a magnet, electrical wire, or any device capable of generating a magnetic field. The oxide coating should never be touched. The tape guides and heads should be kept scrupulously clean.

B. Oscillographs

An oscillograph is a device used to convert analog electrical signals into a semi-permanent or permanent record called an oscillogram.

The heart of the oscillograph is the optical galvanometer. A galvanometer is a voltage-sensitive device that causes a mirror to deflect in proportion to the applied voltage, just as a voltmeter causes a pointer to deflect when

voltage is applied. A light beam is reflected from the mirror onto a moving strip of photosensitive paper. Since the optical arm is long, a small angular movement of the galvanometer mirror causes a relatively large deflection of the light beam on the paper. Figure 30 illustrates the basic elements of an oscillograph.

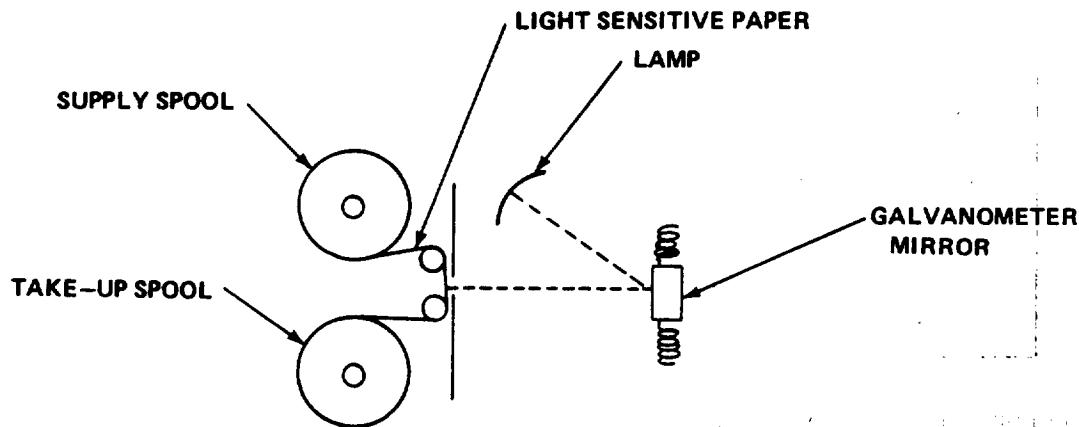


Figure 30. Oscillograph optical elements.

A galvanometer is an electromechanical device. Therefore, it is subject to mechanical limitations of its ability to convert electrical signals into proportional excursions of a light beam. The galvanometer may be thought of as a driven spring-mass system with damping. As such, it is capable of a limited bandwidth of "flat" frequency response. Many different types of galvanometers are commercially available, including those with fluid, magnetic, and electrical damping systems.

Various recording media for oscillograms are available. The light sensitive strip could be photographic film, light sensitive paper, or the newer ultraviolet development paper. The first two types require photographic development processes, with attendant time delay before the data can be viewed. The ultraviolet developing paper exhibits the data traces within a few seconds after exposure to an ultraviolet radiation source, such as a fluorescent lamp. The ultraviolet developing paper has the disadvantage of discoloring when exposed to light and should be stored away from light.

Most oscillographs have a variable speed paper drive system. If the analog trace is to be used for amplitude information, only relatively low paper speeds may be used. If, however, waveshape information is desired, the paper speed must be higher. Depending on the resolution needed 0.254 to 2.54 cm (0.1 to 1.0 inch) of paper per cycle may be necessary. For a 100 Hz

data signal, paper speeds of 10 and 100 inches per second would be required for 0.254 and 2.54 cm (0.1 and 1.0 inch) of paper per cycle, respectively.

Oscillographs are available with up to 36-channel capacity. Although high data channel capacity is possible, channel usage is based on data characteristics. If large amplitude galvanometer deflections are expected, the galvanometer traces should be spaced so that the traces do not cross. If, however, only small trace deflections are expected, larger number of data channels may be used. This is done for ease of trace interpretation.

Other types of oscillographs exist in which optical systems are not used. Rather, the galvanometer element directly moves a mechanical pen which is in contact with the moving paper. As might be expected, the galvanometer mass is much higher than in the optical system and the frequency response is considerably lower. These systems find some application in airplane flutter testing and space vehicle vibration testing where frequencies are on the order of 50 Hz or less.

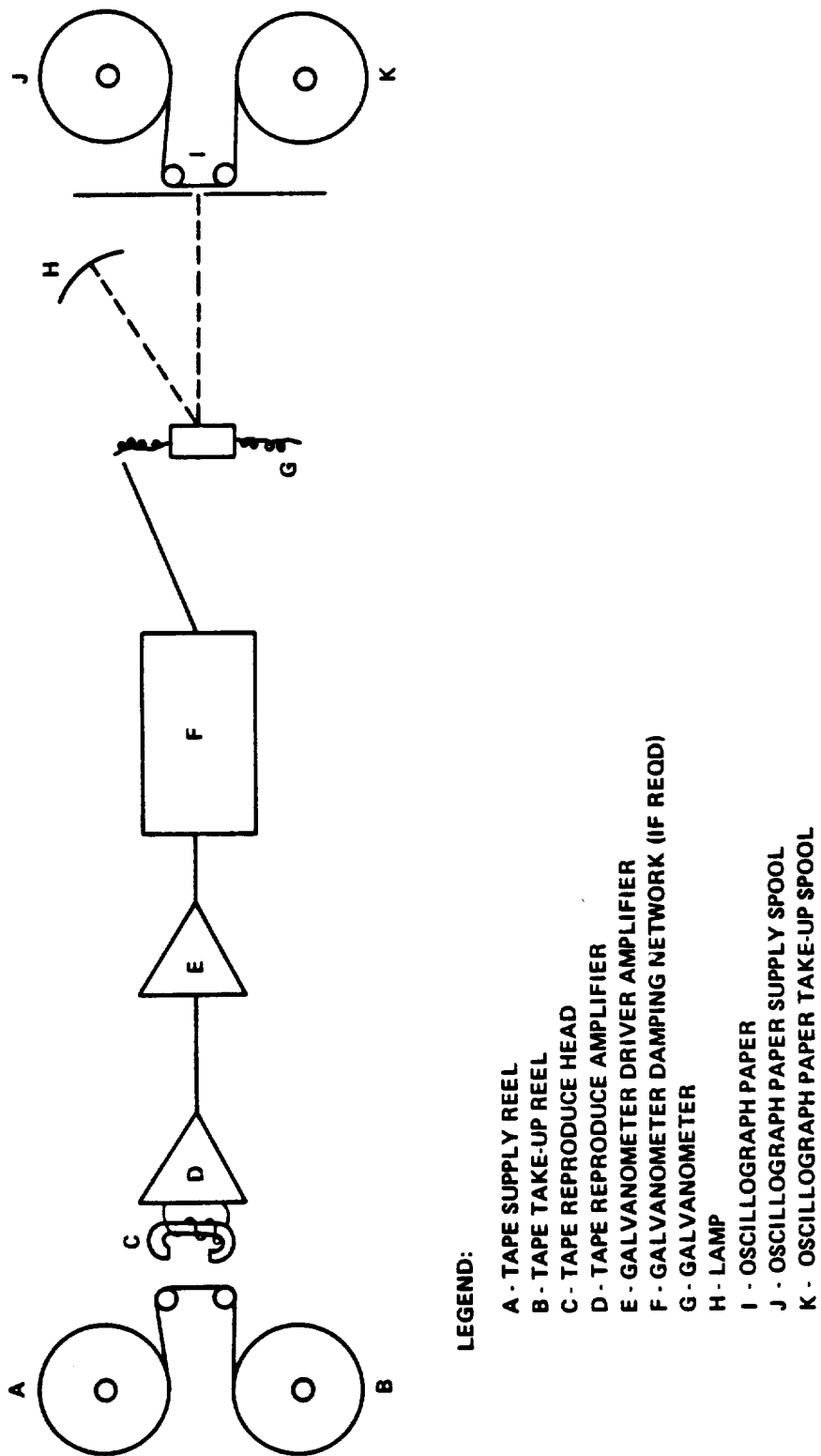
C. Oscillograph – Magnetic Tape System

The following system is required to convert the recorded signal on a magnetic tape to an oscillogram. Figure 31 is a functional block diagram of the system.

The signal from the tape is picked up by the reproduce head and is amplified by the reproduce amplifier. The signal is then fed out of the tape machine into the galvanometer driver amplifier. The galvanometer driver output is fed into an electrical damping network and into the galvanometer. The galvanometer mirror light beam is deflected onto the moving oscillograph paper.

D. X-Y Plotters

The X-Y plotter uses electrical servosystems to produce a pair of crossed motions which produce X-Y plots. The plotter consists of basic balancing circuits plus auxiliary elements to make the instrument versatile. The self-balancing potentiometer circuit compares an unknown external voltage with a stable internal reference voltage. The difference between these voltages is amplified and applied to a servo motor to drive a potentiometer in a direction that will null any difference or error voltage. Accuracy of plots



LEGEND:

- A - TAPE SUPPLY REEL
- B - TAPE TAKE-UP REEL
- C - TAPE REPRODUCE HEAD
- D - TAPE REPRODUCE AMPLIFIER
- E - GALVANOMETER DRIVER AMPLIFIER
- F - GALVANOMETER DAMPING NETWORK (IF REQD)
- G - GALVANOMETER
- H - LAMP
- I - OSCILLOGRAPH PAPER
- J - OSCILLOGRAPH PAPER SUPPLY SPOOL
- K - OSCILLOGRAPH PAPER TAKE-UP SPOOL

Figure 31. Oscillograph-magnetic tape system.

made by this principle is typically 0.1 percent. The full-scale range of the plotter for each axis is obtained with input signals as low as fractions of a millivolt. Thus, the output of many low-level devices, such as thermocouples and strain gages, may be plotted directly without additional amplification.

E. Direct Writing Recorders

A direct writing recorder may be used for slowly changing signals or it may contain significant frequency components up to 5000 Hz. The type of recorder should be selected based on the frequency requirements.

1. X-Y SERVO TYPE

Among the least expensive direct writing recorders are the strip-chart recorders which record analog signals of less than 1 Hz. These recorders usually come with paper widths of 12.7 and 2.54 cm (5 and 10 in.) with one and two writing pens, respectively. The recording paper can be ordinary paper marked by ink pens or temperature sensitive paper marked by a heated stylus. These recorders operate with approximately 0.1 percent accuracy.

2. REVOLVING BAND TYPE

The revolving band type recorder writes directly on electro-sensitive paper. The principle differences in this type and other types of strip-chart recorders are the method of writing and the writing medium. A revolving band rapidly traverses electrically chargeable styli continuously across the slowly-moving electro-sensitive paper at a rate of 100 passes per second. Up to 12 channels are sampled and compared with a precision voltage ramp on each pass. With each pass a corresponding dot for each channel is recorded on the paper at the appropriate point by a high-voltage pulse. The primary advantage of this recorder is the ability to record as many as 12 channels simultaneously.

F. Oscilloscope and Camera

An oscilloscope and camera are often used to record data when unusually high-frequency response is required. The data waveforms are displayed on a cathode ray tube and photographed, usually by a polaroid camera mounted in front of the tube face. An alternate method involves the use of a Memoscope, which is a modified oscilloscope having the ability to store a transient wave and display it continuously on the tube face.

SECTION VIII. DATA REDUCTION

In general, data reduction is the translation of raw information into simplified quantities which describe the information in a manner suitable for engineering analysis and interpretation. For the specific case of flight vehicle vibration data, the available raw information is usually one or more sample amplitude time history records of the vibration response at one or more points on the vehicle structure. The methods employed by MSFC for reducing vibration data are described here, along with appropriate discussions of some general considerations associated with vibration data analysis.

A. Basic Characteristics of Vibration Data

Before data reduction can be pursued in detail, it is necessary to identify certain basic characteristics of the data. In particular, it should be determined if the vibration data are representative of a random process as opposed to a periodic process or other deterministic processes. Perhaps the data represents a combination of both. The procedures for reducing, analyzing, and interpreting data representing a random vibration response are different from those for periodic vibration response. The basic characteristics of periodic and random vibration data will now be discussed.

1. PERIODIC VIBRATION DATA

A periodic function is a special type of deterministic (analytic) function whose amplitude time history repeats itself exactly after a time interval, T_p , called the period. In equation form, a necessary condition for a function $y(t)$ to be periodic is

$$y(t) = y(t + T_p) \quad . \quad (1)$$

This is in contrast to other types of deterministic functions and random processes where equation (1) becomes an inequality. That is,

$$y(t) \neq y(t + T_p) \quad . \quad (2)$$

A periodic function may be expressed by a Fourier series as shown in equation (3), where $f_1 = 1/T_p$ is the frequency in cycles per second (cps).

$$Y(t) = C_0 + C_1 \cos(2\pi f_1 t + \phi_1) + C_2 \cos(4\pi f_1 t + \phi_2) \\ + C_3 \cos(6\pi f_1 t + \phi_3) + \dots = C_0 + \sum_{n=1}^{\infty} C_n \cos(2\pi n f_1 t + \phi_n) \quad (3)$$

In words, equation (3) says that a periodic function consists of a dc component, C_0 , and an infinite number of sinusoidal components having amplitudes C_n and phases ϕ_n . The frequencies of the sinusoidal components are all even multiples of f_1 , which is called the fundamental frequency. Many periodic functions consist of only a few or even a single component. For example, a sine wave has a Fourier series in which all values of C_n are zero except for $n = 1$. In other cases, the fundamental frequency is absent. For example, suppose a periodic function is formed by mixing three sine waves which have frequencies of 60, 75, and 100 Hz. The lowest common multiple is 5 Hz, so the period for the resulting periodic function is $T_p = 0.2$ second. Hence, in the Fourier series for the function, all values of C_n are zero except for $n = 12$, $n = 15$, and $n = 20$.

Many deterministic functions are not periodic. For example, suppose we have the sum of three sine waves which have frequencies of 60, 75, and $300/\pi$. There is no common multiple since $300/\pi$ is an irrational number, so the resulting function is not periodic. However, in actual practice, such non-periodic functions may be closely approximated by a periodic function and expanded into an approximate Fourier series.

2. RANDOM VIBRATION DATA

Unlike periodic functions, the amplitude time history for a random function never repeats itself exactly. Any given sample record represents a unique set of circumstances, and is merely a special example out of a large set of possible records that might have occurred. The collection of all possible records that might have occurred is called an ensemble which forms a random process. Thus, an amplitude time history record for a random vibration response may be thought of as a sample record from a random process.

Since a random process is probabilistic and not an explicit function of time, the prediction of exact amplitudes at some future time is not possible. Thus, a random process must be described in terms of statistical averages as

opposed to exact analytic functions. It is for this reason that the techniques for reducing, analyzing, and interpreting random vibration data are different from those for periodic vibration data.

The properties of a random process may be computed by taking averages over the ensemble at any given time t . For example, the mean value (first moment) of a random process at some time t_1 is computed by taking the instantaneous amplitude of each record of the ensemble at time t_1 , summing the amplitudes, and dividing by the number of records. This computation is illustrated in Figure 32. The mean square value (second moment) at time t_1 , and the correlation between amplitudes at two different times t_1 and t_2 are computed in a similar manner as illustrated in Figures 33 and 34.

For the general case where the mean value, mean square value, and correlation function vary with time, the random process is said to be non-stationary. For the special case where these three properties do not vary with time, the random process is said to be weakly stationary. If all higher moments (i.e., the third moment and up) are also time invariant, the random process is said to be strongly stationary.

If a random process is stationary, the properties of single records in the random process can be computed by taking time averages of the single records as opposed to ensemble averages for the collection of records. The computation of the mean value, mean square value, and correlation function by time averaging is illustrated in Figures 32, 33, and 34. For the general case where these three time averaged properties vary from record to record, the random process is said to be nonergodic. For the special case where these three time averaged properties do not vary from record to record and thus are equal to the corresponding ensemble averaged properties, the random process is said to be weakly ergodic. If all higher moments are also independent of the record used, the random process is said to be strongly ergodic. Note that only stationary random process can be ergodic.

If a vibration response is representative of a nonstationary random process, the properties of the vibration are changing with time and can be completely described only by taking averages over the entire ensemble at every instant of time. If the vibration response is representative of a stationary random process, the properties of the vibration can be described by taking averages over the entire ensemble at any one instant of time. If a vibration response is representative of a stationary and ergodic random process, the properties of the vibration can be described by taking time averages over one record from the ensemble.

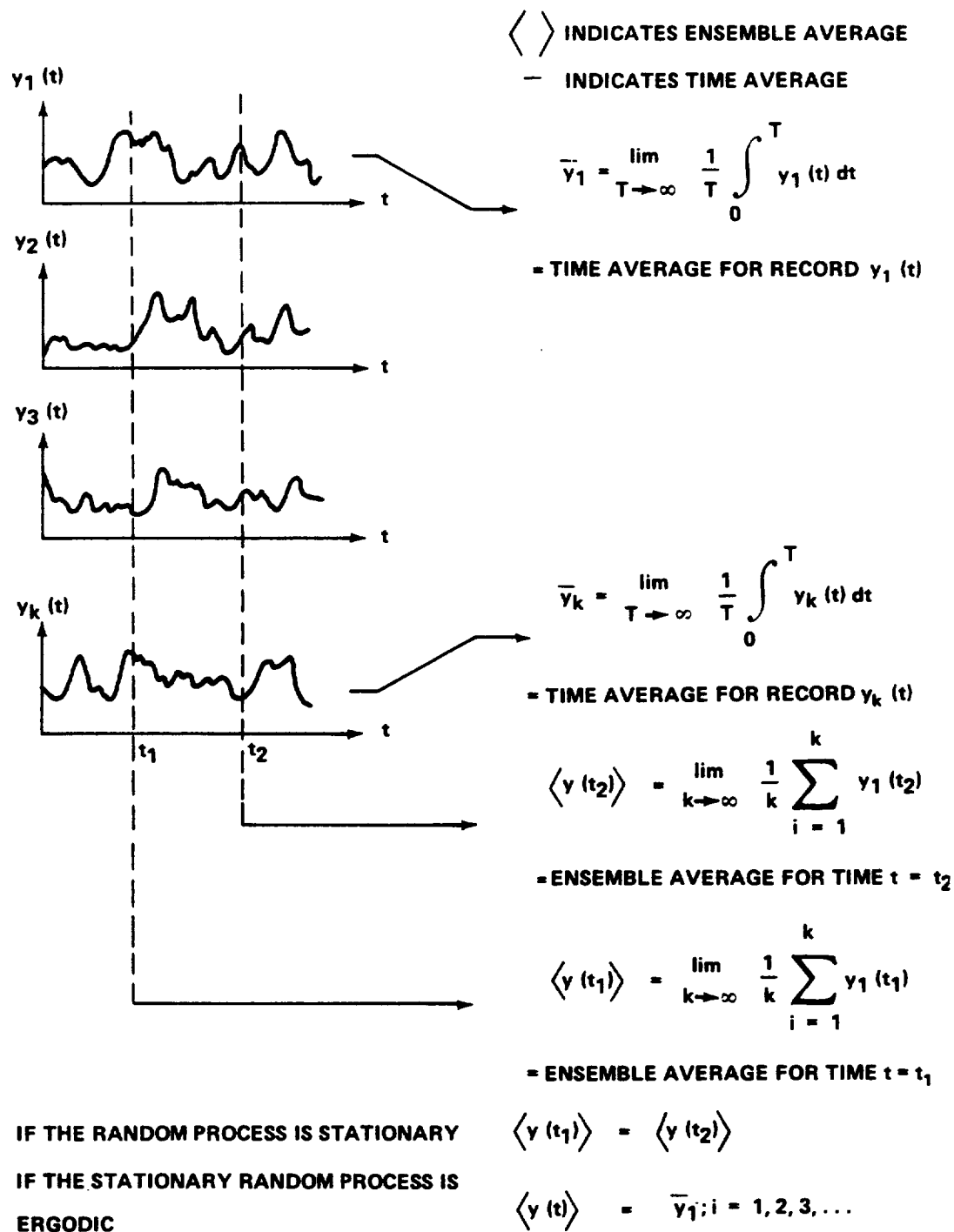
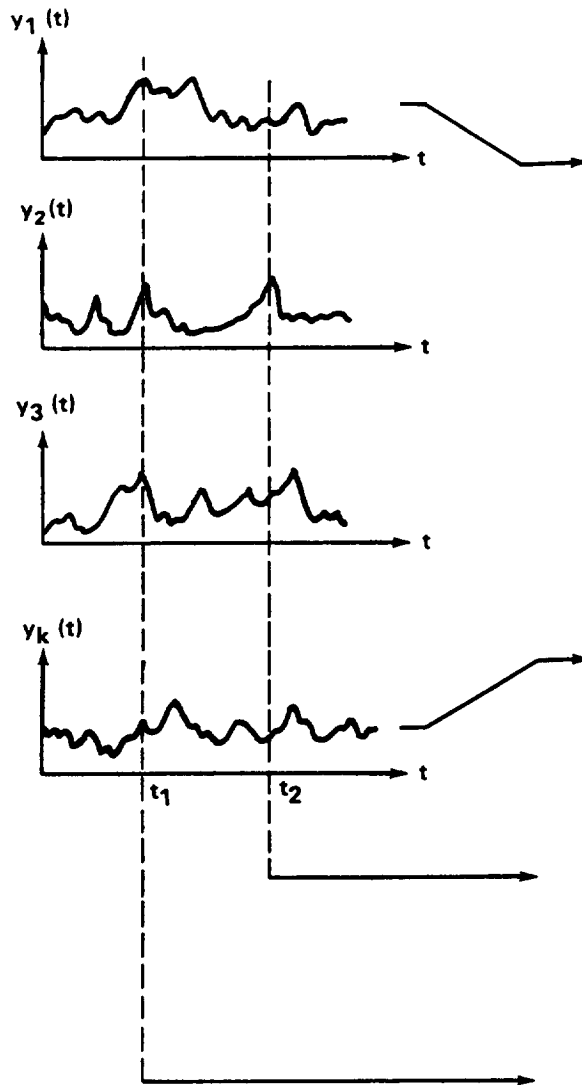


Figure 32. Computation of mean values.

$\langle \rangle$ INDICATES ENSEMBLE AVERAGE
 — INDICATES TIME AVERAGE



$$\overline{y_1^2}(t) = \lim_{T \rightarrow \infty} \frac{1}{T} \int_0^T y_1^2(t) dt$$

= MEAN SQUARE TIME AVERAGE
 FOR RECORD $y_1(t)$

$$\overline{y_k^2} = \lim_{T \rightarrow \infty} \frac{1}{T} \int_0^T y_k^2(t) dt$$

= MEAN SQUARE TIME AVERAGE
 RECORD $y_k(t)$

$$\langle y^2(t_2) \rangle = \lim_{k \rightarrow \infty} \frac{1}{k} \sum_{i=1}^k y_i^2(t_2)$$

= MEAN SQUARE ENSEMBLE
 AVERAGE FOR TIME $t = t_2$

$$\langle y^2(t_1) \rangle = \lim_{k \rightarrow \infty} \frac{1}{k} \sum_{i=1}^k y_i^2(t_1)$$

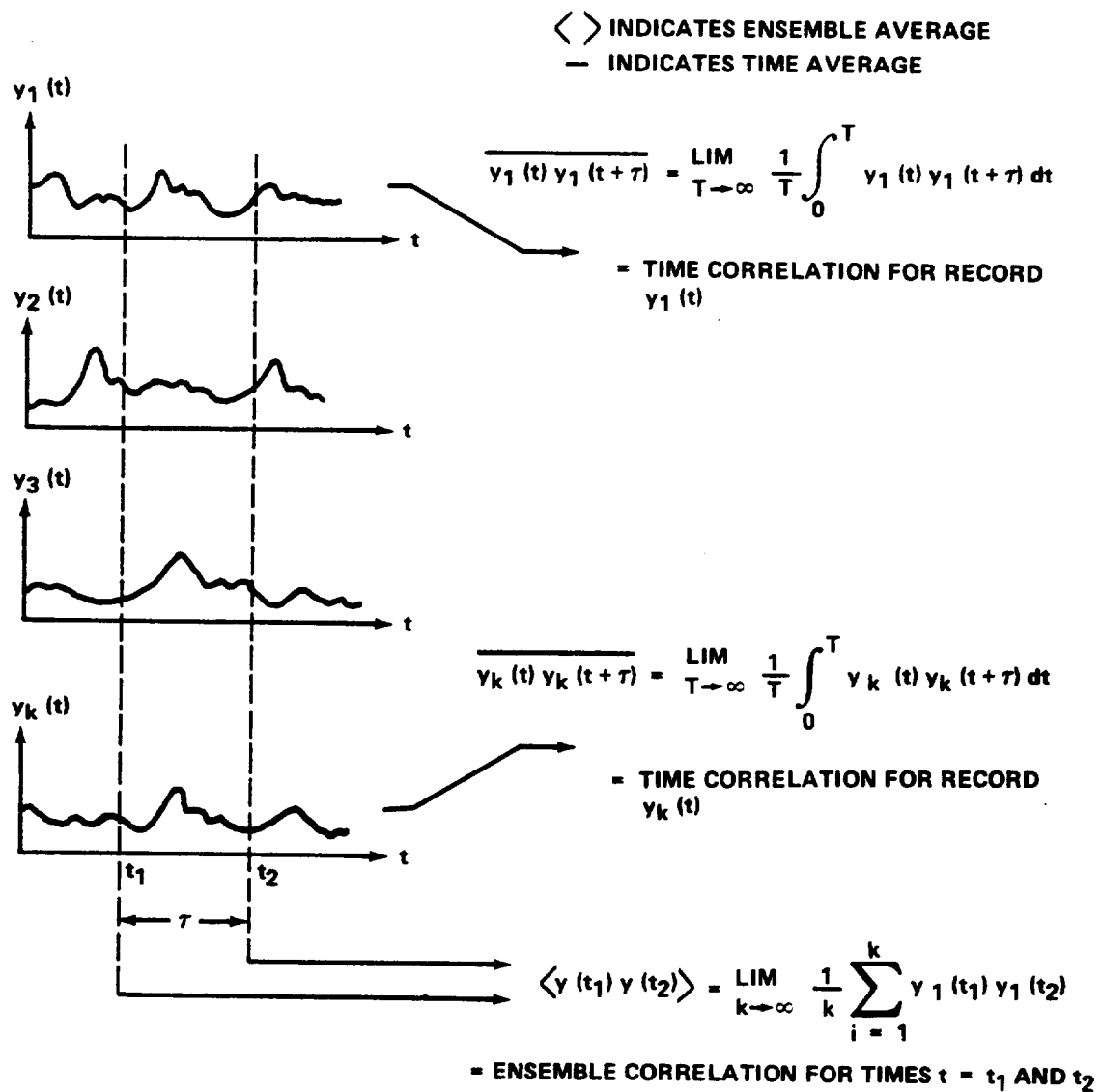
= MEAN SQUARE ENSEMBLE
 AVERAGE FOR TIME $t = t_1$

IF THE RANDOM PROCESS IS STATIONARY,
 IF THE STATIONARY RANDOM PROCESS IS
 ERGODIC,

$$\langle y^2(t_1) \rangle = \langle y^2(t_2) \rangle$$

$$\langle y^2(t) \rangle = \overline{y_i^2}; i = 1, 2, 3, \dots$$

Figure 33. Computation of mean square values.



IF THE RANDOM PROCESS IS STATIONARY, $\langle y(t_1) y(t_2) \rangle = \langle y(t) y(t + \tau) \rangle$.

IF THE STATIONARY RANDOM PROCESS IS ERGODIC,

$$\langle y(t) y(t + \tau) \rangle = \overline{y(t) y(t + \tau)} = R_y(\tau)$$

Figure 34. Computation of autocorrelation values.

For the actual flight vehicle vibration problem, a single record may represent the vibration response at some point on the structure of a given vehicle. The collection of records needed to form an ensemble would then represent the vibration responses at that point occurring during flights of all vehicles of that type. However, data from a large number of vehicles of the same type are rarely available. An ensemble may be contrived by collecting records of the vibration response for repeated flights of the same vehicle, where the time origin of each record is considered to be the start of each flight. Even data of this sort are often difficult to acquire. Usually, vibration data from only a few flights or perhaps just one flight are available. As a result, the vast majority of vibration data reduction is performed by time averaging single sample records.

B. Basic Descriptions of Vibration Data

For any time invariant vibration response, whether it be random, periodic, or a combination of both, the simplest description of the vibration amplitude is given by the mean square value. For a vibration record $y(t)$ of length T , the mean square value \bar{y}^2 is given by

$$\bar{y}^2 = \frac{1}{T} \int_0^T y^2(t) dt \quad (4)$$

where

$T = T_p$ for periodic vibration

$T \rightarrow \infty$ for random vibration.

The positive square root of the mean square value gives the rms (root mean square) value of the vibration; i.e.,

$$y_{\text{rms}} = \sqrt{\bar{y}^2} \quad (5)$$

The mean square value is a measure of both the static and dynamic portions of the vibration amplitude. The static portion of the vibration (the dc component) is defined by the mean value \bar{y} as follows:

$$\bar{y} = \frac{1}{T} \int_0^T y(t) dt \quad (6a)$$

where

$T = T_p$ for periodic vibration

$T \rightarrow \infty$ for random vibration.

The dynamic portion of the vibration is defined by the mean square value about the mean (variance) σ_y^2 as follows:

$$\sigma_y^2 = \frac{1}{T} \int_0^T [y(t) - \bar{y}]^2 dt \quad (6b)$$

where

$T = T_p$ for periodic vibration

$T \rightarrow \infty$ for random vibration.

These three measures of amplitude are related as follows:

$$\bar{y}^2 = \sigma_y^2 + (\bar{y})^2 \quad (7)$$

Hence, if the mean value of the vibration is zero ($\bar{y} = 0$), which is often the case in actual practice, the mean square value and variance will be equal ($\bar{y}^2 = \sigma_y^2$).

Mean square or rms vibration level measurements give only a rudimentary description of the vibration amplitude. For most engineering applications, a more detailed description of the vibration is required. Such detailed descriptions for periodic and random vibration data will now be discussed.

1. PERIODIC VIBRATION DATA

As noted in Paragraph A. of this section, a periodic vibration response can be completely described by a Fourier series which gives the amplitude,

frequency, and phase of all harmonic components of the vibration. However, in actual practice, the amplitudes and frequencies for the harmonic components of a vibration response give a sufficient description for most engineering applications. A knowledge of the associated phase angles is not often required. The description of a periodic vibration response in terms of its harmonic amplitudes and frequencies is given by a discrete frequency spectrum.

A typical discrete frequency spectrum is illustrated in Figure 35. Note that each harmonic component appears in the frequency spectrum as a line which has no bandwidth. The peak amplitudes of the components (C_0 , C_1 , C_2 , etc.) are equivalent to the coefficients in the Fourier series for the periodic vibration as shown in equation (3). The mean value of the vibration is defined by the coefficient C_0 at zero frequency. Note that the mean square value of the vibration is equal to the sum of the mean square values for the individual components plus the square of the mean.

2. RANDOM VIBRATION DATA

If a vibration response is random in nature and assumed to be representative of an ergodic stationary process, a reasonable detailed description of the vibration is obtained from three important properties of random signals. The first is a statistical description of the amplitude characteristics of the vibration, which is called the amplitude probability density function. The second is a statistical description of the time correlation characteristics of the vibration, which is called the autocorrelation function. The third is a statistical description of the frequency composition of the vibration, which is called the power spectral density function. Furthermore, if data from two or more vibration responses are obtained simultaneously, additional information is available from several joint properties. These include joint amplitude probability density functions, cross-correlation functions, cross-power spectral density functions, and coherence functions. These various descriptive properties will now be discussed.

a. Amplitude Probability Density Function

Given a stationary random vibration record $y(t)$ of length T seconds, the first-order amplitude probability density function $p(y)$ is as follows:

$$p(y) = \lim_{T \rightarrow \infty} \lim_{\Delta y \rightarrow 0} \frac{1}{T(\Delta y)} \sum_{i=1}^{\infty} t_i(y, y + \Delta y) \quad (8)$$

$$\bar{y} = c_0$$

$$\overline{y^2} = \frac{1}{2} c_1^2$$

$$\overline{y^2} = c_0^2 + \frac{1}{2} \sum_{i=1}^{\infty} c_i^2$$

$$\sigma_y^2 = \overline{y^2} - (\bar{y})^2 = \frac{1}{2} \sum_{i=1}^{\infty} c_i^2$$

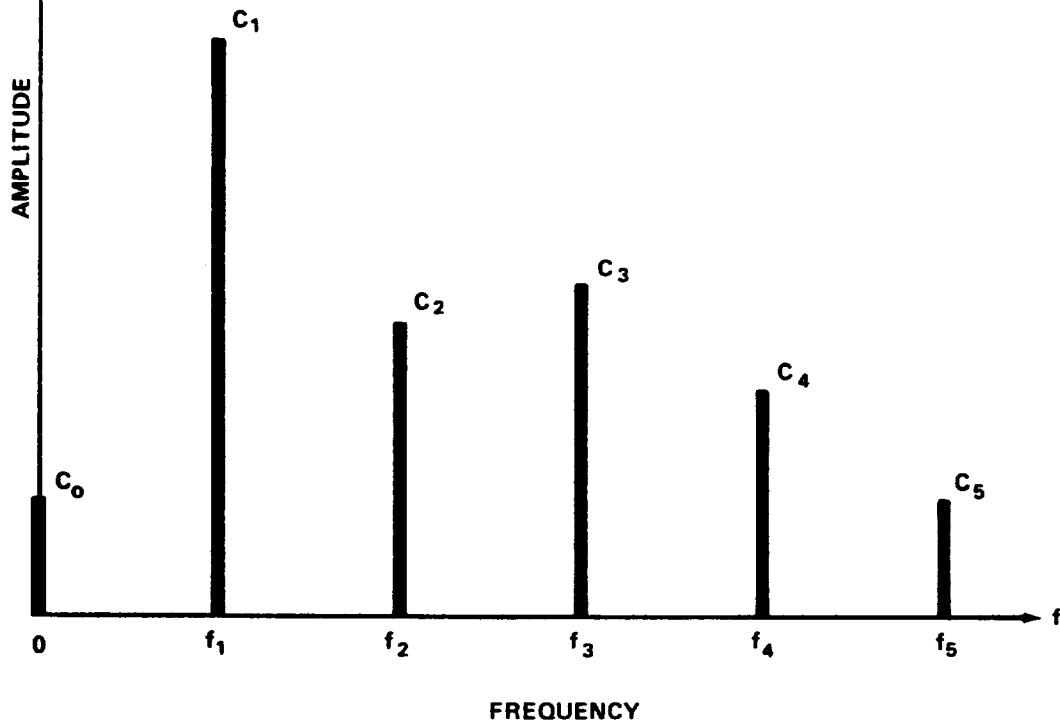


Figure 35. Typical discrete frequency spectrum.

The quantity $t_i(y, y + \Delta y)$ is the time spent by the amplitude within the narrow amplitude interval between y and $y + \Delta y$ during the i th entry into the interval.

A typical probability density plot $[p(y) \text{ versus } y]$ is illustrated in Figure 36. The area under the probability density plot between any two amplitudes y_1 and y_2 is equal to the probability of the vibration response

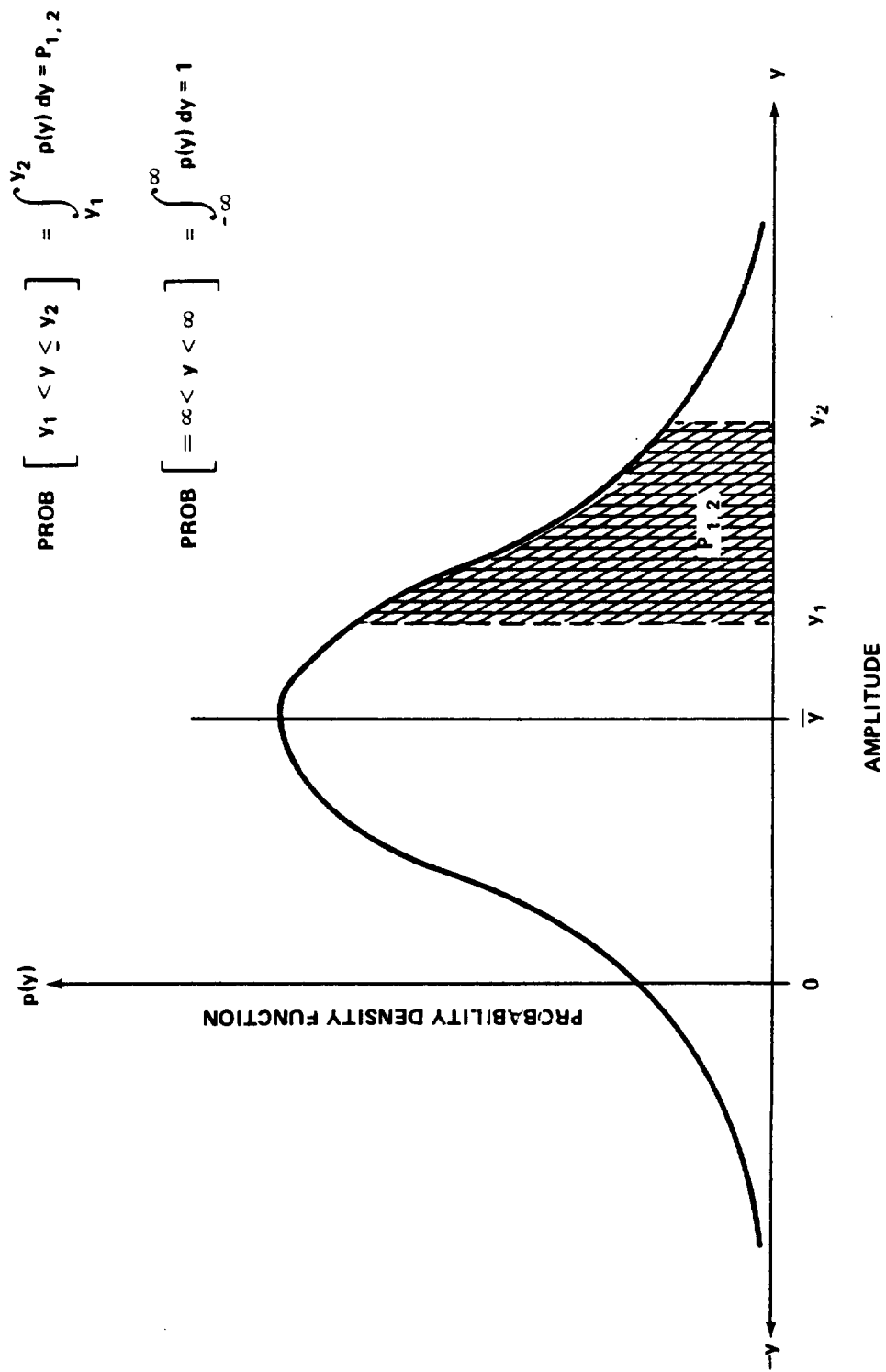


Figure 36. Typical probability density plot.

having an amplitude within that range at any given time. Obviously, the total area under the plot is equal to unity since the probability of the vibration having any amplitude must be one. In other words, it is certain that the vibration response will have some amplitude between plus or minus infinity. Note that the mean value, mean square value, and variance for the vibration are related to the probability density function as follows.

$$\bar{y} = \int_{-\infty}^{\infty} y p(y) dy \quad (9a)$$

$$\bar{y}^2 = \int_{-\infty}^{\infty} y^2 p(y) dy \quad (9b)$$

$$\sigma_y^2 = \int_{-\infty}^{\infty} (y - \bar{y})^2 p(y) dy = \bar{y}^2 - (\bar{y})^2 \quad (9c)$$

b. Autocorrelation Function

Given a stationary random vibration record $y(t)$ of length T seconds, the autocorrelation function $R_y(\tau)$ is as follows:

$$R_y(\tau) = \lim_{T \rightarrow \infty} \frac{1}{T} \int_0^T y(t) y(t + \tau) dt \quad (10)$$

The quantity τ is the time difference in seconds, which is often called the lag time. Note that the autocorrelation function is a real-valued even function which may be either positive or negative.

A typical autocorrelation plot $R_y(\tau)$ versus τ is illustrated in

Figure 37. The autocorrelation function for a vibration response indicates the relative dependence of the vibration amplitude at any instant on the vibration amplitude that had occurred τ seconds before. The maximum value of the autocorrelation function occurs when the lag time is zero. Note that the mean value, mean square value, and variance for the vibration are related to the autocorrelation function as follows:

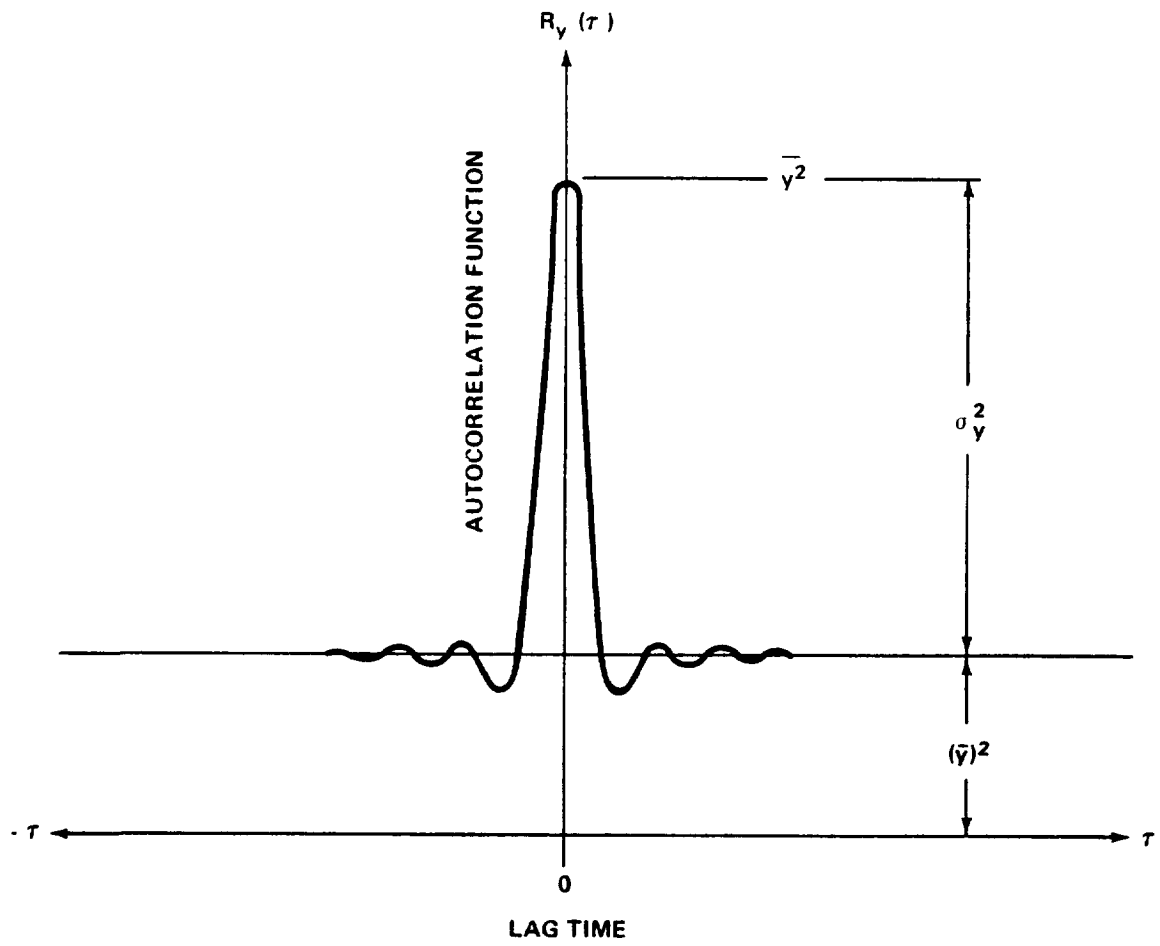


Figure 37. Typical autocorrelation plot.

$$\bar{y} = \sqrt{R_y(\infty)} \quad (11a)$$

$$\bar{y}^2 = R_y(0) \quad (11b)$$

$$\sigma_y^2 = R_y(0) - R_y(\infty) \quad (11c)$$

c. Power Spectral Density Function

Given a stationary random vibration record $y(t)$ of length T seconds, the power spectral density function $G_y(f)$ is as follows:

$$G_y(f) = \lim_{T \rightarrow \infty} \lim_{\Delta f \rightarrow 0} \frac{1}{T(\Delta f)} \int_0^T y_{\Delta f}^2(t) dt \quad . \quad (12)$$

The quantity $y_{\Delta f}^2$ is the square of the amplitudes within the narrow frequency interval between f and $f + \Delta f$. Note that the power spectral density function is a real valued function that is always positive.

A typical power spectrum $[G_y(f) \text{ versus } f]$ is illustrated in Figure 38. The area under the power spectrum plot between any two frequencies f_1 and f_2 is equal to the mean square value of the vibration response within that frequency range. The total area under the plot is equal to the total mean square value of the vibration response. If the vibration response has a non-zero mean value (a dc component), this will appear in the power spectrum as a delta function at zero frequency. The area under the delta function is equal to the square of the mean value. Note that the existence of a delta function at a frequency other than zero would represent a sine wave at that frequency.

It is important to mention that the power spectral density function for a stationary random signal is the Fourier transform of the autocorrelation function. Hence, a power spectrum contains the same basic information as an autocorrelation plot. Furthermore, the power spectrum presents the information in a frequency format which is more convenient for most engineering applications. However, there are special situations where an autocorrelation plot is more useful than a power spectrum. An example is the problem of detecting periodic components in an otherwise random vibration response. These matters are discussed in greater depth in Section IX.

d. Joint Amplitude Probability Density Function

Given two stationary random vibration records, $x(t)$ and $y(t)$, each of length T seconds, the joint amplitude probability density function $p(x,y)$ is as follows:

$$p(x,y) = \lim_{T \rightarrow \infty} \lim_{\substack{\Delta x \rightarrow 0 \\ \Delta y \rightarrow 0}} \frac{1}{T(\Delta x)(\Delta y)} \sum_{i=1}^{\infty} t_i(x, x + \Delta x; y, y + \Delta y) \quad . \quad (13)$$

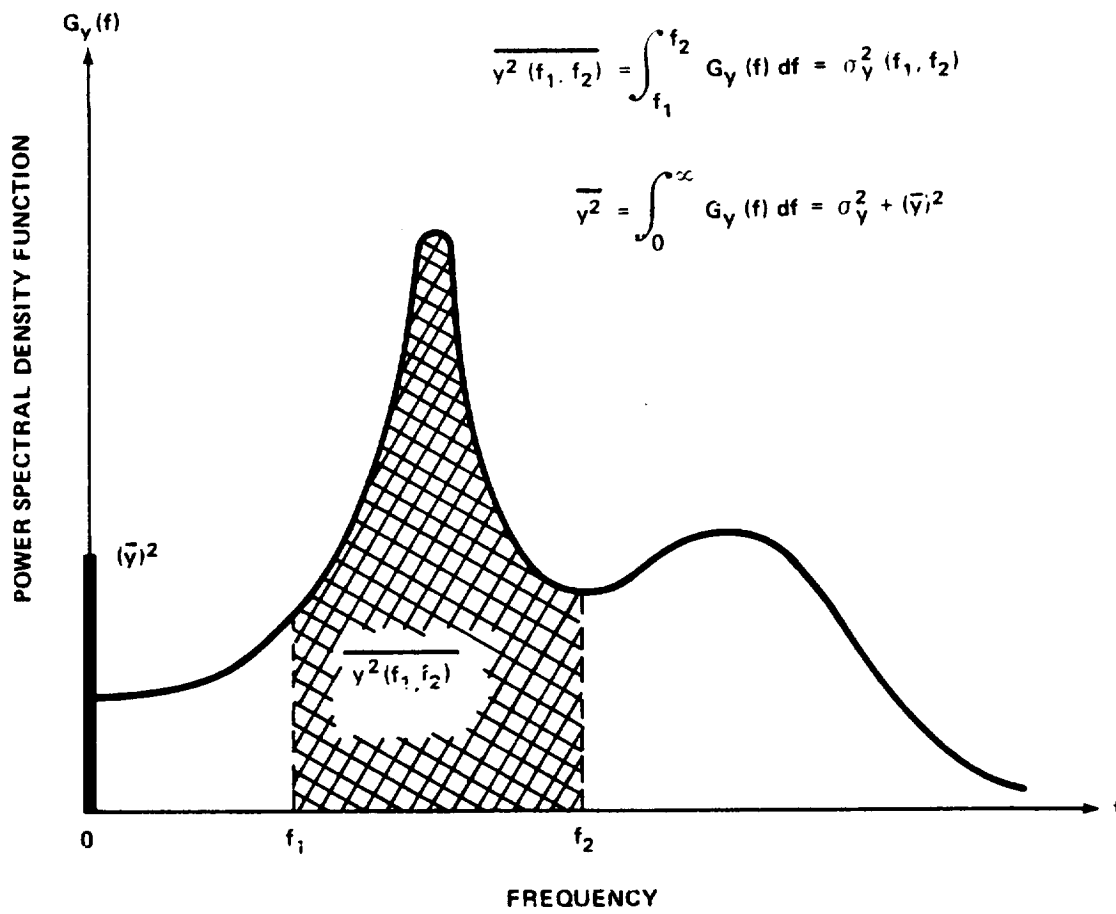


Figure 38. Typical power spectrum.

The quantity $t_i(x, x + \Delta x; y, y + \Delta y)$ is the time spent by the amplitudes $x(t)$ and $y(t)$ when they are simultaneously within the narrow amplitude intervals between x and $x + \Delta x$, and y and $y + \Delta y$, respectively, during the i th simultaneous entry into the intervals.

A typical joint probability density plot [$p(x, y)$ versus x and y] is illustrated in Figure 39. Note that the plot has three dimensions. The volume under the joint probability density plot bounded by the amplitudes x_1 , x_2 , y_1 , and y_2 is equal to the probability that $x(t)$ and $y(t)$ will simultaneously have amplitudes within those ranges at any given time. Obviously, the total volume under the plot is equal to unity since the probability of the two vibration responses simultaneously having any amplitudes must be one.

$$\text{PROB} \left[x_1 < x \leq x_2 ; y_1 < y \leq y_2 \right] = \int_{y_1}^{y_2} \int_{x_1}^{x_2} p(x,y) dx dy = P_{1,2}$$

$$\text{PROB} \left[-\infty < x < \infty ; -\infty < y < \infty \right] = \int_{-\infty}^{\infty} \int_{-\infty}^{\infty} p(x,y) dx dy = 1$$

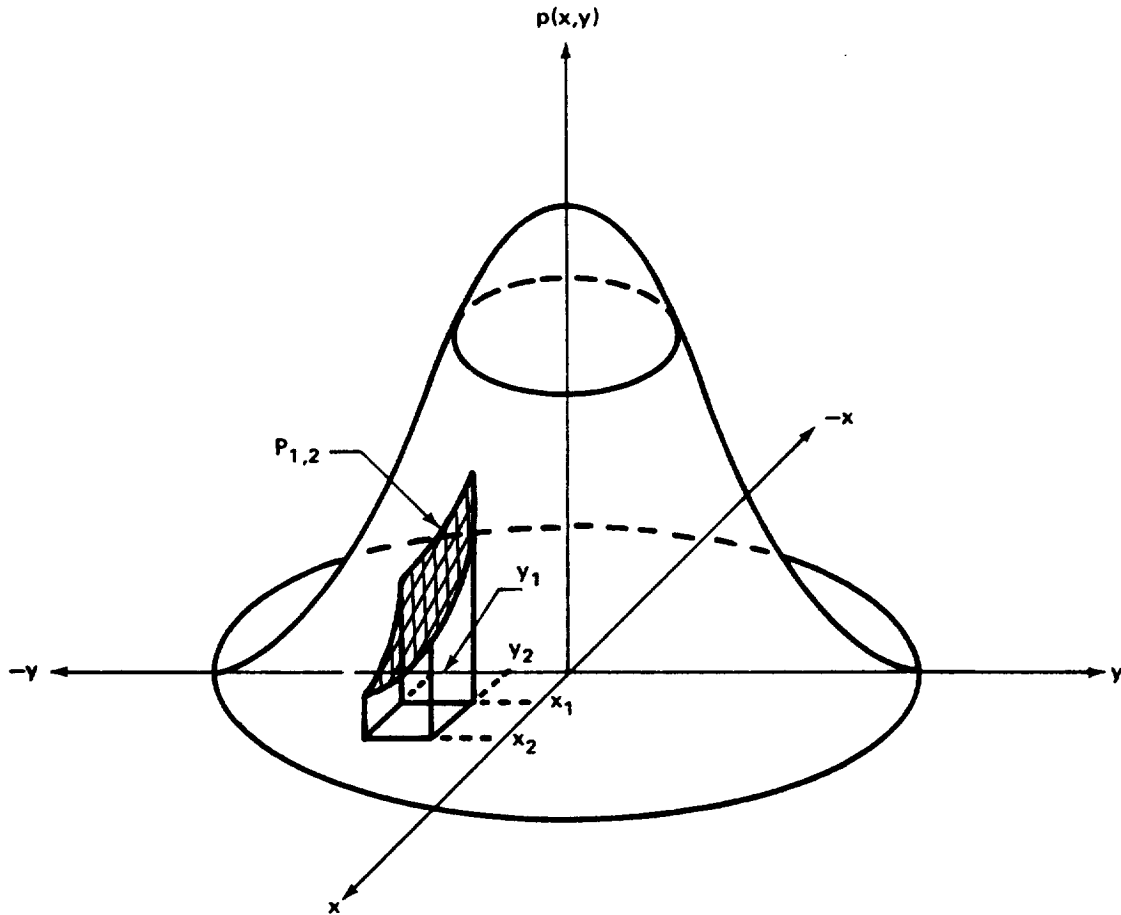


Figure 39. Typical joint probability density plot.

c. Cross-Correlation Function

Given two stationary random vibration records, $x(t)$ and $y(t)$, each of length T seconds, the cross-correlation function $R_{xy}(\tau)$ is as follows:

$$R_{xy}(\tau) = \lim_{T \rightarrow \infty} \frac{1}{T} \int_0^T x(t) y(t + \tau) dt \quad . \quad (14)$$

The quantity τ is the time difference in seconds, which is often called the lag time. Note that the cross-correlation function is real valued but not even, and may be either positive or negative.

A typical cross-correlation plot $|R_{xy}(\tau)|$ versus τ is illustrated in Figure 40. The value of the cross-correlation function for two vibration responses indicates the relative dependence of the amplitude of one vibration response at any instant of time on the amplitude of the other vibration response that had occurred τ seconds before. In actual practice, cross-correlation functions have wide applications to the evaluation of linear structural transfer characteristics. Furthermore, cross-correlation functions furnish a powerful tool for localizing vibration sources by determining time delays and structural transmission paths. These matters are discussed in more detail in Section 7.6 of Reference 20.

f. Cross-Power Spectral Density Function

Given two stationary random vibration records, $x(t)$ and $y(t)$, each of length T seconds, the cross-power spectral density function $G_{xy}(f)$ is as follows:

$$G_{xy}(f) = C_{xy}(f) - jQ_{xy}(f) \quad . \quad (15)$$

The cross-power spectral density function is a complex-valued function with a real part $C_{xy}(f)$ called the co-spectrum, and imaginary part $Q_{xy}(f)$ called the quadspectrum. The co-spectrum and quadspectrum are given by

$$C_{xy}(f) = \lim_{T \rightarrow \infty} \lim_{\Delta f \rightarrow 0} \frac{1}{T(\Delta f)} \int_0^T x_{\Delta f}(t) y_{\Delta f}(t) dt \quad . \quad (15a)$$

$$Q_{xy}(f) = \lim_{T \rightarrow \infty} \lim_{\Delta f \rightarrow 0} \frac{1}{T(\Delta f)} \int_0^{T_{ww}} x_{\Delta f}(t) y_{\Delta f}(t) dt \quad . \quad (15b)$$

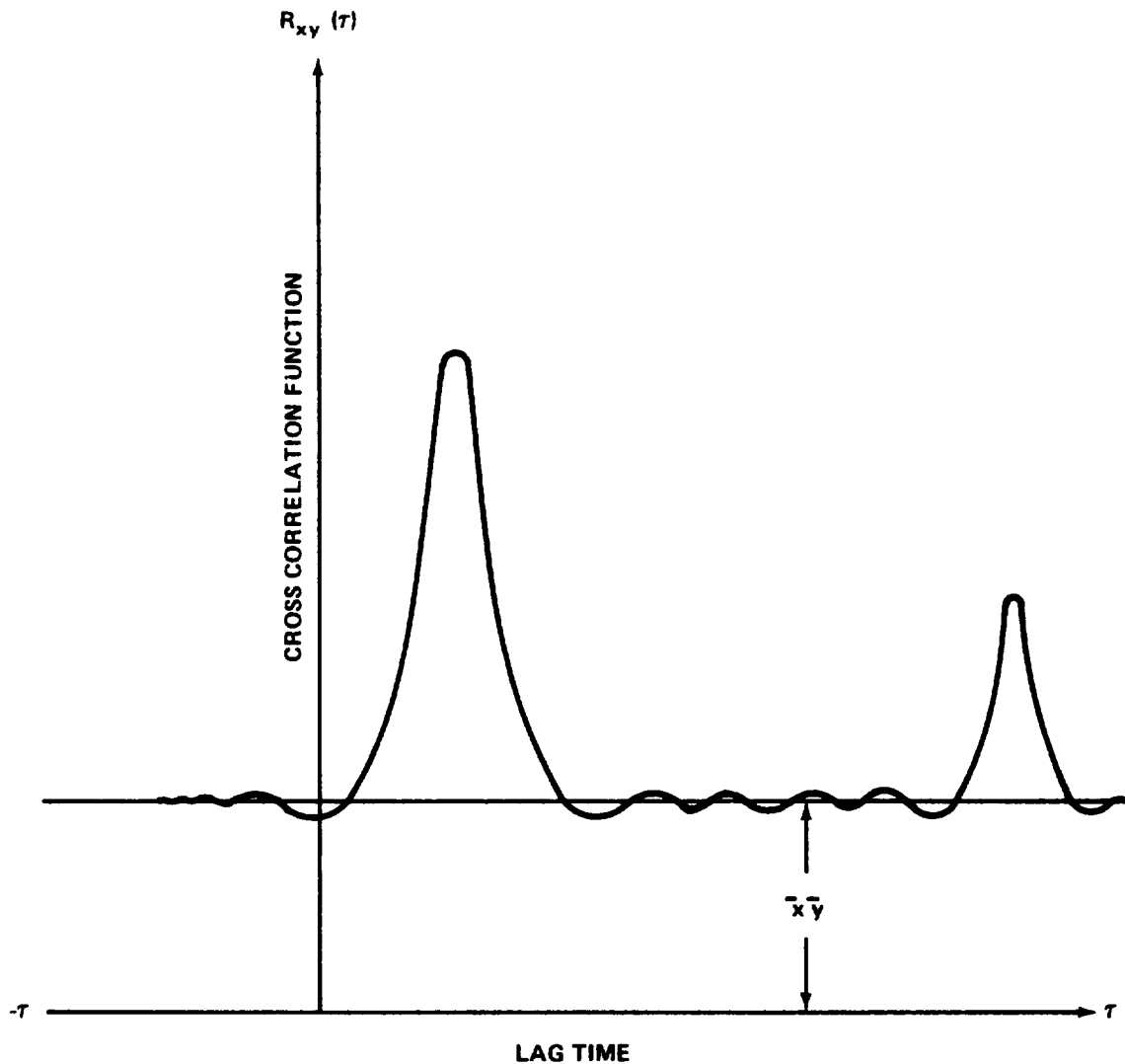


Figure 40. Typical cross correlation plot.

The quantities $x_{\Delta f}(t)$ and $y_{\Delta f}(t)$ are the amplitudes within the narrow frequency interval between f and $f + \Delta f$. The symbol (W) in equation (15b) means that $x(t)$ is 90 degrees out of phase with $y(t)$. Note that both the co-spectrum and quadspectrum may have either positive or negative values.

It is usually more desirable to express the cross-power spectral density function as a vector quantity with a magnitude and phase angle, rather than a complex number as in equation (15). In vector notation, the cross-power spectral density function $G_{xy}(f)$ is given by

$$G_{xy}(f) = |G_{xy}(f)| e^{j\phi_{xy}(f)} \quad (16)$$

where the magnitude term $|G_{xy}(f)|$ and the associated phase angle $\phi_{xy}(f)$ are as follows:

$$G_{xy}(f) = \sqrt{C_{xy}^2(f) - Q_{xy}^2(f)} \quad (16a)$$

$$\phi_{xy}(f) = \arctan \frac{-Q_{xy}(f)}{C_{xy}(f)} \quad (16b)$$

A typical cross-power spectrum $|G_{xy}(f)|$ versus f is illustrated in Figure 41. Cross-power spectral density functions have wide applications to the measurement and evaluation of structural transfer characteristics. The details of such application are beyond the scope of this section. However, several important associations involving the cross-power spectrum for structural input-output relationships will be noted.

Consider a structure (or any other physical system) with a linear frequency response function of $H(f)$. Note that $H(f)$ is a complex-valued function. Let the input excitation be $x(t)$ and the output response be $y(t)$. The following formulas apply:

$$G_{xy}(f) = H(f) G_x(f) \quad (17a)$$

$$G_{yx}(f) = H^*(f) G_x(f) \quad (17b)$$

$$H(f) = \frac{G_{xy}(f)}{G_x(f)} = \frac{G_y(f)}{G_{yx}(f)} \quad (17c)$$

Here, $H^*(f)$ is the complex conjugate of $H(f)$, $G_x(f)$ is the power spectrum of the excitation $x(t)$, and $G_y(f)$ is the power spectrum of the response $y(t)$. It is important to note that $G_{xy}(f) \neq G_{yx}(f)$.

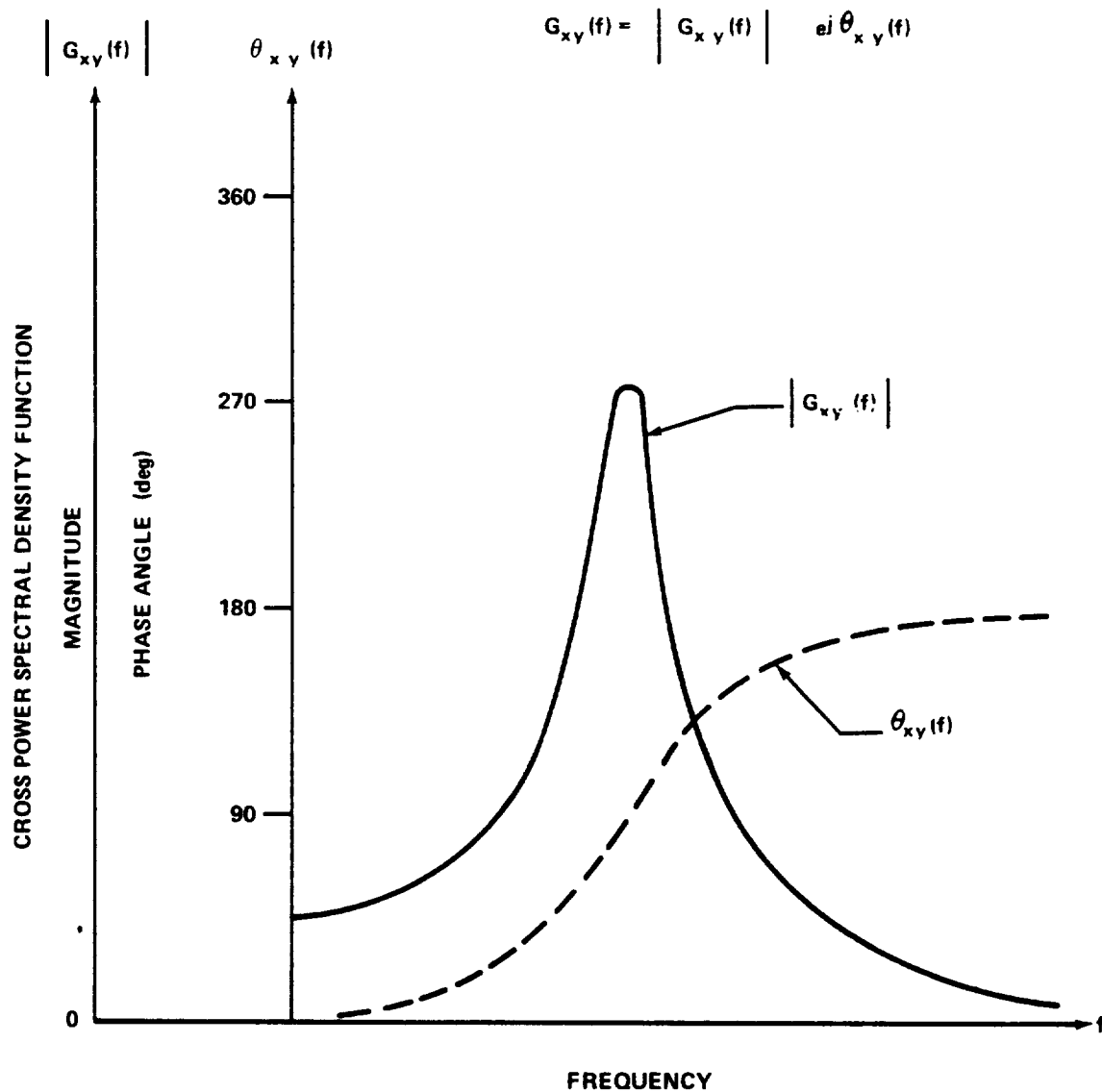


Figure 41. Typical cross-power spectrum.

It was previously mentioned in this section that the power spectral density function and the autocorrelation function for the stationary vibration response are Fourier transform pairs. It should now be noted that the cross-power spectral density function and the cross-correlation function for two stationary vibration responses are also Fourier transform pairs. Hence, both functions contain the same basic information. In general, the time format of the cross-correlation function is more convenient for investigations of

structural transmission paths and time delays while the frequency format of the cross-power spectrum is more convenient for evaluating structural transfer characteristics.

g. Coherence Function

Given two stationary random vibration records, $x(t)$ and $y(t)$, the coherence function $\text{coh}(f)$ is as follows:

$$\text{coh}(f) = \frac{G_{xy}(f) G_{yx}(f)}{G_x(f) G_y(f)} = \frac{|G_{xy}(f)|^2}{G_x(f) G_y(f)} \quad (18)$$

Here $G_x(f)$ and $G_y(f)$ are the power spectra of $x(t)$ and $y(t)$, respectively, and $G_{xy}(f)$ and $G_{yx}(f)$ are the cross-power spectra between $x(t)$ and $y(t)$.

If the two vibration responses are completely uncorrelated (incoherent), the coherence function will equal zero. If the two vibration responses are correlated in a linear manner, the coherence function will equal unity. Hence, if $x(t)$ represents the input excitation to a structure and $y(t)$ represents the output response, the coherence function is a measure of the linearity of the structure. Nonlinearities will produce a coherence function for the input-output relationships which is less than unity. Additive noise in the measurements will also cause the coherence function to be less than unity.

C. General Techniques for Periodic Data Reduction

The basic analog techniques employed by MSFC for periodic vibration data reduction and analysis are now reviewed in terms of general functions. The basic digital techniques employed for vibration data reduction and analysis are presented in Section XII.G.

As noted previously in this section, a periodic vibration response can be completely described (except for phase relationships) by a discrete frequency spectrum which gives the amplitude and frequency of all harmonic components. Given a sample vibration response record in the form of an analog voltage signal, a discrete frequency spectrum for the sampled data may be obtained by using an electronic wave analyzer, or as it is often called, a spectrum analyzer.

There are two basic types of spectrum analyzers. The first type employs a collection of contiguous frequency bandpass filters. The filters may be either constant bandwidth filters or constant percentage filters whose bandwidths are proportional to their center frequencies. When a periodic signal is applied to the bank of filters, each signal passes those frequencies lying within its pass band and excludes all others. The output amplitudes from the filters are then detected and recorded simultaneously as a function of time. The instantaneous output from the filters may also be recorded directly, if so desired. Hence, the spectrum of the applied signal is broken up into as many intervals as there are filters in the bank. This multiple filter type analyzer is sometimes called a real time spectrum analyzer because its operation is substantially instantaneous. This feature constitutes its primary advantage. A secondary advantage is that phase information can be retained if proper calibration procedures are employed. The primary disadvantage of a multiple filter type analyzer is cost. If high resolution is to be obtained, a large number of expensive filters and amplitude detectors must be incorporated in the analyzer. A functional block diagram for a multiple filter type spectrum analyzer is shown in Figure 42.

The second type of spectrum analyzer employs a single narrow frequency bandpass filter. The signal is moved in frequency past the fixed narrow bandpass filter by application of the heterodyne principle. The output amplitude from the filter is detected and recorded as a function of frequency, giving the spectrum for the applied signal. The primary advantage of the single filter type spectrum analyzer is high resolution. Since only a single fixed filter is used, its characteristics can be optimized without adding appreciably to the cost of the analyzer. The primary disadvantage of this single filter type analyzer is that the time required to perform an analysis is relatively long since the entire frequency range of the signal is investigated with only one narrow bandpass filter. It should be noted that single filter spectrum analyzers are usually equipped with several filter selections having different bandwidths to permit flexibility in choosing the resolution desired for a given analysis. A functional block diagram for a single filter type spectrum analyzer is shown in Figure 43.

For either type of spectrum analyzer, the output amplitude detector consists of circuits which compute one or more of three different amplitude functions. These are the peak amplitude, the rectified average amplitude, and/or the mean square amplitude. If the resolution for a given periodic signal analysis is sufficiently sharp to identify each individual frequency component of the signal, the amplitude detection circuit employed is of no direct concern since the outputs from the filter(s) will always be sine waves. The peak, average, and mean square amplitudes for sine waves have fixed relationships to one another, as follows:

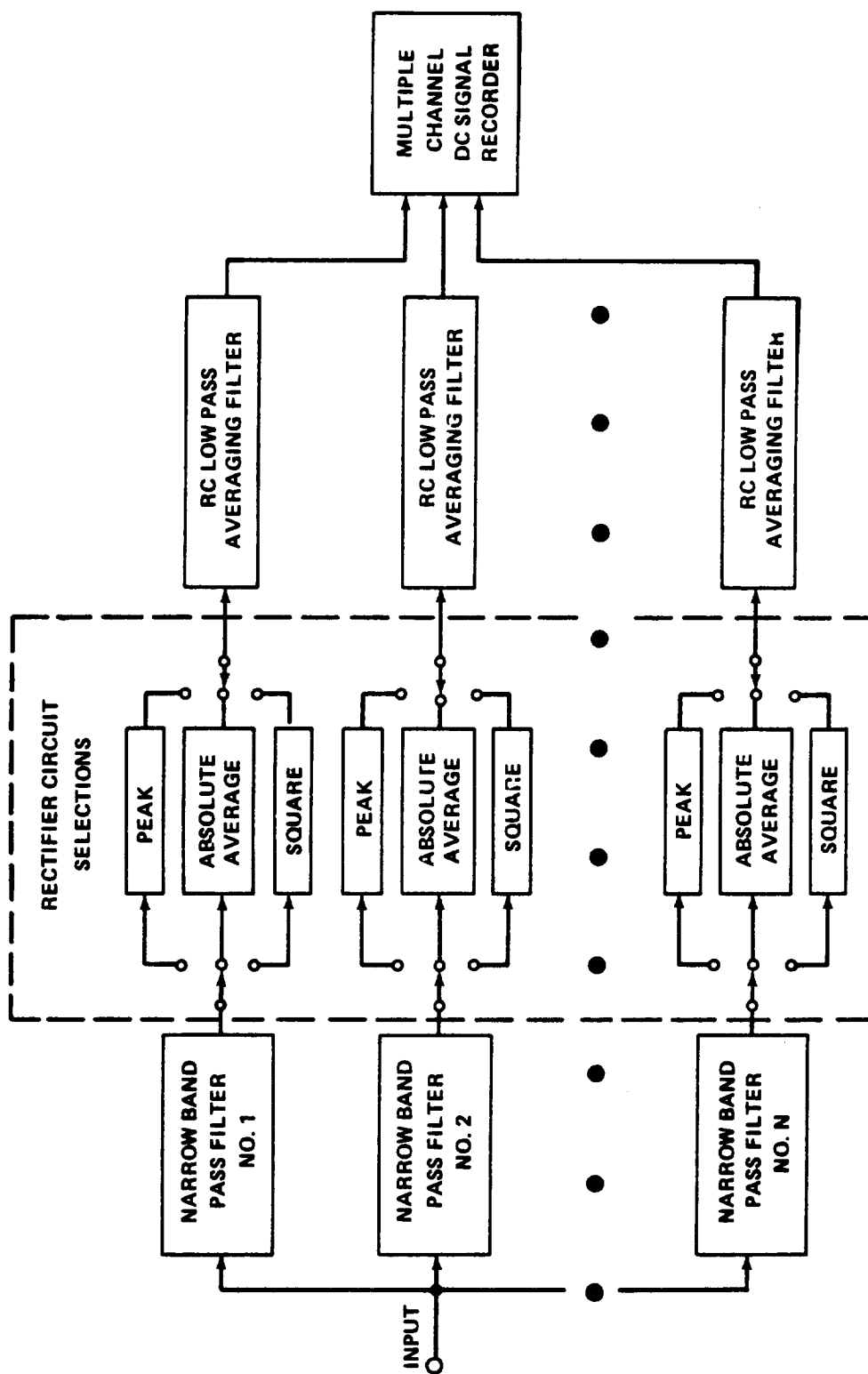


Figure 42. Functional block diagram for multiple filter type spectrum analyzer.

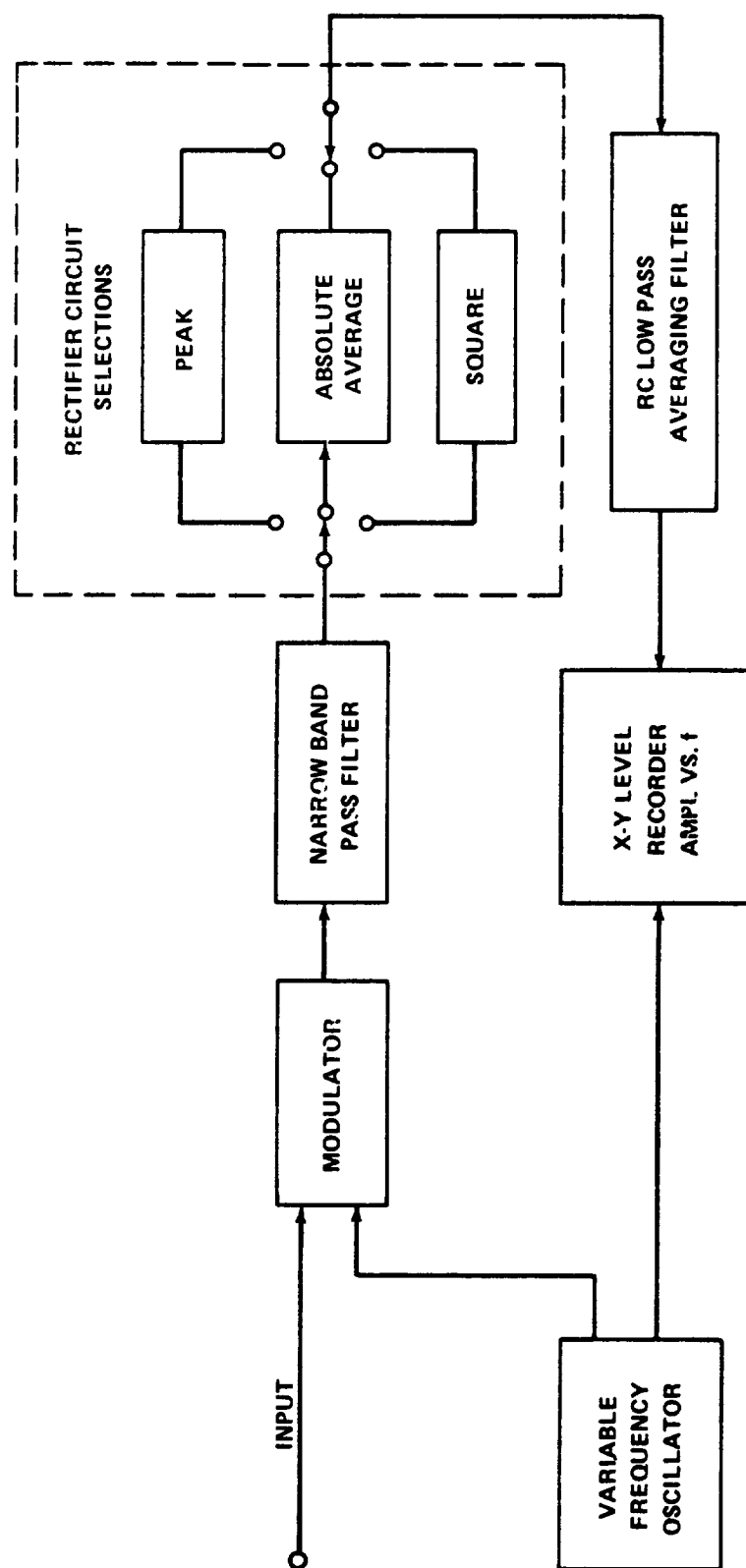


Figure 43. Functional block diagram for single filter type spectrum analyzer.

instantaneous amplitude = $C \sin \omega t$

peak amplitude = C

rectified average amplitude = $0.636 C$ (19)

Mean square amplitude = $0.5 C^2$

root mean square (rms) amplitude = $0.707 C$.

Hence, any one of the three detection circuits may be used and read out in terms of any other amplitude function desired by simply calibrating the readout scale in an appropriate manner. For example, the peak value of the filtered signal may be detected and read out as an rms amplitude by noting that the rms amplitude is equal to 0.707 times the peak amplitude. It is important to emphasize that these relationships apply only when the analysis resolution is sufficiently sharp to isolate individual frequency components. The relationships in equation (19) do not apply to the sum of two or more sine waves.

The practical considerations associated with the analysis of periodic signals are reviewed below. All relationships stated are taken from Reference 20.

1. ANALYSIS ACCURACY

If the various limitations noted in paragraphs 2., 3., and 4. below are observed, the only errors in a spectrum analysis of periodic data are the basic measurement errors inherent in the spectrum analyzer design capabilities and calibration techniques. There are no intrinsic statistical uncertainties or sampling errors associated with the proper reduction and analysis of periodic vibration data.

2. RESOLUTION

The frequency spectrum for a periodic signal is theoretically a discrete line spectrum where each component is a delta function with no bandwidth. However, a spectrum analyzer will display each component as a peak with an apparent bandwidth, which of course will be the bandwidth of the spectrum analyzer filter. Thus, the exact frequency of the signal components will be more accurately defined as the bandwidth of the analyzer filter is made narrower. The accuracy with which the frequencies of individual components are identified is generally referred to as the resolution of the analysis.

It would appear that the best method of analysis would be to use the narrowest possible bandpass filter. However, for the multiple filter type spectrum analyzer, the required number of filters and the associated cost are inversely proportional to the bandwidth of the filters. For the single filter type spectrum analyzer, the required analysis time is inversely proportional to the bandwidth of the filter, as is discussed later. It is important to note, however, that the resolution of any given spectrum analysis should always be sufficient to distinguish between adjacent frequency components. In other words, the analyzer filter bandwidth should always be narrower than the frequency interval between the components of the signal being analyzed. Thus, the general criteria for minimum permissible resolution is

$$B < (1/T_p) \quad (20)$$

where B is the analyzer filter bandwidth in cps and T_p is the period of the vibration data in seconds.

An illustration of a properly resolved spectrum analysis is presented in Figure 44. In this example, $T_p = 1/50$ second, so the maximum permissible bandwidth for acceptable resolution would be $B = 50$ Hz. However, the actual bandwidth used was $B = 2$ Hz resulting in a very precise resolution.

3. SAMPLE RECORD LENGTH

Theoretically, the record length required to perform a spectrum analysis on the sampled periodic vibration data is only T_p seconds long (the length of one vibration period). However, for certain practical reasons, it is desirable that the sample record be very much longer than one period. Multiple filter analyzers are normally employed only when relatively long sample records are involved. However, single filter analyzers are often used to analyze relatively short records.

Analysis of a relatively short sample record with a single filter type spectrum analyzer is usually accomplished by making a continuous loop from the sample record so that the data signal may be continuously applied to the analyzer. The formation of the loop produces, in effect, a fictitious fundamental period for the data. Unless the record length is an exact even multiple of one period T_p , the loop will tend to introduce fictitious frequency components into the analysis. However, these effects become insignificant if the record length is, say, 10 times longer than the period of the vibration data. For

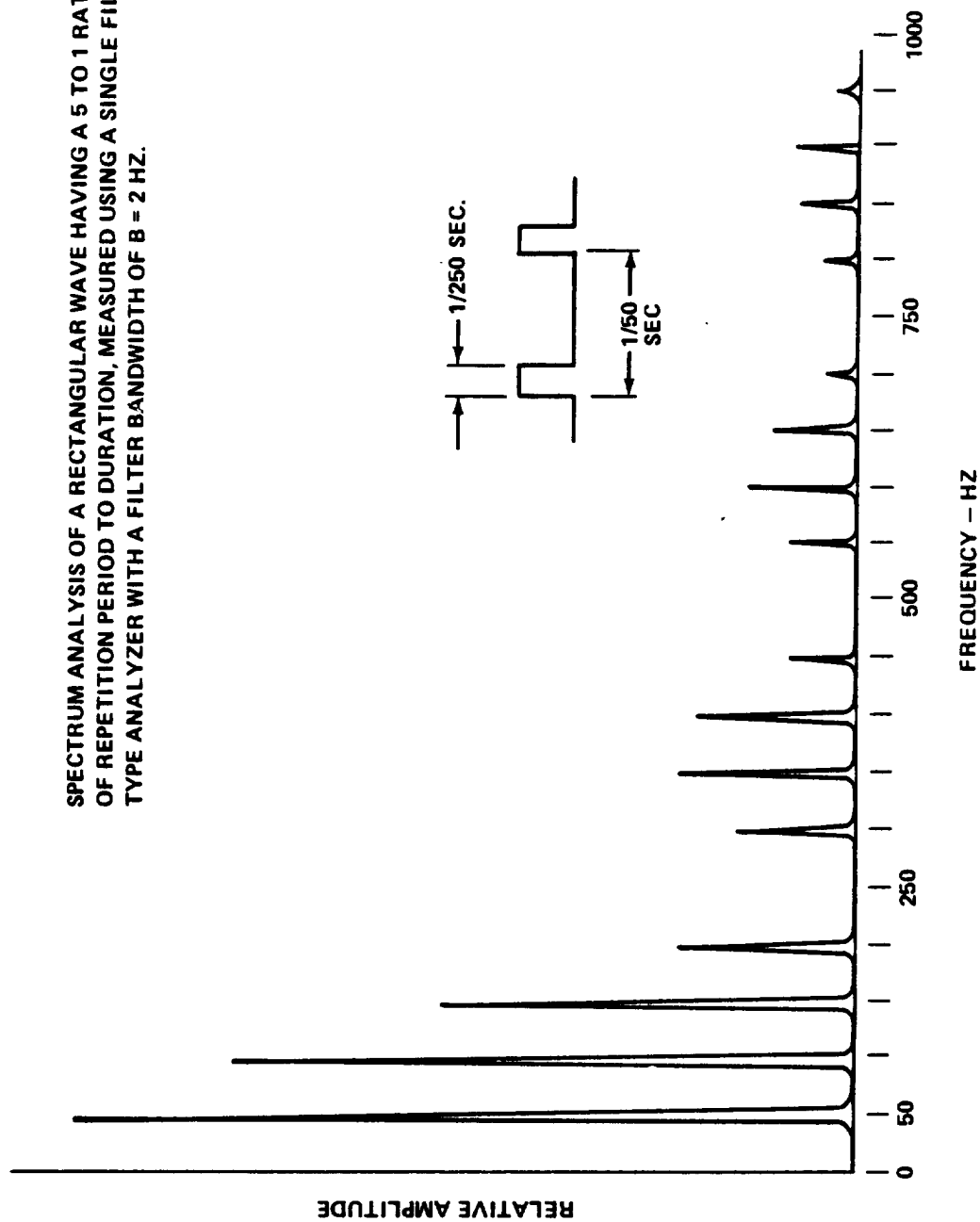


Figure 44. Properly resolved frequency spectrum for periodic data.

example, assume a periodic signal with a fundamental frequency of 25 Hz is to be analyzed. The length of the sample record should be $T > 10 T_p = 0.4$ second.

4. AVERAGING TIME

The peak, average, and/or mean square amplitude detectors incorporated in the spectrum analyzer compute the desired amplitude function by smoothing or time averaging the instantaneous output of an appropriate rectifier circuit (RC). For example, the average amplitude of a signal component is usually measured by a simple ac voltmeter circuit where the component is rectified, and the instantaneous rectified amplitude is averaged by smoothing with an equivalent low-pass RC filter. The equivalent RC time constant of the averaging filter should be longer than the period of the vibration data being analyzed. Thus, a general criteria for the minimum time constant of the averaging filter is

$$K > T_p \quad (21)$$

where K is the equivalent RC time in seconds.

For example, assume a periodic signal with a fundamental frequency of 25 Hz is to be analyzed. The minimum time constant for the averaging filter is $K > T_p = 0.04$ second.

5. SCAN RATE AND ANALYSIS TIME

For the multiple filter type spectrum analyzer, the frequency components of the applied signal are concurrently measured, so the analysis time is substantially instantaneous. However, for the single filter type spectrum analyzer, the frequency components of the applied signal must be individually measured by scanning through the entire frequency range of interest. If the scan is too fast, one of two difficulties may occur.

a. The narrow bandpass filter of the spectrum analyzer will not fully respond to the individual frequency components of the signal.

b. The amplitude detector averaging filter will not fully respond to the individual frequency components of the signal.

The response time for narrow bandpass filters is a function of the exact filter characteristics, but, in general, will be less than $(1/B)$ seconds

where B is the bandwidth of the filter in Hz. Thus, a general criteria for the maximum analysis scan rate based on the analyzer filter response is

$$\text{scan rate} < B^2 \text{ Hz/sec} \quad (22a)$$

The response time for equivalent RC low-pass averaging filters is such that about 98 percent of full response is reached in a time equal to four time constants (4K). Thus, a general criteria for the maximum analysis scan rate based on the averaging filter response is

$$\text{scan rate} < \frac{B}{4K} \text{ Hz/sec} \quad (22b)$$

If the total frequency range for the analysis is F Hz, the minimum analysis time is

$$\text{analysis time} > \frac{F}{B^2} \text{ seconds} \quad (23a)$$

$$\text{analysis time} > \frac{4KF}{B} \text{ seconds} \quad (23b)$$

For example, assume a periodic signal is to be analyzed with a filter bandwidth of B = 10 Hz and an averaging time constant of K = 0.1 second, over a frequency range from near 0 to 2000 Hz (F = 2000 Hz). The maximum scan rate is 25 Hz/sec, since equation (22b) produces the smaller value. Hence, the minimum analysis time is 80 seconds, since equation (23b) produces the larger value.

D. General Techniques for Random Data Reduction

The basic analog techniques employed by MSFC for random vibration data reduction and analysis are now reviewed in terms of general functions. The basic digital techniques employed for vibration data reduction and analysis are presented in Section XII. F.

As noted Paragraph B.2 of this section, a stationary random vibration response can be described in the amplitude domain by a probability density function as given in equation (8), in the time domain by an autocorrelation function as given in equation (10), and in the frequency domain by a power spectral density function as given in equation (12). If two or more vibration response records are available, additional information may be obtained from

a joint probability density function as given in equation (13), a cross-correlation function as given in equation (14), and a cross-power spectral density function as given in equation (15).

The true measurement of the above-mentioned properties requires the determination of a limit as the record length T approaches infinity. Furthermore, the true measurement of probability and power spectral density functions also requires the determination of a limit as either an amplitude interval Δy or a frequency interval Δf approaches zero. Clearly, the determination of these limits is physically impossible. Thus, no real instrument can actually measure the true properties of a random vibration. However, measurements can be performed which produce meaningful estimates for the desired properties. These measurement techniques are now discussed.

1. AMPLITUDE PROBABILITY DENSITY ANALYSIS

Given a sample vibration response record in the form of an analog voltage signal $y(t)$ with a finite length of T seconds, the amplitude probability density function for the vibration response may be estimated from equation (8) as follows:

$$\hat{p}(y) = \frac{\overline{t}_W}{W} \quad . \quad (24)$$

Here, \overline{t}_W is the average portion of the time spent by the signal $y(t)$ within a narrow amplitude interval having a gate width of W volts and a center amplitude of y volts. The hat (\wedge) over $\hat{p}(y)$ means that the measured quantity is only an estimate of $p(y)$, since the record length T and the gate width W are finite. The amplitude probability density function is estimated by the following operations.

- a. Amplitude filtering of the signal by a narrow amplitude gate having a gate width of W volts.
- b. Measurement of the total time spent by the signal within the gate.
- c. Division of the time spent within the gate by the total sampling time, to obtain the average portion of time spent by the signal within the gate.
- d. Division of the average portion of the time spent within the gate by the gate width W .

As the center amplitude of the gate is moved, a plot of the probability density function versus amplitude is obtained.

The above operations are accomplished by an analog amplitude probability density analyzer, which will be called an APD analyzer for simplicity. In general, an APD analyzer measures the time spent by a signal within some narrow amplitude interval by use of a voltage gate (narrow band voltage discriminator) followed by a clock circuit. When the input signal amplitude from the sample record falls within the gate, the clock circuit operates. For all other signal amplitudes, the clock circuit does not operate. The clock circuit output is averaged over the entire time of observation T_a to obtain the average portion of time spent by the signal amplitude within the narrow gate. The required division by the gate width W may be obtained by a proper scale calibration.

There are two basic types of APD analyzers. The first type employs a collection of contiguous voltage gates with equal gate widths. The multiple gate type analyzer measures the probability density within each gate simultaneously to give a plot of probability density versus amplitude. The second type employs a single gate whose center voltage is variable relative to the voltage of the signal. The single gate type analyzer produces a plot of probability density versus amplitude by sweeping (or stepping) the single gate through the entire range of voltage amplitudes of interest. A functional block diagram for a single gate APD analyzer is shown in Figure 45.

The practical considerations associated with amplitude probability density analysis are reviewed below. All relationships stated are taken from Reference 20. Many of the relationships are also studied experimentally in Reference 21.

a. Analysis Accuracy

The analysis of random vibration data involves basic measurement errors due to the analysis equipment design capabilities and calibration techniques, just as is true for the analysis of periodic vibration data. However, the analysis of random data also involves an additional error which is called the statistical uncertainty or probable sampling error. As was mentioned earlier, the data measured from sample records of finite length constitute only statistical estimates of the true properties of the sampled vibration response. The expected deviation of the estimated properties from the actual properties of the random vibration represents the statistical uncertainties associated with the measurements. Thus uncertainty may be defined in terms of a normalized standard deviation for the sampling distribution, which is often called the standard error e .

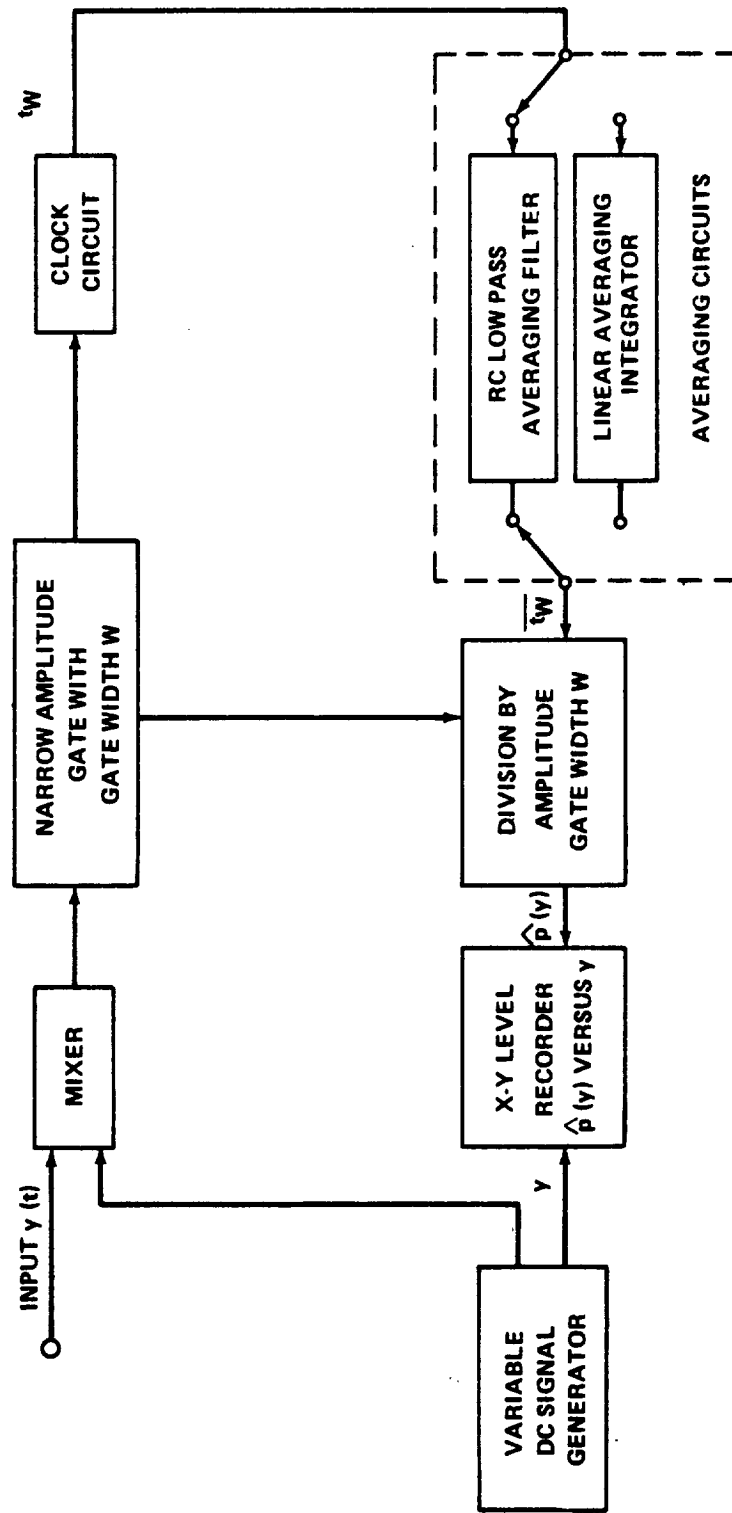


Figure 45. Functional block diagram for amplitude probability density analyzer.

For the specific case of amplitude probability density analysis, the standard error associated with a measured estimate $\hat{p}(y)$ is as follows:

$$e \approx \frac{0.20}{\sqrt{\hat{p}(y) \text{ WBT}}} \quad (25)$$

Here, $\hat{p}(y)$ is the measured probability density, W is the amplitude gate width in relative amplitude units, B is the bandwidth of the signal being investigated, and T is the length of the analyzed sample record in seconds.

Several important features of equation (25) should be noted. First, this expression for the standard error is a simplification of more complicated relationships developed theoretically and empirically in Section 14 of Reference 21. However, equation (25) is an acceptable approximation for most applications. Second, the standard error e is a function of the actual probability density estimate that is measured. Thus, for any given gate width, bandwidth, and record length, the uncertainty of the estimate varies with the amplitude being analyzed. Third, the bandwidth B assumes that the vibration signal has a power spectrum which is uniform between two frequencies B Hz apart, and zero elsewhere. In other words, the signal is assumed to be white noise which has been filtered with an ideal rectangular bandpass filter having a bandwidth B.

The meaning of the standard error e is as follows. Assume a stationary random vibration response with a true probability density function of $p(y)$ is repeatedly sampled at different times, and an estimate $\hat{p}(y)$ is measured for each sample. For about 68 percent of the estimates obtained, the difference between the estimate $\hat{p}(y)$ and the true value $p(y)$ will be less than $\pm e \hat{p}(y)$. Stated in another way, if an estimate $\hat{p}(y)$ is measured, one may say with about 68 percent confidence that the true value $p(y)$ is within the range $(1 \pm e) \hat{p}(y)$. A plot of the standard error e versus the WBT product for various amplitude probability density estimates is presented in Figure 46.

For example, assume an amplitude probability density function is measured from a sample record that is $T = 0$ second long using an APD analyzer with a gate width of $W = 0.1$ volt. Further assume the bandwidth of the signal is $B = 100$ Hz. If a probability density of $p = 0.16$ were measured at the amplitude $y = 1.5$ volt ($y_{\text{rms}} = 1$ volt), the standard error for the estimate

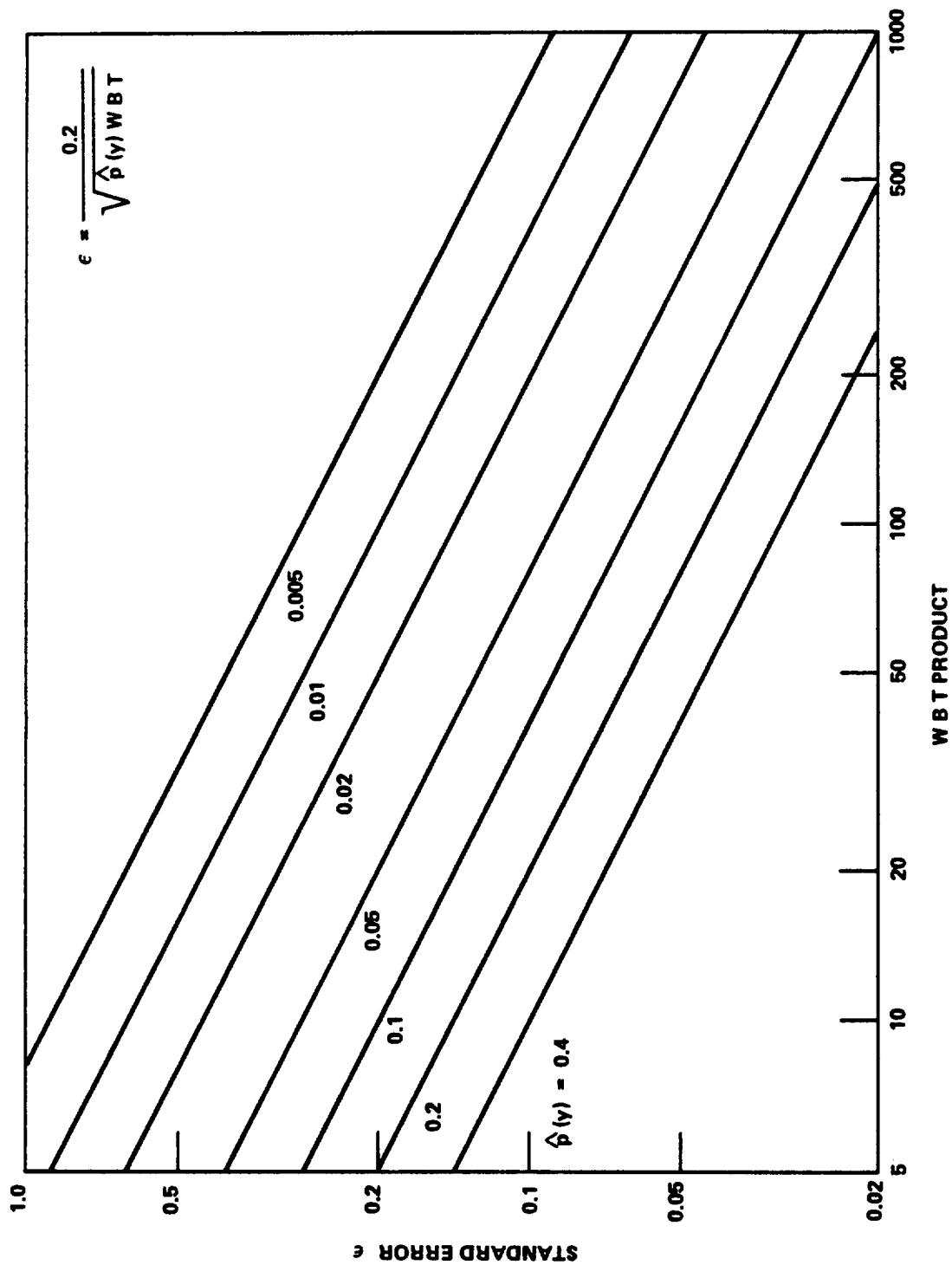


Figure 46. Estimation uncertainty versus WBT product.

would be $e = 0.05$. Hence, one could say with 68 percent confidence that the true probability density at that amplitude is within ± 5 percent of the measured value, or between 0.152 and 0.168.

b. Resolution

Equation (25) shows that the statistical uncertainty of probability density estimates is inversely proportional to the width of the amplitude gate. One might then conclude that improved estimation accuracy can easily be obtained by simply increasing the gate width. However, increasing the gate width reduces the resolution of the analysis; that is, it reduces the ability of the analysis to properly define peaks in the probability density plot. The selection of the analyzer gate width is always a compromise between estimation uncertainty and resolution. A general criterion for proper resolution is a gate width that is less than one-fourth of the rms signal amplitude; that is,

$$W < \frac{1}{4} y_{\text{rms}} \quad (26)$$

where W is the analyzer gate width in volts and y_{rms} is the root mean square value of the signal being analyzed in volts.

c. Sample Record Length

As seen from equation (25), the sample record length T limits the statistical accuracy attainable in an amplitude probability density analysis. The longer the record length, the lower the uncertainty in the resulting probability density estimates. If the statistical uncertainty of a probability density analysis is to be limited to a given desired amount, these matters must be considered before the data are gathered to assure that sample records are sufficiently long.

d. Averaging Time

An APD analyzer computes the portion of time spent by the signal amplitude within the gate by averaging the output of the gate clock circuit. The averaging may be accomplished by true linear integration, called true averaging, or by continuous smoothing with an equivalent low-pass RC filter, called RC averaging. True averaging produces a single probability density estimate after a specific averaging time T_a while RC averaging produces a continuous probability density estimate. If the RC time constant

of the averaging filter is K and the record length T is long compared to K , the continuous estimate at any instant of time has an uncertainty equivalent to an estimate obtained by true averaging over a time interval of $T_a = 2K$.

For the case of true averaging, it is clear that the averaging time T_a should be as long as the record length T if the uncertainty in the resulting estimates is to be kept at a minimum. In other words, all of the information available from the sample record should be employed for the probability density measurement. If T_a is less than T , the uncertainty will be increased since T_a will replace T in equation (25). If T_a is greater than T , as it could be when the sample record is formed into a continuous loop for analysis, the uncertainty will not be decreased from the value given in equation (25) since one is simply looking at the same information more than once.

For the case of RC averaging, minimum uncertainty can be achieved only by making the time constant K very long. However, a long averaging time constant reduces the scan rate and greatly increases the total analysis time, as is discussed in Paragraph D.1.a. of this section. A reasonable compromise is to use an averaging time constant that is at least one-half the record length T .

Thus, the general criteria for the ideal averaging time for a probability density analysis are as follows:

$$\text{for true averaging, } T_a = T \quad (27a)$$

$$\text{for RC averaging, } 2K \geq T \quad (27b)$$

Here, T_a is the true averaging (integration) time in seconds, and K is the time constant of the equivalent RC averaging filter in seconds.

e. Scan Rate and Analysis Time

For the multiple gate type APD analyzer, the probability density is concurrently measured over all amplitudes of interest, so the analysis time is equal to the record length T . However, for the single gate type APD analyzer, the probability density at all amplitudes of interest must be measured by scanning through the desired amplitude range. If the scan is too fast, all the information available at a given amplitude will not be viewed by the analyzer gate over the entire record length, and the statistical uncertainty of the resulting estimate will be increased. If RC averaging is used, the scan rate is further limited because time must be allowed for the RC averaging filter

to respond to abrupt changes in the probability density function. The limitations imposed upon the scan rate by these considerations are as follows:

$$\text{for true averaging, scan rate} < \frac{W}{T_a} \quad (28a)$$

$$\text{for RC averaging, scan rate} < \frac{W}{4K} \quad (28b)$$

Here, T_a is the averaging time in seconds, K is the RC time constant in seconds, and W is the gate width in volts. Hence, scan rate has the units of volts per second.

If the total amplitude range for the APD analysis is A volts, the minimum analysis time is as follows:

$$\text{for true averaging, analysis time} > \frac{T_a A}{W} \quad (29a)$$

$$\text{for RC averaging, analysis time} > \frac{4KA}{W} \quad (29b)$$

For example, assume the amplitude probability density function for a random vibration response is to be estimated from a sample record of length $T = 10$ seconds over an amplitude range from minus four volts to plus four volts ($A = 8$ volts) using an APD analyzer with a gate width of $W = 0.1$ volt. The rms amplitude of the signal is assumed to be 1 volt. If true averaging is used, $T_a = 10$ seconds and the maximum scan rate is 0.01 volt/second.

Hence, the minimum analysis time is 800 seconds or 13.3 minutes. If RC averaging is used, $K \geq 5$ seconds, and the maximum scan rate is 0.005 volt/second. Hence, the minimum analysis time is 1600 seconds, or about 27 minutes.

2. AUTOCORRELATION ANALYSIS

Given a sample vibration response record in the form of an analog voltage signal $y(t)$ with a finite length of T seconds, the autocorrelation function for the vibration response may be estimated from equation (10) as follows:

$$\hat{R}_y(\tau) = \overline{y(t) y(t + \tau)} \quad (30)$$

Here, $\overline{y(t) y(t + \tau)}$ is the average product of the instantaneous signal amplitude at two different times which are τ seconds apart. The hat (\wedge) over $R_y(\tau)$ means that the measured quantity is only an estimate of $R_y(\tau)$, since the record length T is finite. The autocorrelation function is estimated by the following operations:

- a. Delaying the signal by a time displacement equal to τ seconds, called the lag time.
- b. Multiplying the amplitude at any instant by the amplitude that had occurred τ seconds before.
- c. Averaging the instantaneous amplitude product over the sampling time.

As the lag time is moved, a plot of the autocorrelation function versus lag time is obtained.

The above operations are accomplished by an analog autocorrelation function analyzer, which will be called an ACF analyzer for simplicity. In general, an ACF analyzer displaces the signal in time by use of a magnetic signal recorder with a variable lag time between the record and playback. This can be accomplished, for example, with a magnetic drum recorder where the location of the playback head is variable relative to the location of the record head. The input and output of the lag time generator are then multiplied and averaged. The lag time is variable over a range from zero to the longest sampling times that are anticipated. Since the autocorrelation function is an even function, it is not necessary to make measurements with negative lag times. A functional block diagram for an ACF analyzer is shown in Figure 47.

The practical considerations associated with autocorrelation analysis are reviewed below. All relationships stated are taken from Reference 20.

a. Analysis Accuracy

As discussed in Paragraph D.1.a. of this section, the analysis of random vibration data involves not only basic measurement errors, but also a statistical uncertainty inherent in the sampling procedures. Thus, uncertainty may be defined in terms of the standard error e for the sampling distribution. For the specific case of autocorrelation analysis, the standard error associated with a measured estimate $\hat{R}_y(\tau)$ is as follows:

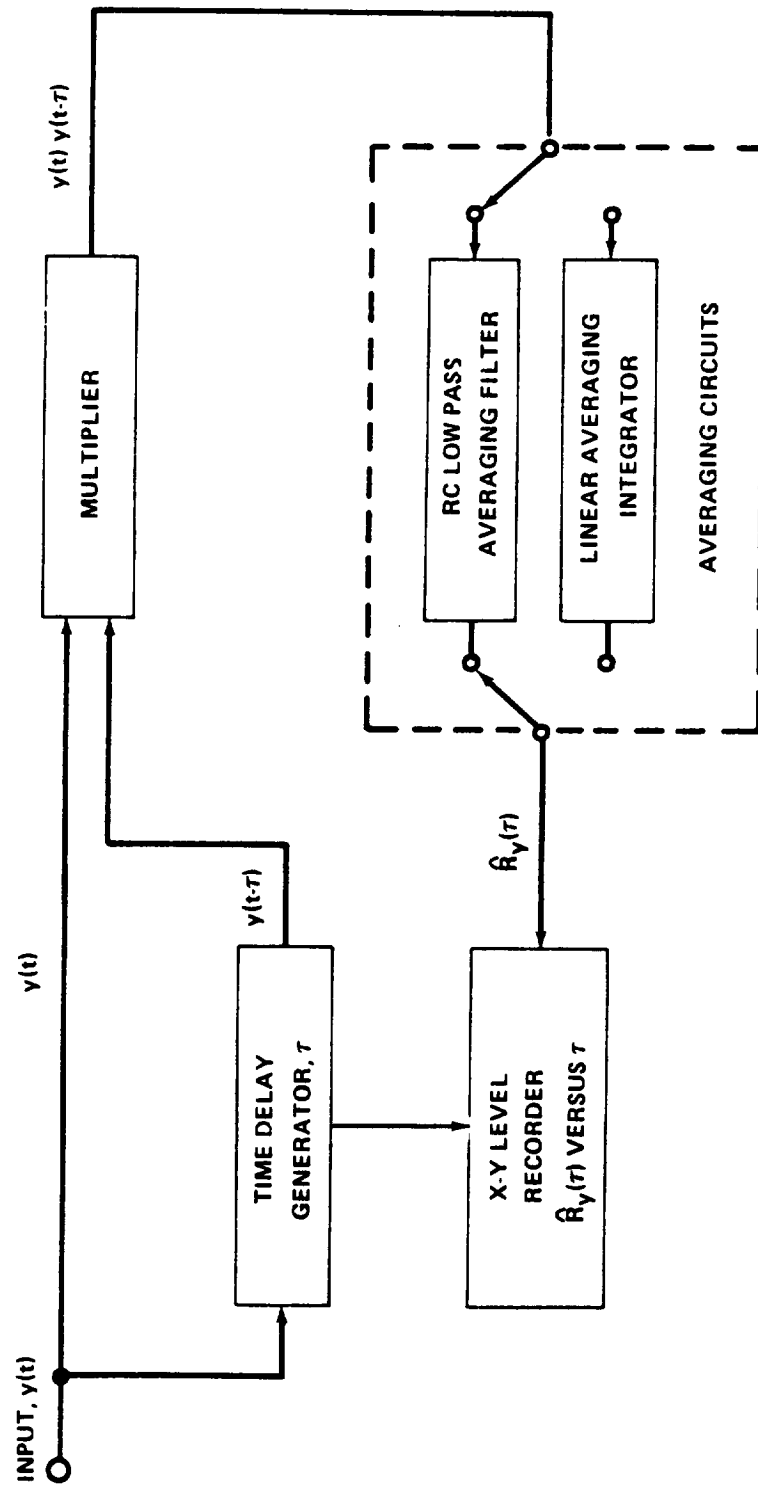


Figure 47. Functional block diagram for autocorrelation analyzer.

$$e \approx \frac{1}{\sqrt{BT}} . \quad (31)$$

Here, B is the noise bandwidth of the signal in Hz and T is the length of the analyzed sample record in seconds. It is assumed in deriving equation (31) that $T \ll \tau$ and that $BT \geq 10$.

Two important features of equation (31) should be noted. First, this expression for the standard error is a conservative approximation which is accurate for lag times near zero. For large lag times, the standard error is not explicitly defined but is somewhat less than the quantity given in equation (31). Second, the bandwidth B is the noise bandwidth of the vibration response signal. The determination of noise bandwidths is covered in Paragraph E. of this section.

The general meaning and interpretation of the standard error e is discussed in Paragraph D.1 of this section. The specific interpretation for autocorrelation analysis is as follows. Assume a stationary random vibration response with a true autocorrelation function of $R_y(\tau)$ is sampled, and an estimate $\hat{R}_y(\tau)$ is measured from the sample. If e is reasonably small, say less than 0.30, it may be said with about 68 percent confidence that the true value $R_y(\tau)$ is within the range $(1 \pm e)R_y(\tau)$. A plot of the standard error e versus the BT product is presented in Figure 48.

For example, assume an autocorrelation function is measured from a sample record that is $T = 10$ seconds long. Further assume the noise bandwidth of the signal is $B = 100$ Hz. The standard error for the resulting estimate is $e \approx 0.032$. Hence, if a measured estimate $\hat{R}_y(\tau)$ at time $\tau = 0$ were about 0.3 volt^2 , it could be said with 68 percent confidence that the true autocorrelation function for that lag time is within ± 3.2 percent of the measured value, or between 0.29 and 0.31 volt^2 .

b. Resolution

As seen from equation (30), the autocorrelation function $\hat{R}(\tau)$ must be estimated at various different lag times τ to obtain a plot of the autocorrelation function versus lag time. The interval between the lag times at which computations are made defines the resolution of the autocorrelation plot. Based upon practical considerations, a general criteria for proper resolution is a lag time interval that is less than one-fourth the reciprocal of the signal bandwidth; that is,

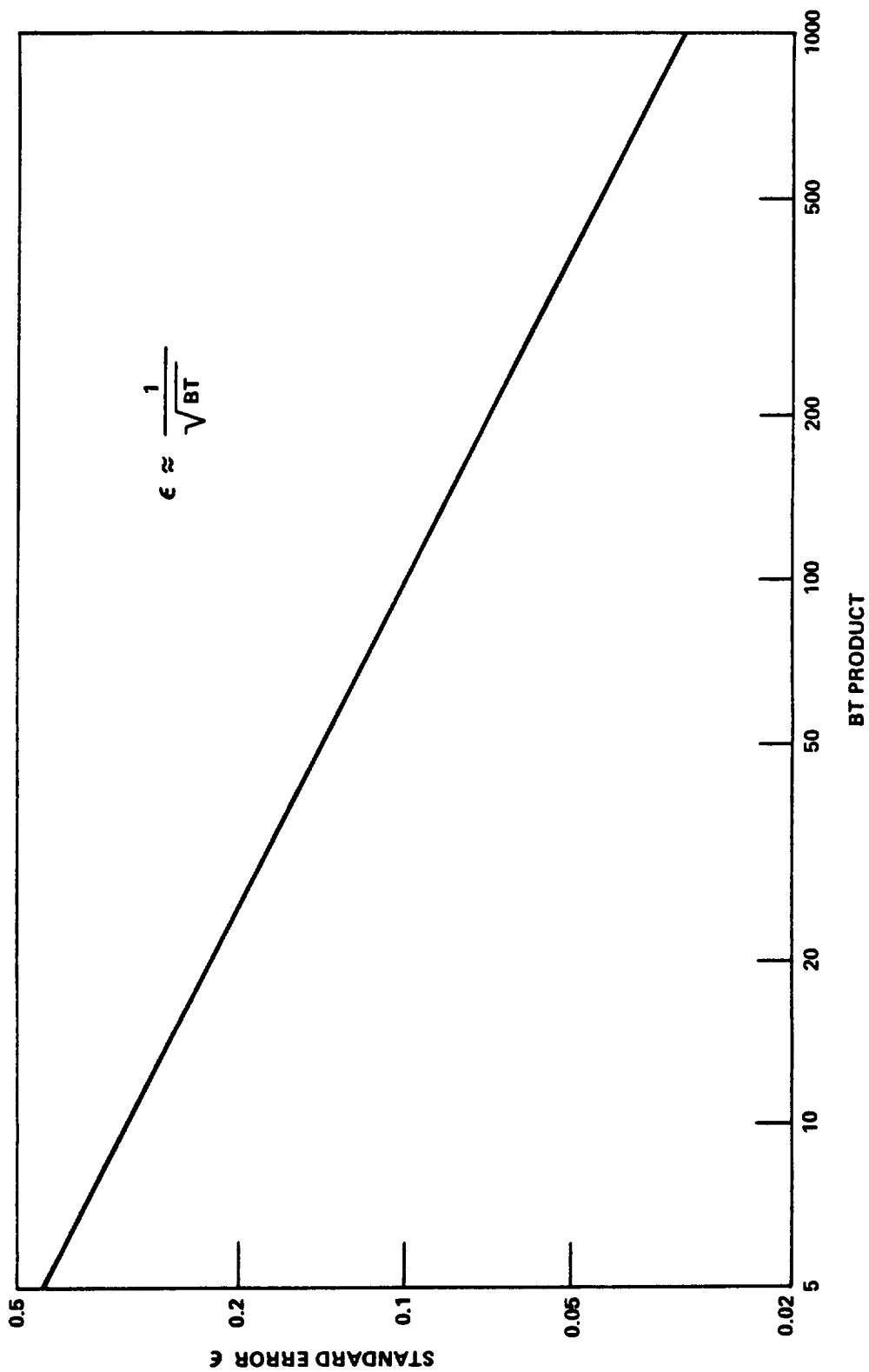


Figure 48. Estimation uncertainty versus BT product.

$$h < \frac{1}{4B} \quad (32)$$

where h is the interval between lag times in seconds and B is the bandwidth of the signal in Hz.

The relationship in equation 8.33 is directly appropriate for the case when an autocorrelation function is computed at specific lag times, $\tau_1, \tau_2 = \tau_1 + h, \tau_3 = \tau_1 + 2h$, etc. However, analog instruments often determine an autocorrelation plot by continuous averaging while the time delay generator makes a continuous scan through the lag time range of interest. For this case, the relationship in equation (32) constitutes the basis for a limit on the lag time scan rate. This limit is discussed in Paragraph e. below.

c. Sample Record Length

As seen from equation (31) the sample record length T determines the statistical accuracy attainable in an autocorrelation analysis. The longer the record length, the lower the uncertainty in the resulting autocorrelation estimates. If the statistical uncertainty of an autocorrelation analysis is to be limited to a given desired amount, these matters must be considered before the data are gathered to assure that sample records are sufficiently long.

d. Averaging Time

An ACF analyzer computes the mean product of the signal amplitudes at two different times by averaging the output of the multiplier circuit. The averaging may be accomplished by true linear integration, called true averaging, or by continuous smoothing with an equivalent lowpass RC filter, called RC averaging. True averaging produces a single autocorrelation estimate after a specific averaging time T_a while RC averaging produces a continuous probability density estimate.

For the reasons presented in Paragraph D.1.d. of this section, the general criteria for the ideal averaging time for an autocorrelation analysis is

$$\text{for true averaging, } T_a = T \quad (33a)$$

$$\text{for RC averaging, } 2K \geq T \quad (33b)$$

Here, T_a is the true integrating time in seconds, and D is the time constant of the equivalent RC averaging filter in seconds.

e. Scan Rate and Analysis Time

The autocorrelation function at all lag times of interest must be measured by scanning through the desired time delay range. This may be done in discrete steps or a continuous sweep. For the case of a stepped scan, if the scan rate is too fast, all the information available at a given lag time will not be analyzed and the statistical uncertainty of the resulting estimate will be increased. For the case of a continuous scan, if the scan rate is too fast, the resolution of the resulting estimate will be reduced. If RC averaging is used, the scan rate is further limited because time must be allowed for the RC averaging filter to respond to abrupt changes in the autocorrelation function. The limitations imposed upon the scan rate by these considerations are as follows:

$$\text{for true averaging, scan rate} < \frac{1}{4BT_a} \quad (34a)$$

$$\text{for RC averaging, scan rate} < \frac{1}{16 BK} \quad (34b)$$

Here, T_a is the averaging time in seconds, K is the RC time constant in seconds, and B is the noise bandwidth in Hz. Hence, scan rate has the units of seconds per second.

If the maximum lag time for the ACF analysis is τ_m seconds where τ_m is relatively small compared to the record length T , the minimum analysis time is as follows:

$$\text{for true averaging, analysis time} > 4BT_a \tau_m \quad (35a)$$

$$\text{for RC averaging, analysis time} > 16 BK \tau_m \quad (35b)$$

For example, assume the autocorrelation function for a random vibration response is to be estimated from a sample record of length $T = 10$ seconds. Further assume the vibration signal has an upper frequency limit of $f_u = 100$ Hz

and that lag times of up to $\tau_m = 1$ second are of interest. If true averaging is used, $T_a = 10$ seconds and the maximum scan rate is 0.00025 second/second. Hence, the minimum analysis time is 4000 seconds or about 67 minutes. If RC averaging is used, $K > 5$ seconds and the maximum scan rate is 0.000125 second/second. Hence, the minimum analysis time is 8000 seconds or about 134 minutes.

3. POWER SPECTRAL DENSITY ANALYSIS

Given a sample vibration response record in the form of an analog voltage signal $y(t)$ with a finite length of T seconds, the power spectral density function for the vibration response may be estimated from equation (12) as follows:

$$\hat{G}_y(f) = \frac{\overline{y^2}_B}{B} \quad . \quad (36)$$

Here, $\overline{y^2}_B$ is the average of the squared instantaneous signal amplitude (mean square value) in a narrow frequency interval having a noise bandwidth of B Hz and a center frequency of f Hz. The hat (\wedge) over $\hat{G}_y(f)$ means that the measured quantity is only an estimate of $G_y(f)$, since the record length T and the bandwidth B are finite. The power spectral density function is estimated by the following operations:

- a. Frequency filtering of the signal by a narrow bandpass filter having a bandwidth of B Hz.
- b. Squaring of the instantaneous amplitude of the filtered signal.
- c. Averaging the squared instantaneous amplitude over the sampling time.
- d. Division of the mean square output by the bandwidth B .

As the center frequency of the bandpass filter is moved, a plot of the power spectral density function versus frequency is obtained. This plot is often called the power spectrum.

The above operations are accomplished by an analog power spectral density analyzer, which will be called a PSD analyzer for simplicity. It is important to note the similarity between the PSD analyzer and a simple spectrum analyzer used for periodic data analysis, as discussed in Section VIII. C. Since the division by the bandwidth B is only a matter of proper scale calibration, the PSD analyzer is nothing more than a spectrum analyzer with a mean square amplitude detection circuit. Thus a PSD analyzer may be used to analyze periodic vibration data as well as random vibration data. However, a simple spectrum analyzer may not be used to analyze random vibration data unless a mean square amplitude detection circuit is available. A peak amplitude detection circuit would obviously produce meaningless results, since a random signal has no specific peak amplitude. An average amplitude detection circuit would produce results that have no real analytical meaning, although the average value of a random signal can be related to the mean square value if the probability density function for the random signal is known. These matters are discussed further in Section VIII. F.

Similar to the spectrum analyzers discussed in Section VIII. C., a PSD analyzer may be either a multiple filter type analyzer employing a bank of contiguous filters, or a single filter type analyzer. A functional block diagram for a single filter type PSD analyzer is shown in Figure 49.

The practical considerations associated with power spectral density analysis are reviewed below. All relationships stated are taken from Reference 20. Many of the relationships are also studied experimentally in Reference 21.

a. Analysis Accuracy

As discussed in Paragraph D.1.a. of this section, the analysis of random vibration data involves not only basic measurement errors, but also a statistical uncertainty inherent in the sampling procedures. This uncertainty may be defined in terms of the standard error e for the sampling distribution. For the specific case of power spectral density analysis, the standard error associated with a measured estimate $\hat{G}_y(f)$ is as follows:

$$e = \frac{1}{\sqrt{BT}} \quad . \quad (37)$$

Here, B is the bandwidth of the PSD analyzer filter in Hz, and T is the length of the analyzed sample record in seconds.

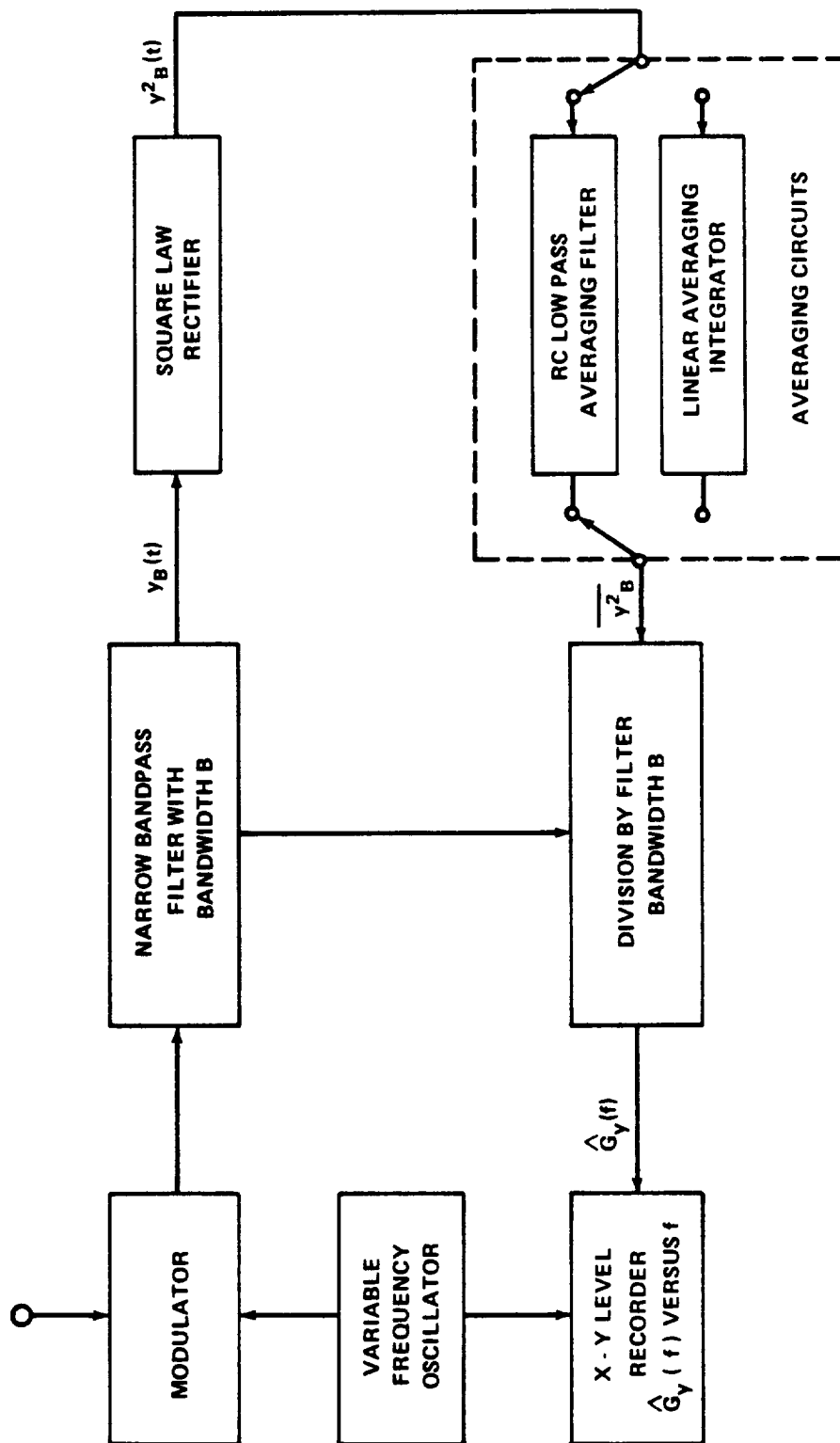


Figure 49. Functional block diagram for power spectral density analyzer.

Note that the uncertainty expression for a power spectral density analysis is similar to the uncertainty expression for an autocorrelation analysis, as given in equation (31). However the interpretation of the bandwidth B in the two expressions is slightly different. For a power spectral density analysis, B is the bandwidth for that portion of the signal spectrum within the frequency range of the PSD analyzer bandpass filter, which is approximately equal to the noise bandwidth of the analyzer filter for a properly resolved power spectral density analysis. The determination of noise bandwidths for filters is discussed in Paragraph E. of this section. For the narrow bandpass filter in most PSD analyzers, the noise bandwidth may be considered equivalent to the half power point bandwidth of the filter.

The general meaning and interpretation of the standard error e is discussed in Paragraph D. 4.a. of this section. The specific interpretation for power spectral density analysis is as follows. Assume a stationary random vibration response with a true power spectral density function of $G_y(f)$ is sampled, and an estimate $\hat{G}_y(f)$ is measured from the sample. If e is relatively small, say less than 0.30, it may be said with about 68 percent confidence that the true value $G_y(f)$ is within the range $(1 \pm e) \hat{G}_y(f)$. A plot of the standard error e versus the BT product is presented in Figure 48.

For example, assume that a power spectral density function is measured from a sample record that is $T = 10$ seconds long using a PSD analyzer with a filter bandwidth of $B = 10$ Hz. The standard error for the resulting estimate is $e \approx 0.10$. Hence, if a measured estimate $\hat{G}_y(f)$ at a given frequency were $0.3 \text{ volt}^2/\text{Hz}$, it could be said with 68 percent confidence that the true power spectral density function for that frequency is within ± 10 percent of the measured value, or between 0.27 and $0.33 \text{ volt}^2/\text{Hz}$.

b. Resolution

Equation (37) shows that the statistical uncertainty of power spectral density estimates is inversely proportional to the bandwidth of the analyzer filter. One might then conclude that improved estimation accuracy can easily be obtained by simply increasing the filter bandwidth. However, increasing the filter bandwidth reduces the resolution of the analysis; that is, it reduces the ability of the analysis to properly define sharp peaks in the power spectrum. The selection of the analyzer filter bandwidth is always a compromise between estimation uncertainty and spectral resolution. It should be further

noted that if there are sharp peaks within the filter bandwidth, the resulting uncertainty will actually be greater than predicted by equation (37). Hence, the emphasis should be placed upon an analyzer bandwidth which will afford proper resolution. A reasonable criteria for proper resolution is a filter bandwidth that is one-fourth the bandwidth (between half power points) of the narrowest peak in the power spectrum; that is,

$$B < \frac{1}{4} (f_2 - f_1) \quad (38)$$

where B is the analyzer filter bandwidth in cps and $(f_2 - f_1)$ is the bandwidth between the half power points of a power spectral density peak in Hz.

c. Sample Record Length

As equation (37) shows, the sample record length T limits the statistical accuracy attainable in a power spectral density analysis. The longer the record length, the lower the uncertainty in the resulting power spectral density estimates. If the statistical uncertainty of a power spectral density analysis is to be limited to a given desired amount, these matters must be considered before the data are gathered to assure that sample records are sufficiently long.

d. Averaging Time

The mean square amplitude detector incorporated in the PSD analyzer computes a mean square value by averaging the instantaneous output of a square law rectifier. The averaging may be accomplished either by true linear integration, called true averaging, or by continuous smoothing with an equivalent low-pass RC filter, called RC averaging. PSD analyzers are usually equipped with both types of averaging circuits. True averaging produces a single power spectral density estimate after a specific averaging time interval T_a , while RC averaging produces a continuous power spectral density estimate.

For the reasons presented earlier, the general criterion for the ideal averaging time for a power spectral density analysis is

$$\text{for true averaging, } T_a = T \quad (39a)$$

$$\text{for RC averaging, } 2K \leq T \quad (39b)$$

Here, T_a is the true integrating time in seconds, and K is the time constant of the equivalent RC averaging filter in seconds.

e. Scan Rate and Analysis Time

For the multiple filter type PSD analyzer, the power spectral density is concurrently measured over all frequencies of interest, so the analysis time is equal to the record length T. However, for the single filter type analyzer, the power spectral density at all frequencies of interest must be measured by scanning through the desired frequency range. If the scan is too fast, one of three difficulties may occur:

1. The statistical uncertainty of the resulting estimate will be increased because all the information available at a given frequency will not be viewed by the analyzer filter over the entire record length.
2. The narrow bandpass filter of the PSD analyzer will not fully respond to a sharp peak in the power spectrum of the signal.
3. If RC averaging is used by the amplitude detector, the averaging filter will not fully respond to sharp peaks in the power spectrum of the signal.

The limitations imposed upon the scan rate by the above mentioned considerations are as follow:

$$\text{for true averaging, scan rate} < \left| \begin{array}{l} \frac{B}{T_a} \\ \frac{B^2}{8} \end{array} \right| \quad \begin{array}{l} (40a) \\ (40b) \end{array}$$

$$\text{for RC averaging, scan rate} < \left| \begin{array}{l} \frac{B}{4K} \\ \frac{B^2}{8} \end{array} \right| \quad \begin{array}{l} (40c) \\ (40d) \end{array}$$

Here, T_a is the averaging time in seconds, K is the RC time constant in seconds, and B is the bandwidth of the PSD analyzer in Hz. Hence, scan rate has the units of Hz per second.

If the total frequency range for the PSD analysis is F Hz, the minimum analysis time is as follows:

$$\text{for true averaging, analysis time} > \left| \begin{array}{l} \frac{FT_a}{B} \\ \frac{8F}{B^2} \end{array} \right. \quad \begin{array}{l} (41a) \\ (41b) \end{array}$$

$$\text{for RC averaging, analysis time} > \left| \begin{array}{l} \frac{4FK}{B} \\ \frac{8F}{B^2} \end{array} \right. \quad \begin{array}{l} (41c) \\ (41d) \end{array}$$

For example, assume the power spectral density function for a random vibration response is to be estimated from a sample record of length $T = 10$ seconds over a frequency range from near 0 to 2000 Hz ($F = 2000$ Hz) using a PSD analyzer filter bandwidth of $B = 10$ Hz. If true averaging is used, $T_a = 10$ seconds and the maximum scan rate is 1 Hz/second, since equation (40a) produces the smaller value. Hence, the minimum analysis time is 2000 seconds or about 33 minutes, since equation (41a) produces the larger value. If RC averaging is used, $K > 5$ seconds and the maximum scan rate is 0.5 Hz/second, since equation (40c) produces the smaller value. Hence, the minimum analysis time is 4000 seconds or about one hour and seven minutes, since equation (41c) produces the larger value.

4. JOINT AMPLITUDE PROBABILITY DENSITY ANALYSIS

Given two sample vibration response records in the form of analog voltage signals $x(t)$ and $y(t)$, each with a finite length of T seconds, the joint amplitude probability density function for the two vibration responses may be estimated from equation (13) as follows:

$$\hat{p}(x, y) = \frac{\overline{t_{W_x} ; t_{W_y}}}{W_x W_y} \quad (42)$$

Here, $\overline{t_{W_x} ; t_{W_y}}$ is the average time spent by the signals $x(t)$ and $y(t)$ while they are simultaneously within the narrow amplitude intervals having gate widths

of W_x and W_y volts and center amplitudes of x and y volts, respectively. The hat ($\hat{}$) over $\hat{p}(x, y)$ means that the measured quantity is only an estimate of $p(x, y)$, since the record length T and the gate widths W_x and W_y are finite. In words, the joint amplitude probability density function is estimated by the following operations:

- a. Individual amplitude filtering of the two signals $x(t)$ and $y(t)$ by narrow amplitude gates having widths of W_x and W_y volts, respectively.
- b. Measurement of the total joint time spent by the two signals while they are simultaneously within the gates.
- c. Division of the total joint time spent within the gates by the total sampling time, to obtain the average portion of time spent by the two signals while they are simultaneously within the gates.
- d. Division of the average portion of time spent within the gates by the product of the gate widths $W_x W_y$.

As the center amplitude of each gate is moved, a three dimensional plot of the joint probability density function versus amplitudes x and y is obtained.

The above operations are accomplished by an analog joint amplitude probability density analyzer, which will be called a joint APD analyzer for simplicity. In general, a joint APD analyzer consists of two simple APD analyzers as discussed in Paragraph D., except the voltage gates in the two analyzers are followed by a single common clock circuit. When the input signal amplitude from one sample record falls within the first analyzer gate while the input signal amplitude from a second sample record simultaneously falls within the second analyzer gate, the clock circuit operates. For all other amplitude combinations, the clock circuit does not operate. As for the simple APD analyzer, the joint APD analyzer may incorporate either multiple pairs of gates or a single pair of gates. A functional block diagram for a single gate pair type joint APD analyzer is shown in Figure 50.

The practical considerations associated with joint amplitude probability density analysis are reviewed below. All relationships stated are based upon material in Reference 20.

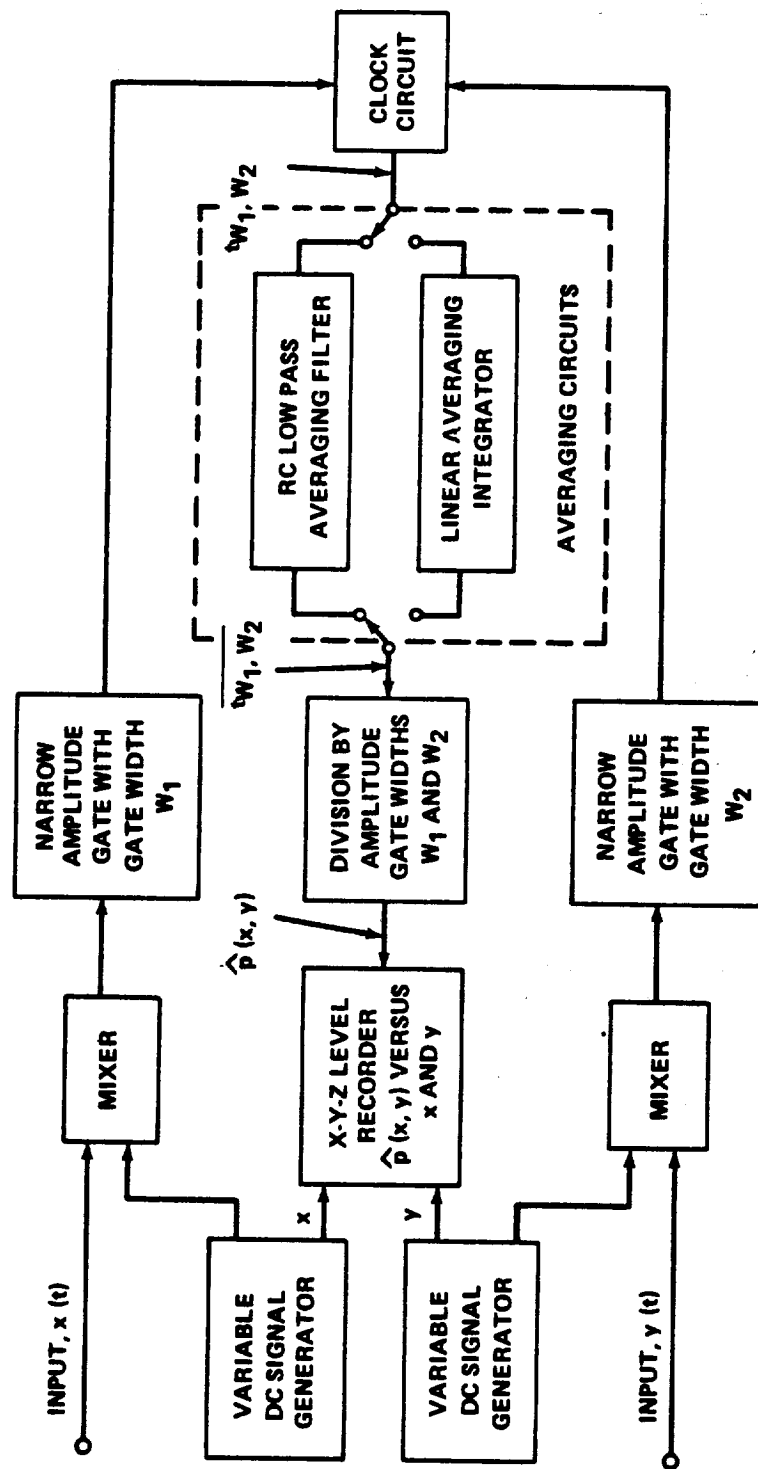


Figure 50. Functional block diagram for joint amplitude probability density analyzer.

a. Analysis Accuracy

The measurement of joint amplitude probability density functions involves a statistical uncertainty just as does the measurement of simple amplitude probability density functions discussed in Paragraph D.1.a. of this section. However, this uncertainty in terms of the standard error e has not been completely evaluated for the case of joint probability density functions. It can only be said that the standard error will be much greater for joint probability density measurement than for simple probability density measurements, given similar signal bandwidths and record lengths.

b. Resolution

c. Sample Record Length

d. Averaging Time

The considerations associated with these three factors are exactly the same as for simple probability density measurements discussed in Paragraphs D.1.a., b., and c.

e. Scan Rate and Analysis Time

The general limitations imposed upon the scan rates for joint probability density analysis are exactly the same as for simple probability density analysis discussed in Paragraph D.1.d. of this section. However, there are two signals whose amplitude ranges must be scanned for a joint probability density analysis. In effect, this means that the gate for signal $x(t)$ must be scanned through the entire amplitude range of interest for $x(t)$, with the gate for signal $y(t)$ fixed at each of the numerous positions required to cover the entire amplitude range of interest for $y(t)$. If the total amplitude range of interest for $x(t)$ and $y(t)$ is A_x and A_y volts, respectively, the minimum analysis time is as follows:

$$\text{for true averaging, analysis time} > \frac{T_a A_x A_y}{W_x W_y} \quad (43a)$$

$$\text{for RC averaging, analysis time} > \frac{4KA_x A_y}{W_x W_y} \quad (43b)$$

Here, T_a is the averaging time in seconds, K is the RC time constant in seconds, and W_x and W_y are the gate widths in volts.

For example, assume that the joint amplitude probability density function for two random vibration responses is to be estimated from two sample records, each of length $T = 10$ seconds, over an amplitude range from minus 4 volts to plus 4 volts ($A_x = A_y = 8$ volts) using a joint APD analyzer with gate widths of $W_x = W_y = 0.1$ volt. The rms amplitude of both signals is assumed to be 1 volt. If true averaging is used, $T_a = 10$ seconds and the maximum scan rate for A_x is 0.01 volt/second for each position of A_y . Hence, the minimum analysis time is 64 000 seconds or 17.8 hours. If RC averaging is used, $K \geq 5$ seconds and the maximum scan rate for A_x is 0.005 volt/second for each position of A_y . Hence, the minimum analysis time is 128 000 seconds or 35.6 hours. These results should be compared with the example following equation (29).

5. CROSS-CORRELATION ANALYSIS

Given two sample vibration response records in the form of analog voltage signals $x(t)$ and $y(t)$, each with a finite length of T seconds, the cross-correlation function for the two vibration responses may be estimated from equation (44) as follows:

$$\hat{R}_{xy}(\tau) = \overline{x(t) y(t + \tau)} = \frac{1}{T} \int_0^T x(t) y(t + \tau) dt \quad (44)$$

Here, $\overline{x(t) y(t + \tau)}$ is the time average cross product of the instantaneous amplitude of the two signals when one signal is displaced in time from the other by τ seconds. The hat (\wedge) over $\hat{R}_{xy}(\tau)$ means that the measured quantity is only an estimate of $R_{xy}(\tau)$, since the record length T is finite. In words, the cross-correlation function is estimated by the following operations:

- a. Delaying the signal $x(t)$ relative to the signal $y(t)$ by a time displacement equal to τ seconds, called the lag time.
- b. Multiplying the amplitude $y(t)$ at any instant by the amplitude $x(t)$ that had occurred τ seconds before.

c. Averaging the instantaneous amplitude product over the sampling time.

As the lag time is moved, a plot of the cross-correlation function versus lag time is obtained.

The above operations are accomplished by an analog cross-correlation function analyzer, which will be called a CCF analyzer for simplicity. In general, a CCF analyzer is exactly the same as the ACF analyzer discussed in Paragraph D.2 of this section, except the direct input to the multiplier and the input to the lag time generator are independent. A functional block diagram for a CCF analyzer is shown in Figure 51.

The practical considerations associated with cross-correlation analysis are reviewed below. All relationships stated are based upon material in Reference 20.

a. Analysis Accuracy

The measurement of cross-correlation functions involves a statistical uncertainty just as does the measurement of autocorrelation functions discussed in Paragraph D.2.a. of this section. For the special case where the two signals being studied have the same bandwidth B , the uncertainty in terms of the standard error e is exactly the same for cross-correlation analysis, given by equation (31). The standard error for cross-correlation measurements has not been completely evaluated for other cases.

b. Resolution

c. Sample Record Length

d. Averaging Time

e. Scan Rate and Analysis Time

The considerations associated with these four factors are exactly the same as for autocorrelation measurements discussed in Paragraphs D.2.b., c., d., and e. of this section.

6. CROSS-POWER SPECTRAL DENSITY ANALYSIS

Given two sample vibration response records in the form of analog voltage signals $x(t)$ and $y(t)$, each with a finite length of T seconds, the cross-power spectral density function for the two vibration responses may be estimated from equation (15) as follows:

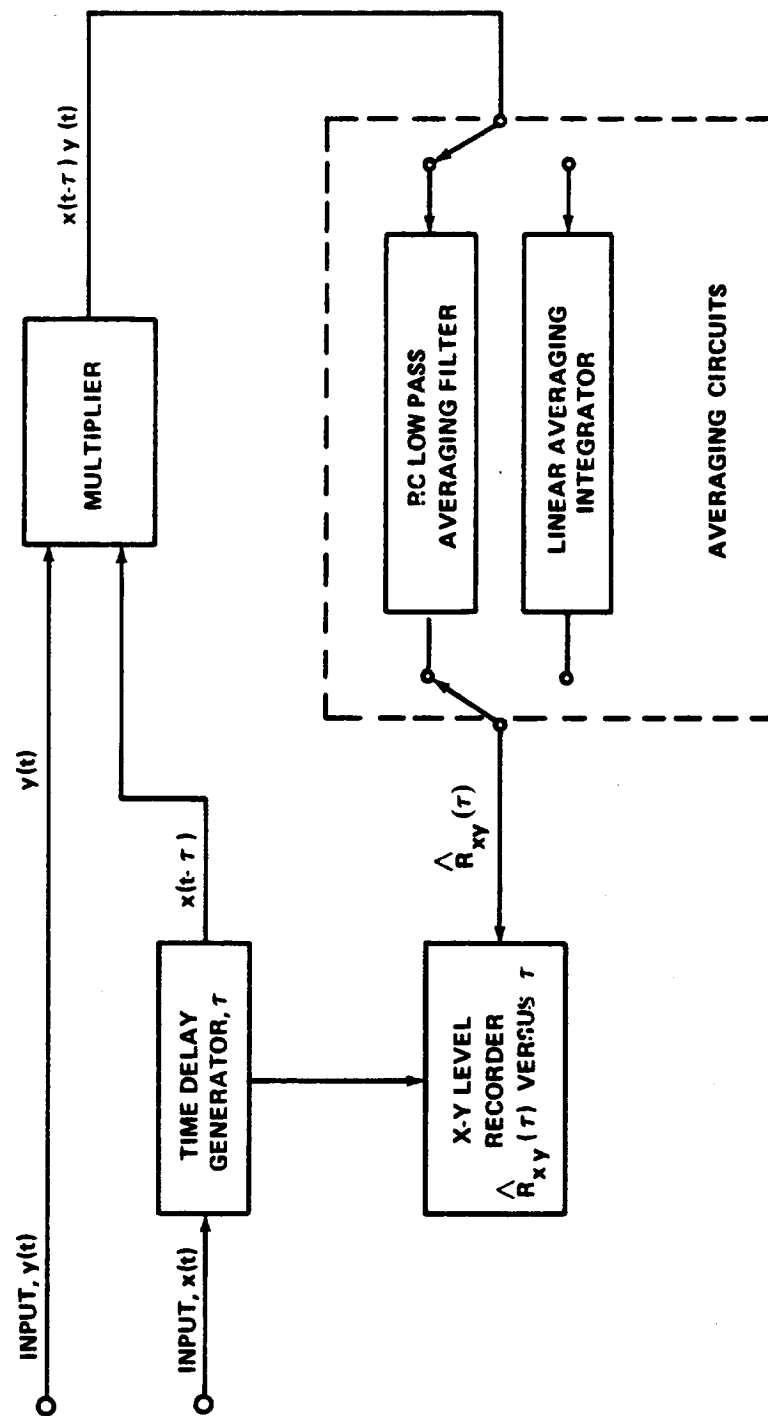


Figure 51. Functional block diagram for cross-correlation analyzer.

$$\hat{G}_{xy}(f) = \hat{C}_{xy}(f) - j\hat{Q}_{xy}(f) \quad (45)$$

$$\hat{C}_{xy}(f) = \frac{\overline{x_B^y B}}{B} \quad (45a)$$

$$\hat{Q}_{xy}(f) = \frac{\overline{\text{VVV} x_B^y B}}{B} \quad (45b)$$

Here, $\overline{x_B^y B}$ is the average product of the instantaneous amplitudes of the two signals, each within a narrow frequency interval having a noise bandwidth of B Hz and a center frequency of f Hz. The symbol (VVV) in equation (45b) means that x(t) is 90 degrees out of phase with y(t). The hat (^) over $\hat{G}_{xy}(f)$ means that the measured quantity is only an estimate of $G_{xy}(f)$, since the record length T and the bandwidth B are finite. The cross-power spectral density function is estimated by the following operations:

- a. Individual frequency filtering of the two signals x(t) and y(t) by narrow bandpass filters having similar bandwidths of B Hz and the same center frequency at any one time.
- b. Multiplying the instantaneous amplitudes of the two filtered signals with no phase shift.
- c. Multiplying the instantaneous amplitudes of the two filtered signals with one shifted 90 degrees out of phase with the other.
- d. Averaging each of the two instantaneous amplitude products over the sampling time.
- e. Division of each of the two mean products by the bandwidth B.

As the center frequency of the two bandpass filters is moved, a plot of the real and imaginary parts of the cross-power spectral density function versus frequency is obtained. This plot is often called the cross-power spectrum.

The above operations are accomplished by an analog cross-power spectral density analyzer, which will be called a cross PSD analyzer for

simplicity. In general, a cross PSD analyzer consists of two simple PSD analyzers as discussed in Paragraph D.1. of this section, except that multipliers replace the squaring circuits and a 90 degree phase shift circuit is added. The narrow bandpass filters in the two component analyzers must be well matched to prevent unwanted phase shifts. As for the simple PSD analyzer, the cross PSD analyzer may incorporate either multiple pairs of filters or a single pair of filters. However, multiple filter pair type analyzers are uncommon because of the high cost and difficulty in matching filters. A functional block diagram for a single filter pair type cross PSD analyzer is shown in Figure 52.

The practical considerations associated with cross-power spectral density analysis are reviewed below. All relationships stated are based upon material in Reference 10.

a. Analysis Accuracy

The measurement of cross-power spectral density functions involves a statistical uncertainty just as does the measurement of power spectral density functions discussed in Paragraph D.3.a. of this section. Furthermore, the individual standard errors associated with the measurement of the real and imaginary parts for a cross-power spectral density function are approximately the same as the standard error for an ordinary power spectral density measurement, as given by equation (37).

b. Resolution

c. Sample Record Length

d. Averaging Time

e. Scan Rate and Analysis Time

The considerations associated with these four factors are exactly the same as for power spectral density measurements discussed in Paragraphs D.3.b., c., d., and e. of this section.

E. Determination of Noise Bandwidth

From Section VIII.D, the estimation of ordinary and cross-power spectra is a function of the noise bandwidth for the analyzer filter. The concept of noise bandwidth is usually associated with the characteristics of filters.

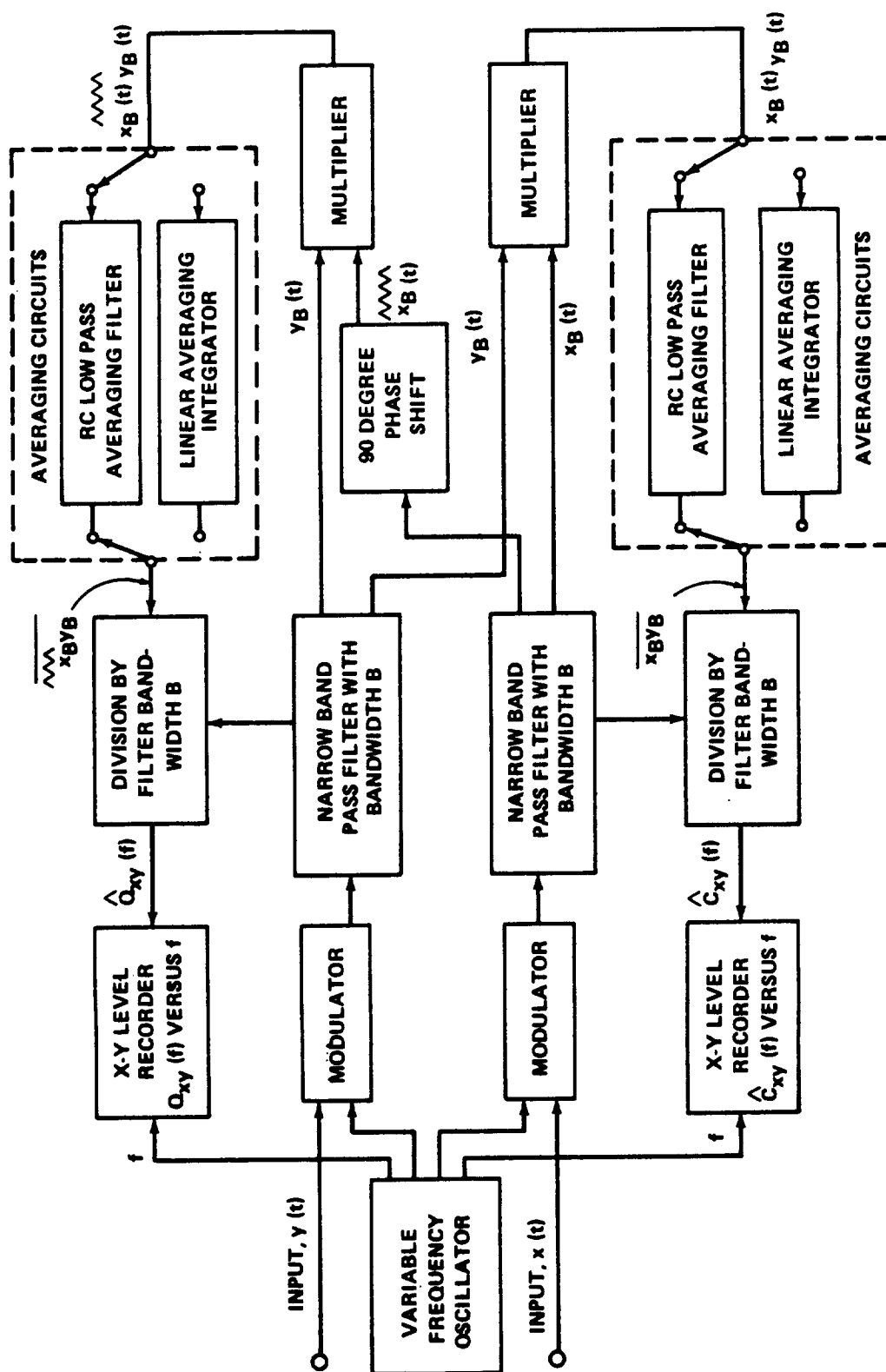


Figure 52. Functional block diagram for cross-power spectral density analyzer.

However, the noise bandwidth concept may also be applied directly to random vibration on response signals.

1. NOISE BANDWIDTH OF FILTERS

Given any real linear filter, the noise bandwidth is defined as that bandwidth of an ideal rectangular filter which would pass the same amount of signal power as the real filter when the input is white noise (a random signal with a uniform power spectrum over all frequencies). If the real linear filter has a complex frequency response function of $H(f)$, the noise bandwidth of the filter is defined mathematically as follows:

$$B = \frac{1}{|H_m|^2} \int_0^{\infty} |H(f)|^2 df \quad (46)$$

Here, $|H(f)|$ is the magnitude of the frequency response function at any frequency f , which is often called the magnitude response function. The term $|H_m|$ is the peak value of the magnitude response function.

For example, assume a filter consists of a single-tuned resonant circuit with a half power point bandwidth of $B_{hp} = 2a$ which is small compared to the filter center frequency f_c . This is effectively a narrow bandpass filter with a cutoff characteristic of 6 dB per octave. The magnitude response function for this filter is given by

$$|H(f)| = \left[\frac{a^2}{a^2 + (f - f_c)^2} + \frac{a^2}{a^2 + (f + f_c)^2} \right]^{1/2} \quad (47)$$

Note that the peak value of $H(f)$ occurs when $f = f_c$ and is approximately equal to unity, as shown below.

$$|H_m| \approx |H(f_c)| = \left[1 + \frac{a^2}{a^2 + 4f_c^2} \right]^{1/2} \approx 1 \text{ if } a \ll f_c \quad (48)$$

Here, the noise bandwidth is given as follows:

$$B = \int_0^{\infty} \left[\frac{a^2}{a^2 + (f + f_c)^2} + \frac{a^2}{a^2 + (f - f_c)^2} \right] df = \pi a \quad . \quad (49)$$

Since the half power point bandwidth is $B_{hp} = 2a$, the relationship between the noise bandwidth and the half power point bandwidth is

$$B = \frac{\pi}{2} B_{hp} \quad . \quad (50)$$

The meaning of equation (50) is as follows. If a white noise input is applied to a single-tuned filter with a half power point bandwidth of B_{hp} Hz, the mean square value of the filter output will be exactly the same as if the filter had an ideal rectangular characteristic with a bandwidth of B Hz as given in equation (50). The importance of the noise bandwidth concept should now be clear. It is a method for reducing any real filter to an equivalent ideal filter with infinitely sharp cutoff characteristics.

The above example illustrates how noise bandwidths may be mathematically determined. However, it is very rare in actual practice to have an explicit equation for the magnitude response function of filters which are being used. Furthermore, the magnitude response function for the bandpass filters used in vibration analysis equipment is often a complicated expression which would make the required integration in equation (46) difficult to accomplish. Fortunately, there are straightforward empirical techniques for measuring the noise bandwidth of real filters which will now be discussed.

2. NOISE BANDWIDTH CALIBRATION PROCEDURE

The noise bandwidth of a filter can be experimentally determined using an oscillator (sine wave signal generator) and a voltmeter, as follows. Apply a sine wave with a known voltage and frequency to the filter, and measure the filter output voltage. The ratio of the output voltage to the input voltage defines the magnitude response function at that frequency; that is,

$$\frac{|Y(f)|}{|X(f)|} = |H(f)| \quad (51)$$

where $|X(f)|$ is the magnitude of the input voltage and $|Y(f)|$ is the magnitude of the output voltage at frequency f . Note that the voltage measurements may be in terms of peak, average, or rms values. It makes no difference as long

as the measurements are consistent. When each measurement in equation (51) is squared, a set of values for $|H(f)|^2$ at various frequencies is obtained. The magnitude response should be measured at a sufficient number of frequencies to permit an accurate plot of $|H(f)|^2$ versus f . The area under this plot, divided by the peak value of the plot, is equal to the noise bandwidth.

For the case when a filter is incorporated in a PSD analyzer, the values for $|H(f)|^2$ at various frequencies can be measured directly by using the mean square value detection circuit in the PSD analyzer. The ratio of the mean square output from the PSD analyzer to the mean square value of the input signal is equal to the square of the magnitude response function; that is,

$$\frac{\overline{y^2(f)}}{\overline{x^2(f)}} = |H(f)|^2 \quad . \quad (52)$$

The following example is based upon an actual noise bandwidth calibration for a multiple filter type PSD analyzer. The filter which was calibrated has a nominal bandwidth of 10 Hz with a center frequency of 35 Hz. The mean square output from the PSD analyzer was measured when a sinusoidal signal was applied to the filter of interest with a constant amplitude and at various frequencies about 1 Hz apart. A block diagram for the calibration test set-up is shown in Figure 53. The resulting plot of $|H(f)|^2$ versus f , as well as the associated plot of $|H(f)|$ versus f , is shown in Figure 54. Note that the plots are displayed on a log-log scale because the skirts of a filter will characteristically appear as straight lines in such a display. This type of display is desirable since it is clearly easier to fit empirical data with straight lines than with curves, as would be required if the plots were displayed on a rectilinear scale.

The plot of $|H(f)|^2$ versus f in Figure 54 has already been properly normalized so that the maximum value is equal to unity; that is, $|H_m| = 1$.

Hence, the noise bandwidth is given directly by the area under the plot. The area under the plot may be determined by noting the value of $|H(f)|^2$ at various frequencies separated by an increment Δf , determining the product $\Delta f |H(f)|^2$ at each frequency noted, and computing the sum of these products. For the plot presented in Figure 54, if the value of $|H(f)|^2$ is noted at frequencies from 24 to 49 Hz in 1-Hz increments, the following results are obtained.

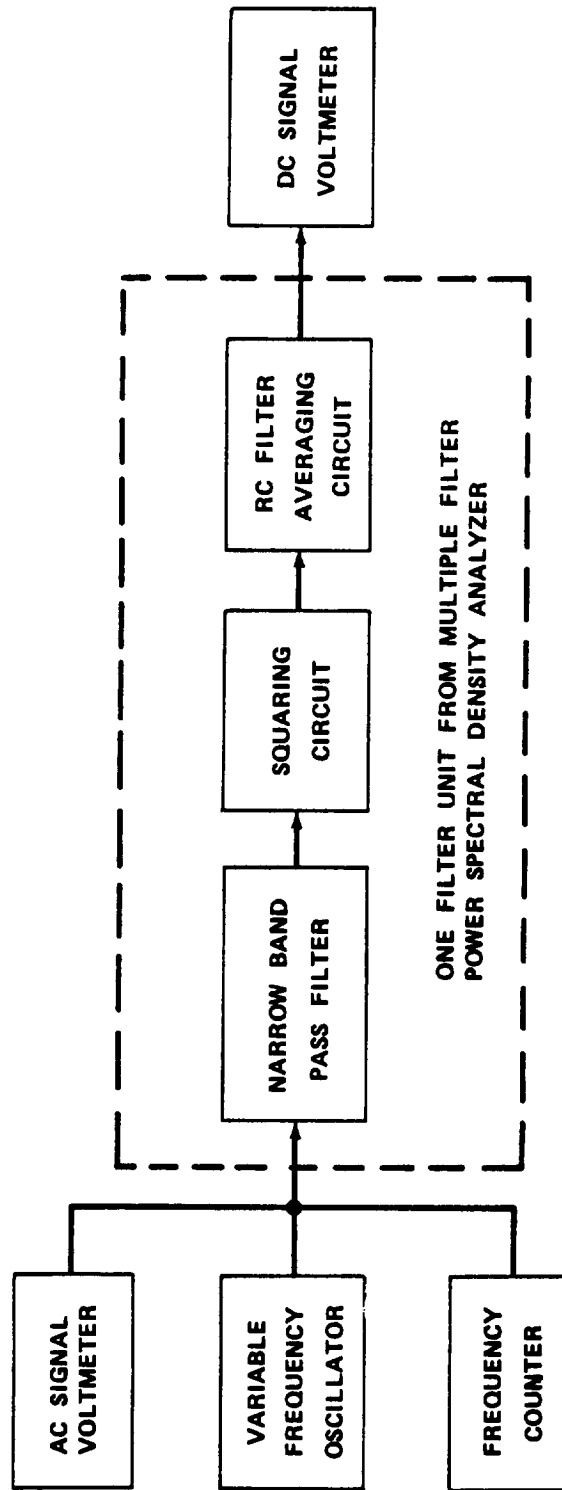


Figure 53. Test setup for filter noise bandwidth calibration.

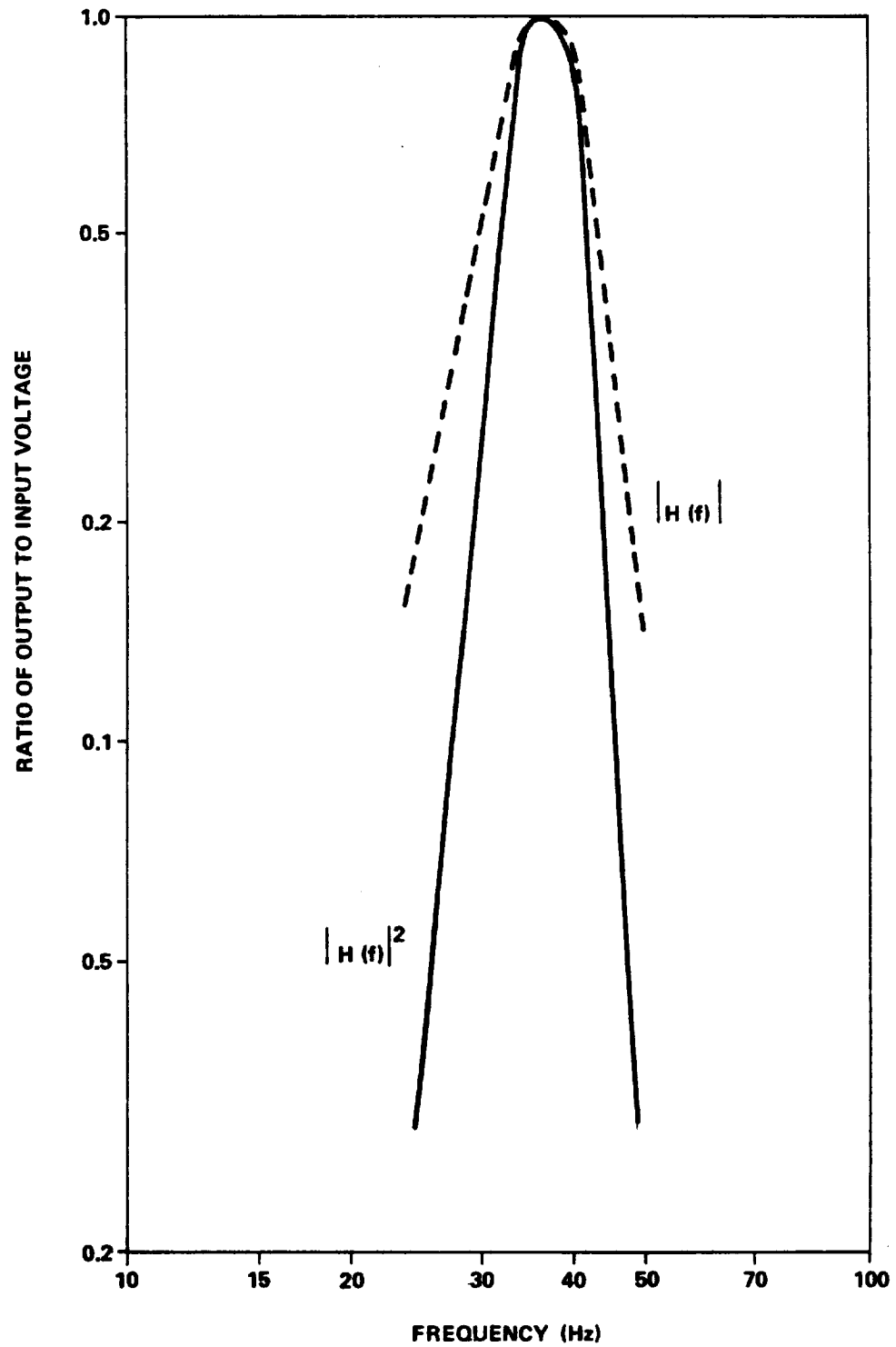


Figure 54. Magnitude response function for bandpass filter.

f	$ H(f) ^2$	Δf	$\Delta f H(f) ^2$	f	$ H(f) ^2$	Δf	$\Delta f H(f) ^2$
25	0.039	1.00	0.039	37	0.99	1.00	0.99
26	0.056		0.056	38	0.96		0.96
27	0.084		0.084	39	0.93		0.93
28	0.12		0.12	40	0.87		0.87
29	0.17		0.17	41	0.74		0.74
30	0.24		0.24	42	0.57		0.57
31	0.34		0.34	43	0.36		0.36
32	0.46		0.46	44	0.22		0.22
33	0.63		0.63	45	0.14		0.14
34	0.80		0.80	46	0.095		0.095
35	0.97		0.97	47	0.058		0.058
36	1.00		1.00	48	0.040		0.040
				49	0.030		0.030
				Total			10.91

The noise bandwidth for the filter employed for the example is $B = 10.9$ Hz. Proper power spectral density measurements will be obtained with this filter by adjusting the bandwidth division resistor for the filter to be equivalent to 10.9 Hz.

The half power points of the filter were also determined during the calibration by noting the frequencies where the value of $|H(f)|^2$ was equal to 0.5. These frequencies were found to be 32.2 and 42.6 Hz. Thus, the half power point bandwidth of the filter is $B_{hp} = 10.4$ Hz. The ratio of the noise bandwidth to the half power point bandwidth is as follows:

$$\frac{B}{B_{hp}} = \frac{10.9}{10.4} = 1.05 \quad . \quad (53)$$

Furthermore, the cutoff rate for the filter is at least 30 dB per octave. These observations are consistent with two general characteristics of the noise bandwidth for bandpass filters, as follows:

- a. In most cases, the noise bandwidth for a bandpass filter is larger than the half power point bandwidth.

b. In most cases, if a bandpass filter has cutoffs of over 30 dB per octave the difference between the noise bandwidth and the half power point bandwidth is less than 5 percent. For such cases, it may be assumed that the noise bandwidth is equal to the half power point bandwidth.

3. ALTERNATE CALIBRATION PROCEDURE

There is another procedure for determining the noise bandwidth of bandpass filters which is simpler than the procedure detailed in Paragraph E.2. of this section, but usually less accurate. This procedure is to measure the mean square output of the filter when the input is a band limited white noise (uniform power spectrum) having a known power spectral density. If the input white noise has a uniform power spectral density of G , and the output has a mean square value of $\overline{y^2}$, the noise bandwidth for the filter is given by

$$B = \frac{\overline{y^2}}{G} \quad . \quad (54)$$

Many commercial random noise generators produce random signals with a reasonably uniform power spectrum, at least over certain frequency ranges. However, there is a problem in determining what the power spectral density for the noise generator signal is for a given output setting. Furthermore, the value $\overline{y^2}$ must be measured using long averaging times to minimize the statistical uncertainty of the measurements. In general, the white noise calibration procedure is not sufficiently accurate to be used as a primary calibration method. However, it is often helpful as a check on a more thorough calibration as detailed in Paragraph E.2. of this section.

4. NOISE BANDWIDTH OF RANDOM SIGNALS

Consider a stationary random vibration response $y(t)$ with a power spectral density function $G_y(f)$. Assume the input excitation $x(t)$ which produces the response has a power spectral density function $G_x(f)$. The following relationship is true:

$$G_y(f) = |H(f)|^2 G_x(f) \quad . \quad (55)$$

Here, $|H(f)|$ is the magnitude response function for the structure, which may be thought of as a mechanical filter. However, for the purposes of data reduction, the individual characteristics of $|H(f)|$ and $G_x(f)$ are of no concern.

For example, it may be assumed that the input $x(t)$ is white noise where $G_x(f) = \text{unity}$, and that the filter has a squared magnitude response function of $|H_1(f)|^2 = |H(f)|^2 G_x(f)$; that is,

$$G_y(f) = |H_1(f)|^2 = |H(f)|^2 G_x(f) \quad . \quad (56)$$

Hence, the response power spectrum is equivalent to the squared magnitude response function for a fictitious filter. It is this reasoning that permits the concept of noise bandwidth to be applied directly to random signals.

By substituting equation (56) into equation (46), the noise bandwidth for a stationary random vibration response $y(t)$ is given by

$$B = \frac{1}{G_m} \int_0^{\infty} G_y(f) df \quad (57)$$

where $G_y(f)$ is the power spectral density function of $y(t)$, and G_m is the maximum value of $G_y(f)$. From Paragraph B.2.c. of this section, it is seen that the integral in equation (56) is equal to the mean square value of $y(t)$. Hence, the following important relationship is obtained:

$$B = \frac{\overline{y^2}}{G_m} \quad . \quad (58)$$

The noise bandwidth of a random vibration response is equal to the mean square value of the vibration divided by the peak power spectral density of the vibration.

F. Practical Considerations for Power Spectra Measurements

Referring to Paragraph D.3. of this section, the measurement of power spectral density functions for random vibration data basically involves the measurement of mean square values in narrow frequency bandwidths, as noted in equation (36). The implication is that the measurement of rectified average values is not proper. In general, this is true. However, mean square values for random data can be obtained from average value measurements if the data are assumed to have a Gaussian (normal) probability density function.

Consider a random signal $y(t)$ with a Gaussian probability density function. The mean square value $\overline{y^2}$ and the rectified average value $\overline{|y|}$ are related as follows:

$$\overline{y^2} = \frac{\pi}{2} (\overline{|y|})^2 = 1.57 (\overline{|y|})^2 \quad . \quad (59)$$

In terms of the rms value,

$$y_{\text{rms}} = \sqrt{\overline{y^2}} = \sqrt{\frac{\pi}{2}} \overline{|y|} = 1.25 \overline{|y|} \quad . \quad (60)$$

From equation (19), the relationship between the rms value and rectified average value for a sine wave is as follows:

$$y_{\text{rms}} = \frac{\pi}{2\sqrt{2}} \overline{|y|} = 1.11 \overline{|y|} \quad . \quad (61)$$

Hence, for the conventional ac voltmeter which detects rectified average values but reads out in rms values for sine waves, the following relationship is true:

$$y_{\text{rms}} = \frac{2}{\sqrt{\pi}} I_{\text{rms}} = 1.13 I_{\text{rms}} \quad . \quad (62)$$

Here, y_{rms} is the true rms level of the random Gaussian signal and I_{rms} is the indicated rms level on the voltmeter scale.

Now consider these associations in terms of power spectral density measurements. Assume a spectral analysis of random vibration data is performed using a PSD analyzer with a rectified average value detection circuit. If the assumption is that the data has a Gaussian probability density function, the mean square value of the data within any narrow bandwidth B is given from equation (59) as follows:

$$\overline{y_B^2} = \frac{\pi}{2} (\overline{|y|_B})^2 \quad . \quad (63)$$

Hence, the power spectral density function at any center frequency f may be estimated from equation (36) as follows:

$$G_y(f) = \frac{\pi}{2B} \overline{(|y|_B)^2} \quad . \quad (64)$$

For a constant bandwidth analysis, the coefficient $\pi/(2B)$ is simply a calibration constant. The required square of the rectified average value $|\bar{y}|$ may be obtained by an appropriate readout scale calibration. In fact, if the analyzer output is passed through a logarithmic converter, the squaring may be accomplished by a proper adjustment of the readout sensitivity.

The only problem with the above procedure is that the Gaussian assumption must be reasonably valid. As the data deviate from the ideal Gaussian form, the ratio of the rms to average value changes and the conversion factor in equation (64) becomes inaccurate. However, the resulting error may not be significant as compared to the statistical uncertainties in the analyzed data. These matters have been considered by many investigators in the past. The general consensus of opinion is that a mean square value measurement capability is not a compelling necessity, but is still very desirable because it does eliminate a possible error from the analysis procedure and simplifies the calibration.

For academic interest, one additional point should be made on this subject. Strong deviations from a Gaussian probability density function in random vibration data are usually associated with nonlinear characteristics of the structure whose response is being measured. The type of deviation from the Gaussian form is a function of the nonlinear characteristic and the parameter being measured. For example, the probability density function for the acceleration response of a hardening spring type structure will tend to show large kurtosis (bunching around the mean value and thickening of the tails). However, the probability density function for the displacement response of the same structure will tend to show small kurtosis (spreading around the mean value and thinning of the tails). These matters are discussed in Section 9 of Reference 21. In any case, the severity of the nonlinear conditions and the resulting deviations of the response amplitudes from the Gaussian form will increase as the response amplitude increases. Hence, the most severe deviations from normality are to be expected at resonant frequencies where the response amplitudes are a maximum. These resonant points which appear as sharp peaks in the response power spectrum might then be expected to display the greatest deviation from the ideal Gaussian form.

However, there is another factor which tends to counteract the nonlinear effects discussed above. It can be shown that narrow bandwidth linear filtering of random signals tends to suppress deviations from the ideal Gaussian form.

In other words, the narrow bandpass filter in the power spectral density analyzer will tend to reduce non-Gaussian amplitude characteristics in the vibration data. However, this effect is only pronounced when the bandwidth of the input signal is wide relative to the bandwidth of the linear filter. For vibration data from a resonant structural response, the bandwidth of the data is quite narrow since it has already been filtered (a resonant structural mode is equivalent to a narrow bandwidth nonlinear filter). Hence, the bandwidth of the analyzer filter must be narrow compared to the bandwidth of the structural resonance before any benefits will be obtained.

G. Multiple Filter Analyzers

The usual wave analyzer employs a single filter which is progressively moved through the spectrum of interest. Time is consumed by this serial process, which can be largely avoided by a parallel process employing a large number of contiguous bandpass filters. With a large number of contiguous band filters each filter acts simultaneously with the others so that the filtering action is essentially done in real time. After filtering and squaring the input function, averaging is necessary, which does consume time. However, the precessive requirements on filtering are removed and this permits a very large time reduction. In practice the penalty imposed is the price of the equipment; the advantage gained is a reduction of analyzing time by an order of 100:1.

A typical multiple filter analyzer is shown in Figure 55. This is of the heterodyne type, which reduces certain problems in filter manufacture. The number of filters employed is of the order of fifty, which are graduated in bandwidth from about 10 to 100 Hz. The band covered is ordinarily 10 Hz to 2000 to 3000 Hz, but this may be extended by altering the frequency of the heterodyne oscillator, enabling a bandwidth of about 10 000 Hz to be obtained. One of the operations shown in Figure 55 is that of squaring and detecting. For some applications the squaring function may be deleted, in which case the output of the analyzer is the averaged absolute value of the spectrum of the function.

In Figure 55, a multichannel display is produced in which the energy in each individual filter is separately shown, producing n records. The usual display device is a multichannel galvanometer oscilloscope. Another type of display can be added to the ensemble of filter records described above. In this case the energy output from each filter channel is stored in its integrator for a preselected integration time, whereupon all channels are read out successively by a commutator and plotted on a graph. This results in a display of integrated

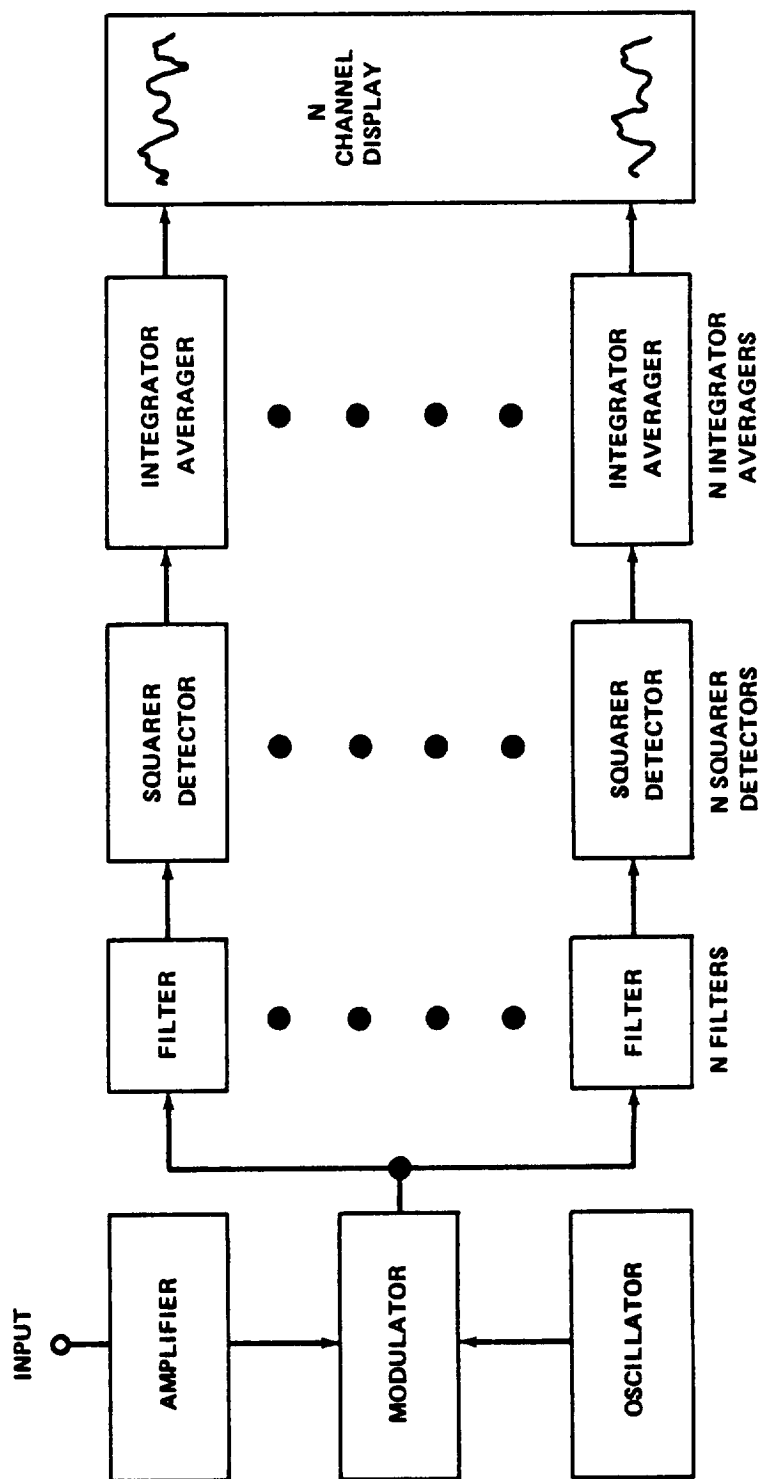


Figure 55. Multiple filter analyzer.

energy versus frequency over the spectrum of interest. The display device can be a conventional X-Y recorder, image storage oscilloscope, card punch, etc. In this manner, successive power spectral density plots may be obtained in intervals of 1 to 2 seconds, an advantage when the stationarity of the process under consideration is in question.

H. A Method of Calibrating a Swept Filter Analyzer or a Multiple Filter Analyzer for Power Spectral Density Analysis

The method of calibrating either a single channel swept filter system or a multiple filter analyzing system is very similar. It consists of the following steps:

1. Feed a calibration sine wave into the analyzer system. This sine wave will have an amplitude proportional to the amplitude of the quantity being measured.
2. Make sure that no bandwidth division is included in the filter system during this set-up time. Dividing a sine wave by the filter bandwidth is misleading and erroneous.
3. Connect the filter output to a suitable recording device. X-Y recorders or oscillograph recorders are acceptable.
4. Since the input sine wave signal, representing a known amplitude of the quantity being measured, was assigned a particular value ($2G$ rms, for instance) then the full-scale X-Y plotter reading would be the squared value of the input. In this case, since the input was $2G$ rms, the output full-scale becomes $4G^2$ (mean square) full-scale.
5. Remove the sine wave calibration signal and apply the random signal which is to be analyzed.
6. Place the bandwidth divisor switch in the circuit.
7. Step 6 has normalized the output so that the plotted amplitude is now in terms of G^2/Hz .

8. With the random signal to be analyzed applied to the input (by means of a type loop recorder-reproducer) the signal is continuously fed into the analyzer while the analyzing system sweeps across the frequency spectrum of interest.

9. The resultant graph is then a plot of power spectral density with the Y axis in terms of G^2/Hz and the X axis in terms of frequency.

These nine steps may be used to calibrate a swept filter system for the analysis of a random wave by using a sine wave of an assigned value for the calibration source. The following method is used to calibrate a multiple filter system for analysis of random waves. Again, a sine wave of an assigned value is used for calibration. Although the same principle is used, there is a slight difference in procedure. In the multiple filter system, the bandwidth divisors are connected at all times. However, one filter in the multiple filter system, usually the narrowest, will not have a bandwidth divisor. It is this filter channel, the one not containing a bandwidth divisor, that is used for the sine wave calibration.

A sine wave of an assigned value is fed to the multiple filter system. However, in this case, the sine wave must be at the frequency of the filter containing no bandwidth divisor. The output of this filter channel is connected to an appropriate recording device. Full-scale again is set up, as in step 4 above. The sine wave calibrating signal is removed and the random wave is connected to the multiple filter system. In the case of wide band white random noise, all filter outputs will be equal in amplitude. This is because all channels have been normalized by bandwidth division. The resulting plot (or in the case of an oscillograph, a multichannel plot) will give the G^2/Hz spectrum amplitude.

In most instances, a white random noise is not applied to the analyzer system; therefore, a flat or equal energy per Hz signal will not be obtained at the output. High peakd may occur which will drive the recorder off scale. In this case, a second analysis run may be necessary. When the data to be analyzed are completely unknown, the chance of driving the recording device over full-scale at some particular frequency is likely. When this does occur, the point at which the recording device is driven off scale is the point at which the system should be recalibrated. The initial calibration has not been wasted, it is merely a first look at the data to see where the peaks do occur and where the system should be calibrated. Some data survey is usually necessary before a final analysis can be made. In some instances, survey may not be required, since the data to be analyzed are known to be very similar to data previously analyzed.

SECTION IX. INTERPRETATION AND EVALUATION OF DATA

Section VIII discussed the general techniques for reducing vibration amplitude time history information into simplified descriptive data. This section is concerned with the proper interpretation and evaluation of the reduced data for applications to structural vibration problems. The desired method for evaluating vibration data is a direct function of the specific engineering problem to be studied. Each particular application usually requires a different emphasis in the interpretation of the data. However, there are certain basic procedures for interpreting and evaluating vibration data which are applicable to nearly all structural vibration problems.

Before measured vibration data can be intelligently interpreted and applied to any problem, it is necessary to know if the data are basically random in nature as opposed to being periodic. If vibration data are to be used for prediction purposes, it is necessary to investigate the time invariance (stationarity) of the data. It is also desirable to determine if the data measured at various different points on a structure or similar structures are equivalent.

In the area of direct engineering applications, the most basic and pertinent interpretations of vibration involve probability density and joint probability density functions, autocorrelation and cross-correlation functions, and power spectral density and cross-power spectral density functions.

Paragraphs A., B., and C. below discuss the procedures for evaluating the randomness, stationarity, and equivalence of vibration measurements. Specific engineering procedures are detailed with numerical examples. Paragraphs D., E., and F. discuss the interpretations and applications of probability density, correlation, and power spectral density functions for single and multiple vibration measurements. The interpretation of each function is illustrated by a numerical example involving a common engineering vibration problem.

A. Evaluation of Randomness

Random vibration is that type of time-varying motion which consists of randomly varying amplitudes and frequencies such that its behavior can be described only in statistical terms. No analytical representation for the vibratory motion is possible. The vibration does not repeat itself after

a finite time period. For all practical purposes, vibration may be considered random unless motion with a periodic form is present.

There are, of course, other types of vibratory motions that are neither random nor periodic. For example, the motion produced by the sum of two or more sine waves is not periodic unless the frequencies for the individual sine waves have a common multiple, as discussed in Section VIII.A.1. However, in actual practice, such a motion may be considered periodic with little error if the available data record is sufficiently long.

If vibration data are purely periodic, the fact is usually obvious by simple observation of an amplitude time history plot. However, when vibration data are a mixture of both random and periodic portions, this fact is often not obvious. There are several different techniques which may be used to detect the presence of periodic components in an otherwise random vibration response. Some of these techniques consist of qualitative inspections of the vibration properties which might be measured from sample records as a normal part of the random data reduction. Other techniques involve the application of a specific quantitative test to sampled data. These techniques will now be discussed.

1. QUALITATIVE TESTS FOR RANDOMNESS

The presence of periodic components in an otherwise random vibration response may often be detected by visual inspection of a power spectral density function, an amplitude probability density function, and/or an autocorrelation function measured from stationary sampled data.

To illustrate how a power spectrum can reveal the presence of a periodic component in an otherwise random signal, refer to Figure 56. In this example, the output of a random noise generator was mixed with a sinusoidal signal. The sinusoidal signal was given an rms amplitude equal to one-twentieth that of the random signal. Plot A which was made using a relatively wide filter gives little or no indication of the presence of the sinusoid. Plot B which was made using a medium filter indicates a possible sinusoid quite clearly. Plot C which was made using a narrow filter gives a strong indication.

Figure 56 illustrates how a highly resolved power spectrum will reveal periodic components as sharp peaks, even when the periodicities are of relatively small intensity. However, a sharp peak in the power spectrum for a vibration response may also represent the narrow band random response of a lightly

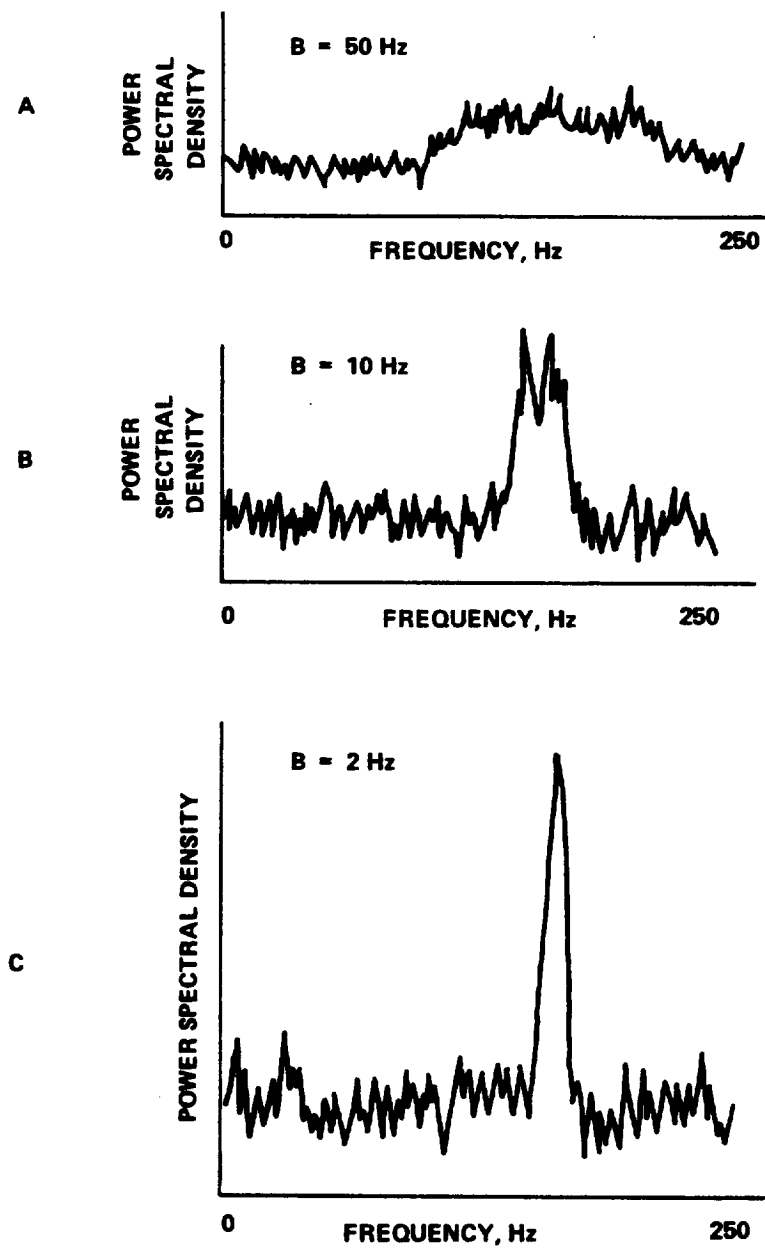


Figure 56. Actual power spectra plots.

damped structural resonance. These two cases can sometimes be distinguished from one another by repeating the power spectral measurement with the narrowest available PSD analyzer filter bandwidth. If the measured spectral peak represents a sine wave, the indicated bandwidth of the peak will always be equal to the bandwidth of the PSD analyzer filter, no matter how narrow the filter is. This method of detection will not work unless the bandwidth for the narrowest PSD analyzer filter is smaller than the bandwidth for a possible narrow band random response peak. For the case of spectral peaks with relatively low center frequencies, say less than 50 Hz, a structural resonance may have a bandwidth of less than 1 Hz, making it very difficult to distinguish from a sine wave.

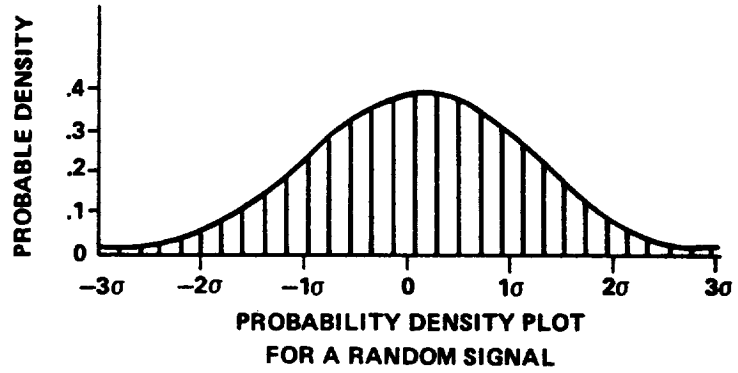
The presence of periodic components in an otherwise random vibration response may also be revealed by an amplitude probability density function for the response. The probability density plots for a sine wave and a random signal are markedly different. A random signal will usually have a probability density function which at least resembles the familiar bell-shaped Gaussian characteristic, while a sine wave has a dish-shaped probability density function. A mixture of the two takes on prominent characteristics of both. This is clearly illustrated by the actual measurements in Plots A, B, and C of Figure 57.

Perhaps the most powerful method of detecting periodicities in an otherwise random vibration response is presented by an autocorrelation plot. For any purely random signal, the autocorrelation function will always approach zero (assuming the signal has no dc component) as the time displacement becomes large. On the other hand, the autocorrelation function for a periodic signal is also periodic, and will continue to oscillate in a steady state manner no matter how large the time displacement becomes. Thus the autocorrelation plot for a signal representing a mixed random and periodic vibration response will decay to a perpetual periodic oscillation as the time displacement becomes large. These matters are illustrated by Plots A, B, and C of Figure 58, and are further discussed with numerical examples in Section IX. E.3.

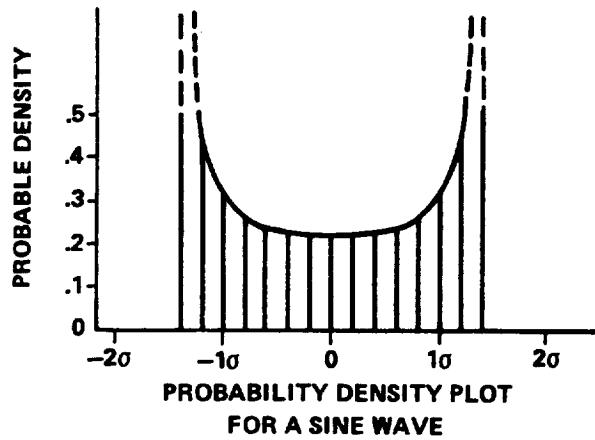
2. QUANTITATIVE TEST FOR RANDOMNESS (VARIANCE TEST)

Quantitative tests for randomness have been developed and studied experimentally in Section 15 of Reference 21. These tests permit a statistical decision, with a defined probable error, to be drawn from rudimentary investigations of a sample vibration response record. The most practical quantitative test for applications to flight vehicle vibration data involves an investigation of

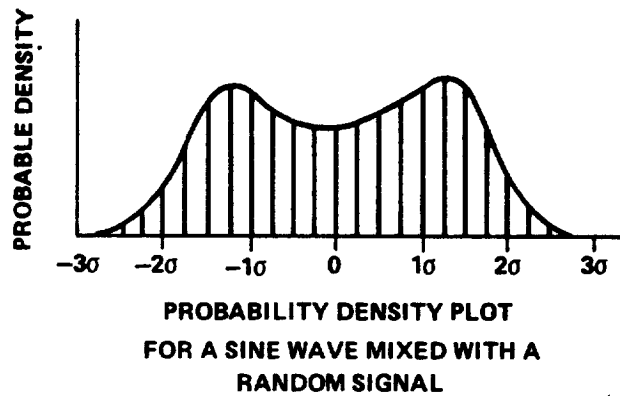
A



B



C



RMS AMPLITUDE OF SINE WAVE = 1.0 VOLTS
RMS AMPLITUDE OF RANDOM SIGNAL = 0.3 VOLTS
RMS AMPLITUDE OF TOTAL SIGNAL = $\sigma = 1.04$ VOLTS

Figure 57. Actual probability density plots.

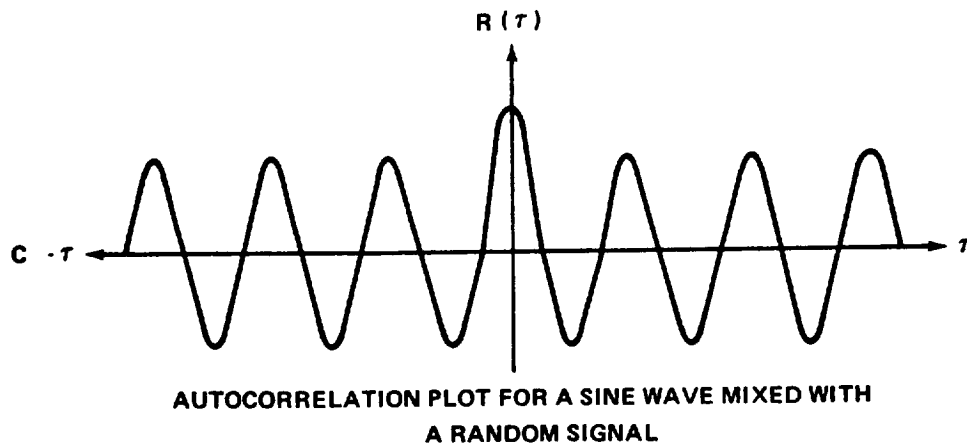
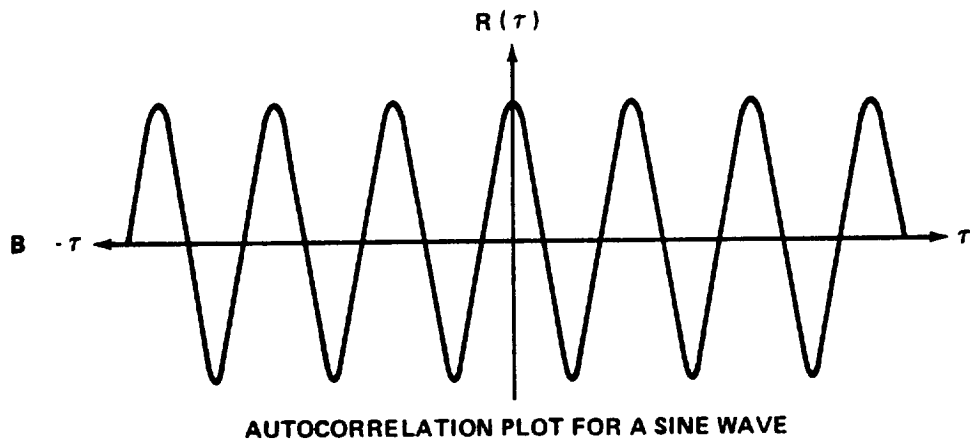
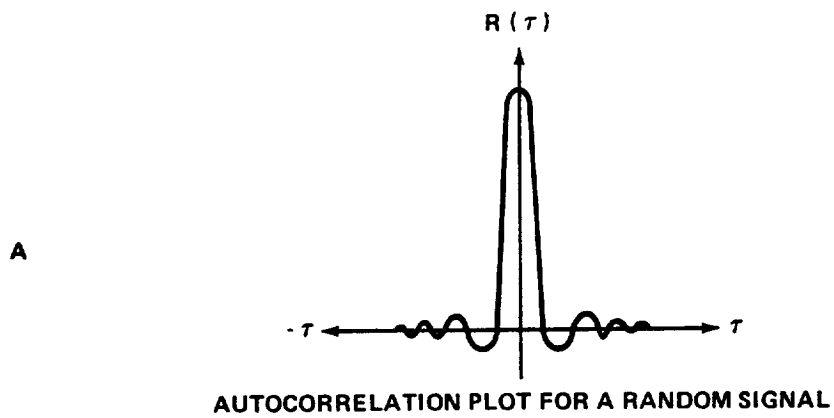


Figure 58. Typical autocorrelation plots.

the variance of narrow band mean square value measurements (or power spectral density measurements). This procedure is identified as Randomness Test B in Reference 21. The principles of that test may be summarized as follows.

As discussed in Paragraph 1 above, the existence of a sinusoid in an otherwise random signal will be revealed by the presence of a sharp peak in a properly resolved power spectrum for the signal. However, a narrow band random signal representing a high Q resonance in a structural vibration response will also appear as a sharp peak in a power spectrum. These two cases can be distinguished from one another by examining repeated measurements of the mean square value for the spectral peak at different times. If the peak represents a sinusoid, mean square measurements taken at different times should be exactly the same except for slight differences due to either or both observational errors and possible sensitivity drift in the measurement equipment. There are no uncertainties or sampling errors associated with measurements of periodic signals.

On the other hand, if the peak is a narrow band random signal (assumed to be stationary), mean square measurements taken at different times will show scatter because of the inherent uncertainties associated with random signal measurements. To be more specific, mean square measurements for a stationary random signal will show scatter or variability which may be defined in terms of a normalized variance ϵ^2 , as follows:

$$\epsilon^2 = \frac{1}{BT_a} \quad . \quad (65)$$

Here, B is the equivalent ideal bandwidth of the random signal in Hz and T_a is the averaging time used to measure a mean square value in seconds. From equation (65), as the bandwidth or averaging time is decreased, the variability of the resulting measurements is increased. These theoretical ideas form the basis for the randomness test outlined here.

Assume a sample record of length T seconds is obtained from a stationary vibration response. Further assume the power spectral density plot estimated from the sample record reveals one or more sharp peaks. Each peak may be tested for randomness by the following procedure:

1. Tune the narrow bandpass filter of the PSD analyzer over a peak of interest so that the narrow frequency range of the peak is isolated from the remainder of the signal.
2. Obtain a collection of mean square measurements by averaging over each of N number of equally long segments of the sample record. Clearly, the required averaging time for each measurement is $T_a = T/N$. For certain theoretical reasons, the number of measurements should be restricted to $N < 0.1 BT$. If averaging is accomplished by continuous smoothing with a low pass RC filter, the resulting continuous mean square measurement time history can be reduced to a collection of discrete mean square measurements by the procedures illustrated in Figure 59.
3. Compute the expected normalized variance ϵ^2 for the collection of mean square measurements, assuming the sampled signal is random, by using equation (65). The bandwidth B in equation (65) is assumed to be the bandwidth for the PSD analyzer filter.
4. Calculate the actual normalized variance ϵ^2 for the collection of mean square measurements by using the following computational formula:

$$\hat{\epsilon}^2 = \frac{\frac{1}{N-1} \left\{ \sum_{i=1}^N \hat{G}_i^2 - \frac{\left[\sum_{i=1}^N \hat{G}_i \right]^2}{N} \right\}}{\left[\frac{1}{N} \sum_{i=1}^N \hat{G}_i \right]^2}$$

GIVEN A SAMPLE RECORD OF LENGTH T SECONDS, A CONTINUOUS RC AVERAGED MEAN SQUARE VALUE MEASUREMENT (OR POWER SPECTRAL DENSITY MEASUREMENT) MAY BE REDUCED TO A COLLECTION OF EQUIVALENT TRUE AVERAGED MEAN SQUARE VALUE MEASUREMENTS AS FOLLOWS. LET THE RC AVERAGING TIME CONSTANT K BE SHORT COMPARED TO THE RECORD LENGTH T ; THAT IS, $K \ll T$. NOW, DIVIDE THE CONTINUOUS MEASUREMENT INTO N EQUAL INTERVALS SUCH THAT EACH INTERVAL IS ABOUT $3K$ OR $4K$ LONG, AS SHOWN BELOW. THE LEVEL OF THE CONTINUOUS MEASUREMENT AT THE END OF EACH INTERVAL WILL CONSTITUTE A DISCRETE MEASUREMENT BASED UPON AN EQUIVALENT TRUE AVERAGING TIME OF $T_a = 2K$. THE INDIVIDUAL READINGS SHOULD BE $3K$ OR $4K$ APART TO ASSURE THAT THEY ARE STATISTICALLY INDEPENDENT.

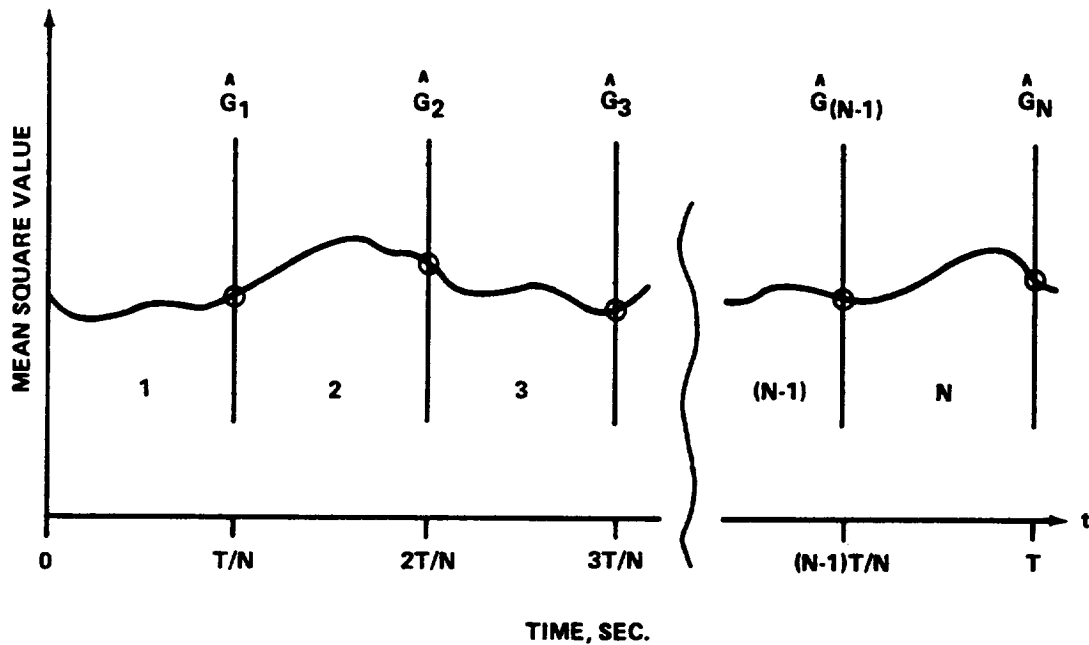


Figure 59. Analysis of continuous mean square value measurements.

$$= \frac{N}{N-1} \left\{ \frac{\sum_{i=1}^N \hat{G}_i^2}{\left[\sum_{i=1}^N G_i \right]^2} - 1 \right\} \quad (66)$$

Here, \hat{G}_i is the i th mean square measurement where $i = 1, 2, 3, \dots, N$.

5. Determine the ratio of the actual and expected normalized variances as follows:

$$R_{\epsilon} = \frac{\epsilon^2}{\epsilon^2} \quad (67)$$

If R_{ϵ} is statistically equivalent to unity, the power spectral density peak being investigated is considered to be the result of a narrow band random vibration response. If R_{ϵ} is significantly less than unity, the power spectral density peak is considered to be the result of a periodic component in the vibration response. The criteria for deciding if R_{ϵ} is equivalent to unity or significantly less than unity is as follows:

$$R_{\epsilon} = 1 \text{ if } R_{\epsilon} > \frac{\chi^2_{(N-1);(1-\alpha)}}{N-1} \quad (68a)$$

$$R_{\epsilon} < 1 \text{ if } R_{\epsilon} < \frac{\chi^2_{(N-1);(1-\alpha)}}{N-1} \quad (68b)$$

Here, $\chi^2_{(N-1);(1-\alpha)}$ is a chi-squared distribution with $N-1$ degrees of freedom. N is the number of measurements employed, and α is the level of significance for the decision. The level of significance defines the probability of erroneously concluding

that the peak represents a sinusoid when in fact it represents a narrow band random signal. An erroneous conclusion of this type is referred to as a Type I error. Clearly, the risk of making a Type I error is reduced by using a smaller value of α in equation (68).

A tabulation of values for χ^2 may be found in most statistics books. Equation (68) is plotted for the levels of significance $\alpha = 0.05$ in Figure 60.

The above step-by-step procedure effectively accomplishes a statistical hypothesis test without going into fundamental details, so that the test may be employed by individuals who do not have a working knowledge of applied statistics. If the procedure is carefully followed, statistically sound decisions will result in most cases.

As noted in Step 5, there is always a risk of concluding that the peak represents a sinusoid when it actually represents a narrow band random signal. This risk defined by α is the probability of making a Type I error. However, there is also a risk of concluding that the peak represents a narrow band random signal when it actually represents a sinusoid. An erroneous conclusion of this type is called Type II error. The Type II error probability associated with the test is a function of certain fundamental considerations which are not discussed here. These considerations are presented in Reference 11. In general terms, the risk of making a Type II error increases as α becomes small and decreases as N becomes large. Thus, the probability of making either a Type I or Type II error will be minimized by using as many measurements as feasible, as long as the number of measurements does not exceed the quantity of 0.1 BT.

It has been noted in paragraphs A.1 and A.2 of this section that the various techniques for detecting periodic components in an otherwise random vibration response are applicable only if the data are stationary. If the various techniques are applied only to that data in the narrow frequency range of sharp power density peaks (as they should be for maximum effectiveness), the stationarity requirement then applies only to the narrow frequency ranges being investigated. However, if a power spectral density peak is not stationary, the peak cannot represent a periodic component since a periodic function is by definition steady state (stationary). Hence, if vibration data do not comply with the stationarity requirement, a test for the presence of periodic components is not really needed since the data by implication contain no periodic components.

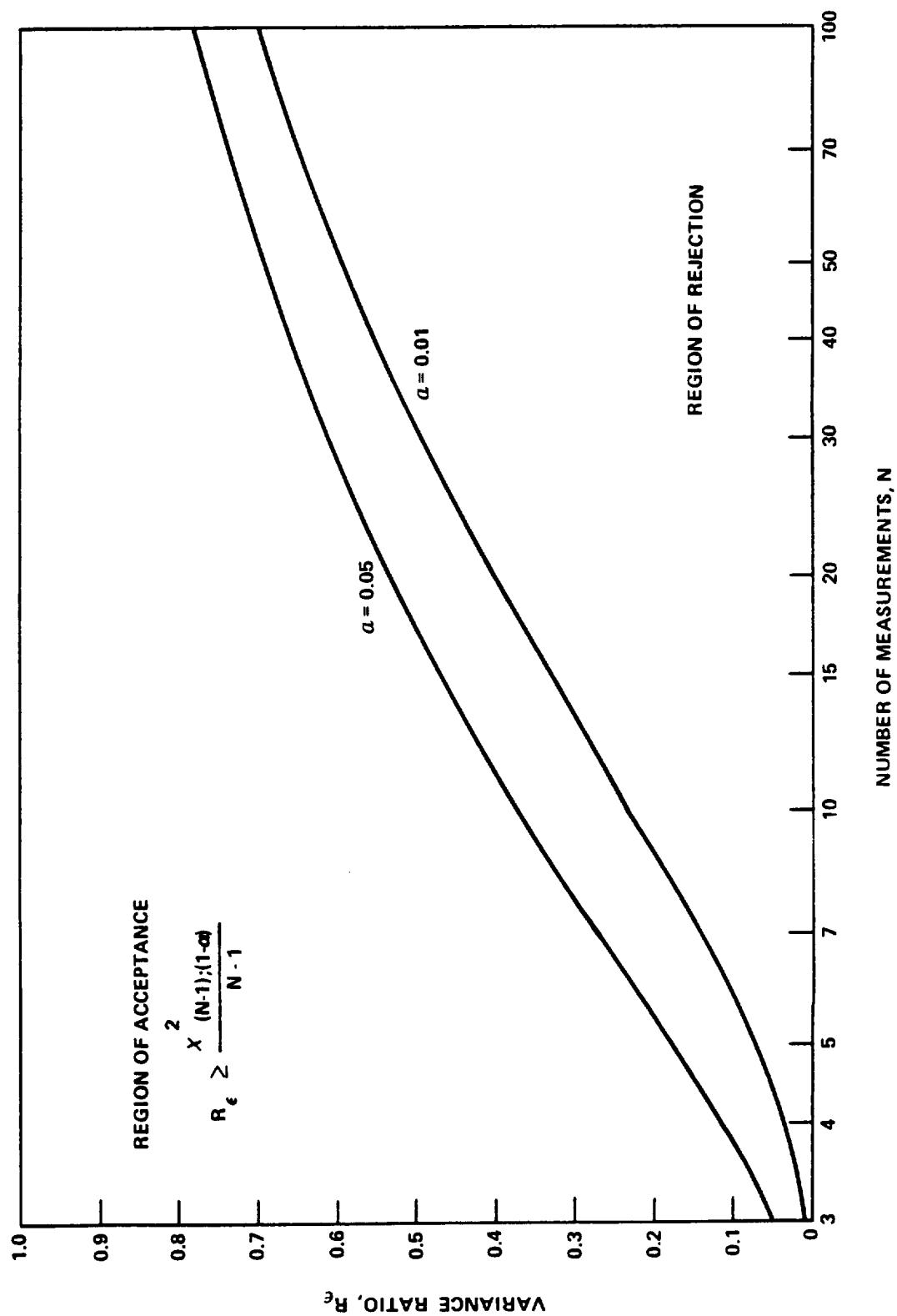


Figure 60. Acceptance regions for randomness test.

Numerical Example:

Assume a sample record of length $T = 10$ seconds is obtained from a vibration response which is believed to be stationary. Further assume the power spectrum measured from the sample record reveals a sharp peak which is to be tested at the $\alpha = 0.05$ level of significance for the presence of a periodic component.

Following the procedure outlined in paragraph A.2. of this section, let a PSD analyzer filter with a bandwidth of $B = 56$ Hz be tuned over the peak to isolate it from the remainder of the signal. Now, let a collection of $N = 31$ power spectral density (mean square value) measurements be obtained from the sample record by averaging over 31 consecutive intervals of $T_a = 0.32$ second. Note that $N = 31 < 0.1 BT = 56$, as it should be. Assume that the resulting measurements are as follow:

Data for Example (a)

Power Spectral Density Measurements G_i , volts² /Hz

1.84	1.09	1.49	1.61
1.56	2.27	2.39	1.64
2.19	2.33	2.10	2.08
2.60	2.70	1.94	1.78
1.37	2.01	2.21	2.49
2.84	1.62	1.80	1.45
1.40	3.08	2.21	1.83
1.83	1.76	1.79	

From equation (65), the expected normalized variance for the measurements if the data is purely random is

$$\epsilon^2 = \frac{1}{BT_a} = 0.056 \quad .$$

From equation (66), the actual normalized variance for the measurements is

$$\hat{\epsilon}^2 = 0.055 \quad .$$

From equation (67), the ratio of the actual to expected normalized variance is

$$R_{\epsilon} = \frac{\hat{\epsilon}^2}{\epsilon^2} = 0.98 \quad .$$

Referring to equation (68) and Figure 60, it is clear that R_{ϵ} is not significantly less than unity at the $\alpha = 0.05$ level of significance. Hence, there is no reason to believe that the power spectral density peak is the result of a periodic component. The peak may be considered to be the result of a narrow band random vibration.

The measurements used for numerical example (a) are taken from Section 15 of Reference 21, and are actual power spectral density measurements for a truly random signal, as indicated by the above test.

Data for Example (b)

Power Spectral Density Measurements G_i , volts²/Hz

1.91	2.25	2.01	1.78
1.68	2.08	1.80	2.13
1.82	1.93	1.89	2.01
2.03	1.92	2.05	2.05
2.07	1.91	1.89	1.71
1.90	2.26	2.03	1.83
1.53	1.76	2.22	1.72
1.55	1.82	2.19	

From equation (66), the actual normalized variance for this set of measurements is

$$\epsilon^2 = 0.0096 \quad .$$

From equation (67), the normalized variance ratio is

$$R_{\epsilon} = 0.17 \quad .$$

Referring to equation (68) and Figure 60, it is clear that R_{ϵ} is significantly less than unity at the $\alpha = 0.05$ level of significance. Hence, there is reason to believe that the power spectral density peak is the result of a periodic component.

The measurements used for numerical example (b) are taken from Section 15 of Reference 21, and are actual power spectral density measurements for a signal consisting of a sine wave buried in noise, as indicated by the above test.

B. Verification of Stationarity

The general concept of stationarity as applied to vibration data is discussed in Section VIII.A.2. It is noted there that the descriptive properties of a random vibration response measured from a sampled vibration over any time interval for which the vibration is stationary. Predictions may be made for future time intervals for stationary data. If the sampled vibration is nonstationary, the data measured from a sample record will reflect only the vibration response properties of that one record alone during that particular time interval when the sample record was obtained. No rigorous predictions may be made for future time intervals when data are nonstationary.

There are two basic procedures for sampling a flight vehicle vibration environment. The first procedure is to obtain a single continuous sample record (at each measurement point of interest) which covers an entire experiment. Continuous sampling is usually employed for experiments involving

short term flight vehicles such as missiles and certain spacecraft. The second procedure is to obtain a collection of short sample records (at each measurement point of interest) which are obtained for various limited time intervals during the experiment. Interval sampling is usually employed for experiments involving long term flight vehicles such as long range bombers.

For the first case where a single continuous sample is available, stationarity means that the vibration response does not change over the length of the sample record (or a specific time interval covered by the sample record). In other words, if the continuous sample record were broken up into many short samples, the descriptive properties measured from each of the various short samples would be equivalent. If this is true, then one set of time invariant properties measured from the entire sample record may be used to describe the sampled vibration.

For the case where a collection of short samples is available, stationarity means that the vibration response is the same for each time interval when a sample is obtained. If this is true, then the collection of samples may be pooled together into one long sample record, and one set of properties measured from the composite sample may be used to describe the sampled vibration. In either case, stationarity effectively means that the properties of a vibration response measured from sample records obtained at different times are equivalent.

For practical purposes, vibration response data may be considered stationary if the mean square values measured from sample records obtained at different times are equivalent. Technically, the mean value and autocorrelation function should also be time invariant. However, the mean value of vibration data is usually zero, and for certain practical reasons, it is unlikely that the autocorrelation function is changing if the mean square value is not changing. Hence, the determination of stationarity can usually be limited to an investigation of mean square values.

In many instances, stationarity or nonstationarity in measured vibration data is obvious. This is particularly true when the uncertainty associated with the measurements is small. For example, if the mean square values measured from a collection of sample records were all within a few percent of one another, the collection of measurements could clearly be considered equivalent without further attention. On the other hand, if a collection of mean square values, each with a measurement uncertainty of only a few percent, displayed scatter if perhaps two or three to one, then the collection of measurements could clearly be considered nonstationary without further attention. The problem

arises when the available data have a relatively high measurement uncertainty due to a narrow bandwidth or short record length. It is often difficult in such cases to distinguish between expected statistical scatter and nonstationarity.

Two different quantitative tests for stationarity are now outlined. The first procedure is based upon a measurement variance test similar to the test for randomness outlined in Paragraph A.2. of this section. This procedure is developed and experimentally studied in Section 16 of Reference 21. The second procedure is based upon nonparametric statistical techniques discussed in Reference 22.

1. VARIANCE TEST FOR STATIONARITY COMBINED WITH RANDOMNESS TEST

This test for stationarity is identical in principle to the test for randomness outlined in Paragraph A.2. of this section. The variance of mean square measurements obtained at different times is compared to the theoretically expected variance for mean square measurements of a stationary random signal. As a lack of randomness will tend to reduce the scatter in repeated mean square measurements, a lack of stationarity will tend to increase the scatter in repeated measurements. Hence, the procedure for applying the variance test for stationarity is the same as the procedures presented for the randomness test in Paragraph A.2. of this section, except for the final decision which is based upon whether or not the ratio R_ϵ is significantly greater than unity rather than significantly less than unity.

The variance test for randomness assumes that the signal being tested is stationary, and the variance test for stationarity requires that the signal being tested is random. It is then logical that the two characteristics of randomness and stationarity should be established jointly by a single test procedure. A combined test does pose one practical problem. The randomness test is most effective when applied to a narrow frequency range obtained by locating a narrow bandwidth filter over a sharp peak in the power spectrum of the signal. On the other hand, a stationarity test should ideally be applied to the entire frequency range of the signal. However, it is often acceptable to test only the sharp spectral peaks for stationarity, since most of the relative power of the vibration response is represented by these peaks. If the peaks in the power spectrum are found to be stationary, it is reasonable to assume the entire signal is stationary for most engineering applications.

Assume a sample record of length T seconds is obtained from a vibration response. Further assume the power spectral density plot estimated from

the sample record reveals one or more peaks. Each peak may be tested for randomness and stationarity by the following procedure:

1. Tune the narrow bandpass filter of the power spectral density analyzer over a peak of interest so that the narrow frequency range of the peak is isolated from the remainder of the signal.
2. Obtain a collection of mean square measurements by averaging over each of N number of equally long segments of the sample record. Clearly, the required averaging time for each measurement is $T_a = T/N$. For certain theoretical reasons, the number of measurements should be restricted to $N < 0.1 BT$. If averaging is accomplished by continuous smoothing with a low pass RC filter, the resulting continuous mean square measurement time history can be reduced to a collection of discrete mean square measurements by the procedures illustrated in Figure 59.
3. Compute the expected normalized variance ϵ^2 for the collection of mean square measurements, assuming the sampled signal is random and stationary, by using equation (65).
4. Calculate the actual normalized variance $\hat{\epsilon}^2$ for the collection of mean square measurements by using the computational formula presented in equation (66).
5. Determine the ratio of the actual and expected normalized variances as follows:

$$R_{\epsilon} = \frac{\hat{\epsilon}^2}{\epsilon^2} \quad . \quad (69)$$

If R_{ϵ} is statistically equivalent to unity, the power spectral density peak being investigated is considered to be the result of a narrow band stationary random vibration response. If R_{ϵ} is significantly less than unity, the power spectral density peak is considered to be nonrandom, and if R_{ϵ} is significantly greater than unity, the power spectral density peak is considered to be nonstationary.

The criteria for deciding if R_ϵ is equivalent to unity or significantly different from unity are as follows:

$$R_\epsilon = 1 \text{ if } \frac{\chi^2(N-1); (1-\alpha/2)}{N-1} \leq R < \frac{\chi^2(N-1); \alpha/2}{N-1} \quad (70a)$$

$$R < 1 \text{ if } R_\epsilon < \frac{\chi^2(N-1); (1-\alpha/2)}{N-1} \quad (70b)$$

$$R_\epsilon > 1 \text{ if } R \geq \frac{\chi^2(N-1); \alpha/2}{N-1} \quad (70c)$$

Here, $\chi^2(N-1)$ is a chi-squared distribution with $N-1$ degrees of freedom, N is the number of measurements employed, and α is the level of significance for the decision. A tabulation of values for χ^2 may be found in most statistics books. Equation (70) is plotted for the levels of significance $\alpha = 0.01$ and $\alpha = 0.05$ in Figure 61. The probable errors associated with a decision are discussed in Paragraph A.2. of this section.

Numerical Example:

Assume a sample record of length $T = 17$ seconds is obtained from a vibration response (the 17 seconds could represent the total length for a collection of sample records obtained at different times). Further assume the power spectrum measured from the sample records obtained at different times). Further assume the power spectrum measured from the sample record reveals a sharp peak which represents most of the relative power of the signal. The peak is to be tested for randomness and stationarity at the $\alpha = 0.05$ level of significance.

Following the procedure outlined in Paragraph B.1. of this section, let a PSD analyzer filter with a bandwidth of $B = 56$ Hz be tuned over the peak to isolate it from the remainder of the signal. Now, let a collection of $N = 31$ power spectral density (mean square value) measurements be obtained by averaging over 31 consecutive intervals of $T_a = 0.54$ seconds. Note that $31 < 0.1 BT = 95$ as it should be. Assume the resulting measurements are as follow:



175

Data for Example (c)

Power Spectral Density Measurements \hat{G}_1 , volt²/Hz

2.25	2.19	2.00	2.21
1.78	3.20	2.23	1.47
2.26	2.30	3.05	2.44
2.07	2.86	2.15	3.28
1.91	2.68	2.36	3.27
2.85	2.15	2.03	2.49
2.00	2.54	2.00	3.43
2.45	2.32	2.57	

From equation (65), the expected normalized variance for the measurements if the data are purely random and stationary is

$$\epsilon^2 = \frac{1}{BT_a} = 0.033 \quad .$$

From equation (66), the actual normalized variance for the measurements is

$$\hat{\epsilon}^2 = 0.038 \quad .$$

From equation (69), the ratio of the actual to expected normalized variance is

$$R_{\epsilon} = \frac{\hat{\epsilon}^2}{\epsilon^2} = 1.15 \quad .$$

Referring to equation (70) and Figure 61, it is clear that R_ϵ is not significantly different from unity at the $\alpha = 0.05$ level of significance. Hence, there is no reason to believe that a periodic component is present or that the signal is nonstationary. The signal may be considered both random and stationary.

The measurements used in numerical example (c) are taken from Section 16 of Reference 21, and are actual power spectral density measurements for a truly stationary random signal, as indicated by the above test.

Now assume that the resulting measurements for the test were as follow:

Data for Example (d)

Power Spectral Density Measurements \hat{G}_i , volts ² /Hz			
2.33	1.24	0.96	2.63
2.03	1.40	1.60	2.25
2.12	1.24	1.37	2.06
1.88	1.22	1.10	2.42
2.20	1.42	1.03	2.27
1.90	1.40	1.62	3.00
2.36	1.39	1.24	2.40
2.61	1.70	2.18	

From equation (66), the actual normalized variance for this set of measurements is

$$\hat{\epsilon}^2 = 0.090 \quad .$$

From equation (69), the normalized variance ratio is

$$R_{\epsilon} = 2.7 \quad .$$

Referring to equation (70) and Figure 61, it is clear that R_{ϵ} is significantly greater than unity for the $\alpha = 0.05$ level of significance. Hence, there is reason to believe the sampled vibration response is nonstationary.

The measurements used for numerical example (d) are taken from Section 16 of Reference 21, and are actual power spectral density measurements for a nonstationary random signal, as indicated by the above test. Specifically, the measurements were obtained from a random signal whose true mean square value changed ± 20 percent relative to an average level (a change of ± 10 percent in the rms amplitude). The rms amplitude of the signal was 10 percent high for the first eight measurements, 10 percent low for the next 15, and 10 percent high for the last 8.

2. NONPARAMETRIC TEST FOR STATIONARITY

This test for stationarity is also based upon an investigation of the scatter or variability of mean square measurements. However, it is only concerned with the number of "runs" which occur in a collection of measurements, and does not require a knowledge of the actual sampling distribution of the measurements. Thus the test is nonparametric.

Assume that a collection of N number of statistically independent mean square values are measured from sampled vibration data. Let the median value of the measurements be determined; that is, the value for which half the measurements are larger and half are smaller. Furthermore, let each measurement that is larger than the median be identified by (+) and each that is smaller than the median be identified by (-). Now arrange the (+) and (-) identifications for the measurements in the proper time sequence.

For example, the resulting sequence for 20 measurements might be as follows:

++	-	+	--	+++	-	+	--	+	--	+	--	.
1	2	3	4	5	6	7	8	9	10	11	12	

A "run" is defined as a sequence of identical symbols which is followed and preceded by a different symbol or no symbol at all. In the above example the number of runs is 12. The total number of runs in a collection of independent measurements obtained at different times gives an indication as to whether or not the quantity being measured is stationary. If very few runs occur, a time trend is indicated. If a great many runs occur, systematic short period fluctuations are indicated.

The application of run theory as a test for stationarity presents three important advantages not afforded by the variance test discussed in Paragraph B.1. of this section.

1. A knowledge of the frequency bandwidth of the signal under investigation is not required.
2. A knowledge of the exact averaging time used to measure the mean square values is not required. Furthermore, there are no restrictions on how long the averaging time should be.
3. It is not necessary for the signal under investigation to be completely random. Valid conclusions are obtained even when periodic components are present in the signal, as long as the fundamental period is short compared to the averaging time used for each mean square measurement.

The above advantages clearly illustrate the broad and simple applicability of the test to vibration data. Actually the test can be applied to a sample record with nothing more than a simple square amplitude detector, such as a true rms voltmeter. No filter or detailed analysis is required. The step-by-step procedure for applying the test is as follows:

1. Obtain a collection of broadband mean square measurements by averaging over each of N number of segments of a sample record. The averaging time for each measurement is of no concern. If averaging is accomplished by continuous smoothing with a low pass RC filter, the resulting continuous mean square measurement time history can be reduced to a collection of discrete mean square measurements by the procedures illustrated in Figure 59.

2. Determine the median of the mean square measurements; that is, the value for which half the measurements are larger and half are smaller.
3. Identify each measurement that is larger than the median by (+) and each that is smaller than the median by (-).
4. With the (+) and (-) identifications for the measurements arranged in proper time sequence, count the number of runs.
5. If the number of runs is either too small or too large, the sample record being investigated is considered to represent a nonstationary vibration response. Otherwise, the sample record is considered to represent a vibration response which is stationary. The criteria for deciding if the number of runs are too small or large is tabulated in Table 6 for various values of N and the level of significance α .

Numerical Example:

Let the data gathered for the numerical examples in Paragraph B.1. of this section be tested for stationarity by application of the run test at the $\alpha = 0.05$ level of significance.

First consider the measurements presented in Example (c). The median value for these measurements is $\hat{G} = 2.30$ volts²/cps. That is, there are 15 measurements with a value greater than 2.30 and 15 measurements with a value less than 2.30. The number of runs in the 31 measurements when considered in a proper time sequence is 16, as shown below:

1	2.25	5	2.19	9	2.00	15	2.21
	1.78		3.20		2.23		1.47
	2.26		2.30		3.05		2.44
	2.07		2.86		2.15		3.28
	1.91		2.68		2.36		3.27
2	2.85	7	2.15	13	2.03	16	2.49
3	2.00		2.54		2.00		3.43
4	2.45	8	2.32	14	2.57		

TABLE 6. RUN TEST FOR STATIONARITY

N	$\alpha = 0.10$		$\alpha = 0.05$		$\alpha = 0.01$	
	lower limit	upper limit	lower limit	upper limit	lower limit	upper limit
8	3	6	-	-	-	-
10	4	7	3	8	-	-
12	4	9	4	9	3	10
14	5	10	4	11	4	11
16	6	11	5	12	4	13
18	7	12	6	13	5	14
20	7	14	7	14	5	15
22	7	16	7	16	5	18
24	8	17	7	18	6	19
26	9	18	8	19	7	20
28	10	19	9	20	7	22
30	11	20	10	21	8	23
32	11	22	11	22	9	24
34	12	23	11	24	10	25
36	13	24	12	25	10	27
38	14	25	13	26	11	28
40	15	26	14	27	12	29
50	19	32	18	33	16	35
60	24	37	22	39	20	41

Referring to Table 6, it is clear that the number of runs is within the range expected for measurements from a stationary signal at the $\alpha = 0.05$ level of significance. Hence, there is no reason to believe that the sampled vibration response is nonstationary. This is a correct conclusion for the data presented in Example (c).

Now consider the measurements presented in Example (d). The median value for these measurements is $\hat{G} = 1.88 \text{ volt}^2/\text{Hz}$. The number of runs in the 31 measurements when considered in the proper time sequence is 3, as shown below :

$$\begin{array}{ccccc}
 1 & \left\{ \begin{array}{l} 2.33 \\ 2.03 \\ 2.12 \\ 1.88 \\ 2.20 \\ 1.90 \\ 2.36 \end{array} \right. & \left\{ \begin{array}{l} 1.24 \\ 1.40 \\ 1.24 \\ 1.22 \\ 1.42 \\ 1.40 \\ \blacktriangledown 1.39 \end{array} \right. & 2 & \left\{ \begin{array}{l} 0.96 \\ 1.60 \\ 1.37 \\ 1.10 \\ 1.03 \\ 1.62 \end{array} \right. & 3 & \left\{ \begin{array}{l} 2.18 \\ 2.63 \\ 2.25 \\ 2.06 \\ 2.27 \\ 2.27 \\ 2.40 \end{array} \right.
 \end{array}$$

Referring to Table 6, it is clear that the number of runs is less than expected for measurements from a stationary signal at the $\alpha = 0.05$ level of significance. Hence, there is reason to believe that the sampled vibration response is nonstationary. This is a correct conclusion for the data presented in Example (d).

Note that the data used for the numerical examples in this section involve relatively large measurement uncertainties. This is done to illustrate how the tests for stationarity are applicable even for data with considerable statistical scatter. Because of the scatter, the fact that the data for Examples (c) and (d) are stationary and nonstationary, respectively, is not immediately obvious by observation.

C. Determination of Data Equivalence

The evaluation of a flight vehicle vibration environment will involve the collection and analysis of many different sample records. These sample records would be gathered as a function of several different variables to obtain appropriate vibration response profiles. For example, a collection of sample records might represent the vibration response for a number of different times during a flight. Hence, the vibration environment can be evaluated as a function of time and structural location. In a similar manner, sample

records might be collected from either or both repeated flights of the same vehicle and flights of different vehicles of the same type. For this case, the specific flight or specific vehicle or both would also be variables in the data analysis.

In any case, an early step in the evaluation of the data should be an investigation for areas of equivalence, so that the number of variables needed to describe the vibration environment can be reduced to a minimum.

As one example, assume the vibration data measured for different flights of a vehicle is not significantly different from flight to flight. Then, the specific flight can be eliminated as a variable in the description of the vibration environment. The sample records obtained for different flights can be pooled together and the vibration environment for the flight vehicle can be described by one set of properties which are applicable to all flights.

For a second example, assume the vibration data measured at various points in a specific structural zone of a vehicle are not significantly different from point to point. Then, the specific point in that zone of the vehicle may be eliminated as a variable in the description of the vibration environment. The sample records obtained for different points in that zone may be pooled together and the vibration environment for that structural zone of the flight vehicle may be described by one set of properties which are applicable to all points in that zone.

Note that the presence or absence of time as a variable determines the stationarity of a vibration response. As described in Subsection B of this section, a stationary vibration response is one whose statistical properties do not vary with time; equivalent. The procedures in Subsection B. of this section for verifying stationarity are simply tests for the equivalence of measurements obtained at different times. Those same procedures can just as well be applied to determine the equivalence of measurements obtained at different locations or on different flights or on different vehicles. However, when a collection of measurements is available which involves two or more variables, there are more powerful statistical procedures for establishing the significant effects of two or more variables simultaneously. These procedures are known as "analysis of variance," and are described in this section.

The two most important variables in the description of a vibration environment are usually time and structural location. Any reduction in the number of different times and locations needed to describe a general vibration environment is clearly desirable. As discussed in Subsection B. of this section, the determination of stationarity may be limited to an examination of mean

square value measurements, for most practical cases. For the same general reasons, the equivalence of vibration data at various structural locations may also be based on an investigation of mean square value measurements, at least for purposes of preliminary evaluation. Hence the following discussions are written assuming that time and location are the variables of interest and that a mean square value is the measured property which defines the vibration environment. However, the general analysis of variance procedures is valid for any measured quantity as a function of any desired variables. In all cases, a requirement is the assumption that the measured quantities in question are normally distributed, or that the measurement errors about some true constant value are normally distributed.

A full discussion on these analyses of variance procedures appears in Section 8 of Reference 21. The material to follow here summarizes some of these procedures and illustrates them with a computational example.

1. ANALYSIS OF VARIANCE PROCEDURES

Basic mathematics for the analysis of variance procedures is as follows. Suppose two sample means \bar{x}_1 and \bar{x}_2 are available where

$$\bar{x}_i = \sum_{j=1}^N x_{ij} ; i = 1, 2 \quad (71)$$

the index $i = 1, 2$ representing two different sets of experiments in each of which $j = 1, 2, \dots, N$ measurements are made. Thus x_{1j} and x_{2j} represent the N sample values in each experiment.

If it is assumed that the underlying populations are normal, and that the sample variances s_1^2 and s_2^2 are estimates of common variance, then the variable

$$t = \sqrt{N} \frac{(\bar{x}_1 - \bar{x}_2)}{\sqrt{s_1^2 + s_2^2}} \quad (72)$$

has a "student's t " distribution with $(N-1)$ degrees of freedom (df). The sample variances are defined by their unbiased estimates

$$s_i^2 = \frac{\sum_{j=1}^N (x_{ij} - \bar{x}_i)^2}{N - 1} \quad ; \quad i = 1, 2 \quad . \quad (73)$$

Note that the number of $df = (N-1)$ is used as a divisor rather than the sample size N . This fact allows a two-tail at the α level of significance by comparing t from equation (72) with a tabulated value of $t_{1-\alpha/2}^{(N-1)}$. If a test among several means \bar{x}_i , $i = 1, 2, \dots, k$ is desired, the situation becomes more complex. All possible combinations of the sample means could be tested, although the level of significance becomes open to question if any combinations fail the test. The analysis of variance procedures offer a solution to this problem.

a. The One-Way Fixed Effects Model

The analysis will now be presented in terms of its simplest form. Assume for example that N measurements of vibration data from each of k points from some flight are available, and that the collection of data is all obtained in a short period of time under identical conditions. It is now desired to test whether the k sample means are all statistically equivalent estimates of some common population mean value μ . That is, the hypothesis is

$$\mu_1 = \mu_2 = \dots = \mu_k = \mu \quad (74)$$

where μ_i represent the respective true mean values. This hypothesis may be cast in a slightly different but equivalent and sometimes more useful form.

Consider each observation to be of the form

$$x_{ij} = \mu + \phi_i + \epsilon_{ij} \quad , \quad \begin{matrix} j = 1, 2, \dots, N \\ i = 1, 2, \dots, k \end{matrix} \quad (75)$$

where μ is the overall mean value, ϕ_i is an effect due to the i th location and ϵ_{ij} is an "error" term assumed to be normally distributed with zero mean and variance σ^2 . In this model the hypothesis becomes

$$\phi_1 = \phi_2 = \dots = \phi_k = 0 \quad . \quad (76)$$

The basis for the test of the hypothesis arises from the fact that two independent estimates of the variance σ^2 may be calculated from the data if the hypothesis is true.

The first of these estimates is obtained from the "within group" variation. That is, define

$$MS_1 = \frac{1}{k} \sum_{i=1}^k s_i^2 \quad (77)$$

which is the average of the k sample variances. This is an unbiased estimate of σ^2 whether or not the hypothesis of equal means is true.

A second estimate is now obtained from the "between group" variation. Define

$$MS_2 = N \frac{\sum_{i=1}^k (\bar{x}_i - \bar{x})^2}{k - 1} \quad (78)$$

where this estimates the population variance as N times the variance of the sample means and \bar{x} is the mean of the k sample means

$$\bar{x} = (1/k) \sum_{i=1}^k \bar{x}_i \quad .$$

Equation (78) is based on the relation

$$\sigma_{\bar{x}}^2 = \frac{\sigma^2}{N} \quad (79)$$

where $\sigma_{\bar{x}}^2$ is the variance of the distribution of sample means computed from samples of size N drawn from a population with variance σ^2 . The variance estimate given by equation (78) will be an estimate of σ^2 if the hypothesis (76) holds. However, if there is a contribution due to nonzero values ϕ_i , then this variance estimate will be enlarged because of this effect. It can be shown that the variance ratio

$$F = \frac{MS_2}{MS_1} \quad (80)$$

has an F distribution with (k-1) and N(k-1) df. Since the estimate MS_2 can only be larger than MS_1 , a one-tail test at the α level of significance may be performed by comparing F from (80) with $F_{1-\alpha}(k-1, N[k-1])$ obtained from a table of the F distribution; that is, if

$$F < F_{\alpha}(k-1, N[k-1]) \quad , \quad (81)$$

the hypothesis of equal means is accepted. The term "fixed effects" stems from the fact that it is assumed that only the effects of k specific fixed points are of interest.

b. One-Way Random Effects Model

In contrast to the fixed effects model, if it is desired to test the hypothesis that the vibration in some extended area of a flight vehicle is the same, then one would select k points at random from this general area. The model is written the same; that is,

$$x_{ij} = \mu + \phi_i + \epsilon_{ij} \quad ,$$

but in this case the ϕ_i are assumed to be k observations of a random variable with zero mean and variance σ_{ϕ}^2 . The hypothesis now is slightly altered and becomes

$$\sigma_{\phi}^2 = 0$$

although the computing procedures and the F ratio remain identical.

c. Two-Way Mixed Effects Model

The specific procedure for the simultaneous test for stationarity and test for equivalence among locations is now presented. Assume that the time period of interest has been subdivided into a large number of small intervals and that r of these intervals have been randomly selected. Also, assume that at each of c specific locations of interest, data is collected during these r intervals. In addition, it is assumed that each of these intervals is stationary and represents a sufficiently long period from which to obtain N independent observations. The data may be conveniently represented as in Table 7. Note that in each cell of the table there are N data values giving a total of Nrc observations.

TABLE 7. VIBRATION DATA LAYOUT FOR TWO-WAY ANALYSIS OF VARIANCE

Time Interval i \ j	Location			
	1	2	...	c
1	x_{11v}	x_{12v}		x_{1cv}
2	x_{21v}	x_{22v}		
...	x_{i1v}	x_{i2v}		
r	x_{r1v}	x_{r2v}		x_{rcv}

$v = 1, 2, \dots, N$

$r = \text{number of rows (times)}$

$c = \text{number of columns (locations)}$

A slightly modified notation for mean values will now be adopted. The symbol $\bar{x}_{ij.}$ will represent an average taken over the values represented by the subscript replaced with a dot; that is, as

$$\bar{x}_{ij.} = \frac{1}{N} \sum_{v=1}^N x_{ijv}$$

It is now assumed that each cell represents a sample of size N from rc separate populations, each normally distributed about a mean μ_{ij} and with a common variance σ^2 . The model becomes

$$x_{ijv} = \mu_{ij} + \epsilon_{ijv} \quad (83)$$

However, the μ_{ij} is postulated to consist of a time effect g_i , a location effect and a possible interaction effect θ_{ij} . The interaction may arise since the joint effect of the two variables taken together may differ from the sum of their separate effects. However, in many particular physical applications, it is unlikely that a significant interaction exists. The location effects h_j are assumed to be due only to the c specific fixed locations; however, the time effects g_i are assumed to be r observations of a random variable with zero mean and variance σ_g^2 . Substituting these terms for μ_{ij} , equation (83) becomes

$$x_{ijv} = \mu + g_i + h_j + \theta_{ij} + \epsilon_{ijv} \quad (84)$$

where all the factors are considered as deviations from the overall mean value μ .

The method for constructing the test of the hypothesis for the one-way analysis of variance still applies in principle to the two-way analysis. One obtains a variance estimate from between locations (columns) variation, an estimate from between times (rows), an estimate from interaction, and finally a within group (or within cell) estimate. Various F tests may then be devised to check the statistically significant interaction effects, locations effect, and time effect. The F ratios are constructed by choosing variance ratios in which the numerator will have a larger expectation than the denominator if the effect being tested for exists (i.e., is nonzero).

The within group mean square is given by the average of all the cell sample variances. That is,

$$MS_1 = \frac{1}{rc} \sum_{i=1}^r \sum_{j=1}^c s_{ij}^2 = \frac{1}{rc(N-1)} \sum_{i=1}^r \sum_{j=1}^c \sum_{v=1}^N (x_{ijv} - \bar{x}_{ij.})^2 \quad (85)$$

$$s_{ij}^2 = \frac{1}{N-1} \sum_{v=1}^N (x_{ijv} - \bar{x}_{ij.})^2 \quad (86)$$

This quantity given an unbiased estimate of σ^2 ; that is, its expected value is σ^2 regardless of whether or not any of the effects are nonzero.

The between locations (columns) variance estimate is

$$MS_4 = \frac{rN}{c-1} \sum_{j=1}^c (\bar{x}_{.j.} - \bar{x}_{...})^2 \quad ; \quad (87)$$

that is, each column mean is based on rN observations, hence the factor rN for estimating an underlying population variance from a sample variance based on means computed from rN observations. This variance estimate will have an expected value of σ^2 if no column effect exists, but otherwise will have an expected value, $E(MS_4)$, given by

$$E(MS_4) = \sigma^2 + N\sigma_{\theta}^2 + \frac{rN}{c-1} \sum_{j=1}^c h_j^2 \quad (88)$$

In equation (88), the term σ_{θ}^2 is the variance attributed to interaction if it exists, and the h_j are fixed column effects if any exist.

The expression for the between times (rows) variance estimate is entirely analogous. Thus

$$MS_3 = \frac{cN}{r-1} \sum_{i=1}^r (\bar{x}_{i..} - \bar{x}_{...})^2 \quad (89)$$

The expected value, $E(MS_3)$, of the between rows variance estimate is given by

$$E(MS_3) = \sigma^2 + Nc \sigma_g^2 \quad . \quad (90)$$

The interaction sum of squares is obtained by considering the identity

$$\begin{aligned} x_{ijv} - \bar{x} &= (\bar{x}_{ij.} - \bar{x}_{i..} - \bar{x}_{.j.} + \bar{x}_{...}) + (\bar{x}_{i..} - \bar{x}_{...}) \\ &\quad + (\bar{x}_{.j.} - \bar{x}_{...}) + (x_{ijv} - \bar{x}_{ijv.}) \quad . \end{aligned} \quad (91)$$

The sum of squares corresponding to each of the last three terms in equation 9.27 have already been accounted for by equations (85), (87), and (89). The interaction mean square is therefore

$$MS_2 = \frac{1}{(r-1)(c-1)} \sum_{i=1}^r \sum_{j=1}^c (\bar{x}_{ij.} - \bar{x}_{i..} - \bar{x}_{.j.} + \bar{x}_{...})^2 \quad . \quad (92)$$

This expression can be shown to have an expected value of σ^2 if there is no interaction effect, but otherwise will be increased by the factor $N\sigma_\theta^2$; that is,

$$E(MS_2) = \sigma^2 + N\sigma_\theta^2 \quad . \quad (93)$$

All the foregoing equations are summarized in the analysis of variance table, Table 8.

By inspecting the expected mean square values, the various F tests are seen to be as follow:

TABLE 8. TWO-WAY ANALYSIS OF VARIANCE TABLE

Source	Sum of Squares	df	Mean Square	Expected Mean Square
Between columns (locations)	$SS_4 = rN \sum_{j=1}^c (\bar{x}_{.j.} - \bar{x}_{...})^2 \dots$	$c-1$	$MS_4 = \frac{SS_4}{c-1}$	$\sigma^2 + N\sigma_\theta^2 + \frac{rN}{c-1} \sum_{j=1}^c h_j^2$
Between rows (times)	$SS_3 = cN \sum_{i=1}^r (x_{i..} - \bar{x}_{...})^2 \dots$	$r-1$	$MS_3 = \frac{SS_3}{r-1}$	$\sigma^2 + Nc\sigma_g^2$
Interaction	$SS_2 = \frac{r}{N} \sum_{i=1}^r \sum_{j=1}^c (\bar{x}_{ij.} - \bar{x}_{i..} - \bar{x}_{.j.} + \bar{x}_{...})^2 \dots$	$(r-1)(c-1)$	$MS_2 = \frac{SS_2}{(r-1)(c-1)}$	$\sigma^2 + N\sigma_\theta^2$
Within cells	$SS_1 = \sum_{i=1}^r \sum_{j=1}^c \sum_{v=1}^N (x_{ijv} - \bar{x}_{ij.})^2$	$rc(N-1)$	$MS_1 = \frac{SS_1}{rc(N-1)}$	σ^2
Total	$SS_T = \sum_{i=1}^r \sum_{j=1}^c \sum_{v=1}^N (x_{ijv} - \bar{x}_{...})^2 \dots$	$rcN-1$	$MS_T = \frac{SS_T}{rcN-1}$	-----

(

(

	<u>Variance Ratio</u>	<u>df for F</u>
(a) Locations :	$F = \frac{MS_4}{MS_2}$	$(c-1, [r-1][c-1])$
(b) Times :	$F = \frac{MS_3}{MS_1}$	$(r-1, rc [N-1])$
(c) Interaction :	$F = \frac{MS_2}{MS_1}$	$([r-1][c-1], rc[n-1])$

The various hypotheses are accepted at the α level of significance if the computed F is less than the appropriate tabulated value of $F_{1-\alpha} (m, n)$ where M and n are the df as indicated above.

d. Computational Procedure

The quantities given in Table 8 are more conveniently calculated by the following equivalent computational procedure:

1. Calculate within cells totals W_{ij} where

$$W_{ij} = \sum_{v=1}^N x_{ijv}; \quad i = 1, 2, \dots, r \\ j = 1, 2, \dots, c \quad .$$

2. Calculate row totals R_i where

$$R_i = \sum_{j=1}^c W_{ij}; \quad i=1, 2, \dots, r \quad .$$

3. Calculate column totals C_j where

$$C_j = \sum_{i=1}^r W_{ij}; \quad j = 1, 2, \dots, c \quad .$$

4. Calculate overall total T:

$$T = \sum_{i=1}^r R_i = \sum_{j=1}^c C_j \quad .$$

5. Calculate "crude" total sum of squares (i.e., the original values squared as opposed to deviations from an appropriate mean value squared).

$$CSS_T = \sum_{i=1}^r \sum_{j=1}^c \sum_{v=1}^N x_{ijv}^2 \quad .$$

6. Calculate the correction factor due to the mean for transforming crude sums of squares to squared deviations about an appropriate mean value

$$CF = \frac{T^2}{rcN}$$

7. Calculate crude between column sum of squares

$$CSS_4 = \frac{1}{rN} \sum_{j=1}^c C_j^2 \quad .$$

8. Calculate crude between row sum of squares

$$CSS_3 = \frac{1}{cN} \sum_{i=1}^r R_i^2 \quad .$$

9. Calculate crude within cell sum of squares

$$CSS_W = \frac{1}{N} \sum_{i=1}^r \sum_{j=1}^c W_{ij}^2 \quad .$$

10. Calculate between column sum of squares

$$SS_4 = CSS_4 - CF \quad .$$

11. Calculate between rows sum of squares

$$SS_3 = CSS_3 - CR \quad .$$

12. Calculate total sum of squares

$$SS_T = CSS_T - CF \quad .$$

13. Calculate within cells sum of squares

$$SS_1 = CSS_T - CSS_W \quad .$$

14. Calculate interaction sum of squares

$$SS_2 = SS_T - SS_1 - SS_3 - SS_4 \quad .$$

15. Calculate mean squares

$$MS_1 = SS_1 / rc(N-1) \quad MS_3 = SS_3 / (r-1)$$

$$MS_2 = SS_2 / (r-1)(c-1) \quad MS_4 = SS_4 / (c-1) \quad .$$

The hypothesis of stationarity is accepted (at the α level of significance)
if

$$F = \frac{MS_3}{MS_1} < F_{1-\alpha} (r-1, rc[N-1]) \quad .$$

The hypothesis of no difference between the chosen locations is accepted if

$$F = \frac{MS_4}{MS_2} < F_{1-\alpha} (c-1, [r-1][c-1]) \quad .$$

The hypothesis of no interaction between time and location may also be tested. In many problems there is no physical reason to suspect any interaction. This hypothesis is accepted if

$$F = \frac{MS_2}{MS_1} < F_{1-\alpha} ([r-1][c-1], rc[N-1]) \quad .$$

2. COMPUTATIONAL EXAMPLE

The data listed in Table 9 represent actual experimental results outlined in Reference 21. The data are taken from a nonstationary process and the different locations represent repetitions of the experiment.

As can be seen from the data, $r = 5$, $c = 5$, and $v = 3$ for this example. Therefore, $rcN = 75$ for the total number of observations. Since the data involved here are nonstationary but equivalent from location to location, the hypothesis of stationarity should be rejected and the hypothesis of no difference between locations should be accepted. Also the hypothesis of no interaction between time and location should be accepted.

The calculations will now be performed in the exact sequence given in Paragraph C.1.d. of this section.

1. Within cells totals

$$W_{11} = 8.34 \quad W_{12} = 7.76 \quad W_{13} = 7.29 \quad W_{14} = 7.70 \quad W_{15} = 6.74$$

$$W_{21} = 9.00 \quad W_{22} = 7.47 \quad W_{23} = 7.72 \quad W_{24} = 7.44 \quad W_{25} = 6.26$$

TABLE 9. EXPERIMENTAL RESULTS

<div><div>c</div><div>r</div></div>		Location				
		1	2	3	4	5
Time Interval	1	3.54	2.36	2.55	2.50	2.32
		2.29	3.00	2.17	2.92	1.94
		2.51	2.40	2.57	2.28	2.48
	2	2.86	2.46	1.91	3.21	1.95
		2.87	2.68	3.10	2.14	1.92
		3.27	2.33	2.71	2.09	2.39
	3	1.97	3.98	2.24	2.24	3.32
		2.20	2.32	2.72	2.55	2.69
		3.04	2.28	1.76	2.62	3.00
	4	2.06	1.60	1.74	2.18	1.86
		1.52	2.00	1.62	1.66	2.73
		1.70	2.25	1.80	2.32	2.15
	5	2.22	2.02	1.90	2.05	2.00
		2.02	2.11	1.54	1.85	1.68
		1.82	2.43	2.51	1.79	1.76
Data from Reference 21, pp. 16-28, representing nonstationary data equivalent from point-to-point (experiment-to-experiment) r=5, c=5, v=3.						

$$W_{31} = 7.21 \quad W_{32} = 8.58 \quad W_{33} = 6.72 \quad W_{34} = 7.41 \quad W_{35} = 9.01$$

$$W_{41} = 5.28 \quad W_{42} = 5.85 \quad W_{43} = 5.16 \quad W_{44} = 6.16 \quad W_{45} = 6.74$$

$$W_{51} = 6.06 \quad W_{52} = 6.56 \quad W_{53} = 5.95 \quad W_{54} = 5.69 \quad W_{55} = 5.44$$

2. Row totals

$$R_1 = 37.83 \quad R_2 = 37.89 \quad R_3 = 38.93 \quad R_4 = 29.19 \quad R_5 = 29.70$$

3. Column totals

$$C_1 = 35.89 \quad C_2 = 36.22 \quad C_3 = 32.84 \quad C_4 = 34.40 \quad C_5 = 34.19$$

4. Overall total

$$T = 173.54$$

5. Crude total sum of squares

$$CSS_T = 420.0338$$

6. Correction factor due to mean

$$CF = 401.5484$$

7. Crude between columns and squares

$$CSS_4 = 402.0508$$

8. Crude between row sum of squares

$$CSS_3 = 407.7635$$

9. Crude within cell sum of squares

$$CSS_W = 411.5505$$

10. Between columns sum of squares

$$SS_4 = 402.0508 - 401.5484 = .5024$$

11. Between rows sum of squares

$$SS_3 = 407.7635 - 401.5484 = 6.2151$$

12. Total sum of squares

$$SS_T = 420.0338 - 401.5484 = 18.4854$$

13. Within cells sum of squares

$$SS_1 = 420.0338 - 411.5505 = 8.4833$$

14. Interaction sum of squares

$$SS_2 = 18.4854 - 15.2008 = 3.2846$$

15. Mean squares

$$MS_1 = \frac{8.4833}{50} = .16967 \quad MS_3 = \frac{6.2151}{4} = 1.5538$$

$$MS_2 = \frac{3.2846}{16} = .20529 \quad MS_4 = \frac{.5024}{4} = .12560$$

$$MS_T = \frac{18.4854}{74}$$

The results are displayed in Table 10.

Three values from a table of the F distribution are now necessary. The hypotheses will be tested at the $\alpha = 5$ percent level of significance. These values are $F_{.95}(4, 50) = 2.57$, $F_{.95}(4, 16) = 3.01$, and $F_{.95}(16, 50) = 1.86$.

TABLE 10. RESULTS

Source	Sum of squares	df	Mean Square	Expected Mean Square
Between Locations	.5024	4	.12560	$\sigma^2 + 3\sigma_\theta^2 + \frac{15}{4} \sum_{j=1}^5 h_j^2$
Between Times	6.2151	4	1.5538	$\sigma^2 + 15\sigma_g^2$
Interaction	3.2846	16	.20529	$\sigma^2 + 3\sigma_\theta^2$
Within Cells	8.4833	50	.16967	σ^2
Total	18.4854	74	.24980	-----

Test of hypothesis of stationarity:

$$F = \frac{MS_3}{MS_1} = \frac{1.5538}{.16967} = 9.1578 > F_{.95}(4, 50) = 2.57$$

Since the computed F is larger than $F_{.95}(4, 50)$, the hypothesis of stationarity is rejected at the 5 percent level of significance.

Test of hypothesis of no difference between locations:

$$F = \frac{MS_4}{MS_2} = \frac{.12560}{.20529} = .61182 < F_{.95}(4, 16) = 3.01.$$

Since the computed F is smaller than $F_{.95}(4, 16)$, the hypothesis of no difference between locations is accepted at the 5 percent level of significance.

Test of hypothesis of no interaction between time and location:

$$F = \frac{MS_2}{MS_1} = \frac{.20529}{.16967} = 1.2099 < F_{.95}(16, 50) = 1.86$$

Since the computed F is smaller than $F_{.95}(16, 50)$, the hypothesis of no interaction between time and location is accepted as expected at the 5-percent level of significance.

This concludes the computational example.

D. Interpretation and Application of Amplitude Probability Density Functions

1. FIRST-ORDER PROBABILITY DENSITY FUNCTIONS

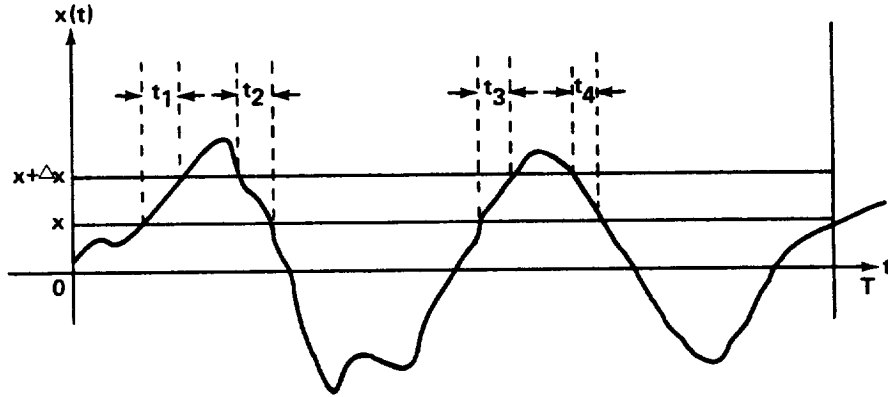
The first-order probability density function is defined in Section VIII. B.2 but will be repeated here for convenience. The general definition of a continuous probability density function in statistical terms is as follows. Let $r = r(\alpha)$ be a continuous random variable which is defined as a real valued function of α where the behavior of α is determined by chance. A (first-order) probability density function, $p_r(x)$, is defined by the condition,

$$p_r(x) dx = \text{Prob} [x < r(\alpha) < x + dx] \quad (94)$$

where x is a specific value of the random variable r . The probability density function $p_r(x)$ should not be confused with the (cumulative) probability distribution function $P_r(x)$ which is related to $p_r(x)$ by the equation

$$P_r(x) = \int_{-\infty}^x p_r(t) dt \quad (95)$$

For the case of a stationary random process, consider a single representative member, $x(t)$, of this process as follows:



An estimate of the probability that $x(t)$ assumes particular amplitude values between x and $(x + \Delta x)$ for a record of finite length T may be obtained from the ratio $\Delta t/T$ where Δt is the total time spent by $x(t)$ in the range $(x, x + \Delta x)$. In equation form

$$\text{Prob } [x < x(t) \leq x + \Delta x] \approx \frac{1}{T} \sum_{i=1}^k t_i = \frac{\Delta t}{T} \quad (96)$$

where t_i is the time spent by $x(t)$ in the range $(x, x + \Delta x)$ during its i th passage through this range. If one replaces $x(t)$ by R to distinguish between the random variable $R = x(t)$ and a special value x , then for small Δx one can define a (first-order) amplitude probability density function $p(x)$ such that

$$\text{Prob } [x < R \leq x + \Delta x] \approx p(x) \Delta x \quad (97)$$

It is understood that $p(x)$ in actuality also depends on R but this dependence is not noted in the interest of simplicity.

More precisely, one defines $p(x)$ by the limiting operation

$$p(x) = \lim_{\Delta x \rightarrow 0} \frac{\text{Prob}[x < R \leq x + \Delta x]}{\Delta x} = \lim_{\Delta x \rightarrow 0} \left[\lim_{T \rightarrow \infty} \frac{1}{T} \left(\frac{\Delta t}{\Delta x} \right) \right]. \quad (98)$$

In actual measurements one only works with finite T and nonzero Δx so that only the estimate given by equation 9.32 is obtained which contains associated statistical errors. (See Section VIII.D.1. for a discussion of these problems.)

In terms of $p(x)$, the mean value of $x(t)$ is given by

$$\bar{x} = \int_{-\infty}^{\infty} x p(x) dx. \quad (99a)$$

The mean square value is

$$\bar{x}^2 = \int_{-\infty}^{\infty} x^2 p(x) dx \quad (99b)$$

while the variance, or second moment about the mean, is

$$\sigma_x^2 = \int_{-\infty}^{\infty} (x - \bar{x})^2 p(x) dx = \bar{x}^2 - (\bar{x})^2. \quad (100)$$

The positive square root of the variance is called the standard deviation. Moments about the mean (central moments) of order higher than the second are defined in an exactly analogous way. If all moments of a probability distribution are known, then the distribution is completely specified. The amplitude probability distribution function is defined using equation (95).

a. Special Distributions

The application of amplitude probability density functions lies in the fact that if the function is completely known, certain probability statements of

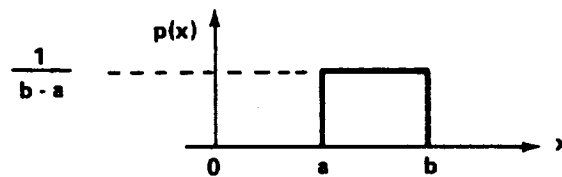
interest may be made which state where the amplitude of a signal may be expected to lie. Certain special density functions often occur in practice which allow quantitative probability statements to be easily made. Three of these will now be discussed.

1. Uniform (Rectangular) Distribution

One of the simplest probability density functions is the uniform or rectangular function. A random variable R is said to follow a uniform (or rectangular) distribution over the interval $(a < x < b)$ if its probability density function is given by

$$p(x) = \begin{cases} \frac{1}{b-a} & a \leq x \leq b \\ 0 & \text{otherwise} \end{cases} \quad (101)$$

See the drawing below.



The mean μ and variance σ^2 of this distribution are

$$\mu = \frac{a+b}{2} \quad (102)$$

$$\sigma^2 = \frac{(b-a)^2}{12} .$$

2. Normal (Gaussian) Distribution

The Gaussian probability density function is defined by the equation

$$p(x) = \frac{1}{\sigma \sqrt{2\pi}} e^{-\left(\frac{x-\mu}{\sigma}\right)^2} \quad (103)$$

and has a mean value μ and variance σ^2 . An important feature of this distribution is because it is completely characterized by its mean and variance since it may be shown that all higher moments are functions of the first and second. Probability statements are made in terms of the mean and standard deviation. For example, if μ and σ are known, then

$$\text{Prob } [x > \mu + 3\sigma] \approx .00135 \quad (104)$$

The normal distribution is tabulated in almost any statistics book. Since the mean and variance completely describe this distribution, if a set of experimental data may be assumed to be normally distributed, an estimate of the mean and variance obtained from this data is all that is needed to specify the distribution. A picture of the Gaussian probability density function appears in Section XIV.

3. Rayleigh (Radial Normal) Distribution

The Rayleigh probability density function is given by

$$p(x) = \begin{cases} (x/v^2) \exp(-x^2/2v^2) & , \quad x \geq 0 \\ 0 & , \quad x < 0 \end{cases} \quad (105)$$

This distribution is completely characterized by the parameter v . The mean of this distribution is $(\pi/2)^{\frac{1}{2}} v$ while the variance is $v^2 (4-\pi)/2$. The Rayleigh probability density function is not widely tabulated. However, the Rayleigh probability distribution function is simply an exponential function which is available. A picture of the Rayleigh probability density function appears in Section XIV.

B. Applications

1. Tests of Assumptions

A major reason for experimentally obtaining an estimate of an amplitude probability density function is to verify that some useful assumption about the theoretical form of the distribution is correct. For example, the assumption of the existence of a normal distribution is very often invoked in obtaining simple useful theoretical results. A plot of the amplitude density function can provide a visual, "quick look," verification of this assumption if the plot follows the symmetrical, bell-shaped form characteristic of the Gaussian density function. A quantitative method for more precisely testing this assumption based on the analog plot of the density function and the statistical errors associated with the measurements is given in Section 17 of Reference 21. If the data are available in a digital form, the chi-square test described in Section XIV.F provides an alternate quantitative method. Just being able to visually determine if the density function is unimodal (i.e., has a single peak) and monotonic on either side of this mode allows certain probability statements to be made. See Section 6.2.3 of Reference 20.

2. Range of Expected Variations

If a well-known density function can be assumed to properly fit the experimental data, then probability statements can usually be made in terms of the mean and standard deviation. However, if the data do not seem to be well represented by some theoretical distribution, then the probability statements may have to be derived directly from the observed density function.

For example, assume some piece of equipment must be mounted on a structure and relatively little clearance will be available. Also suppose that the structure will be subjected to random vibration and that amplitudes that would cause contact of the equipment with the surrounding equipment are unacceptable. It is then desirable to be able to estimate the probability of amplitudes occurring at any given instant which are great enough in magnitude to cause this contact. An experiment with the structure should then be performed and an experimental estimate of the amplitude probability density function obtained. If c is the amplitude that must not be exceeded, then one desires the probability

$$P(x < c) = \int_c^{\infty} p(x) dx \quad . \quad (106)$$

If this number is very small such that the probability of contact at any given instant is minimal, no further action is necessary. However, if the probability of contact is unacceptably large, corrective action must be taken. The probability given by equation (106) is over-simplified because an uncertainty in the estimate of the density function exists. This uncertainty is given by equation (25) and must be allowed for in an engineering application.

An exact analogous situation occurs if a piece of equipment is to be placed on a resilient mount and either bottoming of the mount is unacceptable or large enough amplitudes to cause striking of nearby equipment or structures is catastrophic. The procedure is precisely the same as described in the preceding paragraph and the amplitude probability density function is the crucial information.

Note, that for both the above applications, the probability statements are good for only a given instant of time. Other statements about the probability of exceeding a certain value within a certain length of time (e.g., a flight of T seconds) may be made if the distribution of extreme values of amplitude is considered.

3. Probability of Exceeding Specified Level

Narrow frequency bandwidth random vibration responses are characteristic of lightly damped structural systems with a single predominate mode of vibration; that is, single degree-of-freedom systems. For example, the response of a resiliently mounted piece of equipment to broad band random excitation will produce a narrow bandwidth random vibration response of the entire equipment on the mounts. The center frequency for the response will be the resonant frequency for the mounted equipment. Very often, continuous elastic structures may also be treated as a single degree-of-freedom systems for purposes of analysis to obtain approximate results for various dynamics problems. These matters are developed further in Paragraph F. of this section. It is only necessary to note here that a narrow frequency bandwidth vibration response is common in many engineering problems.

If the probability density function, $p(x)$, for a narrow frequency band response (output) is known, and if the instantaneous amplitude and velocity are assumed to be statistically independent, then the probability density function of the peak amplitudes, $p_p(x)$, may be computed [23] from the formula

$$p_p(x) = \frac{-p'(x)}{p(0)} \quad . \quad (107)$$

More directly, the probability of exceeding a critical peak amplitude, a_c , is given by the equation

$$\begin{aligned} P_p(a_c) &= \int_{a_c}^{\infty} p_p(x) dx = \text{Prob} [\text{positive peak value} \geq a_c] \\ &= \frac{p(a_c)}{p(0)} = \alpha_a \quad . \end{aligned} \quad (108)$$

If the frequency of a narrow band random vibration is f_r , the expected number of times that a peak with an amplitude greater than a_c will occur per second is

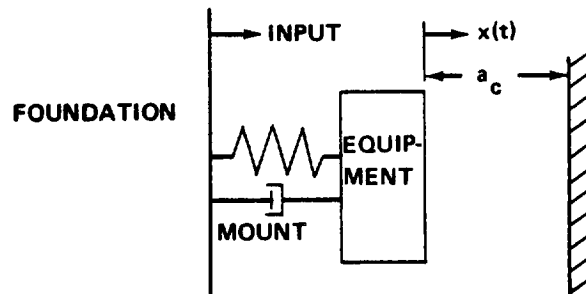
$$\bar{N}_a = \alpha_a f_r \quad . \quad (109)$$

Hence, the mean time between peaks (MTBP) with an amplitude greater than a_c is

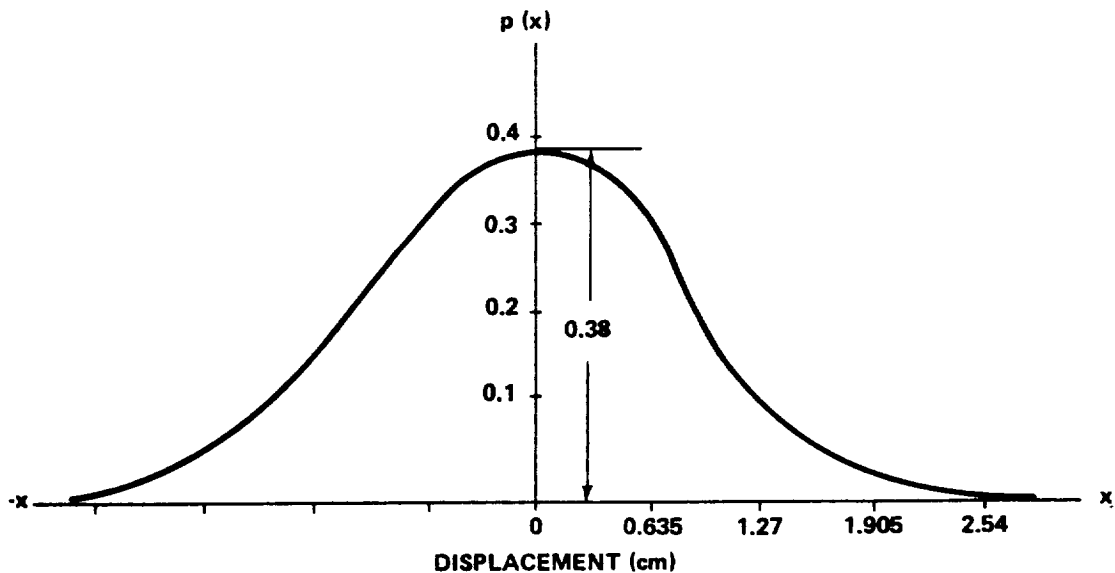
$$\text{MTBP} = \frac{1}{\alpha_a f_r} \quad . \quad (110)$$

If the occurrence of a peak greater than a_c is expected to be damaging, then it is clear that the MTBP for the critical peak amplitude should be very long.

To illustrate these points, consider the case of a resiliently mounted piece of equipment located in a flight vehicle where space is limited. The problem is to determine how much distance must be allowed between the equipment and the neighboring structure to minimize the likelihood of a collision. Assume that the resiliently mounted equipment is a single degree-of-freedom system (not necessarily linear) with a resonant frequency of about $f_r = 20$ Hz. Further assume that the vibration response displacements of the neighboring structure are negligible compared to the response displacements of the equipment. A model for the problem is shown below.



Now assume that the response displacement for the equipment has an rms value of 0.635 cm (0.25 inch) and a probability density function of the form shown below.



As seen from the drawing, the height of the probability density function $x = 0$ is $p(0) = 0.38$. From equations (108) and (109) the height of the probability density function at the critical displacement a_c is given by

$$p(a_c) = \alpha_a p(0) = \frac{p(0)}{(MTBP)f_r} = \frac{0.019}{MTBP}$$

where MTBP is the desired mean time between collisions in seconds.

The desired value for MTBP is a function of the total time which the equipment is exposed to vibration. Assume for this example that the flight vehicle is a missile where the total exposure time to pertinent vibration is 5 seconds. Further assume that an MTBP of 10 times the total exposure time is considered acceptable. Then, the desired MTBP is 50 seconds and the necessary value for $p(a_c)$ is

$$p(a_c) = 0.00038.$$

The critical displacement a_c may now be obtained directly from the probability density plot for the response displacement associated with a probability density of $p(a_c) = 0.00038$.

It should be noted that the actual measurement of probability density functions at extreme amplitudes involves a great deal of statistical uncertainty unless long experiments are performed. The accuracy of probability density measurements is discussed in Section VIII.0.1. In the drawing shown before, the final solution to the problem requires the determination of a displacement amplitude with a specific probability density based upon measured data. In reality, the resulting value for a_c would have confidence intervals associated with it because of the statistical uncertainties in the measurement of $p(x)$.

4. Fatigue Problems

Metal fatigue considerations also involve a direct application of the amplitude probability density function. In this case, amplitude is related to a stress level which in turn is related to fatigue damage. The application of

Miner's Rule is the usual method which essentially states that fatigue life is used up proportionately at the various stress levels. That is, if 10 000 cycles result in failure at stress level a_1 and 20 000 cycles result in failure at stress level a_2 , then either 5000 cycles at level a_1 or 10 000 cycles at stress level a_2 would use 50 percent of the fatigue life of the metal. Actually, the probability density function for peak amplitudes is critical for this problem. This is in fact one of the major applications of the Rayleigh distribution since it may be shown that a narrow band response with a Gaussian probability density function for its instantaneous amplitudes has a Rayleigh probability density function for its peak amplitudes. The fatigue problem is treated in greater depth in Section 9 of Reference 20.

2. JOINT PROBABILITY DENSITY FUNCTIONS

Consider a pair of records $R = x(t)$ and $S = y(t)$. Also consider the pair of events that R falls in the interval $(x, x + \Delta x)$ and, simultaneously, S falls in the interval $(y, y + \Delta y)$. The joint probability for the occurrence of these two may be estimated by determining the fraction of time per unit time that these two events coincide. For records of finite length T , this estimate is given by

$$\text{Prob}[x < R \leq x + \Delta x, y < S \leq y + \Delta y] \approx \frac{\Delta t}{T} \quad (111)$$

where Δt represents the amount of time that these two events coincide.

The joint probability density function $p(x, y)$ is then defined by the condition

$$\text{Prob}[x < R \leq x + \Delta x, y < S \leq y + \Delta y] \approx p(x, y) \Delta x \Delta y \quad (112)$$

The exact value is obtained by taking limits; that is,

$$p(x, y) = \lim_{\substack{\Delta x \rightarrow 0 \\ \Delta y \rightarrow 0}} \frac{\text{Prob}[x < R \leq x + \Delta x, y < S \leq y + \Delta y]}{(\Delta x)(\Delta y)} \quad (113)$$

$$p(x, y) = \lim_{\substack{\Delta x \rightarrow 0 \\ \Delta y \rightarrow 0}} \lim_{T \rightarrow \infty} \frac{\Delta t}{R(\Delta x)(\Delta y)} \quad (114)$$

It must be kept in mind that, in practice, T is finite and Δx , Δy are nonzero so that only an estimate of equation (114) is obtained which has associated statistical uncertainties.

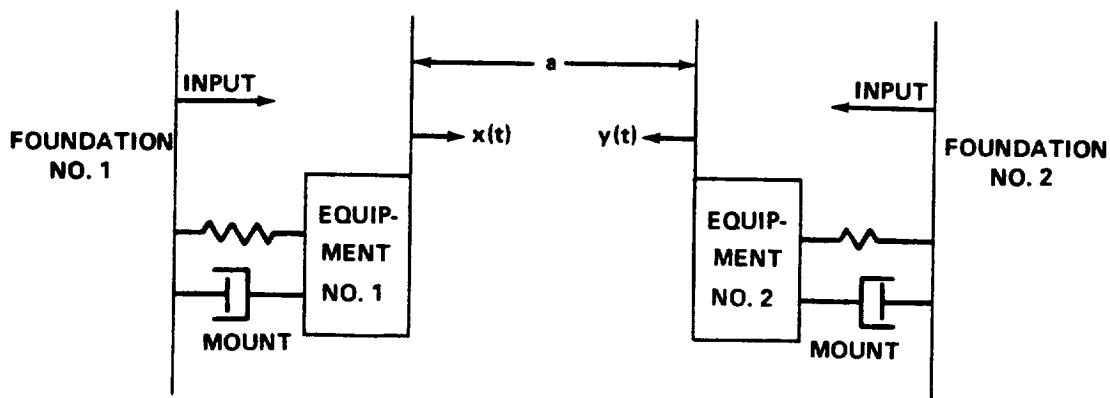
Application:

Analogous to the single variable case, the probability of $x(t)$ exceeding the level α and $y(t)$ exceeding the level β may be given by the relation

$$\text{Prob}[x > \alpha, y > \beta] = \int_{\beta}^{\infty} \int_{\alpha}^{\infty} p(x, y) dx dy \quad (115)$$

Joint density functions require much more effort to calculate and have not been widely applied in engineering practice. However, the applications for the single variable case can be easily extended.

Consider the example for first order density functions where one wants to evaluate the chance of a resiliently mounted piece of equipment contacting an obstructing structure when its mounting is randomly excited. Suppose the problem is extended to two pieces of equipment resiliently mounted and facing each other. See the drawing that follows.



The probability desired here is that $x + y$ exceeds a . This is given by

$$\text{Prob}[x + y > a] = 1 - \int_{-\infty}^a \int_{-\infty}^{a-y} p(x, y) dx dy \quad (116)$$

The double integral is taken to the left of the line $x + y = a$. This would have to be evaluated numerically if the density function is given as experimental results. Even if the density function was available in analytical form, the integration may have to be performed by numerical methods.

The lower limits of the integral in equation (116) are written as $-\infty$. However, as indicated in the drawing, there would be no amplitudes existing beyond the mounting surfaces. Therefore, the density function would be zero below these limits allowing one to write zero limits in equation (116).

If the density function is given digitally as a two-dimensional frequency histogram such as described in Section XIV, equation (116) could be easily evaluated. One merely needs to count the number of observations lying to the right of the line $x + y = a$. Results of analog displays would have to be arranged and interpreted in a similar manner.

3. CONDITIONAL PROBABILITY DENSITY FUNCTIONS

A conditional probability density function relates the occurrence of two events to the probability of occurrence of one of these events. In particular, for the pair of records $R = x(t)$ and $S = y(t)$ one may write equation (111) as

$$\begin{aligned} \text{Prob}[x < R \leq x + \Delta x, y < S \leq y + \Delta y] \\ = \text{Prob}[x < R \leq x + \Delta x] \cdot [\text{Prob } y < S \leq y \\ + \Delta y \mid x < R \leq x + \Delta x] \quad . \end{aligned} \quad (117)$$

In equation (117), $\text{Prob}[x < R \leq x + \Delta x]$ is the first-order probability of equation (97) while $\text{Prob}[y < S \leq y + \Delta y \mid x < R \leq x + \Delta x]$ is the conditional probability that S lies in the interval $(y, y + \Delta y)$ given that R lies in the interval $(x, x + \Delta x)$.

Analogous to equations (97) and (112), a conditional probability density function $p(y \mid x)$ may be estimated by

$$\text{Prob}[y < S \leq y + \Delta y \mid x < R \leq x + \Delta x] \approx p(y \mid x) \Delta y. \quad (118)$$

Assuming $p(x)$ to be different from zero, the analogy to the previous cases is extended and

$$p(y \mid x) = \lim_{\Delta y \rightarrow 0} \frac{\text{Prob}[y < S \leq y + \Delta y \mid x < R \leq x + \Delta x]}{\Delta y} = \frac{p(x, y)}{p(x)}. \quad (119)$$

Again, as in the previous cases, measurement of the conditional probability density function is subject to statistical uncertainties.

Applications:

The complete evaluation of $p(y \mid x)$ requires a tremendous amount of effort. This requires measurement of $\text{Prob}[y < S \leq y + \Delta y \mid x < R \leq x + \Delta x]$ for all intervals $\Delta x, \Delta y$ that cover the entire range of interest. This effectively amounts to the evaluation of a density function of y given any specific x and vice versa if $p(y \mid x)$ is desired. The evaluation is actually quite similar but somewhat more extensive than that of a joint density function.

The conditional probability density function might be applied to aid the interpretation of the autocorrelation behavior of a random process. For example, consider a random process $x(t)$, and let $y(t)$ be $x(t)$ delayed by some value τ ; that is, $y(t) = x(t + \tau)$. One can now obtain values of $p(y \mid x_0)$ as a function of τ for some fixed x_0 . For a specific value x_0 and a value of τ for which the autocorrelation function is relatively large, the variability of $p(y \mid x_0)$ would be comparatively small. This in effect allows the interpretation of the conditional probability in a predictive sense.

In a special case, the conditional probability can be computed directly. For example, assume the random process $x(t)$ has a normal density function with mean $\mu = 0$ and variance σ^2 . Assuming the process is stationary, then if $y(t) = x(t + \tau)$ is the second process, $y(t)$ will have mean value $\mu = 0$ and variance σ^2 also. The first-order normal density function $p(x)$ is given by equation (103) and the joint normal density function $p(x, y)$ is

$$p(x, y) = \frac{1}{2\pi\sigma_x\sigma_y\sqrt{1-\Gamma_{xy}^2}} \exp \left[\frac{1}{2(1-\Gamma_{xy}^2)} \left(\frac{x^2}{\sigma_x^2} - 2\frac{\Gamma_{xy}}{\sigma_x\sigma_y}xy + \frac{y^2}{\sigma_y^2} \right) \right] \quad (120)$$

where

$$\sigma_x^2 = E[x^2] \quad ; \quad \sigma_y^2 = E[y^2] \quad (121)$$

$$\Gamma_{xy} = \frac{E[xy]}{\sigma_x\sigma_y} \quad (122)$$

Letting $\Gamma = \Gamma_{xy}$, the conditional probability density for y given x is then

$$p(y|x) = \frac{p(x,y)}{p(x)} = \frac{1}{\sigma_y\sqrt{2\pi}\sqrt{1-\Gamma^2}} \exp \left[\frac{-1}{2(1-\Gamma^2)} \left(\frac{y}{\sigma_y} - \Gamma \frac{x}{\sigma_x} \right)^2 \right] \quad (123)$$

For the special case at hand $\sigma_x = \sigma_y = \sigma$ and equation (121) reduces to

$$p(y|x) = \frac{1}{\sigma\sqrt{2\pi}\sqrt{1-\Gamma^2}} \exp \left[\frac{-1}{2\sigma^2(1-\Gamma^2)} (y - \Gamma x)^2 \right] \quad (124)$$

The correlation coefficient Γ is the normalized value of the autocorrelation function evaluated at τ . Therefore, for a fixed x one can consider equation (120) as giving probability density functions for y as a function of τ .

Numerical Example

Assume that at $\tau = .5$ sec, $\Gamma = .80$. Assume also $x = 2\sigma$, and it is desired to find the probability that y lies between $y_1 = 1.95\sigma$ and $y_2 = 2.05\sigma$. For convenience, assume the variables have been standardized so that they have unit variance. One now wants to compute

$$\text{Prob}(1.95 < y \leq 2.05 | x) = \int_{1.95}^{2.05} p(y | x) dy$$

with $p(y | x)$ given by equation (124). This may be approximated numerically. First, for $y = 1.95$,

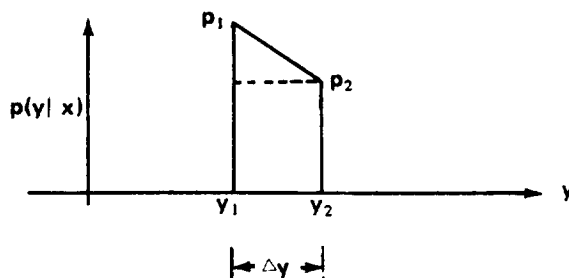
$$\begin{aligned} P_1 = p(1.95 | 2.00) &= \frac{1}{\sqrt{2\pi}\sqrt{.36}} \exp \left[\frac{-1}{2(.36)} (1.95 - 2.00[.80])^2 \right] \\ &= .66490 \exp [-.17014] \\ &= (.66490) (.84355) = .56088 \end{aligned}$$

Also, for $y = 2.05$

$$\begin{aligned} p_2 = p(2.05 | 2.00) &= .66490 \exp \left[\frac{-1}{.72} (2.05 - 2.00[.80])^2 \right] \\ &= .66490 \exp [-.28125] \\ &= (.66490) (.75484) = .50189 \end{aligned}$$

Now, the integral of equation (119) may be approximated by the following formula with $\Delta y = 0.10$ as shown in the drawing below. Note that area is essentially that of a trapezoid.

$$\int_{y_1}^{y_2} p(y | x) dy \approx (p_1 + p_2) \frac{\Delta y}{2}$$



Substituting the values for p_1 and p_2 computed above, one obtains

$$\text{Prob } (1.95 < y < 2.05 | 2.00) \approx (p_1 + p_2) \frac{\Delta y}{2}$$

$$= (.56088 + .50189) .05 = .053$$

Therefore, given $x = 2.00$, the probability of y lying in the interval 1.95 to 2.05 is approximately .053 or 5.3 percent.

E. Interpretation and Application of Correlation Functions

Correlation functions for random processes are divided into two types. First, the autocorrelation function which is obtained by correlating a record with itself, where one portion of the record is displaced in time relative to the second portion. The more general case, the cross-correlation function, is obtained by correlating two distinct random records, the second record of which is displaced in time relative to the first record. The cross-correlation function includes the autocorrelation function as a special case. In general, these functions depend both on the instant of time at which they are measured in addition to the time displacement. However, for stationary random

processes (that is, processes which are invariant under a translation of the time axis), the correlation functions depend only on the time displacement. The subsequent discussion and results hold only for stationary or for stationary ergodic random processes. The word "ergodic" indicating that time averages on one long record can replace ensemble (statistical) averages.

1. AUTOCORRELATION FUNCTIONS

Let $\{x_k(t)\}$ represent a random process and let angular brackets $\langle \rangle$ denote ensemble averages taken over the index k ; that is, averages of the functions making up the random process computed at a given time t . Also assume that the mean value of the process (and of each individual record) is zero. The autocorrelation function, $R_{xx}(\tau)$, of the stationary random process is then defined by

$$R_{xx}(\tau) = \langle x_k(t) x_k(t+\tau) \rangle \quad (125)$$

If the process is ergodic, the ensemble averages are replaced by time averages on a single member of the process, $x(t)$, and the autocorrelation function may be defined by the more practical formula below.

$$R_{xx}(\tau) = \overline{x(t)x(t+\tau)} = \lim_{T \rightarrow \infty} \frac{1}{T} \int_{-T/2}^{T/2} x(t) x(t+\tau) dt \quad (126)$$

In equation (126) the bar over $x(t)x(t+\tau)$ indicates time averaging. In practice, of course, only estimates of equation (126) can be obtained since T must be finite. This error and other inaccuracies give rise to basic statistical uncertainties in the measurement of $R_{xx}(\tau)$ which must be taken into account in interpreting experimentally obtained values of $R_{xx}(\tau)$. These statistical uncertainties are discussed in detail in Section VIII.D.2.

The definition given by equation (126) applies to random data. For periodic data, the infinite average is not necessary and the correlation function is defined by

$$R_{xx}(\tau) = \frac{1}{T} \int_{-T/2}^{T/2} x(t) x(t + \tau) dt \quad (127)$$

where the T is the period of $x(t)$. For example, assume $x(t)$ is a sine wave; that is,

$$x(t) = A \sin (2 \pi f_0 t + \theta) \quad (128)$$

where $T = 1/f_0$. The autocorrelation function for this case is given below.

$$\begin{aligned} R_{xx}(\tau) &= \frac{1}{T} \int_{-T/2}^{T/2} A^2 \sin (2 \pi f_0 t + \theta) \sin [2 \pi f_0 (t + \tau) + \theta] dt \\ &= \frac{A^2}{T} \int_{-T/2}^{T/2} \sin (2 \pi f_0 t + \theta) [\sin (2 \pi f_0 t + \theta) \cos (2 \pi f_0 \tau) \\ &\quad + \sin (2 \pi f_0 \tau) \cos (2 \pi f_0 t + \theta)] dt \\ &= \frac{A^2 \cos (2 \pi f_0 \tau)}{T} \int_{-T/2}^{T/2} \sin^2 (2 \pi f_0 t + \theta) \\ &\quad + \frac{A^2 \sin (2 \pi f_0 \tau)}{T} \int_{-T/2}^{T/2} \sin (2 \pi f_0 t + \theta) \cos (2 \pi f_0 t + \theta) dt . \end{aligned}$$

Now the integral of $\sin^2 (2 \pi f_0 t + \theta)$ taken over its period is $T/2$ while the integral of the product of the sine and cosine is zero due to their orthogonality. The final result is therefore

$$R_{xx}(\tau) = \frac{A^2}{2} \cos (2 \pi f_0 \tau) \quad . \quad (129)$$

For cases of narrow band noise in many physical problems, the autocorrelation function is often given by a damped exponential of the form

$$R_{xx}(\tau) = Ae^{-k|\tau|} \cos 2\pi f_0\tau \quad (130)$$

where A and k are positive constants. In the case of wide band noise, $R_{xx}(\tau)$ has a sharp maximum at $\tau = 0$ and falls off rapidly to zero on either side. Figure 62 gives an illustration of these three cases. Several properties of the autocorrelation function in general are useful in their interpretation and are noted here. Namely,

$$R_{xx}(-\tau) = R_{xx}(\tau) \quad (131)$$

$$|R_{xx}(\tau)| \leq R_{xx}(0) = \overline{x^2(t)} \text{ for all } \tau \quad (132)$$

If $x(t)$ is random, then

$$\lim_{\tau \rightarrow \infty} R_{xx}(\tau) = 0 \quad (133)$$

The correlation coefficient $\Gamma_{xx}(\tau)$, which lies between -1 and +1 is defined by

$$\Gamma_{xx}(\tau) = \frac{R_{xx}(\tau)}{R_{xx}(0)} \quad (134)$$

The coefficient $\Gamma_{xx}(\tau)$ gives a measure of the linear relation of $x(t)$ to $x(t + \tau)$. Therefore, the correlation function may be interpreted as giving a quantitative measure of the degree of linear dependence between a function and

itself measured τ time units later. One interpretation of $\Gamma_{xx}^2(\tau)$ is as follows. $\Gamma_{xx}^2(\tau)$ is that fraction of the variance of $x(t + \tau)$ which is attributable to the linear relation of $x(t + \tau)$ to $x(t)$. The quantity $[1 - \Gamma_{xx}^2(\tau)]$ is the fraction of the variance of $x(t + \tau)$ that is unexplained by $x(t)$ and is attributable to some other source.

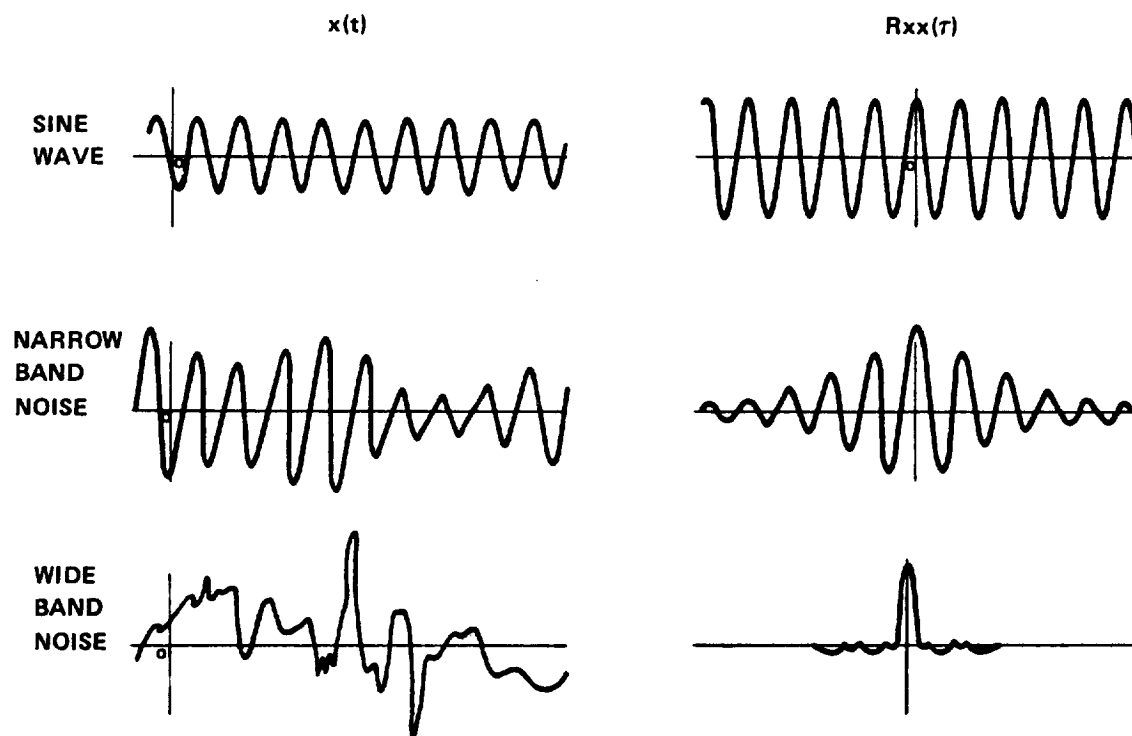


Figure 62. Illustration of typical autocorrelation functions.

2. CROSS-CORRELATION FUNCTIONS

Let $\{x_k(t)\}$ and $\{y_k(t)\}$ denote two stationary random processes. The cross-correlation function $R_{xy}(\tau)$ between $\{x_k(t)\}$ and $\{y_k(t)\}$ is then defined by

$$R_{xy}(\tau) = \langle x_k(t) y_k(t + \tau) \rangle \quad . \quad (135)$$

For ergodic processes the ensemble average of equation (135) may be replaced by a time average of single members of the processes and $R_{xy}(\tau)$ is alternatively defined by

$$R_{xy}(\tau) = \overline{x(t)y(t+\tau)} = \lim_{T \rightarrow \infty} \int_{-T/2}^{T/2} x(t)y(t+\tau) dt \quad . \quad (136)$$

As for the case of the autocorrelation function, statistical uncertainties will exist in any estimate of equation (136) due to finite averaging time and other inaccuracies. The same considerations discussed in Section VIII.D.2 for the autocorrelation function apply to the case of the cross-correlation function.

The relations given by equations (131), (132), and (133) for the autocorrelation function do not hold in general for the cross-correlation function. However, similar relations do exist and are given below.

$$R_{xy}(\tau) = R_{yx}(-\tau) \quad (137)$$

$$|R_{xy}(\tau)| \leq [R_{xx}(0) R_{yy}(0)]^{\frac{1}{2}} \text{ for all } \tau \quad ; \quad (138)$$

that is, $R_{xy}(\tau)$ is not an even function as is $R_{xx}(\tau)$, although when $x(t)$ and $y(t)$ are interchanged, symmetry about the vertical axis exists. Equation (138) is the analogous statement to equation (132), and, in fact, equation (132) is a special case of equation (138). An additional relation for the cross-correlation function is as follows:

$$|R_{xy}(\tau)| \leq \frac{1}{2} [R_{xx}(0) + R_{yy}(0)] \quad . \quad (139)$$

Note that this relation also will give equation (132) as a special case.

A cross-correlation coefficient may be defined which gives the simple correlation coefficient of equation (134) as a special case; that is,

$$\Gamma_{xy}(\tau) = \frac{R_{xy}(\tau)}{[R_{xx}(0) R_{yy}(0)]^{\frac{1}{2}}} \quad (140)$$

The quantity $\Gamma_{xy}(\tau)$ is bounded by +1 and -1 as can be seen by applying equation 9.74.

3. APPLICATIONS

Auto- and cross-correlation functions have been applied in the past to many different physical problems. Such areas have been involved as improving tracking radar reception, aircraft position finding, electroencephalogram analysis, and many facets of vibration data analysis. Two underlying features are fundamental to most applications. These are the determination of time delays and the determination of an underlying functional relationship resulting in large correlations.

(a) Example. Detection of Sine Wave in Noise (Autocorrelation)

As an example of detecting a functional relationship obscured by noise which is important to vibration analysis, the detection of a sine wave in noise will be illustrated. Assume the presence of a sinusoid $x(t) = A \sin 2\pi f_0 t$ with $A = 0.0254 \text{ cm}$ (.010 inch) and $f_0 = 100 \text{ Hz}$. Also assume narrow band noise, $n(t)$, is present at $f_0 = 100 \text{ cps}$ with a mean square value $A^2/2 = 32.258 \text{ cm}^2$ ($5 \times 10^{-5} \text{ in.}^2$). The autocorrelation function of the sinusoid is given by equation 9.65 which is $R_{xx}(\tau) = 32.258 \times 10^{-5} [\cos 2\pi(100)\tau] \text{ cm}^2$ for the example at hand. The autocorrelation function for narrow band noise for this example is assumed to be given by equation (130) which is $R_{nn}(\tau) = 5 \times 10^{-5} e^{-30\tau} \cos [2\pi(100)\tau]$. The constant c equals $32.258 \times 10^{-5} \text{ cm}^2$ ($5 \times 10^{-5} \text{ in.}^2$) since c must be the mean square value determined by letting $\tau = 0$. The constant k of equation (129) is arbitrarily assumed to be 30 rad/sec for this example which is a typical value.

Assume that $x(t)$ and $n(t)$ are independent. Then if $y(t) = x(t) + n(t)$, the autocorrelation function for $y(t)$ is given by

$$R_{yy}(\tau) = R_{xx}(\tau) + R_{nn}(\tau) \quad (141)$$

Since $R_{xx}(\tau)$ is a cosine function and $R_{nn}(\tau)$ is a cosine exponential which goes to zero as τ gets large, the $R_{xx}(\tau)$ term will dominate in equation (141) for large τ ; that is, the following equation holds.

$$\lim_{T \rightarrow \infty} \frac{R_{xx}(\tau)}{R_{yy}(\tau)} = 1 \quad (142)$$

One says that $R_{xx}(\tau)$ and $R_{yy}(\tau)$ are asymptotically equal. This means, that when the autocorrelation function is plotted, it will start to look like $R_{xx}(\tau)$ for large τ instead of decreasing to zero as pure noise would. This is illustrated in Figure 63 for the special case described. One should note that an actual autocorrelation plot would contain many irregularities due to statistical uncertainties and other inaccuracies. However, the basic underlying shape would appear as pictured in Figure 63.

(b) Example. Detection of Prominent Vibration Transmission Path
(Cross-correlation)

Assume that it is desired to attempt to determine whether the most prominent vibration response on a structure is a result of transmission via wave propagation through the structure or is due to acoustic transmission via the surrounding air. For simplicity in the example, it will be assumed that structural path lengths are great enough compared to the wave length of the vibration so that any structural transmission is by wave propagation (Fig. 64).

If the distance of transmission through the air is assumed to be 3.048 m 10 feet (and phase shifts at interfaces are ignored), a peak in the cross-correlation function $R_{xy}(\tau)$ would be expected at

$$\tau = \frac{3.048 \text{ m}(10 \text{ ft})}{304.8 \text{ m/sec}(1000 \text{ ft/sec})} = 0.01 \text{ sec}$$

where the speed of sound is taken to be approximately 304.8 m/sec (1000 feet per second).

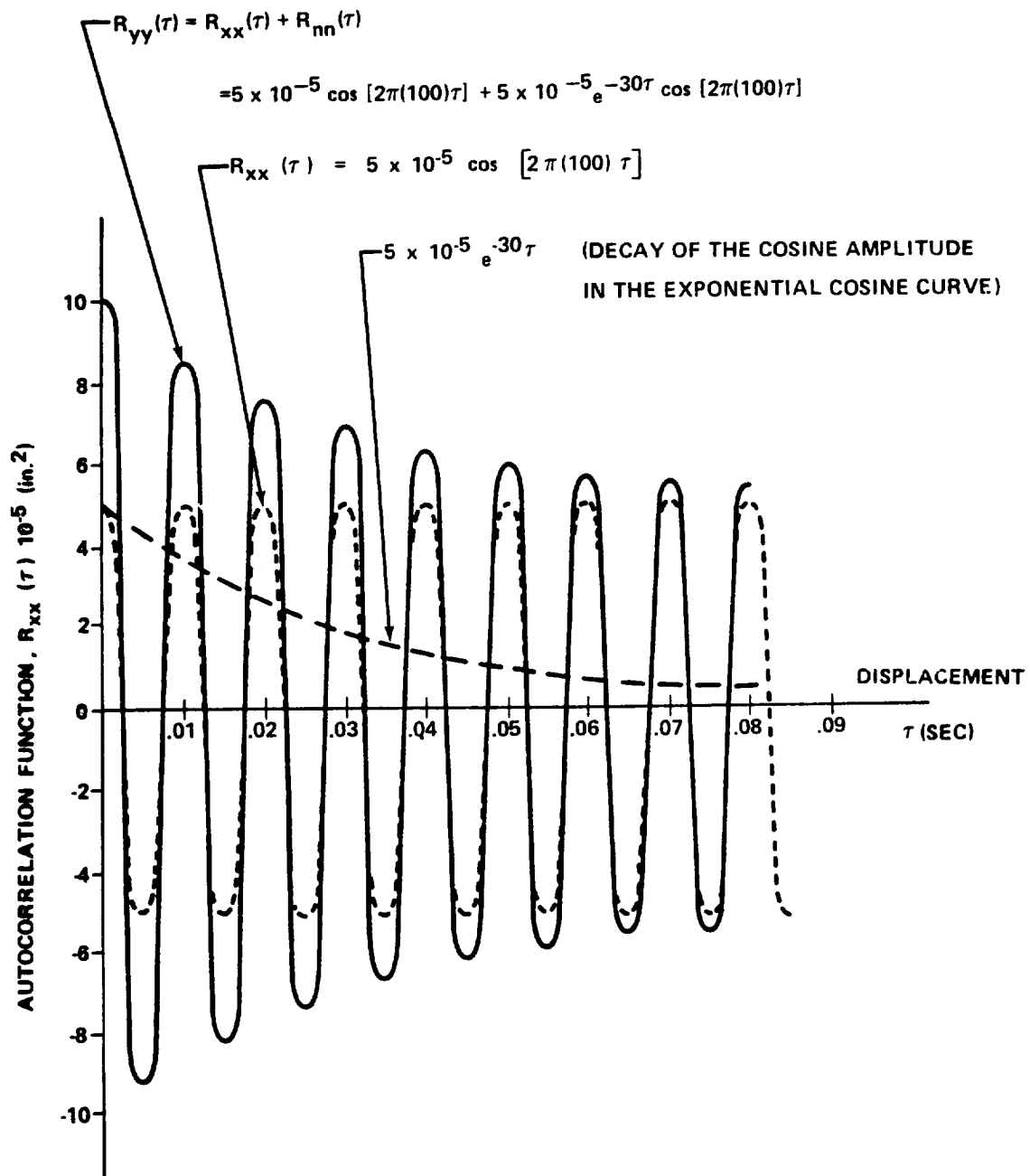


Figure 63. Autocorrelation function for sine wave plus noise.

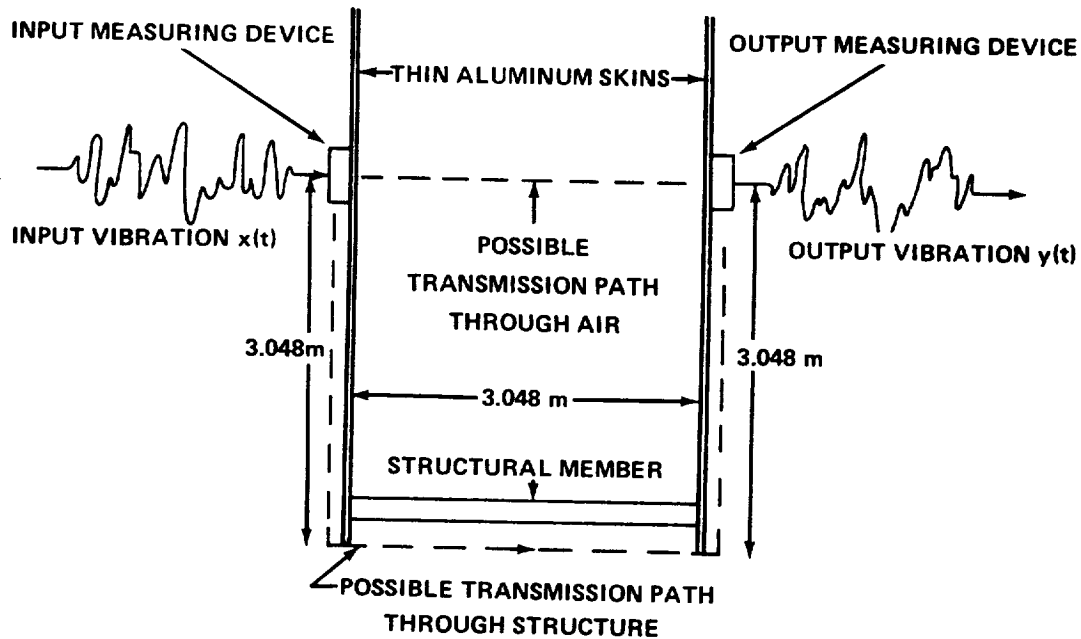


Figure 64. Transmission path determination example.

Wave propagation through the aluminum structure is assumed to occur at a speed of approximately 4572 m/sec (15 000 feet per second). Therefore, if significant vibration transmission occurs through the structure, a peak in the cross-correlation function $R_{xy}(\tau)$ would be expected at

$$\tau = \frac{9.144 \text{ m (30 ft)}}{4572 \text{ m/sec (15 000 ft/sec)}} = 0.002 \text{ sec}$$

since the structural path is 9.144 m (30 feet) long.

Suppose now that measurements of the input $x(t)$ and the output $y(t)$ are obtained. An estimate of the cross-correlation function, $R_{xy}(\tau)$, is then obtained via an approximation to equation (136). The cross-correlation function might then appear as pictured in Figure 65. The interpretation would be that a strong correlation exists between $x(t)$ and $y(t)$ at a delay of $\tau = .010$ second, indicating the major energy is being transmitted acoustically. A secondary peak appears at $\tau = .002$ second, indicating a weaker relation because of the direct transmission through the structure.

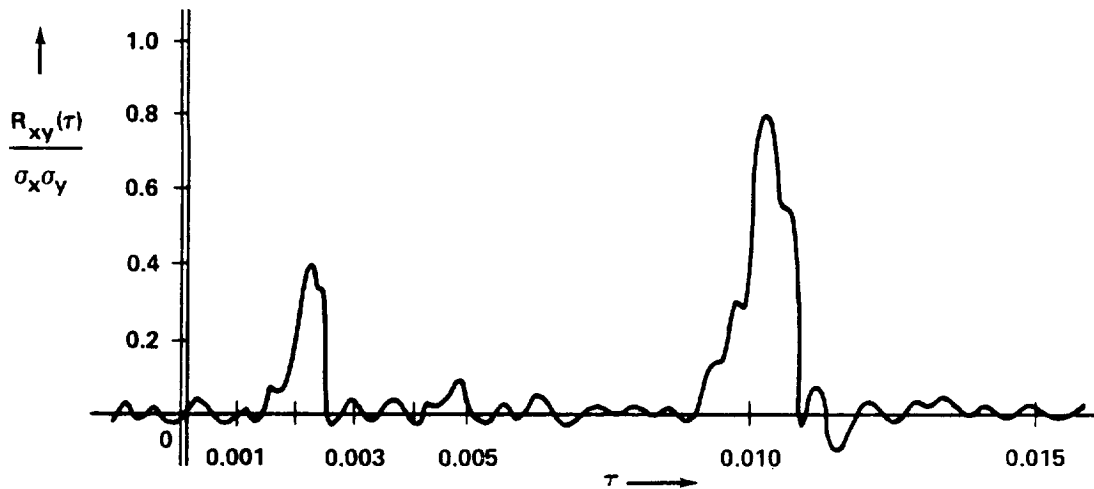


Figure 65. Possible normalized cross-correlation function for transmission path example.

The example given here greatly oversimplifies the problem, of course. A considerable amount of structural engineering analysis would be required to actually determine the structural response and its effect on transmission delays. Also, statistical analysis is required in the proper determination of the correlation function and its associated uncertainties. However, the basic approach to the problem would remain the same.

(c) Example. Detection Theory

A more theoretical application of correlation techniques arises in detection theory. If it is assumed that a given input signal is obscured by white noise, it can be shown that the optimum linear filter takes the form of a correlator except for a constant factor. In this situation the input which consists of signal plus white noise is multiplied by a stored version of the signal it is desired to detect. This gives the optimum output where maximum output signal-to-noise power ratio is the optimization criteria.

F. Interpretation and Application of Power Spectral Density Functions

The ordinary and cross-power spectral density functions are important concepts for both practical vibration data analysis problems and for theoretical structural analysis problems. In a theoretical context, the areas of application for power spectra are effectively the same as for correlation functions, since the two properties for stationary vibration data are Fourier transform pairs.

However, in a practical context, the frequency format of power spectra is easier to interpret for many applications, just as the time format of correlation functions is easier to interpret for certain applications discussed in Paragraph E. of this section.

Ordinary and cross-power spectra are discussed here primarily in terms of their relationships to idealized structures. Hence, it is appropriate to first review the dynamic characteristics of idealized structures before proceeding.

1. RESPONSE CHARACTERISTICS FOR IDEALIZED STRUCTURES

An idealized structure is defined as one which has constant parameters, and is linear between two points of interest called the excitation (input) point and the response (output) point. A structure has constant parameters if all fundamental properties such as mass, stiffness, damping, and geometry are invariant with time, and the surrounding environment. A structure is linear if the response characteristics are additive and homogeneous. The term additive means that the response to a sum of excitations is equal to the sum of the responses to the individual excitations. The term homogeneous means that the response to a constant times the excitation is equal to the constant times the response to the excitation.

Given an idealized structure, the weighting function $h(\tau)$ associated with the structure is defined as the response (output function) of the idealized structure to a unit impulse input function and is measured as a function of time, τ , from the moment of occurrence of the impulse input. For physically realizable systems, it is necessary that $h(\tau) = 0$ for $\tau < 0$ since the response must follow the input. The usefulness of the concept of the weighting function is because of the following: an idealized structure is completely characterized by its weighting function in the sense that given any arbitrary input as a function of time $x(t)$ and known for all t , the system output $y(t)$ is determined by the equation

$$y(t) = \int_0^{\infty} h(\tau) x(t - \tau) d\tau \quad ; \quad (143)$$

that is, the value of the output function, $y(t)$, at time t is given as a weighted linear (infinite) sum over the entire past history of the input $x(t)$.

If $x(t)$ is an input to the structure for only a finite fixed time T , then

$$y(t) = \int_0^T h(\tau) x(t - \tau) d\tau \quad . \quad (144)$$

If $x(t)$ exists only for $t \geq 0$, then

$$y(t) = \int_0^t h(\tau) x(t - \tau) d\tau \quad (145)$$

since

$$\int_t^\infty h(\tau) x(t - \tau) d\tau = 0 \quad ;$$

that is, for $t - \tau < 0$, or $\tau > t$, $x(t - \tau) = 0$. Hence the above equation.

The idealized structure may alternatively be characterized by its frequency response function $H(f)$ which is defined as the Fourier transform of $h(\tau)$,

$$H(f) = \int_0^\infty h(\tau) e^{-j2\pi f\tau} d\tau \quad (146)$$

where f is measured in cycles per unit time. The lower limit is zero instead of $-\infty$ since $h(\tau) = 0$ for $\tau < 0$. The replacement of the weighting function with the frequency response function may be made since there is a one-to-one correspondence between classes of suitably restricted functions and their Fourier transforms; that is, two different weighting functions will not give the same frequency response function. The restrictions on $h(\tau)$ are that $h(\tau)$ and its derivative $h'(\tau)$ must be piecewise continuous on every finite interval (a, b) , and that $|h(\tau)|$ must be integrable on $(-\infty, \infty)$. It should be noted that the frequency response function is a special case of the transfer function of a structure given by the Laplace transform of $h(\tau)$ in which case $e^{-j2\pi f\tau}$ in equation (146) is replaced by $e^{-p\tau}$ where p is a general complex variable.

The frequency response function is of great interest since it contains amplitude magnification and phase shift information. Since $H(f)$ is complex valued, the complex exponential (polar) notation may be used; that is,

$$H(f) = |H(f)| e^{j\phi(f)} \quad (147)$$

where $|H(f)|$ is the absolute value of $H(f)$ and $\phi(f)$ the argument of $H(f)$. The absolute value $|H(f)|$, which is often called the gain factor, measured the amplitude magnification when the input to the structure is a sinusoid while the angle $\phi(f)$, which is often called the phase factor, gives the corresponding phase shift.

This result may be easily seen by consideration of the complex input

$$\begin{aligned} x(t) &= a e^{j2\pi ft} = A e^{j\theta} e^{j2\pi ft} \\ &= A \cos(2\pi ft + \theta) + j A \sin(2\pi ft + \theta) \end{aligned} \quad (148)$$

Note that the real part of equation (148), $A \cos(2\pi ft + \theta)$ is a general sinusoidal input with amplitude A and a phase angle θ with respect to some time origin. By definition, an idealized structure is linear which implies the real part of the output response is due to only the real part of the input excitation, and likewise for the imaginary parts. Hence, any result obtained for the complex function contains the same result for the real part of the function as a special case. These facts allow the concrete physical interpretation to be placed on the frequency response function of equation (147), even though it is a complex valued quantity.

Substituting equation (148) into equation (143) gives

$$\begin{aligned} y(t) &= \int_0^{\infty} h(\tau) a e^{j2\pi f(t-\tau)} d\tau \\ &= a e^{j2\pi ft} \int_0^{\infty} h(\tau) e^{-j2\pi f\tau} d\tau \\ &= x(t) H(f) \end{aligned}$$

or, once can write

$$y(t) = A |H(f)| e^{j[2\pi ft + \theta + \phi(f)]} \quad (149)$$

which illustrates the amplification by the gain factor $|H(f)|$ and phase shift by the phase factor $\phi(f)$ of the sinusoidal input.

Certain other symmetry properties are worthwhile to note, namely,

$$H^*(f) = \int_0^\infty h(\tau) e^{j2\pi f\tau} d\tau = H(-f) \quad (150)$$

where $H^*(f)$ is the complex conjugate of $H(f)$. Also, this relation gives

$$H^*(f) = |H(f)| e^{-j\phi(f)}$$

$$H(-f) = |H(-f)| e^{j\phi(-f)}$$

which implies

$$|H(f)| = |H(-f)| \quad (151)$$

and

$$-\phi(f) = \phi(-f) \quad (152)$$

Another important relationship is that given the input $x(t)$, the weighting function $h(t)$, and output $y(t)$, then

$$Y(f) = H(f) X(f) \quad (153)$$

where $Y(f)$ and $X(f)$ are the Fourier transforms of $y(t)$ and $x(t)$, respectively. This may be shown directly as follows.

$$Y(f) = \int_{-\infty}^{\infty} \left[\int_{-\infty}^{\infty} h(\tau) x(t - \tau) d\tau \right] e^{-j2\pi ft} dt$$

Now, multiplying and dividing by $e^{-j2\pi f\tau}$ and rearranging terms gives

$$Y(f) = \left(\int_{-\infty}^{\infty} h(\tau) e^{-j2\pi f\tau} d\tau \right) \int_{-\infty}^{\infty} x(t - \tau) e^{-j2\pi f(t - \tau)} dt$$

The desired result is obtained by the change of variable $u = t - \tau$ and $du = d\tau$ in the righthand integral.

The following important fact is seen immediately. If one idealized structure described by $H_1(f)$ is followed in succession by another idealized structure described by $H_2(f)$ where the second structure does not load the first, then the overall structure is described by $H(f)$ where

$$H(f) = H_1(f) H_2(f)$$

This is true since

$$Y(f) = H_1(f) X(f)$$

and

$$Z(f) = H_2(f) Y(f) = H_2(f) [H_1(f) X(f)]$$

$$= [H_2(f) H_1(f)]$$

$$= H(f) X(f)$$

This implies that

$$| H(f) | = | H_1(f) | | H_2(f) |$$

$$\phi(f) = \phi_1(f) + \phi_2(f) \quad (154)$$

so that in cascaded idealized structures, the gain factors multiply and the phase factors add when it is assumed that the two structures are decoupled.

Note that use is often made of the complex exponential notation since it conveniently displays amplitude magnification and phase shift information. This is merely polar coordinate notation in the complex plane, however, under certain conditions the $x = u + iv$ form of notation may conveniently illustrate certain information in a useful manner. In this case, $\text{Re}(x) = u$ and $\text{Im}(x) = v$ are defined as the real and imaginary parts of the complex variable x . This alternative interpretation is illustrated in the material which follows.

2. IDEALIZED STRUCTURE WITH MOTION EXCITATION

Consider the case of a structure which is subjected to a foundation motion excitation. Assume that the structure can be represented by a simple linear lumped parameter system consisting of a mass, spring, and dashpot as shown in Figure 66.

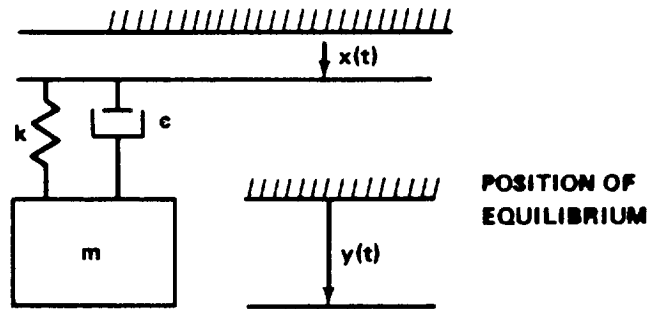


Figure 66. Idealized structure with motion excitation.

In Figure 66, k is the spring constant in N/m, c is the viscous damping coefficient in Ns/m, and m is the mass in kg-sec²/inch. The term $x(t)$

is the excitation measured in any units of motion desired (displacement, velocity, acceleration, strain, etc.), and $y(t)$ is the response measured in the same units. The model in Figure 66 might represent some secondary structure in a flight vehicle (simplified to only one degree-of-freedom) which is subjected to random vibration of a primary supporting structure. The problem is to determine an appropriate frequency response function for this model.

From basic dynamics, the sum of all forces acting on the mass in Figure 66 must equal zero; that is,

$$F_k(t) + F_c(t) + F_m(t) = 0 \quad (155)$$

where

$$\begin{aligned} F_k(t) &= -k [y(t) - x(t)] &&= \text{spring force} \\ F_c(t) &= -c [\dot{y}(t) - \dot{x}(t)] &&= \text{damping force} \\ F_m(t) &= -m \ddot{y}(t) &&= \text{inertial force} \\ \dot{y}(t) &= dy(t)/dt &&= \text{velocity} \\ \ddot{y}(t) &= d^2y(t)/dt^2 &&= \text{acceleration} \end{aligned}$$

Now assume the foundation motion is sinusoidal such that $x(t) = X_1 \sin 2\pi ft$. It will be more convenient here to use complex numbers instead of trigonometric functions. From the identity, $e^{j\theta} = \cos \theta + j \sin \theta$, it follows that a sinusoidal function may be expressed by $\sin \theta = \text{Im} [e^{j\theta}]$. Using this notation, the assumed foundation motion is

$$x(t) = \text{Im} [X_1 e^{j2\pi ft}] \quad (156)$$

From equations (155) and (156), the resulting equation of motion for the structure is as follows:

$$m \ddot{y}(t) + c \dot{y}(t) + ky(t) = \text{Im} [(k + j2\pi fc) X_1 e^{j2\pi ft}] \quad (157)$$

The particular solution to equation (157) will yield the desired steady state response $y(t)$.

Now assume a solution to equation (157) in the general form of a sinusoidal response as follows:

$$y(t) = Y_1 \sin(2\pi ft + \phi) = \text{Im} [Y_1 e^{j(2\pi ft + \phi)}] \quad (158)$$

Here Y_1 is the peak value of the response and ϕ is the phase angle between the response and the sinusoidal excitation. When equation (158) is substituted into equation (157), the following relationship is obtained:

$$\begin{aligned} & \text{Im} [-(2\pi f)^2 m + j2\pi fc + k] Y_1 e^{j(2\pi ft + \phi)} \\ &= \text{Im} [(k + j2\pi fc) X_1 e^{j2\pi ft}] \end{aligned} \quad (159)$$

Hence, the particular solution to equation (157) is given from equations 9.94 and (159) as follows:

$$y(t) = \text{Im} \left[\frac{(k + j2\pi fc) X_1 e^{j2\pi ft}}{k - (2\pi f)^2 m + j2\pi fc} \right] \quad (160)$$

It is desirable to write equation (160) in a different form by introducing two definitions

$$\zeta = \frac{c}{c_c} \quad \text{where} \quad c_c = 2\sqrt{km} \quad (161a)$$

$$f_n = \frac{1}{2\pi} \sqrt{\frac{k}{m}} \quad (161b)$$

The term c_c in equation (161a) is called the "critical damping coefficient" and the ratio ζ is called the "damping ratio." The term f_n in equation (161b) is called the "undamped natural frequency." When the relationships in equation (161) are substituted into equation (160), the following result is obtained:

$$y(t) = \text{Im} \left[\frac{\left(1 + j2\zeta \frac{f}{f_n}\right) X_1 e^{j2\pi ft}}{1 - \left(\frac{f}{f_n}\right)^2 + j2\zeta \frac{f}{f_n}} \right] \quad (162)$$

When equation (162) is converted from complex notation to trigonometric notation, the following result is obtained.

$$y(t) = \frac{\sqrt{1 + \left[2\zeta \frac{f}{f_n}\right]^2} X_1 \sin(2\pi ft + \phi)}{\sqrt{\left[1 - \left(\frac{f}{f_n}\right)^2\right]^2 + \left[2\zeta \frac{f}{f_n}\right]^2}} \quad (163a)$$

where

$$\phi = -\arctan \left[\frac{2\zeta \left(\frac{f}{f_n}\right)^3}{1 - \left(\frac{f}{f_n}\right)^2 + 4\zeta^2 \left(\frac{f}{f_n}\right)^2} \right] \quad (163b)$$

Note next that the frequency response function for this problem may be written as

$$H(f) = |H(f)| e^{j\phi(f)},$$

where the gain factor $|H(f)|$ is given by the ratio of the response amplitude to the excitation amplitude, and the phase factor $\phi(f)$ is given by the phase shift between the response and excitation. Hence, from equations (158) and (163b), the gain factor $|H(f)|$ is given by

$$|H(f)| = \frac{Y_1}{Y_1} = \frac{1 + \left[2\zeta \frac{f}{f_n} \right]^2}{\sqrt{\left[1 - \left(\frac{f}{f_n} \right)^2 \right]^2 + \left[2\zeta \frac{f}{f_n} \right]^2}} \quad (164)$$

and $\phi(f)$ is as given by equation (163b). The general result is illustrated in Figure 67.

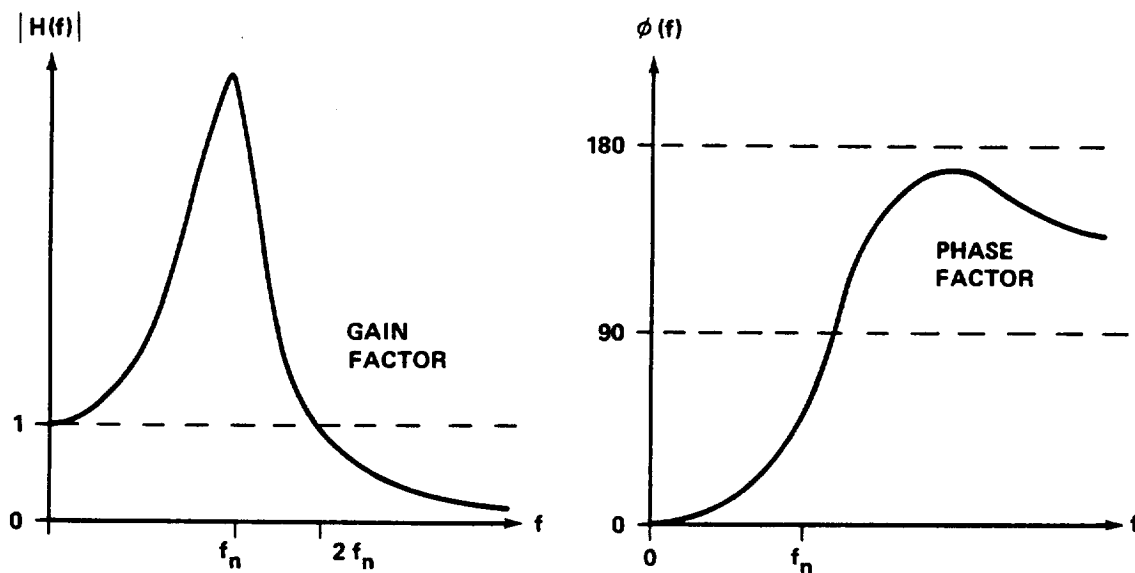


Figure 67. Gain and phase factors for frequency response functions.

The frequency response function $H(f)$ for this problem may also be written directly from equation (162) in the following form. This is often called the "transmissibility function" for the single degree-of-freedom system.

$$H(f) = \frac{1 + j2\zeta \frac{f}{f_n}}{1 - \left(\frac{f}{f_n}\right)^2 + j2\zeta \frac{f}{f_n}} \quad (165)$$

Equation (165) may be written as a complex number $w = u + iv$, where the real and imaginary parts are as follows:

$$H(f) = \text{Re} [H(f)] + j \text{Im} [H(f)] \quad (166)$$

where

$$\text{Re}[H(f)] = \frac{1 - \left(\frac{f}{f_n}\right)^2 + \left(2\zeta \frac{f}{f_n}\right)^2}{\left[1 - \left(\frac{f}{f_n}\right)^2\right]^2 + \left[2\zeta \frac{f}{f_n}\right]^2} \quad (166a)$$

$$\text{Im}[H(f)] = \frac{-2\zeta \left(\frac{f}{f_n}\right)^3}{\left[1 - \left(\frac{f}{f_n}\right)^2\right]^2 + \left(2\zeta \frac{f}{f_n}\right)^2} \quad (166b)$$

The general result for this type of presentation is illustrated in Figure 68.

There are other frequency response functions which are applicable to a simple idealized structure for different interpretations which should not be confused with the transmissibility function of equation (165). For example, assume the response parameter of interest in Figure 66 is the relative motion $z(t) = y(t) - x(t)$. The appropriate frequency response function which relates a motion excitation $x(t)$ to a relative motion response $z(t)$ is as follows:

$$H(f) = \frac{(f/f_n)^2}{1 - \left(\frac{f}{f_n}\right)^2 + j2\zeta \frac{f}{f_n}} \quad (167)$$

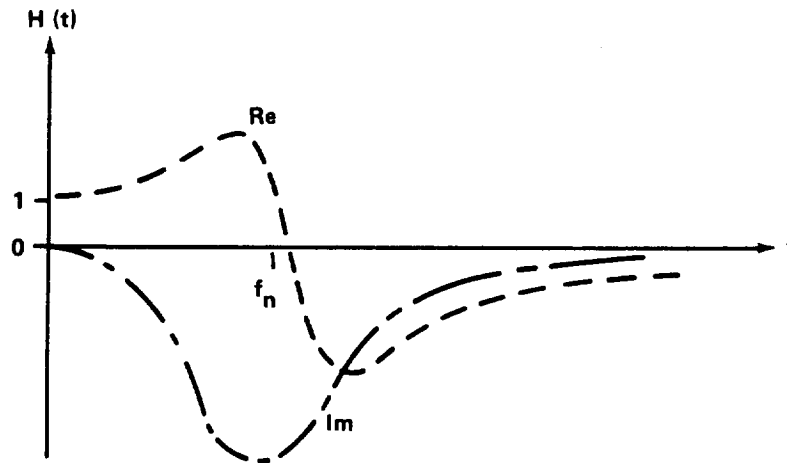


Figure 68. Real and imaginary parts for frequency response function.

For a second different example, assume the response of a simple structure to a force excitation is of interest, as illustrated in Figure 69.

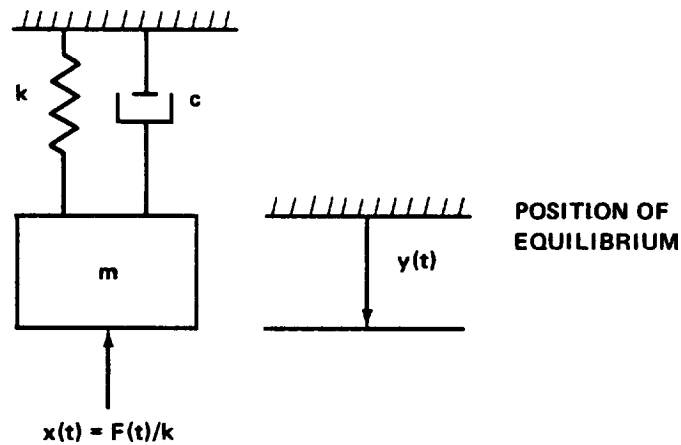


Figure 69. Simple idealized structure with force excitation.

Here, the excitation $x(t)$ is a force excitation which is normalized to displacement units, and $y(t)$ is the response displacement. The appropriate frequency response function which relates a force excitation $x(t)$ to a absolute response displacement $y(t)$ is then as follows:

$$H(f) = \frac{1}{1 - \left(\frac{f}{f_n}\right)^2 + j2\zeta \frac{f}{f_n}} \quad (168)$$

3. ORDINARY POWER SPECTRAL DENSITY FUNCTIONS

Given a stationary random vibration record $y(t)$ of length T seconds the ordinary power spectral density function $G_y(f)$ is defined in Section VIII.B.2.C. as follows:

$$G_y(f) = \lim_{T \rightarrow \infty} \lim_{\Delta f \rightarrow 0} \frac{1}{T(\Delta f)} \int_0^T y_{\Delta f}^2(f, t) dt \quad (169)$$

The quantity $y_{\Delta f}^2(f, t)$ is the square of the instantaneous amplitude within the narrow frequency interval between f Hz and $f + \Delta f$ Hz.

One must be careful in the interpretation of equation (169) in that, although it is a physically appealing definition, there are frequency filtering operations implied in the definition of the quantity $y_{\Delta f}^2(f, t)$ which are not explicitly indicated in the definition of $G_y(f)$. The definition of the spectral density given by equation (169) is very satisfactory from the measurement point of view in that it describes a direct physical approach to obtaining $G_y(f)$. Of course, T will always be finite and Δf will be nonzero in actual practice. These matters are discussed in detail in Section VIII.D.3.

A definition more appropriate in analytical studies is obtained by considering the Fourier transform of the autocorrelation function $R_y(\tau) \equiv R_{yy}(\tau)$. See paragraph D. of this section for a definition of $R_y(\tau)$. To be specific, define a function $S_{yy}(f) \equiv S_y(f)$ where f ranges over $-\infty < f < \infty$ by the relation

$$S_y(f) = \int_{-\infty}^{\infty} e^{-j2\pi f\tau} R_y(\tau) d\tau \quad . \quad (170)$$

Equation (170) may be simplified by the following procedure:

$$\begin{aligned} \int_{-\infty}^{\infty} e^{-j2\pi f\tau} R_y(\tau) d\tau &= \int_{-\infty}^{\infty} R_y(\tau) \cos 2\pi f\tau d\tau \\ &\quad - j \int_{-\infty}^{\infty} R_y(\tau) \sin 2\pi f\tau d\tau \quad . \end{aligned} \quad (171)$$

Use the fact now that $R_y(\tau)$ is an even function and $\sin 2\pi f\tau d\tau$ is an odd function. That is, $R_y(\tau) = R_y(-\tau)$ and $\sin 2\pi(-\tau) = -\sin 2\pi f\tau$. Then, the imaginary term in equation (171) is zero since it is the integral of an odd function between symmetric limits. This is shown mathematically by

$$\begin{aligned} \int_{-\infty}^{\infty} R_y(\tau) \sin 2\pi f\tau d\tau &= \int_{-\infty}^{\infty} R_y(\tau) \sin 2\pi f\tau d\tau + \int_0^{\infty} R_y(\tau) \sin 2\pi f\tau d\tau \\ &= \int_0^{\infty} R_y(-\tau) \sin 2\pi f(-\tau) d\tau \\ &\quad + \int_0^{\infty} R_y(\tau) \sin 2\pi f\tau d\tau = 0 \quad . \end{aligned}$$

Therefore,

$$S_y(f) = \int_{-\infty}^{\infty} R_y(\tau) \cos 2\pi f\tau d\tau \quad (172)$$

The quantity $S_y(f)$ is a two-sided mathematical idealization which covers the frequency interval from minus infinity to plus infinity. Note that $S_y(f)$ is actually fictitious since negative frequencies are physically unrealizable. However, $S_y(f)$ is related to the physically realizable one-sided power spectral density function $G_y(f)$ which exists only for $f \geq 0$ as follows.

Define

$$\begin{aligned} G_y(f) &= S_y(f) + S_y(-f) = 2S_y(f) \quad \text{for } f \geq 0 \\ &= 0 \quad \text{for } f < 0 \end{aligned} \quad (173)$$

Then, the following relationship is true:

$$G_y(f) = 4 \int_0^{\infty} R_y(\tau) \cos 2\pi f\tau \, d\tau \quad (174)$$

The equivalence of equations (169) and (174) is proved in Reference 24. These equivalent relationships are fundamental to the proper interpretation and application of power spectral density functions, as will now be shown.

Consider an idealized structure with a weighting function $h(\tau)$. If an excitation of $x(t)$ is applied to the structure, the response $y(t)$ is given by

$$y(t) = \int_{-\infty}^{\infty} h(\tau) x(t - \tau) \, d\tau \quad (175)$$

Then, the power spectrum for the response is as follows:

$$S_y(f) = \int_{-\infty}^{\infty} e^{-2\pi f\tau} R_y(\tau) \, d\tau = \int_{-\infty}^{\infty} e^{-2\pi f\tau} E[y(t) y(t + \tau)] \, d\tau$$

$$\begin{aligned}
&= \int_{-\infty}^{\infty} \int_{-\infty}^{\infty} \int_{-\infty}^{\infty} e^{-2\pi f \tau} h(\alpha) h(\beta) E[x(t-\alpha) x(t+\tau-\beta)] d\alpha d\beta d\tau \\
&= \int_{-\infty}^{\infty} \int_{-\infty}^{\infty} \int_{-\infty}^{\infty} h(\alpha) e^{2\pi f \alpha} h(\beta) e^{-2\pi f \beta} R(\tau+\alpha-\beta) \\
&\quad e^{-2\pi f(\tau+\alpha+\beta)} d\alpha d\beta d\tau .
\end{aligned}$$

Noting that τ , α , and β are dummy variables, a change of variable $t = \tau + \alpha - \beta$, $dt = d\tau$, can be made so that the equation may be factored to obtain the following result:

$$S_y(f) = H(f) H^*(f) S_x(f) = |H(f)|^2 S_x(f) . \quad (176)$$

In equation (176), $H(f)$ is the frequency response function for the structure between the excitation and the response, $H^*(f)$ is the complex conjugate of $H(f)$, and $|H(f)|$ is the magnitude of $H(f)$ or the gain factor for the structure. The quantity $S_x(f)$ is the two-sided mathematical power spectral density function for the excitation. In terms of the physically realizable power spectra for the excitation and response, equation (176) becomes

$$G_y(f) = |H(f)|^2 G_x(f) . \quad (177)$$

The result presented in equation (177) is extremely important and illustrates the fundamental value of power spectra concepts for structural vibration problems. In words, the power spectrum for the vibration response of an idealized structure is equal to the power spectrum for the excitation multiplied by the square of the gain factor for the structure. Given any two of the quantities in equation (177), the third can be determined. For example, if the frequency response function for a structure is known, the power spectrum

for the response can be computed given the power spectrum for the excitation, and vice versa. Also, if the power spectra for the excitation and response are known, the gain factor for the structure (but not the phase factor) can be computed.

Referring to equation (172), the inverse Fourier transform for the power spectral density function is

$$R_y(\tau) = \int_{-\infty}^{\infty} S_y(f) \cos 2\pi f\tau \, df = \int_0^{\infty} G_y(f) \cos 2\pi f\tau \, df \quad . \quad (178)$$

The mean square value of the signal is equal to the autocorrelation function for zero time displacement ($\tau=0$). Hence, the following relationship ensues directly.

$$\overline{y^2} = R_y(0) = \int_0^{\infty} G_y(f) \, df \quad . \quad (179)$$

The total mean square value for a random vibration is equal to the total area under the power spectrum for the vibration. The rms vibration amplitude is equal to the square root of the area. Furthermore, if only those frequencies in the range between f_a and f_b Hz are of interest,

$$\overline{y^2}(f_a, f_b) = \int_{f_a}^{f_b} G_y(f) \, df \quad (180)$$

$\overline{y^2}(f_a, f_b)$ is defined as the mean square value of a random vibration in the frequency range from f_a to f_b Hz and is equal to the area under the power spectrum for the vibration between those frequency limits. The corresponding rms vibration amplitude is equal to the square root of the area.

Numerical Example:

Consider a structure between two points of interest on a flight vehicle. Assume the fundamental natural frequency and damping ration for the structure are

$$f_n = 100 \text{ Hz}$$

$$\zeta = 0.025$$

Further assume that one end of the structure is subjected to a vibration $x(t)$ which, when measured in acceleration units, has a reasonably uniform power spectral density function of

$$G_x(f) = 0.01 \text{ g}^2/\text{Hz}$$

over a frequency range from $f \ll 100$ to $f \gg 100$ Hz. Note that $g = 9.804 \text{ m/sec}^2$ (386 inches/sec²). The problem is to determine the power spectrum and rms amplitude for the response acceleration at the other end of the structure.

Assuming that the structure may be represented by a simple idealized structure as shown in Figure 66, the appropriate gain factor for the structure is given by equation (164), in that section. For a natural frequency of $f_n = 100$ Hz and damping ratio of $\zeta = 0.025$, the gain factor is

$$|H(f)| = \frac{1 + \left(\frac{0.05 f}{100}\right)^2}{\sqrt{\left[1 - \left(\frac{f}{100}\right)^2\right]^2 + \frac{0.05 f}{100}}}$$

From equation (177), the power spectral density function for the response acceleration will be as follows:

$$G_y(f) = \frac{\left[1 + \left(\frac{0.005 f}{100}\right)^2\right] 0.01}{\left[1 - \frac{f}{100}\right]^2 + \left[\frac{0.005 f}{100}\right]^2} \text{ g}^2/\text{Hz}$$

A plot for the response power spectrum is presented in Figure 70.

The total mean square value for the response acceleration will be given in general terms as follows.

$$\begin{aligned}\overline{y^2} &= \int_0^{\infty} G_y(f) df = \int_0^{\infty} |H(f)|^2 G_x(f) df \\ &= \int_0^{\infty} \frac{\left[1 + \left(2\zeta \frac{f}{f_n}\right)^2\right] G_x(f)}{\left[1 - \left(\frac{f}{f_n}\right)^2\right]^2 + \left[2\zeta \frac{f}{f_n}\right]^2} df \quad . \quad (181)\end{aligned}$$

For the special case where $G_x(f)$ is a constant (hypothetically for all frequencies), equation (181) can be integrated by the method of residues to obtain the following solution:

$$\overline{y^2} = \frac{\pi f_n (1 + 4\zeta^2) G_x}{4\zeta} \approx \frac{\pi f_n G_x}{4\zeta} \quad \text{for } \zeta \ll 1 \quad . \quad (182)$$

Substituting the proper values for this problem into equation (182) gives the following result:

$$\overline{y^2} = \frac{\pi (100) (0.01)}{4(0.025)} = 31.4 g^2 \quad .$$

Hence the rms response acceleration is

$$y_{\text{rms}} = 5.6 g = 55.88 \text{ m/sec}^2 (2200 \text{ in./sec}^2) .$$

Note that the value for $\overline{y^2}$ could also be obtained by graphically measuring the area under the response power spectrum in Figure 70.

4. CROSS-POWER SPECTRAL DENSITY FUNCTIONS

Given two stationary random vibration records, $x(t)$ and $y(t)$, each of length T seconds, the cross-power spectral density function $G_{xy}(f)$ is defined in Section VIII.B.2.f. as follows:

$$G_{xy}(f) = C_{xy}(f) - jQ_{xy}(f) \quad (183)$$

where

$$C_{xy}(f) = \lim_{T \rightarrow \infty} \lim_{\Delta f \rightarrow 0} \frac{1}{T(\Delta f)} \int_0^T x_{\Delta f}(f, t) y_{\Delta f}(f, t) dt \quad (183a)$$

$$Q_{xy}(f) = \lim_{T \rightarrow \infty} \lim_{\Delta f \rightarrow 0} \frac{1}{T(\Delta f)} \int_0^T \tilde{x}_{\Delta f}(f, t) y_{\Delta f}(f, t) dt \quad (183b)$$

The quantities $x_{\Delta f}(f, t)$ and $y_{\Delta f}(f, t)$ are the instantaneous amplitudes within the narrow frequency interval between f Hz and $f + \Delta$ Hz. The symbol \tilde{x} in equation (183b) means that $x(t)$ is 90 degrees out of phase with $y(t)$.

From equation (183), the cross-power spectrum is a complex valued quantity with a real part $C_{xy}(f)$ called the cospectrum and an imaginary part $Q_{xy}(f)$ called the quadspectrum. The definition of $G_{xy}(f)$ in equation (183) is satisfactory from the measurement point of view in that it describes a direct physical approach to obtaining $G_{xy}(f)$, just as equation (169) describes a direct physical approach to obtaining the ordinary power spectrum $G_y(f)$. Of course, T will always be finite and Δf will be nonzero in actual practice. These matters are discussed in detail in Section VIII.D.f.

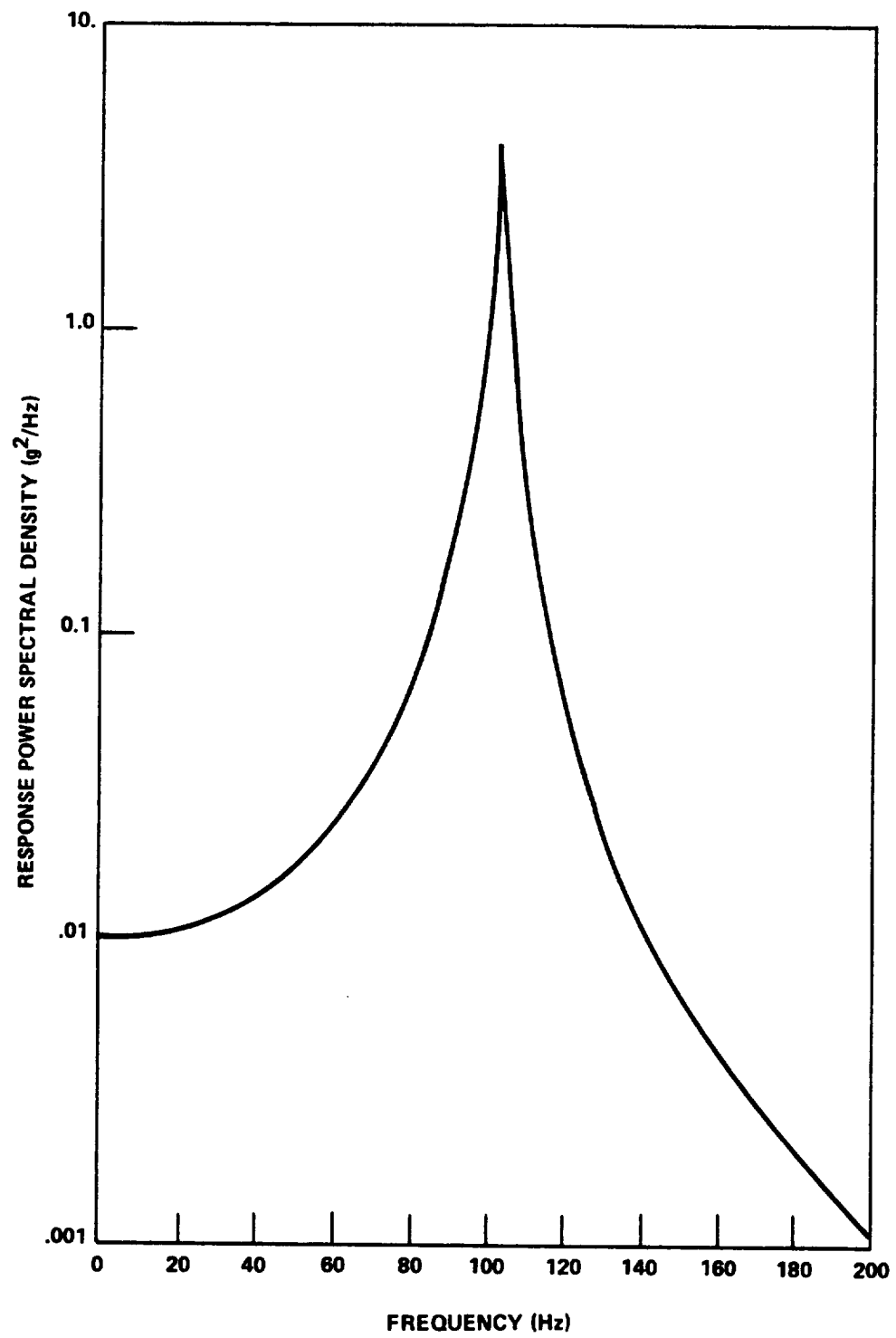


Figure 70. Response power spectrum for simple structure.

The cross-power spectrum is a generalization of the ordinary power spectrum as the cross-correlation function is a generalization of the auto-correlation function. Hence, the most direct definition is an analogy to equation (170); that is, define

$$S_{xy}(f) = \int_{-\infty}^{\infty} e^{-j2\pi f\tau} R_{xy}(\tau) d\tau \quad (184)$$

where $R_{xy}(\tau)$ is the cross-correlation function defined in Paragraph D. of this section. Because $R_{xy}(\tau)$ is not an even function, the imaginary portion of this transform does not vanish in general, and therefore $S_{xy}(f)$ is a complex number. As before $S_{xy}(f)$ is a two-sided mathematical idealization which covers the frequency interval from minus infinity to plus infinity. A physically realizable cross-power spectral density function $G_{xy}(f)$ is given by

$$G_{xy}(f) = C_{xy}(f) - jQ_{xy}(f) = 2S_{xy}(f) \quad ; \quad f \geq 0 \quad (185)$$

$$= 0 \quad \text{for } f < 0$$

Referring to equation (184), it can be shown from the $\sin 2\pi ft$ and $\cos 2\pi ft$ parts of the Fourier transform that the cospectrum is an even function of f while the quadspectrum is an odd function of f ; that is,

$$C_{xy}(f) = C_{xy}(-f) \quad (186)$$

$$Q_{xy}(f) = -Q_{xy}(-f)$$

Also, from the symmetry property of the cross-correlation function, $R_{xy}(-\tau) = R_{yx}(\tau)$, it follows immediately that

$$\begin{aligned}
C_{xy}(f) &= \int_0^{\infty} [R_{xy}(\tau) + R_{yx}(\tau)] \cos 2\pi f \tau d\tau \\
&= \frac{1}{2} [G_{xy}(f) + G_{xy}(-f)]
\end{aligned} \tag{187}$$

$$\begin{aligned}
Q_{xy}(f) &= \int_0^{\infty} [R_{xy}(\tau) - R_{yx}(\tau)] \sin 2\pi f \tau d\tau \\
&= \frac{j}{2} [G_{xy}(f) - G_{xy}(-f)]
\end{aligned}$$

In the above equations, it is sufficient to obtain the functions for $f \geq 0$ since the symmetry properties in equations (186) yield the results for $f < 0$.

A further relation for the cross-power spectrum may be obtained from the symmetry properties of the cross-correlation function. (See Paragraph E.2. of this section.)

$$G_{xy}(-f) = G_{xy}^*(f) = G_{yx}(f) \tag{188}$$

Here, $G_{xy}^*(f)$ is the complex conjugate of $G_{xy}(f)$. From basic considerations, it can be shown that $G_{xy}(f)$ satisfies the following important inequality:

$$|G_{xy}(f)|^2 \leq G_x(f) G_y(f) \tag{189}$$

Now consider an idealized structure with a weighting function $h(\tau)$. Assume that an excitation $x(t)$ with a power spectral density function $G_x(f)$ is applied to the structure producing a response $y(t)$. By the same procedures used in Paragraph F.2. of this section, it can be shown that

$$G_{xy}(f) = H(f) G_x(f) \tag{190}$$

where $H(f)$ is the frequency response function for the structure between the excitation and the response.

The physical interpretations for cross-power spectral density functions are similar in part to the applications for cross-correlation functions. Specifically, a cross-power spectrum will reveal dependence (or coherence) between two vibration records. That is, if two random vibration responses, $x(t)$ and $y(t)$, are completely independent and unrelated to one another, the cross-power spectrum for the two responses will be zero at all frequencies. On the other hand, if the two vibrations are related, the dependence must be due to some structural connection between the points where the vibrations occur. For this case, a nonzero cross-power spectrum will be measured which is associated with the frequency response function for the structure between the points.

Consider the case where a vibration response $y(t)$ at some point on a structure is the result solely of the vibration response $x(t)$ at some other point. Clearly, $x(t)$ may be considered an excitation which produces a response $y(t)$. The frequency response function between the two points will be given directly by equation (190). This points out the most important application for cross-power spectral density functions; that is, the determination of frequency response functions for structures from measured vibration data.

Because the interpretations for cross-power spectral density functions are closely associated with structural frequency response functions, it is often desirable to present a cross-power spectrum in the form of a magnitude and phase angle as follows:

$$G_{xy}(f) = C_{xy}(f) - jQ_{xy}(f) = |G_{xy}(f)| e^{j\theta_{xy}(f)} \quad (191)$$

$$|G_{xy}(f)| = \sqrt{C_{xy}^2(f) + Q_{xy}^2(f)} \quad (192)$$

$$\theta_{xy}(f) = \arctan \frac{-Q_{xy}(f)}{C_{xy}(f)} \quad (193)$$

By presenting the frequency response function $H(f)$ in terms of the gain factor $|H(f)|$ and the phase factor $\phi(f)$, equation (190) becomes

$$|G_{xy}(f)| e^{j\theta_{xy}(f)} = |H(f)| e^{j\phi(f)} G_x(f) \quad . \quad (194)$$

Hence, the following input-output relationship exists:

$$|G_{xy}(f)| = |H(f)| G_x(f) \quad (195)$$

$$\theta_{xy}(f) = \phi(f) \quad .$$

The cross-power spectrum for an excitation and response has a magnitude equal to the power spectrum for the excitation multiplied by the gain factor for the structure, and a phase factor equal to the phase factor for the structure. Note that the phase angle $\theta_{xy}(f)$ can be used to determine time delays, as would be obtained from a cross-correlation function. The time delay $\tau_{xy}(f)$ between the excitation and response at any frequency f is given by

$$\tau_{xy}(f) = \frac{\theta_{xy}(f)}{2\pi f} \quad . \quad (196)$$

Numerical Example:

Consider a structure between two points of interest on a flight vehicle, as discussed for the example in Paragraph F.2. of this section; that is, assume that the structure may be represented by a simple idealized structure as shown in Figure 66, with a natural frequency of $f_n = 100$ Hz and a damping ratio of $\zeta = 0.025$. Further, assume that the structure is subjected to a vibration excitation which, when measured in acceleration units, has a reasonably uniform power spectral function of $G_x(f) = 0.01 \text{ g}^2/\text{Hz}$ over a frequency range from $f \ll 100$ to $f \gg 100$ Hz. The problem is to determine the cross-power spectrum for the response acceleration relative to the excitation, and the time delay between the response and excitation at the frequency $f = 100$ Hz.

From equations (191) and (195), the cross-power spectrum is given by

$$G_{xy}(f) = |G_{xy}(f)| e^{j\theta_{xy}(f)}$$

where

$$G_{xy}(f) = 0.01 |H(f)| g^2 / \text{Hz}$$

$$\theta_{xy}(f) = \phi(f) \text{ radians}$$

The appropriate gain factor and phase factor for the structure is given by equation (163). Substituting from equation (163) and noting that $f_n = 100 \text{ Hz}$ and $\zeta = 0.025$, the cross-power spectral density function is as follows:

$$|G_{xy}(f)| = \sqrt{\frac{0.1 \left[1 + \left(\frac{0.05f}{100} \right)^2 \right]}{\left[1 - \left(\frac{f}{100} \right)^2 \right]^2 + \left[\frac{0.05f}{100} \right]^2}}$$

$$\theta_{xy}(f) = -\arctan \left[\frac{0.05 \left(\frac{f}{100} \right)^3}{1 - \left(\frac{f}{100} \right)^2 + 0.0025 \left(\frac{f}{100} \right)^2} \right]$$

For the frequency $f = 100 \text{ Hz}$, the phase angle for the cross-power spectrum is

$$\theta_{xy}(100) = -\arctan(20) = 1.52 \text{ radian.}$$

Hence, from equation (196), the time delay between the excitation and response at $f = 100 \text{ Hz}$ is as follows:

$$\tau_{xy} = \frac{1.52}{200\pi} = 0.0024 \text{ second} .$$

5. COHERENCE FUNCTIONS

The application of cross-power spectra concepts as a tool for measuring the frequency response functions for structures is best implemented with aid of a real-valued quantity called the coherence function. The coherence function $\gamma_{xy}^2(f)$ is defined as follows:

$$\gamma_{xy}^2(f) = \frac{|G_{xy}(f)|^2}{G_x(f)G_y(f)} . \quad (197)$$

For an idealized structure (constant parameter linear system) where a response $y(t)$ is due solely to an excitation $x(t)$, the coherence function for $x(t)$ and $y(t)$ will be unity for all frequencies. This can be shown from equations 9.113 and 9.126 as follows:

$$\gamma_{xy}^2(f) = \frac{|G_{xy}(f)|^2}{G_x(f)G_y(f)} = \frac{G_x^2(f)|H(f)|^2}{G_x(f)|H(f)|^2G_x(f)} = 1 . \quad (198)$$

If a response $y(t)$ is not because of an excitation $x(t)$, [that is, $y(t)$ and $x(t)$ are independent], the coherence function for $x(t)$ and $y(t)$ will be zero for all frequencies. If a response $y(t)$ is only partially because of an excitation $x(t)$, the coherence function will have some value between zero and unity which indicates the amount of dependence or coherence between the $x(t)$ and $y(t)$. Hence, the coherence function furnishes information similar to that available from the correlation coefficient discussed in Paragraph E.1. of this section.

The coherence function may be thought of as a ration of two particular estimates for the square of the gain factor for a structure between two points of interest. To be specific, consider equation (177) as giving one estimate

$$|\hat{H}(f)|_1^2 = \frac{G_y(f)}{G_x(f)} \quad (199)$$

and equation (195) as giving a second estimate

$$|\hat{H}(f)|_2^2 = \frac{|G_{xy}(f)|^2}{G_x^2(f)} \quad (200)$$

where x and y are data from the two points involved. The hat (^) above the symbols is used to indicate that these are estimates for $|H(f)|$ based upon the measured data. If one takes the ratio of these two estimates, the coherence function is obtained.

$$\frac{|\hat{H}(f)|_2^2}{|\hat{H}(f)|_1^2} = \frac{|G_{xy}(f)|^2 G_x(f)}{G_x^2(f) G_y(f)} = \gamma_{xy}^2(f) \quad (201)$$

It should be noted that $|\hat{H}(f)|$ in the above equations will equal the correct gain factor $|H(f)|$ for the structure in question only if underlying assumptions are satisfied. Specifically, the structure must truly represent a constant parameter linear system and the measurements must be free of extraneous noise.

As noted earlier in equation (189), cross-power spectra satisfy the inequality

$$|G_{xy}(f)|^2 \leq G_x(f) G_y(f) \quad (202)$$

Hence, the coherence function is bounded by

$$0 \leq \gamma_{xy}(f) \leq 1 \quad . \quad (203)$$

Note that the coherence function can never be greater than unity. Equation (198) shows that the coherence is unity if the underlying assumptions, including linearity, are valid. The coherence function may be thought of as a measure of linearity, are valid. The coherence function may be thought of as a measure of linearity in the sense that the function attains this maximum value of unity for all frequencies if the structure is linear. Hence, if the coherence function is less than unity, one possible cause might be the lack of linear dependence between the excitation and response.

However, the reverse statement does not follow from what has been presented here. That is, the above argument does not prove that the coherence function will necessarily be less than unity for a nonlinear system, although in fact this is considered to be true. As mentioned before, the presence of unwanted extraneous noise in power spectra measurements will also influence the resulting coherence function and cause its value to be less than unity. These important matters will now be discussed.

a. Noisy Measurements of Frequency Response Functions.

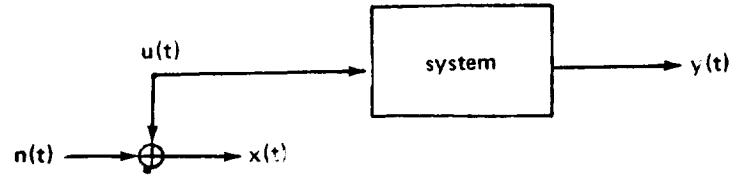
The effect of additive noise on frequency response function estimates is developed here. The coherence function plays a crucial role in these considerations. Three cases are of concern:

1. Uncorrelated noise occurring in the input measuring device.
2. Uncorrelated noise occurring in the output measuring device.
3. Uncorrelated noise occurring in both the input and output measuring devices.

The third is clearly the most important and contains the other two as special cases. However, they are presented in the indicated sequence for simplicity.

Case 1. Noise in the Input Measuring Device

Let $x(t)$ represent a measurement of the input to a system. Assume that this measurement is made up of the true signal $u(t)$ which passes through the system, and a noise component $n(t)$ which is uncorrelated with either the input or output.



The measured input is given by the equation

$$x(t) = u(t) + n(t) \quad . \quad (204)$$

It is easily shown that the power spectral density function and cross-power spectral density function for the signal and uncorrelated noise are additive. The following equations hold true.

$$G_x(f) = G_u(f) + G_n(f) \quad (205)$$

$$G_{xy}(f) = G_{uy}(f) + G_{ny}(f) = G_{uy}(f) = H(f) G_u \quad (206)$$

since

$$G_{ny}(f) = 0 \quad .$$

For this case the coherence function between $x(t)$ and $y(t)$ is

$$\gamma_{xy}^2(f) = \frac{|G_{xy}(f)|^2}{G_x(f) G_y(f)} = \frac{G_u^2(f) |H(f)|^2}{G_x(f) |H(f)|^2 G_u(f)}$$

$$= \frac{G_u(f)}{G_x(f)} = \frac{1}{1 + [G_n(f)/G_u(f)]} < 1 \quad (207)$$

This relationship clearly shows that any noise present in the input measuring device reduces the coherence function to less than unity. Also, as the input signal to measuring device noise ratio becomes small, the coherence function becomes small. If the noise power spectral density function is much less than the signal power spectral density function, that is $G_n(f) \ll G_u(f)$, then equation (207) may be put in a simpler form,

$$\gamma_{xy}^2(f) \approx 1 - [G_n(f)/G_u(f)] \quad (208)$$

The gain factor estimates $\hat{|H(f)|_1}$ and $\hat{|H(f)|_2}$ given by equations (199) and (196), respectively, are related to the true gain factor by the following equations:

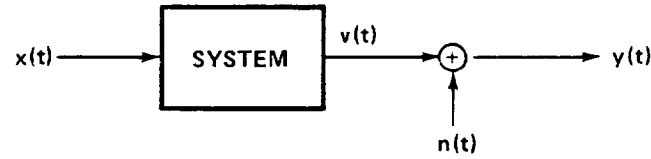
$$|H(f)|^2 = \frac{G_y(f)}{G_u(f)} = \frac{G_y(f)}{G_x(f)} \cdot \frac{G_x(f)}{G_u(f)} = |H(f)|_1^2 \frac{1}{\gamma_{xy}^2(f)} \quad (209)$$

$$\begin{aligned} |H(f)| &= \frac{|G_{uy}(f)|}{G_u(f)} = \frac{|G_{xy}(f)|}{G_u(f)} = \frac{|G_{xy}(f)|}{G_x(f)} \frac{G_x(f)}{G_u(f)} \\ &= \hat{|H(f)|_2} \frac{1}{\gamma_{xy}^2(f)} \end{aligned} \quad (210)$$

One should be careful to note that the square of the gain factor is involved in equation (209) as compared to the unsquared gain factor occurring in equation (210).

Case 2 . Noise in the Output Measuring Device

In this case $x(t)$ is input to the system, $v(t)$ is the output, and $y(t)$ is the measured output which contains a noise component $n(t)$ due to the output measuring device.



The output $y(t)$ is given by

$$y(t) = v(t) + n(t) \quad (211)$$

where $n(t)$ is assumed to be uncorrelated with $x(t)$ or $y(t)$. The simple and cross spectral relations become

$$G_y(f) = G_v(f) + G_n(f) = |H(f)|^2 G_x(f) + G_n(f) \quad (212)$$

$$G_{xy}(f) = G_{xv}(f) = H(f) G_x(f) \quad (213)$$

It follows that the coherence function between $x(t)$ and $y(t)$ is given by

$$\gamma_{xy}^2(f) = \frac{|H(f)|^2 G_x(f)}{G_y(f)} = \frac{G_v(f)}{G_y(f)} = \frac{1}{1 + [G_n(f)/G_v(f)]} < 1 \quad (214)$$

As in Case 1, if any noise is present, the coherence function is strictly less than one, and is inversely proportional to the output measuring device noise to true output signal ratio. If $G_n(f) \ll G_v(f)$, then

$$\gamma_{xy}(f) \approx 1 - [G_n(f)/G_v(f)] \quad . \quad (215)$$

The analogous relations to equations (209) and (210) are

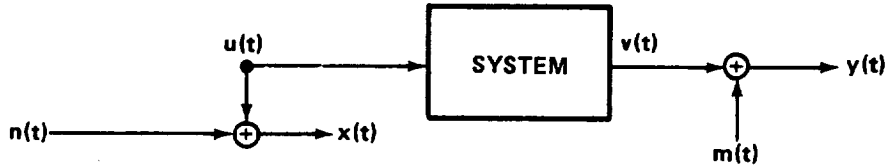
$$|H(f)|^2 = \frac{G_v(f)}{G_x(f)} = \frac{G_v(f)}{G_y(f)} \frac{G_y(f)}{G_x(f)} = |\hat{H}(f)|_1^2 \gamma_{xy}^2(f) \quad (216)$$

$$|H(f)| = \frac{|G_{xv}|}{G_v} = \frac{|G_{xy}|}{G_x} = |\hat{H}(f)|_2 \quad . \quad (217)$$

The above relation, equation (217), would appear to indicate that use of the cross spectral estimate gives a direct measure of the gain factor. However, it will be shown later that reduced statistical confidence must be placed on the measurement when the coherence function becomes less than unity.

Case 3. Noise in Both Input and Output Measuring Devices

For this case the measured input $x(t)$ and measured output $y(t)$ are composed of the true signals $u(t)$ and $v(t)$ and noise components $n(t)$ and $m(t)$, respectively.



The measured input and output are given by

$$x(t) = u(t) + n(t)$$

$$y(t) = v(t) + m(t) \quad . \quad (218)$$

The spectral relations are

$$\begin{aligned}
 G_x(f) &= G_u(f) = G_n(f) \\
 G_y(f) &= G_v(f) + G_m(f) \\
 G_{xy}(f) &= G_{uv}(f)
 \end{aligned}
 \tag{219}$$

The coherence function for this case is

$$\begin{aligned}
 \gamma_{xy}^2(f) &= \frac{|G_{xy}(f)|^2}{G_x(f)G_y(f)} = \frac{|G_{uv}(f)|^2}{[G_u(f) + G_n(f)][G_v(f) + G_m(f)]} \\
 &= \frac{|G_{uv}(f)|^2}{G_u(f)G_v(f) \left[1 + \frac{G_u(f)G_m(f)}{G_u(f)G_v(f)} + \frac{G_n(f)G_v(f)}{G_u(f)G_v(f)} + \frac{G_n(f)G_m(f)}{G_u(f)G_v(f)} \right]} \\
 &= \frac{1}{1 + (N_1/G_1) + (N_2/G_2) + (N_1/G_1)(N_2/G_2)} < 1
 \end{aligned}
 \tag{220}$$

where

$$\begin{aligned}
 N_1 &= G_n(f) & G_1 &= G_u(f) \\
 N_2 &= G_m(f) & G_2 &= G_v(f)
 \end{aligned}
 \tag{221}$$

This formula illustrates the behavior that would be expected when reasoning from the two simpler cases; that is, as the instrument noise to input and output signal ratios decrease, the coherence function approaches unity.

Simple formulas directly relating the coherence function and gain factor estimates to the true gain factor do not exist for this third case. However, slightly different types of formulas are given below.

$$|\hat{H}(f)|_2 = \frac{|G_{xy}(f)|}{G_x(f)} = \frac{|G_{uv}(f)|}{G_u(f) + G_n(f)} = \frac{|H(f)|}{1 + [G_n(f)/G_u(f)]}$$

or

$$|H(f)| = |\hat{H}(f)|_2 (1 + [G_n(f)/G_u(f)]) \quad . \quad (222)$$

Also,

$$\begin{aligned} \gamma_{xy}^2(f) |\hat{H}(f)|_1^2 &= \frac{|G_{xy}(f)|^2}{G_x G_y} \frac{G_y}{G_x} = \frac{G_u^2(f) |H(f)|^2}{G_x G_y} \frac{G_y}{G_x} \\ &= |H(f)|^2 \frac{G_u^2(f)}{G_x^2(f)} \end{aligned}$$

or

$$|H(f)|^2 = \gamma_{xy}^2(f) \frac{G_x^2(f)}{G_u^2(f)} |\hat{H}(f)|_1^2 \quad . \quad (223)$$

b. Confidence Limits Based on Coherence Function

For the cases considered above, an estimate of the true frequency response function may be obtained from the measured functions $G_{xy}(f)$ and $G_x(f)$. Let the measured frequency response function be

$$\hat{H}(f) = \frac{G_{xy}(f)}{G_x(f)} = |\hat{H}(f)| e^{j\hat{\phi}(f)} \quad (224)$$

As mentioned previously, although equation (217) apparently gives a direct estimate of $h(f)$, reduced statistical confidence must be placed on the results. This is illustrated as follows. It has been shown in Reference 25 that to a very close approximation,

$$\begin{aligned} \text{Prob} \left[\left| \frac{\hat{H}(f) - H(f)}{H(f)} \right| < \sin \epsilon \text{ and } |\hat{\phi}(f) - \phi(f)| < \epsilon \right] \\ \approx 1 - \left[\frac{1 - \gamma_{xy}^2(f)}{1 - \gamma_{xy}^2(f) \cos^2 \epsilon} \right]^k \end{aligned} \quad (225)$$

where k is the number of degrees of freedom (df).

The number k is given by

$$k = 2BT = \frac{2N}{m} \quad (226)$$

B = bandwidth

T = total record length in time

N = total number of observations

m = maximum lag number in autocorrelation estimate.

Equation (225) is displayed in Figure 71 which follows, with k as a function of $\gamma_{xy}^2(f)$. Figure 71 gives three sets of curves; one set for $P = .90$, $P = .85$, and $P = .80$ when $\epsilon = .05$ radians; one set when $\epsilon = .10$ radians; and, one set when $\epsilon = .15$ radians. Since $\sin \epsilon \approx \epsilon$ for these small values of ϵ , the curves are satisfactory for a gain factor accuracy of 5, 10, and 15 percent, and a phase angle accuracy of .05, .10, and .15 radians which are approximately 2.9, 5.7, and 8.6 degrees.

The application of these curves to determine a sample size necessary to measure a frequency response function with a desired accuracy is somewhat limited at times. This is because the coherence function is not known in advance, and therefore must be estimated. However, a conservative choice is usually in order. In this case the above relations will be practical guidelines.

(a) Example. Iterative Determination of $H(f)$

A possible application of the coherence function is as follows. Suppose a linear system is under consideration, and it is desired to estimate the frequency response function with a known accuracy. First, one would measure the coherence function by measuring the input and output power spectra separately as well as the input/output cross-power spectra. Now, with a first estimate of the coherence function, the approximate number of degrees of freedom needed to measure the frequency response function to the accuracy desired would be determined. Next, $H(f)$ is estimated under these experimental conditions. A new coherence function measurement would now be available giving improved information and the process could be repeated, continuing the iterations until desired results were obtained.

(b) Example. Sample Size Requirement

A second application of Figure 71 is as follows. Suppose the measuring instrument noise is known, or is estimated. Also, assume that based on this knowledge and approximate expected power spectra of the input and output, the coherence function of the system is estimated to be $\gamma^2 = 0.8$. Now assume that a maximum 5 percent error in the gain factor measurement with a corresponding maximum 3-degree error in the phase is considered acceptable when there is a confidence of 90 percent of measuring these quantities that accurately. That is, $\gamma_{xy}^2(f) = .8$, $\epsilon = .05$, and $P = .90$. How many degrees of freedom are needed for the measurements? Figure 71 is entered at the $\gamma^2 = .8$ value, and the intersection with the top curve corresponding to $P = .90$ and $\epsilon = .05$ is noted. The value of k is then read off the

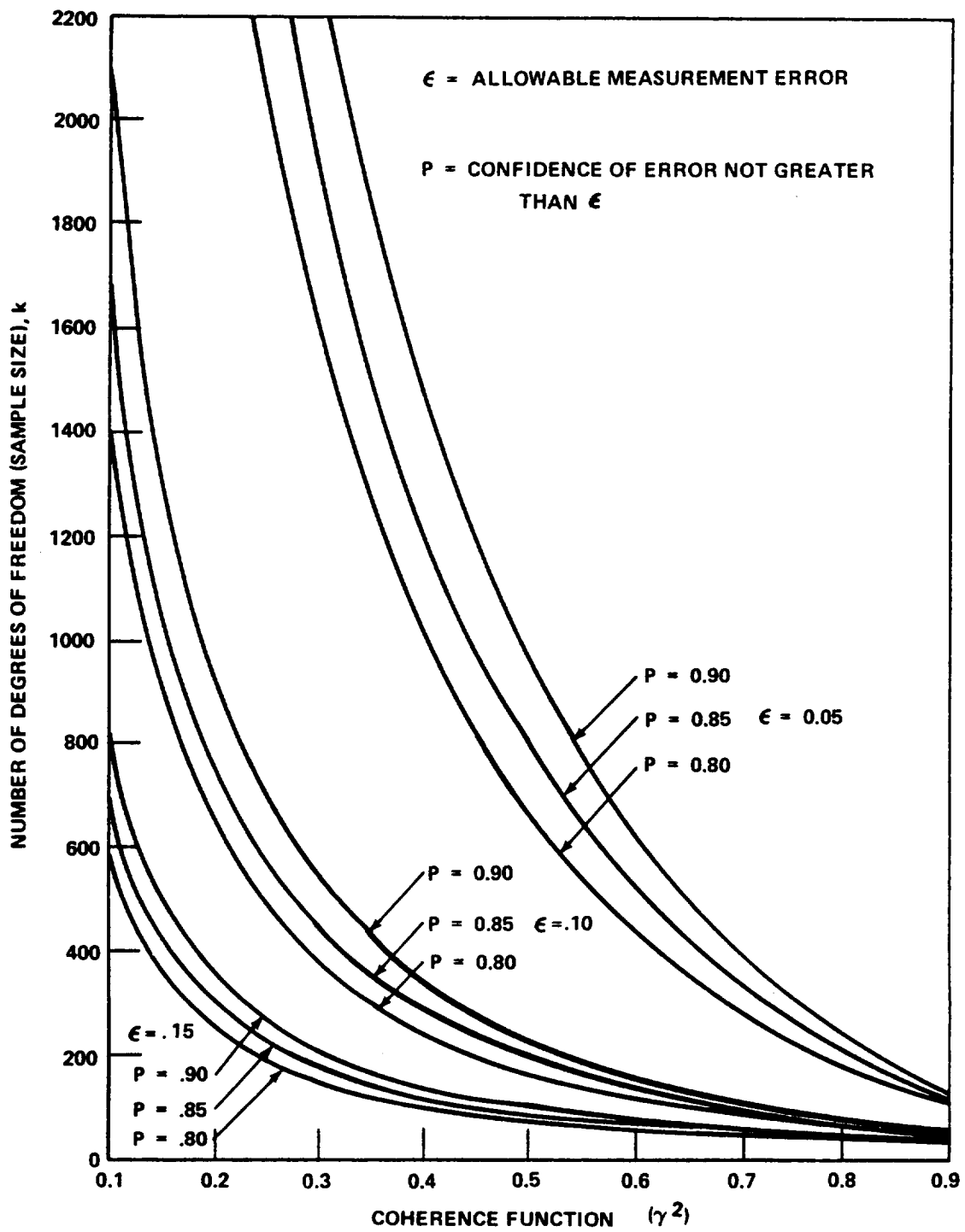


Figure 71. Data for frequency response function measurement confidence.

vertical scale which is approximately $k = 240$. Therefore, about 240 df are needed to measure the frequency response function under these given conditions.

(c) Example. Measurement Bias Correction

As the preceding analysis shows, the coherence function is a useful quantity in the general consideration of frequency response functions and their measurement. If the noise in the input/output measuring equipment is known, then the frequency response function can be properly determined. As can be seen by the formula given, quite misleading and biased results could be obtained if no attention is paid to measurement noise. For example, assume one wants to experimentally determine in the laboratory the frequency response function of a linear system. Assume that the noise in the output measuring device is known to be negligible, but the input device noise is not. Then the formulas for Case 1 would apply. First one must determine the input measuring device noise power spectral density which should be approximately constant for most situations. Then one must apply a stationary random input to the system and determine the input and output power spectral density functions. From knowledge of these quantities, equations (199), (203), (207), and (209) could be applied to determine the gain factor as well as knowledge of the uncertainty in its measurement.

The above illustration applies to laboratory measurements of frequency response functions where random input signals are used. In general, frequency response functions are commonly measured in the laboratory using sinusoidal inputs. The resulting data analysis for sinusoidal signals are straightforward without involving power spectra and cross-power spectra functions. However, the employment of random signal inputs can greatly reduce the total test time required for a frequency response function measurement. This follows because the needed information is obtained simultaneously at all frequencies of interest, whereas with sinusoidal inputs, a separate test is required at each frequency of interest.

SECTION X. ACOUSTIC, VIBRATION, AND SHOCK TESTS

A. Acoustic Tests

It is the policy of MSFC to qualify acoustically some of the space vehicle structures and components. In general, any single component or structure susceptible to acoustic impingement will be acoustically tested separately from other qualification tests. This is accomplished by testing assemblies to the latest acoustic specifications which are generated on an individual, rather than a general, basis. In some instances, however, components may be tested to the same specification if they are to be located in the same zone of the vehicle.

The acoustic test specification is obtained by one of two methods. If no actual flight or static firing data are available, the acoustic environment at the specimen location is estimated using presently available prediction techniques ("Methods of Flight Vehicle Noise Prediction," WADC TR58-343, Volumes I and II and NASA memorandum R-P&VE-SVE-64-191). These techniques take into account the number and size of the engines, significant flow parameters, location of the specimen, flight time, and other pertinent factors. If reliable acoustic data are available from static firings and/or flights of similar vehicles, the test specifications may be generated from the measured rather than the predicted acoustic environment. From the acoustic environment, the external and internal design criteria can be determined. The exposure durations based upon operational phases are given in the design criteria. For example, the exposure duration to a static firing spectrum will vary for the different stages. For a particular stage, it will be the total of the exposure durations of all the static firings of that stage. In general, there is more than one acoustic design criterion for each location. This is because different spectra and noise levels are generated at launch, during static firings, and during the flight of the vehicle. The test specification is determined from a consideration of the exposure durations and the design criteria; hence, it is ensured that the test specification spectrum will contain all of the important features of the design criteria.

The time duration of the test is obtained by adding the times of the design criteria, unless one design criterion overall level is much higher than the others. In this case, the high level design criterion time is taken as the test specification time. As an alternative, high level and low level tests may be specified so that a compatibility can be attained between the test levels and

operational exposure durations. In some instances, the available acoustic testing facilities may not be capable of producing the test spectrum overall level, and it is, therefore, necessary to test at a lower acoustical level for a longer period. The increase in testing time is determined from calculations based upon the random fatigue curve for the specimen material.

The tolerances allowed during the acoustical qualification test are as follows:

(a) The test time shall be within -0 to $+10$ percent of the time set forth in the test specifications;

(b) The overall sound pressure level and the individual $1/3$ -octave band levels measured at the specimen location shall be within -0 to $+4$ dB of the levels set forth in the test specifications (without the test specimen installed).

The specimen must be instrumented with a sufficient number of strain gages, accelerometers, and microphones to enable such things as mode shapes, transmission loss, panel response, and strain levels to be measured with some degree of accuracy and reliability. During the test runs, all information from these measurements is stored on magnetic tape for future reduction.

Preliminary test runs include calibration checks, linearity checks, and sine sweeps at levels lower than the test specification. After this, the specimen is tested to the acoustic test specification with frequent inspections between the test runs. After the initial period of acoustical qualification, the specimen. This additional testing is important if a limited number of samples is available for the initial test, so that the statistics of failure probability can be taken into account. Doty ("Fatigue Life Safety Margin," Wyle Technical Memorandum 65-24, dated December 30, 1965) gives the additional testing requirements as a function of probability of survival, number of specimens, and standard deviation from the logarithmic normal distribution. For example, testing two samples for a probability of survival of 99 percent and a standard deviation of 0.225, the test time should be increased by eight. Throughout all tests, the specimen is inspected regularly and thoroughly, and if any failures occur, the testing is stopped to allow a complete inspection and fatigue check. If it is practicable, acoustical qualification tests are to be carried out in a reverberation room.

In addition to acoustical qualification tests, other acoustical tests are conducted to determine such parameters as noise reduction, acoustic absorption, reverberation time, structural response, etc. A number of separate conditions will affect these parameters; therefore different test systems are required to study each individual effect. The basic methods used in this field of structural testing are listed below.

1. IN-FLIGHT ACOUSTIC TESTS

During the flight of space vehicles, a continuous record of the acoustic field inside and outside the vehicle is obtained from strategically placed microphones. From the data obtained during these flights, the noise reduction produced by the structure and the response of the structure can be calculated. These results can also be compared with the values obtained using prediction methods. This comparison leads to more accurate prediction methods.

2. STATIC FIRING TESTS

During the static firing of a vehicle, measurements of the sound level at the surface of the vehicle are recorded using microphones attached to the structure. The instantaneous phase relationship of the sound pressure, at any two or more points on the surface of the vehicle, can be measured for a given frequency and a correlation curve (see Section XII for definition) may be calculated. This correlation curve can be used to predict the response of the structure to the acoustic field. The greatest structural response, for any particular mode, occurs when the shape of the acoustic correlation curve corresponds to the mode shape of the structure.

Other microphones located in the near and far field during static firings are used to measure the intensity of the acoustic field on buildings and other structures near the test stand. Acoustical tests may also be conducted by placing the test specimen in the acoustical field generated by the static firing of a vehicle or single engines. To assist in this method of testing, a Mobile Acoustic Research Laboratory (MARL) has been constructed at MSFC. Large space vehicle structures may be mounted on the MARL, which is then placed in the vicinity of a static firing.

3. MODEL TESTS

Small rocket engines can be tested in a "field" containing a radial array of many microphones. The sound pressure level distribution (directivity) can be determined from these measurements. With a knowledge of the size and power of the small model rocket engine, one can often predict the sound output of larger engines. This test system is also very useful for investigating other effects, such as the combustion instability in a rocket engine.

4. REVERBERATION CHAMBER TESTS

Under some circumstances, it is possible to use a reverberation chamber to obtain information on acoustic fatigue. The test specimen is placed within a room which has walls constructed of a hard reflecting material. Sound energy is fed into the room from an intense sound source, such as a siren or an air modulator. Multiple reflections within the room produce a reverberant field with a high sound pressure level. The structure under test has strain gages and microphones attached to its surface which give a continuous record of the strain induced by the incident acoustic field.

Some reverberation rooms have additional facilities to enable the response of a structure to be determined in tests involving simultaneous vibration temperature and pressure variations in addition to the acoustic field.

Experiments to measure the transmission loss of a panel are carried out in a reverberation room with the specimen mounted between the reverberation room and an anechoic room. Microphones placed either side of the panel can then be used to record the sound attenuation and the transmission loss of the panel at a given frequency.

5. PANEL TESTING TECHNIQUES

Sections of space vehicles, or separate panels, can be acoustically tested by subjecting the specimen to an acoustic field in a progressive wave chamber. This normally is driven by a high intensity sound source, such as a siren or an air modulator, the output of which may be fed into an exponentially progressive wave chamber or tube which is often terminated anechoically. Test specimens can be fitted into the side wall of the wave chamber and will receive acoustic energy at grazing incidence. Other panels, and larger structures, placed at the outlet of the horn will receive sound waves with varying angles of incidence.

Acoustic, vibration, and stress measurements are taken during the period of the test using microphones, accelerometers, and strain gages mounted on the surface of the specimen.

6. ROCKET SLED TESTS

The response of full-scale or model structures to the acoustic field produced by aerodynamic effects can be determined on a rocket sled test. The specimen is mounted on a sled structure which is propelled along a track at transonic or supersonic speeds. Continuous measurements are recorded from microphones, pressure transducers, and strain gages mounted on the specimen; these measurements are used to measure the sound level, panel response, and fatigue. Other techniques can be used to detect the pressure of shock waves in the vicinity of the test panel.

B. Shock And Vibration Tests

Vibration and shock tests at MSFC are conducted on space vehicle components, structural items, and complete vehicles. These tests use electromagnetic and hydraulic shakers, and various types of shock test machines. Some tests are conducted according to formalized written specifications while other tests are for research purposes. These research tests are useful during the development phase of hardware and they increase the probability of success during qualification, reliability testing, and actual flight.

MSFC is capable of conducting almost any conceivable shock and vibration test representing realistic environments. Most testing does not involve special techniques or equipment, but rather a creative test design, using established test equipment and techniques. Transducers are available to give voltage analogs for vibratory displacement, velocity, acceleration, pressure, stress, and other quantities. These transducers are available in a vast variety of sensitivities and vibration characteristics. High speed photography, stroboscopic lighting, calibrated microscopes and telemicroscopes are other measurement methods.

Vibration data may be read out on voltmeters, oscilloscopes, or x-y recorders, recorded on oscillographs and magnetic tapes, or fed directly into computers for instant analysis.

Environmental tests may be natural, such as transportation and handling, or simulated by using a shock or vibration generator. The design or systems

engineer should not hesitate to request any test which would be of aid in producing or improving the desired final item.

Although testing of vehicle components is the major activity, vibration testing of large structural items and complete vehicles is also accomplished at MSFC. These structural tests are not usually run to establish the strength of the vehicle under vibratory loading, but are conducted to establish the natural frequencies of the vehicle and the associated mode shapes and relative deflections of the parts.

To date, the most ambitious vibration tests were conducted on full scale prototype sections of the Saturn I, IB, and V vehicles. A typical test setup is shown in Figure 72. The complete assemblies were excited by both sinusoidal and random excitation and the response characteristics were obtained.

1. SHOCK MACHINES

Space vehicles are subjected to high level transient excitation at various times during vehicle life. Shock testing is necessary to insure component reliability. The problems involved in defining the shock environment and simulating this environment in the laboratory are very complex. Because of the complexity of this problem, two different approaches to shock test definition have evolved. The first, and simplest approach, is to define the test environment in terms of the type of shock machine to be used and the procedure to be followed in executing the test. The second, and presently more popular approach, is to define the test environment in terms of an acceleration time history (or the associated response spectrum) to which a specimen must be subjected.

Two types of shock test machines are presently available at MSFC; a drop test machine, and a hydraulic-pneumatic shock test machine. The drop test machine (Fig. 73) consists of a table upon which the specimen is mounted and a rigid mass upon which the table falls. The table is raised by cables to a predetermined height, then automatically released. The height from which the table is released determines the velocity change. The shape of the shock pulse can be varied by placing rubber pads or triangular-shaped lead pellets on the rigid mass. A brake restricts any rebound motion of the table.

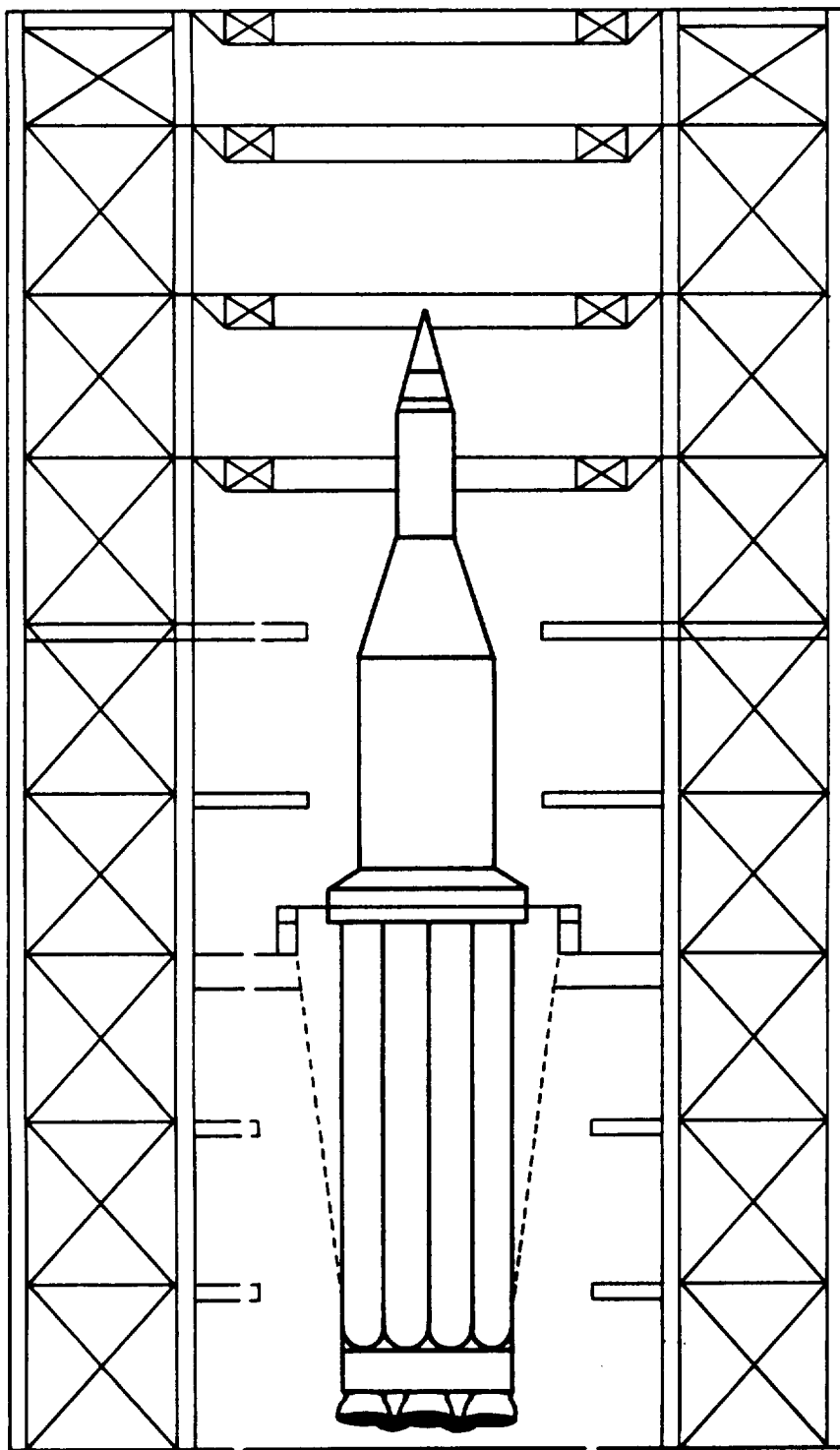


Figure 72. Mode test setup for saturn vehicle.

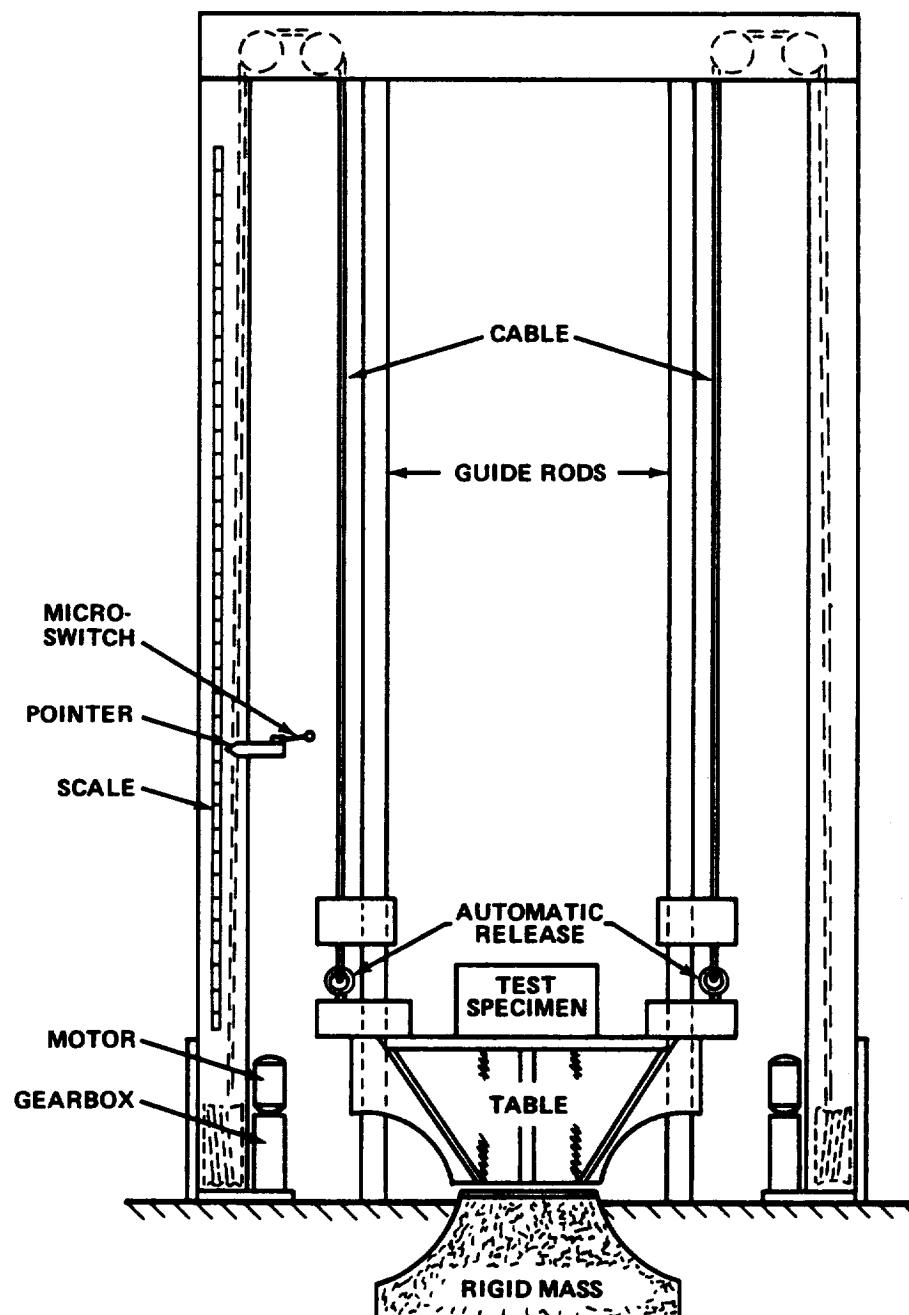


Figure 73. Drop-test shock machine.

The hydraulic-pneumatic shock machine illustrated schematically in Figure 74 is capable of producing a great variety of acceleration wave shapes, amplitudes, and time bases. The machine develops its thrust through differential gas pressures acting on two faces of a thrust piston in a closed cylinder. With reference to Figure 74, operation of the machine is described as follows. A relatively low gas pressure is maintained in the top gas chamber which forces the thrust piston against a seal ring seated on its base. In preparation for firing, compressed nitrogen gas is introduced into the lower chamber to equalize the force on the top face of the thrust piston. Any increase of pressure in the lower chamber upsets this equilibrium, opens the seal at the orifice and causes the piston to rise. Instantly, the entire bottom area of the piston is exposed to the lower chamber gas pressure. A thrust on the piston results, which is controlled by the geometry of the acceleration metering pin. This limited duration thrust is transmitted to the test specimen by the thrust column. The forward motion of the thrust piston is arrested as the piston approaches the deceleration orifice. The deceleration of the piston, and thus the specimen, is controlled by the deceleration metering pin.

2. ELECTRODYNAMIC SHAKER

The electrodynamic shaker, because of its versatility, is the work horse of the vibration test laboratories at MSFC. Shakers are adaptable to many configurations for different types of testing. They can be used individually for component testing, in series for large structural testing, for certain types of shock testing, or in combination with a slip table. Slip tables are presently of the granite type or the hydrostatic bearing type. They are used to relieve the shaker head of the static load imposed by a heavy test specimen and to help obtain unidirectional inputs.

The shaker operates on the same principle as an electromagnetic speaker in an ordinary radio. Basically, the shaker or vibrator (Fig. 75) is composed of an armature and a powerful, electrically energized field magnet. When alternating current is passed through the armature windings, and direct current is passed through the field magnet windings, a strong magnetic force is generated between them. This force causes the armature to move in a direction perpendicular to the plane of the table surface. The amplitude and direction of the force is dependent upon the magnitude and direction of the armature current, respectively. The amplitude and direction of the force in the armature determines the acceleration of the table surface. However, the acceleration measured at the table surface or specimen control point is not a direct linear function of the force generated by the armature current. Resonant modes of the specimen armature combination tend to distort the input acceleration level.

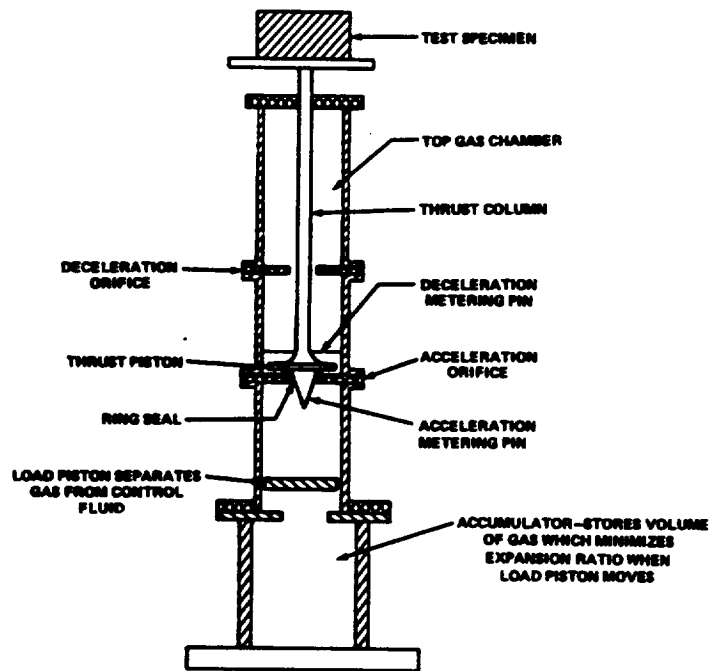


Figure 74. Hydraulic - pneumatic shock machine.

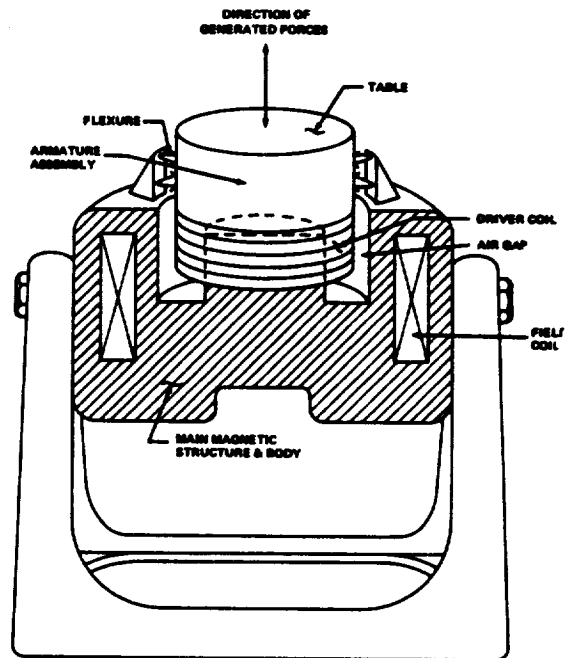


Figure 75. Electromagnetic vibration shaker.

If the specimen to be tested is less massive than the armature, the specimen will have little effect on the acceleration of the table. However, the first effect of a large mass is to decrease the overall acceleration on the table in accordance with the equation $G = \frac{F}{W}$, where W is the weight in grams, G is acceleration in gravity units, M/SU^2 and F is the force rating of the shaker in newtons. The second effect of a large mass is to lower the frequency of the resonance so that the mass supplies a force to the armature. This force may be in phase with lead, or lag the armature force, and will therefore distort the table acceleration waveform.

Special provisions are usually made in an electronic network for adjusting the input signal to the power amplifier to compensate for electrical and armature structural responses. Figure 76 is presented to indicate the general behavior of a loaded and unloaded armature over the usable frequency range.

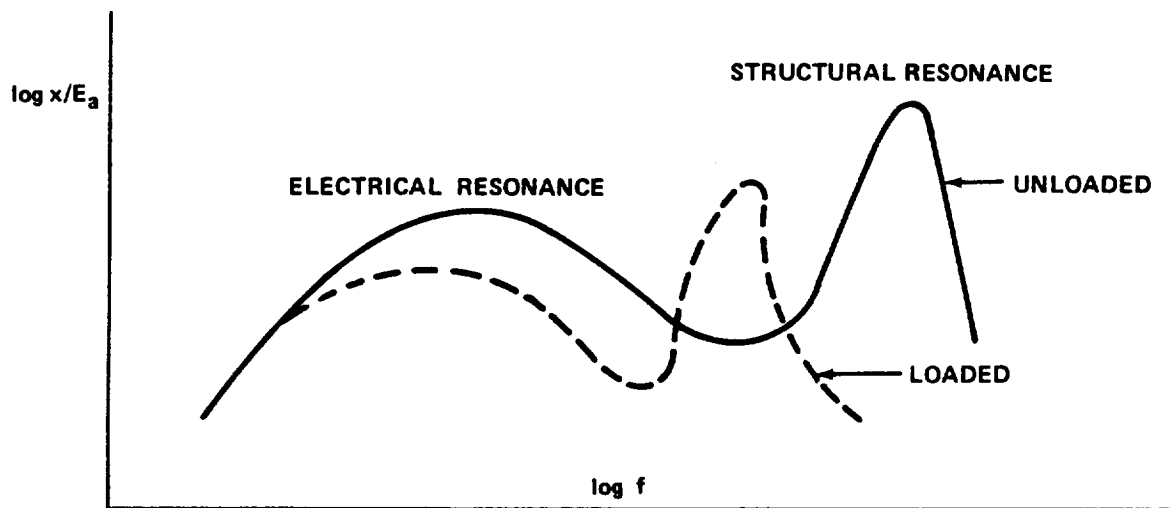


Figure 76. Armature behavior over usable frequency range.

The steady state or average current (force) in the armature is limited by the resistive power losses (heat generated) which the armature is capable of dissipating. The peak current (force) is limited by the voltage that the armature can withstand without breakdown in the insulation. Vibrators designed for random vibration can withstand peak forces of approximately three times the average force.

These vibrators, or force generators, range in weight from 18.14 to 15 872.5 kg and in-force output from 5.337 to 133 440 nts. Generally, the costs of electromagnetic vibrators are much greater than mechanical vibrators (eccentrics). More elaborate auxiliary support equipment, such as amplifiers, power supplies, and controls, are needed for electromagnetic vibrators than for mechanical shakers. The desirability of the electromagnetic vibrator lies in its versatility and usable frequency range of up to 3 kc. An electromagnetic vibrator can generate very complicated waveforms such as broad band random vibrations.

The thruster is another type of electrodynamic shaker which is in use at MSFC. Because of its relatively small size, a number of these vibrators can be used to apply inputs at various points around a large structure. This machine eliminates large, heavy fixtures and minimizes structure/shaker resonant coupling because of the high natural frequency of the thruster's light armature.

3. SINUSOIDAL-SWEEP TESTING

The sine sweep tests consist of applying a sinusoidal motion to the specimen and slowly varying the frequency at some predetermined rate. In order to produce sinusoidal motions at the exciter table, it is necessary to generate electrical signals proportional to the desired accelerations. The signal source for sine sweep testing is the sine oscillator (Fig. 77). The oscillator generates a low power sine wave signal whose amplitude and frequency are controllable by the operator. This low power signal is supplied to the power amplifier where its energy is increased to a level sufficient to drive the vibration exciter. If the oscillator signal through the power amplifier was applied to the exciter and a frequency sweep made at some constant output voltage, we might expect the table acceleration to vary as shown in Figure 76. Since it usually is desirable to maintain some specified acceleration on the table and since the frequency response function of the exciter-amplifier (Fig. 76) is generally unknown before the test, there must be some means of automatically maintaining the table acceleration level at the desired value. The simplest means to accomplish this is to measure the table acceleration and allow the operator to adjust the oscillator output to maintain the desired acceleration level. In practice, this oscillator adjustment is performed automatically. The desired acceleration level is programmed into the vibration controller and the monitored table acceleration is compared to it. Differences between the desired and measured levels are corrected either by increasing or decreasing the controller output. The additional capability to control displacement at low frequencies is usually included in

the sine control system. Such a capability allows the operator to control constant displacement levels at those frequencies where the exciter is displacement-limited. As the frequency is increased and reaches a point where the acceleration is the desired value, the automatic control switches to maintain a constant acceleration rather than constant displacement. The frequency at which the automatic control switches from displacement to acceleration is known as the "crossover" frequency.

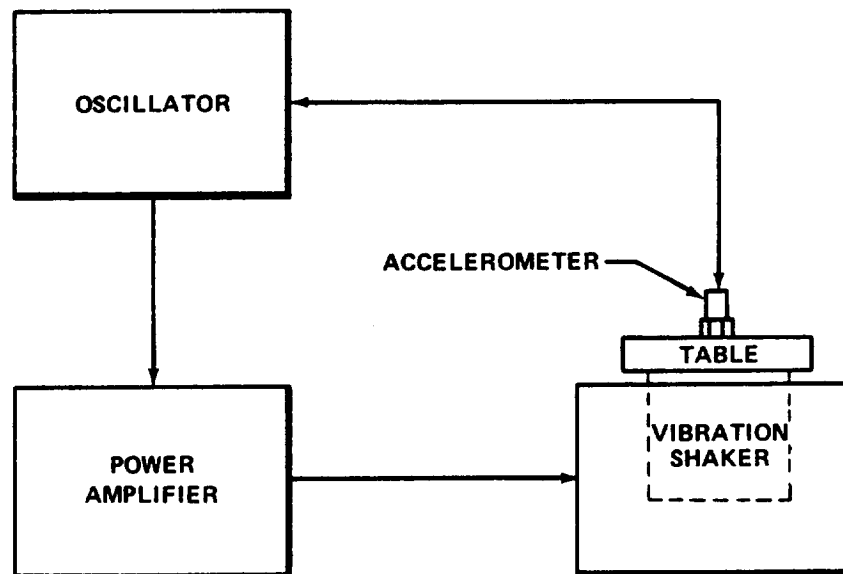


Figure 77. Functional block diagram of sinusoidal sweep generating system.

4. RANDOM VIBRATION TESTING

The use of random vibration testing, occasionally called random noise or white noise testing, is increasing rapidly. Random vibration is similar to many environments measured on aircraft, guided missiles, and space vehicles.

The random vibration test equipment configuration shown in Figure 78 is obviously more complex than the sine test equipment configuration. This complexity is necessary because the load-influenced transfer function of the amplifier-exciter must be compensated at all frequencies simultaneously. Because the random signal contains all frequencies within its bandwidth limits, a sequential equalization, like that employed in the sine test system, is not possible. One equalization system uses wave-shaping circuits ("peak-notch filters") inserted in the signal path. This system requires a determination of the amplifier-exciter (load) transfer function by using a low level

sine sweep prior to equalization. Once the transfer function is determined, the wave shaping circuits are adjusted to generate the inverse transfer function of the system, resulting in a table acceleration with a relatively flat frequency response. Spectrum shaping is accomplished by inserting other wave shaping circuits with the desired transfer characteristics. The "peak-notch equalizer" system is declining in popularity because of the complex setup procedure necessary and its lack of automatic control.

The automatic equalization configuration shown in Figure 78 is presently in use at MSFC. In this scheme, equalization is accomplished by controlling the energy in each of many continuous narrow bandwidths. The wide-band random signal from the noise generator is passed into a bank of continuous filters. The output of each filter is fed into an automatic control amplifier. From the amplifier, the signal is fed into a mixer and then to the power amplifier. The output of the table-mounted (control) accelerometer is adjusted (the spectrum is shaped) by the operator. The output of each analyzer filter is then compared to the desired value. The difference signal is used to adjust the output from the corresponding automatic control amplifier resulting in a spectrum at the table shaped to the desired value. The additional capability to monitor and record the energy value within each filter is included in the equalizer. Set-up time is reduced since the equalization takes place as the test is begun. It is necessary only to program the desired spectrum shape and level prior to the test.

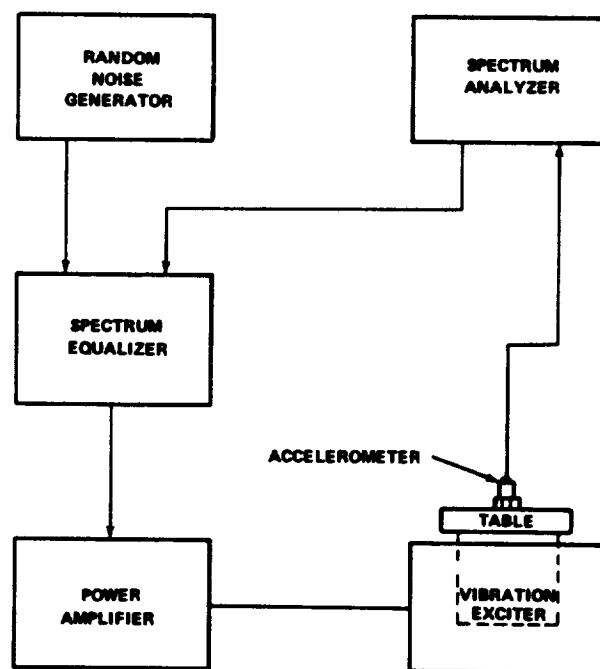


Figure 78. Functional diagram of a random vibration generating system.

SECTION XI. VIBRATION AND ENVIRONMENTS AND TEST SPECIFICATIONS

A. Stage and Vehicle Vibration and Shock Criteria

It is imperative that the vibration environment of future vehicles be predicted prior to design and development so that satisfactory design and test procedures can be established. These criteria are essential to the establishment of high reliability standards necessary for man rated vehicles. The precise prediction of these environments is highly complex and may not be reached soon. However, based on measured data and a few simplifying assumptions, adequate predictions may be obtained provided the necessary assumptions and limitations are realized by the user.

Localized vibration originates primarily from four sources of excitation:

1. Mechanically induced vibration from rocket engine fluctuation which is transmitted throughout the vehicle structure.
2. Acoustic pressures generated by rocket engine operation.
3. Aerodynamic pressure created by boundary layer fluctuations.
4. Self excited machinery or components, etc.

Restricting notation to vibrational power quantities, the total vibration at any point on the vehicle may be expressed as

$$P_T = P_{/mech} + P_{/ae} + P_{/mach}$$

where / denotes the vibrational power caused by the indicated source. The powers add arithmetically since vibrational power is proportional to the mean square cyclic response. An exact analysis of structural response would necessitate an accurate description of each individual source and the manner in which they combine. In most cases only one source is the primary forcing function. Hence, the remaining sources may be considered negligible in regard to the total dynamic response at any instant of time. However, an expression is given [equation (229)] which provides an estimate for combined driving functions.

Rocket vehicle structure may be separated into two dynamic categories:

I. Structure susceptible to acoustic and/or aerodynamic pressures (i.e., skin panels).

II. Structure not susceptible to acoustic and aerodynamic pressures (i.e., structural beams).

The dynamic analysis of these two groups are obviously handled by two different techniques. Each is explained below.

Type I

This group of structures may be subdivided into three sections:

I(a). Skin panels. A panel is defined as a section of skin bounded by radial and longitudinal stiffeners. This type of structure is directly excited by impinging acoustic pressures. The direction normal to the panel face exhibits the most severe vibratory response; consequently, this is the direction usually considered when referring to panel vibrations.

I(b). Skin stiffeners (such as ring frames and stringers). This type of structure is not directly excited by acoustic forces but is driven by the motion of adjacent panels. Thus the stiffeners are indirectly forced by impinging acoustic pressures.

I(c). Bulkheads. These skin segments form the upper and lower extremities of vehicle propellant tanks. The bulkheads are further subdivided into:

I(c)-1. Forward bulkheads

I(c)-2. Aft bulkheads

The added mass of liquid loading greatly reduces the vibration amplitudes experienced by the aft bulkheads; consequently, the two bulkheads are treated separately.

The equation for predicting the vibration environment of acoustically (or aerodynamically) susceptible structure is [26]

$$G_n = G_r \left(\frac{p_n}{p_r} \right) \left(\frac{\rho_r t_r}{\rho_n t_n} \right) \sqrt{F} = G_r \left(\frac{p_n}{p_r} \right) \left(\frac{\rho_r t_r}{\rho_n t_n} \right) \sqrt{\frac{W_n}{W_n + W_c}} \quad (227)$$

where

G_n = the vibration response of the new vehicle structure at a particular station number. The term G is the acceleration due to cyclic motion divided by the acceleration of gravity g_0 . Since rocket vibrations contain many frequencies the response magnitude (G) is specified in spectral form.

G_r = the known vibration response of a reference vehicle structure. This value has been determined by many measurements and is also presented on a spectral basis. Further, this parameter should be obtained from unloaded structure (i. e., structure which does not reflect the effects of component mass loading).

t_r = the thickness of the skin associated with G_r .

ρ_r = the skin weight density of the reference structure.

p_r = the impinging acoustic (or aerodynamic) pressure which is driving the reference structure.

t_n = the skin thickness¹ associated with G_n .

ρ_n = the skin weight density associated with G_n .

p_n = the acoustic (or aerodynamic) pressures impinging upon the new vehicle structure. This pressure must also be predicted.

F = A factor which accounts for the attenuation effects produced by incorporating additional mass into the existing system.

W_n = weight of basic structure.

W_c = component weight mounted on W_n .

1. For corrugated or sandwich structure this parameter is an equivalent thickness.

Equation (227) applies to random rms composite values or to sinusoidal values. For the mean square spectral value, the total expression is simply raised to the second power. This expression is applicable to localized vibratory environments and is valid for all materials. It is invalid when considering large sections of vehicle structure (i.e., entire cylindrical tank). However, the static loading of these large sections is the critical design factor and localized dynamics thereby produce only negligible effects.

Referring again to equation (227), P_n represents the maximum pressure impinging upon the vehicle at any time. Three conditions must be considered, one of which will result as the maximum.

1. Captive-firing environments (applicable to boosters and upper stages).
2. On-pad acoustic environments.
3. The period of maximum aerodynamic pressure (occurs subsequent to Mach one; therefore, the combining of engine generated acoustics and boundary layer pressures do not have to be considered).

Type II

Now consider the Type II structure. This structure may be subdivided into two sections.

II(a). Structural beams such as I beams, etc. The components mounted in this section would not primarily be affected by acoustic pressures but by rocket engine vibrations.

II(b). Rocket engine components. These components may again be subdivided into three sections:

II(b)-1. Combustion chamber section. This section includes the components mounted on the chamber dome or side case.

II(b)-2. Turbopump section. This section includes the components located on the propellant pumps.

II(b)-3. Actuator assembly. The components located in this region are mounted on the actuator struts or actuator rods.

The equation for predicting vibrations of these structural types is

Type II(a)

$$G_n = G_r \sqrt{\frac{(NTV)_n}{(NTV)_r} \frac{W_r}{W_n}} F = G_r \sqrt{\frac{(NTV)_n}{(NTV)_r} \left(\frac{W_r}{W_n + W_c} \right)} \quad (228a)$$

Type II(b)

$$G_n = G_r \sqrt{\frac{(TV)_n}{(TV)_r} \frac{W_r}{W_n}} F = G_r \sqrt{\frac{(TV)_n}{(TV)_r} \left(\frac{W_r}{W_n + W_c} \right)} \quad (228b)$$

where

G_n = the vibration response of the new structure. This is considered an input to a component mounted on this structure.

G_r = the vibration response of a reference structure. This environment is determined by measured data acquired from unloaded structure.

NTV_n = number of engines, thrust and exhaust velocity of rocket engine associated with the stage under consideration in the new vehicle.

NTV_r = number of engines, thrust and exhaust velocity of rocket engine associated with a reference vehicle.

$F = \frac{W_n}{W_n + W_c}$ = an attenuation factor which takes into account the effects of component mass loading.

W_n = the structural weight corresponding to G_n .

W_r = the structural weight corresponding to G_r .

W_c = the weight of component to be mounted on W_n .

Equation (228) applies to random rms composite values or to sinusoidal values. For the mean square spectral density value the total expression is simply squared. For Type II(b) structure, clustering does not generally affect engine vibrations; therefore N_r and N_n are not considered. Also, for Type II structure, only once case is considered the maximum. This case is the firing (either captive or inflight) of that particular stage under consideration. The vibration transmitted from other stage firings (i. e., booster to upper stages) is negligible compared to that stage operation. Thus, with a knowledge of the necessary rocket engine parameters and structural mass characteristics, the vibratory environment of a new vehicle is shown in Figure 79.

The methods and techniques presented herein will provide satisfactory estimates of the vibratory environment associated with any particular problem. These techniques are considered indicative of the present state-of-the-art and will permit adequate environmental estimates with only a few simple calculations. It is not imperative that the user thoroughly understand the philosophy behind the methods. He should, however, realize the necessary requirements and limitations. A summary of the principal limitations regarding these techniques is given below.

1. The techniques do not apply to entire structure such as an entire rocket engine assembly or large structural members. They do, however, apply to components and other items of equipment mounted on these structures.

2. These methods are not applicable for prediction of combined environments such as excitation due to propellant flow and engine vibration combined. In some remote cases the type of structure may not be clearly defined or excitation may be both acoustically and mechanically induced. In these cases the two methods may be combined and a certain percentage assigned to each method depending upon degree of structural susceptibility to acoustic and mechanical excitation. Employment of the respective percentages is left to the discretion of the user.

$$G_{n_t} = \sqrt{X\%G_{n_I}^2 + Y\%G_{n_{II}}^2}$$

where

G_{n_t} = the resultant combined environment

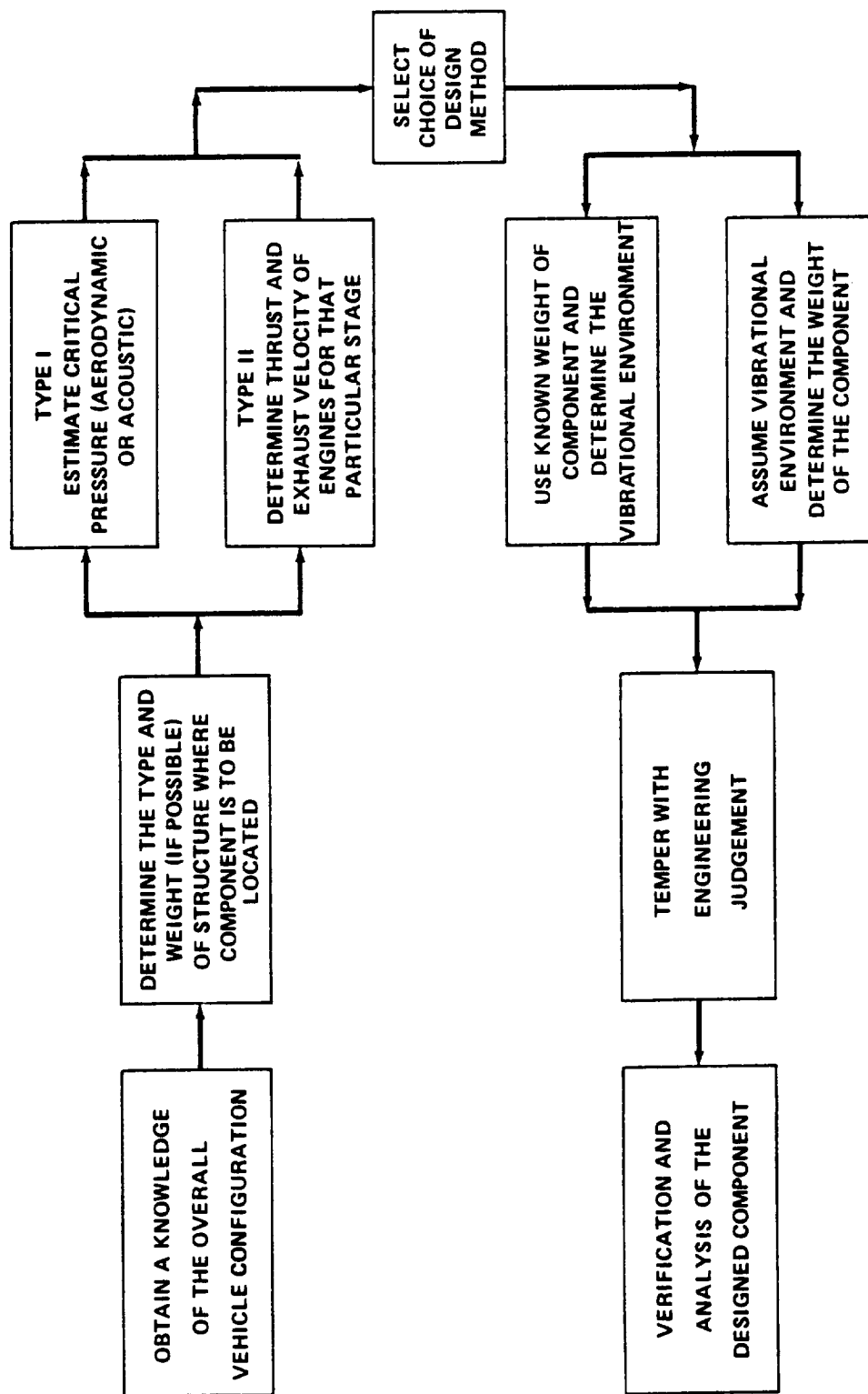


Figure 79. Flow chart for determining the vibration environment of a new vehicle structure.

G_{n_I} = the environment obtained from using Type I methods

$G_{n_{II}}$ = the environment obtained from using Type II methods

and

$$X\% + Y\% = 1.0 \text{ or } 100\%$$

3. This method does not provide frequency characteristics of the new structure. The method is based on the fact that similar structure has similar response characteristics. Precise frequency calculations tend to complicate the problem and it is doubtful that the results would justify the time and effort required. The calculation of the component natural frequency is, within itself, possibly a simple problem. In the actual system, however, this frequency is coupled with the support structure frequency characteristics. The determination of structure-component coupling effects is a highly complex requirement. Consequently, adequate frequency calculations and evaluation of these effects require considerable time and effort.

These techniques rely upon typical structural configurations which have been sufficiently defined by measured data. Subsequent statistical analyses describe the dynamic characteristics of the structure with statistical certainty. Thus, with only a knowledge of the structural geometry and mass characteristics, the anticipated dynamic environment may be established. These techniques are applicable to most rocket vehicle structure — including corrugated and sandwich skin construction provided an equivalent flat plate thickness may be determined.

The predicted environments represent a statistical estimation since the reference spectra should be established by statistical techniques. Consequently, the probability of the actual environment not exceeding the predicted environment of a future vehicle is established with a confidence level indicative of the necessary vehicle mission. This does not infer that the predicted environment will accurately correspond to a single measured environment. Certainly, some of the measured responses of a new vehicle will be significantly lower than the predicted. This is to be expected since the criterion is such that the prediction will envelope the greater percentage of the situations. However, this problem is elevated somewhat by the techniques utilized of separating rocket vehicle structure into eight basic categories — each possessing essentially similar dynamic characteristics. This reduced the variance so that the mode value (point of maximum occurrence) is not greatly less

than the higher confidence limits. Therefore, the higher percentage criterion may be used without the concern of over conservatism in regard to a specific problem.

B. Payload Vibration and Shock Criteria

The techniques previously described have been altered to provide vibration design and test criteria for launch vehicle payloads and payload components. A new criteria philosophy was deemed necessary because: (1) The type of structure in the payload area is grossly different from the launch vehicle structure, (2) the payloads and payload components will not be subjected to static firing tests and therefore require test criteria that possess the high degree of confidence dictated by their "one-shot" use, and (3) their use environment can be simulated better by random vibration criteria. The new techniques generate five types of vibration criteria:

1. Vehicle dynamics.
2. Sine evaluation.
3. High level random.
4. Low level random.
5. Shock.

These criteria are designed to simulate as nearly as possible the expected flight environments. The specific purposes of each of these criteria are as follows:

1. Vehicle dynamics criteria consist of sinusoidal vibration levels designed to simulate the vibration environment induced by launch vehicle bending and torsion and by engine ignition and thrust variations.
2. Sine evaluation criteria consist of sinusoidal vibration levels designed to evaluate the component's dynamic response characteristics when it is subjected to vibration levels less severe than the maximum anticipated levels but of sufficient magnitude to induce significant dynamic responses.
3. High-level random criteria are random vibration levels designed to evaluate the component's performance when subjected to an input representative of the maximum anticipated spectral intensity of the environment.

4. **Low-level random criteria** are random vibration levels designed to evaluate the component's performance when subjected to an input representative of the maximum anticipated energy of the environment.

5. **Shock criteria** are shock levels designed to simulate the maximum anticipated shock environment on damage equivalence basis.

Each of these criteria is calculated using the predicted vehicle dynamics, acoustically induced vibration, and shock environments. The following paragraphs outline how the particular environments are predicted and subsequently used for criteria development.

The vehicle dynamics environment is predicted using a mathematical model of the launch vehicle and payload. The model is forced with inputs representative of the actual vehicle forcing functions; i. e., wind loads, engine ignition/cutoff forces, and release and separation forces. The maximum response of the payload at each significant frequency is computed with these modal responses being considered as the vehicle dynamics environment. The environment is enveloped to generate the sinusoidal vehicle dynamics criteria.

Vibration data for the reference structure are gathered and statistically summarized. These summaries, consisting of an envelope of the maximum spectral intensities and an envelope of the average spectral intensities, are extrapolated to the new structural configuration. The extrapolation relationships used are the same as for launch vehicle components [reference equation (227)], except that the extrapolation relationship is a function of the acoustic pressure at each frequency rather than the overall acoustic pressure. As a result of these calculations, a predicted maximum and average vibration spectrum is generated. These spectra are used to generate the following criteria:

1. The high-level random criteria are generated by enveloping the maximum spectral intensities.

2. The low-level random criteria are generated by reducing the envelopes obtained in 1. to possess the maximum statistical composite value of all the data samples.

3. The sine evaluation criteria are generated by computing, from the maximum spectral intensities, an equivalent g response factor (GRF). This factor is obtained from

$$GRF_i = 1.2 \sqrt{g_i f_i}$$

where

g_i = maximum spectral intensity in any spectral increment i .

f_i = frequency associated with the i^{th} spectral increment.

The equivalent g response factor at each frequency is plotted, and a sine sweep level is calculated that passes beneath all plotted points.

Measured shock environments from similar payload structure are analyzed, and a prediction based on these analyses is made for the new structure. The analysis is performed in the shock (response) spectrum domain and therefore generates shock spectrum criteria that are expected to induce damage equivalent to that induced by the predicted environment.

SECTION XII. THEORETICAL CONSIDERATIONS

The preceding sections of this manual have described basically the methods and facilities employed to obtain, reduce, evaluate, and utilize vibration data. This section, however, presents a different approach. It contains applicable reference material for a theoretical and statistical look at vibration analysis.

The sequence of information presented by the following main paragraphs does not necessarily indicate the relative importance of the paragraphs. In some cases a main paragraph may be considered a separate entity, not having to follow any particular preceding paragraph.

A. Vibration Terms – Their Meanings and Uses

1. DISPLACEMENT, VELOCITY, AND ACCELERATION

Vibration measurements can be in terms of displacement, velocity, or acceleration. The easiest measurement to understand is that of displacement, or the magnitude of motion of the body being studied. Where the rate of motion (frequency of vibration) is low enough, the displacement can be measured directly with a dial-gage micrometer. When the motion of the body is great enough, its displacement can be measured with a common scale.

In its simplest case, the displacement may be considered as simple harmonic motion; that is, a sinusoidal function having the form

$$x = A \sin \omega t \quad (230)$$

where A is a constant, ω is 2π times the frequency, and t is the time as shown in Figure 80. The maximum peak-to-peak displacement (the quantity indicated by a dial gage) is $2A$, and the root mean square (rms) displacement is $A/\sqrt{2}$ ($=0.707A$). The average (full-wave rectified average) value of the displacement is $2A/\pi$ ($=0.636A$) while the "average double amplitude" (a term occasionally encountered) would be $4A/\pi$ ($=1.272A$). Displacement measurements are significant when deformation and bending of structures are studied.

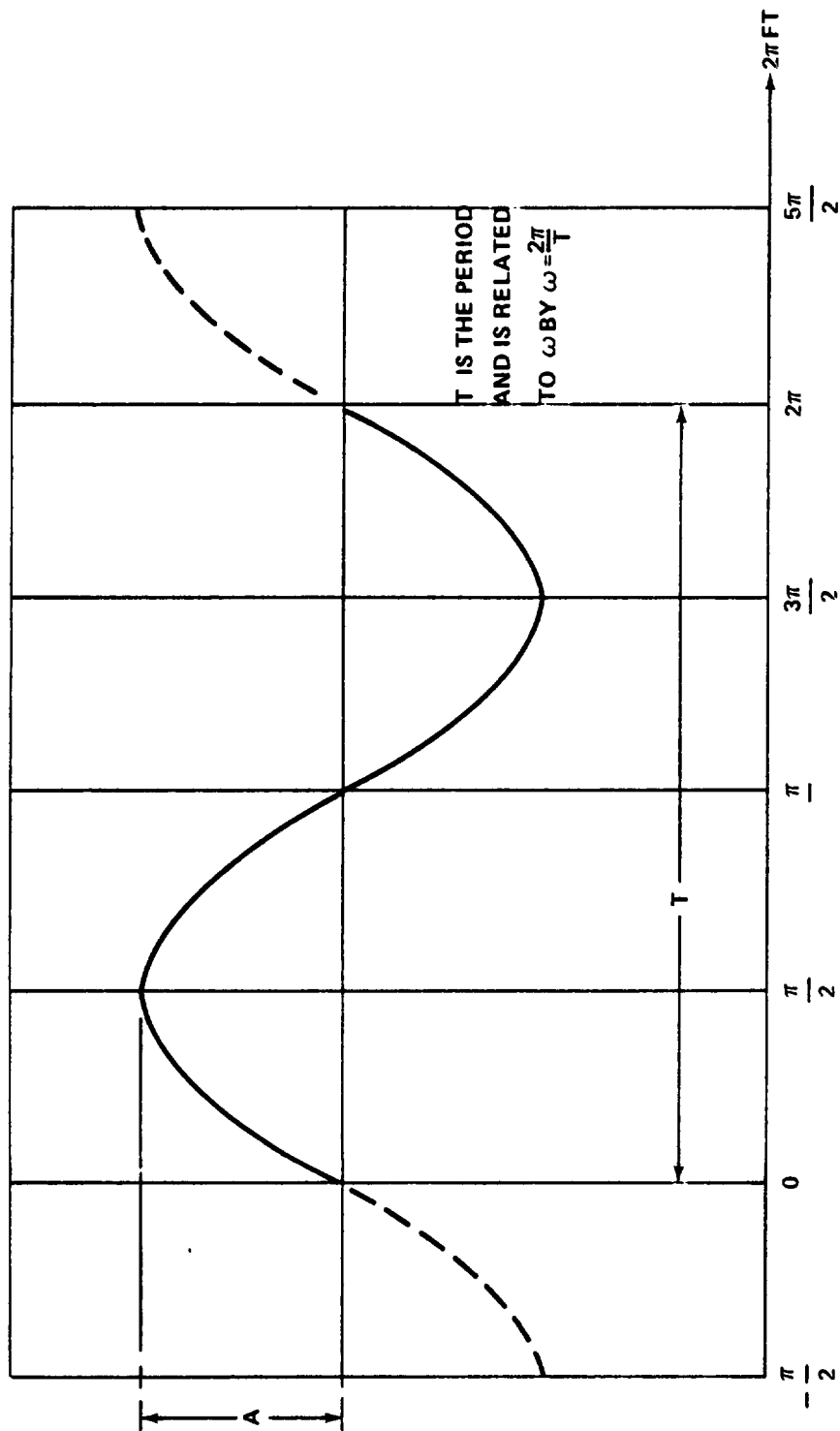


Figure 80. Sinusoidal function $x = A \sin \omega t$.

In many other practical problems, however, displacement is not the important property of the vibration. A vibrating mechanical part will radiate sound in much the same way as does a loudspeaker. In general, the velocities of the radiating part (which corresponds to the cone of the loudspeaker) and the air next to it will be the same, and if the distance from the front of the part to the back is large compared to one-half of the wavelength of sound in air, the actual sound pressure in air will be proportional to the velocity of the vibration. The sound energy radiated by the vibrating surface is the product of the velocity squared and the resistive component of the air load. Under these conditions, particularly where noise is important, it is the velocity of the vibrating part and not its displacement which is of greatest importance.

Velocity is the time rate of change of displacement, or the first derivative of displacement with respect to time, so that for the sinusoidal vibration in equation (230) the velocity is

$$v = \frac{dx}{dt} = \omega A \cos \omega t \quad . \quad (231)$$

Thus, the velocity is proportional not only to the displacement but also to the frequency of the vibration.

In many cases of mechanical vibration, and particularly where mechanical failure is a consideration, the actual forces set up in the vibrating parts are important factors. Newton's laws of motion state that the acceleration of a given mass is proportional to the applied force, and that this force produces a resulting reacting force which is equal but opposite in direction. Members of a vibrating structure, therefore, exert forces on the total structure that are a function of the masses and the accelerations of the vibrating members.

Acceleration measurements are important where vibrations are sufficiently severe to cause actual mechanical failure. Acceleration is the second derivative of the displacement with respect to time or the first derivative of velocity with respect to time. That is,

$$a = \frac{dv}{dt} = \frac{d^2x}{dt^2} = -\omega^2 A \sin \omega t \quad . \quad (232)$$

The acceleration, therefore, is proportional to the displacement and to the square of the frequency.

There is another use for acceleration measurements. The analogy cited above concerning the loudspeaker covers the usual case where the cone or baffle is large compared to the wavelength of the sound involved. In most machines the relationship does not hold, since relatively small parts are vibrating at relatively low frequencies. This may be compared to a small loudspeaker without a baffle. At low frequencies the air may be "pumped" back and forth from one side of the cone to the other with a very high velocity, radiating much sound energy because of the very low air load, which has a reactive mechanical impedance. Under these conditions the accelerations measurement provides a better measure of the amount of noise radiated than does a velocity measurement.

2. SUMMARY

Displacement measurements are used only in instances where the actual amplitude of motion of the parts is important. This would include those cases where the dynamic loading because of the operating machinery in a factory may cause unsafe deflections in flooring and walls or where large amplitudes of motion might actually cause parts to strike together, thus causing damage or serious rattle. The deflections observed at the center of a wall panel or beam, for example, can give useful information about the stresses acting in these members. The displacement is not directly a measure of surface strain of the member but is rather an integrated indication of the strain. The strain measured by the usual strain gage is minute elongation or compression of material between points an inch or so apart; in contrast, the displacement measurement referred to above is the bending of material over a distance of several feet.

Velocity measurements are generally used in noise problems where the radiating surfaces are comparatively large with respect to the wavelength of the sound.

Acceleration measurements are the most practical where actual mechanical failure of the parts involved is of importance and in many noise problems, particularly those involving small machinery. A general purpose vibration meter, therefore, must be able to measure all three vibration characteristics.

3. NON-SINUSOIDAL VIBRATION

Equations (230), (231), and (232) represent only sinusoidal vibrations, but, as in the case of the other complex waves, complex periodic vibrations

can also be represented as a Fourier series of sinusoidal vibrations. These simple equations may, therefore, be expanded to include as many terms as desirable in order to express any particular type of vibration. It will be noted that, since velocity is proportional to frequency, and acceleration is proportional to the square of the frequency, the higher frequency components in a vibration are progressively more important in velocity and acceleration measurements than in displacement readings.

B. Random Process and Probability Distribution

An example of a random experiment may be illustrated by tossing a single die to determine how many spots will be on the top face after each toss. A record of the number of spots that show after each toss is illustrated in Figure 81.

This graphical result is called a sample function, and a collection of many of these sample functions forms an ensemble. If many of the random experiments are repeated, the ensemble of sample functions is an example of a random process. In the case of the die, the number of spots showing or

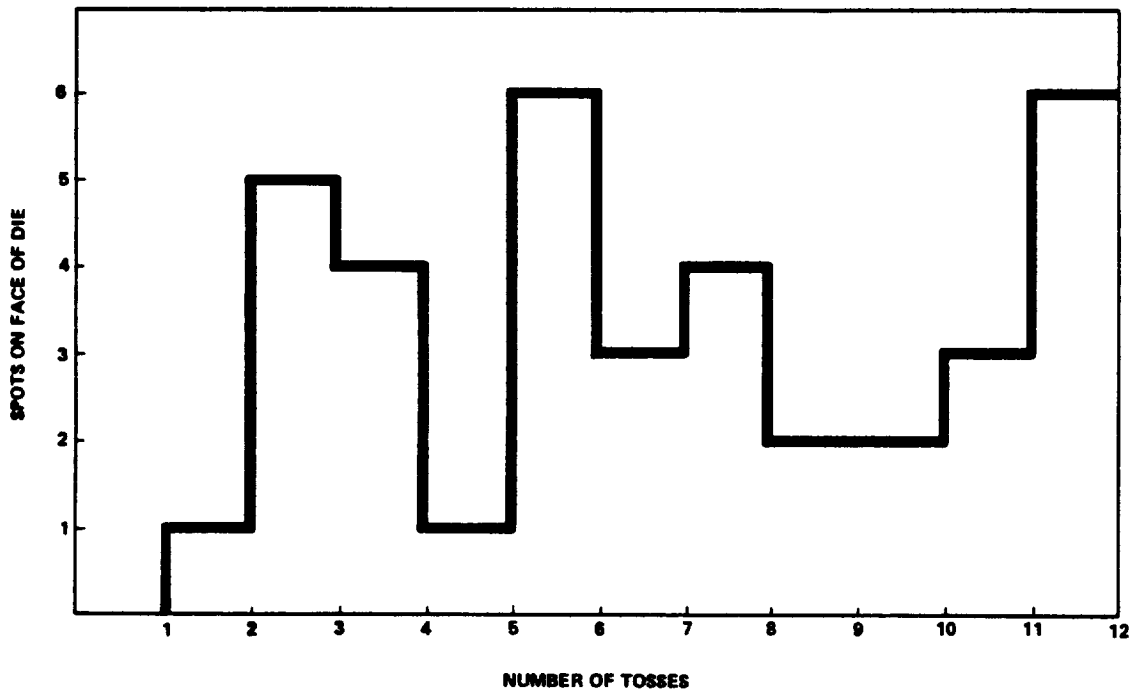


Figure 81. Record of a random experiment with a die.

the value measured is an example of a random variable. If x is a random variable, it may be noted that any function of x such as x^2 , e^x , or $x^{1/2}$ is a random variable.

Since there are only six sides to a die, the random variable in this case has only six possible values, and is a discrete random variable.

However, if for the experiment a measurement had been chosen with an infinite number of possible results, a continuous random variable would have been defined. Continuing the experiment, the ensemble is observed and the number of times the value one occurs on the first toss is counted, and is denoted n_1 . Let N denote the total number of sample functions. Then the relative frequency of the occurrence of one on the first toss is denoted by n_1/N . Now if N becomes very large, then n_1/N will approach a limiting value. Then the value of n_1/N as $N \rightarrow \infty$ is the probability of "one" occurring on the first toss of the die. This probability is written $P(1)$. A more general expression may be written

$$\begin{aligned} P(x_k) &= \text{probability that } x \text{ has the value } x_k \text{ on the first toss} \\ &= \lim_{N \rightarrow \infty} \frac{n_k}{N} \end{aligned} \quad (233)$$

where n_k is the number of times the value x_k occurs on the first toss among the N sample functions.

The complete set of values $P(x_k)$ for all possible values of k is called the probability distribution of the discrete random variable x . A plot of the probability distribution of a discrete random variable is shown in Figure 82.

From the above:

- a. The probability of a certain event = 1
- b. The probability of an impossible event = 0
- c. $0 \leq P(x_k) \leq 1$

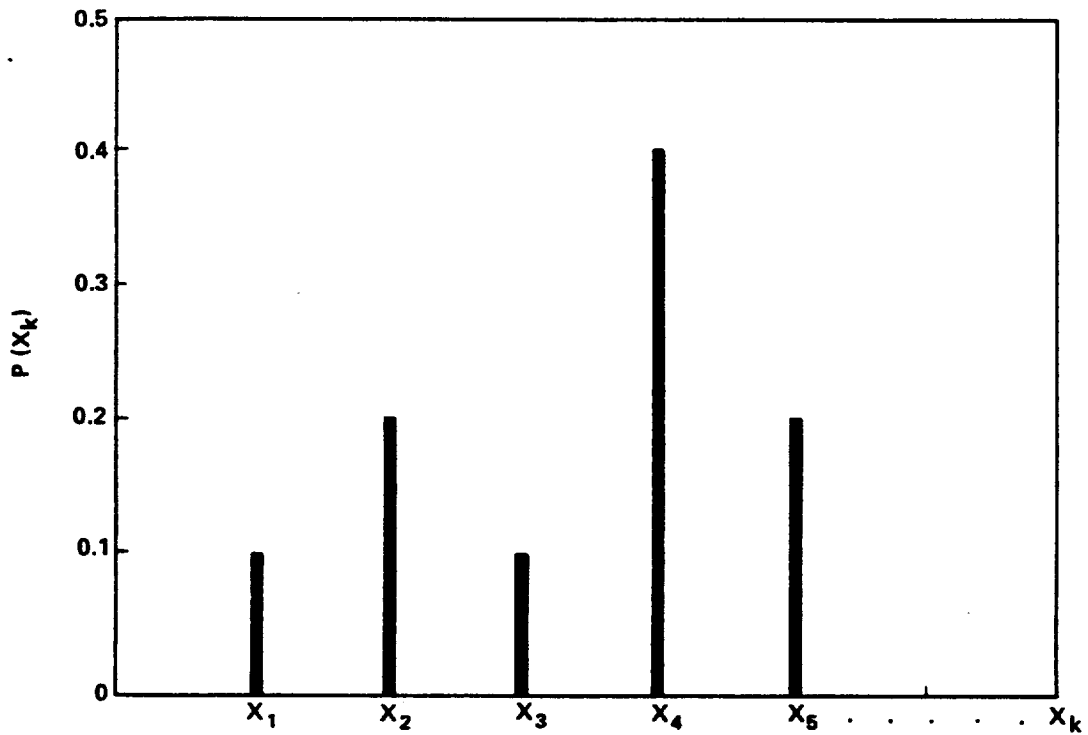


Figure 82. Probability distribution of a discrete random variable.

d. When different values of x are mutually exclusive,

$$P(x_1 \text{ or } x_2 \text{ or } x_k \text{ or } \dots) = P(x_1) + P(x_2) + P(x_k) \quad . \quad (234)$$

e. If the random variable can take on no more than M possible values,

$$\sum_{k=1}^M P(x_k) = 1 \quad (235)$$

f. A probability distribution function for a discrete random variable may be defined as follows (Fig. 83):

$$P(x \leq X) = \sum P(x_k) \quad (236)$$

$$g. \quad P(x \leq +\infty) = 1, \quad P(X \leq -\infty) = 0$$

$$h. \quad \text{If } b > a, \text{ then } P(x \leq b) - P(x \leq a) = P(a < x \leq b) \geq 0.$$

Extending the above concept to continuous random variables, a probability distribution function is shown as a smooth curve rather than a step function (Fig. 84). Now the probability distribution of the discrete case is replaced by the probability density function which is defined as the derivative of the probability distribution function and is denoted by the symbol $p(x)$. The continuous functions and the discrete case have similar properties except the sums now become integrals.

$$a. \quad F(x \leq X) = \int_{-\infty}^X p(x) dx \quad (237)$$

$$b. \quad \int_{-\infty}^{\infty} p(x) dx = 1 \quad (238)$$

$$c. \quad \int_a^b p(x) dx = P(a < x \leq b) \text{ for } b \geq a \quad (239)$$

Now there are two means of expressing our random process:

a. An ensemble of sample functions may be constructed (Fig. 85).

b. The probability distribution of the values for any particular toss n may be given. This is written

$$P\left[x_k^{(n)}\right].$$

The above expression simply means the probability that x has the value x_k in the n th toss. In the case of the tossed die, the probability of a three turning up on the 10th toss is written

$$P\left[x_3^{(10)}\right] \text{ where } x_3 = 3.$$

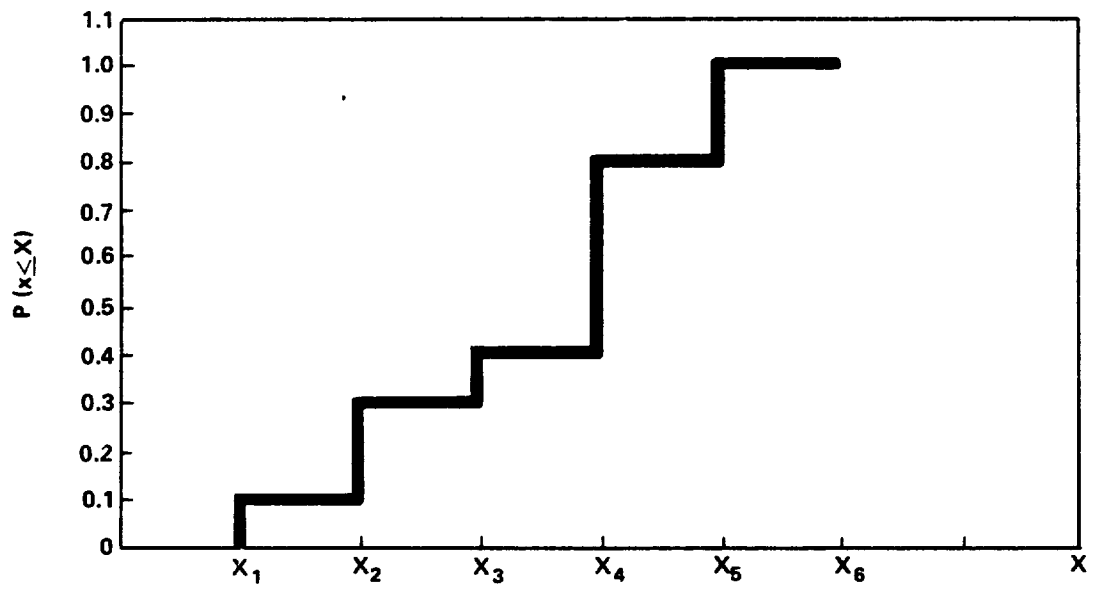


Figure 83. Probability distribution for a discrete random variable.

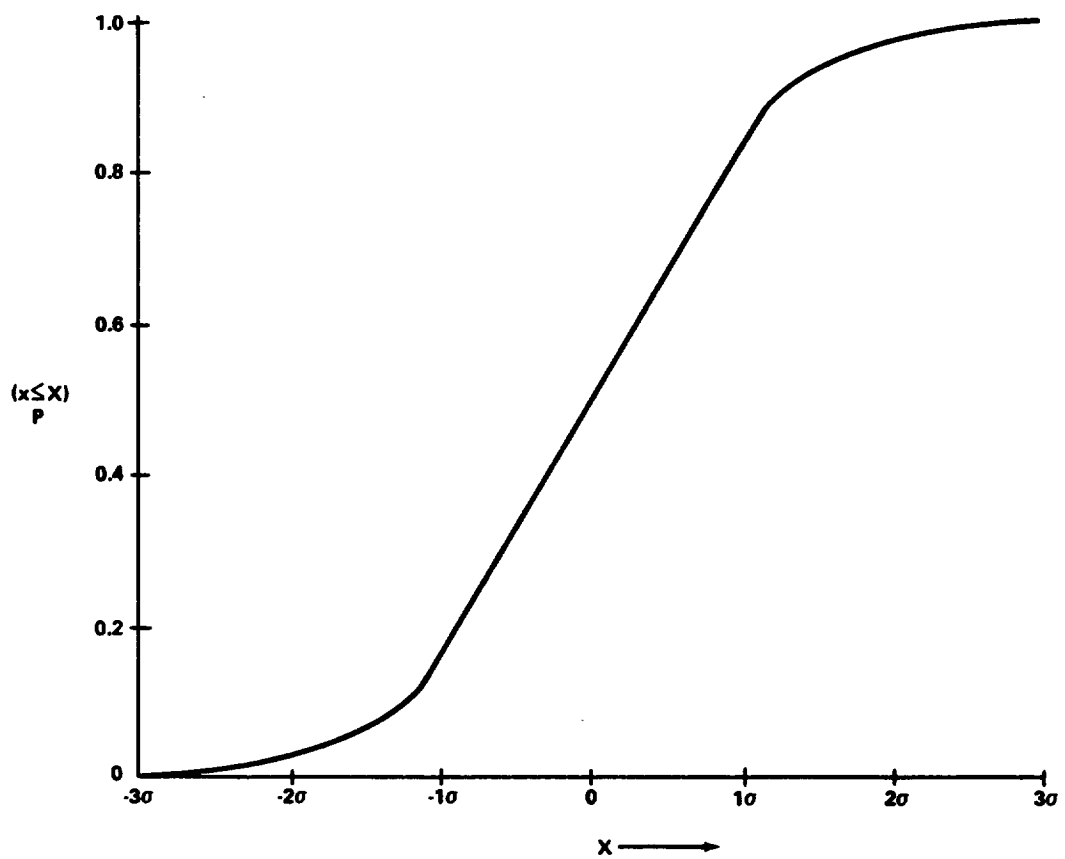


Figure 84. Probability distribution function for continuous random variable.

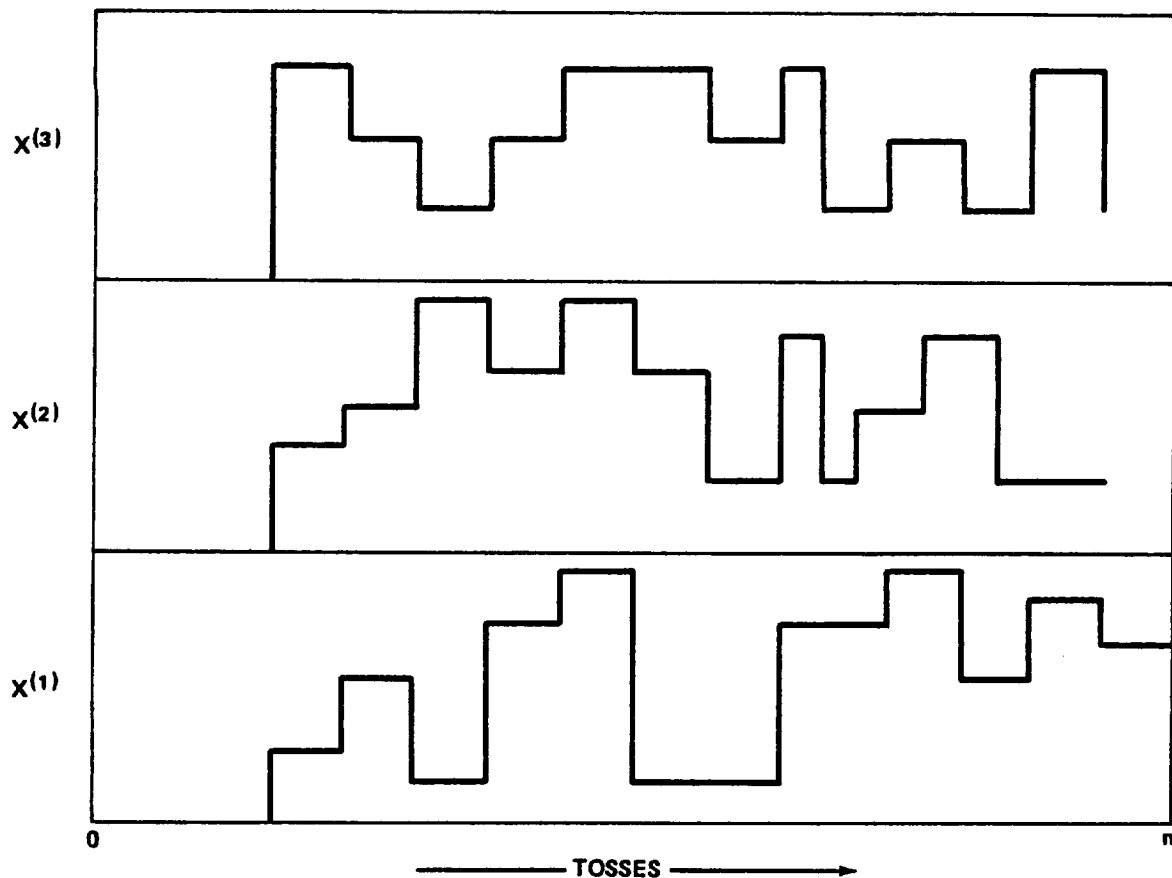


Figure 85. Ensemble of sample functions.

The probability applies to a particular toss since the experiment is across the process, and each toss of the die is an experiment and what happens on toss $(n + 1)$ is not dependent on the results of toss n . Therefore,

$$P\left[x_3^{(10)}\right] = P\left[x_3^{(11)}\right] = \dots = P\left[x_3^{(n)}\right] .$$

From the above, the random process may be completely specified by determining the probability distribution in any toss n .

However, it is noted that all random experiments are not independent. The type of random process to be considered eventually is definitely not one where successive tosses (or successive intervals) are independent. For example, consider a large number of spinners whose angular positions can be refined to an infinite number of possible results, and make the choice of the spinner used in a particular interval dependent upon the result of the

experiment for the preceding interval. The probability distribution $P[x_k^{(n)}]$ for all possible values of k during the n th interval may be specified, but nothing has been said about the dependence of the $(n - 1)$ interval. The probability distribution for all k and all n may be determined and still not show the interdependence between intervals. To do this the concept of joint and conditional probability distributions are introduced.

1. JOINT PROBABILITY DISTRIBUTIONS

Consider a pair of intervals 1 and 2, where the random variable x assumes the values x_i and x_j , respectively, denoted by $x_i^{(1)}$, $x_j^{(2)}$. Again examine N sample functions. Let $n_{i,j}^{(1,2)}$ denote the number of times the combination $x_i^{(1)}$, $x_j^{(2)}$ occurs among the N sample functions. Then, the joint probability is defined by

$$P[x_i^{(1)}, x_j^{(2)}] = \lim_{N \rightarrow \infty} \frac{n_{i,j}^{(1,2)}}{N} \quad (240)$$

As before, it follows that

$$0 \leq P[x_i^{(1)}, x_j^{(2)}] \leq 1 \quad (241)$$

If $x_i^{(1)}$ has I possible values, and $x_j^{(2)}$ has J possible values, then

$$\sum_{i=1}^I \sum_{j=1}^J P[x_i^{(1)}, x_j^{(2)}] = 1 \quad (242)$$

Also, the previous probability

$$P[x_i^{(1)}] = \sum_{j=1}^J P[x_i^{(1)}, x_j^{(2)}] \quad (243)$$

which states the probability of a particular value x_i in the first interval is equal to the sum of its joint probabilities with all possible values of $x_j^{(2)}$ in the second interval.

Similarly,

$$P[x_j^{(2)}] = \sum_{i=1}^I P[x_i^{(1)}, x_j^{(2)}] \quad (244)$$

Second order distribution functions may now be obtained from the joint probabilities. Also, higher order distribution functions may be obtained from higher-order joint probabilities defined by

$$P[x_i^{(1)}, x_j^{(2)}, x_k^{(3)}, \dots]$$

2. CONDITIONAL PROBABILITY DISTRIBUTIONS

Second order distribution functions may now be obtained from the joint probabilities. Also, higher order distribution functions may be obtained from higher-order joint probabilities defined by

$$P[x_j^{(2)} \mid x_i^{(1)}]$$

where the terms following the vertical bar are given terms.

As before, consider N sample functions. Let $n_i^{(1)}$ be the number of times x_i occurs in interval 1, and let $n_{i,j}^{(1,2)}$ be the number of times the combination $x_i^{(1)}, x_j^{(2)}$ occurs. Then

$$P[x_j^{(2)} \mid x_i^{(1)}] = \lim_{N \rightarrow \infty} \frac{n_{i,j}^{(1,2)}/N}{n_i^{(1)}/N} = \frac{P[x_i^{(1)}, x_j^{(2)}]}{P[x_i^{(1)}]} \quad (245)$$

is expressed as the ratio of the probability that both $x_i^{(1)}$ and $x_j^{(2)}$ will occur divided by the probability that $x_i^{(1)}$ will occur. The above result, of course, required that $P x_i^{(1)} \neq 0$. This result can be written in the equivalent form

$$P \left[x_i^{(1)}, x_j^{(2)} \right] = P \left[x_i^{(1)} \right] P \left[x_j^{(2)} \mid x_i^{(1)} \right] \quad (246)$$

For certain cases, the conditional probability

$$P \left[x_j^{(2)} \mid x_i^{(1)} \right] = P \left[x_j^{(2)} \right] \quad (247)$$

independent of the given information that $x_i^{(1)}$ has occurred. In this case, the random variables $x^{(1)}$ and $x^{(2)}$ are said to be independent. Now

$$P \left[x_i^{(1)}, x_j^{(2)} \right] = P \left[x_i^{(1)} \right] P \left[x_j^{(2)} \right] \quad (248)$$

and the joint probabilities are specified from the first-order probabilities.

The concept of joint and conditional probabilities for discrete random variables may be extended to continuous random variables in the form of joint and conditional probability density functions. Considering an ensemble of sample functions which are continuous functions of time, as for example an accelerometer signal, a complete description of the random process requires a specification of the joint probability density function $P(x_{t_1}, x_{t_2}, \dots, x_{t_n})$

for every choice of times t_1, t_2, \dots, t_n and for every finite n . Since this is nearly impossible for a completely arbitrary random process, it is necessary to seek means to simplify the specification of the random process and determine the average value of the sample function in a particular interval. This is

$$\frac{x_1 n_1 + x_2 n_2 + \dots + x_m n_m}{N}$$

As $N \rightarrow \infty$, this becomes

$$x_1 P(x_1) + x_2 P(x_2) + \dots + x_M P(x_M)$$

and is written

$$\sum_{k=1}^M x_k P(x_k) \quad .$$

The above defines the statistical average, ensemble average, or expectation of the random variable x and is noted by

$$E[x] = \sum_{k=1}^M x_k P(x_k) \quad . \quad (249)$$

Extending the above for a continuous random variable, using a probability density function $p(x)$,

$$E[x] = \int_{-\infty}^{\infty} x p(x) dx \quad . \quad (250)$$

Considering a function $f(x)$ of the random variable x ,

$$E[f(x)] = \int_{-\infty}^{\infty} f(x) p(x) dx \quad . \quad (257)$$

An important class of functions is

$$E[x^n] \quad , \quad \text{where } n = 1, 2, 3, \dots, n, \text{ and integer}$$

$$x^n = \text{power of } x \quad .$$

These are the nth moments by analogy with mechanics.

$E[x]$, the cg line location, is called the mean

$E[x] = m$ (the symbol for the mean)

$E[(x - E(x))^2]$ is the variance

$E[(x - E(x))^2] = E[(x - m)^2] = \sigma^2$ (the symbol for variance)

Also, it can be shown that $\sigma^2 = E[x^2] - m^2$,

$\sqrt{\sigma^2} = \sigma$ (called the standard deviation).

For a stationary random process, σ^2 is a measure of the ac component power, m^2 is a measure of the dc component power, and $E[x^2]$ is a measure of the total power.

Up to this point, only averages of a single variable have been discussed. Extending the discussion to a pair of x and y of discrete random variables.

$$E[f(x,y)] = \sum_{i=1}^I \sum_{j=1}^J f(x_i, y_j) P(x_i, y_j) \quad (252)$$

and for continuous random variables

$$E[f(x,y)] = \int_{-\infty}^{\infty} \int_{-\infty}^{\infty} f(x,y) p(x,y) dx dy \quad (253)$$

The functions of the form

$$E[(x - m_x)^k (y - m_y)^n]$$

are called joint central moments. This particular one is the (k, n) th joint central moment. Also, measuring the interdependence of x and y , the term covariance is assigned when $k = n = 1$; i. e.,

$$E[(x - m_x)(y - m_y)]$$

C. Random Processes in Vibration Analysis

The random variable x has been introduced as the value resulting from a random experiment. The values of x as sample functions were then grouped to form an ensemble. Also, it was noted that x could have either discrete or continuous values. The discrete form was used to introduce new concepts because it is easier to understand from a physical viewpoint.

Emphasis is now shifted from general considerations to the specific type of random process as applied to vibration work; that is, continuous random processes as a function of time.

Considering the ensemble of such functions (Fig. 86), the probability distribution of x at time t_1 and x at t_2 may be described. Also, joint properties of $x_{t_1} = x(t_1)$ and $x_{t_2} = x(t_2)$ may be described. To describe the joint properties an ensemble average is used. The particular ensemble average

$$E[x(t_1) x(t_2)] = R(t_1, t_2) \quad (254)$$

is called the autocorrelation function and is symbolized by $R(t_1, t_2)$ since this result, in general, is a function of both t_1 and t_2 . The autocorrelation function provides a measure of the interrelation of $x(t_1)$ and $x(t_2)$.

Up to this point, probability functions and ensemble averages at particular times (which is across the ensemble of sample functions) have been discussed. However, to obtain an ensemble of sample functions would require the firing of a large number of vehicles. Now consider the necessary conditions for the time average of one sample function to equal the ensemble average across the sample functions of an ensemble.

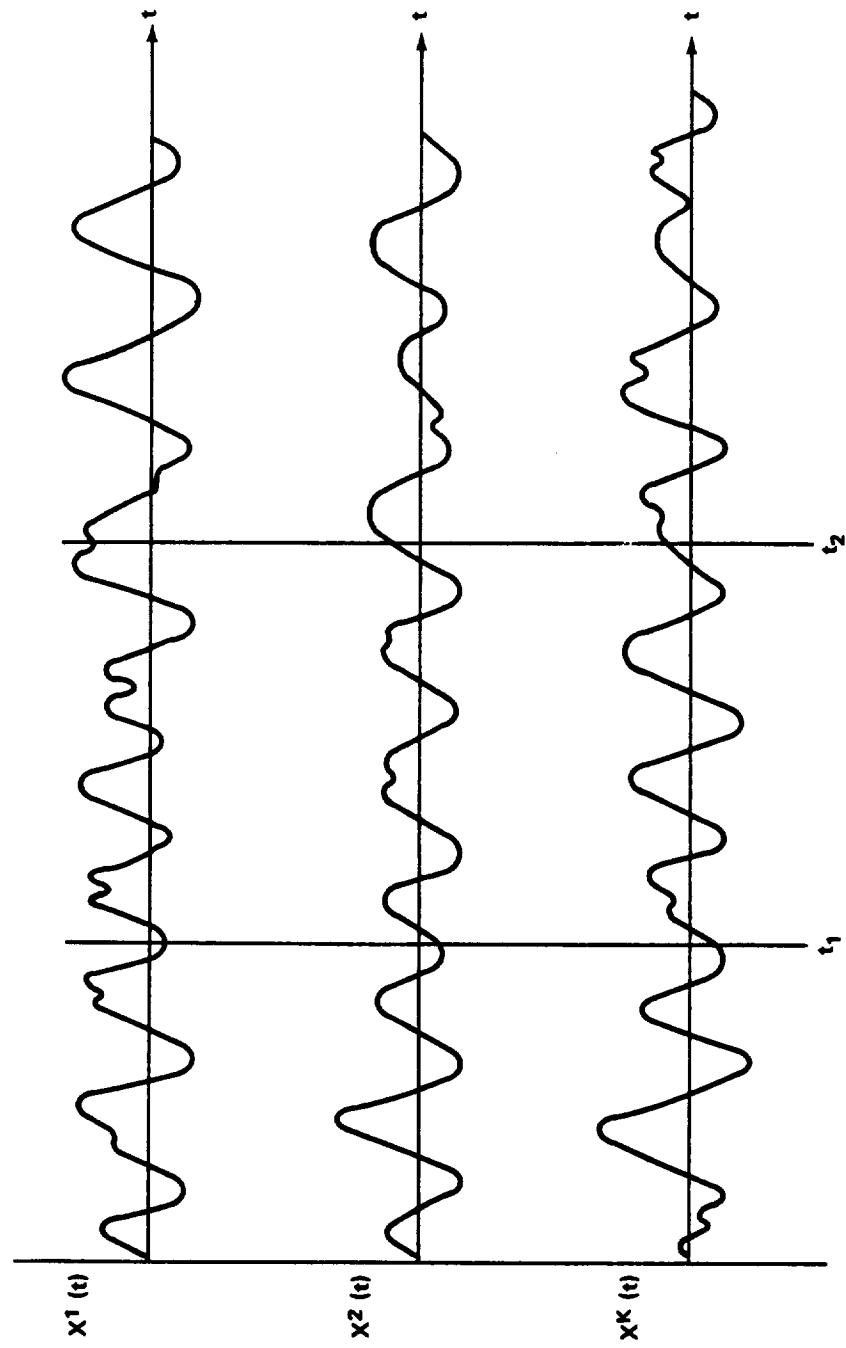


Figure 86. Ensemble of continuous random processes as a function of time.

The average along one sample function is called the time average. The time average, denoted by $\overline{x(t)}$, of a sample function $x(t)$ of length $2T$ is defined by

$$\overline{x(t)} = \lim_{T \rightarrow \infty} \frac{1}{2T} \int_{-T}^T x(t) dt \quad . \quad (255)$$

In general, this result depends upon the particular sample function chosen. The parameter t , of course, is averaged out so that this result is no longer a function of t .

The average across the ensemble is the statistical average previously defined, which at $t = t_1$ is

$$E[x(t_1)] \quad .$$

In general, this result depends upon the particular time, $t = t_1$, chosen.

It should be noted that

$$\overline{x(t)} = E[x(t_1)]$$

when random processes are both stationary and ergodic. These concepts are defined below.

A random process is stationary if the joint probability density depends only on time differences and not on the time origin; that is, for all translations in time t ,

$$P[x(t_1), x(t_2), \dots, x(t_n)] = P[x(t_1 + t), x(t_2 + t), \dots, x(t_n + t)] \quad (256)$$

which simply means we can start averaging the function at any point. In particular $E[x(t_1)]$ is now the same for all t_1 .

A random process is ergodic if it is stationary and if all sample functions are similar such that time averages on any sample function are statistically equivalent to corresponding ensemble averages over the ensemble of sample functions.

For a stationary process the autocorrelation function $R(t_1, t_2)$ becomes a function of the time difference $t_2 - t_1$ only; that is, $R(t_2 - t_1)$. The time difference is represented usually by τ . Therefore, for a stationary process, letting $\tau = t_2 - t_1$,

$$R(t_1, t_2) = R(t_2 - t_1) = R(\tau) = E[x(t_1) x(t_1 + \tau)] \quad ,$$

independent of t_1 .

Now if a random process is ergodic, then any function of the process is ergodic. So

$$\langle f[x(t_1)] \rangle = E[f(x(t_1))] = E[f(x(t))] \quad . \quad (257)$$

Therefore, for an ergodic process

$$E(\tau) = E[x(t) x(t + \tau)] \quad (258)$$

where

$$R(\tau) = \lim_{T \rightarrow \infty} \frac{1}{2T} \int_{-T}^T x(t) x(t + \tau) dt \quad . \quad (259)$$

Thus the time average of the product of a function at a time t and a time $t + \tau$ is the autocorrelation function, noted by

$$R(\tau) = \overline{f(t) f(t + \tau)} \quad .$$

The autocorrelation function of a stationary process has the following properties:

$$a. \quad R(0) = E x^2(t) = \sigma^2 + m^2$$

$$b. \quad R(0) \geq R(\tau) = R(-\tau)$$

$$c. \quad \lim_{T \rightarrow \infty} R(\tau) = m^2$$

Result (a) is the mean square value of $x(t)$ at any time t . Result (b) states that $R(\tau)$ is an even function of τ with a maximum value at $\tau = 0$. Result (c) assumes that $x(t)$ and $x(t + \tau)$ are statistically independent for large τ . If the mean value $m = 0$, then result (a) shows that the mean square value equals the variance, and the root mean square value equals the standard deviation.

D. Amplitude and Frequency Distribution in Random Noise

Many of the most severe vibration environments encountered in current vehicles result from noise generated aerodynamically by the interaction of the propulsion jet with the atmosphere and from pressure fluctuations in the turbulent boundary layer which surrounds the vehicle during flight. Both of these forcing functions contain energy at all frequencies throughout a relatively wide bandwidth, and the amplitudes of both vary in a random fashion.

Usually, the amplitude probability distribution in a random noise forcing function follows the normal or Gaussian probability law. This has been generally supported by analysis of the two forcing functions mentioned above. Also, it is usually assumed that the random forcing function is both stationary and ergodic. To assume stationarity the statistical properties of the function must be assumed to not vary with time; therefore, any two samples taken from a single continuous record of the function must appear statistically equivalent. To assume ergodicity, any sample taken from a single continuous record of the function must be statistically equivalent to the entire record of the function. When stationarity and ergodicity exist, the average properties of each sample of any record are similar and do not vary with time, and this permits the use of the time averages rather than sample or ensemble averages. Also, these requirements permit use of Fourier transforms to relate the statistical autocorrelation of the forcing function with its frequency spectrum.

Many of the random forcing functions which are encountered during launch and flight vary with time and are neither stationary nor ergodic. However, the time history function can be divided into several shorter time periods in which the function is reasonably stationary. When the length of these shorter time periods is not sufficiently large compared to the time period of the response, large variations can be expected between the responses at differing times, because the sample length is not long enough to give the true averages.

When the force input to a linear single degree-of-freedom system is random, the response is also random. If the force contains energy at all frequencies over a relatively wide frequency range which includes the resonant frequency of the system, the energy at frequencies near the resonant frequency will be magnified. Therefore, the response will appear to be approximately sinusoidal with an amplitude which varies randomly with time. Figure 87 illustrates a sample of the response of a panel to random noise excitation. It is assumed that the instantaneous amplitudes x are distributed normally with a zero mean and standard deviation x_r . The normal probability density for (x/x_r) is shown at the bottom of Figure 87. The probability, or the proportion of time that (x/x_r) is between (x_1/x_r) and $(x_1/x_r) + (\Delta x/x_r)$, is the product of the probability density at (x_1/x_r) and the interval $(\Delta x/x_r)$. Note that the quantity x_r equals the root mean square value here since the mean value is zero.

The probability density for the peak response x_0 of the lightly damped single degree-of-freedom system are distributed for very narrow bandwidths in accordance with the Rayleigh distribution. The Rayleigh probability density for (x_0/x_r) is illustrated in the upper portion of Figure 87. Comparing the normal and the Rayleigh probability density functions, it is clear that the probability of a zero instantaneous amplitude is higher than the probability of any other value as illustrated by the normal probability density function. However, it is improbable that the peak amplitude in any cycle equals zero, as illustrated by the Rayleigh probability density function where the most probable peak amplitude is seen to be approximately the rms amplitude, $(x_0/x_r) = 1$.

The probability distribution functions for these two distributions are given in Figure 88. The probability distribution is the integral of the probability density and gives the probability that the amplitude ratio is less than or equal to any value of the ratio. Thus, for the normal distribution of

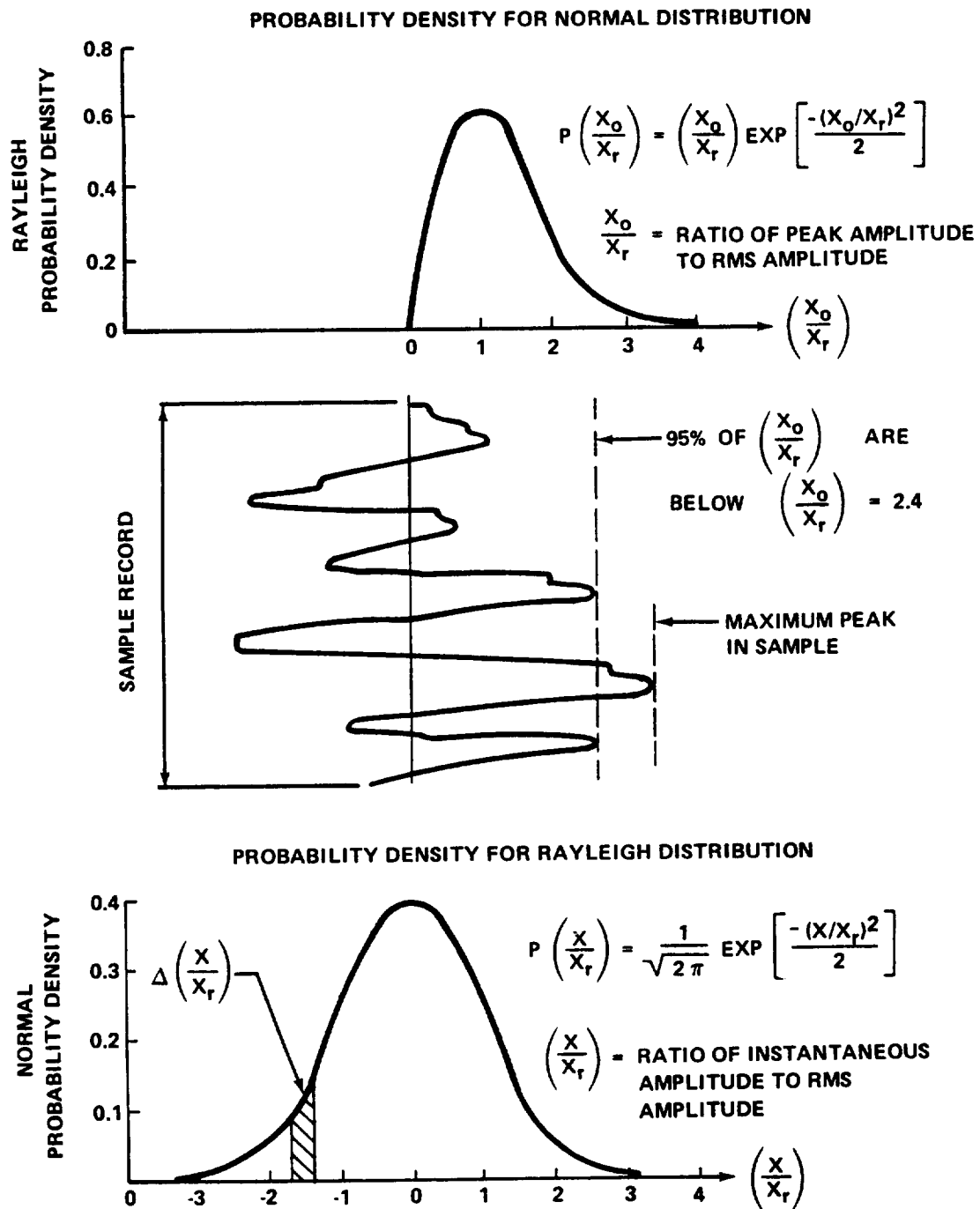


Figure 87. Sample of response of a panel to random noise excitation.

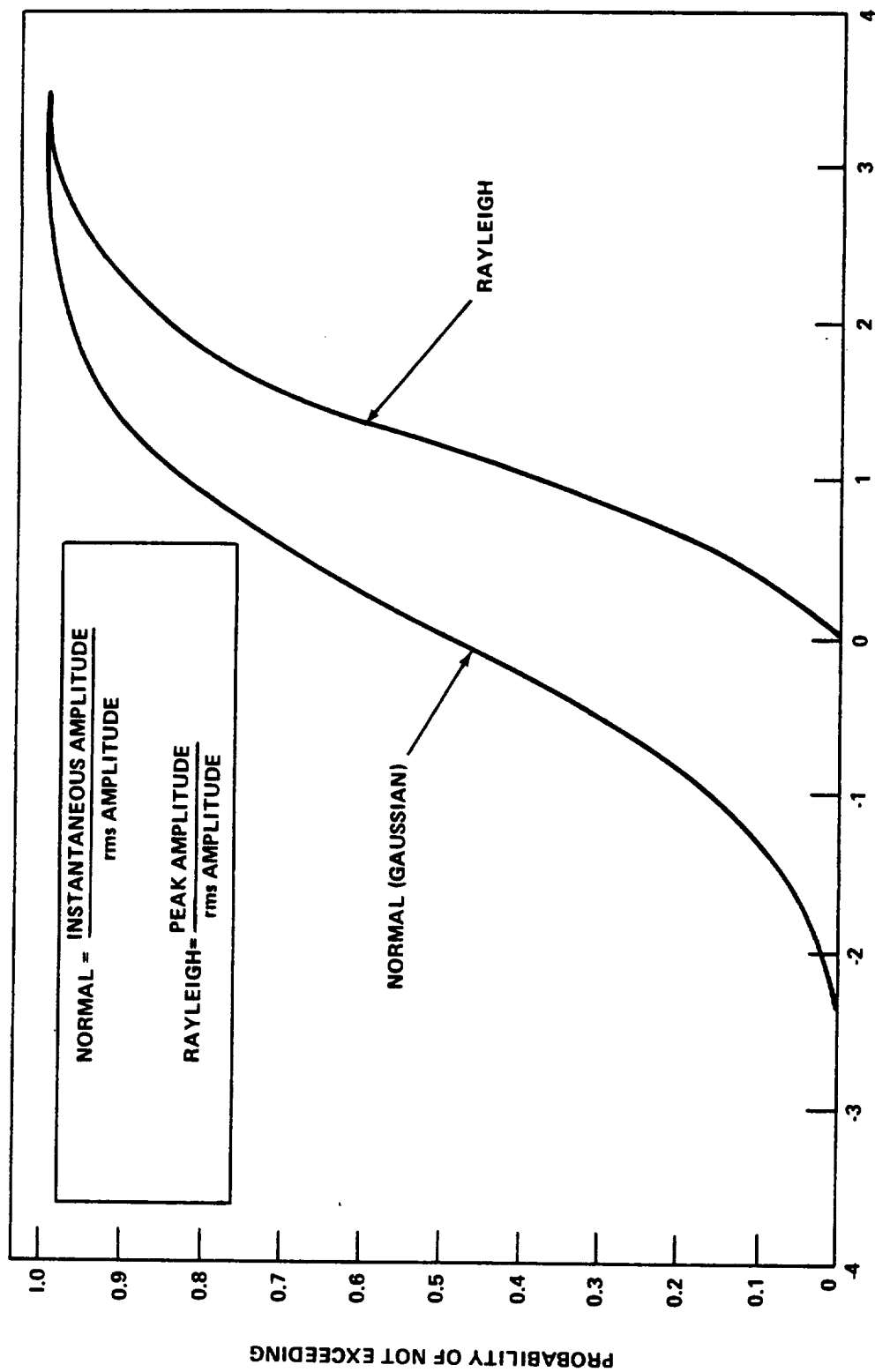


Figure 88. Normal and Rayleigh probability distribution functions.

amplitudes, it is equally probable that the instantaneous amplitude will be positive or negative relative to the mean of zero. Further, 85 percent of the instantaneous amplitudes (absolute values) are less than the root mean square (rms) value. For the Rayleigh distribution, 39 percent of the peak amplitudes are less than the rms amplitude, 50 percent are less than 1.18 times the rms value, 86 percent are below 2.0 times the rms value, and 99 percent are below 3.0 times the rms value. The sample response in Figure 87 shows that the maximum peak amplitude occurred at the 99-percent level and three peaks equal or exceed the 95-percent level.

However, the Rayleigh distribution will be expected only in the single degree-of-freedom system. When additional degrees-of-freedom exist in the system, additional resonant frequencies will exist. The response will be more complex and the peak amplitudes will tend to be more normally distributed about the mean amplitude (Ref. 20, Section 4.9.3). However, if the data are fed through a relatively narrow filter, the peak amplitudes from the filter will tend to produce a Rayleigh distribution.

The distribution of (peak) amplitudes in a random forcing function or response can be conveniently described in terms of the root mean square amplitude. However, the importance of the distribution of (peak) amplitudes relative to the rms amplitude cannot be over emphasized for the vibration engineer. This distribution adds another dimension to the analysis of vibration data: the evaluation of a vibration environment for either equipment or structure, and the selection of test methods for the determination of equipment or structural reliability. The necessity of this added dimension results directly from the fact that the majority of equipment malfunctions occur at the maximum peak amplitudes and a disproportionate amount of the fatigue damage to structure is caused by the relatively infrequent peaks.

1. FREQUENCY AND POWER PROPERTIES

To determine the response of the single degree-of-freedom system to a random forcing function, it is necessary to define the frequency distribution as well as the amplitude distribution of the random input. The instantaneous power dissipated by damping equals the instantaneous damping force times the instantaneous velocity of the motion. Therefore, the average damping power (P_d) which is dissipated between time t_1 and t_2 is the integral of the instantaneous power during the time interval divided by the duration of the interval, or

$$P_d = \frac{1}{(t_2 - t_1)} \int_{t_1}^{t_2} c \dot{x}^2 dt \quad (260)$$

where $c \dot{x}$ is the instantaneous damping force and \dot{x} is the instantaneous velocity.

Since c is a constant (when viscous damping can be assumed), the damping power equals c times the average or mean value of the square of the velocity during the time interval. Hence the equation for P_d could be written

$$P_d = c \overline{\dot{x}^2} \quad (261)$$

where $\overline{\dot{x}^2}$ is the mean square velocity (or the square of the rms velocity). It is convenient to utilize the concept of damping power in the definition of the frequency distribution of the random forcing function or response. For example, consider a random forcing function which contains force components at all frequencies within the frequency region between f_1 and f_2 , and which excites a single degree-of-freedom system consisting of only a viscous damper. If the damper were separated from the forcing function by a series of unity gain filters covering the frequency range between f_1 and f_2 , each with bandwidth Δf , the power dissipated in the damper resulting from the portion of the forcing function passed through the filter of frequency f_a is

$$\Delta P_a = c \overline{\dot{x}_a^2} \quad (262)$$

where $\overline{\dot{x}_a^2}$ is the mean square velocity resulting from the portion of the forcing function of bandwidth Δf centered on frequency f_a .

The power spectral density (PSD) at frequency f_a is simply the damping power per cycle per second, or

$$PSD = \frac{\Delta P_a}{\Delta f} = \frac{c \overline{\dot{x}_a^2}}{\Delta f} = c \overline{\dot{x}^2}(f_a) \quad (263)$$

and the total power P_d between frequencies f_1 and f_2 is the sum of the mean square velocity per cycle per second times the bandwidth Δf and the damping constant c throughout the frequency range

$$P_d = \sum_{f_1}^{f_2} (\text{PSD}) \Delta f = \sum_{f_1}^{f_2} c \overline{\dot{x}^2(f)} \Delta f \quad . \quad (264)$$

Because of the convenience of the power spectral density approach the term is often applied to accelerations or displacements as well as velocities. Further, when applied to these other quantities, it is tacitly assumed that the value of c is unity and the result becomes the power spectral density of the function (either in displacement, x ; velocity, \dot{x} ; or acceleration, \ddot{x}). To avoid confusion, it is often preferred to speak of mean square value (displacement, velocity, or acceleration, depending on the quantity used) per cycle per second rather than power spectral density. This distinction allows the reservation of the word "power" for actual mechanical power.

The response of a single degree-of-freedom system, with frequency response function $H(\omega)$ and spring constant k , to an applied random forcing function which is characterized by a continuous distribution of mean square force per cycle per second, $\overline{F^2(f)}$, is given by the sum of the mean square response associated with each narrow frequency band Δf . However, it is desirable to use the mean square force per radian per second, which is $\overline{F^2(f)}/2\pi$ and the bandwidth Δ . Then

$$\overline{x^2(f)} = \frac{\overline{F^2(f)}}{2\pi k^2} |H(\omega)|^2 \Delta \omega \quad (265)$$

and the total mean square response, $\overline{x^2}$, is the sum of the response in each $\Delta\omega$, from ω_1 to ω_2 :

$$\overline{x^2} = \frac{1}{2\pi} \sum_{\omega_1}^{\omega_2} \frac{\overline{F^2(f)}}{k^2} |H(\omega)|^2 \Delta \omega \quad . \quad (266)$$

When the forcing function is constant throughout the resonant frequency range, it can be shown that the total mean square response is given by

$$\overline{x^2} = \frac{Q \omega_n \overline{F^2(f)}}{4k^2} = \frac{\omega_n}{4Q} Q^2 \frac{\overline{F^2(f)}}{k^2} \quad (267)$$

where $\omega_n = 2\pi f_n$ equals the natural angular frequency of free undamped oscillations and $Q = |H(\omega_n)|$. The total mean square response equals an effective response bandwidth $(\omega_n/4Q)$ times Q^2 and times the mean square force per cycle per second divided by the square of the spring constant. This mean square resonant response $\overline{x^2}$ to a random forcing function of constant $\overline{F^2(f)}$ differs from its mean square response to a sinusoidal forcing function of mean square value $\overline{F^2}$, which coincides with the natural frequency and has the same magnitude as $\overline{F^2(f)}$ simply by the effective response bandwidth $(\omega_n/4Q)$.

Hence, the mean square resonant response to a random forcing function of constant $\overline{F^2(f)}$ is proportional to Q times the mean square per cycle value of the forcing function; whereas in the sinusoidal case, the mean square response is Q^2 times the mean square value of the forcing function. This provides an important and practical distinction between these two situations.

E. Vibration Excitation Sources

Vibration excitation sources and their characteristics are discussed in Section VIII and are considered here in a general fashion to show their role in the overall vibration problem and to indicate possible areas of difficulty.

These sources of excitation can be divided into four major categories: acoustic noise, various types of aerodynamic disturbances, free atmospheric disturbances, and mechanical disturbances. Each of these categories consists of essentially different types of disturbances which create a wide variety of forces on the structure, and may include localized forces acting at fixed points, pressure disturbances over areas of the structure ranging from the relatively small to those of the entire vehicle external skin, and

forces and pressures which are essentially stationary (spatially) or propagating over the structure.

Excitation sources are often defined by quasi-sources parameters which do not always define the actual source phenomenon, but which partly describe the effects which these stimuli create on the structure. As an example, rocket engine acoustic excitation is often defined in terms of the distribution of sound pressure level over the skin. Also, rocket engine combustion instabilities are defined in terms of the force acting on some structural link attached to the engine.

It is usually assumed that the various sources of excitation can be considered as independent in predicting structural response. However, for similar types of sources, such as aerodynamic sources, coupling may occur which, because of nonlinearities, will produce a combined source whose characteristics are different from those of the original sources. For example, coupling may occur between attached shock waves, boundary layer disturbances, base pressure fluctuations, and acoustic noise. For refined predictions, such coupling effects may be of considerable interest.

The response of certain structural elements of the vehicle constitutes a second type of coupling which can alter the characteristics of the excitation source. Burning instabilities of liquid rocket engines, for example, may induce excitation of the fuel feed lines which in turn cause pressure fluctuations in the combustion chamber. Mechanically-induced vibrations originating within certain equipment items will feed back through the equipment and may, under some circumstances, alter the internal unbalanced forces causing the response. Skin panel responses to boundary layer disturbances form another example of this type of coupling by altering the shape and thickness of the boundary layer and by producing additional pressure fluctuations which travel downstream to further alter the boundary layer.

Response of the structure is also important in the production of new sources of excitation. The additional sources may in some cases be of secondary importance, such as the acoustic noise generated within the closed pressurized vehicle by skin response to external acoustic excitation. On the other hand, response of the entire structure to free atmospheric disturbances can produce significant aerodynamic forces resulting from angle of attack changes which clearly are not part of the original sources of excitation.

It is desirable to isolate the source parameters from those of the propagation or excitation-to-force transfer parameters, and also to determine the source-to-source coupling, the response-to-source coupling, and the

response-to-source initiation parameters. This may be very difficult to do at the present time and for many types of excitation and structures this may never be feasible. However, conceptually this does represent a more systematic approach to the overall description of what is generally classified as excitation sources.

Since the sources of excitation often consist of random-type phenomena, the description must be statistical.

Random forces, or force components, are definable only in terms of the statistical averages of estimated or measurable properties of the force, such as the mean, mean square, correlation functions, and power spectral density functions. Well defined forces do not in themselves present any difficulty in the vibration response problem, and can usually be treated separately from the random forces.

It would seem that a complete description of random force functions will never be attained under any circumstances and fortunately, for practical engineering applications, this will be unnecessary. However, improvements can and should be made to advance the state-of-the-art by investigating more statistical averages than are presently used. Justification for this lies in the fact that the accurate prediction of structural fatigue life depends upon the accuracy of response predictions, which can be made with no greater degree of certainty than that of the information used to describe stimulus and transfer properties.

1. STATISTICAL PROPERTIES OF THE RANDOM FORCE $F(t)$

Of the statistical averages presently used, the most common are concerned with the amplitude $F(t)$ of an oscillatory, unidirectional random force acting at a fixed point and containing a continuous spectrum of frequencies with arbitrary phasing. Although the statistical averages are difficult and time consuming to obtain in practice (unless electronic computing devices are used), the necessary expressions and concepts are easily established.

Statistical averages must be determined from a sample of data obtained from repeated experiments or trials of the same random process. For the case being discussed, this sample data would consist of a set of N records, $F_k(t)$, ($k = 1, 2, 3, \dots, N$), obtained from measurements of $F(t)$ at some fixed point x and direction ψ on the vehicle over the same time period for repeated flights of the same type vehicle. For example, a flush-mounted

microphone located at a given position on the vehicle skin could record the amplitude variation of sound pressure level at x during numerous launchings or flights. Different vehicles (even the same type of vehicle in design and performance) will have slightly different characteristics and will often be launched under varying conditions of thrust, trajectory, weather, etc. The characteristics of the random process causing $F(t)$ will thus change from record to record, and it may be impossible to obtain two records of the same random process. Unless the variation between the different records is very significant, the individual random processes occurring during each flight could be thought of as being part of a more general random process whose variation is sufficiently broad to include the variations between the different force amplitude-time records.

By knowing the time scale equivalence between the various $F_k(t)$ records and by aligning these time coordinates along a vertical scale, the force amplitudes $F_k(t)$, as shown in Figure 89 constitute an ensemble. This ensemble statistically represents the random process which characterizes $F(t)$.

Unless the simplifying assumptions of stationarity and ergodicity (discussed later) are imposed on this random process, the statistical averages of $F(t)$ will vary with time and hence must be determined from this ensemble by averaging over the amplitudes $F_k(t_i)$ for each fixed time t_i , say t_1, t_2, t_3, \dots . The mathematical expressions for the mean, mean square, standard deviation, autocorrelation function, and power spectral density function are listed below for a general nonstationary, nonergodic force function $F(t)$. These expressions are given for the exact case in terms of known probability density functions, $P_F(z, t)$, and for the approximate case where these are not known.

The symbol $E[A]$ is used here to denote the expected or mean value of the random variable A .

Mean:

$$E[F(t_i)] = \langle F(t_i) \rangle = \int_{-\infty}^{\infty} z P_F(z, t_i) dz \approx \frac{1}{N} \sum_{k=1}^N F_k(t_i) \quad . \quad (268)$$

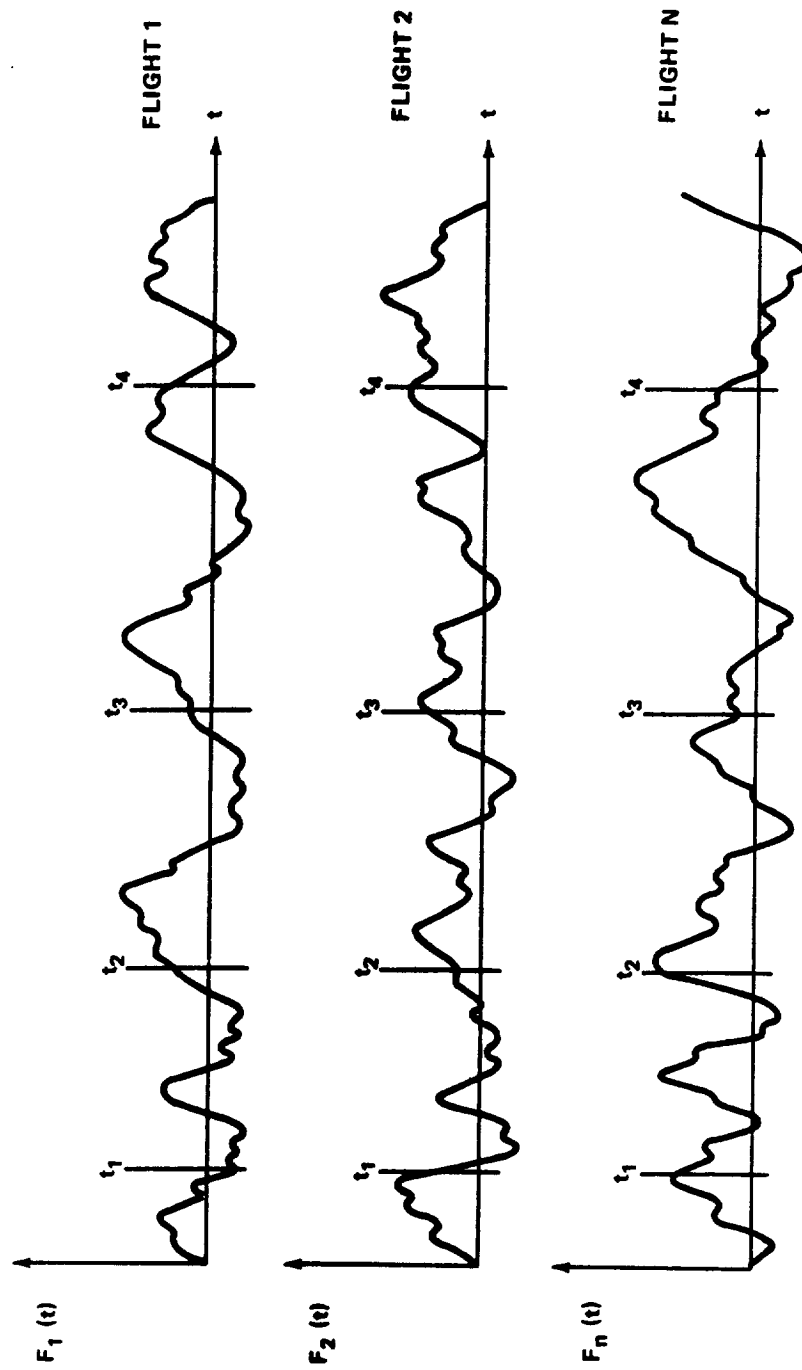


Figure 89. Ensemble of measured time histories of force.

Mean square:

$$E [F^2(t_i)] = \langle F^2(t_i) \rangle = \int_{-\infty}^{\infty} z^2 p_F(z, t_i) dz \approx \frac{1}{N} \sum_{k=1}^N F_k^2(t_i) \quad (269)$$

Note that the above nonstationary mean and mean square values are functions of time.

Standard deviation:

$$\sigma(t_i) = \sqrt{F^2(t_i) - F(t_i)^2} \quad (270)$$

Nonstationary autocorrelation function:

$$\begin{aligned} R_F(t_i, t_j) &= E[F(t_i) F(t_j)] = \langle F(t_i) F(t_j) \rangle \\ &= \int_{-\infty}^{\infty} \int_{-\infty}^{\infty} z_1 z_2 p_F(z_1, t_i; z_2, t_j) dz_1, dz_2 \\ &\approx \frac{1}{N} \sum_{k=1}^N F_k(t_i) F_k(t_j) \quad (271) \end{aligned}$$

Nonstationary power spectral density:

$$S_F(f_i, f_j) = \int_{-\infty}^{\infty} \int_{-\infty}^{\infty} R_F(t_i, t_j) e^{j2\pi(f_i t_i - f_j t_j)} dt_i dt_j \quad (272)$$

Note that the nonstationary autocorrelation function is a function of both t_i and t_j , and the nonstationary power spectral density function is a function of both f_i and f_j .

The first-order probability density function $p_F(z, t_i)$ is the probability density function for the amplitude $F(t)$ at time $t = t_i$ and $p_F(z, t_i) dz$ equals the probability that at $t = t_i$ the amplitude F lies in the interval $z < F < z + dz$. The joint probability density function $p_F(z_1, t_i; z_2, t_j)$ is the joint probability density function for $F(t)$, which multiplied by $(dz_1)(dz_2)$ equals the probability that F lies in both the intervals.

$$z_1 < F < z_1 + dz_1 \text{ at } t = t_i$$

$$z_2 < F < z_2 + dz_2 \text{ at } t = t_j$$

The $p_F(z, t_i)$ functions are estimated by sampling the various $F_k(t)$ records for fixed values of $t = t_i$, and constructing the usual relative frequency-of-occurrence graphs. The joint probability density function $p_F(z_1, t_i; z_2, t_j)$ is a function of two variables, z_1 and z_2 , and hence is geometrically described by a surface. The larger the data sample size, N , and the smaller amplitude intervals tested, the more accurately the force probability density functions can be determined.

It is often assumed that the random process being characterized is stationary. This implies that the averages are invariant with respect to time. Thus, the ensemble mean $\langle F(t) \rangle$ and mean square $\langle F^2(t) \rangle$ may be determined at any time t . All of the force amplitude $F_k(t)$ used to obtain these averages must correspond to the same value of t . The autocorrelation function, which generally depends upon two values of t , say t_i and t_j , will now depend only upon the time difference τ between t_i and t_j . The mathematical expressions for the first few statistical averages, shown above, reduce to the following simpler forms for a stationary random process:

Letting t_0 be equal to any time, one obtains the following results.

Mean:

$$E[F] = \langle F \rangle = \int_{-\infty}^{\infty} z p_F(z, t_0) dz \approx \frac{1}{N} \sum_{k=1}^N F_k(t_0) \quad (273)$$

Mean square:

$$E [F^2] = \langle F^2 \rangle = \int_{-\infty}^{\infty} z^2 p_F(z, t_0) dz \approx \frac{1}{N} \sum_{k=1}^N F_k^2(t_0) . \quad (274)$$

Standard deviation:

$$\sigma = \sqrt{\langle F^2 \rangle - \langle F \rangle^2} . \quad (275)$$

Stationary autocorrelation function:

$$\begin{aligned} R_F(\tau) &= E [F(t_0) F(t_0 + \tau)] \int_{-\infty}^{\infty} \int_{-\infty}^{\infty} z_1 z_2 p_F(z_1, t_0; z_2, t_0 + \tau) dz_1 dz_2 \\ &\approx \frac{1}{N} \sum_{k=1}^N F_k(t_0) F_k(t_0 + \tau) . \end{aligned} \quad (276)$$

Stationary power spectral density (two-sided):

$$S_F(f) = \int_{-\infty}^{\infty} R_F(\tau) e^{-i2\pi f\tau} d\tau ; -\infty < f < \infty . \quad (277)$$

The above two-sided power spectral density function $S_F(f)$ is an even function of f , defined for negative f as well as positive f . The one-sided realizable power spectral density function $G_F(f)$ is defined only for positive f and is related to $S_F(f)$ by the expression

$$\begin{aligned}
G_F(f) &= 2 S_F(f) & 0 \leq f < \infty \\
&= 0 & f < 0
\end{aligned} \tag{278}$$

thus,

$$G_F(f) = 2 \int_{-\infty}^{\infty} R_F(\tau) e^{-j2\pi f\tau} d\tau \quad ; \quad 0 \leq f < \infty \quad . \tag{279}$$

For a stationary random process, the autocorrelation function $R_F(\tau)$ is an even function τ ; that is, $R_F(-\tau) = R(\tau)$. Hence the above power spectral density functions are given by

$$\begin{aligned}
S_F(f) &= 2 \int_0^{\infty} R_F(\tau) \cos 2\pi f\tau d\tau \quad ; \quad -\infty < f < \infty \\
G_F(f) &= 4 \int_0^{\infty} R_F(\tau) \cos 2\pi f\tau d\tau \quad ; \quad 0 \leq f < \infty \quad .
\end{aligned} \tag{280}$$

The inverse relations yield

$$\begin{aligned}
R_F(\tau) &= \int_0^{\infty} G_F(f) \cos 2\pi f\tau df \\
&= \frac{1}{2} \int_{-\infty}^{\infty} S_F(f) \cos 2\pi f\tau df \quad .
\end{aligned} \tag{281}$$

If the ensemble is composed of time records of $F(t)$ which are sufficiently long, the ensemble statistical averages may change significantly with time. For example, suppose that $F(t)$ shown in Figure 90 is typical of other records in the ensemble. The random process associated with this $F(t)$ will be nonstationary if it is not compensated for by other records in the ensemble. However, it may be segmented into time intervals, $(0, t_1)$, (t_1, t_2) , (t_2, \dots) , such that during each interval the random process can be assumed stationary. Stationary statistical averages can then be determined for each segment. Only one record of the ensemble is shown here, but it is assumed that this one is typical of most of the $F_k(t)$ records in the ensemble, with respect to the locations of the ends of the stationary segments. If this record is not typical of all but a negligibly small number of the N ensemble records, then considerable error may be introduced by assuming stationarity over these segments.

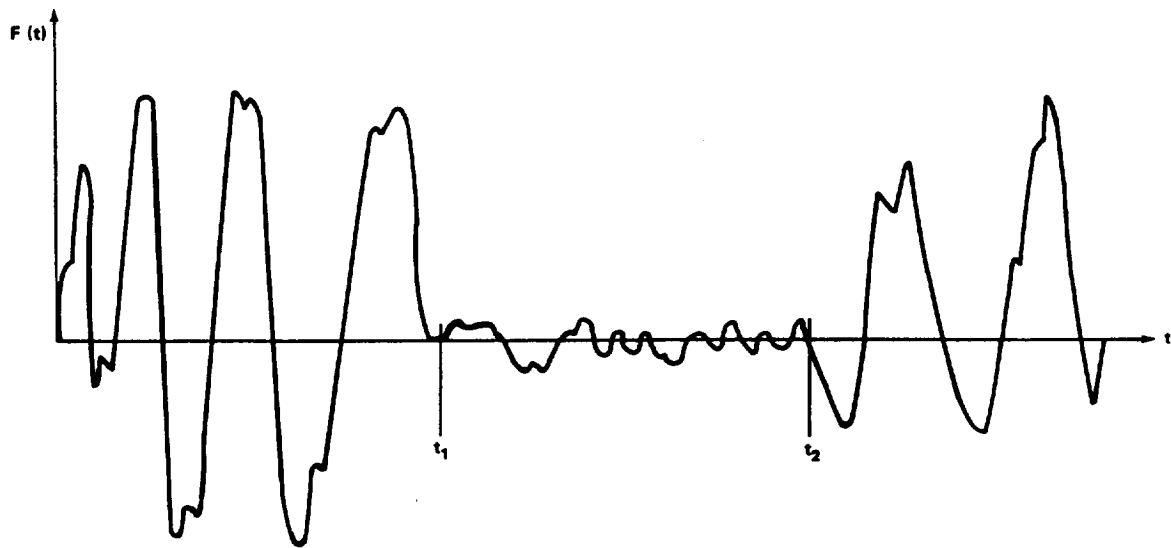


Figure 90. Time record of a nonstationary random force function.

A further simplifying assumption is usually made that the random process which characterizes $F(t)$ is ergodic. The combined assumptions of stationarity and ergodicity imply, in addition to the invariance of the ensemble statistical averages with time, that any one of the $F_k(t)$ samples of $F(t)$ is statistically equivalent to the entire ensemble. Thus the statistical averages defining the random force function $F(t)$ may be obtained by timewise integrations, thereby eliminating the immediate requirement for the probability density functions. The mathematical expressions for the statistical averages then become:

Mean:

$$E [F] = \overline{F} = \lim_{T \rightarrow \infty} \frac{1}{2T} \int_{-T}^T F(t) dt \quad . \quad (282)$$

Mean square:

$$E [F^2] = \overline{F^2} = \lim_{T \rightarrow \infty} \frac{1}{2T} \int_{-T}^T F^2(t) dt \quad . \quad (283)$$

Autocorrelation:

$$R_F(\tau) = E F(t) F(t + \tau) = \lim_{T \rightarrow \infty} \frac{1}{2T} \int_{-T}^T F(t) F(t + \tau) dt \quad . \quad (284)$$

Power spectral density:

$$G_F(f) = 2S_F(f) = 4 \int_0^{\infty} R_F(\tau) \cos 2\pi f\tau d\tau \quad ; \quad 0 \leq f < \infty \quad . \quad (285)$$

Although the probability density functions are not required in obtaining the statistical averages of $F(t)$ for a stationary and ergodic random process, these functions are of importance and should be determined. A method has already been outlined for approximating these functions from ensemble samplings. Time averages are often used when an adequate and representative ensemble is not available. Hence when the assumptions of stationary and ergodicity are imposed, the probability density functions may have to be obtained from a single time record of $F(t)$. The method previously presented for approximating $p_F(z, t)$ is still valid, except that $p_F(z, t)$ becomes $p_F(z)$, and the data sample would consist of say N' values, $F(t_k)$,

($k = 1, 2, \dots, N'$), of $F(t)$ measured at even intervals of time as shown in Figure 91. It is important that Δt be sufficiently small to ensure that the highest frequency amplitude variations are weighted equally with those of the lower frequencies. Bendat [24] indicates that at least two sample readings per cycle should be made for the highest frequencies and that 10 to 20 sample readings per cycle might be practical estimates.

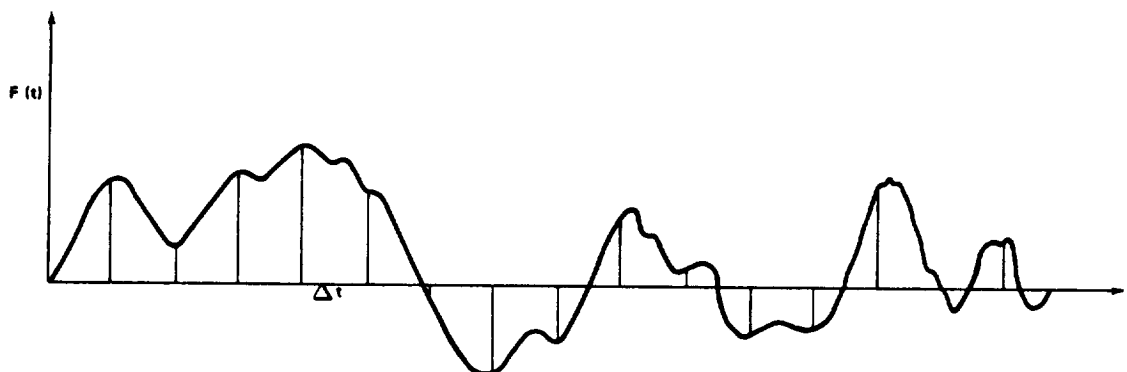


Figure 91. Amplitude sampling of $F(t)$ at even intervals of time.

Stationarity of the random process assumes, by definition, that the effects of all starting transients can be neglected and, hence, that the process has always occurred with no changes in its statistical properties (i.e., it began at $t = -\infty$). Also, the exact statistical averages of the random process can only be obtained if the sample size is infinite, which necessitates infinitely long records. For practical applications, this type of precision is unwarranted and sufficiently accurate results can be obtained for finite, but large, data samplings.

Some degree of nonstationarity exists in most random processes which have a physical origin, so that ensemble averages should be used in determining the statistical properties of $F(t)$. This, however, is undesirable at the present time for a number of reasons. First, the quantity of data generally available for statistical analysis, in practice, is often meager and of limited accuracy. This is partially due to the difficulties encountered in duplicating any given random process, which thus restricts the number of ensemble sample records that accurately represent the particular random process being investigated. Even though either numerous records or long time records or both may be available, they may contain spurious information introduced by the influence of other random or nonrandom physical processes.

Secondly, when adequate and accurate representative samplings are available, the data reduction can be a heavy task. It would thus certainly be necessary to use high speed digital computers if a statistical analysis of any quality were to be made.

Finally, there is a great desire on the part of analysts to take full advantage of the simpler time averaging expressions which are valid for stationary and ergodic random processes. Analog computing techniques are readily available and relatively easy to program, which can efficiently determine at least the first few, and most important, statistical averages. The assumptions of stationarity and ergodicity are therefore widely used with segmented time records as a first approximation of the statistical averages.

The block diagrams shown in Figure 92 illustrate the simple procedure for obtaining the mean, mean square, autocorrelation function, and power spectral density function for a single time record $F(t)$ by means of electronic analog techniques. The function $F(t)$ must be fed into the circuitry from magnetic tape.

In practice, the length of the time records of $F(t)$ may be relatively short, and in real time may contain only one second or less of recorded data. To increase the sample size, the ends of the magnetic tape may be joined, forming a loop, which can then be repeatedly analyzed electronically as a continuous uninterrupted $F(t)$ signal. This effectively increases the time duration of a random process and assumes that the process is stationary.

If a number of representative samples of $F(t)$ are available, and if electronic analog techniques are to be employed, the statistical averages may be evaluated as time averages for each record and the set of statistical results obtained from all of the samples may then be further averaged as an ensemble. For example, if the mean value $\overline{F_k}$ has been determined for each of N records ($k = 1, 2, 3, \dots, N$), by the time averages,

$$\overline{F_k} = \frac{1}{T} \int_0^T F_k(t) dt \quad . \quad (286)$$

The ensemble mean $\overline{\overline{F}}$ of all the N records is given by the expression

$$\overline{\overline{F}} = \frac{1}{N} \sum_{k=1}^N \overline{F_k} \quad . \quad (287)$$

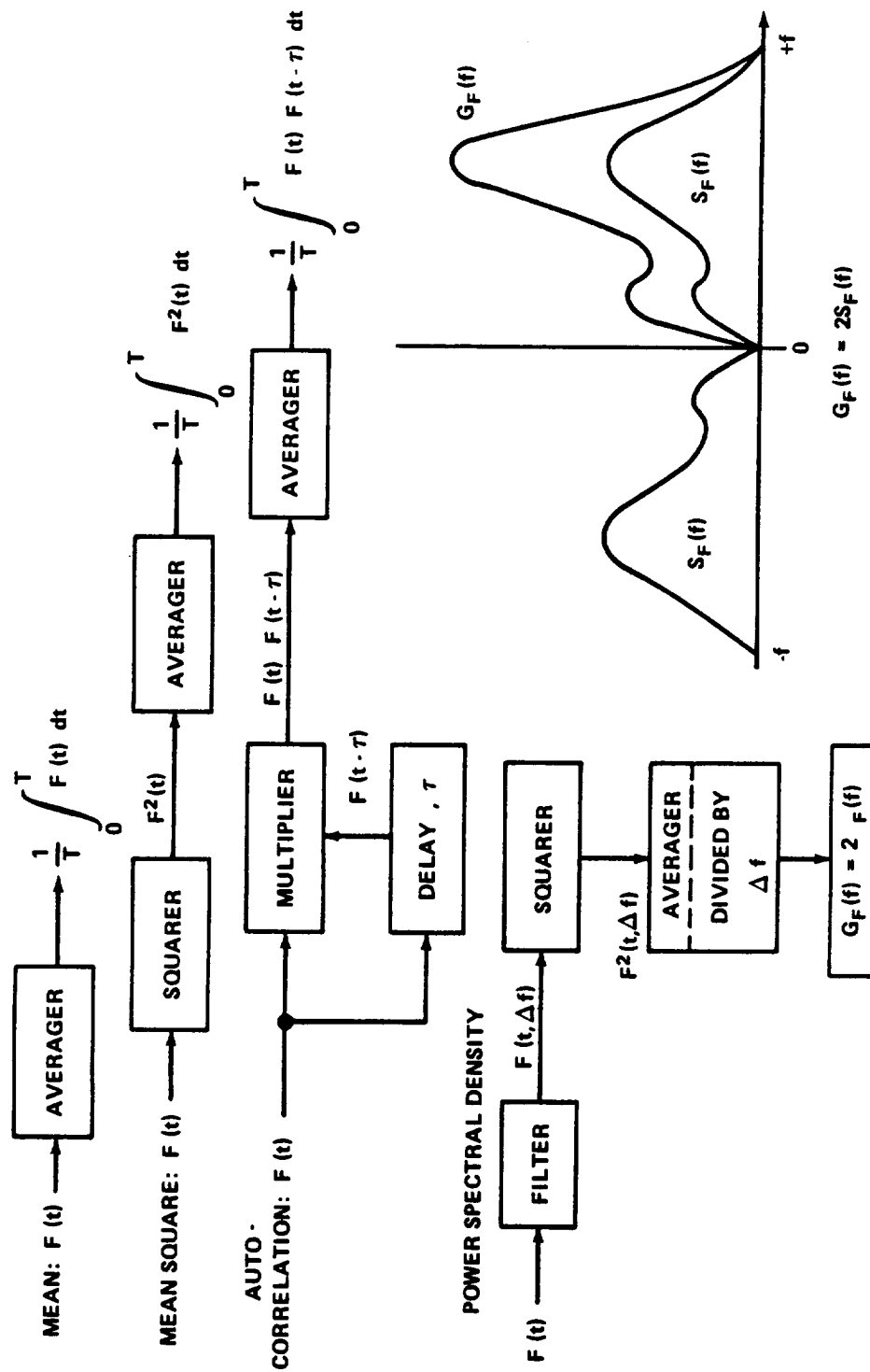


Figure 92. Block diagrams of electronic analog CCTS for computing statistical averages.

Similarly for the mean square and autocorrelation function:

$$\overline{F_k^2} = \frac{1}{T} \int_0^T F_k^2(t) dt \quad (288)$$

$$R_{F_k}(\tau) = \frac{1}{T} \int_0^T F_k(t) F_k(t+\tau) dt \quad (289)$$

Then, the ensemble average yields

$$\overline{F^2} = \frac{1}{N} \sum_{k=1}^N \overline{F_k^2} ; R_F(\tau) = \frac{1}{N} \sum_{k=1}^N R_{F_k}(\tau) \quad (290)$$

The ensemble power spectral density function would then be most conveniently determined from the resultant autocorrelation function $R_F(\tau)$ using the expression

$$G_F(f) = 2 S_F(f) = 4 \int_0^{\infty} R_F(\tau) \cos 2\pi f \tau d\tau ; 0 \leq f < \infty \quad (291)$$

If in future analyses, computing equipment and programs become available to determine both ensemble and time averages for segmented records, the choice of the proper method to use should be based upon the number of samples available and the length of these samples. Bendat [24] indicates that many samples of short records are more appropriately analyzed by ensemble techniques, with time averages employed for a small number of long records.

2. INTERPRETATION OF STATISTICAL AVERAGES OF $F(t)$

All of the above expressions for the mean, mean square, and autocorrelation function are independent of frequency, and therefore represent the statistical averages of $F(t)$ over all frequencies that are contained in $F(t)$.

This type of information is of limited value as it does not show the relative importance of possible high amplitude persisting frequency components of $F(t)$, nor the general distribution of power throughout the frequency range of $F(t)$. Since structural response is strongly dependent upon the frequency of excitation, it is necessary to determine these statistical averages for certain discrete frequencies and frequency bands. For example, the power spectral density function is one of the statistical averages used to describe the mean square of $F(t)$ in terms of its frequency components. In the following discussion of the properties of the statistical averages of $F(t)$, particular attention will be given to spectral characteristics of these averages.

The components of $F(t)$ contained within certain frequency bands or at discrete frequencies are obtained in practice by filtering techniques. If $F(t)$ is stored on magnetic tape, it can be passed through a set of electrical filters which transmit only those frequencies within the bandwidth of the filter. The action of these filters is closely associated with the Fourier series and Fourier transform, which display the theoretical frequency components of a function. The convenient mathematical forms provided by Fourier methods are very useful in explaining the actual frequency content of $F(t)$ and in the interpretation of results obtained by filtering. It is important to consider briefly the spectral properties of $F(t)$ itself and the problem of filtering before considering the spectral properties of the statistical averages of $F(t)$. The following discussion is not intended to be mathematically rigorous or sufficiently precise to include all possible types of functions. The arguments presented are directed toward the practical aspects of the problem.

Consider first that the function $F(t)$ is well defined of period $2T$ and contains a finite number of constant peak amplitude frequency components which remain unchanged for all time (i.e., from $t = -\infty$ to $t = +\infty$). Such a function is stationary and can be expressed by the finite Fourier series,

$$\begin{aligned}
 F(t) &= \frac{a_0}{2} + \sum_{n=1}^N (a_n \cos \omega_n t + b_n \sin \omega_n t) \\
 &= c_0 + \sum_{n=1}^N c_n \cos (\omega_n t + \varphi_n)
 \end{aligned} \tag{292}$$

where

$$c_n = \sqrt{a_n^2 + b_n^2} = \text{peak amplitude of the } n\text{th angular frequency component } \omega_n = 2\pi f_n = 2\pi f_0 \text{ where } f_0 = (1/2T).$$

$$c_0 = a_0/2$$

$$\phi_n = \tan^{-1} (b_n/a_n) = \text{phase angle of the } n\text{th frequency component.}$$

$$a_n = \frac{1}{T} \int_{-T}^T F(t) \cos \omega_n t dt$$

$$b_n = \frac{1}{T} \int_{-T}^T F(t) \sin \omega_n t dt \quad (293)$$

$$\omega_n = n\omega_0, \omega_0 = \frac{2\pi}{2T} = \text{basic Fourier angular frequency.}$$

All of the a_n 's, b_n 's, and c_n 's will be zero except for those which correspond to values of ω_n which appear as discrete frequencies in $F(t)$.

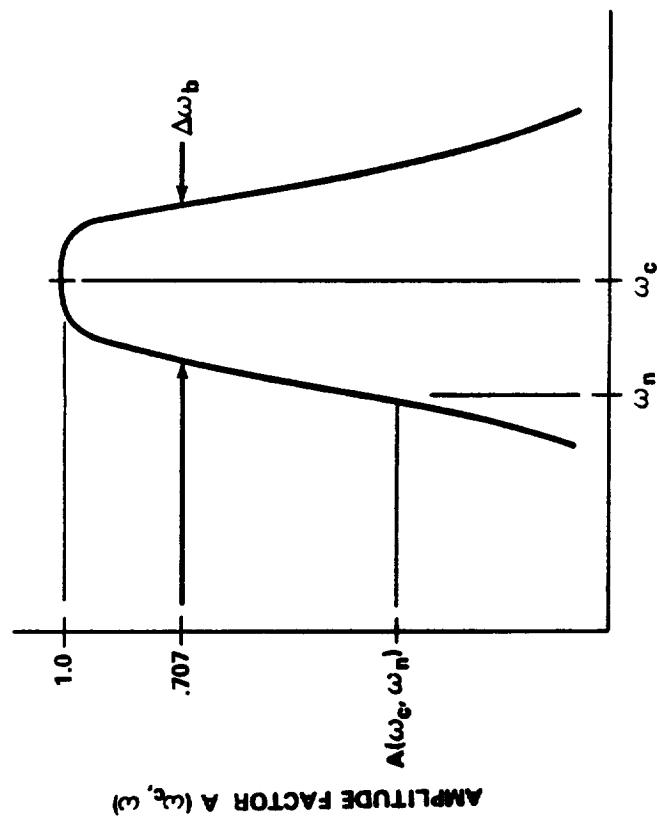
The amplitudes of the various frequency components are easily obtained for an $F(t)$, known to contain only discrete frequencies, by electrically filtering $F(t)$ through a variable frequency bandpass filter of bandwidth $\Delta\omega_b = 2\pi\Delta f_b$.

The block diagram in Figure 92 shows the essential equipment required for this process and Figure 93 shows a plot of the typical characteristics of such a filter relative to some centerband frequency ω_c .

The amplitude of each filtered frequency component of $F(t)$ is given by the product

$$c_n (\text{filtered}) = A(\omega_c, \omega_n) c_n. \quad (294)$$

Thus, each filtered amplitude c_n may be obtained by sweeping ω_c through the entire frequency range of interest so that ω_c is made to coincide, one at a time, with each of the frequencies ω_n . If the bandwidth is sufficiently



$\Delta\omega_b$ = BANDWIDTH OF BAND PASS FILTER

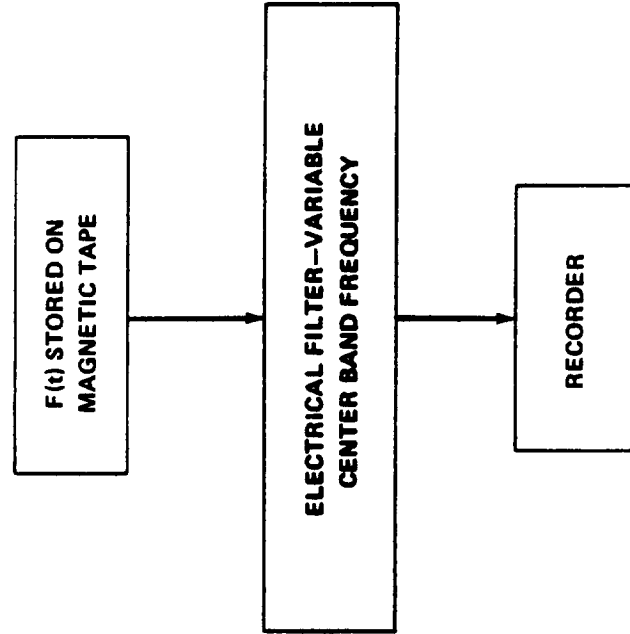


Figure 93. Typical filter characteristic.

narrow, only one frequency component will be transmitted to the recorder for each fixed ω_c , and the filtered wave in each case will be a pure sinusoid of constant peak amplitude. If, however, more than one frequency component is transmitted, the filtered wave will be modulated and the individual amplitudes of the unfiltered wave may be more difficult to obtain. Therefore, it may be desirable to use narrower bandwidth filters to separate close frequencies. A lower practical limit to the bandwidth does exist, but these limitations are not discussed here.

Finally, the information obtained by filtering out the discrete frequency components of $F(t)$ can be presented in the form of a bar graph as in Figure 94. Only the component amplitudes c_n are shown, as phase data is generally not obtained in present data reduction systems. For many dynamic problems, it is important that the phasing be known, and in the future it will be desirable to measure this quantity. This phasing, for a periodic function, can be obtained from the above time integrations for a_n and b_n .

The above finite Fourier series can be extended to include functions having period $2T$ which contain an infinite number of frequencies which are all multiples of the basic angular frequency π/T .

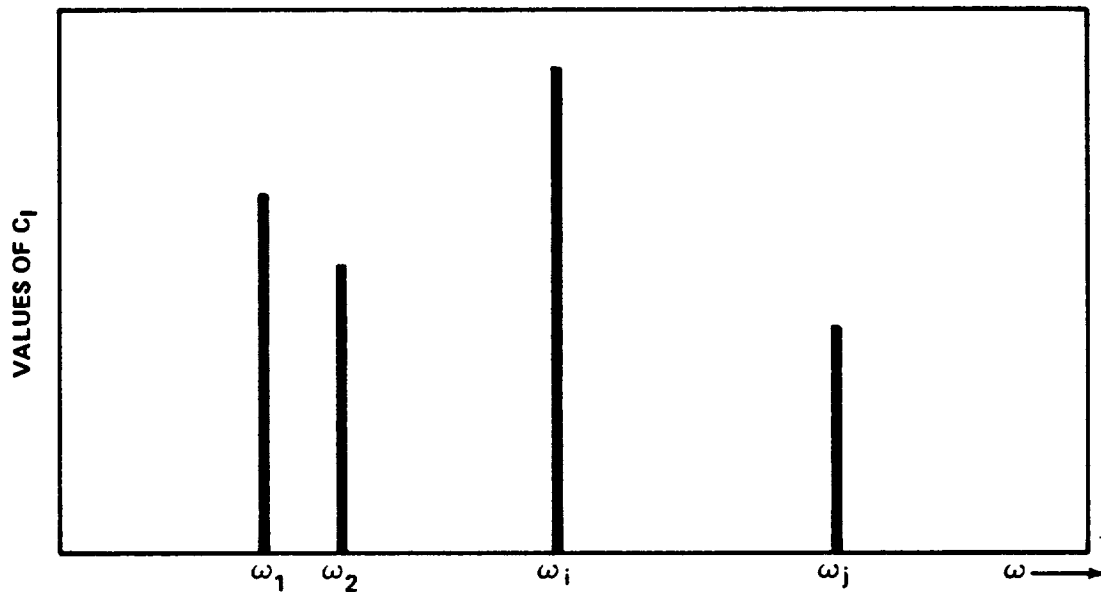


Figure 94. Bar graph of the amplitude of filtered discrete frequency components.

Generally, the function $F(t)$ is random and has no finite period (i.e., $T \rightarrow \infty$). This is true for both stationary and nonstationary random functions. Such functions cannot be represented by the Fourier series as they contain a continuous band of frequencies which are not multiples of some basic frequency. (For an infinite period, this basic frequency is zero.) The spectral characteristics of the function must be described by either its Fourier transform or by its power spectral density function. It is assumed here that neither the transform nor the spectrum function are trivially zero or infinite in amplitude.

Following the approach used by Bendat, the above Fourier series ($N \rightarrow \infty$) can be rewritten in the complex form

$$F(t) = \sum_{n=-\infty}^{\infty} A_n e^{j\omega_n t} \quad \omega_n = 2\pi f_n ; j = \sqrt{-1}$$

$$A_n = \frac{1}{2T} \int_{-T}^T F(t) e^{-j\omega_n t} dt = \frac{1}{2} (a_n - jb_n), \quad n \neq 0 \quad (295)$$

$$A_0 = a_0/2, \quad |A_n|^2 = c_n^2/4$$

where ω_0 is equal to π/T , and $F(t)$ is of period $2T$.

As the period T approached infinity, $T \rightarrow \infty$, the basic frequency ω_0 approaches zero, which shows that more and more frequencies are contained in $F(t)$. Thus, the coefficient A_n , and hence a_n and b_n , approach zero, which implies that the amplitude c_n of the individual frequency components also approach zero. However, as $T \rightarrow \infty$, the ratio $2\pi A_n/\omega_0$ becomes the Fourier transform

$$\lim_{\omega_0 \rightarrow 0} \frac{2\pi A_n}{\omega_0} = \int_{-\infty}^{\infty} F(t) e^{-j\omega t} dt = \mathcal{F}_F(\omega) \quad (296)$$

The Fourier transform of $F(t)$, when it exists, may therefore be used to describe the frequency characteristics of nonperiodic functions. This transform exists for a limited case of nonstationary functions, where the total energy associated with these functions is finite. Typical examples of these functions are isolated pulses of various shapes, or a finite train of pulses. Examples of the Fourier transform for three types of pulses are presented in Figure 95.

If $F(t)$ contains a sinusoidal component of nonzero amplitude at some frequency $\bar{\omega}$, then the Fourier transform $\mathcal{F}_F(\omega)$ will exhibit an infinite spike at $\bar{\omega}$.

For stationary nonperiodic random processes, the total energy associated with $F(t)$ is infinite and the above Fourier transform is also infinite. In this case the spectral properties of $F(t)$ are displayed by the use of the one-sided realizable power spectral density function $G_F(\omega)$. Formally, this function may be defined as

$$G_F(\omega) = \lim_{T \rightarrow \infty} \frac{|\mathcal{F}_F(\omega)|^2}{T} \quad (297)$$

Although $|\mathcal{F}_F(\omega)|$ is infinite, this ratio exists and is finite for nonperiodic $F(t)$. If $F(t)$ contains a sinusoidal component at frequency $\bar{\omega}$, then $G_F(\omega)$ will exhibit an infinite spike at the frequency. For nonstationary functions, where the Fourier transform exists, the power spectral density function will be zero, except for periodic components where it will exhibit infinite spikes. Since well-defined oscillatory functions contain periodicities, it is not possible to show a diagram of some analytical function and its corresponding power spectral density. Such spectrums must be determined from a statistical analysis of a recorded function resulting from some physical random phenomenon.

It is now clear that the filtering techniques used for functions which contain a continuous band of frequencies must be altered somewhat from those discussed above for periodic functions. Because the amplitude of each frequency component is zero for such functions (except for additional discrete sinusoids), it is necessary to filter a narrow band of frequencies and determine the statistical averages of the amplitude of the filtered signal over all frequencies in that narrow band. Since it is more desirable to use electrical filters, with the function $F(t)$ stored on magnetic tape, the time averages associated with

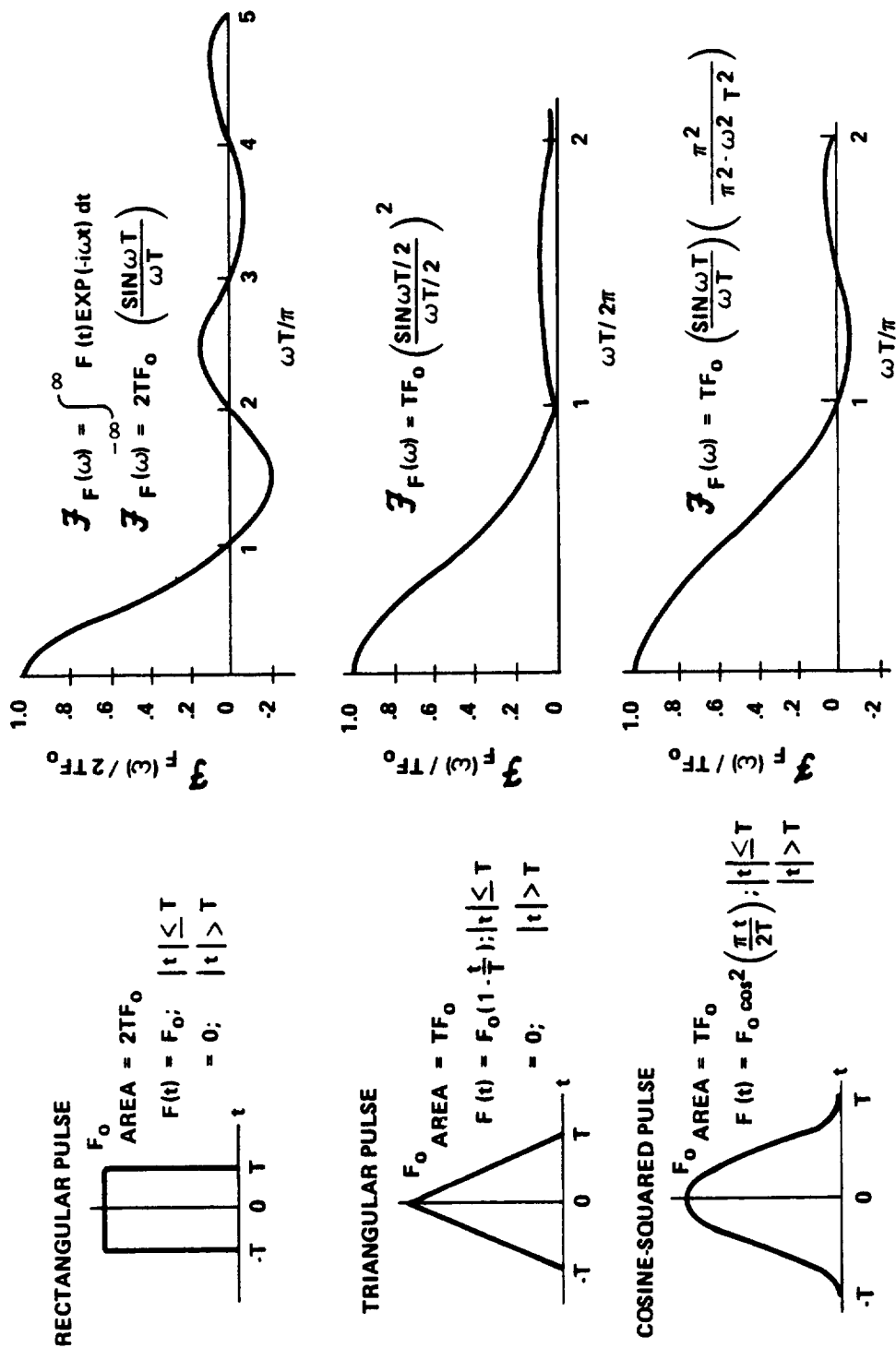


Figure 95. Finite isolated pulses and their Fourier transforms.

stationary and ergodic processes are preferred over ensemble averages because of available electronic analog methods for determining these averages. The above discussion shows that the nonstationary functions which are of practical interest (i. e. , those containing a finite amount of energy) are transients that appear in the form of isolated pulses and shocks. These are difficult to filter because of the small sample sizes available – usually one or two records which are small fractions of a second in length. The following discussion of the statistical averages of the frequency components of $F(t)$ will then be confined to stationary and ergodic random process, or those processes for which the assumptions of stationary and ergodicity closely approximate the actual conditions.

In many random processes occurring in nature, the mean value of the oscillating amplitude of a random variable, say $F(t)$, is approximately equal to zero. Also, the time variation of the amplitudes of the individual frequency components of $F(t)$ will have a near zero mean value. The assumption that the mean is zero is widely used in practice. Whether or not this assumption is valid naturally depends upon the random variable being considered. For example, the distribution of the amplitude peaks of $F(t)$ may be Rayleigh, which cannot have a zero mean.

The mean square value $\overline{F^2}$ of $F(t)$ has a special physical interpretation that is fundamental in spectral analyses. The instantaneous power dissipated by a resistor R is an electrical network equals I^2R or E^2/R , where E is the voltage drop across the resistor and I is the resistor current. Analogously, the instantaneous power $P(t)$ dissipated in a structure having viscous damping c and vibratory velocity v equals cv^2 or $AF^2(t)$, where A is a constant of proportionality. The average power P_{avg} is the time average (mean of the instantaneous power),

$$P_{avg} = \frac{1}{T} \int_0^T P(t) dt = \frac{A}{T} \int_0^T F^2(t) dt \quad (298)$$

and hence is proportional to the mean square value $\overline{F^2}$ of $F(t)$.

$$P_{avg} = A \overline{F^2} ;$$

that is, a knowledge of overall mean square value of the applied force $F(f)$ indicates the amount of power being dissipated in a linear structure, to within a constant of proportionality.

To broaden the use of the power concept so that the techniques which have been developed for its application can be extended to include random variables, for which true damping power does not exist, the proportionality constant A is dropped and the mean square value of the random variable is called the total average power of the variable. It may be more appropriate for such cases to retain the "mean square" terminology. Both of these will be used here to avoid possible confusion with existing terminology used in the referenced literature.

The mean square value is particularly useful in dealing with near discrete frequency, random amplitude components of $F(t)$. For the well-behaved periodic function, the discrete frequency components have constant peak amplitudes. For a near discrete frequency with random amplitude, it is not practical to determine all of the many Fourier coefficients required to define this component. Instead, a narrow band filter is used to obtain these near discrete components and the mean square value of the amplitude of each such frequency is obtained.

The equivalent sinusoidal amplitude in terms of the Fourier coefficients is given by the relation

$$\Delta \overline{F^2(\omega_n)} = \frac{1}{2} c_n^2 = \text{mean square value of a true sinusoid with amplitude equal to } c_n.$$

The total average power P_{avg} for all of the near discrete components is equal to the arithmetic sum of the power $\Delta P(\omega_n)$ of each component.

$$P_{\text{avg}} = \sum_n \Delta P(\omega_n) = \sum_n \Delta \overline{F^2(\omega_n)} \quad . \quad (299)$$

The graph (Fig. 96) of the mean square value of the individual frequency components is similar to that of Figure 94 where the Fourier amplitude

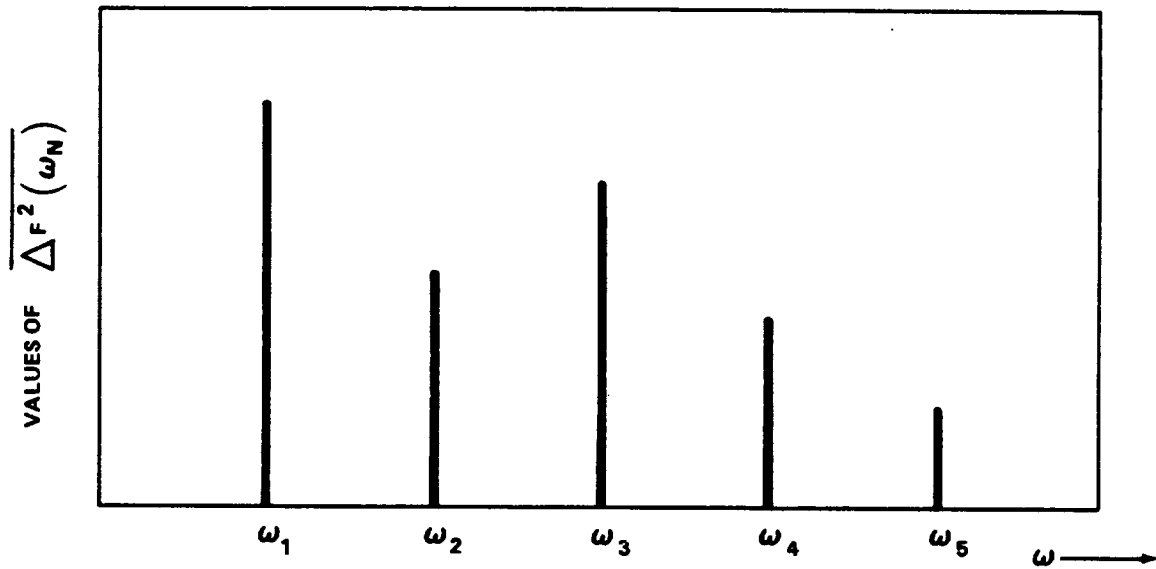


Figure 96. Bar graph of the mean square amplitudes of discrete frequency components.

coefficients are displayed for each sinusoidal component of $F(t)$. Just as did these Fourier coefficients, the mean square value of each frequency component, and hence the power in each component, decreases to zero when the number of frequencies contained in $F(t)$ increases to a continuous band of frequencies. This assumes, of course, that no finite amplitude discrete frequencies are present. To eliminate this difficulty, it is usual to consider the mean square value over a finite frequency range of continuous frequency components, and to divide this quantity by the frequency band. In the limit, as the frequency band decreases to zero, this ratio becomes a mean square spectral density function with respect to frequency and is usually called the power spectral density function $G_F(\omega)$.

Mathematically expressed:

$$G_F(\omega) = \lim_{\Delta\omega \rightarrow 0} \frac{\overline{F^2(\Delta\omega)}}{\Delta\omega} = \lim_{\Delta\omega \rightarrow 0} \frac{P_{\text{avg}}(\Delta\omega)}{\Delta\omega} \quad (300)$$

where

$F^2(\Delta\omega)$ = mean square amplitude over all frequencies in Δ

$P_{\text{avg}}(\Delta\omega)$ = total average power over all frequencies in $\Delta\omega$.

The total average power contained in all frequency components in $F(t)$ is therefore given by the equation

$$P_{\text{avg}} = \overline{F^2} = \int_0^{\infty} G_F(\omega) d\omega \quad . \quad (301)$$

The physical interpretation of the mean square statistical average of $F(t)$ is now evident in terms of the definition of power presented above.

The power spectral density function $G_F(\omega)$ is also related to the autocorrelation function $R_F(\tau)$, as shown in the previous expressions for the statistical averages. For a stationary and ergodic process, reciprocal relations exist in terms of the Fourier transform. These convenient mathematical relations are as follows:

$$G_F(\omega) = \frac{1}{2\pi} G_F(f) = \frac{2}{\pi} \int_0^{\infty} R_F(\tau) \cos \omega\tau d\tau$$

$$R_F(\tau) = \int_0^{\infty} G_F(\omega) \cos \omega\tau d\omega \quad . \quad (302)$$

These relationships are not easily explained by physical arguments and are not discussed further in this document.

The stationary autocorrelation function $R_F(\tau)$ of a single time function $F(\tau)$ also has a special interpretation which is important in determining response of the structure. Basically, this function shows quantitatively the agreement between the function $F(t)$ at time t and at time $t + \tau$ [i.e., between the functions $F(t)$ and $F(t + \tau)$]. When $\tau = 0$, the two functions are in perfect agreement at every point and the correlation between the two is as large as possible. Thus,

$$R_F(0) \cong |R_F(\tau)| .$$

It is to be noted that $R_F(0)$ is equal to the mean square value $\overline{F^2}$ of $F(t)$. A non-negative correlation coefficient, $C_F(\tau)$, is a convenient measure of the relative correlation of $F(t)$ with itself. This coefficient is defined here as follows:

$$C_F(\tau) = \left| \frac{R_F(\tau)}{R_F(0)} \right| . \quad (303)$$

Thus, $C_F(\tau)$ may have any values between 0 and 1. $C_F(\tau) = 1$ indicates perfect correlation, $C_F(\tau) = 0$ indicates no correlation, and values of $C_F(\tau)$ between 0 and 1 indicate partial correlation.

The validity of this concept of correlation is easily shown by considering a simple sine wave of the form

$$F(t) = C \sin (\omega t - \phi) .$$

The non-negative correlation coefficient $C_F(\tau)$ for this case is

$$C_F(\tau) = \left| \frac{\frac{C^2}{2T} \int_{-T}^T \sin(\omega t + \phi) \sin(\omega t + \omega \tau + \phi) dt}{\frac{C^2}{2T} \int_{-T}^T \sin^2(\omega t + \phi) dt} \right|$$

$$= \left| \frac{\frac{1}{2} C^2 \cos \omega \tau}{\frac{1}{2} C^2} \right| = |\cos \omega \tau| \quad (304)$$

A plot of $C_F(\tau)$ is presented in Figure 97, and it will be valuable to compare this ideal coefficient with those obtained in practice for random functions.

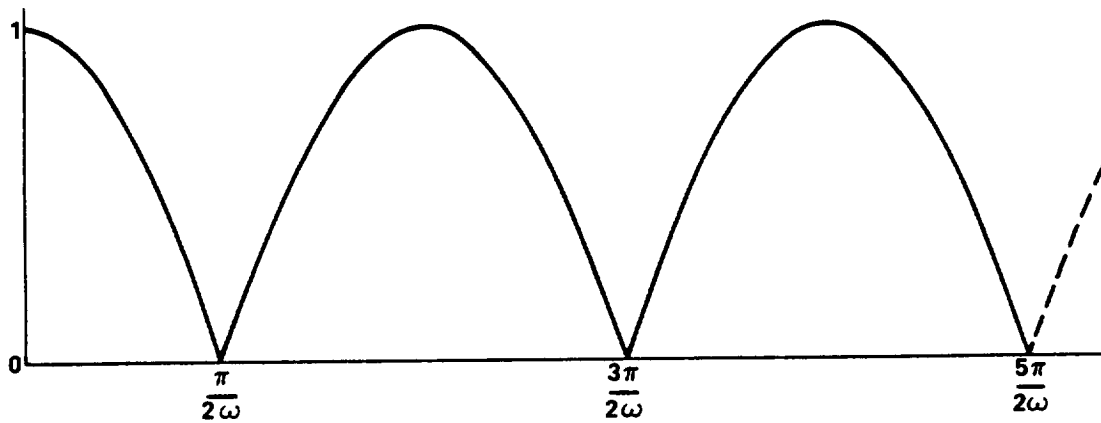


Figure 97. The correlation function $C_F(\tau)$ of a sinusoid is the absolute value of a cosinusoid $C_F(\tau) = |\cos \omega \tau|$.

In contrast to a well-behaved periodic function, the correlation coefficient for random white noise is zero for all $\tau \neq 0$. "White" noise is a descriptive term for a random process whose power spectral density function is a constant over all frequencies.

F. Digital Vibration Analysis

The process of digitizing consists of converting continuous data into discrete numbers. There are two main parts involved in a digitization pro-

cedure. The first part is sampling, which is defining the points at which the data is observed. It is important to have a sufficient number of samples to describe properly the significant information in high frequencies. On the other hand, sampling at points which are too close together will yield correlated and highly redundant data, and increase greatly both the labor and cost of calculations. To cut down the number of samples, one should decrease the sampling rate to the lowest rate which will avoid aliasing errors.

To be specific on aliasing, if the time interval between samples is h seconds, then the sampling rate is $(1/h)$ samples per second. The useful data will be from 0 to $(1/2h)$ Hz since frequencies in the data which are higher than $(1/2h)$ Hz will be folded into the lower frequency range from 0 to $(1/2h)$ Hz and confused with data in this lower range. The frequency

$$f_c = \frac{1}{2h} \quad (305)$$

is known as the Nyquist frequency. Folding of the frequency axis is illustrated on Figure 98. For example, if $f_c = 100$ Hz, then data at 170, 230, 370, and 430 Hz would not be distinguished from data at 30 Hz.

The second part in a digitizing procedure is the matter of quantization, which is the actual conversion of the observed values to numerical form. No matter how fine the scale, a choice between two consecutive values is required. This matter is illustrated on Figure 99. In this figure one would choose $(a + 1)$ as the closest numerical value to the desired time value.

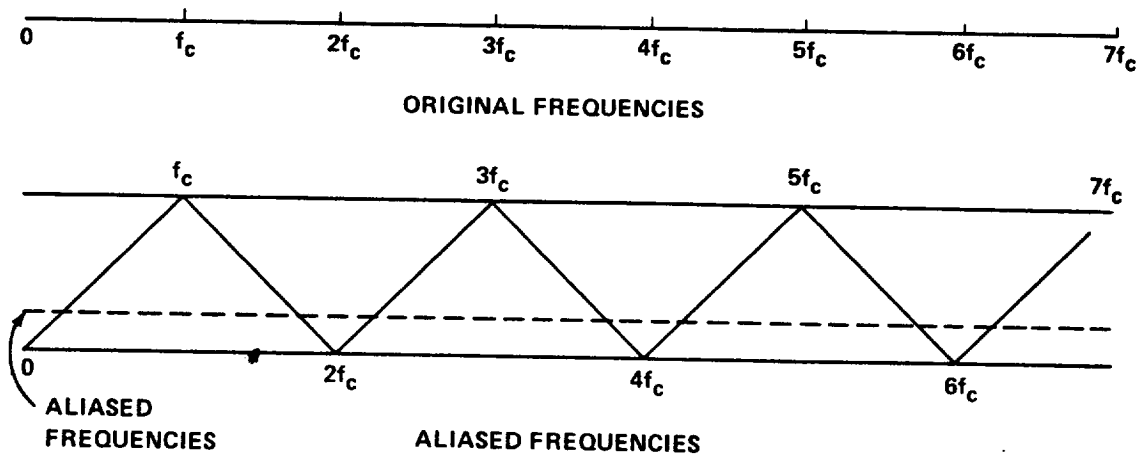


Figure 98. Illustration of folding about the nyquist cutoff frequency f_c .

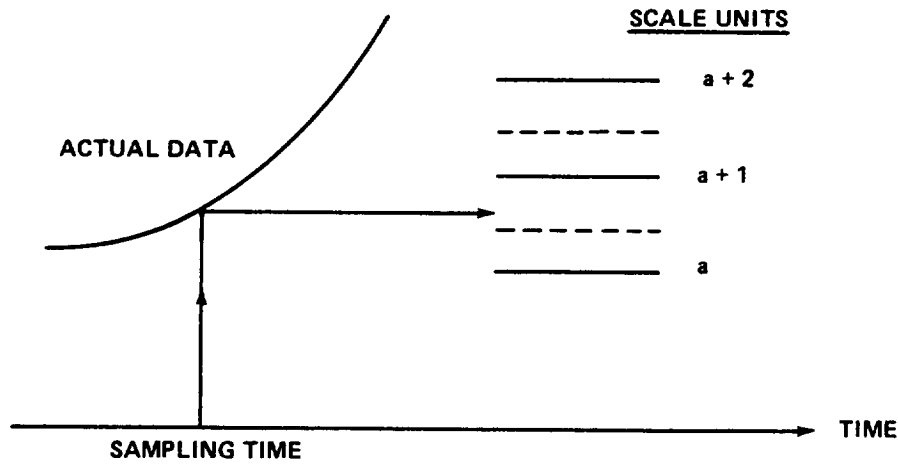


Figure 99. Illustration of quantization error.

If one assumes that the quantization errors follow a uniform probability distribution over one scale unit, then these errors will have a mean value of zero and a standard deviation (rms value) of approximately 0.3 scale unit. This can be considered as an rms noise error on desired signal measurements. For example if the rms value of a signal is quantized at 300 scale units, then since the rms value of the noise is 0.3 scale unit, one would have an rms noise-to-signal ratio here of 0.001.

1. BASIC STATISTICAL ANALYSIS

a. Data values u_i are found at points $i = 1, 2, \dots, N$. These points are a distance h apart and determine the cutoff frequency $f_c = (1/2h)$.

b. Mean value

$$\bar{u} = \frac{1}{N} \sum_{i=1}^N u_i \quad (306)$$

where

N = number of data samples

u_i = data values at points $i = 1, 2, 3, \dots, N$.

The true mean value is denoted usually by μ . The quantity u is called the sample mean value and is an estimate of μ . So that subsequent formulas and calculations may be simplified, it is convenient to transform the data to have a zero mean value. That is, define quantities x_i by the relation

$$x_i = u_i - u \quad , \quad i = 1, 2, \dots, N \quad . \quad (307)$$

This computation would be necessary later for other procedures and is most optimally performed at this time.

c. Standard deviation

$$s = \sqrt{\sum_{i=1}^N \frac{(x_i)^2}{N-1}} \quad (308)$$

where

N = number of data samples

x_i = transformed data values at points $i = 1, 2, 3, \dots, N$.

The quantity s is called the sample standard deviation. The sample variance is denoted by s^2 . The true standard deviation is denoted usually by σ , and the true variance is denoted by σ^2 .

d. Standardization. A further transformation on the data may be convenient at this time if the computer calculations are to be performed with fixed, as opposed to floating, arithmetic. Multiplying the transformed values, x_i , by $1/s$ yields

$$y_i = \frac{1}{s} x_i \quad , \quad i = 1, 2, \dots, N \quad . \quad (309)$$

This results in final data with a sample mean of zero and a sample standard deviation of unity.

The scaling problem is eased in fixed point arithmetic since the data may now be considered to lie in the range $y_i \leq 7$. Actually the probability of values greater than three or four in absolute value is negligible in most

cases. If floating point arithmetic is used, there is no particular advantage to having the division by s . It must be noted that the division by s corresponds to a scale change so that output data for plotting and the like would have to be later scaled appropriately. Also, for large amounts of data, the complete standardizing is costly computational timewise since N divisions are required if there are N data points.

e. Skewness coefficient (C_s)

$$C_s = \sum_{i=1}^N \frac{(x_i)^3}{N s^3} \quad (310)$$

where

s = sample standard deviation

N = number of data samples

x_i = transformed data values $u_i - \bar{u}$.

The true skewness coefficient for a normal distribution is zero.

f. Kurtosis coefficient (C_k)

$$C_k = \sum_{i=1}^N \frac{(x_i)^4}{N s^4} \quad (311)$$

where

s = sample standard deviation

N = number of data samples

x_i = transformed data values $u_i - \bar{u}$.

The true kurtosis coefficient for a normal distribution is 3.0.

g. Probability density function

$$f(x) = \frac{d F(x)}{dx} \quad (312)$$

where

$f(x)$ = probability density function

$F(x)$ = probability distribution function .

The number of observations and the percentage of data in each of k class intervals are tabulated. To later optimally apply a χ^2 goodness-of-fit test of the data to the Gaussian and Rayleigh distributions, the number of class intervals should be chosen as indicated in Table 11.

TABLE 11. OPTIMUM NUMBERED CLASS INTERVALS k
AS A FUNCTION OF THE SAMPLE SIZE N .

N	0-299	300-499	500-699	700-899	900-1249	1250-1749	1750-∞
k	16	20	24	27	30	35	39

h. Probability distribution function

$$f(x) = \int_{-\infty}^x f(x) dx \quad (313)$$

where

$f(x)$ = probability density function

$F(x)$ = probability distribution function

$F(-\infty) = 0$; $F(\infty) = 1.0$.

The cumulative number of observations and the cumulative percentage of data in each class interval are tabulated.

i. Gaussian (normal) probability density function

$$\phi(x) = \frac{1}{\sigma\sqrt{2\pi}} \exp \left[\frac{-x^2}{2\sigma^2} \right] \quad (314)$$

where

the true mean value is zero

σ = true standard deviation (estimated by s , the sample standard deviation).

Thus,

$$\phi(x) \approx \frac{1}{s\sqrt{2\pi}} \exp \left[\frac{-x^2}{2s^2} \right] \quad (315)$$

The density function $\phi(x)$ is evaluated at the midpoints of the k class intervals determined in 7 above.

j. Gaussian probability distribution function

$$\Phi(x) = \int_{-\infty}^x \phi(x) dx \quad (316)$$

where

$\phi(x)$ = Gaussian probability density function

$\Phi(x)$ = Gaussian probability distribution function.

The Gaussian distribution function should be evaluated at the $k-1$ class interval end points.

k. Rayleigh probability density function

$$c(x) = \frac{x}{\sigma^2} \exp \left[\frac{-x^2}{2\sigma^2} \right] \quad (317)$$

where

σ = true standard deviation (estimated by s , the sample standard deviation).

Thus,

$$c(x) \approx \frac{x}{s^2} \exp \left[\frac{-x^2}{2s^2} \right] \quad (318)$$

The density function $c(x)$ is evaluated at the midpoints of the k class intervals.

1. Rayleigh probability distribution function

$$C(x) = \int_{-\infty}^x c(x) dx \quad (319)$$

where

$c(x)$ = Rayleigh probability density function
 $C(x)$ = Rayleigh probability distribution function.

The distribution function $C(x)$ is evaluated at the $k - 1$ class interval end points.

m. Tests for normality

(1) χ^2 Goodness-of-fit test

Let p_i be the percentage of observations in the i th class interval. These values are obtained when the density function histogram is tabulated in Step g. Let ΔA_i be the area under the Gaussian density function curve in the i th class interval. Note that these quantities are effectively obtained during Steps i and j. The statistic

$$\chi^2 = N \sum_{i=1}^k \frac{p_i^2}{\Delta A_i} \quad (320)$$

is distributed as χ^2 with $k - 3$ degrees of freedom (df).

(2) Moment test

The skewness and kurtosis coefficients C_s and C_k given by equations (310) and (311) may be used as an additional test

for normality. The sampling distributions for C_s and C_{k-3} are tabulated for the .01 and .05 levels of significance in Reference 27, where they are denoted by γ_1 and γ_2 , respectively.

n. Test for Rayleigh distribution

The procedure is identical to that outlined in m(1) above except that the ΔA_i values are obtained from Steps k and l. Also, due to the fact that only one parameter, namely s^2 , is necessary to define the Rayleigh distribution, the statistic computed from equation 14.92 will be distributed as χ^2 with $k - 2$ df.

2. FOURIER SERIES REPRESENTATION

If a sample record $x(t)$ is periodic of period T , that is, $x(t) = x(t + T)$ for all t , and if one assumes $f_0 = (1/T)$ is the fundamental frequency, then $x(t)$ can be represented by the series

$$x(t) = \frac{a_0}{2} + \sum_{n=1}^{\infty} (a_n \cos 2\pi n f_0 t + b_n \sin 2\pi n f_0 t) \quad (321)$$

where

$$a_n = \frac{2}{T} \int_0^T x(s) \cos 2\pi n f_0 s \, ds \quad (322)$$

$$b_n = \frac{2}{T} \int_0^T x(s) \sin 2\pi n f_0 s \, ds \quad (323)$$

Assume $x(t)$ of length T is sampled at an even number N equally spaced points a distance h apart where h has been selected to produce a sufficiently high frequency cutoff $f_c = (1/2h)$. Let

$$x_n \equiv x(nh) \quad ; \quad n = 1, 2, \dots, N.$$

One may calculate the finite analog of a Fourier series which will pass through the N data points [28]. For any point t in the interval $(0, T)$, one obtains

$$x(t) = A_0 + \sum_{n=1}^{N/2} A_n \cos \frac{2\pi nt}{T} + \sum_{n=1}^{(N/2)-1} B_n \sin \frac{2\pi nt}{T} \quad . \quad (324)$$

At the particular points $t = kh$, $k = 1, 2, \dots, N$

$$x_k = x_{kh} = A_0 + \sum_{n=1}^{N/2} A_n \cos \frac{2\pi nk}{N} + \sum_{n=1}^{(3N/2)-1} B_n \sin \frac{2\pi nk}{N} \quad . \quad (325)$$

The coefficients A_n and B_n are given by

$$A_0 = \frac{1}{N} \sum_{k=1}^N x_k = 0$$

$$A_n = \frac{2}{N} \sum_{k=1}^N x_k \cos \frac{2\pi nk}{N}, \quad n = 1, 2, \dots, \frac{N}{2} - 1$$

$$A_{N/2} = \frac{1}{N} \sum_{k=1}^N x_k \cos \pi \quad (326)$$

$$B_n = \frac{1}{N} \sum_{k=1}^N x_k \sin \frac{2\pi nk}{N}, \quad n = 1, 2, \dots, \frac{N}{2} - 1 \quad .$$

Note that $A_0 = 0$ when the sample mean $\bar{x} = 0$ which is the situation here. In the above formulas,

N = number of data samples

x_k = data values at $k = 1, 2, \dots, N$

A_n = finite analog of Fourier cosine coefficient

B_n = finite analog of Fourier sine coefficient

h = time interval between samples

$f_c = (1/2h)$ = cutoff frequency

T = period

$f_0 = (1/T)$ = fundamental frequency .

One should note that for large N the computational requirements for determining the coefficients A_n and B_n become quite overwhelming. However, the determination of the coefficients might still be of enough interest to justify the necessary computations.

a. Choice of Sample Size N

Certain formulas presented in Reference 20 can aid in the selection of the optimum sample size N to minimize later data processing. For example, assume that a set of power spectrum measurements $\{G_x(f)\}$ at a particular value of f follows a normal (Gaussian) distribution. Let $G_x^*(f)$ be the true value and let Δp be defined such that

$$\text{Prob} \left[\left| \frac{G_x^*(f) - G_x(f)}{G_x^*(f)} \right| \leq \Delta p \right] \geq p. \quad (327)$$

It can be shown that under certain conditions

$$\Delta p \approx \frac{\alpha_p}{\sqrt{BT}} \quad (328)$$

where α_p is the p percent value for a normal distribution defined by

$$\text{Prob} \left(-\alpha_p < x \leq \alpha_p \right) = p. \quad (329)$$

In equation (329), x is a normally distributed random variable with zero mean and unit standard deviation. The quantity T in equation (328) is the total time period over which the data is taken, and B is the resolution bandwidth.

To illustrate how the sample size N is related to the BT product which these samples represent, an example will be calculated. Suppose that the error of the power spectral density estimate at non-zero frequencies is to be no more than $\Delta p = 30$ percent at an 80-percent confidence level ($\alpha_p = 1.3$); that is, in a sequence of repeated experiments, at least 80 percent of the estimates will have an error no larger than 30 percent. The BT product is then determined as

$$BT = \left(\frac{\alpha_p}{\Delta p} \right)^2 \approx 18.7.$$

Assume now that frequencies up to $f_c = 2000$ Hz are of interest and a resolution bandwidth $B = 10$ Hz has been chosen. The maximum lag number m is then calculated from the equation

$$m = \frac{2f_c}{B} = \frac{2(2000)}{10} = 400.$$

Also, the time interval h between samples is given by

$$h = \frac{1}{2f_c} = \frac{1}{2(2000)} = .00025 \text{ sec.}$$

The total record time is

$$T = \frac{1}{B} \left(\frac{\alpha_p}{\Delta_p} \right)^2 = \frac{1}{10} (18.7) = 1.87 \text{ sec.}$$

One then calculates the total number of observations N to be collected from the equation

$$N = \frac{T}{h} = \frac{1.87}{0.00025} = 7.480 \times 10^3 = 7480.$$

This number is applicable to nonzero frequencies. For $G_x(0)$, one requires twice as many observations to maintain the same error risks.

Further experimental design considerations, such as the determination of the resolution bandwidth B , are discussed in Section VIII and in Reference 20.

3. AUTOCORRELATION FUNCTION

For a sampled data $\{u_n\}$, $n = 1, 2, \dots, N$, from a record $x(t)$ which is stationary, the estimated autocorrelation function at the points $t = rh$, $r = 0, 1, 2, \dots, m < N$, will be defined using the transformed data values $u_n - \bar{u}$ by the formula

$$R_r \equiv R_x(rh) = \frac{1}{N-r} \sum_{n=1}^{N-r} (u_n - \bar{u}) (u_{n+r} - \bar{u}) = \frac{1}{N-r} \sum_{n=1}^{N-r} x_n x_{n+r}$$

$$\approx \frac{1}{N-r} \sum_{n=1}^{N-r} u_n u_{n+r} - (\bar{u})^2 \text{ if } N \gg r \quad (330)$$

where

$u_n = u(nh) = \text{data values at } n = 1, 2, \dots, N$

$\bar{u} = \text{sample mean value}$

$r = \text{lag number} = 0, 1, 2, \dots, m < N$

$m = \text{maximum lag number}$

$x_n = u_n - \bar{u} = \text{transformed data values.}$

Note that the mean value $\bar{x} = 0$.

The maximum lag number m determines the later frequency bandwidth f resolution for the power spectral density function in the frequency interval $(0, f_c)$. This resolution bandwidth is given by

$$B = \frac{2 f_c}{m} \quad . \quad (331)$$

The resolution bandwidth B is twice the range found by dividing the frequency interval $(0, f_c)$ into m equally spaced parts (f_c/m) apart. Thus from knowledge of f_c , one can choose m in advance so as to have a desired B . For small statistical uncertainty in later estimates of the power spectral density function, one should choose $m \ll N$ since the maximum number of statistical degrees of freedom associated with these estimates is given by $(2N/m)$. On the other hand, high resolution (i.e, small B) will result if m is large. Thus a compromise choice for m is necessary in practice.

The autocorrelation function may take on negative as well as positive values. A normalized value for the autocorrelation function is obtained by dividing R_r by R_0 where

$$R_0 = R_x(0) = \frac{1}{N} \sum_{n=1}^N (x_n)^2 \quad . \quad (332)$$

Note that the quantity R_0 is a sample estimate of the true mean square value in the data. The quantity R_0 is related to the (unbiased) sample variance s^2 by the relation

$$R_0 = \frac{N-1}{N} s^2 . \quad (333)$$

Thus for large N , there is negligible difference between R_0 and s^2 .

When R_r is normalized, one obtains the quantity (R_r/R_0) which will be between plus and minus one; that is

$$-1 \leq (R_r/R_0) \leq 1.$$

4. POWER SPECTRAL DENSITY FUNCTION

For sampled data from a record $x(t)$ which is stationary with $x = 0$, (i.e., as occurs for transformed data values $x_n = u_n - \bar{u}$), a "raw" estimate of its realizable one-sided power spectral density function $G(f)$; that is, $G(f)$ is non-zero only for $f \geq 0$, is given for an arbitrary f in the range $0 \leq f \leq f_c$ by

$$G_x(f) = 2h \left[R_0 + 2 \sum_{r=1}^{m-1} R_r \cos \left(\frac{\pi r f}{f_c} \right) + R_m \cos \left(\frac{\pi m f}{f_c} \right) \right] \quad (334)$$

where

h = time interval between samples

R_r = value of autocorrelation function at lag r using the transformed data values $x_n = u_n - \bar{u}$

m = maximum lag number

$f_c = (1/2h)$ = cutoff frequency.

The total mean square value in the record in the frequency range $0 \leq f \leq f_c$ is given by

$$\int_0^{f_c} G_x(f) df = R_0 \equiv R_x(0) . \quad (335)$$

This quantity $G_x(f)$ should not be confused with a nonrealizable two-sided power spectral density function $S_x(f)$ which is defined for negative as well as positive f by

$$S_x(f) = S_x(-f) = \frac{G_x(f)}{2} \quad . \quad (336)$$

Here

$$\int_{-f_c}^{f_c} S_x(f) df = R_x(0) \quad . \quad (337)$$

The values of the function $G(f)$ should be calculated only at the $(m+1)$ special frequencies

$$f = \frac{kf_c}{m} ; \quad k = 0, 1, 2, \dots, m. \quad (338)$$

This will provide $(m/2)$ independent spectral estimates since spectral estimates at points less than $(2f_c/m)$ apart will be correlated. At these special frequency points,

$$G_k = G_x\left(\frac{kf_c}{m}\right) = 2h \left[R_0 + 2 \sum_{r=1}^{m-1} R_r \cos\left(\frac{\pi rk}{m}\right) + (-1)^k R_r \right] \quad (339)$$

The index k is called the harmonic number ($k = 0, 1, 2, \dots, m$), and the quantity G_k is the "raw" estimate of the power spectral density function at the frequency $f = (kf_c/m)$. The quantities G_k will be non-negative for all k .

A convenient check formula is

$$R_x(0) = \frac{1}{2hm} \left[\frac{1}{2} G_0 + \sum_{k=1}^{m-1} G_k + \frac{1}{2} G_m \right] \quad . \quad (340)$$

A "refined" estimate of the power spectral density may be found by further frequency smoothing called "Hanning [29]". Let \tilde{G} represent this "refined" estimate. Then at the $(m+1)$ frequencies $f = (kf_c^k/m)$; $k = 0, 1, 2, \dots, m$, one obtains

$$\begin{aligned}\tilde{G}_0 &= 0.5 G_0 + 0.5 G_1 \\ \tilde{G}_k &= 0.25 G_{k-1} + 0.5 G_k + 0.25 G_{k+1}; k = 1, 2, \dots, m-1 \\ \tilde{G}_m &= 0.5 G_{m-1} + 0.5 G_m\end{aligned}\quad (341)$$

Other "refined" estimates may be obtained which are more complicated than the above. These provide different bias and uncertainty errors which are preferred for certain applications. These values for \tilde{G}_k should be used as the final estimates here for $G(f)$ at the frequencies $f = (kf_c/m)$; $k = 0, 1, 2, \dots, m$.

5. JOINT STATISTICAL ANALYSIS OF TWO RECORDS

In the following formulas the assumption will be that two records $x(t)$ and $y(t)$ are stationary and exist only for $0 \leq t \leq T$. Choose a sampling time interval $\Delta t = h$ time units apart, which in so doing induces a desired corresponding frequency cutoff $f_c = (1/2h)$. Let the respective sample values for $x(t)$ and $y(t)$ be denoted by

$$\left. \begin{aligned}u_n &= u(nh) \\ v_n &= v(nh)\end{aligned} \right\} \quad \begin{aligned}n &= 1, 2, 3, \dots, N \\ T &= Nh\end{aligned}\quad (342)$$

The first quantities to compute are the sample mean values

$$\bar{u} = \frac{1}{N} \sum_{n=1}^N u_n \quad \bar{v} = \frac{1}{N} \sum_{n=1}^N v_n$$

Choose a maximum lag number m which will give a desired frequency resolution $B = (2f_c/m) \approx (1/hm)$ as well as a desired number of degrees of freedom $(2N/m)$. The autocorrelation functions and power spectral density functions are calculated for x and y in terms of the transformed data separately according to the formulas listed previously. Formulas to calculate their joint cross-correlation functions and cross-power spectral functions in terms of the transformed data will now be given where the transformed data are defined as before by

$$x_i = u_i - \bar{u} \text{ and } y_i = v_i - \bar{v}; i = 1, 2, 3, \dots, N.$$

6. CROSS-CORRELATION FUNCTIONS

$$R_{xy}(rh) = \frac{1}{N-r} \sum_{n=1}^{N-r} (x_n)(y_{n+r})$$

$$R_{yx}(rh) = \frac{1}{N-r} \sum_{n=1}^{N-r} (y_n)(x_{n+r}) \quad (343)$$

where

$$r = 0, 1, 2, \dots, m \text{ and } m = \text{maximum lag number.}$$

Note that the two cross-correlation functions R_{xy} and R_{yx} differ by the interchange of the x_n and y_n sample values.

The cross-correlation functions $R_{xy}(rh)$ and $R_{yx}(rh)$ may be normalized to have values between plus and minus one by dividing them by $\sqrt{R_x(0)}\sqrt{R_y(0)}$. This defines a cross-correlation coefficient

$$\Gamma_{xy}(rh) = \frac{R_{xy}(rh)}{\sqrt{R_x(0)} \sqrt{R_y(0)}} \quad (344)$$

such that $-1 \leq \Gamma_{xy}(rh) \leq 1$.

For later determination of the cross-power spectral density function between x and y, calculate the two quantities

$$\begin{aligned} A_{xy}(rh) &= \frac{1}{2} [R_{xy}(rh) + R_{yx}(rh)] \\ B_{xy}(rh) &= \frac{1}{2} [R_{xy}(rh) - R_{yx}(rh)] \end{aligned} \quad (345)$$

7. CROSS-POWER SPECTRAL DENSITY FUNCTION

The cross-power spectral density function is a complex-valued quantity defined by

$$G_{xy}(f) = C_{xy}(f) - jQ_{xy}(f); j = \sqrt{-1} \quad (346)$$

where $C_{xy}(f)$ is called the cospectral density function and $Q_{xy}(f)$ is called the quadrature spectral density function. An equivalent representation for $G_{xy}(f)$ is

$$G_{xy}(f) = |G_{xy}(f)| e^{j\Theta_{xy}(f)} \quad (347)$$

where $|G_{xy}(f)|$ is the absolute value of $G_{xy}(f)$ and $\Theta_{xy}(f)$ is the phase angle contained in $G_{xy}(f)$.

Other identities are

$$\begin{aligned}
 |G_{xy}(f)|^2 &= C_{xy}^2(f) + Q_{xy}^2(f) \\
 C_{xy}(f) &= |G_{xy}(f)| \cos \Theta_{xy}(f) = C_{yx}(f) \\
 Q_{xy}(f) &= -|G_{xy}(f)| \sin \Theta_{xy}(f) = -Q_{yx}(f) \\
 \Theta_{xy}(f) &= -\tan^{-1} [Q_{xy}(f)/C_{xy}(f)] .
 \end{aligned}
 \tag{348}$$

Raw estimates from sampled data for the cospectral density function and the "quadrature" spectral density function may be found as follows. Formulas are for realizable one-sided spectra which are non-zero only for $f \geq 0$.

At an arbitrary value of f in the range $0 \leq f \leq f_c$ raw estimates are

$$\begin{aligned}
 C_{xy}(f) &= 2h \left[A_{xy}(0) + 2 \sum_{r=1}^{m-1} A_{xy}(rh) \cos \left(\frac{\pi rf}{f_c} \right) \right. \\
 &\quad \left. + A_{xy}(mh) \cos \left(\frac{\pi mf}{f_c} \right) \right]
 \end{aligned}
 \tag{349a}$$

$$\begin{aligned}
 Q_{xy}(f) &= 2h \left[2 \sum_{r=1}^{m-1} B_{xy}(rh) \sin \left(\frac{\pi rf}{f_c} \right) \right. \\
 &\quad \left. + B_{xy}(mh) \sin \left(\frac{\pi mf}{f_c} \right) \right] .
 \end{aligned}
 \tag{349b}$$

These functions should be calculated only at the $(m+1)$ special frequencies

$$f = \frac{kf_c}{m} ; k = 0, 1, 2, \dots, m .$$

At these frequencies, one obtains

$$C_k = C_{xy}(kf_c/m) = 2h \left[A_{xy}(0) + 2 \sum_{r=1}^{m-1} A_{xy}(rh) \cos \left(\frac{\pi rk}{m} \right) + (-1)^k A_{xy}(mh) \right] \quad (350)$$

$$Q_k = Q_{xy}(kf_c/m) = 4h \sum_{r=1}^{m-1} B_{xy}(rh) \sin \left(\frac{\pi rk}{m} \right) \quad (351)$$

Refined estimates of both $C_{xy}(f)$ and $Q_{xy}(f)$ may now be calculated as before by using the "Hanning" method [30]. This yields

$$\begin{aligned} \tilde{C} &= 0.5 C_0 + 0.5 C_1 \\ \tilde{Q} &= 0.5 Q_0 + 0.5 Q_1 \quad k = 1, 2, \dots, m-1 \\ \tilde{C}_k &= 0.25 C_{k-1} + 0.5 C_k + 0.25 C_{k+1} \\ \tilde{Q}_k &= 0.25 Q_{k-1} + 0.5 Q_k + 0.25 Q_{k+1} \\ \tilde{C}_m &= 0.5 C_{m-1} + 0.5 C_m \\ \tilde{Q}_m &= 0.5 Q_{m-1} + 0.5 Q_m \end{aligned} \quad (352)$$

Now, since $G_{xy}(f) = C_{xy}(f) - jQ_{xy}(f)$, at the special frequencies $f = (kf/m)$; $k = 0, 1, 2, \dots, m$, one obtains the refined estimates

$$\begin{aligned} \tilde{G}_{xy}(f) &\equiv \tilde{G}_{xy}(kf/m) = \tilde{C}_k - j\tilde{Q}_k = |\tilde{G}_{xy}(f)| e^{j\theta_{xy}(f)} \\ |\tilde{G}_{xy}(f)|^2 &= \tilde{C}_k^2 + \tilde{Q}_k^2 \\ \tilde{\theta}_{xy}(f) &= -\tan^{-1}(\tilde{Q}_k/\tilde{C}_k) \end{aligned} \quad (353)$$

These values for $|\tilde{G}_{xy}|$ and $\tilde{\Theta}_{xy}$ should be used as the final estimates here for $|G_{xy}|$ and Θ_{xy} at the frequencies $f = (kf_c/m)$; corresponding to the harmonic numbers $k = 0, 1, 2, \dots, m$.

8. TRANSFER FUNCTION PROPERTIES FOR LINEAR SYSTEMS

Assume now that $x(t)$ is the input to a linear system, characterized by its frequency response function $H(f)$, and $y(t)$ is the output from this linear system. The frequency response function $H(f)$ is a complex-valued function defined by

$$H(f) = \int_0^{\infty} h(\tau) e^{-j2\pi f \tau} d\tau \quad (354)$$

where $h(\tau) = 0$ for $\tau < 0$ is called the weighting function or unit impulse response function of the system. An equivalent representation for $H(f)$ is

$$H(f) = |H(f)| e^{j\phi(f)} \quad (355)$$

where $|H(f)|$ indicates the gain factor of the system at frequency f , and $\phi(f)$ indicates the corresponding phase shift at frequency f .

A basic result between stationary input power spectra $G_x(f)$, linear systems $H(f)$, and stationary output power spectra $G_y(f)$ is

$$G_y(f) = |H(f)|^2 G_x(f) \quad (356)$$

Another basic result using the stationary cross-power spectra $G_{xy}(f)$ is given by

$$G_{xy}(f) = H(f) G_x(f) \quad (357)$$

This latter equation reduces to two relations by equating real and imaginary parts, namely,

$$|G_{xy}(f)| = |H(f)| G_x(f)$$

$$\Theta_{xy}(f) = \phi(f) \quad . \quad (358)$$

One can derive also the relation

$$\frac{G_{xy}(f)}{G_{yx}(f)} = e^{j2\phi(f)} \quad . \quad (359)$$

from which to determine the phase factor $\phi(f)$.

At the special frequencies $f = (kf_c/m)$; $k = 0, 1, 2, \dots, m$, the gain factor and the phase shift are estimated by

$$|\tilde{H}_k| = \frac{|\tilde{G}_{xy}(f)|}{\tilde{G}_k} = \frac{(\tilde{C}_k^2 + \tilde{Q}_k^2)^{1/2}}{\tilde{G}_k}$$

$$\phi_k = -\tan^{-1}(\tilde{Q}_k/\tilde{C}_k) \quad . \quad (360)$$

9. COHERENCE FUNCTION

A coherence function $\gamma_{xy}^2(f)$ is defined between the stationary records $x(t)$ and $y(t)$ by the relation

$$\gamma_{xy}^2(f) = \frac{|G_{xy}(f)|^2}{G_x(f) G_y(f)} \quad ; \quad G_x(f) \neq 0, G_y(f) \neq 0 \quad (361)$$

where

$G_x(f)$ = power spectral density function of $x(t)$ at frequency f

$G_y(f)$ = power spectral density function $y(t)$ at frequency f

$G_{xy}(f)$ = cross-power spectral density function between $x(t)$ and $y(t)$ at frequency f .

The coherence function satisfies the inequality $0 \leq \gamma_{xy}^2(f) \leq 1$ for all f . It is unity when $x(t)$ and $y(t)$ are linearly related, and it is zero when $x(t)$ and $y(t)$ are incoherent at a frequency f .

At the special frequencies $f = (kf_c/m)$; $k = 0, 1, 2, \dots, m$, the coherence function is estimated by

$$\tilde{\gamma}_k^2 = \frac{\tilde{C}_k^2 + \tilde{Q}_k^2}{\tilde{G}_{k,x} \tilde{G}_{k,y}} \quad (362)$$

10. JOINT AND CONDITIONAL PROBABILITY DISTRIBUTIONS

As an adjunct to calculations of interest for two random records, such as the cross-correlation function and the cross-power spectral density function, one may also calculate joint and conditional probability density functions.

a. Joint Probability Density Function

The joint probability density function

$$f(x, y) = \frac{\partial}{\partial y} \left[\frac{\partial}{\partial x} F(x, y) \right] \quad (363)$$

where

$f(x, y)$ = joint density function

$F(x, y)$ = joint distribution function.

This may be obtained in the form of a two dimensional histogram. That is, each variable is divided into an appropriate number of class intervals and the number of observations and the percentage of data in each rectangle is recorded. See Figure 100 for an illustration as to how such a tabulation might appear.

		1	1	2	1	1	0	1	0
		3	4	5	7	6	3	2	1
1		2	7	15	19	13	6	2	1
3		4	8	18	25	16	8	4	2
		3	6	14	17	16	6	3	1
1		2	5	6	8	5	5	1	0
0		1	1	2	3	2	2	1	0

Figure 100. Two-dimensional histogram representing $f(x,y)$. (Number in each square represents observed frequency.)

b. Joint Probability Distribution Function

The joint probability distribution function

$$F(x,y) = \int_{-\infty}^x \int_{-\infty}^y f(u,v) dv du \quad (364)$$

where

$f(x,y)$ = joint density function

$F(x,y)$ = joint distribution function

$$F(-\infty, x_2) = F(x_1, -\infty) = 0 ; F(\infty, \infty) = 1$$

The distribution function is tabulated by first accumulating the number of observations and percentages in the x direction and then in the y direction for the final cumulative rectangle entries.

C. Joint Gaussian Distribution

Let P denote the normalized covariance matrix for the variables x and y; that is,

$$P = \begin{vmatrix} 1 & -\Gamma_{xy}(0) \\ -\Gamma_{yx}(0) & 1 \end{vmatrix} = \begin{vmatrix} \frac{R_{xx}(0)}{\sqrt{R_x(0)}\sqrt{R_x(0)}} & \frac{-R_{xy}(0)}{\sqrt{R_x(0)}\sqrt{R_y(0)}} \\ \frac{-R_{yx}(0)}{\sqrt{R_y(0)}\sqrt{R_x(0)}} & \frac{R_{yy}(0)}{\sqrt{R_y(0)}\sqrt{R_y(0)}} \end{vmatrix} .$$

(365)

Note that $\Gamma_{xy}(0) = \Gamma_{yx}(0)$ and is termed the correlation coefficient of x and y. Let x be a vector defined by

$$x = \begin{pmatrix} \frac{x}{s_x} & , & \frac{y}{s_y} \end{pmatrix}$$

and let

$$x' = \text{transpose of } x.$$

The two dimensional (sample) normal density function is then given by

$$f(x) = \frac{\exp\left\{\frac{-1}{2|P|} xPx'\right\}}{2\pi |P|} \quad (366)$$

where

$$|P| = \det P = 1 - \Gamma_{xy}^2(0). \quad (367)$$

The quadratic form xPx' replaces the squared exponent x^2 in the one dimensional case. The two dimensional (joint) Gaussian distribution is therefore a function of five parameters $\bar{x} = 0$, $\bar{y} = 0$, s_x , s_y , and $\Gamma_{xy}(0)$. All these quantities are available from previous calculations, the means being zero, of course, because of the previously applied transformation $x = u - \bar{u}$, etc. The bivariate normal distribution is most easily described in terms of "equi-probability ellipses". If one considers the points that give a constant value to the density function, it is seen that they form an ellipse

$$\begin{aligned} \frac{1}{2|P|} xPx' = \frac{1}{2 \left[(1 - \Gamma_{xy}^2(0)) \right]} & \left[\left(\frac{x}{s_x} \right)^2 - \Gamma_{xy}(0) \left(\frac{x}{s_x} \right) \left(\frac{y}{s_y} \right) \right. \\ & \left. + \left(\frac{y}{s_y} \right)^2 \right] = c^2 \end{aligned} \quad (368)$$

where c^2 is a constant. It can be shown that the mass in the whole plane outside the ellipse is

$$\int_c^\infty 2c e^{-c^2} dc = e^{-c^2} \quad (369)$$

Therefore, ellipses might be plotted for the 50, 75, 95, and 99 percent values; that is, ellipses which include all but 50, 25, 5, and 1 percent of the observations.

The values for c^2 corresponding to these values are given in Table 12.

TABLE 12. VALUES OF c^2 FOR EQUIPROBABILITY ELLIPSES

Percent of Observations Included in Ellipse	Corresponding Value of c^2
50	0.693
75	1.386
95	2.996
99	4.605

For a moderate positive value of $\Gamma_{xy}(0)$, the ellipses might take the form shown in Figure 101. If $\Gamma_{xy}(0) = 0$, they become circles and for $\Gamma_{xy}(0) = \pm 1$, a degenerate case of straight lines arises.

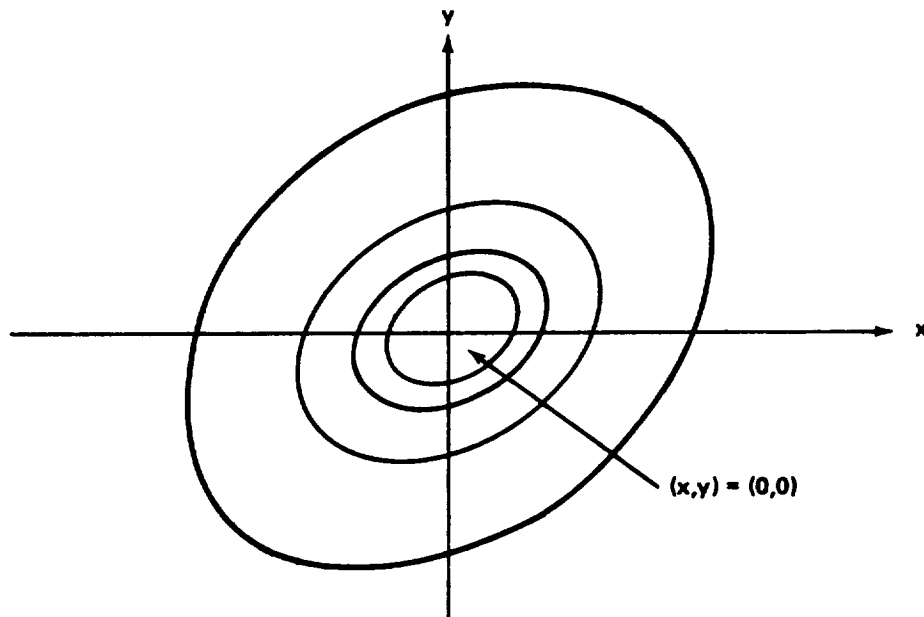


Figure 101. Typical equiprobability ellipses.

The proper method of plotting would be from the parametric equations of an ellipse. This requires several steps:

1. Eliminate the xy term in equation (368) of the ellipse by a rotation of coordinates through the proper angle.
2. Calculate the semimajor axis a and semiminor axis b of the ellipse.
3. Plot the values as a function of Θ from the parametric equations

$$x = a \cos \Theta$$

$$y = b \sin \Theta.$$

The details of obtaining the angle necessary to rotate out the xy term and for computing the axes a and b may be found in standard texts on analytic geometry.

d. Conditional Probability Density

The conditional density function for y given x , $f(y | x)$ (that is, for a specific value of x) is

$$f(y | x) = \frac{f(x, y)}{f(x)} \quad (370)$$

where

$$\begin{aligned} f(y | x) &= \text{conditional density function of } y \text{ given } x \\ f(x, y) &= \text{joint density function of } x \text{ and } y \\ f(x) &= \text{density function of } x (\text{assumed } \neq 0) . \end{aligned}$$

This is obtained by choosing a column of the two dimensional histogram for the joint density function, and normalizing each entry by dividing by the total number (or total percentage) in that column. That is, for each class interval of x one may obtain a conditional density function.

To obtain conditional densities for x given y , one uses rows instead of columns.

11. SUMMARY OF FUNCTIONS FOR TWO RECORDS

The preceding work is summarized in Figures 102 and 103 which show the order for computing desired functions for two records $x(t)$ and $y(t)$. In the transfer function calculation, $x(t)$ is considered as an input and $y(t)$ as an output through a linear system.

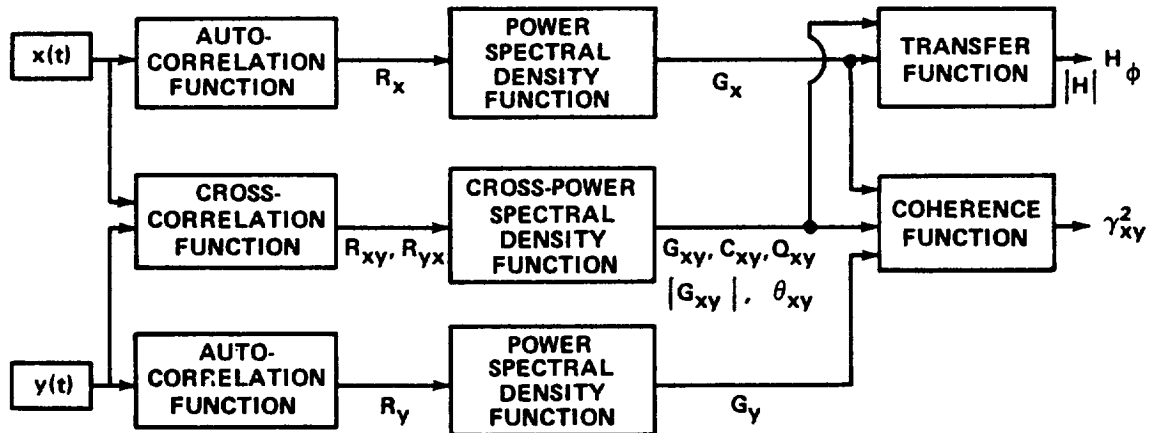


Figure 102. Functions to be computed for two records.

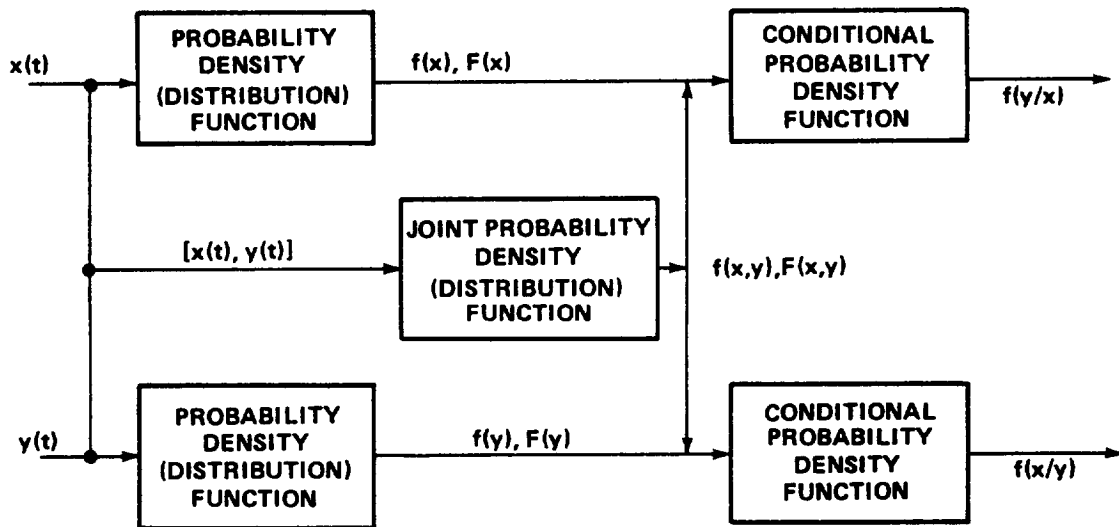


Figure 103. Joint probability functions for two records.

12. DIGITAL COMPUTER PROGRAM FLOW CHARTS

The flow charts on the following pages give the operations to be performed by the digital computer program for the statistical analysis of vibration data. The essential sequence of the operations should be approximately as indicated if all of the preceding analysis is desired. Other routines can be added to incorporate additional desired tests, such as tests for randomness and stationarity. Also, if only certain parts of the program are requested, such as power spectra alone, these can be computed directly by omitting intervening steps dealing with other information.

13. COMPUTER TIME ESTIMATES

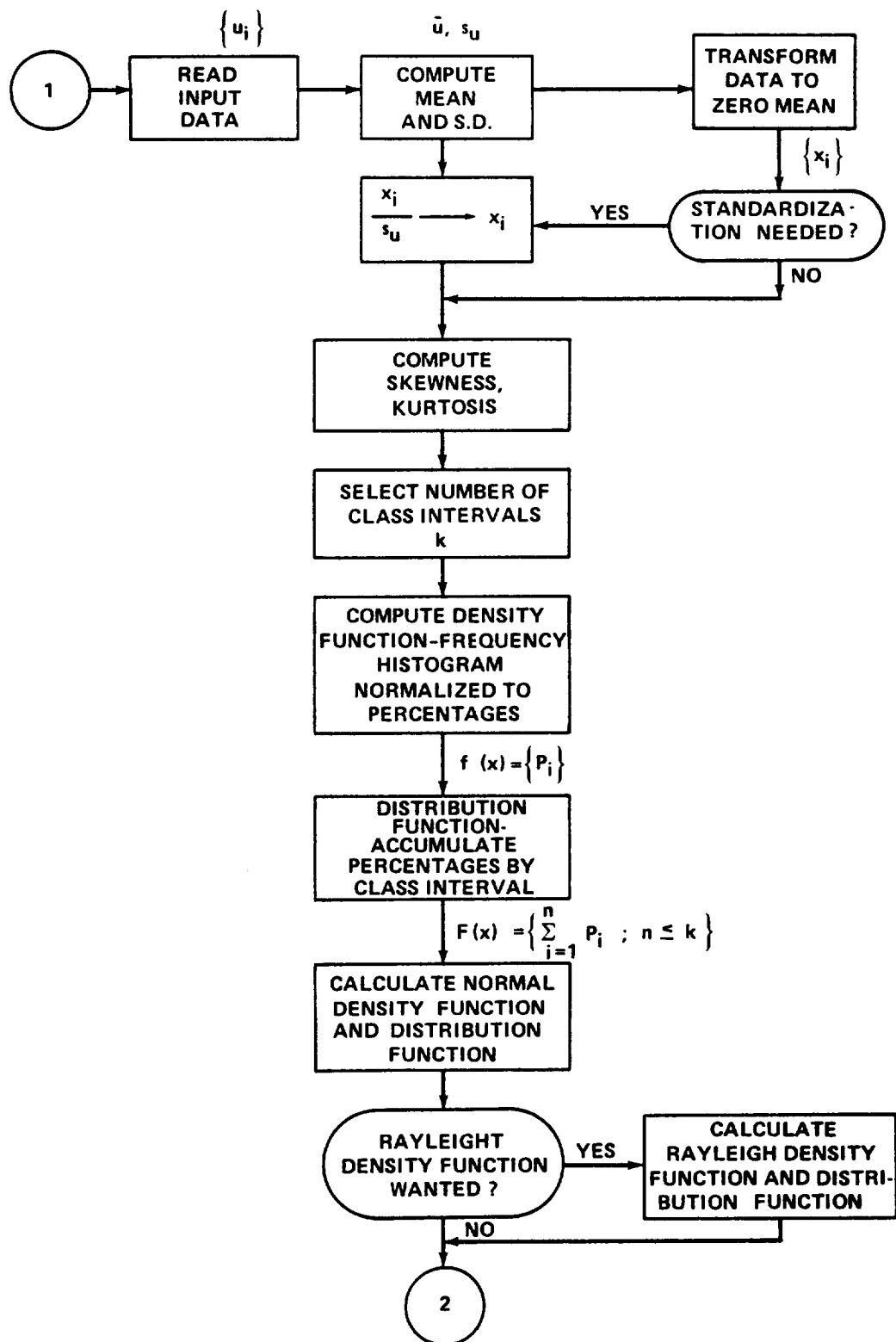
Table 13 gives some computing time estimates in terms of the number of operations required. The load-store-indexing operations are grouped together as are add and subtract. About a 30 percent factor to account for programming overhead should be added into final estimates. This is to allow for the necessary branching, control, etc., all of which is not accounted for. Estimates for the construction of the probability densities and distributions are not included because of their high dependence on the method of coding. Input/output operations and setup time are not included and, of course, these might be the preponderant factors when relatively small amounts of data are involved. An example based on fixed-point IBM-7090 operation times as indicated is included in the figure. This is given with and without the Fourier series because of its effect in the overall times.

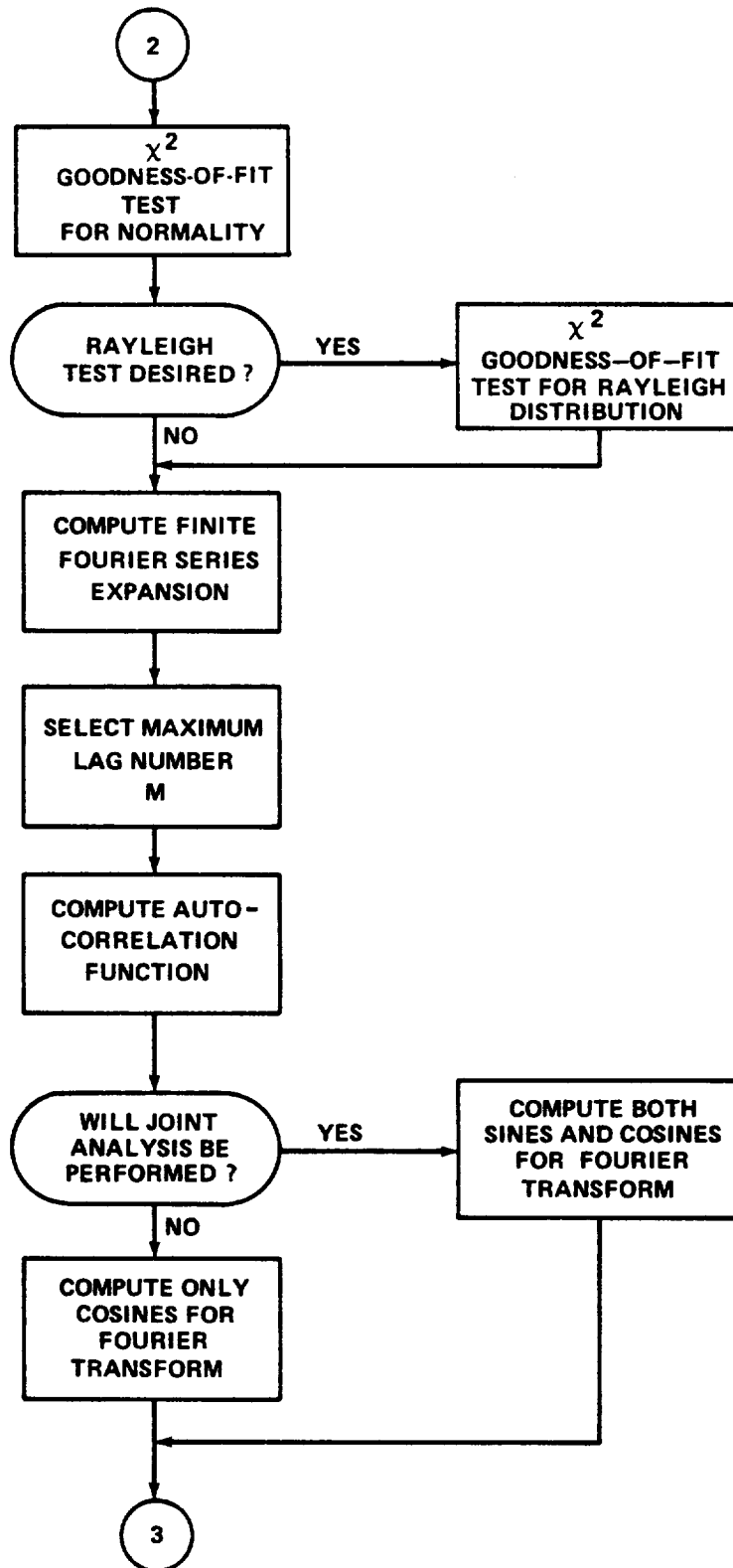
14. COMPUTATIONAL DETAILS

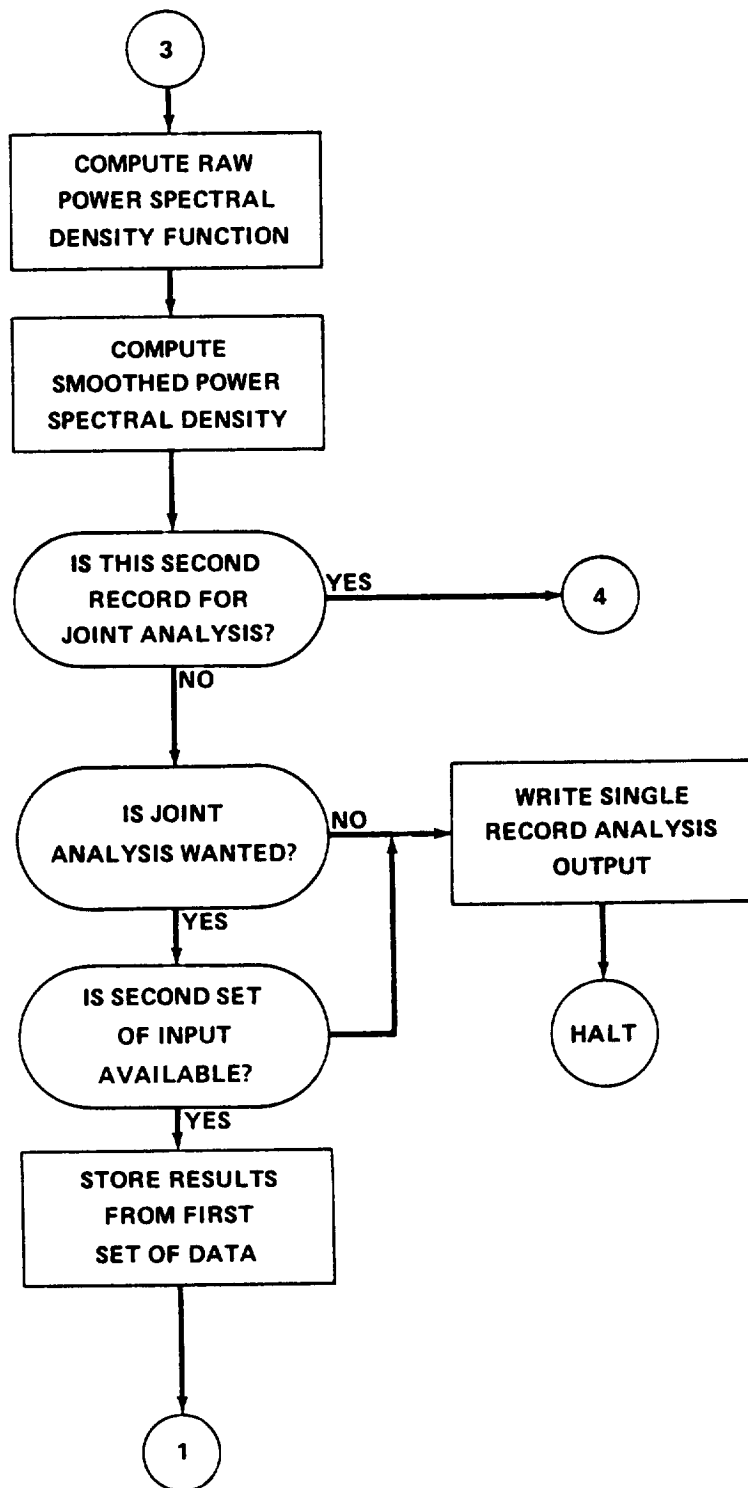
Certain aspects of the programming involved for the vibration data analysis are discussed in this section. Most items are concerned with minimization of computation time. This might not be particularly significant when relatively small amounts of data are involved since such things as input/output time might overshadow the actual computation time. However, when large amounts of input data exist, the computational time becomes quite significant and proper attention to certain computational techniques can result in considerably reduced program execution time with the resulting economy of operation.

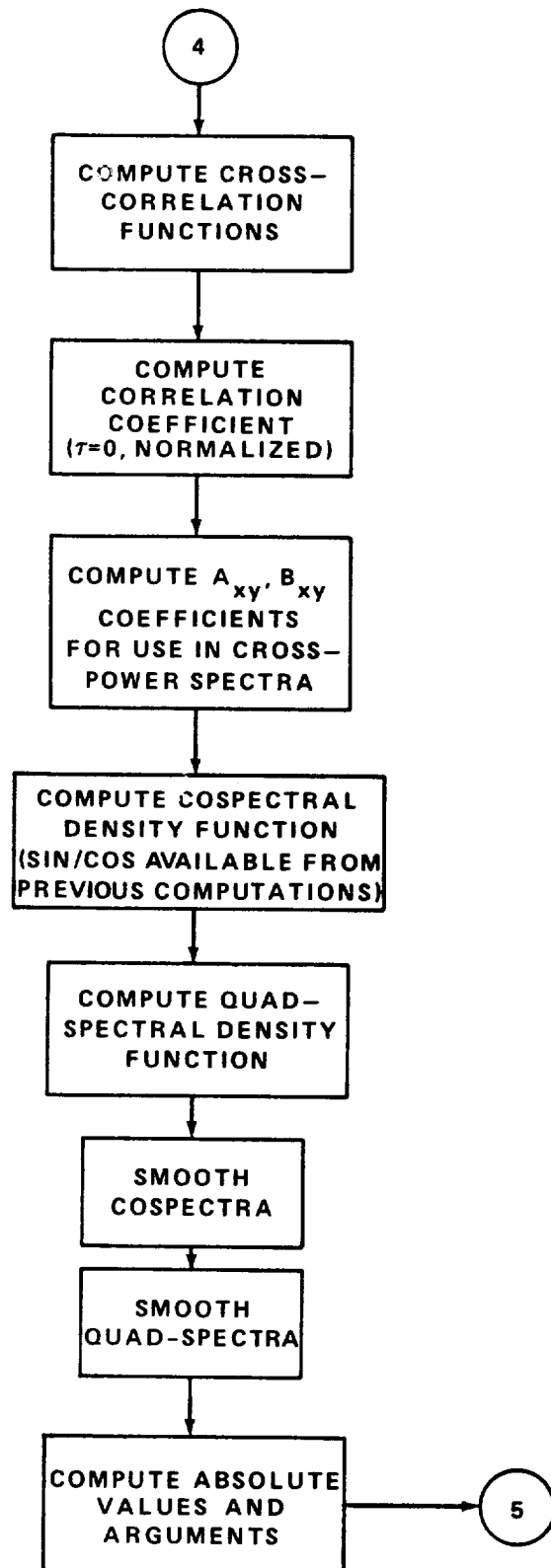
a. Fourier Coefficients and Sine Cosine Evaluation

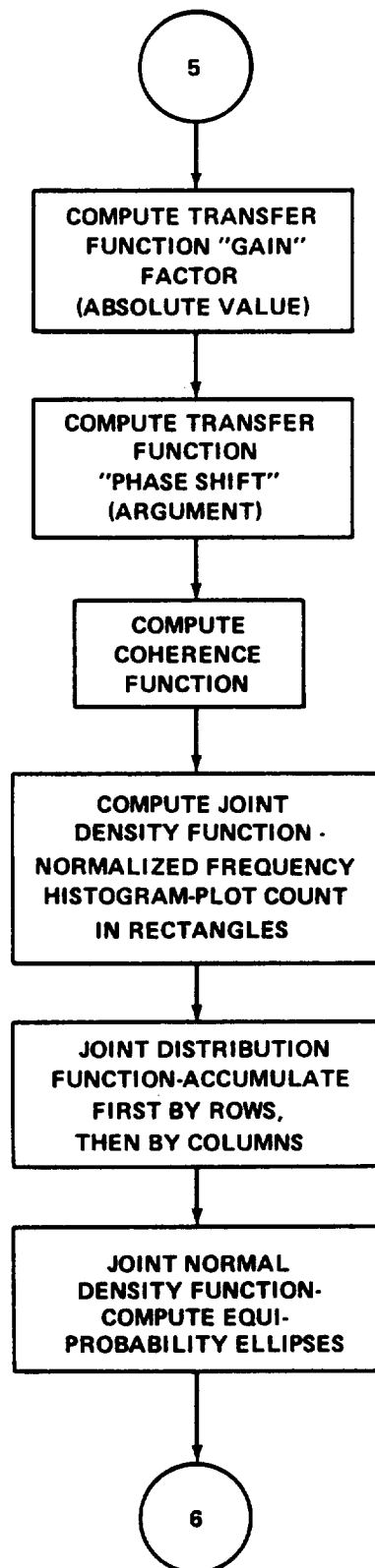
An efficient recursive procedure for generating the coefficients of the finite Fourier series is described in Chapter 24 of Reference 31. A portion











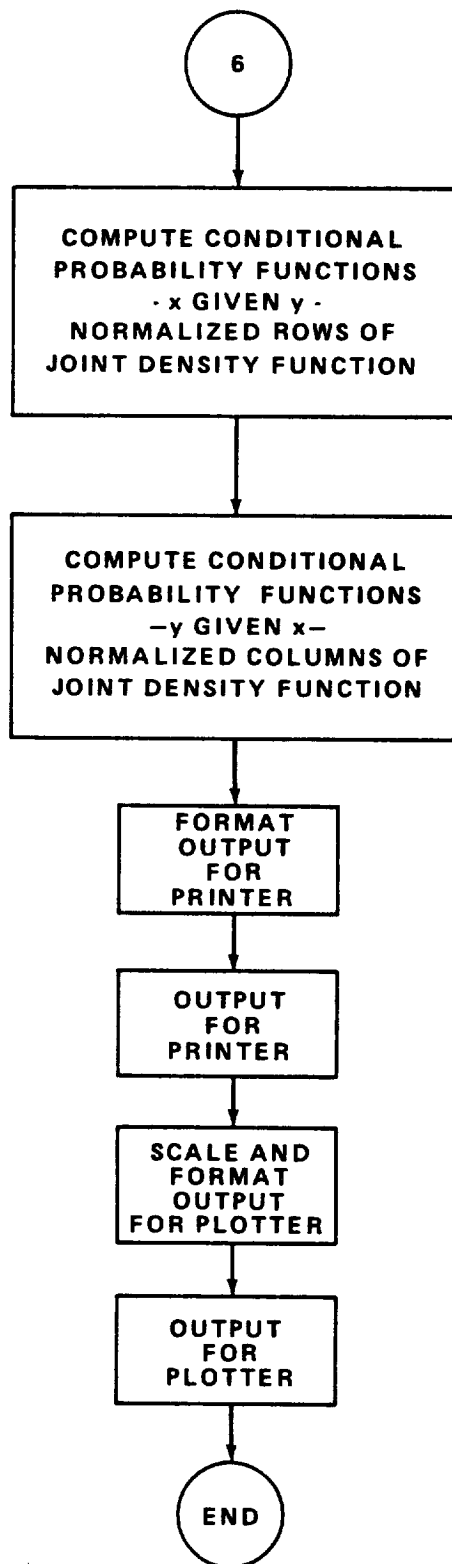


TABLE 13. TIME ESTIMATES FOR DIGITAL VIBRATION PROGRAM

Operation	Load, Store, Index 4.36 μ s	Add, Subtract 4.36 μ s	Multiply 24.85 μ s	Divide 30.52 μ s	e^x 309 μ s	\sin/\cos 257 μ s	\tan^{-1} 360 μ s	$\sqrt{\quad}$ 193 μ s	Sample Totals in ms
Mean		N		1					4 391
Transfer to Zero Mean	2 N	N							13 080
Standard Deviation	4 N	N	N	1				1	243 043
Skewness	4N	N	N	1					242 850
Kurtosis	4N	N	N	1					242 850
Probability Density									-----
Probability Distribution									-----
Normal Density Function	4k	k	k	k	k				15 447
Normal Distribution									-----
χ^2	4k	k	k + 1	k					3 460
Rayleigh Distribution	6k		2k	2k	k				17 388
Fourier Series ^a	12+29(N+1)+14(N+1)2N		1+14(N+1) +8(N+1)2N			2			221 927 623
Autocorrelation Function	$(m+1)(N - \frac{m}{2})4$		$(m+1)(N - \frac{m}{2})$	m					21 947 600
Sine/Cosines	2m	m	m			2			38 444
Spectral Density Function	3m(m+1)	m(m+1)	m						723 506
Smoothing	8(m-1)	2(m-1)							8 684
Cross- Correlation Functions	Twice Autocorrelation								42 996 046
Cross-power Spectra	4(m-1)(m+1)	(m+1)(2m-1)	(m-1)(m+1)						2 066 398
Smoothing	16(m-1)	4(m-1)							20 849
Transfer Function	8(m+1)	m+1	2(m+1)	2(m+1)			m+1	m+1	144 795
Coherence Function	6(m+1)		m+1	m+1					19 884
Joint Probability									-----

N = total number of observations

m = maximum lag number

k = number of class intervals

Sample Total

290 678 786 ms

= 4.845 min.

Sample Total without
Fourier series

68 751 163 ms

= 1.146 min.

For sample time estimates N = 1000

m = 200

k = 40

a. Estimates taken from Reference 31.

of this procedure may also be easily adapted for calculation of the coefficients necessary in the Fourier transform to obtain the cross-power spectra from the cross-correlation function. The procedure is now described with some minor modifications from the way it appears in the above mentioned reference.

First consider for each $n = 1, \dots, (N/2) - 1$, the numbers $U_{kn} = U_{k,n}$ defined recursively by

$$U_{N+2,n} = U_{N+1,n} = 0$$

$$U_{kn} = x_k + (2 \cos \frac{2\pi n}{N}) U_{k+1,n} - U_{k+2,n} . \quad (371)$$

It can be shown that the Fourier coefficients are then given by

$$A_n = \frac{2}{N} (U_{1n} \cos \frac{2\pi n}{N} - U_{2n})$$

$$B_n = \frac{2}{N} (U_{1n} \sin \frac{2\pi n}{N}) . \quad (372)$$

The term $A_0 = 0$, of course, and $A_{N/2}$ is still defined as before by

$$A_{N/2} = \frac{1}{N} \sum_{k=1}^N x_k \cos k\pi . \quad (373)$$

An essential part of the procedure makes necessary the computation of only $\cos (2\pi/N)$ and $\sin (2\pi/N)$. Subsequent values, $\cos (2\pi n/N)$ and $\sin (2\pi n/N)$, may be generated recursively from the formulas,

$$\cos (n+1) \frac{2\pi}{N} = \cos \frac{2\pi}{N} \cos n \frac{2\pi}{N} - \sin \frac{2\pi}{N} \sin n \frac{2\pi}{N}$$

$$\sin (n+1) \frac{2\pi}{N} = \sin \frac{2\pi}{N} \cos n \frac{2\pi}{N} + \cos \frac{2\pi}{N} \sin n \frac{2\pi}{N}$$

$$n = 1, 2, \dots, N/2 \quad . \quad (374)$$

The angle range is from 0 to π , but the range 0 to $\pi/4$ suffices to define all necessary function values. Therefore, for $n > N/8$, subsequent function values may be obtained from such relations as

$$\sin \left(\frac{\pi}{2} - \Theta \right) = \cos \Theta$$

$$\cos \left(\frac{\pi}{2} - \Theta \right) = \sin \Theta$$

$$\sin (\pi - \Theta) = \sin \Theta$$

$$\cos (\pi - \Theta) = -\cos \Theta \quad .$$

This further reduces the computing requirements from four multiplies and two adds to either an interchange or changing sign or both of previously generated values. The associated coding would become more involved however.

The computing procedure is finally very simply described.

- (1) Set $n = 1$, compute $\sin \frac{2\pi}{N}$, $\cos \frac{2\pi}{N}$.
- (2) Compute U_{1n} and U_{2n} recursively as given by equation (371).
- (3) Compute A_n and B_n from equations (372).
- (4) Compute $\sin (n+1) \frac{2\pi}{N}$, $\cos (n+1) \frac{2\pi}{N}$ by equations (374).
- (5) Test n to see if finished, if not increment n by one and return to (2).
- (6) Evaluate $A_{N/2}$ directly from its defining equation (373).

The computations may be further speeded by performing the summations of the values associated with the like sines or cosines in advance; that is, consider the expression

$$\begin{aligned}\alpha &= x_1 \cos \frac{2\pi}{N} + x_{(N-2)/2} \cos \frac{2\pi(N-2)/2}{N} \\ &= (x_1 - x_{(N-2)/2}) \cos \frac{2\pi}{N}\end{aligned}$$

since

$$\cos \frac{2\pi(N-2)/2}{N} = \cos \frac{N\pi-2\pi}{N} = \cos \left(\pi - \frac{2\pi}{N} \right) = -\cos \frac{2\pi}{N}.$$

The second version of the equation is evaluated faster since one multiply is eliminated. Similar factoring may be performed for other parts of the sequence. See Reference 32 for complete details. The program required to implement this, of course, becomes fairly complicated.

The method of sine-cosine evaluation may be employed to advantage in the cross-power spectra calculations. However, the remainder of the procedure leads to less efficient computational methods because different coefficients, A_{xy} and B_{xy} , arise in evaluating the cross-power spectra equations.

b. Correlation Function Computation

Depending upon the accuracy of the input data, it may be worthwhile to take advantage of the variable length multiply feature found on some digital computers. A digital computer usually performs a multiply essentially by shifting and adding. The variable length feature merely stops this process prior to the time that a number of shifts equal to the word length of the machine have been performed. For the IBM-7090, the maximum multiply time is $30.52 \mu s = 14$ machine cycles. The average time is given in the machine reference manual as 11.6 cycles or $25.29 \mu s$. This is because actual execution time is a function of sequences of zeros that occur in one of the factors.

To illustrate the use of the variable multiply, assume it is known that the input data consist of a maximum of 15 binary digits (bits). A count $C = 15$ is therefore used in the multiply instruction. The maximum multiply time would be $(C/3) + 3 = 8$ cycles. If it is assumed that a proportional amount of the difference between the maximum and average times is saved on the average, the average time would be

$$8 - \frac{15}{35} (2.4) = 6.97 \text{ cycles} = 15.19 \mu\text{s} .$$

Depending on the results of further programming analysis, a shift would probably be necessary to properly scale the data for subsequent summations. A shift of less than 16 places requires 2 cycles = $4.36 \mu\text{s}$, which would result in an effective multiply time of $19.55 \mu\text{s}$. This number is still significantly less than the full multiply time when a tremendous number of multiplies are necessary. This situation can, of course, occur in calculation a correlation function based large amounts of data.

Further methods for auto and cross-correlation function evaluation are described in Reference 32. These methods are based on the assumption that data accuracy is relatively small (that is, say 10 bits as arises from typical analog to digital conversion), and the amount of data is quite large. Then, by initial scanning of the data, an optimum computing method may be determined which amounts to factoring out common values in the cross products to save multiplies. This programming becomes quite involved as a program-writing program is necessary.

c. Power Spectral Density Computations

A small amount of computing time may be saved in the power spectral density smoothing. One notes that the smoothing formulas require $0.5 G_i$, and $0.25 G_i$, where the G_i are the raw estimates. Therefore, one should omit the factor of two which occurs in the formula for G_i , thereby computing $G_i/2$ directly for later smoothing. This, of course, only saves shifting instructions on a binary digital computer since shifting right or left is equivalent to multiplying or dividing by two, respectively.

d. Probability Density Function Construction

The construction of the single variable density function requires that the total interval of values on which the function is observed be divided into k class intervals. After the number k is selected, one must establish the end points of each of the intervals. Next, a count of the number of observations lying in each of these intervals must be determined.

There are, of course, many ways of establishing the end points of the k class intervals. One method would be as follows:

1. Determine the sample range $R = u_{\max} - u_{\min}$.
2. Calculate $\Delta u = R/k$.
3. Let the intervals be $(-\infty, u_{\min}]$

$$\begin{aligned} & (u_{\min}, u_{\min} + \Delta u] \\ & (u_{\min} + \Delta u, u_{\min} + 2\Delta u] \\ & (u_{\max} - \Delta u,] \end{aligned}$$

where the notation $(x, y]$ indicates the lower limit strictly greater than x , but the upper limit less than or equal to y .

A second method is as follows:

1. Compute \bar{u} and s_u
2. Compute $\frac{6s_u}{k} = \Delta u$.

That is, consider a six-standard deviation range of values.

$$\begin{aligned}
 3. \quad \text{Let the intervals be } & (-\infty, \bar{u} - 3s_u + \frac{\Delta u}{2}] \\
 & (\bar{u} - 3s_u + \frac{\Delta u}{2}, \bar{u} - 3s_u + \frac{3\Delta u}{2}] \\
 & \vdots \\
 & (\bar{u} + 3s_u - \frac{\Delta u}{2}, \infty]
 \end{aligned}$$

In cases where the data are transformed to have a zero mean (that is, $x_i = u_i - \bar{u}$, $\Delta x = \Delta u$, $s_x = s_u$), the intervals simplify to:

$$\begin{aligned}
 & (-\infty, 3s_x + \frac{\Delta x}{2}] \\
 & (3s_x + \frac{\Delta x}{2}, -3s_x + \frac{3\Delta x}{2}] \\
 & \vdots \\
 & (3s_x - \frac{\Delta x}{2}, \infty]
 \end{aligned}$$

The factor $\Delta x/2$ is included to keep the intervals centered at the $\pm 3s_x$ points. The range $6s_x$ should not be used for sample sizes under about 1500. The range should be decreased so that, assuming a normal distribution,

$$\text{Prob } x > \text{Upper limit} \quad N > 2;$$

that is, there should be an expected frequency of at least two in the tail intervals. This requirement is mainly for the χ^2 goodness-of-fit test.

The actual counting of the number of observations per interval could be done most easily if the data is sorted beforehand. Then the procedure becomes a matter of comparing the sequence of observed values against the upper limit of an interval until a value exceeds the interval upper limit. Counts could be established, for example, by storing index register contents when the comparison fails, and then later computing differences. However, whether or not a complete initial sort is worthwhile requires more analysis.

The two-dimensional density function is obtained in essentially the same way except that two limits must be checked. This, of course, greatly increases the computing time requirements.

SECTION XIII. VIBRATION RESPONSE ANALYSIS

In this section, the basic analytic methods for determining the dynamic response of structure are presented. These methods are the basic tools used by vibration and acoustic engineers for structural analysis. Structural analysis methodology is a vast subject encompassing a broad spectrum of mathematical knowledge and its application to structural theory. To cover this much material in one section of a single book would be impossible without a systematic policy of condensation. In this section condensation of material is considerable in areas where prior knowledge is assumed or when references are readily available. Derivations are included when essential to understanding the material.

More detailed descriptions will be presented on less familiar topics such as superposition leading to the treatment of random inputs and the development of the Duhamel integral (sometimes called the superposition integral or the convolution integral), equivalent systems, transient-steady state relationship, orthogonality, matrix theory application, vector and tensor applications and an introduction to non-linear systems. Basic mathematical considerations are included at the end of this section.

In most cases the presentation of material is addressed to the theoretical analysis of structure for application to dynamic analysis. Applications involving judgement considerations are included in Section XIV. The output of a theoretical analysis is usually in some form of response or transfer function. Application of these functions is used in many vibration and acoustic problems such as environment derivation, loads computation, natural frequency identification, flight data validation, and test data interpretation. The latter application is further divided into modal frequency tests, impedance tests (a special application of equivalent systems) and qualification tests. Furthermore, the contents of this section are limited to classical mechanics except for some areas such as response of a panel to acoustic inputs where the theoretical result is modified by empirical test data.

A. Review of Fundamentals

A physical system experiences vibration when subjected to time-varying external forces. Suppose a vibrating system has N_p particles where a particle is defined as mass concentrated at a point and the rotational properties of each point about its center are neglected. At any specific time, three coordinates are required to define the position of each particle. If the system

of particles is in a free-free condition, the system is said to have $3N_p$ degrees of freedom where N_p is equal to the number of particles. If any of the particles are restrained in any direction due to external constraints, then the degrees of freedom are less than $3N_p$ by the number of constraints, N_k . The degrees of freedom are defined then as the number of independent position quantities required to define the location of any particle in the system at some time. Therefore,

$$\text{Degrees of Freedom} = 3N_p - N_k \quad .$$

1. CONSERVATIVE FORCE FIELDS

Webster [33] states: "If the forces depend on the velocities or on anything besides the coordinates, the system is not conservative." Stated in another way, the potential energy function is a function of the coordinates only; that is,

$$V = V(x, y, z)$$

which leads to Webster's defining equation for a conservative force.

$$dV = \frac{\partial V}{\partial x} dx + \frac{\partial V}{\partial y} dy + \frac{\partial V}{\partial z} dz \quad . \quad (375)$$

There are four methods for testing a force function to see if it is conservative. If the force function possesses any one of the following, it is conservative:

- a. It is the gradient of a scalar function.
- b. The line integral of the tangential component around any regular closed curve is zero.
- c. The line integral of the tangential component along any curve wholly in the defined domain of the force, extending from a point P to a point Q is independent of the path.
- d. The curl of the vector field F is 0; that is,

$$\vec{\nabla} \times \vec{F} = 0 \quad . \quad (376)$$

The more rigorous definition given above is required in the analysis of more complex systems such as found in fluid dynamics. In practical engineering analysis of structure, a system without damping is conservative.

2. NATURAL FREQUENCY AND RESONANCE

The natural frequency of vibration of a system is the frequency of a free vibration. A system experiences free vibration if the vibration continues after the forcing function is removed.

Resonance occurs when a system experiences an external driving force with a frequency that coincides with one of the natural frequencies of the system or when the imaginary parts of the impedance vectors cancel.

3. HARMONICS

Assume a system has a number of possible vibration frequencies, $f_1, f_2, f_3, \dots, f_n$ such that:

$$f_2 = 2f_1,$$

$$f_3 = 3f_1,$$

.

.

.

$$f_n = nf_1$$

.

Then the fundamental frequency f_1 is called the first harmonic, f_2 is the first overtone or the second harmonic, f_3 is the second overtone or the third harmonic, and the n^{th} frequency is the n^{th} harmonic or the $(n-1)^{\text{th}}$ overtone.

4. SYSTEM LINEARITY

A vibratory system is said to be linear and time invariant if the equations of motion describing the system take the form of linear differential equations with constant coefficients. A system with a single degree of freedom can be described in terms of a single second-order differential equation. A two-degree-of-freedom system can be described by a pair of coupled second-order differential equations and a system of n degrees of freedom requires n equations.

A linear differential equation by definition is one that contains the dependent variable and its derivatives to the first degree only. Using D to represent the differential operator, d/dx , the general form of a linear differential equation can be written as

$$(a_0 D^n + a_1 D^{n-1} + \dots + a_{n-1} D + a_n) y = F \quad . \quad (377)$$

If $F = 0$ then the equation is said to be homogeneous since each term is to the first degree in y or one of its derivatives. For a vibratory system to be linear, the coefficients must be constants.

All discussion in this section is addressed to linear systems except for Paragraph G which presents an introduction to non-linear dynamics.

5. RANDOM REPRESENTATIONS

For a linear system superposition is rigorously applicable and becomes a powerful engineering tool. Churchill [34] gives the following theorem on superposition. "Any linear combination of two solutions of a linear homogeneous differential equation is again a solution." A random vibration may be considered to be a composite of an infinite number of sinusoidal vibrations. Since a Fourier series contains an infinite number of sinusoids, each of which is a singular solution to a different equation, a Fourier series can be used to solve a random vibration problem using superposition. Eliminating the lower frequency terms in a Fourier series and considering superposition of the remaining sinusoids, the solution for a random input follows. It will be shown that the response of the system can be defined for sinusoidal input and applied to the solution for a random input.

Exactly the same result is obtained when a truncated portion of a random signal is considered. In this case the power spectral density is derived for an infinite time interval through the Fourier transform and the solutions are identical with the periodic series discussed above. A little subjective reasoning verifies this conclusion. A periodic signal with the lower frequency terms neglected and a truncated random signal of infinite length are one and the same for representing random inputs in dynamic analyses. In the paragraphs that follow, the root mean square/power spectral density relation is developed for the periodic and non-periodic case.

The periodic and non-periodic random solutions are also related to the transient solution, because if the response of a linear system is known for one input it is known for every input. Proof is shown through the transfer function defined as the ratio of the Laplace transformed output to the Laplace transformed input. This is discussed in Paragraphs C.3 and H.2 of this section.

a. Periodic Functions

A random environment used for an analysis can be represented by a periodic function if certain restrictions are observed. Since each term of a Fourier series is periodic, the sum of these terms is also periodic. For vibration analysis and data reduction the periodic character of the series can be neglected provided the lower frequency terms in the series are edited out of the analysis. In general, the error is reduced to negligible magnitude if the first 20 frequencies are ignored. If the period under consideration is T seconds, the first frequency is $1/T$ Hz and the 20th frequency is $20/T$ Hz. Suppose the lowest frequency of interest is 5 Hz; thus,

$$\frac{20}{T} = 5 \quad T = 4 \text{ seconds}$$

If the lowest frequency of interest is 20 Hz, T can be 1 second.

In Reference 35 the development of this approach is covered in some detail. When the Fourier series is equated to the G_{rms} by squaring the series, the following result is obtained

$$G_{rms} = \left[\sum_{0}^n \frac{a_n^2 T}{2} \Delta f \right]^{\frac{1}{2}} \quad (378)$$

G_{rms} = acceleration root mean square

Δf = frequency increment

a_n = coefficient of each term in the series

T = time interval

If $\Delta f \rightarrow df$ the summation becomes an integral,

$$G_{\text{rms}} = \left[\int_{f_1}^{f_2} \text{PSD } df \right]^{\frac{1}{2}} \quad (379)$$

PSD = power spectral density, g_2/Hz . Thus, the PSD is related to the G_{rms} for any frequency increment. The superposition principle permits solutions to random input problems by considering the combined effect of sinusoids. An analog spectrum analyzer performs an analysis in electrical units using the above equation. Conversion to g's follows from the calibration.

b. Non-Periodic Functions

Exactly the same conclusion is reached by considering a truncated random signal and using an autocorrelation function.

Suppose a single sample of random data is of duration T . The temporal average is obtained by averaging with respect to time along the sample. The temporal mean square is given by

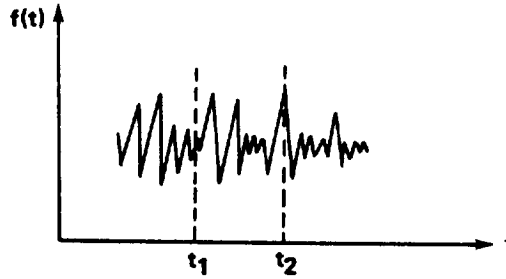
$$\langle f^2(t) \rangle = \frac{1}{T} \int_{-\frac{T}{2}}^{\frac{T}{2}} [f^2(t)] dt \quad (380)$$

If the $f(t)$ is defined for all time, then the above equation is evaluated by taking the limit as $T \rightarrow \infty$. For such a function, a temporal autocorrelation function is defined by

$$\begin{aligned} \phi(\tau) &= \langle f(t) f(t + \tau) \rangle \\ &= \lim_{T \rightarrow \infty} \frac{1}{T} \int_{-\frac{T}{2}}^{\frac{T}{2}} f(t) f(t + \tau) dt \quad (381) \end{aligned}$$

When $f(t)$ is only defined for a finite interval, a similar expression exists. The integral on the right side may be used without the limit as $T \rightarrow \infty$ provided $f(t)$ is defined from $t_1 = T/2$ to $t_2 = T/2 + \tau$. Such a finite average would most often be used for incremental values of τ which are small compared to T . The function $\phi(0)$ is just the temporal mean square.

Consider a stationary random process as given below on the interval from t_1 to t_2 .



If τ_{\max} is defined to be $t_2 - t_1$, an autocorrelation value

$$E[x(t_1) x(t_2)] = R(\tau) \quad (382)$$

results in a function of τ when all values of τ are considered. A frequency distribution of $R(\tau)$ can be stated by a standard transformation using the following relation:

$$R(\tau) = \int_{-\infty}^{\infty} S(\omega) e^{i\omega\tau} d\omega \quad (383)$$

The function $S(\omega)$ has the form of the Fourier transform of $R(\tau)$.

$$S(\omega) = \frac{1}{2\pi} \int_{-\infty}^{\infty} R(\tau) e^{-i\omega\tau} d\tau \quad (384)$$

$S(\omega)$ is a non-negative even function of ω (symmetric about the ordinate). Suppose that $t_2 \rightarrow t_1$ which means $\tau \rightarrow 0$. Then $R(\tau) = R(0)$.

$$R(\tau) = R(0) = 2 \int_0^{\infty} S(\omega) d\omega \quad . \quad (385)$$

$R(0)$ is the mean square of the process for it is the sum over all frequencies of $S(\omega) d\omega$. Therefore, $S(\omega)$ may be thought of as a mean square spectral density. Changing from a circular frequency to a linear frequency gives

$$\begin{aligned} R(0) &= E \{ [X(t)]^2 \} \\ &= \int_0^{\infty} W(f) df \end{aligned} \quad (386)$$

where $X(t)$ represents an acceleration process and $W(f)$ has units of g^2/Hz or power spectral density.

Looking at equation (381)

$$R(0) = \lim_{T \rightarrow \infty} \frac{1}{T} \int_{-\frac{T}{2}}^{\frac{T}{2}} f^2(t) dt \quad . \quad (387)$$

This last relationship shows that to obtain a true mean square spectral density, $f(t)$ is averaged over a long time; also $\Delta W \rightarrow 0$ as $T \rightarrow \infty$.

In problems of interest, the power spectral density is not integrated over all positive values of frequencies because usually a finite range of frequencies is all that is important. Therefore, the equation is normally used in the form given below:

$$\int_{f_1}^{f_2} W(f) df = \lim_{T \rightarrow \infty} \frac{1}{T} \int_{-\frac{T}{2}}^{\frac{T}{2}} f^2(t) dt \quad . \quad (388)$$

The term on the left is the square of the G_{rms} value if $W(f)$ is power spectral density. This last statement is presented because the above equation is a general relationship and $W(f)$ could be a function other than power spectral density. Rewriting the last equation in terms of G_{rms} yields

$$G_{\text{rms}} = \left[\int_{f_1}^{f_2} W(f) df \right]^{1/2} \quad (389)$$

This is the same result that was obtained in Equation (379). The digital analysis of random data follows the developments in the foregoing paragraphs.

B. Equation of Motion – Steady State

1. NEWTON'S LAW

Newton's second law of motion may be stated the following way: The time rate of change of momentum is proportional to the resultant force and is in the direction of that force. As a general rule for most vibration problems the mass is constant and thereby

$$\sum F_x = m \frac{d}{dt} (V) = m\ddot{x} \quad (390)$$

The quantity $m\ddot{x}$, a product of the mass and acceleration, is called the inertia force. Equation (390) can also be stated as the summation of forces in the x-direction minus the inertia force is zero. In this form, the equation represents d'Alembert's principle. The state of motion of mass at any instant may be considered as a state of equilibrium, thereby reducing the problem to its static equivalent.

This law of motion can be used to establish the equation of motion for any degree-of-freedom vibrating system. However, for simple illustration purposes the equation of motion for a one-degree-of-freedom system will be derived.

Consider the viscous damped spring-mass system excited by a harmonic force as shown in Figure 104. For an applied force and motion down-

ward, the forces acting on the mass in the free-body sketch are shown in Figure 104.

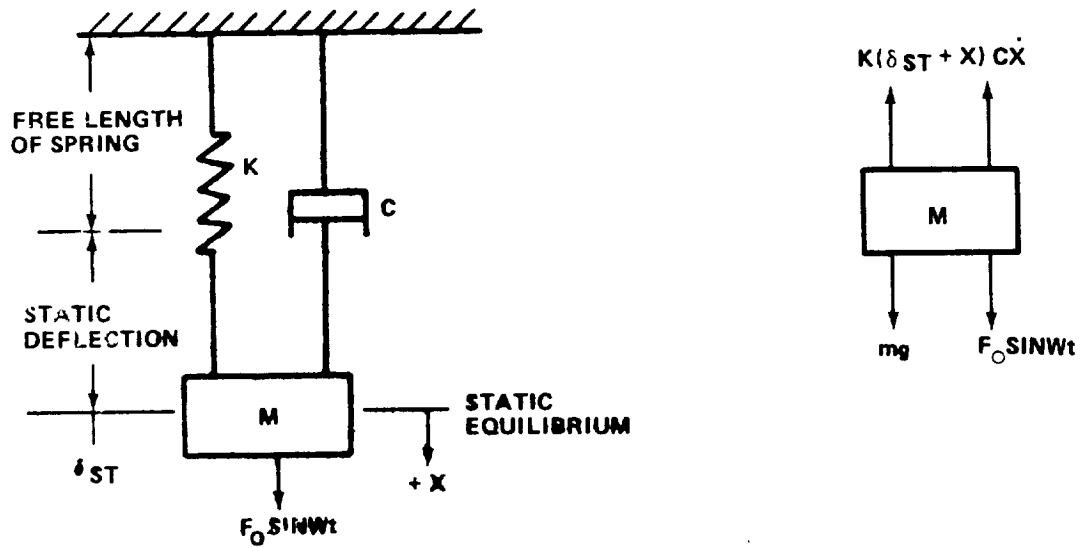


Figure 104. Generalized model: one-degree-of-freedom system.

Considering the motion in the x -direction, the equation of motion of this system is

$$\begin{aligned} m\ddot{x} &= \sum (\text{Forces in } x\text{-Direction}) \\ &= mg + F_0 \sin \omega t - k(\delta_{ST} + x) - c\dot{x} \end{aligned} \quad (391)$$

Before an excitation force is applied to the mass, the gravitational attraction mg is equal to the static spring force $k\delta_{ST}$; therefore

$$m\ddot{x} + c\dot{x} + kx = F_0 \sin \omega t \quad (392)$$

The general solution of the above second order linear differential equation is the sum of the complementary function $X_c(t)$ and the particular integral $X_p(t)$; that is,

$$X = X_c + X_p \quad (393)$$

A solution $X_c = A e^{DT}$ satisfies the corresponding homogeneous equation

$$m\ddot{x} + c\dot{x} - kx = 0 \quad . \quad (394)$$

Substituting $D = dx/dt$ in the differential equation results in a simple quadratic which will, in general, be satisfied by two values of D ,

$$D_{1,2} = \frac{1}{2m} \left(-c \pm \sqrt{c^2 - 4km} \right) \quad (395)$$

and the complementary equation consists of a linear combination of two solutions, namely,

$$X_c = a_1 e^{D_1 t} + a_2 e^{D_2 t} \quad (396)$$

where a_1 and a_2 are arbitrary constants depending on the initial conditions.

The complementary solution of a damped vibrating system describes free motion if the damping is low enough to make D_1 and D_2 complex numbers. Critical damping is the value of "c" which separates the vibration and non-vibrating system; that is, the radical of equation (395) will become zero. Thus, the critical damping is expressed as

$$C_c = 2\sqrt{km} = 2m\omega_n \quad . \quad (397)$$

Damping of a vibrating system is often specified in terms of the ratio of damping to the critical damping, expressed as c/c_c where

$$\frac{c}{c_c} = \frac{c}{2\sqrt{km}} \quad . \quad (398)$$

The ratio c/c_c is more commonly referred to as the damping factor and is given the symbol ζ .

The previous development describes a typical stable vibrating system which occurs when the damping factor is positive. If the damping factor is greater than one the values of D_1 and D_2 will be real, distinct and negative because $\zeta^2 - 1$ will be less than ζ . Thus, the complementary equation would be

$$X_c = a_1 e^{-D_1 t} + a_2 e^{-D_2 t} \quad (399)$$

No matter what the initial conditions are for this particular case there will be no oscillatory motion. The motion, called aperiodic, will diminish exponentially as time increases.

For the special case where $\zeta = 1$, both of the roots are negative and are equal to $-\omega_n$, yielding the complementary equation

$$X_c = (a_1 + a_2 t) e^{-\omega_n t} \quad (400)$$

which is again aperiodic and will diminish exponentially with time.

If the damping factor, ζ , is less than one, the roots D_1 and D_2 will be complex conjugates of the form and a vibration exists

$$D = -\zeta \omega_n \pm j \sqrt{1 - \zeta^2} \omega_n \quad (401)$$

where $j = \sqrt{-1}$. At this point it is convenient to define the term $\omega_n \sqrt{1 - \zeta^2}$. Since ζ is a ratio of damping coefficients, the term $\omega_n \sqrt{1 - \zeta^2}$ defines the frequency of oscillation, ω_d . This frequency is less than the undamped natural frequency of the system.

The complementary equation for a stable vibration system ($0 < \zeta < 1$) can be expressed in a simpler form by using the frequency of oscillation ω_d and Euler's formula

$$e \pm i \theta = \cos \theta \pm i \sin \theta \quad ; \quad (402)$$

that is,

$$X_c = e^{-\zeta \omega_n t} (A_1 \cos \omega_d t + A_2 \sin \omega_d t)$$

or

$$X_c = A e^{-\zeta \omega_n t} \sin(\omega_d t + \phi) \quad (403)$$

where A_1 , A_2 , ϕ and A are arbitrary constants determined from the initial conditions. These constants are related by $A = \sqrt{A_1^2 + A_2^2}$ and $\phi = \tan^{-1} A_1/A_2$. The complementary equation for ζ less than one describes harmonic motion and will diminish exponentially with time.

Since all the cases discussed have exponential decay, the motion described by the complementary equation is classified as transient motion except when $\zeta = 0$, then the amplitude will not diminish as time increases.

To determine the particular integral and complete the general solution, a method called "Method of Undetermined Coefficients for Finding Particular Integrals" can be used. The following rule is found in Reference 36. If $f(t)$ is a function for which repeated differentiation yields only a finite number of independent derivatives, then, in general, a particular integral X_p can be found by assuming X to be an arbitrary linear combination of $f(t)$ and all its independent derivatives, substituting this expression into the differential equation determining the arbitrary constants in X in such a way that the resulting equation is identically satisfied.

Using the above rule a particular solution in the form

$$X = A \cos \omega t + B \sin \omega t \quad (404)$$

is substituted in the differential equation (392) yields

$$\begin{aligned} X_p &= \frac{F_0}{\sqrt{(\omega c)^2 + (k - \omega^2 m)^2}} \sin(\omega t - \phi) \\ &= \frac{F_0/k}{\sqrt{(2 \zeta \omega/\omega_n)^2 + [1 - (\omega/\omega_n)^2]^2}} \sin(\omega t - \phi) \quad . \end{aligned} \quad (405)$$

The total solution is the sum of the complementary and particular solution. In time the complementary solution vanishes and only the particular solution remains for the steady state condition.

The ratio X/X_0 is defined as the magnification factor κ and is written

$$\kappa = \frac{X}{X_0} \frac{1}{\sqrt{(2\zeta r)^2 + (1 - r^2)^2}} \quad (406)$$

where

r = the frequency ratio ω/ω_n

$$X_0 = F_0/K \quad .$$

The phase angle equation is

$$\phi = \tan^{-1} \frac{2\zeta r}{1 - r^2} \quad . \quad (407)$$

From studying the particular integral, the following conclusions can be made:

- a. The frequency of the response is the same as the excitation frequency and the motion is harmonic. Therefore, this motion is called steady-state motion.
- b. The particular integral does not contain arbitrary constants. Thus, the steady-state response is independent of the initial conditions.
- c. As can be seen by the solution of the particular equation, the steady-state response amplitude is a function of the frequency and amplitude of the excitation. The ratio X/X_0 is the magnification factor κ .
- d. At resonance ($\omega/\omega_n = 1$) the damping factor ζ alone limits the amplitude of the system.
- e. The response $X \sin(\omega t - \phi)$ and the excitation $F_0 \sin \omega t$ do not reach maximum values simultaneously. At resonance the phase angle equals 90 degrees. The phase angle varies with excitation frequency because of the presence of the damping factor.

Figures 105 and 106 illustrate in a linear form, plots of the magnification factor κ and the phase angle ϕ as a function of the frequency ratio r for various amounts of damping.

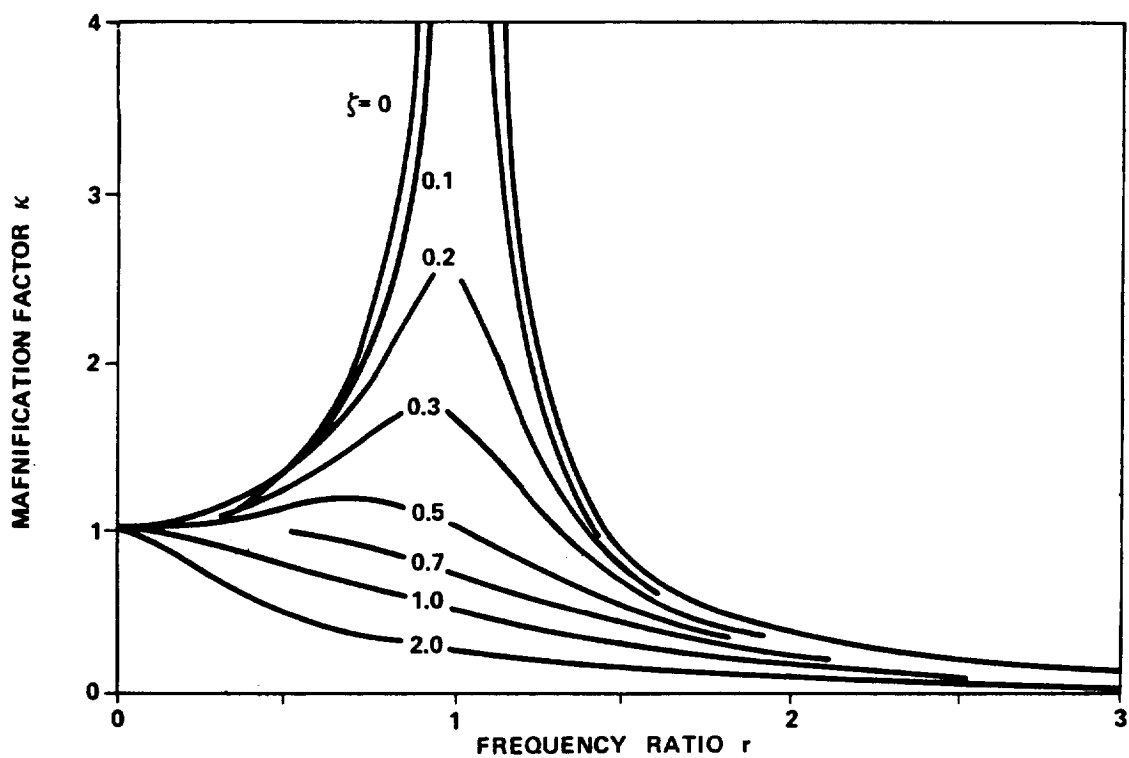


Figure 105. Magnification factor versus frequency ratio.

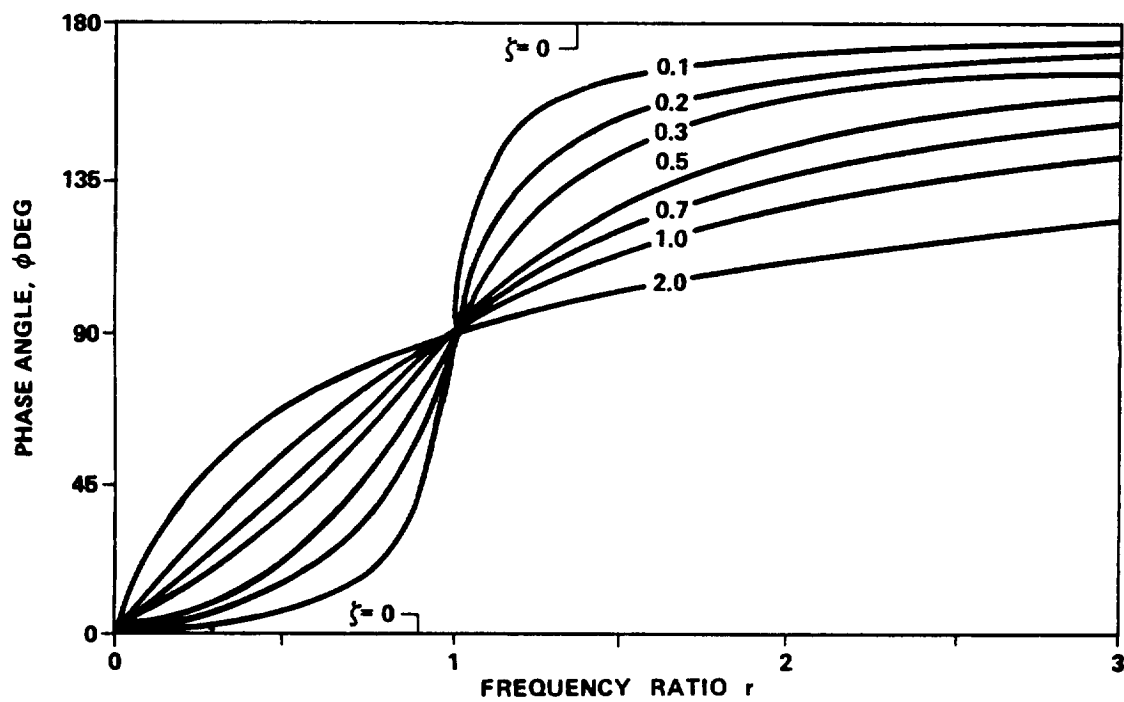


Figure 106. Phase angle versus frequency ratio.

Frequently, this same information is presented in log-log form and is commonly referred to as Bode plots. Figures 107 and 108 represent examples of typical Bode plots.

Another useful plot for the same presentation is known as the Nyquist plot, Figure 109. The length of the vector $|X/X_o e^{c\phi}|$ is the magnification factor while the phase angle ϕ is the vector inclination with the real axis.

2. ENERGY EQUATIONS

Previously, a second order, nonhomogeneous, ordinary differential equation of motion for a vibration system was derived and an algebraic solution was obtained. Another method to obtain the differential equation for the undamped free vibration is through the concept of total energy [37].

With an undamped free vibration system there is no forcing function and no energy dissipation due to viscous damping. Therefore, the systems energy content will remain constant.

Conservation of energy requires that the sum of the potential and kinetic energies be equal to a constant at all times for a conservative system. The potential energy results from the strain energy of the spring neglecting the mass of the spring and the kinetic energy is the energy resulting from the velocity of the mass.

Consider the undamped free vibration spring-mass system as shown in Figure 110. Assume that the mass m is displaced from the static equilibrium position in the positive x direction and then released. The system's potential energy changes due to the displacement. This change is equal to the change in strain energy in the spring minus the potential energy of the mass when there is a change in elevation. Therefore, the potential energy is defined by the term U and is expressed as

$$U = \int_0^X (\text{Total Spring Force}) dx - mgx \quad . \quad (408)$$

In Figure 110, giving spring force versus spring deformation, the potential energy is the cross-hatched area of the plot. The total spring force is the sum of the static deflection plus the force due to displacement. Thus,

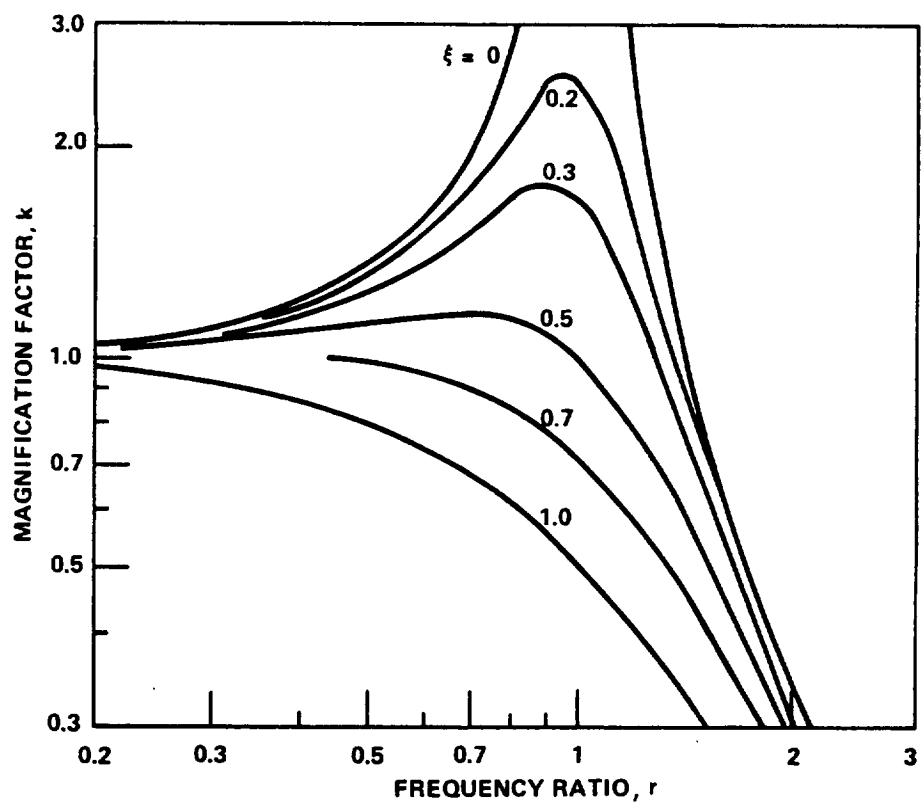


Figure 107. Bode plot (κ versus r).

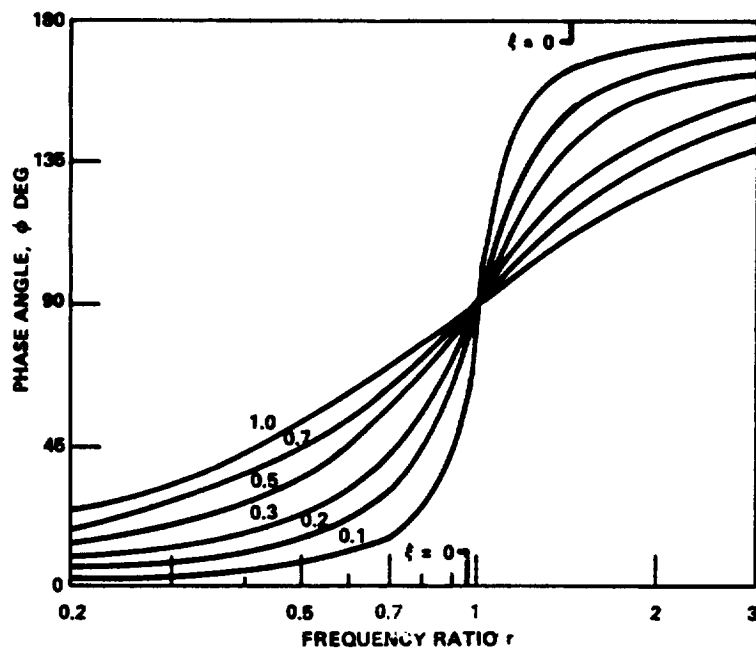


Figure 108. Bode plot (ϕ versus r).

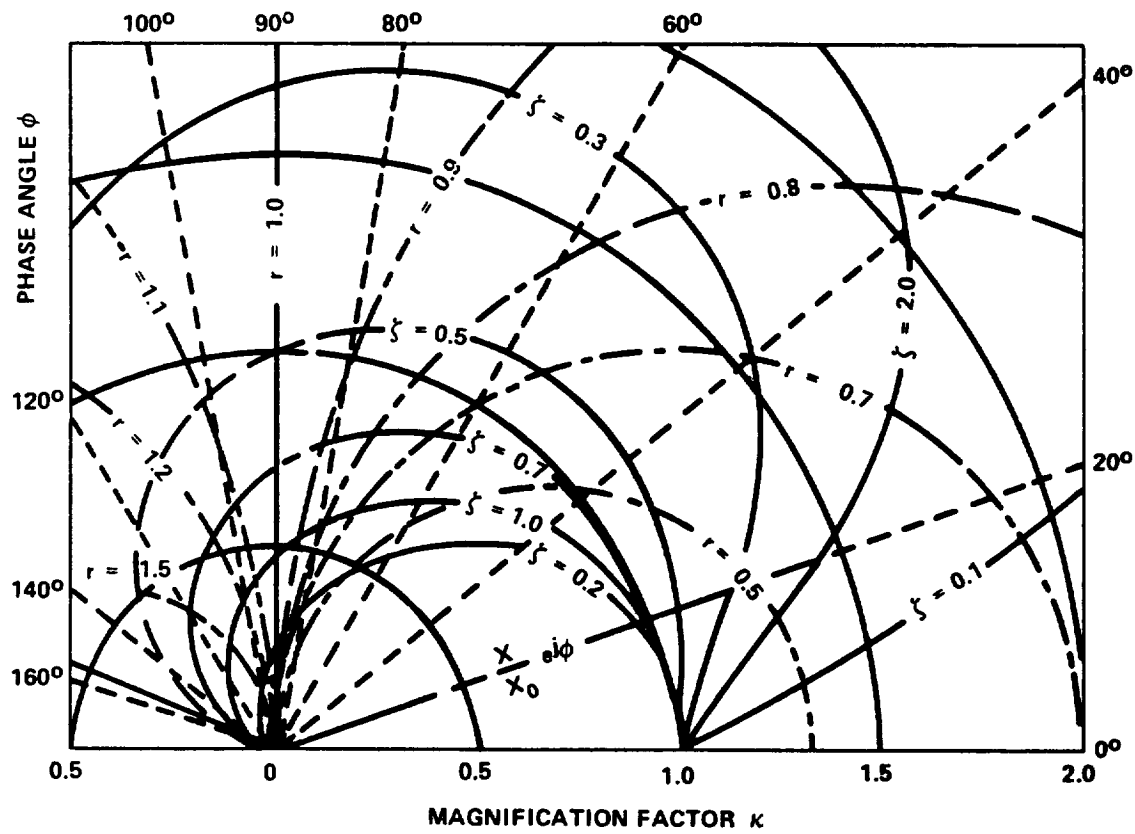


Figure 109. Nyquist plot.

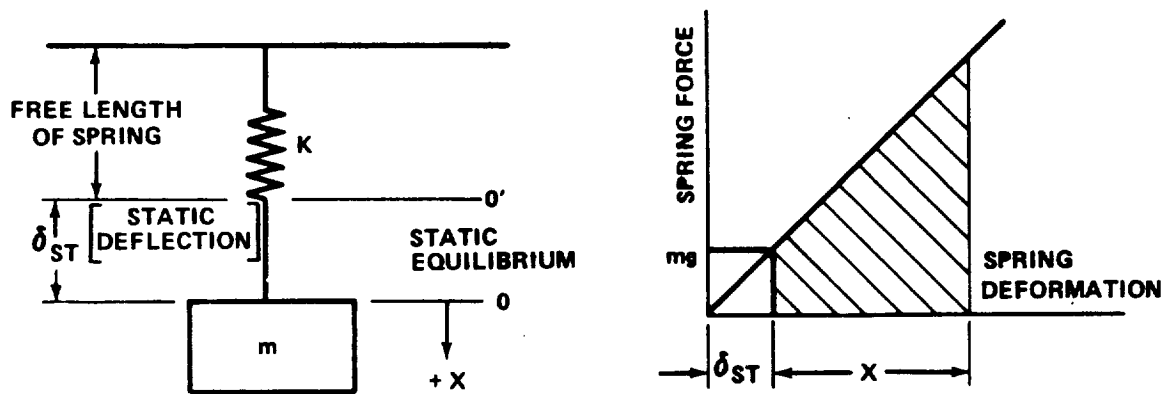


Figure 110. Potential energy in a spring.

by subtracting out the term mgx , the net potential energy in the spring is obtained. The evaluation of the integral is

$$\begin{aligned} U &= \int_0^x (mg + kx) dx - mgx \\ &= \frac{1}{2} kx^2 \end{aligned} \quad (409)$$

Assuming that the mass of the spring is negligible when compared with the block of mass m , the kinetic energy T is defined as

$$T = \frac{1}{2} m\dot{x}^2 \quad (410)$$

Recalling that the total energy of the system was constant, the time derivative of the total energy is zero.

$$T + U = \text{Constant}$$

$$\frac{d}{dt} [T + U] = \frac{d}{dt} \left[\frac{1}{2} m\dot{x}^2 + \frac{1}{2} kx^2 \right] = 0 \quad (411)$$

Since the velocity cannot be equal to zero for all time, the solution follows from the discussion in Paragraph 1. of this subsection.

3. LAGRANGE'S EQUATIONS

The equations of motion for a complex vibrating system can be derived by utilizing Newton's laws as developed in Paragraph 2. of this subsection. A more powerful tool for this type of analysis is the Lagrangian method.

The object of Lagrange's equations of motion is to express the equations in terms of generalized coordinates and generalized forces. The transformation of Cartesian coordinates to a set of generalized coordinates can be very involved. Also the forces used in Newton's laws are vector quantities and are difficult to handle in complex systems. Thus, the Lagrangian method permits the equations of motion to be derived using basic energy expressions. Energy is a scalar quantity and can be expressed in

any convenient set of coordinates. Lagrange's equations will be derived using the concepts of virtual displacements and d'Alembert's principle as developed in Reference 37.

It is necessary to set up a theory of generalized coordinates and assuming that there are as many generalized coordinates as Cartesian coordinates. Consider a dynamic system of p mass particles with n degrees of freedom. Each particle m_i will have the Cartesian coordinates x_i , y_i , and z_i ($i = 1, 2, \dots, p$) and can be described by a set of generalized coordinates (q_1, q_2, \dots, q_n) . The Cartesian coordinates can be expressed as functions of the generalized coordinates. This reflects the general case in which coordinate coupling exists, that is, the axes of the coordinate system are nonorthogonal. Therefore, the Cartesian coordinates are related to the generalized coordinates

$$\begin{aligned}x_i &= x_i(q_1, q_2, \dots, q_n) \\y_i &= y_i(q_1, q_2, \dots, q_n) \\z_i &= z_i(q_1, q_2, \dots, q_n)\end{aligned}\quad (413)$$

With a system of particles described by a set of generalized coordinates, q_1, q_2, \dots, q_n , the time derivative \dot{q}_k of any coordinate q_k will be called the generalized velocity associated with this coordinate. The generalized velocity of the Cartesian coordinate x_i is the corresponding component \dot{x}_i of the velocity of the i^{th} particle located by this coordinate. Extending the concept further the original velocity components \dot{x}_i , \dot{y}_i , and \dot{z}_i of equation (413) can be expressed in terms of the generalized components and velocities by differentiating equation (413).

$$\begin{aligned}\frac{\partial x_i}{\partial t} = \dot{x}_i &= \frac{\partial x_i}{\partial q_1} \frac{dq_1}{dt} + \frac{\partial x_i}{\partial q_2} \frac{dq_2}{dt} + \dots + \frac{\partial x_i}{\partial q_n} \frac{dq_n}{dt} \\ \frac{\partial y_i}{\partial t} = \dot{y}_i &= \frac{\partial y_i}{\partial q_1} \frac{dq_1}{dt} + \frac{\partial y_i}{\partial q_2} \frac{dq_2}{dt} + \dots + \frac{\partial y_i}{\partial q_n} \frac{dq_n}{dt}\end{aligned}$$

$$\frac{\partial z_i}{\partial t} = \dot{z}_i = \frac{\partial z_i}{\partial q_1} \frac{dq_1}{dt} + \frac{\partial z_i}{\partial q_2} \frac{dq_2}{dt} + \dots + \frac{\partial z_i}{\partial q_n} \frac{dq_n}{dt} .$$

These three equations can be simplified to the following expressions:

$$\dot{x}_i = \sum_{j=1}^n \frac{\partial x_i}{\partial q_j} \dot{q}_j \quad (414a)$$

$$\dot{y}_i = \sum_{j=1}^n \frac{\partial y_i}{\partial q_j} \dot{q}_j \quad (414b)$$

$$\dot{z}_i = \sum_{j=1}^n \frac{\partial z_i}{\partial q_j} \dot{q}_j . \quad (414c)$$

Consider the i^{th} particle m_i with its Cartesian coordinates x_i , y_i and z_i . If the components of the applied forces acting on the particle m_i are X_i , Y_i , and Z_i , then the work done by these forces to move the particle a distance of δx_i , δy_i and δz_i is equal to the sum of the products of the component forces and their δ -displacements. Therefore, from the principle of virtual work, the virtual work is

$$\delta W = \sum_{i=1}^p (X_i \delta x_i + Y_i \delta y_i + Z_i \delta z_i) = 0 . \quad (415)$$

From Reference 37, d'Alembert's principle may be stated as such: "Every state of motion may be considered at any instant as a state of equilibrium if the inertia forces are taken into consideration." Utilizing the concept of d'Alembert's principle, equation (415) can be written as

$$\delta W = \sum_{i=1}^p (X_i \delta x_i + Y_i \delta y_i + Z_i \delta z_i)$$

$$= \sum_{i=1}^p m_i (\ddot{x}_i \delta x_i + \ddot{y}_i \delta y_i + \ddot{z}_i \delta z_i)$$

or

$$\begin{aligned} \delta W &= \sum_{i=1}^p (X_i \delta x_i + Y_i \delta y_i + Z_i \delta z_i) \\ &= \sum_{i=1}^p m_i (\ddot{x}_i \delta x_i + \ddot{y}_i \delta y_i + \ddot{z}_i \delta z_i) = 0 \end{aligned} \quad (416)$$

It is necessary to analyze each of the terms in equation (416). The first is expressed in terms of Cartesian coordinates and is the work done by the components of the applied forces. To express this form in terms of generalized coordinates the infinitesimal variations, δx_i , δy_i , and δz_i must be evaluated.

This is accomplished by realizing that

$$\delta x_i = \sum_{j=1}^n \frac{\partial x_i}{\partial q_j} \delta q_j \quad (417a)$$

$$\delta y_i = \sum_{j=1}^n \frac{\partial y_i}{\partial q_j} \delta q_j \quad (417b)$$

$$\delta z_i = \sum_{j=1}^n \frac{\partial z_i}{\partial q_j} \delta q_j \quad (417c)$$

Substituting these equations into the first term of equation (416) yields

$$\begin{aligned} \delta W &= \sum_{i=1}^p \left[X_i \sum_{j=1}^n \frac{\partial x_i}{\partial q_j} \delta q_j + Y_i \sum_{j=1}^n \frac{\partial y_i}{\partial q_j} \delta q_j \right. \\ &\quad \left. + Z_i \sum_{j=1}^n \frac{\partial z_i}{\partial q_j} \delta q_j \right] \end{aligned}$$

or

$$\delta W = \sum_{j=1}^n Q_j \delta q_j \quad (418)$$

where Q_j is,

$$Q_j = \sum_{i=1}^p \left(X_i \frac{\partial x_i}{\partial q_j} + Y_i \frac{\partial y_i}{\partial q_j} + Z_i \frac{\partial z_i}{\partial q_j} \right) \quad (419)$$

The definition of Q_j is called the generalized force corresponding to the generalized coordinate q_j . In order to express the second term of equation (416) in generalized coordinates, it is necessary to first introduce the kinetic energy function T as

$$T = \frac{1}{2} \sum_{i=1}^p m_i (\dot{x}_i^2 + \dot{y}_i^2 + \dot{z}_i^2) \quad (420)$$

Differentiating this equation with respect to \dot{x}_i , \dot{y}_i , \dot{z}_i and then with respect to time and using these results in conjunction with equation (417), the second term of equation (416) can be written as

$$\delta W = \sum_{j=1}^n \sum_{i=1}^p \left[\frac{d}{dt} \left(\frac{\partial T}{\partial \dot{x}_i} \right) \frac{\partial x_i}{\partial q_j} + \frac{d}{dt} \left(\frac{\partial T}{\partial \dot{y}_i} \right) \frac{\partial y_i}{\partial q_j} + \frac{d}{dt} \left(\frac{\partial T}{\partial \dot{z}_i} \right) \frac{\partial z_i}{\partial q_j} \right] \delta q_j \quad (421)$$

Equation (421) can be simplified if the following relation is used for x_i and equivalent expressions for y_i and z_i :

$$\frac{d}{dt} \left(\frac{\partial T}{\partial \dot{x}_i} \right) \frac{\partial x_i}{\partial q_j} = \frac{d}{dt} \left(\frac{\partial T}{\partial \dot{x}_i} \right) \frac{\partial x_i}{\partial q_j} + \frac{\partial T}{\partial \dot{x}_i} \frac{\partial \dot{x}_i}{\partial q_j}$$

or

$$\frac{d}{dt} \left(\frac{\partial T}{\partial \dot{x}_i} \right) \frac{\partial x_i}{\partial q_j} = \frac{d}{dt} \left(\frac{\partial T}{\partial \dot{x}_i} \frac{\partial x_i}{\partial q_j} \right) - \frac{\partial T}{\partial \dot{x}_i} \frac{\partial \dot{x}_i}{\partial q_j} \quad (422)$$

Substitution of these expressions for x_i , y_i and z_i into equation (421) results in the following equation

$$\begin{aligned} \delta W = \sum_{j=1}^n \sum_{i=1}^p \left[\frac{d}{dt} \left(\frac{\partial T}{\partial \dot{x}_i} \frac{\partial x_i}{\partial q_j} + \frac{\partial T}{\partial \dot{y}_i} \frac{\partial y_i}{\partial q_j} + \frac{\partial T}{\partial \dot{z}_i} \frac{\partial z_i}{\partial q_j} \right) \right. \\ \left. - \left(\frac{\partial T}{\partial \dot{x}_i} \frac{\partial \dot{x}_i}{\partial q_j} + \frac{\partial T}{\partial \dot{y}_i} \frac{\partial \dot{y}_i}{\partial q_j} + \frac{\partial T}{\partial \dot{z}_i} \frac{\partial \dot{z}_i}{\partial q_j} \right) \right] \delta q_j \quad (423) \end{aligned}$$

This equation can be simplified further by using the expressions for x_i , y_i and z_i in equation (414) and also realizing that

$$\frac{\partial \dot{x}_i}{\partial \dot{q}_j} = \frac{\partial x_i}{\partial q_j}, \quad \frac{\partial \dot{y}_i}{\partial \dot{q}_j} = \frac{\partial y_i}{\partial q_j}, \quad \frac{\partial \dot{z}_i}{\partial \dot{q}_j} = \frac{\partial z_i}{\partial q_j} \quad (424)$$

Substitution of equation (424) into (423) will produce the following expression for δW :

$$\begin{aligned} \delta W = \sum_{j=1}^n \sum_{i=1}^p \left[\frac{d}{dt} \left(\frac{\partial T}{\partial \dot{x}_i} \frac{\partial x_i}{\partial \dot{q}_j} + \frac{\partial T}{\partial \dot{y}_i} \frac{\partial y_i}{\partial \dot{q}_j} + \frac{\partial T}{\partial \dot{z}_i} \frac{\partial z_i}{\partial \dot{q}_j} \right) \right. \\ \left. - \left(\frac{\partial T}{\partial \dot{x}_i} \frac{\partial \dot{x}_i}{\partial q_j} + \frac{\partial T}{\partial \dot{y}_i} \frac{\partial \dot{y}_i}{\partial q_j} + \frac{\partial T}{\partial \dot{z}_i} \frac{\partial \dot{z}_i}{\partial q_j} \right) \right] \delta q_j \quad (425) \end{aligned}$$

From equation (420) the kinetic energy function in Cartesian coordinates is a function of the velocities \dot{x}_i , \dot{y}_i and \dot{z}_i . This expression for the

kinetic energy can be differentiated with respect to \dot{q}_j and q_j , and after comparing the results of this operation with equation (425), it can be seen that

$$\delta W = \sum_{j=1}^n \left[\frac{d}{dt} \left(\frac{\partial T}{\partial \dot{q}_j} \right) - \frac{\partial T}{\partial q_j} \right] \delta q_j \quad . \quad (426)$$

Previously, an expression for δW was derived as a function of a generalized force Q_j . This expression, equation (418), when equated with equation (426) yields the following equations of motion commonly referred to as Lagrange's equations.

$$\frac{d}{dt} \left(\frac{\partial T}{\partial \dot{q}_j} \right) - \frac{\partial T}{\partial q_j} = Q_j \quad . \quad (427)$$

At this point it is necessary to discuss the generalized force in more detail. For a complex vibrating system the generalized force can consist of three distinct forces:

- a. An applied force that is applied externally to the system
- b. A spring force because of a change in potential energy of the system
- c. A damping force which is due to the dissipation of energy in a damper.

The potential energy of a system is a function of the generalized coordinates as shown in the equation

$$U = \frac{1}{2} \sum_{i=1}^n \sum_{j=1}^p k_{ij} q_i q_j \quad (428)$$

and if this equation is differentiated with respect to q_i the following expression gives the generalized spring force

$$Q_j = - \frac{\partial U}{\partial q_j} = - \sum_{i=1}^n k_{ij} q_i \quad . \quad (429)$$

The dissipation function D can be analogous with the potential energy function defined as

$$D = \frac{1}{2} \sum_{i=1}^n \sum_{j=1}^p c_{ij} \dot{q}_i \dot{q}_j \quad . \quad (430)$$

When this function is differentiated with respect to q_j the generalized force for the dissipation function is

$$Q_j = - \frac{\partial D}{\partial \dot{q}_j} = - \sum_{i=1}^n c_{ij} \dot{q}_i \quad . \quad (431)$$

Now it can be seen that the generalized force for a complex vibrating system is comprised of three distinct forces. Thus, Lagrange's equations of motion can be expressed in a more general form and is given below

$$\frac{d}{dt} \frac{\partial T}{\partial \dot{q}_j} - \frac{\partial T}{\partial q_j} + \frac{\partial D}{\partial \dot{q}_j} + \frac{\partial U}{\partial q_j} = Q_j \quad . \quad (432)$$

The subscripts $j = 1, 2, \dots, n$ are the number of generalized coordinates of the system, and Q_j is the applied force for each generalized coordinate.

Whenever the system is conservative and since the potential energy function is a function only of the generalized coordinates, equation (432) can be written

$$\frac{d}{dt} \frac{\partial L}{\partial \dot{q}_j} - \frac{\partial L}{\partial q_j} = 0 \quad (432a)$$

where $L = T - U$ and is known as the Lagrangian operator.

The primary advantage of Lagrange's equations is that the equations represent a uniform way of writing the equations of motion of a system and these equations are independent of the coordinate system used.

4. INFLUENCE COEFFICIENTS

In the preceding paragraphs, Newton's second law of motion and energy relationships were used to derive the equations of motion for a

vibrating structure. Another commonly used and very convenient approach for systems with many degrees of freedom is the method of influence coefficients. The equations of motion may be written in terms of influence coefficients and solved to obtain numerical values for natural frequencies and mode shapes. This method is an application of the Lagrangian use of generalized coordinates and is widely used for the analysis of complex structures.

The method of influence coefficients is based upon linearity. The "inertia force" associated with the vibratory motion of each element of mass causes a certain motion at all other mass elements in the system. Then the deflection at each mass element is the sum of the effects from all the inertia forces. This effect is described by an array of numbers called influence coefficients.

An influence coefficient, denoted α_{ij} , is a parameter having the dimension of compliance or reciprocal of stiffness. It is defined as the static deflection of a system at position i due to a unit force applied at position j when the unit force is the only force acting. Hence the influence coefficient is a measure of the elastic properties of a system. Influence coefficients are conveniently used to keep account of all the induced deflections due to various applied forces and to set up the differential equations of motion for the system.

The values of the influence coefficients are obtained for a given system by applying a unit static load at point j and finding the resulting deflection in the direction of the load at point i . The deflections, and therefore influence coefficients, are obtained using the methods of static analysis (see examples in Section XIV.B.5). For a system with n degrees of freedom, the number of influence coefficients will be n^2 . However, only $n(n+1)/2$ will have different values, because of reciprocity, $\alpha_{ij} = \alpha_{ji}$. Reciprocity is based on the fact that the strain energy or stored work in an elastic system is the same for both cases. As an illustration of reciprocity, consider the simply supported beam shown in Figure 111 in which two vertical forces F_1 and F_2 are applied at positions 1 and 2.

The influence coefficients for this illustration are α_{11} , α_{12} and α_{21} . The deflection at position 1 due to the force F_2 applied at position 2 is $F_2 \alpha_{12}$. Extending this concept the deflections at points 1 and 2 of the system due to the applied loads F_1 and F_2 are written in terms of influence coefficients as

$$\begin{aligned} x_1 &= \alpha_{11} F_1 + \alpha_{12} F_2 \\ x_2 &= \alpha_{21} F_1 + \alpha_{22} F_2 \end{aligned} \quad (433)$$

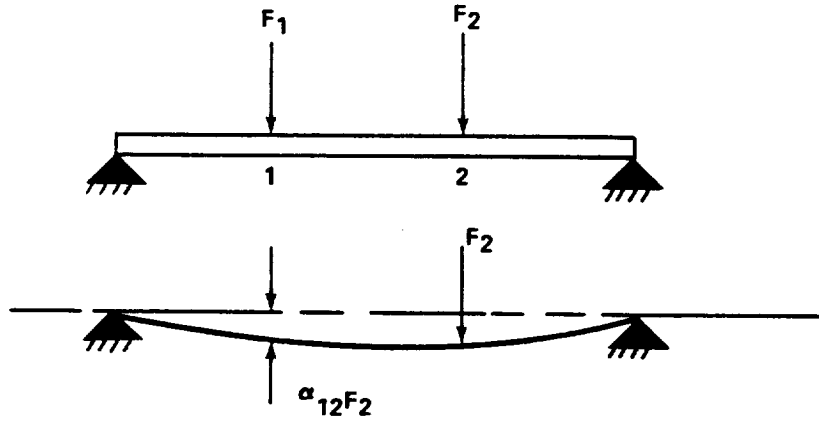


Figure 111. Simply supported beam with two loads.

For proof of reciprocity consider that the procedure of loading is separated into two steps. First, when F_1 is applied alone, the potential energy in the beam is $\frac{1}{2} F_1^2 \alpha_{11}$. When F_2 is then applied, the additional deflection at position 1 due to the force F_2 is $F_2 \alpha_{12}$. The work done by F_1 corresponding to this deflection is $F_1(F_2 \alpha_{12})$. The total potential energy in the system is then

$$U = \frac{1}{2} F_1^2 \alpha_{11} + F_1(F_2 \alpha_{12}) + \frac{1}{2} F_2^2 \alpha_{22} \quad . \quad (434)$$

The last two terms of this equation represent the additional potential energy which is due to the application of F_2 .

Second, when the force F_2 is applied to station 2 and then the force F_1 is applied to station 1, the total potential energy of the system is

$$U = \frac{1}{2} F_2^2 \alpha_{22} + F_2(F_1 \alpha_{21}) + \frac{1}{2} F_1^2 \alpha_{11} \quad . \quad (435)$$

The last two terms of this equation are due to the application of F_1 .

Since the total energy and the product $F_1 F_2$ is the same, α_{12} must equal α_{21} and reciprocity is proven for this simple case. Note that α_{11} does not equal α_{22} because F_1 does not equal F_2 in the general case.

While the previous illustration is based on static forces acting on a weightless beam, it should be realized that the reasoning applies equally

well to any linear spring type system, and the forces could be inertia loads developed by point masses.

Using influence coefficients, the equations for a linear system with dynamic loads can now be written. Assuming a harmonic motion

$$x_j = x_{jo} \sin \omega t$$

and

$$\ddot{x}_j = -x_{jo} \omega^2 \sin \omega t$$

a set of algebraic equations can be written for a system of n elements of mass.

$$x_1 = \alpha_{11} (m_1 \omega^2 x_1) + \alpha_{12} (m_2 \omega^2 x_2) + \dots + \alpha_{1n} (m_n \omega^2 x_n)$$

$$x_2 = \alpha_{21} (m_1 \omega^2 x_1) + \alpha_{22} (m_2 \omega^2 x_2) + \dots + \alpha_{2n} (m_n \omega^2 x_n)$$

$$\begin{array}{ccccccc} \cdot & \cdot & \cdot & \cdot & \cdot & \cdot & \cdot \\ \cdot & \cdot & \cdot & \cdot & \cdot & \cdot & \cdot \\ \cdot & \cdot & \cdot & \cdot & \cdot & \cdot & \cdot \end{array} \quad (436)$$

$$x_n = \alpha_{n1} (m_1 \omega^2 x_1) + \alpha_{n2} (m_2 \omega^2 x_2) + \dots + \alpha_{nn} (m_n \omega^2 x_n) .$$

Dividing through the above equations by ω^2 and collecting the coefficients of the variables x_i , the set of equations may be rearranged as follows:

$$\left(\alpha_{11} m_1 - \frac{1}{\omega^2} \right) x_1 + (\alpha_{12} m_2) x_2 + \dots + (\alpha_{1n} m_n) x_n = 0$$

$$(\alpha_{21} m_1) x_1 + \left(\alpha_{22} m_2 - \frac{1}{\omega^2} \right) x_2 + \dots + (\alpha_{2n} m_n) x_n = 0$$

$$\begin{array}{ccccccc} \cdot & \cdot & \cdot & \cdot & \cdot & \cdot & \cdot \\ \cdot & \cdot & \cdot & \cdot & \cdot & \cdot & \cdot \\ \cdot & \cdot & \cdot & \cdot & \cdot & \cdot & \cdot \end{array} \quad (437)$$

$$(\alpha_{n1} m_1) x_1 + (\alpha_{n2} m_2) x_2 + \dots + \left(\alpha_{nn} m_n - \frac{1}{\omega^2} \right) x_n = 0 \quad .$$

These are linear homogeneous equations and are satisfied if the determinant of the coefficients of x_i in the above equation vanishes as follows:

$$\begin{vmatrix} \left(\alpha_{11} m_1 - \frac{1}{\omega^2} \right) & (\alpha_{12} m_2) & \dots & (\alpha_{1n} m_n) \\ (\alpha_{21} m_1) & \left(\alpha_{22} m_2 - \frac{1}{\omega^2} \right) & \dots & (\alpha_{2n} m_n) \\ \cdot & \cdot & & \cdot \\ \cdot & \cdot & & \cdot \\ \cdot & \cdot & & \cdot \\ (\alpha_{n1} m_1) & (\alpha_{n2} m_2) & \dots & \left(\alpha_{nn} m_n - \frac{1}{\omega^2} \right) \end{vmatrix} = 0 \quad .$$

The above determinant, called the characteristic equation, will result in an equation of n^{th} degree in $1/\omega^2$, leading to n natural frequencies of the system. The mode shapes can then be determined from equation (437) by substituting in the natural frequencies and solving for the amplitude ratios. The solution of the frequency equation for n greater than 2 is normally performed on a computer. For additional discussion of matrix theory and application, see Paragraphs B.5 and I.3. of this section.

5. MATRIX METHODS

The use of matrices in the study of multi-degree-of-freedom systems has become an accepted language in vibrations and is widely used, especially when digital computers are available. Matrix methods, common in vibration work, follows. The material presented here is found in References 37 and 38. A review of applicable matrix theory is presented in Paragraph H.4. of this section.

For a linear system with multi-degree-of-freedom, the equations of motion for free undamped vibration are

$$m_{11} \ddot{q}_1 + m_{12} \ddot{q}_2 + \dots + m_{1n} \ddot{q}_n + k_{11} q_1 + k_{12} q_2 + \dots + k_{1n} q_n = 0$$

$$m_{21} \ddot{q}_1 + m_{22} \ddot{q}_2 + \dots + m_{2n} \ddot{q}_n + k_{21} q_1 + k_{22} q_2 + \dots + k_{2n} q_n = 0$$

.....

$$m_{n1} \ddot{q}_1 + m_{n2} \ddot{q}_2 + \dots + m_{nn} \ddot{q}_n + k_{n1} q_1 + k_{n2} q_2 + \dots + k_{nn} q_n = 0$$

where

m_{nn} = generalized mass

q_n = generalized coordinate

k_{nn} = stiffness coefficient .

These equations can be written more concisely in matrix notations as

$$M\{\ddot{q}\} + K\{q\} = \{0\} \quad (438)$$

where

$$M = \begin{bmatrix} m_{11} & m_{12} & \dots & m_{1n} \\ m_{21} & m_{22} & \dots & m_{2n} \\ \dots & \dots & \dots & \dots \\ m_{n1} & m_{n2} & \dots & m_{nn} \end{bmatrix} \quad K = \begin{bmatrix} k_{11} & k_{12} & \dots & k_{1n} \\ k_{21} & k_{22} & \dots & k_{2n} \\ \dots & \dots & \dots & \dots \\ k_{n1} & k_{n2} & \dots & k_{nn} \end{bmatrix} \quad \{\ddot{q}\} = \begin{bmatrix} \ddot{q}_1 \\ \ddot{q}_2 \\ \vdots \\ \ddot{q}_n \end{bmatrix}$$

and

$$\{q\} = \begin{bmatrix} q_1 \\ q_2 \\ \vdots \\ q_n \end{bmatrix}$$

$\{q\}$ is called the coordinate vector, $M = [m_{ij}]$ is called the mass matrix, and $K = [k_{ij}]$ is called the stiffness matrix.

More generally, a linear system with applied excitation can be described by a matrix equation of the form

$$M \{\ddot{q}\} + C \{\dot{q}\} + K \{q\} = \{Q\} \quad (439)$$

where $\{Q\}$ are the generalized forces corresponding to the generalized coordinates $\{q\}$, and $[C]$ is the viscous damping matrix of the same order as $[M]$ and $[K]$.

The above equation applies to all linear constant parameter vibratory systems, and the specifications of any particular system are contained in the coefficient matrices $[M]$, $[C]$ and $[K]$. The type of excitation is described by the column matrix $\{Q\}$. The individual terms in the coefficient matrices have the following significance:

m_{ij} is the momentum component at i due to a unit velocity at j
 c_{ij} is the damping force at i due to a unit velocity at j
 k_{ij} is the elastic force at i due to a unit displacement at j .

In certain applications it is more convenient to deal with $[K]^{-1}$, the inverse of the stiffness matrix, than with $[K]$. The elements of $[K]^{-1}$, α_{ij} , will then represent a unit displacement at i due to a unit force applied at j and are seen to be the influence coefficients discussed in the previous section. $[K]^{-1}$ itself is sometimes called the flexibility matrix.

The previous general discussion applied to a n -degree-of-freedom system expressed in terms of the generalized coordinates. As an example, a two-degree-of-freedom system described in terms of the more familiar displacement coordinates will be presented. The differential equation, in matrix format, is written as

$$[m] \{\ddot{x}\} + [c] \{\dot{x}\} + [k] \{x\} = \{f(t)\} .$$

For natural frequency determination c_1 , c_2 , $f_1(t)$ and $f_2(t)$ all must be set equal to zero. The solution, assumed to be sinusoidal, expressed in matrix format, is

$$\begin{bmatrix} x_1 \\ x_2 \end{bmatrix} = \begin{bmatrix} a_1 \\ a_2 \end{bmatrix} \sin \omega_n t \quad . \quad (440)$$

Since $\sin \omega_n t$ is not always zero

$$(-\omega_n^2 [M] + [K]) \{a\} = \{0\} \quad . \quad (441)$$

For a practical vibration, the amplitudes a_1, a_2 cannot be zero and the remaining quantity $(-\omega_n^2 [M] + [K])$ must be zero. Expanding into determinant form

$$\begin{vmatrix} (k_1 + k_2 - \omega_n^2 m_1) & -k_2 \\ -k_2 & (k_2 - \omega_n^2 m_2) \end{vmatrix} = 0 \quad (442)$$

and into algebraic form

$$m_1 m_2 \omega_n^4 - (k_2 m_1 + k_1 m_2 + k_2 m_2) \omega_n^2 + k_1 k_2 = 0 \quad . \quad (443)$$

This is a quadratic in ω_n^2 and can be solved by the quadratic formula to yield the two natural frequencies which are the positive values.

The values ω_n^2 are termed the eigenvalues (particular values) of the matrix $[M]^{-1} [K]$ which is called the dynamic matrix. This can be seen if equation (441) is put in the form of an eigenvalue equation obtained by writing equation (439) in the form

$$\omega_n^2 [M] \{a\} = [K] \{a\} \quad (444)$$

and multiplying both sides by $[M]^{-1}$ to obtain

$$[M]^{-1} [K] \{a\} = \omega_n^2 \{a\} \quad . \quad (445)$$

This is the usual form for an eigenvalue equation with ω_n^2 representing the eigenvalues and $\{a\}$ representing the eigenvectors corresponding to the mode shapes.

An iteration technique is sometimes used to determine the eigenvalues. When using the iteration technique, equation (441) is written in still another form obtained by a technique similar to equation (445).

$$[K^{-1} M] \{a\} = \lambda \{a\} \quad (446)$$

where

$$\lambda = \frac{1}{\omega_n^2} .$$

The technique of iteration utilizes an initial estimate for the mode shape of vibration. The matrix equation is then expanded. The resulting column is now normalized; i.e., reducing one of the amplitudes to unity by dividing each term of the column by the particular amplitude. The process is then repeated with the normalized column as the new estimate until the amplitudes for the first mode converge to a value of acceptable accuracy. The fundamental frequency can then be found directly from the matrix equation. For the next higher mode shapes and natural frequencies, the orthogonality principle (Paragraph H.5 of this section) is used to obtain a new matrix equation that is free from any lower modes. The iterative procedure is then repeated.

6. COORDINATE COUPLING

Coordinate coupling occurs when a force is transmitted by spring or dashpot to more than one coordinate of the system. In other words, the displacement of one mass will be felt by another mass in the same system through the coupled elements.

There are two types of coupling action, generally referred to as stiffness coupling due to static displacements and mass coupling due to inertia forces. These two types of coupling will be discussed by the following example.

A two-degree-of-freedom system is shown in Figure 112 and consists of a mass m and two springs of stiffness k_1 and k_2 . Any two independent coordinates, such as x and ϕ from any origin, can be used to specify the configuration of the system.

Considering Figure 112 with coordinates (x, ϕ) and assuming small oscillations, the equations of motion are

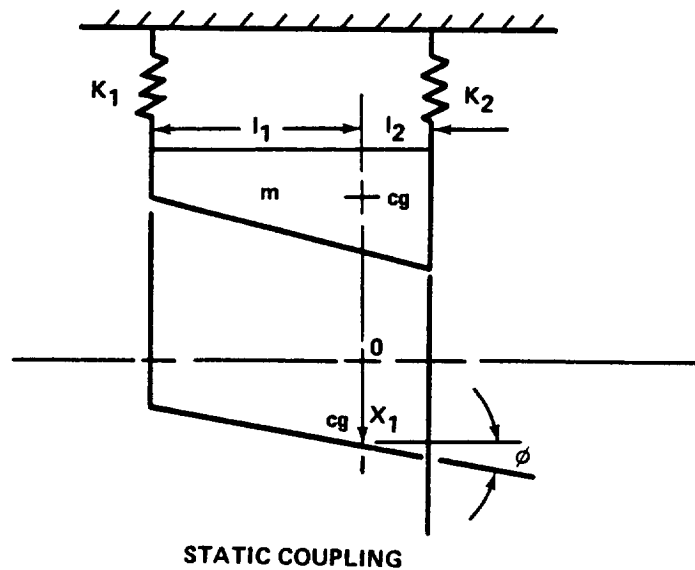


Figure 112. Two-degree-of-freedom system.

$$m\ddot{x} + (k_1 + k_2)x - (k_1 l_1 - k_2 l_2)\phi = 0 \quad (447)$$

$$J\ddot{\phi} + (k_1 l_1^2 + k_2 l_2^2)\phi - (k_1 l_1 - k_2 l_2)x = 0$$

Each of the above equations contain terms of both x and ϕ and are therefore interdependent on each other. The motions of the mass will be independent of each other only if the coupling term $(k_1 l_1 - k_2 l_2)$ is equal to zero; i.e., the center of gravity is located so that $k_1 l_1 = k_2 l_2$. Otherwise, the resultant motion of the mass will consist of both rectilinear and rotational components when either a displacement or torque is applied through the center of gravity of the body as an initial condition.

In the example described in Figure 112, the origin was chosen to correspond with the center of gravity of the mass m . If the origin were chosen at any other location, mass terms as a function of both coordinates will appear in the equations and the system would then be mass coupled in addition to stiffness coupled.

The terms uncoupled modes and coupled modes often appear in vibration terminology. These terms are used in reference to coupled systems. Sometimes in analysis or test the system is artificially constrained to make one or more of the coordinates zero, resulting in an uncoupled mode. While the uncoupled mode is of interest particularly in understanding the dynamics of the system, the uncoupled and coupled modes are not the same.

7. PLATES

The bending properties of a plate depend to a large extent on its thickness as compared with its other dimensions. Timoshenko [39] uses thickness to classify plates into three types:

- a. Thin plates with small deflections.
- b. Thin plates with large deflections.
- c. Thick plates.

The assumptions, or a statement of second order terms neglected, are made during the analysis for each of the classes of plates. In this paragraph, a simple example of the first class from Reference 39 is discussed.

Consider a plate of uniform thickness h bounded by a constraint on two edges and free on two edges and take the x - y plane as the middle plane of the plate before loading. Let the y axis coincide with one of the longitudinal edges of the plate and the z axis be downward as shown in Figure 113.

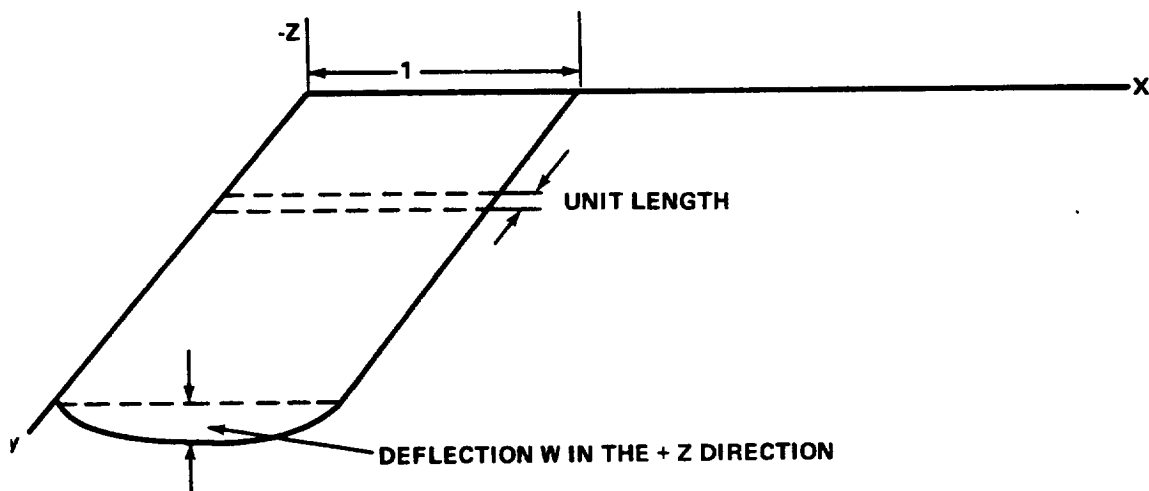


Figure 113. Thin plate with small deflection.

If the width of the strip is l and the depth is h , then the strip may be assumed to be a bar of rectangular cross section of length l and depth h . It is assumed that the cross sections of the bar remain plane during bending and only a rotation with respect to their neutral axes is considered. If no normal forces are applied to the end sections of the bar, the neutral surface of the

bar coincides with the middle surface of the plate, and the unit elongation of a fiber parallel to the x axis is proportional to its distance z measured from the middle surface.

The deflection curve is given by $-d^2W/dx^2$, where W is the deflection of the bar in the z direction and is assumed to be small compared with the length of the bar 1. The unit elongation of a fiber at a distance z from the middle surface is denoted by ϵ_x and is given by

$$\epsilon_x = -z \frac{d^2W}{dx^2} \quad (448)$$

as shown in Figure 114a.

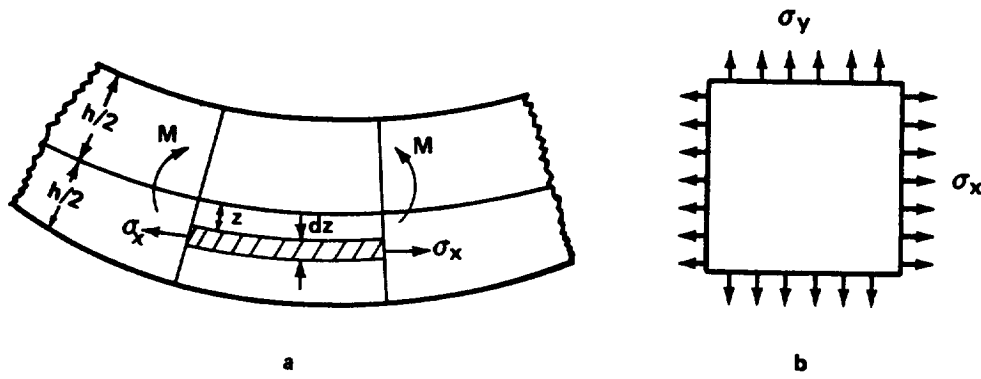


Figure 114. Plate element free body.

Applying Hooke's law, the unit elongations ϵ_x and ϵ_y in terms of the normal stresses σ_x and σ_y acting on the shaded element in Figure 114b are given by

$$\epsilon_x = \frac{1}{E} [\sigma_x - \nu \sigma_y] \quad (449)$$

$$\epsilon_y = \frac{1}{E} [\sigma_y - \nu \sigma_x]$$

where E is the modulus of elasticity and ν is Poisson's ratio. Since the lateral strain is zero, the second equation therefore gives

$$\epsilon_y = 0$$

$$\sigma_y = \nu \sigma_x$$

and

$$\epsilon_x = \frac{1}{E} - (1 - \nu^2) \sigma_x \quad . \quad (450)$$

For the stress

$$\sigma_x = \frac{E \epsilon_x}{1 - \nu^2} = \frac{E}{1 - \nu^2} \left(z \frac{d^2 W}{dx^2} \right) \quad . \quad (451)$$

If the plate were subjected to either tensile or compressive forces acting in the x-direction and uniformly distributed along the longitudinal sides of the plate, the direct stress would have to be added to the stress due to bending.

The bending moment in the strip is obtained by direct integration.

$$M = \int_{-\frac{h}{2}}^{\frac{h}{2}} \sigma_x z \, dz = - \frac{E h^3}{12(1 - \nu^2)} \frac{d^2 W}{dx^2} \quad . \quad (452)$$

Let

$$D = \frac{E h^3}{12(1 - \nu^2)} \quad .$$

Then the equation for the deflection curve of the elemental strip is given by

$$D \frac{d^2 W}{dx^2} = -M \quad . \quad (453)$$

The flexural rigidity of the plate D is the quantity that replaces the term EI in the differential equation for beams.

Therefore, the deflection of the plate depends on an integration of equation (453). The solution of the problem includes the definition of the

boundary. The boundary may be simply supported (free to rotate), constrained (not free to rotate) or somewhere in between.

If the boundary is constrained on all four sides, the curvature equation assumes a more complex form and axial stress must be considered. For circular plates, polar coordinates are used. More details on these problems are found in the references.

C. Equations of Motion – Transients

In the previous paragraphs, the response of a system to a sinusoidal input or combinations of sinusoidal inputs was developed. An input consisting of one or more sinusoids or a truncated random disturbance of infinite length is classified as steady state. In this paragraph, the equations of motion are developed for a transient input. A definition of a transient is difficult to state. One definition of a transient can be formulated from the discussion in Paragraph A.5.2 of this section. In Paragraph A.5.2 of this section, the time period of the disturbance T was assumed to be infinite for the steady state input. If the time T cannot be assumed to be infinite, the input is a transient. Thus, for a transient, the exact time of initiation and cessation of the disturbance is pertinent to the response.

The response to transients is represented by an expression called in the literature as the *faltung* Duhamel, or convolution integral. This integral can be developed directly from the equation of motion or by superposition. Both methods of development will be presented.

1. DUHAMEL INTEGRAL – EQUATIONS OF MOTION

The derivation which follows is performed for a single degree-of-freedom system with damping. Consider the equation of equilibrium as discussed in Paragraph B.1 of this section with a forcing function F .

$$m\ddot{x} + c\dot{x} + kx = F$$

where the initial conditions are $x = \dot{x} = 0$ when $t = 0$ and the force F begins to act.

With these initial conditions, the solution to this equation is

$$x = \frac{F}{k} \left[1 - e^{-\omega_n \frac{c}{2k} t} \left(\frac{c}{2k} \frac{\omega_n}{q} \sin qt + \cos qt \right) \right] \quad (454)$$

where

$$\omega_n = \sqrt{\frac{k}{m}}$$

and

$$q = \sqrt{\frac{k}{m} - \frac{c^2}{4m^2}} = \omega_n \sqrt{1 - \frac{c^2}{c_0^2}} .$$

If the force is withdrawn after an instant of time, δt , the response will be the sum of the expression above and a similar expression where the force is negative and applied at $t = \delta t$. The effect of these two forces is the same as F_1 acting during the interval where $0 \leq t \leq \delta t$. The first term in each equation cancels each other and the remaining terms take a functional form of

$$x = f(t) - f[t + (-\delta t)] . \quad (455)$$

Using the Taylor's series expansion for this form of the expression for x and neglecting higher orders of δt yields

$$x = \frac{d f(t)}{dt} \delta t . \quad (456)$$

Substituting in equation (454), x as the function of t , provides the response equation

$$x = \frac{F_1 \delta t}{mq} e^{-\omega_n \frac{c}{c_0} t} \sin qt . \quad (457)$$

The above expression describes the response at time t resulting from a single force applied at $t = 0$ and removed at $t + \delta t$. If the force is applied at $t = \tau$, the response at t becomes

$$x = \frac{F_1 \delta t}{mq} e^{-\omega_n \frac{c}{c_0} (t-\tau)} \sin q (t-\tau) . \quad (458)$$

By allowing $F_1 \delta t$ to approach $F(\tau) d\tau$ and integrating the above expression results in one form of Duhamel's integral

$$x = \int_0^t F(\tau) h(t-\tau) d\tau \quad (459)$$

where $F(\tau)$ is the forcing expression and $h(t-\tau)$ contains all the system parameters. The above expression can be integrated by parts

$$x = h(t-\tau) \int_0^t F(\tau) d\tau - \int_0^t \left[\int_0^t F(\tau) d\tau \right] d[h(t-\tau)] .$$

Suppose the integral part, $\int F(\tau) d\tau$, is defined as zero for all time of the integration interval except a small increment from $-\epsilon$ to ϵ . Suppose also the value of the integral is one when integrated between $-\epsilon$ and ϵ .

$$\int_{-\epsilon}^{\epsilon} F(\tau) d\tau = 1 \quad (460)$$

where ϵ is a very small quantity. Equation (460) defines an impulse. Using this specialized force the response becomes

$$x = h(t-\tau) - \int_0^t d h(t-\tau) \quad (461)$$

The second term is zero since $h(t-\tau)$ is a step function. The response is $h(t-t)$ for the specific system considered which is nothing more than the motion of a single degree-of-freedom system with damping. It is shown in Reference 34 that the same result is obtained for a system of multiple degrees of freedom.

If the force is not a single impulse but a general shape that can be constructed from a set of impulses, general shape is represented by an integration of the first term of equation (461).

$$x(t) = \int_0^t F(\tau) h(t-\tau) d\tau \quad (462)$$

Equation (462) is the common form of the transient integral. Negative time is not considered.

2. DUHAMEL'S INTEGRAL — SUPERPOSITION

Exactly the same result is obtained by superposition and direct reasoning. This is the derivation most often presented in text books. An individual forcing element is considered to be an impulse as defined above

$$\int_{-\epsilon}^{\epsilon} \delta(\tau) d\tau = 1 \quad (463)$$

The complete force can be considered a superposition of impulses and in an interval of time

$$F(\tau) = \sum \delta(\tau) \Delta \tau \quad . \quad (464)$$

Let $h(t-\tau)$ be the response of the system to a single impulse. The response to a force $F(\tau)$ contains a number of impulses, each is acting on the system at a different time.

$$x(t) = \sum \delta(\tau) h(t-\tau) \Delta \tau \quad (465)$$

or in the limit

$$x(t) = \int_0^t F(\tau) h(t-\tau) d\tau \quad . \quad (466)$$

This equation is identical to the previously derived expression and also represents the response at t for a force operating on the system in an interval of time represented by a function of τ .

3. TRANSIENT/STEADY STATE RELATIONSHIP

The response of a linear constant parameter system for any input was derived in Paragraph C.1 of this section, and resulting in equation (466), the Duhamel equation

$$x(t) = \int_0^t F(\tau) h(t-\tau) d\tau \quad . \quad (467)$$

An alternate and interchangeable form of equation (467) can be written with the time delay associated with the forcing term in the integral. Equation (467) then becomes

$$x(t) = \int_0^t F(t-\tau) h(\tau) d\tau \quad . \quad (468)$$

The forcing function is then established to be an exponential steady state input of the form

$$F(t-\tau) = e^{i\omega(t-\tau)} \quad (469)$$

where ω = radians per second.

Equation (469) is substituted and the $e^{i\omega\tau}$ term is brought outside the integral since the integration is over the variable τ .

$$x(t) = e^{i\omega t} \int_0^t e^{-i\omega\tau} h(\tau) d\tau \quad (470)$$

For a steady state periodic input, the integration limits can be considered infinite and the integral defines the Laplace transform of the weighting function $h(\tau)$. The Laplace transform, as suggested from the name, transforms the problem from the time domain into the frequency domain (see Paragraph H.2. of this section) and $x(t)$ is related to $x(\omega)$.

$$x(\omega) = e^{i\omega t} L[h(\tau)] \quad (471)$$

As seen from equation (471), $L[h(\tau)]$ = Laplace transform. The Laplace transform of the weighting function is a quantity that is easily obtained from an analysis or from an actual test. However, it should be noted that the input is an exponential and not a sinusoid. The weighting function itself in the time domain is the inverse transform

$$L^{-1} \left[\frac{x(\omega)}{e^{i\omega t}} \right] = h(\tau) \quad (472)$$

Without a computer, the evaluation of the inverse transform required by equation (472) for typical $x(\omega)/e^{i\omega t}$ ratios would be very cumbersome for anything but the simplest dynamics system. However, with the advent of the digital computer, this approach becomes practical. In addition, the weighting function can be used with equations (462) and (468) to determine the response of the system to any transient input.

D. Equations of Motion – Acoustic Impingement

1. RESPONSE EQUATION DERIVATION

Consider a spherical sound wave that has traveled unimpeded a long distance from a sound source, whose "crests" are in a plane perpendicular

to the direction of propagation. Such waves represent the simplest three-dimensional wave and may be expressed in the form

$$f(r - ct) \quad (473)$$

where

$$\begin{aligned} r &= \text{radial distance from the source} = (x^2 + y^2 + z^2)^{1/2} \\ c &= \text{velocity of the propagated wave} \\ t &= \text{time} \end{aligned}$$

A simplification of the more general case is obtained when a plane wave is considered. For this special case the fronts are always perpendicular to the x-axis, and the one dimensional wave is of the form

$$f(x - ct) \quad (474)$$

The parameters describing this wave at some point in time and distance from the source are expressed by

$$\delta = - \frac{\partial \xi}{\partial x} \quad (475)$$

where

$$\begin{aligned} \delta &= \text{change in density} \\ \xi &= \text{displacement} \end{aligned}$$

This equation satisfies the requirement of conservation of matter. The change in density is equal to the rate of change of displacement $\partial \xi / \partial x$. From the thermodynamic gas laws relating the change in pressure to the change in density

$$P = \gamma c P_o \delta \quad (476)$$

where

$$\begin{aligned} P &= \text{pressure} \\ c &= \text{specific heat (1.40 for air)} \\ P_o &= \text{atmospheric pressure} \end{aligned}$$

and for equilibrium

$$\rho \frac{\partial^2 \xi}{\partial t^2} = \rho \frac{\partial u}{\partial t} = - \frac{\partial P}{\partial x} \quad (477)$$

where

$$\begin{aligned} \rho &= \text{mass density} \\ u &= \text{velocity} \end{aligned}$$

which provides the net force ($\partial p / \partial x$) acting on the medium in terms of mass and its acceleration.

Combining equations (475), (476), and (477), expressions for ξ , ρ , δ and the change in temperature ΔT in a plane sound wave are obtained.

$$\frac{\partial^2 \xi}{\partial x^2} = \frac{1}{c^2} \frac{\partial^2 \xi}{\partial t^2} \quad (478a)$$

$$\frac{\partial^2 P}{\partial x^2} = \frac{1}{c^2} \frac{\partial^2 P}{\partial t^2} \quad (478b)$$

$$\frac{\partial^2 \delta}{\partial x^2} = \frac{1}{c^2} \frac{\partial^2 \delta}{\partial t^2} \quad (478c)$$

where

$$c = \left(\frac{P_o \gamma c}{\rho} \right)^{1/2}$$

$$\delta = - \frac{\partial \xi}{\partial x}$$

and

$$P = P_o \gamma c \delta = \rho c^2 \frac{\partial \xi}{\partial x} .$$

Now

$$\Delta T = \left(1 - \frac{1}{\gamma c} \right) \frac{T_p}{p_o} = (\gamma c - 1) \frac{\partial \xi}{\partial x} T . \quad (479)$$

The displacement, density, and pressure are parameters of the same wave with a velocity c . For the purpose of illustration, the parameters can be considered three separate waves propagating without change of shape and with a velocity c . The three waves are not independent, but are related by equilibrium, continuity, and thermodynamics through the equations above. If the particle velocity is known, density and pressure can be determined.

The average energy of a volume of gas due to passage of a plane wave is

$$W = \frac{1}{2} \rho \iiint \left[\left(\frac{\partial \xi}{\partial t} \right)^2 + c^2 \left(\frac{\partial \xi}{\partial x} \right)^2 \right] dx dy dz \text{ ergs} \quad (480)$$

For a simple harmonic wave of frequency ω this equation can be expressed in terms of pressure P alone

$$W = \frac{1}{2} \rho c^2 \iiint \left[\left(\frac{c}{\omega} \right)^2 \left(\frac{\partial P}{\partial x} \right)^2 + P^2 \right] dx dy dz \quad (481)$$

The rate at which the energy is being transmitted along the wave per square centimeter of wavefront is called the intensity I of the sound wave. This will equal the excess pressure P on the square centimeter, multiplied by the velocity of the gas particle

$$P \left(\frac{\partial \xi}{\partial t} \right) = -\rho c^2 \frac{\partial \xi}{\partial x} \frac{\partial \xi}{\partial t} \text{ ergs/sec/cm}^2 \quad (482)$$

If the wave is a simple harmonic function; i.e.,

$$f(x - ct) = P \cos (\omega t - kx) \quad (483)$$

where

P = maximum pressure

ω = angular frequency

k = wave number defined by a spatial period $2\pi/k$ or λ (commonly referred to as wave length).

The expressions for pressure, energy, and intensity follow the sign convention of a wave moving to the right, having a maximum pressure P +

$$P_+ = P_+ e^{i(\omega t - kx)} \quad (484a)$$

$$\xi_+ = A_+ e^{i(\omega t - kx)} \quad (484b)$$

$$\frac{\partial \xi}{\partial t} = U_+ e^{i(\omega t - kx)} \quad (484c)$$

where

$$K = \frac{2\pi f}{c}, \quad A_+ = -\left(\frac{P_+}{2\pi i f \rho c}\right), \quad U_+ = \frac{P_+}{\rho c}.$$

Now

$$P_+ = \rho c \left(\frac{\partial \xi}{\partial t} \right) \quad (485a)$$

$$W_+ = \frac{P_+^2}{2\rho c^2} = \frac{1}{2} \rho U_+^2 \quad (485b)$$

$$I = \frac{P_+^2}{2\rho c} = \frac{1}{2} \rho c U_+^2. \quad (485c)$$

For an example, consider a wave moving from the right and impinging on an interface or rigid surface and assume the angle of incidence is perpendicular to the surface. The total pressure developed on the surface is the superposition of the incident wave and the reflected wave designated by P_- .

$$P = P_+ e^{i(\omega t + kx)} + P_- e^{i(\omega t + kx)} \quad (486)$$

and

$$\frac{\partial \xi}{\partial t} = \frac{1}{\rho c} \left[P_+ e^{i(\omega t - kx)} - P_- e^{i(\omega t + kx)} \right] \quad (487a)$$

$$W = \frac{1}{2\rho c^2} (P_+^2 + P_-^2) \quad (487b)$$

$$I = \frac{1}{2\rho c} (P_+^2 + P_-^2). \quad (487c)$$

In practical acoustic impingement problems, the medium dynamics couples with the surface dynamics to form a very complex system. Because of the complexity of this acoustic and structural dynamics, the analysis is often augmented by empirical data.

2. PANEL RESPONSE TO RANDOM ACOUSTIC NOISE

In Paragraph 1. of this subsection, the basic acoustic impingement equations were presented. The summary of that paragraph was that the basic equations are often modified by empirical data. In this paragraph additional analysis procedures are presented. These equations contain terms that are more accurately evaluated by experiment.

Equations for the net vibration response at any point in a panel structure can be written from the cumulative effect of all of the oscillatory forces acting on the panel. Forces applied at discrete points induce local vibrations at the points of application. These local vibrations are transmitted along structural paths and are superimposed on other vibrations in accordance with their relative amplitudes and phases. Looking at the panel response problem in this manner, it is convenient to employ the space-time correlation functions, since these functions include phase relationships.

Consider the panel structure shown in Figure 115. The deflection of point j due to a pressure at i is

$$\delta_j^{(i)}(t) = A_i \int_0^t p_i(\tau) h_j^{(i)}(t-\tau) d\tau \quad (488)$$

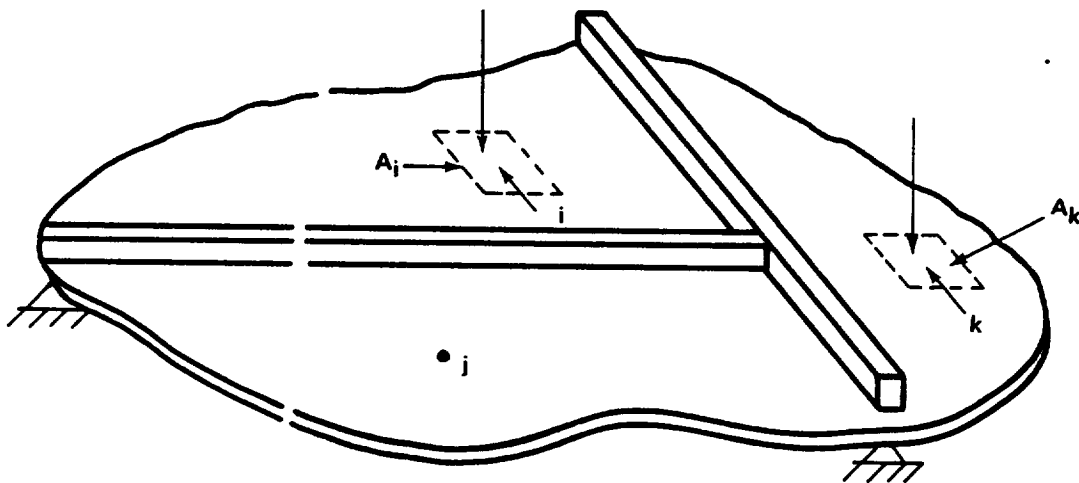


Figure 115. Panel structure.

The deflection at j due to a pressure at k is

$$\delta_j^{(k)}(t) = A_k \int_0^{t'} p_k(\tau) h_j^{(k)}(t-\tau) d\tau \quad (489)$$

where h symbolizes the weighting function.

Equations (488) and (489) are applications of the Duhamel integral. The cross correlation, or measure of phase, between these two components of deflections at j is

$$R_{\delta_j}^{(ik)}(\theta) = \lim_{T \rightarrow \infty} \frac{1}{T} \int_0^T \delta_j^{(i)}(t) \delta_j^{(k)}(t+\theta) dt \quad (490)$$

where θ is the time lag.

If the variables are changed by letting

$$\begin{aligned} \epsilon_1 &= t - \tau & \epsilon_2 &= t + \theta - \tau = t' - \tau \\ d\epsilon_1 &= -d\tau & d\epsilon_2 &= -d\tau \end{aligned}$$

the responses become

$$\delta_j^{(i)}(t) = A_i \int_{-\infty}^{\infty} p_i(t-\epsilon_1) h_j^{(i)}(\epsilon_1) d\epsilon_1 \quad (491)$$

$$\delta_j^{(k)}(t+\theta) = A_k \int_{-\infty}^{\infty} p_k(t-\epsilon_2+\theta) h_j^{(k)}(\epsilon_2) d\epsilon_2 \quad (492)$$

and the cross correlation for components of deflection at j due to pressures at i and k becomes

$$R_{\delta_j}^{(ik)}(\theta) = A_i A_k \int_{-\infty}^{\infty} \int_{-\infty}^{\infty} R_{p_{ik}}(\theta - \epsilon_2 + \epsilon_1) h_j^{(i)}(\epsilon_1) h_j^{(k)}(\epsilon_2) d\epsilon_1 d\epsilon_2 \quad (493)$$

The total deflection at j is

$$\delta_j(t) = \sum_{i=1}^n \delta_j^{(i)}(t) \quad . \quad (494)$$

After a time lag, θ , the total deflection is

$$\delta_j(t-\theta) = \sum_{k=1}^n \delta_j^{(k)}(t-\theta) \quad . \quad (495)$$

In order to obtain the power spectral density function, the autocorrelation function for deflection at j is first written

$$R_{\delta_j}(\theta) = E \left[\sum_i^n \sum_k^n \delta_j^{(i)}(t) \delta_j^{(k)}(t+\theta) \right] \quad (496)$$

where $R_{\delta_j}(\theta)$ = autocorrelation function. Referring to Paragraph A. 5.b. of this section, the power spectral density is directly written

$$\begin{aligned} \Phi_{\delta_j}(\omega) &= \frac{1}{\pi} \int_{-\infty}^{\infty} R_{\delta_j}(\theta) e^{-i\omega\theta} d\theta \\ &= \frac{1}{\pi} \int_{-\infty}^{\infty} \sum_i^n \sum_k^n R_{\delta_j}^{(ik)}(\theta) e^{-i\omega\theta} d\theta \\ &= \sum_i^n \sum_k^n \frac{1}{\pi} \int_{-\infty}^{\infty} R_{\delta_j}^{(ik)}(\theta) e^{-i\omega\theta} d\theta \end{aligned}$$

where $\Phi_{\delta_i}(\omega)$ = power spectral density. This latter expression can be extended by a summation on the cross power spectral density function to include all inputs

$$\Phi_{\delta_j}(\omega) = \sum_i^n \sum_k^n \Phi_{\delta_j}^{(ik)}(\omega) \quad . \quad (498)$$

It is now required to express the cross spectral density function in terms of the structure. This may be done as follows:

$$\Phi_{\delta_j}^{(ik)}(\omega) = \frac{1}{\pi} \int_{-\infty}^{\infty} R_{\delta_j}^{(ik)}(\theta) e^{-i\omega\theta} d\theta \quad (499a)$$

$$\Phi_{\partial_j}^{(ik)}(\omega) = A_i A_k \int_{-\infty}^{\infty} R_{p_{ik}}(\theta - \epsilon_2 + \epsilon_1) e^{-i\omega(\theta - \epsilon_2 + \epsilon_1)} d\theta \quad (499b)$$

$$\int_{-\infty}^{\infty} h_j^{(i)}(\epsilon_1) e^{-i\omega\epsilon_1} d\epsilon_1 \int_{-\infty}^{\infty} h_j^{(k)}(\epsilon_2) e^{-i\omega\epsilon_2} d\epsilon_2$$

where A_i, A_k = areas at i and k . The first integral of Equation (499b) is the power spectral density, $H_j^{(i)}$ represents the second equation, and $H_j^{*(i)}(\omega)$ represents the last integral. Or

$$\Phi_{\delta_j}^{(ik)}(\omega) = A_i A_k \Phi_{p_{ik}}(\omega) H_j^{*(i)}(\omega) H_j^{(k)}(\omega) \quad (500)$$

Now substituting for $\Phi_{\delta_j}^{(ik)}(\omega)$,

$$\Phi_{\delta_j}^{(ik)}(\omega) = \sum_i^n \sum_k^n A_i A_k \Phi_{p_{ik}}(\omega) H_j^{*(i)}(\omega) H_j^{(k)}(\omega) \quad (501)$$

The deflection power spectrum at j is stated in Equation (501). The summation of the product of these areas over which the pressures act, the power spectrum of those pressures and the weighting functions represent all input sources. Expressing the power spectral density functions for deflection in matrix form:

$$\begin{bmatrix} \Phi_{\delta_j}(\omega) \end{bmatrix} = \begin{bmatrix} H_j^{*(i)}(\omega) \end{bmatrix} (A_i) \begin{bmatrix} \Phi_{p_{ik}}(\omega) \end{bmatrix} (A_k) \begin{bmatrix} H_j^{(k)}(\omega) \end{bmatrix} \quad (502)$$

(mx1) (mxn) (nxn) (nxn) (nxn) (nxm)

where

$$\begin{bmatrix} H_j^{*(i)}(\omega) \end{bmatrix} = \begin{bmatrix} H_j^{*(k)}(\omega) \end{bmatrix}^T$$

and T indicates the transpose. The areas and pressure power spectra are measurable or calculable. The impulse responses of deflection can be obtained as follows. Assume there are δ_i degrees of freedom. The equations of motion can then be written as

$$\begin{matrix} \begin{pmatrix} M_{ik} \end{pmatrix} \begin{pmatrix} \ddot{\delta}_i \end{pmatrix} + \begin{pmatrix} C_{ik} \end{pmatrix} \begin{pmatrix} \dot{\delta}_i \end{pmatrix} + \begin{pmatrix} K_{ik} \end{pmatrix} \begin{pmatrix} \delta_i \end{pmatrix} = \begin{bmatrix} F(t) \end{bmatrix} \\ \begin{pmatrix} nxn \end{pmatrix} \quad \begin{pmatrix} nx1 \end{pmatrix} \end{matrix} \quad (503)$$

Taking Laplace transforms

$$\begin{matrix} \begin{bmatrix} S^2 \begin{pmatrix} M_{ik} \end{pmatrix} + S \begin{pmatrix} C_{ik} \end{pmatrix} + \begin{pmatrix} K_{ik} \end{pmatrix} \end{bmatrix} \begin{bmatrix} \delta_i^{(v)} \end{bmatrix} = \begin{pmatrix} 0 \\ 0 \\ 1^{(v)} \\ 0 \\ \vdots \end{pmatrix} \\ \begin{bmatrix} L \begin{bmatrix} \delta_i^{(v)} \end{bmatrix} \end{bmatrix} = \begin{bmatrix} S^2 \begin{pmatrix} M_{ik} \end{pmatrix} + S \begin{pmatrix} C_{ik} \end{pmatrix} + \begin{pmatrix} K_{ik} \end{pmatrix} \end{bmatrix}^{-1} \begin{pmatrix} 0 \\ 0 \\ 1^{(v)} \\ 0 \\ \vdots \end{pmatrix} \end{matrix} \quad (504)$$

where

v = any point

S = Laplace variable.

The Laplace transforms of the responses to unit impulses at each mode are

$$\begin{pmatrix} \delta_i^{(v)} \end{pmatrix} = \begin{bmatrix} S^2 \begin{pmatrix} M_{ik} \end{pmatrix} + S \begin{pmatrix} C_{ik} \end{pmatrix} + \begin{pmatrix} K_{ik} \end{pmatrix} \end{bmatrix}^{-1} \quad (505)$$

The complex frequency response matrices are obtained by

$$\lim_{s \rightarrow i\omega} \left[(\delta_i^{(v)}) \right] = \left[H_i^{(k)}(\omega) \right] ,$$

or

$$\left[H_i^{(k)}(\omega) \right] = \left[-\omega^2 [M_{ik}] + i\omega [C_{ik}] + [K_{ik}] \right]^{-1} . \quad (506)$$

This can be carried further, if desired, to forces in the structure and to stresses. For example:

$$\{F\} = [K_{ik}] \{\delta_i\} \quad (507)$$

and

$$\{f\} = [b] \{F\} = [b] [K_{ik}] \{\delta_i\} . \quad (508)$$

The power spectra of stress then are

$$\begin{aligned} \{\Phi_f(\omega)\} &= [b] [K_{ik}] \left[H_j^{(k)}(\omega) \right] [A_i] \left[\Phi_{p_{ik}} \right] [A_k] \left[H_j^{*(i)}(\omega) \right] \\ &\quad [K_{ik}]^T [b]^T \end{aligned} \quad (509)$$

where

f = stress

b = factor converting deflection to stress

k = deflection times stiffness.

The pressure power spectra can be calculated. Consider the following: The virtual work done on a panel by the acoustic pressure field is

$$\delta\omega = \int_0^a \int_0^b p(x, y, t) \sum_m \sum_n \Phi_{mn}(x, y) \delta q_{mn}(t) \quad (510)$$

where

x, y = coordinates

q = generalized deflection.

The generalized force in the mn mode is

$$Q_{mn}(t) = \frac{\partial(\delta\omega)}{\partial(\delta q_{mn})} = \int_0^a \int_0^b p(x, y, t) \Phi_{mn}(x, y) dx dy \quad (511)$$

By definition, the cross correlation of the generalized forces in two pairs of modes (mn and rs) is

$$\begin{aligned} R_{Q_{mn} Q_{rs}}(\tau) &= \lim_{T \rightarrow \infty} \frac{1}{2T} \int_T^T Q_{mn}(t) Q_{rs}(t+\tau) dt \quad (512) \\ &= \lim_{T \rightarrow \infty} \frac{1}{2T} \int_T^T \left[\int_0^a \int_0^b p(x, y, t) \Phi_{mn}(x, y) dx dy \right] \\ &\quad \left[\int_0^a \int_0^b p(x_1, y_1, t+\tau) \Phi_{rs}(x_1, y_1) dx dy \right] dt. \end{aligned}$$

Rearranging,

$$\begin{aligned} R_{Q_{mn} Q_{rs}}(\tau) &= \int_0^a \int_0^b \int_0^a \int_0^b \left[\lim_{T \rightarrow \infty} \frac{1}{2T} \int_T^T p(x, y, t) p(x_1, y_1, t+\tau) dt \right] \\ &\quad \Phi_{mn}(x, y) \Phi_{rs}(x_1, y_1) dx dx_1 dy dy_1 \quad (513) \end{aligned}$$

where a and b are dimension limits of the panel. The cross power spectrum of the generalized force is then

$$\Phi_{Q_{mn} R_{rs}}(\omega) = \frac{1}{\pi} \int_{-\infty}^{\infty} R_{Q_{mn} R_{rs}}(\tau) e^{-i\omega\tau} d\tau \quad (514)$$

Equation (502) is the basic equation for calculating panel response. This response is in terms of power spectral density. The weighting functions are obtained from equation (506). These weighting functions can be computed from laboratory measurements. The areas are easily obtained and the power spectra of the pressures are an input.

E. Application and Examples – Direct Steady State Forcing

1. LUMPED PARAMETER SYSTEMS

The analysis of a structure necessitates the selection of an idealized model of the structure. Most often this idealization consists of lumping the mass into discrete points and considering the remainder of the system weightless springs. The constructed model should have dynamic characteristics similar to the system under analysis.

Several lumped parameter analysis methods are available. One method, influence coefficients, was presented in some detail in Paragraph B.4. of this section. Other methods will be only briefly discussed in this paragraph since these methods are often discussed in detail in the common texts on vibration. These methods are:

- a. Stodola.
- b. Rayleigh or energy.
- c. Holzer and Myklestad.

a. Stodola Method

The Stodola method was originally developed to determine the lateral vibrations of turbine rotors, but can be extended as a method of obtaining either the bending or torsional natural frequencies and modes of nonuniform vibrating beams.

The Stodola method initially assumes a mode shape usually based upon static deflection. Starting with the inertial loading of the system, successive integrations produce the deflection of the beam due to dynamic loading. The process essentially consists of solving equation (394) by trial and without damping. An iteration or two utilizing previously calculated deflections as the assumed deflection converges to a constant ratio of the assumed deflections to the calculated deflections. The natural frequency of the first mode is found by multiplying the initially assumed frequency by the average of the ratios of the mass element deflections.

Consider a beam at any time t , the inertia loading is proportional to mass, frequency squared and the deflection curve $y(x)$. If a deflection curve $y(x)$ is arbitrarily chosen and ω arbitrarily set equal to unity, then a deflection curve can be determined by using the equivalent static load. Starting with the beam loading, successive integrations give the shear, bending moment, slope and deflection. The result will be $g_1(x)$, a new deflection curve. Using $y_1(x)$ as a deflection curve, the process of successive integration is repeated and another deflection curve, $y_2(x)$, is obtained. The operation is repeated until two successively determined deflection curves are of constant ratio to each other at each point on the beam. The final curve represents the fundamental mode of the beam.

b. Rayleigh Method

In Paragraph B. 2. of this section, the energy of a vibrating system was discussed. The energy method is combined with the procedure of successive iterations to form the Rayleigh method. In this respect the Rayleigh method is similar to the Stodola method.

If a beam is represented by a series of lumped masses W_1/g , W_2/g , $W_3/g \dots W_n/g$, and the system is considered to be conservative or undamped, the maximum strain energy can be determined from the work done by these loads. The first approximations are provided by determining the static deflections y_1 , y_2 , $y_3 \dots y_n$ and applying the deflections to the energy equations. For a lumped mass system

$$T_{\max} = \sum_{i=1}^n \frac{1}{2} \frac{W_i}{g} \omega^2 y_i^2 \quad \text{Kinetic energy} \quad (515a)$$

$$U_{\max} = \sum_{i=1}^n \frac{1}{2} W_i y_i \quad \text{Potential energy.} \quad (515b)$$

By equating equations (515a) and (515b), the frequency is established as

$$\omega^2 = g \frac{\sum_{i=1}^n W_i y_i}{\sum_{i=1}^n W_i y_i^2} \quad (516)$$

where

W_n = lumped masses

y_n = deflection at each mass.

The deflection can be determined for the first approximation by any one of several strength of materials methods. A second set of deflections is obtained from the resulting frequency, ω . The iterations are then continued until the desired accuracy is obtained.

c. Holzer Method

Holzer's method can be used to calculate higher modes in addition to the fundamental mode. In this outline of the Holzer method, a torsional model will be used.

Consider a vibration system represented by a series of disks connected by shafts of stiffness $K_1, K_2, K_3 \dots K_n$ and vibrating with frequency ω . The external torque required to maintain the vibration is zero at all system natural frequencies. The external torque required will not be zero for frequencies other than the natural frequencies. The amplitude of a disk is assumed to remain constant while an external torque is computed. If the external torque required to excite a system is plotted as a function of frequency, a natural mode will be identified at every point on the plot where the curve crosses the abscissa.

The Holzer method can be applied to both bending and torsional mode solutions; however, it is primarily used to solve torsional mode problems due to the laborious calculations required for bending mode solutions.

d. Myklestad Method

The Myklestad method is similar to the Holzer method in that a trial frequency must be assumed and, after including the mass and stiffness of the beam or shaft, a residual function results. This residual function may be a slope or bending moment. After two or more iterations a curve of the residual function, similar to the torque remainder curve of the Holzer method is plotted against the assumed frequency. The zero points of this function identify the natural frequencies of the system.

The procedure is more involved than the Holzer method because the assumed frequency must satisfy the four boundary conditions of bending moment, shear, slope, and deflection. For any assumed frequency, ω_n , the bending moment and displacement diagrams can be constructed to satisfy three of the four boundary conditions. By plotting the fourth boundary condition against ω , the natural frequency, ω_n , will occur when this remainder equals zero.

2. DISTRIBUTED PARAMETER SYSTEMS

Examples of mechanical systems that have their masses and elastic forces distributed are cables, rods, beams, plates, shells, membranes, etc.

Distributed systems have an infinite number of degrees of freedom and natural frequencies. Each natural frequency has an unique mode shape, which is known as its characteristic function or normal function. A transient or steady state forced vibration generally will excite many or all of these frequencies in combination. The net response of a particular point is the combined effect of all modes.

The differential equation for the transverse vibration of beams is derived as follows. Consider a beam of uniform section, weight and stiffness as shown in Figure 116. From Figure 116,

$$dV = -f(x)$$

$$\frac{dM}{dx} = V$$

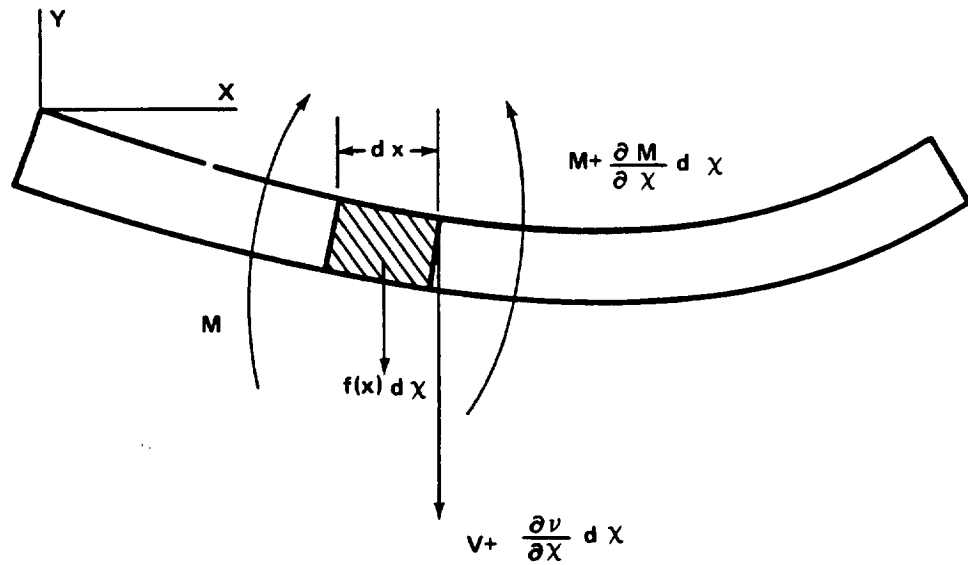


Figure 116. Beam element, free body section.

$$M = -EI \frac{d^2 y}{dx^2}$$

where

V = shear

M = bending moment

EI = flexural rigidity

$f(x)$ = distributed loads per unit length.

Combining the free body equations gives

$$\frac{d^2 M}{dx^2} = \frac{dV}{dx} = -f(x) \quad . \quad (517)$$

Therefore

$$\frac{d^2}{dx^2} \left(EI \frac{d^2 y}{dx^2} \right) = f(x) \quad . \quad (518)$$

The distributed load $f(x)$ on the beam is the inertia load and equals the product of its mass and acceleration. Its direction is opposite to the acceleration so that

$$f(x) = -\frac{w}{g} \frac{\partial^2 y}{\partial t^2} \quad . \quad (519)$$

If the beam vibrates harmonically and the acceleration is $\omega^2 y$, then the distributed load $f(x)$ becomes

$$f(x) = \frac{w}{g} \omega^2 y \quad . \quad (520)$$

Thus, the differential equation for a distributed parameter beam is

$$\frac{d^4 y}{dx^4} - \frac{w}{g} \frac{\omega^2}{EI} y = 0 \quad .$$

From differential equations a solution of the type

$$y = X(x) T(t) \quad (522)$$

can be assumed. Substituting this equation into the fourth order differential equation gives the result

$$\frac{X^{IV}(x)}{X(x)} = \frac{W}{gEI} \frac{T^{IV}(t)}{T(t)} = -\lambda^2$$

where λ is a constant. Thus, two linear homogeneous differential equations are obtained

$$X^{IV}(x) + \lambda^2 X(x) = 0 \quad (524)$$

$$T^{IV}(t) + \lambda^2 \frac{gEI}{w} T(t) = 0 \quad . \quad (525)$$

The general solution of equation (523) is

$$X = C_1 e^{\lambda x} + C_2 e^{-\lambda x} + C_3 e^{i\lambda x} + C_4 e^{-i\lambda x} \quad (526)$$

and expressed in terms of trigonometric functions is

$$X = B_1 \cosh \lambda x + B_2 \sinh \lambda x + B_3 \cos \lambda x + B_4 \sin \lambda x \quad . \quad (527)$$

The values of the constants can be determined for any given type of beam from the boundary conditions. For a deflected beam y is the deflection, dy/dx is the slope, d^2y/dx^2 is a function of the bending moment, and d^3y/dx^3 is the shear function. The end boundary conditions depend on the type of supports that are used for the beam. The four main categories of end boundary conditions are pinned, clamped, sliding and free.

An illustration of the determination of natural frequencies and mode shapes of a uniform beam follows. Assume a beam of length L and pinned at both ends. The boundary conditions for a pinned end beam are: When $x = 0$ or $x = L$, then $y = 0$ and $d^2y/dx^2 = 0$. For the assumed solution to satisfy these conditions, it is necessary that XT vanish when $x = 0$ or $x = L$ for all t and that $T'(0) = 0$, where $T'(0)$ is the initial velocity of any point along the length of the beam. Since the beam is at rest, initially, $T'(0)$ must be zero. Substituting these conditions into equation (527) gives

$$B_1 + B_3 = 0$$

$$B_1 = B_3 \quad .$$

Therefore, B_1 and B_3 are zero and

$$X = B_2 \sinh \lambda x + B_4 \sin \lambda x \quad .$$

For the other boundary condition $y = 0$ when $x = L$ and $d^2y/dx^2 = 0$ the results are as follows:

$$X = 0 = B_2 \sinh \lambda L + B_4 \sin \lambda L$$

$$X'' = 0 = B_2 \lambda^2 \sinh \lambda x - B_4 \lambda^2 \sin \lambda x \quad .$$

Thus,

$$B_2 \sinh \lambda L = 0$$

$$B_4 \sin \lambda L = 0 \quad .$$

Since $\sinh \lambda L$ cannot equal zero, B_2 must equal zero. Since the deflection of the beam is always zero when $x = L$, any values of λL whose sine equals zero will satisfy the equation. Therefore, the equation

$$B_4 \sin \lambda L = 0$$

is satisfied when $L = N$ since B_4 cannot always be zero. The letter N is the number of the natural frequency or mode shape. Now λ can be evaluated to be $\lambda = N/L$, and the first part of the assumed solution will be

$$X(x) = B_4 \sin \frac{N\pi}{L} x \quad . \quad (528)$$

Solving equation (525) by similar means and using the value of λ it can be shown that the second part of equation (522) is

$$T = C \cos N^2 \pi^2 \sqrt{\frac{gEI}{wL^4}} t \quad . \quad (529)$$

This gives the general solution as

$$y = B_N \sin \frac{N\pi x}{L} \cos N^2 \pi^2 \sqrt{\frac{gEI}{wL^4}} t \quad . \quad (530)$$

The value of B_N is the maximum displacement or the amplitude of the free vibration. It is dependent upon the initial conditions of displacement and velocity.

A similar analysis can be made on other types of beams if the end boundary conditions are known. The boundary conditions can be found in many vibration text books.

3. EXPERIMENTAL DETERMINATION OF SYSTEM PARAMETERS FOR THIN WALLED CYLINDERS

Under MSFC research contracts, analytic and experimental work was performed on thin walled cylinders with and without attached weights. Detail results of this work are described in References 40, 41, 42, and 43. In this paragraph a summary of the results are presented.

The program was directed toward the development of methods to predict dynamic responses of a pressurized-ring and stringer-stiffened cylinder to which concentrated mass items are attached. This type of structure is typical of a launch vehicle which is exposed to mechanical and acoustical random vibrations. The program combined analytical and empirical methods to predict frequencies and mode shapes of simple cases then continued to more complex structures.

In order to make a realistic analysis, experiments were conducted to determine the significant parameters contributing to the dynamic response of pressurized stiffened cylinders with and without attached concentrated mass. Some of the dynamic properties determined from experiments are summarized below:

a. The structural damping of the cylinder measured from test data was found to be low (generally less than one percent of critical).

b. The dynamic response of the unweighted pressure stiffened cylinder consisted of many non-sinusoidal circumferential waves involving the stringers and several longitudinal waves with modes at the frames. The stringers did not greatly influence modes at the higher modes.

c. As the magnitude of attached weights was increased, the modal response became increasingly localized. Treating the stiffened cylinder with an attached mass as a single-degree-of-freedom system, a simple empirical method was devised to calculate the fundamental frequency f.

$$f = \frac{1}{2\pi} \sqrt{\frac{K(386.4)}{W_e + W_a}} \quad (531)$$

where

W_a = added weight

W_e = effective cylinder weight

K = spring constant .

All parameters were empirically determined [40]. This empirical formulation is satisfactory in making a first estimate of the fundamental frequency. However, the model is considered incomplete and attempts to apply this formula outside the limited range of structural parameters from which they were derived is not recommended.

a. Analytical Methods and Assumptions

A more complete analytical method was developed to predict mode shapes and resonant frequencies of pressurized cylinders with ring frames, stringers, and attached mass. The analysis was substantiated by tests and supported by empirical data.

Two approaches were used to analyze the cylinder [43]. One approach considers the stringers as discrete elements (discrete analysis) supporting the shell and the other assumed the stringer spread uniformly over the surface to produce an orthotropic shell. The dynamic analysis of the ring and stringer stiffened pressurized cylinder was based upon the energy method using Lagrange's equation (Paragraph B.3. of this section).

$$\frac{d}{dt} \left(\frac{\partial T}{\partial \dot{q}_i} \right) + \frac{\partial U}{\partial q_i} = 0 \quad (532)$$

where

T = potential energy of the system
 U = kinetic energy of the system
 q = generalized coordinates
 i = 1, 2, 3 .

From an assumed vibratory motion of the structure, the potential and kinetic energy excursions from the initial pressurized state were determined for the cylinder with no attached weight. The potential energy of the system is the integrated strain energy of the shell, stringers, and rings. The total kinetic energy is the integrated kinetic energy of the shell, stringers, and rings.

The frequencies and mode shapes of cylinders with an attached weight, ΔW , were determined by accounting for the potential and kinetic energy of the added weight for each mode, combining with the potential and kinetic energies for orthogonal modes of the cylinder and applying the results to Lagrange's equation. The displacements of the attached weight were expressed in terms of the generalized model function at the point of attachment. The assumed mode shapes were of the form

$$\mu = q_{kl}^{(1)} \cos k\theta \cos \lambda_1 x$$

$$V = q_{kl}^{(2)} \sin k\theta \sin \lambda_1 x$$

$$W = q_{kl}^{(3)} \cos k\theta \sin \lambda_1 x$$

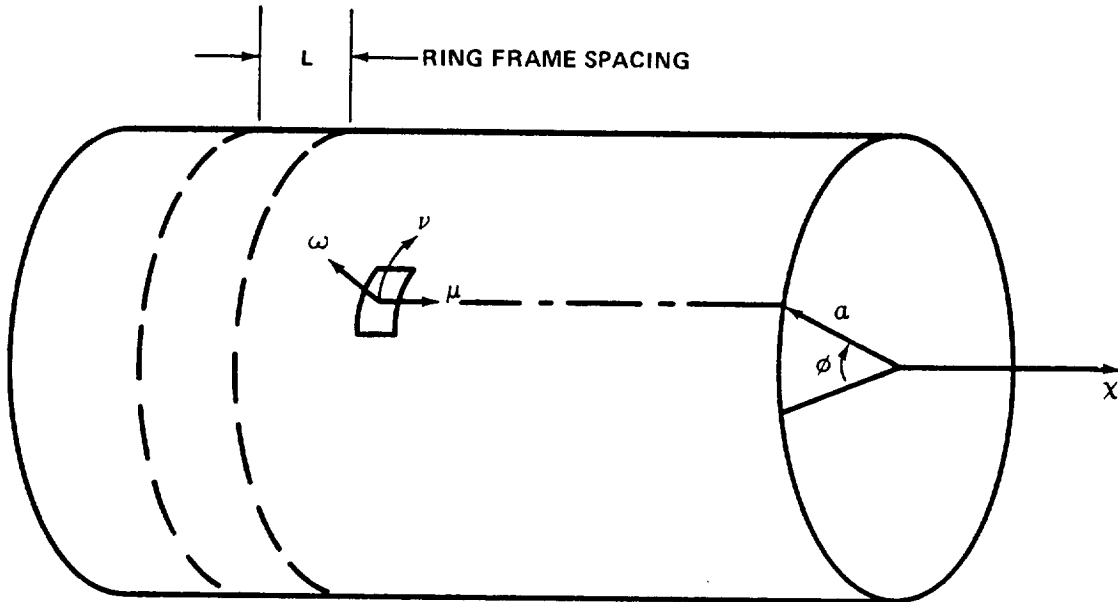
where

$q_{kl}^{(i)}$ = generalized coordinate (function of time only)

$i = 1, 2, 3$

k and l = circumferential and longitudinal wave numbers, respectively.

Figure 117 illustrates the cylinder geometric and displacement field.



NOTE:

CYLINDRICAL COORDINATE $\phi \ a \ \chi$
 CORRESPONDING DISPLACEMENTS $v \ \omega \ \mu$
 RADIUS a = CONSTANT

Figure 117. Cylinder geometry and displacement field.

For the actual analysis, assumptions were required. Classification of these assumptions led to two types of analyses: discrete and orthotropic.

1. Discrete Analysis

For the discrete analysis, the energy due to the stringers are summed with the skin energy. Specific assumptions for this analysis include:

a. The shells are considered thin and Love-type strain-displacement relationships with Donnell large deflection terms are used to account for nonlinear effects due to pressurization.

b. The nonlinear effects caused by pressurization arise from an axisymmetric static stress state within the cylinder (i.e., membrane stresses developed in the skin). The effects of pressurization adequately included without considering localized bending due to rings, end fixity, or stringers.

c. The ring frames are considered sufficiently rigid such that their potential energy is negligible in comparison to the stringer and shell potential energies.

d. The frequencies for unweighted, stiffened cylinders can be predicted by employing the mode shapes of unstiffened cylinders with Rayleigh-Ritz energy methods.

e. The resulting eigenvalue equations may be linearized while still retaining nonlinear effects.

2. Orthotropic Analysis

For the orthotropic analysis, the mass and stiffness of the stringer and the skin are combined to form an orthotropic shell. The orthotropic shell is then treated as a single thickness cylinder. Two additional assumptions are required for the orthotropic analysis:

a. The stringers are sufficiently small and closely spaced such that their stretching and bending stiffnesses and mass contribution can be "smeared out" uniformly (with the skins) around the cylinder.

b. The nonlinear effects caused by pressurization can be obtained from the axisymmetric static stress state of the combined stringer and the shell idealizations. This assumption replaces the second assumption listed under discrete analysis.

Using either the discrete or orthotropic analysis, the kinetic and potential energies are idealized and the summations of the energy terms are applied to Lagrange's equation (Paragraph B.3. of this section). The resulting equation in matrix form is

$$\omega_c^2 \left(\begin{bmatrix} & 0 \\ M_j & \end{bmatrix} + [\Delta M] \right) \{q_j^{(3)}\} = \begin{bmatrix} & 0 \\ m_j \omega_j^2 & \end{bmatrix} \{q_j^{(3)}\} \quad (533)$$

where

ω_c = the resonance of the cylinder coupled with the attached weight

$\begin{bmatrix} & 0 \\ M_j & \end{bmatrix}$ = the diagonal dynamic matrix associated with the cylinder structure

$[\Delta M]$ = the matrix associated with the attached weight

$\{q_j^{(3)}\}$ = the generalized normal coordinates

$\begin{bmatrix} & 0 \\ m_j \omega_j^2 & \end{bmatrix}$ = the product of the diagonal dynamic matrix and the eigenvalue ω_j^2 for the unweighted cylinder for each j^{th} mode or j^{th} l, k combination.

For the unweighted cylinder, eigenvalues, ω^2 , and eigenvectors, $q^{(i)}$, were first determined for various values of l and k. M_j and ΔM were then computed and inserted into equation (533). The n by n system of algebraic equations, represented by equation (533), was solved for the coupled eigenvalues, ω_c^2 , and the eigenvectors, $q_j^{(3)}$, using a computerized iteration scheme [42].

In the following paragraphs, comparisons are made of analytical and experimental results. The conditions under which the analytical assumptions are valid are discussed for both the discrete and orthotropic approach. For cylinders having a large attached weight compared with the cylinder stiffness on improved analysis, see Paragraph E.3.c. of this section.

Test methods and the approach to testing used for these analyses are presented in the references. The following paragraphs present discussions of the results of the tests and analytical work for dynamic response of cylinders with stringers and attached weights, response of cylinders to discrete frequency mechanical excitation and response of cylinders to acoustic excitation.

b. Effect of Stringers and Attached Weight

The dynamic response analysis of a stiffened, pressurized cylinder with attached concentrated weights using Lagrangian energy methods, gave satisfactory results when applied to cylinders with many stiff stringers. This method also gave satisfactory results when applied to stringerless cylinders and cylinders with rings but without stringers, the analysis loses accuracy as the attached weight increases. The large discrepancy in predicted frequency and mode shape due to heavy weights was attributed to the slow convergence of the trial modes used to represent the sharply cusped response of the cylinder in the immediate vicinity of the weight. The frequency calculations for the unstiffened cylinder appear highly sensitive to small discrepancies in the longitudinal mode shape. Agreement of experimental and theoretical natural frequency was poor for the fundamental frequency, but good at the higher modes. This was attributed to the sensitivity of fundamental frequency to small changes in added weights which strongly effects the local mode shape.

For cylinders with stringers, the increased stiffness somewhat reduced the large error in predicting the longitudinal mode shape especially in the localized area near the added weight. Thus, the assumed mode shapes appear satisfactory for stringer stiffened cylinders even with the heavier attached weight. Trial mode shape functions with more rapid decay in the longitudinal direction may improve predictions for the unstiffened cylinder.

Test results on the cylinder with only ring frames confirmed that the rings were sufficiently rigid to contain the responses within the bay that was dynamically excited. Therefore, isolating a single bay between rings (assumption c) and performing the analysis as a ringless cylinder of shorter length was justified.

From the discrete stringer analysis the unweighted cylinder had the fundamental frequency occurring at $k = 12$ circumferential full waves, with antinodes at each stringer. The orthotropic analysis did not show this. Other than the fundamental resonance there seemed to be little relation between the number of shell stringers and k , the number of circumferential waves.

The results of a parametric study demonstrated the importance of a discrete analysis when few stringers are present in the structure. The simpler orthotropic analysis was satisfactory only when a "sufficient" number of stringers were employed in the stiffened cylinder. It is difficult to define what a "sufficient" number of stringers is because it depends on the stiffness ratio of stringer to shell, spacing, and other factors. The substitution of the simpler orthotropic model for the discrete stringer-shell idealization must be made with caution.

c. Improved Analysis

In order to improve the accuracy of the analysis technique, another analysis [41] was developed to predict the dynamic response of a ring stiffened pressurized cylinder with attached concentrated weight but with no stringers. This improved analysis was directed toward reducing the large error in predicting the highly cusped localized response of stringerless cylinders in the vicinity of the attached weight.

This analysis employs a variational technique and the principle of minimum potential energy to form the equations of motion and boundary conditions. Love's first approximation and Donnell type nonlinear terms were assumed for the strain-displacement relations.

A computer program [43], based upon the improved analysis, is presently capable of computing the resonant frequencies of pressurized cylinders with ring frames and attached mass. Mode shape prediction, also a part of the program, has not yet been completed. Analytical and experimental fundamental resonant frequency results show good agreement for all weights considered and for mid bay and quarter bay attachment points between ring frames. Satisfactory predictions require a Fourier series order of truncation $N^* = 75$.

d. Response to Discrete Frequency Mechanical Excitation

An analysis was developed [41] to express the steady state response of a cylinder shell to applied external sinusoidal forcing functions using the method of normal modes and energy methods. The derivation considered an unloaded cylindrical shell with damping and was extended to include the effects of added concentrated weights. This analysis was used to predict driving point and transfer mobilities versus frequency.

Driving point mobilities showed fair correlation with experimental results at frequencies below the above resonance. Transfer mobility correlated poorly with experimental values. Since only the fundamental mode shape value of the transfer point was considered, knowledge of the shell modes in the vicinity of the resonant frequency of the weight may be required in order to improve the accuracy of the transfer mobility prediction.

e. Response to Acoustic Excitation

The response analysis of a cylindrical shell for an acoustical pressure environment should include an area integration of the pressure over the surface of the shell, as well as an integration of the pressure over a frequency spectrum, if the acoustical environment is random. However, the test program has shown that when the shell is loaded with a relatively heavy discrete weight, the primary resonance is characteristic of a single-degree-of-freedom system. Only the shell surface in the vicinity of the mass has any appreciable responses. Therefore, an approximate analytical estimation of the response of a shell with a discrete mass to acoustic pressure excitation may be obtained by considering only a small shell surface in the vicinity of the mass. It appears that if the shell is excited acoustically within this small shell area, the response of the mass at its resonant frequency should not differ markedly from that obtained in an acoustic environment encompassing the entire shell. An analysis was developed [41] to estimate the velocity response of the discrete mass to acoustic noise, channeled within a square area that includes the mass.

1. Discrete Frequency Acoustic Excitation

Acoustic tests were conducted [41] using discrete frequency acoustic noise, directed at 232.25 cm^2 (36 in.^2) area containing a concentrated weight. Correlation of predicted results was fair considering the accuracy of measured data and the difference between the assumed point loading on the weight and the distributed (pressure) loading over an area. Also, the analysis assumes that the weight responds as a single-degree-of-freedom system and coupling of higher frequency modes are negligible. Part of the difference between experimental and analytical results may be attributed to these higher frequency modes.

2. Random Acoustic Excitation

The response of the cylinder excited by a reverberant random acoustic excitation was predicted [41] based upon a transfer function obtained from the discrete frequency acoustic tests.

The predicted rms response of the weight was $0.19 G_{rms}$ as compared to the experimental value of $0.64 G_{rms}$. The disagreement between the experimental and predicted response may be attributed to the following factors:

a. The prediction of the response of the weight was based on the assumption that the transfer function obtained from the sinusoidal acoustic test was an estimate of the transfer function. This is predicted on the assumption of linearity of the steady state response of the weight to a sinusoidal pressure excitation of the cylindrical shell; i.e., that the ratio of g/psi is constant for any amplitude of pressure excitation. However, the shell characteristics may be such that a nonlinear relationship exists between the acceleration response and the acoustic pressure excitation, resulting in a departure from the transfer function used in the analysis. It was also assumed that the transfer function obtained from the channeled sinusoidal acoustic horn test is an approximation to the transfer function of the weight excited by random acoustic environment encompassing the entire shell. While this is predominantly the case, it is to be expected that with more of the shell surface exposed to the acoustic environment (either random or sinusoidal), additional shell modes may affect the acceleration response of weight to the acoustic pressure environment.

b. The data used in the analysis were accurate to within ± 2 Hz on the frequency scale and to within ± 10 percent on the response scale. A shift in the noise by 1.5 Hz resulted in the predicted rms acceleration response of the weight from $0.19 g's$ (rms) to $0.31 G_{rms}$ compared to an experimental value of $0.64 G_{rms}$.

The utilization of the experimental transfer function obtained from the channeled sinusoidal acoustic noise in the reverberation chamber test did result in a prediction within a factor of two to four of the experimental rms response of the weight. (Recent studies of transfer functions obtained from acoustic test chambers indicate a variation due to the mode of testing; i.e., reverberant, free field, or progressive wave.)

f. Conclusions

Analytical and experimental studies summarized in these paragraphs and described in References 40 through 44, provide useful background on the understanding of the dynamic response of stiffened cylinders with attached weights. Analytical methods were developed to predict mode shapes and

natural frequencies. Experiments were addressed to the verification of system parameters used in the analysis.

4. EXPERIMENTAL DETERMINATION OF LOCAL STRUCTURE TO BE USED IN LABORATORY TESTING

The presentation in Paragraph 3. above covered the response of complete cylinders to acoustic impingement. The test cylinders were designed as research specimens to help identify the pertinent parameters required for analysis. In this paragraph structural approaches more typical of a large space vehicle are discussed. Both the segment approach and the model approach are presented.

Like the previous paragraph, this paragraph presents a summary of work performed under MSFC contracts. Detail reports of this work are in References 45 through 48.

Critical components, mounted to the shell structures of the present-day launch vehicles, are subjected to high vibration and acoustic environments during boost and atmospheric flight. Vibration testing is essential in establishing confidence in the successful operation of the components under these extreme environments. It would be economically advantageous to be able to vibration test these components using representative shell segments instead of testing large portions of the vehicle. An important aspect of any test requirement is to simulate the localized dynamic characteristics of the segment and the components. The purpose of this program was to investigate the feasibility of the segment test approach and to develop techniques in design and testing of shell segments (with mounted components) from typical large structures.

To evaluate the feasibility of the segment testing approach, analytical and experimental studies were performed on flexibly supported flat plates, models of complete shells of revolution, model segmented shells, a full-scale shell of revolution and a full scale segment. Structures from the Saturn V launch vehicle were used in this study. Model shells include the following portions of the Saturn V launch vehicle:

- a. Instrument Unit.
- b. S-II thrust cone structure and forward skirt.
- c. S-IC oxidizer tank upper bulkhead.

A rectangular plate is used to analytically and experimentally study the effects of various boundary and restraint conditions on dynamic response. Complete model shells were used to study dynamic responses and to estimate the boundary conditions for their segments. Model segments are used to verify design of the boundary restraints. Model results are correlated with data from full-scale tests on the complete cylindrical section and segments of the Instrument Unit.

a. Plate Boundary Restraint Study

The effects of boundary conditions on a test structure were investigated [45] by studying dynamic response of a rectangular plate with various conditions of free edges and elastic point supports. This investigation also serves as a starting point for developing analyses for a segmented shell with point supports and concentrated weight attachments.

The finite difference method was used to solve the vibration problem of a flexible-point-supported plate. The plate was considered to have spring supports at discrete points along the edge of the plate. These supports were assumed to have spring and viscous damping restraint against deflection, but no restraint against rotation (no bending moment). To determine the natural frequencies and the corresponding mode shapes, loading was considered as inertial loading of the plate. Provisions can be made for additional loading due to concentrated mass attached to the plate.

The finite difference method transforms the partial differential equation and boundary conditions into a finite difference equation in terms of normal displacement at selected grid points. Additional grid points were used beyond the plate boundary. The problem was reduced to eigenvalue matrix formulation and the numerical solution of the final matrix equation yielded the modal and frequency data of the rectangular plate. The computer programs for the solution of the plate analysis are given in Reference 45.

A 50.8 x 60.96 x 0.317 cm (20 by 24 by 1/8 inch) rectangular aluminum plate, flexibly supported at discrete points, was tested to determine its natural frequencies and corresponding mode shapes. The supports had restraints against normal deflection but not against rotation. The spring stiffnesses and locations were varied to determine their effect upon response. The plate was mechanically excited.

It was found that the wave patterns and resonant frequencies of a plate which is continuously supported along its edges could be approximated for some modes by using discrete point supports.

Although the behavior of the plate close to the edges was unpredictable in many cases, the behavior in the interior of the plate was, in general, predictable. The detail test results, given in Reference 45, strongly suggest the desirability to use the finite difference method to analyze flexibly supported rectangular plates and segmented shells. Also, simulating continuous boundary conditions of segmented shells with the more practical discrete point supports is justified.

b. Shell Dynamic Analysis

To investigate the overall shell dynamic behavior prior to segmentation, four scale models were fabricated based on various parts of Saturn V structures. Duplicate models were made for segmentation purposes. The scale models which were manufactured and tested are listed below:

- a. Instrument Unit, 1:6.67 scale.
- b. S-II thrust cone including simulated rocket engines, 1:10 scale.
- c. S-II forward skirt including LOX tank upper bulkhead, 1:10 scale.
- d. S-IC LOX tank upper bulkhead including partial cylindrical shell structure, 1:10 scale.

The detail technique in scale model design is described in Section V of Reference 46. Structural details and experimental data on the models are given in Reference 45.

Analytical and experimental programs were conducted to determine the vibration and dynamic response behavior of the shell structures. In the analytical phase, partial differential equations were established along the shell meridian. The dependent variables include three displacement components, the angle of rotation and the four shell internal stress components in the same directions as the four displacement variables.

The stress variables are the transverse shear, the membrane stresses and the meridian bending moment. For each circumferential harmonic number, the equations were solved numerically to yield proper modal and frequency

data. The dynamic effects of the stringers and the ring stiffeners were handled differently. For the stringers which were located along the shell meridians, their stiffness was averaged and merged with the shell to form a mean stiffness. For the ring stiffeners, the dynamic impedances were formulated individually. The impedances were represented in terms of the increments of the shell internal stresses as functions of the local displacements. These increments were introduced into the differential equations at the ring stiffener locations during numerical integration. The computer program to execute the integration and typical modal and frequency data for shell structure models are presented in Reference 47.

In the experimental phase, the complete model sections, with and without mass attachments, were subjected to the same external discrete frequency forcing function. The resonant frequencies, mode shapes of the basic structure and acceleration measurements of the lumped masses simulating the shell components were recorded. For each point of mass attachment, a measurement of mechanical point impedance was made over the frequency range of interest for use in verification of dynamic similarity of partitioned models. The strain response along lines of planned segmentation were determined using the analytical program. This provided information necessary to define the edge reactions of segmented structures.

As would be expected, the natural frequencies for the loaded shell models were shifted to lower values as compared to the unloaded models. In many cases the general patterns of both the response and impedance plots were essentially unchanged in the frequency range of up to 500 Hz except for the frequency shift. At higher frequency the attached mass appears to suppress the response.

A comparison of experimental results with analytical prediction is not made in Reference 45. Perhaps this comparison is made in Reference 27 which was not available at the time this summary prepared.

c. Shell Scale Model Design Procedure

To design shell scale models for dynamic investigation, it is important to establish specific similitude relations. The similitude relations are used to define dimensions, materials, mass, stiffness and other parameters in model design. They are also used to interpret the model dynamic response data and to predict the corresponding responses in the full scale structure.

A number of scale models were designed and tested. In one case, the scale dynamic response data were compared with the full scale structure data. In general, the procedure has been found satisfactory and should be useful in applying to other shell structures. Vibration tests on full scale segmented shell structure with mounted components were successfully conducted by making use of the scale model data acquired previously. The general scaling laws and considerations are described in Section V of Reference 46.

d. Segmented Shell Dynamic Analyses, Design, and Test

The vibration analysis [48] of a flexibly supported shell segment is a generalization of the finite difference technique applied to the rectangular plate. A cross stiffened shell element with attached masses and flexible supports were formulated into equilibrium equations. Grid points were assumed which covered the shell segment and the neighboring areas. The matrix formulation and numerical solution are illustrated in Reference 48. A modified and improved finite difference computer program is given in Section II of Reference 46. Design and test results of segmented shells are given in Reference 48. In general, the analytical data generated by the computer program compared favorably with the test data.

e. Conclusions and Recommendations

The feasibility of performing vibration tests on shell mounted components using a segmented shell structure has been demonstrated. A design procedure and related guidelines necessary to use the segmented shell test approach for large structures was formulated by combining analytical studies with scale model and full scale experimental investigations.

Experimental results indicate that the method of controlling structure response amplitudes is dependent on the inherent damping in the segmented specimen. For structures where sufficient friction and damping exist, no additional damping devices are needed to control vibration amplitudes. For structures where the inherent damping in the segmented piece is relatively small, vibration amplitudes may be controlled by regulating the input vibration level. Where damping is small, damping devices may be installed at the supporting points to control the response amplitudes. Also, when segmenting a structure, the design and location of the flexible supports have a significant effect on the dynamic responses of the structure. Therefore, when considering vibration tests on large and expensive structures, it is advisable to conduct a scale model investigation prior to final segment selection and edge support design and fabrication.

In the vibration test performed, mechanical vibration inputs were applied by attaching the exciter directly to the specimen. Inputs were controlled by monitoring amplitude at selected locations. In certain tests it may be desirable to mount the flexibly-supported specimen on a very rigid fixture and apply vibration through this fixture. It is expected that the same basic design criteria and techniques for the specimen are also applicable when rigid fixtures are used.

The analytical study on the modal responses of the complete and segmented shell supplied a guideline and gave insight to the problems involved. The finite difference method possesses desirable features in dealing with singly and doubly curved shell structures and proved applicable to investigating the modal behavior of a segmented and flexibly-supported shell.

When selecting shells for segmented component qualification tests, it is advisable to start with hardware where substantial experiences have been accumulated from tests of unsegmented structures. By combining these resources with the developed analytical techniques and scale model experiments, considerable savings in time and costs may be realized in conducting vibration tests on segmented shells of large structures.

F. Equivalent Systems

An equivalency between mechanical, electrical and acoustical systems will be presented in this paragraph. Mechanical and acoustical systems are often presented and studied by means of their equivalent electric circuits partly for experimental reasons and partly for convenience. The equivalent electrical system is obtained by comparing the equations of motion for the mechanical and acoustical systems. Systems are analogous if their differential equations are mathematically the same. When the differential equations are the same, the corresponding terms in each of the equations are analogous.

1. PRINCIPLES OF EQUIVALENCY

Equivalency between mechanical, electrical and acoustical systems originate from two fundamental laws:

- a. D'Alembert's principle for the mechanical and acoustical system.
- b. Kirchoff's law for the electrical system.

D'Alembert's principle states that the sum of the forces applied to a body are zero. Kirchoff's laws state that the sum of all voltages around any closed circuit is zero, and the sum of the currents entering a point is equal to the sum of the currents leaving the point. The latter statement is analogous to the statement that the charge does not collect at the point.

Using D'Alembert's principle the differential equation for the mechanical and acoustical system is derived. For the mechanical system

$$m\ddot{x} + r_m \dot{x} + \frac{1}{C_m} x = F e^{i\omega t} \quad (534)$$

where

m = mass
 r = mechanical resistance
 C_m = mechanical compliance
 $F e^{i\omega t}$ = applied force.

For an acoustical system consisting of an enclosed container with an opening subjected to an oscillating force,

$$M\ddot{X} + r_A \dot{X} + \frac{1}{C_A} X = P e^{i\omega t} \quad (535)$$

where

M = inertance
 r_A = acoustical resistance
 C_A = acoustical capacitance
 $P e^{i\omega t}$ = external applied acoustical pressure.

For an electrical circuit consisting of an inductance, resistance and capacitor in series, the equation of motion obtained by using Kirchoff's laws

$$L \ddot{q} + r_e \dot{q} + \frac{1}{C_E} q = E e^{i\omega t} \quad (536)$$

where

L = inductance
 r_e = electrical resistance
 C_E = electrical capacitance
 q = charge
 $E e^{i\omega t}$ = voltage.

All of the above equations have a common form

$$S \ddot{X} + R \dot{X} + \frac{1}{C} X = H e^{i\omega t} \quad (537)$$

The solution to this equation in terms of the first derivative of the dependent variable is given by

$$\dot{X} = \frac{H e^{i\omega t}}{R + i \left(\omega S - \frac{1}{\omega C} \right)} \quad (538)$$

The equation may be put in a different form by multiplying both numerator and denominator by the complex conjugate of the denominator.

$$\dot{X} = \frac{H R - i \left(\omega S - \frac{1}{\omega C} \right) e^{i\omega t}}{R^2 + \left(\omega S - \frac{1}{\omega C} \right)^2} \quad (539)$$

or

$$\dot{X} = (L + iN) H \quad (539a)$$

The impedance for the system is defined

$$Z = (L + iN)^{-1} \quad \text{Impedance}$$

and

$$ZX = H \quad (540)$$

Thus, the impedance equation represents a common parameter applicable to mechanical, acoustical and electrical systems.

2. IMPEDANCE AND MOBILITY

The impedance is defined to be the complex ratio of voltage to current for the electrical system, force to velocity for the mechanical system and volume velocity to sound pressure for the acoustic system. The impedance for a system is a characteristic quantity for the system and is independent of other systems that may be connected to it. Therefore, the impedance is a very useful quantity to describe a particular system.

Mobility is defined for the acoustic system to be the complex ratio of sound pressure to volume velocity which is the reciprocal of the impedance. For a mechanical system, the mobility is the complex ratio of the velocity to the force. For an electrical system, the mobility is the complex ratio of the current to the voltage and is called admittance.

Since new elements may be deleted or added without rewriting a complete set of new equations, impedance and mobility are two important quantities for a systems analysis.

Considering any combination of mechanical, acoustical, or electrical systems, satisfying equation (540), the total impedance can be obtained by direct addition or reciprocal addition. For a series connection the impedances are directly added, and for a parallel connection the reciprocals of the impedances are added to obtain the reciprocal of the combination. If mobility is used, the parallel connection is summed by direct addition, and the reciprocal of the total mobility is obtained by adding the reciprocals of each portion.

The full exploitation of the impedance/mobility approach in testing demands very careful measurement. Significant progress has been made in developing experimental methods for measuring impedance.

3. GENERAL DISCUSSION OF EQUIVALENT SYSTEMS

In addition to the specific equivalent relationships through mechanical impedance in equation (540), other equivalencies are used. All of these equivalencies are, of course, related by the proper conversions.

a. Electrical Analogies to Mechanical Systems

There are two electrical analogies for mechanical systems:

1. The voltage force or mass inductance.
2. The current force or mass capacitance.

The current-force analogy has the advantage that both the electrical circuit and the mechanical circuit are of the same form. The following tabulation from Reference 49 presents the analogous quantities between the electrical system and mechanical system.

Mechanical System	Electrical System	
	Voltage-force Analogy	Current-force Analogy
D'Alembert's principle	Kirchhoff's voltage law	Kirchhoff's current law
Degree of freedom	Loop	Node
Force applied	Switch closed	Switch closed
F Force (lb) nt	v Voltage (volt)	i Current (ampere)
m Mass (lb-sec ² /in.) kg	L Inductance (henry)	C Capacitance (farad)
z Displacement (in.) m	q Charge (coulomb)	$\Phi = \int v \, dt$
\dot{x} Velocity (in./sec) m/sec	i Loop current (ampere)	v Node voltage (volt)
c Damping (lb-sec/in.) N/M	R Resistance (ohm)	1/R Conductance (mho)
k Spring (lb/in.) g/m	1/C 1/Capacitance	1/L 1/Inductance
Coupling element	Element common to two loops	Element between nodes

In using the voltage-force analogy, if the mechanical elements are in series, the electrical elements are in parallel. If the mechanical elements are in parallel, the electrical elements are in series.

For the current-force analogy, the mechanical elements are in series when the electrical elements are in series and a similar scheme exists for elements in parallel. In the current-force analogy, velocity across is analogous to voltage across and force through is analogous to current through.

b. Acoustical Circuits

Acoustical circuits are usually more difficult to represent pictorially than mechanical or electrical circuits because the circuit elements are more difficult to identify. One of the analogies between acoustic and electrical systems is to choose pressure analogous to voltage and a volume velocity analogous to current. This seems to be a reasonable choice since a volume of fluid flows through the acoustic element and there exists a sound pressure differential across the element.

c. Acoustic Mass

Acoustic mass is a quantity proportional to mass but has the dimensions of km/m^4 . It is associated with a specific mass of air accelerated by a net force which acts to displace the gas without appreciably compressing it. The important idea here is acceleration without compression. An acoustic mass may be represented by a tube filled with gas. Using Newton's second law for the mass,

$$P(t) = M \frac{dU(t)}{dt} \quad (541)$$

where $P(t)$ is the instantaneous pressure difference in $\text{Newton's}/\text{m}^2$ between the ends of the mass undergoing acceleration, M is the acoustic mass in km/m^4 of the gas undergoing acceleration and $U(t)$ is the instantaneous volume velocity of the gas in cubic meters per second across any cross-sectional plane in the tube. The steady state value for P is

$$P = j\omega MU \quad (542)$$

where P and U are complex quantities in rms.

d. Acoustic Compliance

Acoustic compliance is expressed in m^5/N . It is associated with a volume of air that is compressed by a net force without an appreciable average displacement of the center of gravity of air in the volume. This acoustic element is represented by an enclosed volume of air V with an opening for entrance of pressure variations. In equation form

$$P(t) = \frac{1}{C} \int U(t) dt \quad (543)$$

where C is the acoustical compliance.

e. Acoustical Resistance and Acoustical Responsiveness

An acoustic resistance is associated with the dissipative losses occurring when there is a viscous movement of a quantity of gas through a fine-mesh screen or through a small tube. The reciprocal of the acoustical resistance is the acoustic responsiveness. The pressure drop across this element is the acoustic responsiveness. The pressure drop across this element is

$$P(t) = R_A U(t) = \frac{1}{r_A} U(t) \quad (544)$$

where R_A is the acoustical resistance and r_A is the acoustic responsiveness.

f. The Acoustical/Electrical Analogy

Acoustic transmission systems are not analogous to mechanical systems in such a simple manner. Therefore, acoustical/electrical analogies will be discussed.

The two variables frequently used in the discussion of an acoustic transmission system are the sound pressure P at the particular surface and the volume V of gas through the surface due to acoustic pressure. The acoustic impedance (defined on a particular surface) is the complex quotient of P and V . Therefore,

$$Z = \frac{P}{V} \quad \text{or} \quad V = \frac{P}{Z} \quad (545)$$

which is similar to $I = E/Z_e$ in electrical circuitry. However, if the acoustic impedance Z_c were defined as the quotient of V and P

$$Z_c = \frac{V}{P} \text{ or } V = Z_c P \quad (546)$$

which is similar to the electrical equation

$$E = IZ_e \quad (547)$$

Therefore, the analogy between the acoustic and electrical circuit depends on how the acoustic impedance is defined. The two analogies are really impedance and mobility analogies. The difficulty that arises in the construction of the acoustic circuit is whether the elements are in series or parallel. As an example, suppose a number of transmission tubes terminate or originate in a common junction point. This is similar to a number of electric lines entering a common junction box which may be connected to either a series or parallel configuration in the box. If Z_c is defined as P/V then the transmission tubes appear to be in parallel since they experience the same sound pressure. However, if the impedance is defined as V/P , then the tubes seem to be in series for each has the same acoustic pressure again. One justification for using the impedance as P/V , which looks like $Z_e = E/I$ in electrical terminology, is that the sum of the volume displacements to any junction is zero. This is similar to Kirchoff's second law for the electromotive force around a mesh. For the analogy,

$$V = PZ_A \rightarrow E = IZ_e \quad (547a)$$

A tube with an open end is represented by an open circuited line, while a tube with a closed end is similar to a short circuited line. The analogy to choose is difficult; the literature states that the two analogies are about equal in useability.

G. Non-Linear Vibrations

Because of its complexity, non-linear effects in vibration are largely ignored by practicing engineers; however, the picture is changing. As the performance demands of space vehicles continually become more intense and

as materials having non-linear properties are introduced, a better understanding of these phenomena are likely to become necessary. Thus, this introduction to the subject is provided in the vibration manual. It is not the intent of this paragraph to provide practical methods for solving non-linear vibration problems, but to accomplish two objectives. First, the intent is to provide information leading to an understanding of the phenomena so it can be recognized intelligently and dealt with accordingly. Second, the introduction provided here will hopefully lead to an expanded study of the subject by the practicing engineers and eventually to a methodology of non-linear vibrations that can be normally applied to space vehicle problems. With this in mind, a separate bibliography on non-linear vibrations is provided in addition to the list of references.

1. GENERAL

Linear equations of vibrations, defined in Paragraph A.1. of this section, arise when the motions can be assumed small so that forces, such as the restoring force of a spring or damping, are linear in the displacement or velocity. As long as the results of such equations agree favorably with experiment, the equations are useful and have the advantage that new solutions may be derived by the appropriate superposition of a number of known solutions of the equations. When the amplitude of the driving force or the amplitude of vibration becomes large, and the results from the linear equations no longer agree with experiment, then this new behavior must be analyzed by non-linear equations.

Solutions to non-linear equations cannot be found with the generality of the linear solutions. Before resorting to numerical integration, however, it is profitable to investigate some of the properties of the solution graphically and analytically. For a single degree of freedom, the rough sketching of a trajectory starting with initial conditions in a velocity-displacement plane will indicate the possibility of periodic motion. For conservative systems, a first integral may be found without too much difficulty leading to energy surfaces whose singularities may reveal considerable information about the nature of the solutions. Such methods of attacking non-linear problems may be described as topological or geometric.

In most mechanical vibration problems, non-linear phenomena occur when the amplitudes become larger and the non-linear terms are associated with certain physical parameters which are usually small. The procedure of attacking such problems differs little from linear problems since this class of non-linear problems may be solved by perturbation methods such as

those of Poincare, Cylden and Lindstedt, and Kryloff and Bogoluiboff [50, 51] in which the equations are reduced to a set of linear inhomogeneous differential equations. Another method which is nearly equivalent, is the iteration method in which the linearized solution is substituted into the non-linear terms of the differential equations yielding a set of inhomogeneous linear equations.

The concept of mechanical impedance, which is the ratio of driving force to velocity expressed as a complex function of the frequency, does not carry over directly into non-linear problems. Response curves, in which the amplitude is plotted against frequency, and the trajectories as shown in the phase plane play a somewhat similar role in non-linear steady state vibrations as impedance provides in the linear case.

2. PHENOMENA CAUSED BY NON-LINEARITY

There are a number of phenomena which can be accounted for in no other way than by the consideration of non-linearity. Some of these are briefly outlined below and expanded in the subsequent paragraphs. It is often found, for example, that the vibration frequency of a system depends upon the amplitude of the vibration. It may be observed that a system driven at a particular frequency may also vibrate at a lower frequency which is an integral fraction of the driving frequency. This is referred to as subharmonic response. A related phenomenon is the combination frequencies. A non-linear system driven by two separate frequencies may exhibit not only frequencies which are multiples of the two driving frequencies but also frequencies which are the sum and difference of these frequencies. Another is the jump phenomenon. This can only be explained by the presence of damping with the non-linearity of a vibrating system. Such a non-linear system, driven at constant amplitude but with the frequency varying gradually over a given range, may suddenly jump to a different mode of vibration with a higher or lower amplitude. Reversing the frequency change will not necessarily cause the system to pass through the same mode of vibration but will produce a jump at a different frequency. For this reason, the jump phenomenon is also called "hysteresis resonance."

3. THE NON-LINEAR RESTORING FORCE

These phenomena and some of the methods of attacking non-linear equations by considering the differential equation for a mass supported by a spring with a non-linear restoring force are illustrated. For a single degree of freedom, the differential equation is given by

$$m d^2x/dt^2 + c_0 dx/dt + k_1x + k_2x^3 = 0$$

or

$$d^2x/dt^2 + c dx/dt + \omega_0^2x + kx^3 = 0 \quad (547b)$$

where x is the displacement, k_1 and k_2 the spring constants, c the damping constant, m the mass of the vibrating object, and t the time. The quantity ω_0 is the natural frequency of the linear system, and k is a constant that introduces the effect of a non-linear restoring force. The symbol k , as used here, should not be confused with the k used in previous paragraphs for the restoring force in the linear case.

If $k > 0$, then the spring is hard, while for $k < 0$, the spring is soft. The value $k = 0$ is the linear spring. If k is assumed small, then the equations may be described as quasi-linear, since the non-linear solution reduces, for vanishingly small values of k , to a solution of the linear equation.

4. ENERGY CURVES FOR CONSERVATIVE SYSTEMS (PHASE-PLANE)

For a conservative system where there is no damping, equation (547b) with $c = 0$ can be integrated once after multiplying the equation through by dx/dt . This leads to

$$(dx/dt)^2/2 + \omega_0^2x^2/2 + kx^4/4 = E \quad (547c)$$

where E is the total energy of the system. If $dx/dt = v$, then equation (544) becomes

$$\omega_0^2x^2 + kx^4/2 + v^2 - 2E = 0 \quad (547d)$$

This can be represented by a curve in the x, v plane for each value of E and fixed k or by a surface in the x, v, E space. When $k > 0$, all curves of constant E form a non-intersecting family of closed curves around the origin as seen in Figure 118. For the linear spring, these curves are ellipses. However, when $k < 0$, then the curves of constant E form closed curves only in the finite region containing the origin as seen in Figure 119. The origin in both Figures 118 and 119 is a singular point and is related to the minimum point on the energy surface in the x, v, E space. It corresponds to the minimum energy and is the greatest lower bound of E for which any motion of the system exists. This point is called a vortex point since a family of non-intersecting curves encircle it like the streamlines in a free fluid vortex.

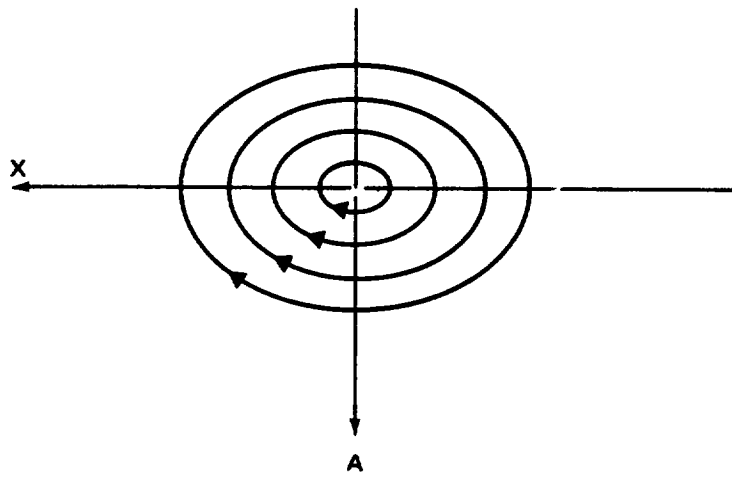


Figure 118. Lines of constant energy in the phase plane for the hard spring, $K > 0$.

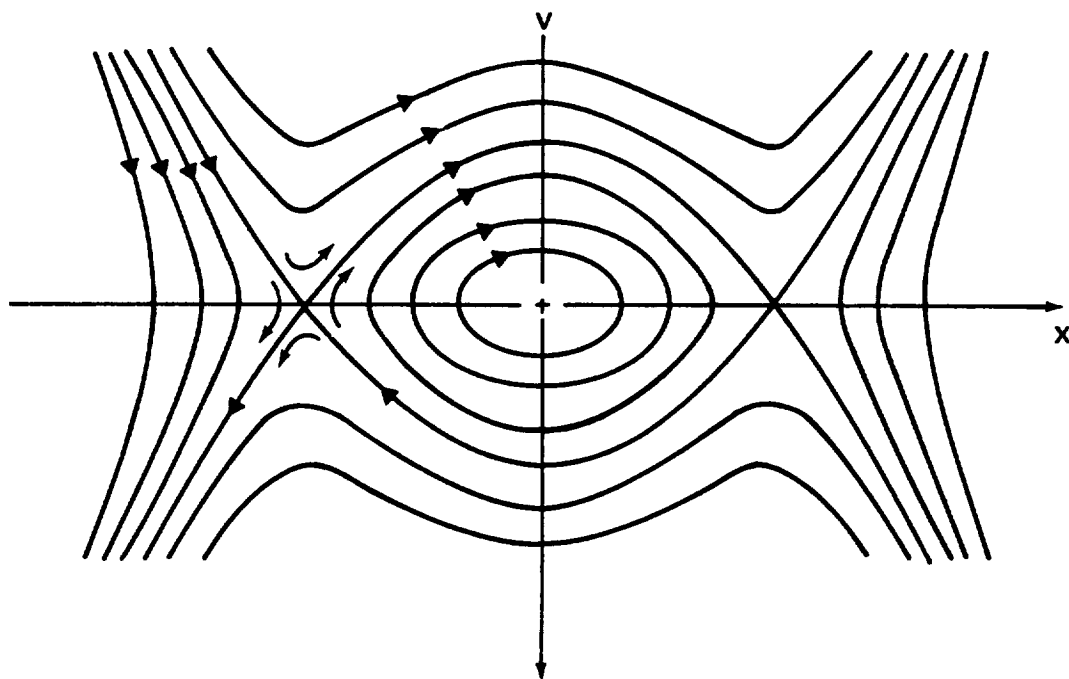


Figure 119. Lines of constant energy in the phase plane for the soft spring, $K < 0$.

The maximum displacement occurs when the velocity v vanishes. Solving for this value of x yields

$$x_m^2 = \left[-\omega_0^2 + \sqrt{-\omega_0^4 + 4Ek} \right] / k \quad . \quad (547e)$$

Note that maximum displacements occur for all values of E and ω for the hard spring, $k > 0$, for which all the trajectories are closed curves. However, for the soft spring, $k < 0$, the values of E and k must be restricted to

$$\omega_0^2 \geq -4Ek \quad . \quad (547f)$$

The equality with $v = 0$ designates the saddle points on the surface in the x, v, E plane of equation (544a). The curves of constant E passing through them in Figure 119 divide the plane into regions of periodic and non-periodic motion. For this reason, the curve is called a separatrix.

Because of the symmetry in ω and x , the time for a period in the oscillation is given by solving the energy equation for dv/dt and integrating with respect to x from 0 to x_m , or

$$T = 4 \int_0^{x_m} \frac{dx}{\sqrt{2E - \omega_0^2 + kx^2/2}} \quad . \quad (547g)$$

This may be easily expressed in terms of an elliptic integral by setting $x = x_m \cos \theta$. This leads to

$$2E - (\omega_0^2 + kx^2/2)x^2 \equiv \frac{k}{2} (x_m^2 - x^2) (b^2 + x^2)$$

$$\frac{k}{2} (x_m^2 - b^2) = -\omega_0^2$$

$$T = 4 \int_0^{\pi/2} \frac{d\theta}{\sqrt{kx_m^2 + 2\omega_0^2 + kx_m^2 \sin^2 \theta}} \quad . \quad (547h)$$

Note that when $k < 0$ the period increases with amplitude of vibration while for $k > 0$, the period decreases. The motion along the separatrix starting from $x = 0$ to the saddle point is vanishingly slow from the integrand it follows that the integral diverges when x_m^2 is set equal to $-\omega_0^2/k$.

When damping occurs no simple energy relation exists. For specific initial conditions, the x, v plane may be sketched by the method of isoclines or by numerical integration. These trajectories may spiral toward the origin indicating that the motion damps out eventually. The method of trajectories in the phase plane, although not furnishing a complete solution, gives much qualitative information on the nature of the solution. For motion with a single degree of freedom, the phase plane method is practical but it becomes more complicated when applied to systems having more degrees of freedom. These will not be treated here but similar methods for higher degrees of freedom were developed by Ku [52].

5. PHASE PLANE — LIMIT CYCLE

The phase plane method was applied by Van der Pol on an equation with non-linear damping in the form

$$m d^2x/dt^2 + k[(dx/dt)^2 - 1] dx/dt = 0 \quad . \quad (549)$$

In this equation true damping occurs for $dx/dt > 1$ and energy is supplied to the motion when the velocity is small. Thus, when motion occurs at small velocity the negative damping provides energy to the motion until the velocity increases to a point where the motion becomes highly damped and slows down rapidly. This type of oscillatory motion is called relaxation oscillation. Plotting the trajectories in the phase plane, Van der Pol discovered that when the motion was started at any point in the plane, the trajectory eventually coincided with a definite closed curve called a "limit cycle." For such a non-linear motion the eventual motion does not depend upon the initial condition of the problem but is determined by the limit cycle curve in the phase plane. If any trajectory starting from any point in the plane spirals to the limit cycle as the time t increases, then the motion is stable. A mechanical example of limit cycle oscillation is the simple escapement mechanism in a spring-wound clock or watch.

6. LIENARD PLANE

Another geometric method uses what is described as the Lienard plane. Consider the equation

$$d^2x/dt^2 + f(x) dx/dt + g(x) = 0 \quad (550)$$

and introduce the function

$$F(x) = \int_0^x f(x) dx \quad (551)$$

$$y = dx/dt - F(x) \quad (552)$$

In terms of x and y the differential equation may be expressed in the following form:

$$dy/dx = g(x)/[y-F(x)] \quad (553)$$

Levinson and Smith [53] showed that there is only one closed trajectory when the functions $F(x)$ and $g(x)$ have the following properties:

- a. All functions are continuous and $F(x)$ and $g(x)$ are odd in x where $g(x)$ has the same sign as x .
- b. $F(x)$ has a single positive zero x_0 , and for $x > x_0$ it increases monotonically and is positive.
- c. $F(x)$ goes to infinity with x .

7. ITERATION METHOD — RESPONSE CURVES

To illustrate the importance of damping in hysteresis resonance, the periodic solution of a driven non-linear spring and mass without damping is found. Usually the frequency of the driving force is known in advance of the solution but for this problem it is convenient to determine it later. Accordingly, equation (543) is written in the form

$$\ddot{x} + \omega^2 x = (\omega^2 - \omega_0^2)x - kx^3 + F \cos \omega t \quad (554)$$

Let the initial approximation be $x_0 = A \cos \omega t$. Then substituting this solution into the left right-hand side leads to the following equation for the second approximation x_1 :

$$\ddot{x}_1 + \omega^2 x_1 = \left[(\omega^2 - \omega_0^2) A - \frac{3kA^3}{4} + F \right] \cos \omega t - \frac{kA^3}{4} \cos 3\omega t \quad (555)$$

If x_1 is to be periodic, then the coefficient of $\cos \omega t$ must vanish since this term in the integration yields the secular term $t \cos \omega t$. Hence,

$$\omega^2 = \omega_0^2 + \frac{3kA^2}{4} - \frac{F}{A} \quad (556)$$

This relation gives the frequency of the driving force in terms of the amplitude of vibration and the amplitude of the driving force. Integrating equation (555) yields

$$x_1 = A \cos \omega t + \frac{KA^3}{32\omega^2} \cos 3\omega t \quad (557)$$

Response curves for the vibrations are obtained by plotting the amplitude of the vibration A versus frequency ω for constant values of the driving force. This is shown in Figure 120 for the hard spring and in Figure 121 for the soft spring. Note that the phase of the amplitude changes by π when the frequency changes from values below to values above the natural frequency of the linear system.

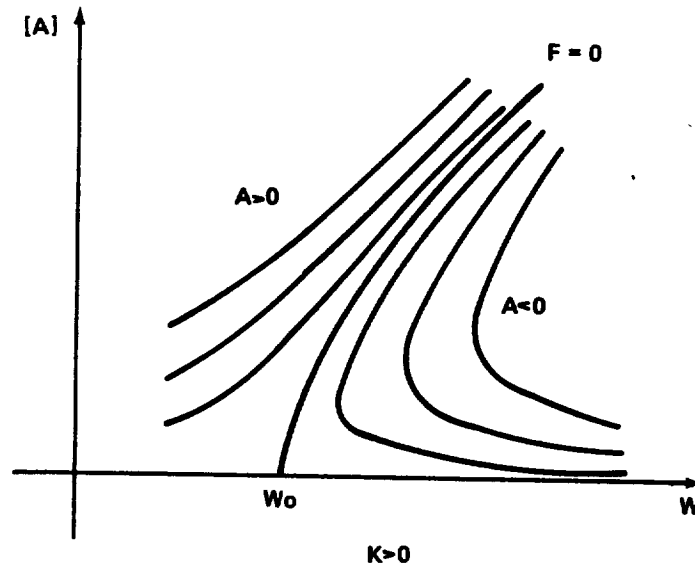


Figure 120. Response curves for the hard spring.

8. ITERATION METHOD WITH DAMPING-JUMP PHENOMENON

The effects of damping on the response curve for the non-linear spring will be considered next. There will be a change in phase between the driving

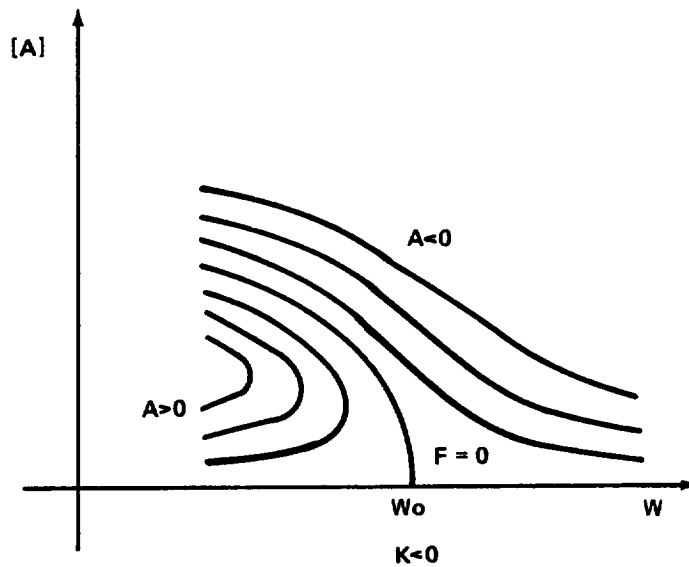


Figure 121. Response curves for the soft spring.

force and the response of the system due to the influence of viscous damping. The phase of the response was chosen leaving the phase of the driving force to be determined later. Accordingly, the equation becomes

$$\ddot{x} + c\dot{x} + \left(\omega_0^2 x + kx^3 \right) = H \cos \omega t - G \sin \omega t \quad . \quad (558)$$

Let $x = A \cos \omega t$ be the response. Substituting the approximation into the equation, using the trigonometric identity, $\cos 3x = 4 \cos^3 x - 3 \cos x$, and equating coefficients of $\sin \omega t$ and $\cos \omega t$ on the right and left sides of the equation yields

$$\begin{aligned} (\omega_0^2 - \omega^2) A + \frac{3kA^3}{4} &= H \\ c\omega A &= G \end{aligned} \quad . \quad (559)$$

From this it can be seen that with damping, no external force implies no motion since $A = 0$ from $H = G = 0$. The magnitude of the driving force is $F = G^2 + H^2$, and the equation for the response curves becomes

$$F^2 = \left[(\omega_0^2 - \omega^2) A + \frac{3kA^3}{4} \right]^2 + c^2 A^2 \omega^2 \quad . \quad (560)$$

The amplitude A for fixed values of F is plotted in Figure 122. Note that each curve of constant F has two vertical tangents. If for a given amplitude of the driving force the frequency is decreased, the amplitude will vary continuously until the first vertical tangent is reached at which the amplitude will jump to the higher value on the same curve (Fig. 123). The amplitude will vary continuously for lower values of frequency. However, when the frequency is increased again retracing the same curve, the amplitude will vary continuously until the first vertical tangent is reached at which the amplitude will drop suddenly to the value on the lower part of the curve as shown in Figure 123. Since the response of the system is not the same in the two directions of frequency variation, this phenomenon is often referred as hysteresis resonance.

9. SUBHARMONIC RESPONSE

In the iteration procedure for the equation without damping the additional iterations yield higher harmonics in the solution. Because of the presence of these higher harmonics, not found in the linear solution, it is possible to have a response of the system at a frequency which is a fraction of the driving frequency. This phenomenon is called subharmonic response. Since the frequency at which this phenomenon occurs is not known, then the variable $\theta = \omega t$ is introduced. The differential equation then becomes

$$\omega^2 x'' + \omega_0^2 x + kx^3 = F \cos \theta \quad . \quad (561)$$

Consider a solution in the form

$$x = \sum_{n=1}^{\infty} a_n \cos \frac{2n-1}{3} \theta \quad . \quad (562)$$

Substitution of this solution into the differential equation using the trigonometric identities

$$\begin{aligned} \cos^3 \theta / 3 &= 3/4 \cos \theta / 3 + 1/4 \cos \theta \\ \cos^3 \theta / 3 \cos \theta &= 1/4 \cos \theta / 3 + 1/2 \cos \theta \\ \cos \theta / 3 \cos^2 \theta &= 1/2 \cos \theta / 3 + \dots \\ \cos^3 \theta &= 3/4 \cos \theta + \dots, \end{aligned} \quad (563)$$

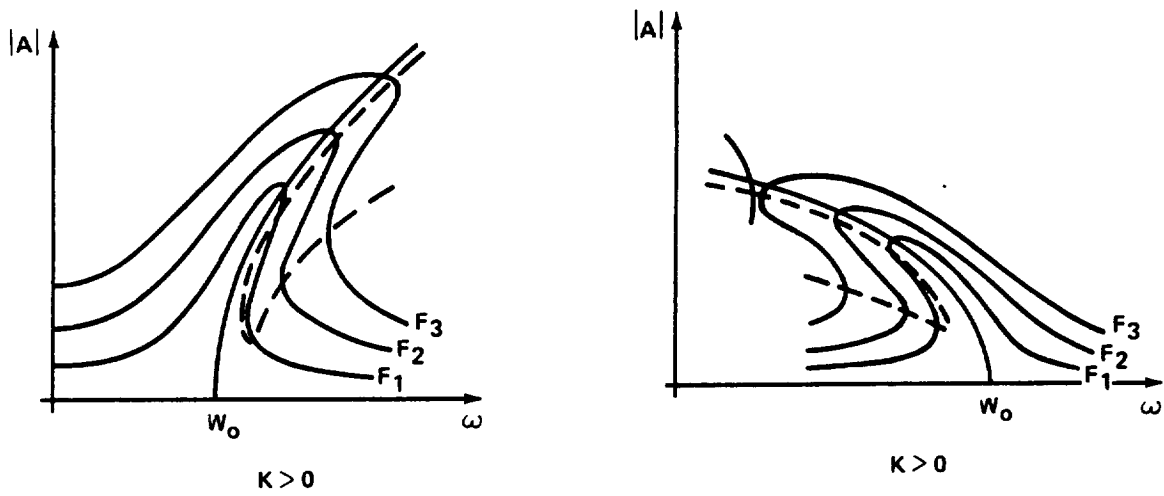


Figure 122. Response curves for the non-linear spring with damping.

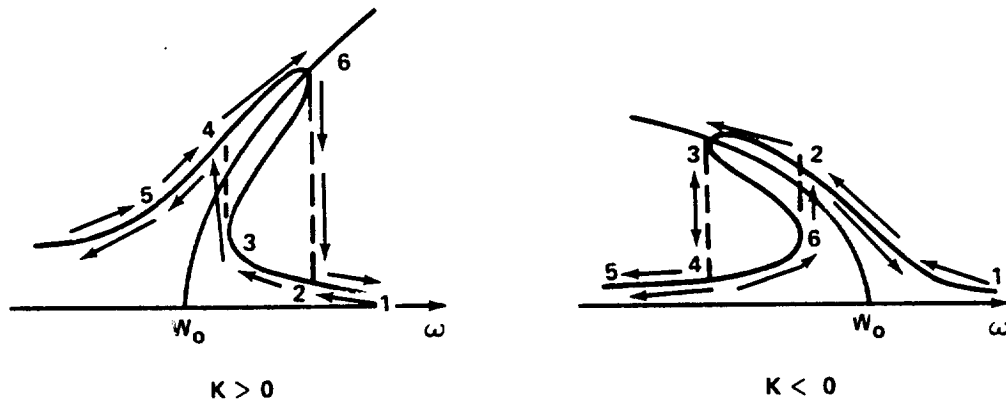


Figure 123. Jump phenomenon or hysteresis resonance for the non-linear spring with damping.

and equating the coefficients of each $\cos(2n-1) \theta/3$ equal to zero yields for the first two terms

$$a_1(\omega_0^2 - \omega^2/a) + (3k/4) (a_1^3 + a_1^3 + a_1^2 a_2 + 2a_1 a_2^2) = 0$$

$$a_2(\omega_0^2 - \omega^2) + (k/4) (a_1^3 + 6a_1^2 a_2 + 3a_2^3) = F \quad . \quad (564)$$

As a guide for exploring these equations the linear case is considered first, $k = 0$, yielding

$$a_2 = F/(\omega_0^2 - \omega^2)$$

from the second equation and either

$$a_1 = 0$$

or

$$\omega = 3\omega_0$$

from the first. If $\omega = 3\omega_0$, then a_1 may be arbitrarily prescribed and is the natural frequency term of the system added to the driving frequency term. Hence, for $k \neq 0$, a_1 and F should be fixed but a_2 and ω are functions of a_1 .

Solving the first of the two expressions for ω^2 and the second for the a_2 not multiplied by k , after eliminating ω^2 by the first equation, yields

$$\begin{aligned} \omega^2 &= 9\omega_0^2 + (27k/4) (a_1^2 + a_1 a_2 + a_2^2/a_1 + 2a_2^2) \\ a_2 &= -F/8\omega_0^2 + (k/32\omega_0^2) (a_1^3 - 21a_1^2 a_2 - 27a_2^2 a_1 - 51a_2^3) \end{aligned} \quad (565)$$

The linear solution as a first approximation to the above equation is now considered. The linear solution is followed by an iteration to find the next approximation of order k . Setting $\omega = 3\omega_0$ and $a_2 = -F/8\omega_0^2 = a$ in the preceding two equations leads to

$$\omega^2 = 9\omega_0^2 + \frac{27k}{4} (a_1^2 + aa_1 + 2a^2) \quad (566)$$

$$a_2 = a + \frac{K}{32\omega_0^2} (a_1^3 - 21a_1^2 a - 27a^2 a_1 - 51a^3) \quad (567)$$

Equation (566) represents an ellipse in the ω, a_1 plane when $k > 0$ and a hyperbola for $k < 0$. This relation also has a maximum at $a_1 = -a/2$ when $k < 0$ and a minimum for $k > 0$. For $a_1 = -a/2$, from equation (566),

$$\omega^2 = 9(\omega_0^2 + 2lk a^2/16) \quad . \quad (568)$$

Therefore, for $k < 0$ the subharmonic response must have

$$\omega \leq \sqrt[3]{\omega_0^2 + 2lka^2/16} \quad (569)$$

and for $k > 0$

$$\omega \geq \sqrt[3]{\omega_0^2 + 2lka^2/16} \quad . \quad (570)$$

For this particular problem, subharmonic resonance at a frequency three times the natural frequency of the linear system does not exist.

Subharmonic response also occurs for the non-linear spring with damping. Details are found in Stoker [54]. The damping constant must be small of the order of k and must satisfy the inequality

$$c < \frac{3}{32} \frac{|ka_1 F|}{\omega_0^3} \quad . \quad (571)$$

The foregoing discussion is intended only to suggest in a limited way the basic types of analysis which might be applied to find the solution on non-linear differential equations associated with vibrations. Considerable literature is available where these concepts are presented in greater detail. One of the earliest books written on the subject of non-linear equations is Andronov and Chaikin [50]. Two books by Minorsky [55, 56] summarize and extend the classical methods of Poincare, Rayleigh and others. Stoker [54] has treated non-linear vibrations with one degree of freedom. A book especially devoted to the solution of practical problems is Reference 52. Much advanced research in the understanding of non-linear vibrations is available in the works of the

researchers at RIAS (a division of The Martin Company) and published in the five volumes [51]. An extensive bibliography of papers dealing with specific problems is also provided. The classical papers on non-linear analysis such as those of Poincare, Rayleigh, and Van der Pol are contained in the bibliography.

H. Supporting Mathematics

Some of the supporting mathematics are presented separately in this paragraph. The contents of this paragraph are addressed more to a general treatment of the subject rather than the specific applications contained in preceding paragraphs of this section.

1. INFINITE SERIES

A finite series is of the form

$$x_1 + x_2 + x_3 + \dots + x_n$$

where each term is formed by some definite rule and x_n is a specific termination. For cases where this generating rule is supposed to apply over and over indefinitely, the number of terms is unlimited. This unlimited set of terms forms an infinite series which may be written as

$$y_1 + y_2 + y_3 + \dots y_n + \dots$$

where y_n = an arbitrary termination. Using a summation convention, the infinite series has the form

$$S = \sum_{i=1}^{\infty} y_i \quad . \quad (572)$$

If a limit exists the sum of an infinite series is defined as the limit of the sum of a finite number of terms, as the number of terms approaches infinity. This is denoted by

$$\text{Sum} = \lim_{n \rightarrow \infty} S_n \quad .$$

If this limit exists, the series is said to converge; if the limit does not exist, the series diverges. Methods to test for convergency or divergency are thoroughly discussed in the literature.

One important application of the infinite series arises in the solution of differential equations. The application of the infinite series to the solution of differential equations gives rise to the invention of transcendental functions such as circular functions, hyperbolic functions, Bessel functions, etc.

The general Taylor series given below is used to expand or represent functions that are continuous and have all continuous derivatives. The Taylor series is given by

$$y = f(x) = f(a) + \sum_{n=1}^{\infty} \frac{(x-a)^n f^n(a)}{n!} \quad (573)$$

where $f^n(a)$ is the n^{th} derivative of $f(x)$ evaluated at the point a . For the expansion about the arbitrary point (a) to be valid, $f(z)$ and $f^n(z)$ have to be continuous. If a is zero (expansion about the origin), then the Taylor series degenerates into a Maclaurin series given by

$$y = f(x) = f(o) + \sum_{n=1}^{\infty} \frac{x^n f^n(o)}{n!} \quad (573a)$$

Note that in both of these series, n is an integer so that x always appears to some "integer" power. However, in some differential equations, such as Bessel's equation, x may appear as $x^{p/q}$ where q is not one. To take care of this possibility the functional form of the solution is changed from a Taylor series [57] by assuming that

$$y = x^c \left[f(a) + \sum_{n=1}^{\infty} \frac{(x-a)^n f^n(a)}{n!} \right] \quad (574)$$

This allows for terms such as $f(x) = (x)^{3/4}$, etc. This last equation is the form used in the solution of most differential equations and is due to Frobenius [36]. If the solution is in the form of a pure Taylor series, then $c = 0$. Thus,

an infinite series may be used to approximate a general function. This idea is especially advantageous in the solution of differential equations when the exact solution is not readily obtainable by standard methods.

Infinite series theory is also applied to expressions that are exact solutions. If an exact solution is known, the expression can be stated in terms of an infinite series. This operation is often performed to simplify an exact expression by isolating and then eliminating second order effects. An excellent example of this application is the reasoning leading to equation (456).

2. LAPLACE TRANSFORMS

Although the Laplace transform exists for any function possessing the properties listed below, the vibration engineer normally applies the theory to functions of time. Therefore, the discussion in this paragraph is presented for functions of time.

The Laplace transform of a function $f(t)$ exists only if $f(t)$ is piecewise continuous in every finite interval in the region $t \geq 0$ and if the function is of exponential order.

a. Piecewise Continuous - A function $f(t)$ is piecewise continuous in the interval $0 \leq t \leq T_1$ if the interval can be divided into a finite number of sub-intervals, in each of which $f(t)$ is continuous, and if $f(t)$ approaches a finite limit as t approaches either end point of the interval.

b. Exponential Order - A function $f(t)$ is of exponential order if there exists some real number α_0 such that $\lim_{t \rightarrow \infty} f(t) e^{-\alpha t} = 0$ where $\alpha > \alpha_0$.

The Laplace transformation of $f(t)$ is denoted by $L[f(t)] = F(s)$ and is defined by the following integral

$$F(s) \equiv \int_0^{\infty} e^{-st} f(t) dt \quad . \quad (575)$$

The integral transforms a t domain to an s domain and has wide application in the solution of differential equations. The inverse transform of $F(s)$ is equal to $f(t)$ and is denoted by

$$f(t) = {}^{-1}\{F(s)\} \quad . \quad (576)$$

Thus, a correspondence is established between a function in the time domain and its transform in the s domain. This correspondence is used by engineers to solve differential equations in addition to the direct transformation tool such as the application in Paragraph C.3. of this section.

Before proceeding with the solution to a differential equation by the Laplace transform, a few brief comments on the Fourier transform are in order. The Fourier transform and the Laplace transform are similar but not generally equivalent. In the Laplace transform the multiplier operator s is, in general, a complex number with real and imaginary parts. The multiplier number in the Fourier transform contains only the imaginary part. Therefore, the Laplace transform contains a built-in convergence factor.

For the application of Laplace transforms to the solution of a linear differential equation, consider the following equation

$$m\ddot{x} + b\dot{x} + cx = u(t) \quad . \quad (577)$$

Consider the operator $\{d/dt\}$ and denote it by D . Then

$$L\{Df(t)\} = \int_0^{\infty} e^{-st} Df(t) dt \quad . \quad (578)$$

This integral can be evaluated by successive integrating by parts to yield

$$\begin{aligned} L\{D^n f(t)\} = & s^n F(s) - s^{n-1} f(0) - s^{n-2} Df(0) + \dots \\ & - sD^{n-2} F(0) - D^{n-1} (f(0)) \quad . \end{aligned} \quad (579)$$

Substituting in the Laplace transform for each term yields

$$(ms^2 + bs + c) F(s) = \frac{1}{s} \quad (580)$$

and

$$F(s) = \frac{1}{s} \left[\frac{1}{ms^2 + bs + c} \right] \quad . \quad (581)$$

The solution to the differential equation is obtained from equation (581) by means of partial fractions and taking the inverse Laplace transform of the portions that are found in tables.

For some application of the Laplace transform to the solution of a differential equation, the resulting algebraic solution contains the product of two functions. In order to obtain the inverse transform of the product of two functions, the convolution integral is used.

Consider the functions $f(x)$ and $f(x-t)$ where $f(x-t)$ represents a translation of the function $f(x)$ t units in the positive direction. The following result exists and is proven in Reference 58:

$$L[f(x-t)] = e^{-st} [f(x)] = e^{-st} F(s) \quad . \quad (582)$$

Now consider the product of two Laplace transformations. Define

$$L[f(t)] = F(s)$$

$$L[g(x)] = G(s)$$

and

$$F(s) G(s) = \int_0^{\infty} f(t) \int_0^{\infty} e^{-sx} f(x-t) dx dt \quad .$$

Rearranging terms yields

$$F(s) G(s) = \int_0^{\infty} e^{-sx} \left[\int_0^{\infty} f(t) f(x-t) dt \right] dx \quad . \quad (583)$$

The term in brackets looks much like the convolution integral defined as

$$f(t) * g(t) = \int_0^x f(t) g(t) dt \quad (584)$$

where $g(t)$ here is $f(x-t)$. Therefore the product of $F(s)$ and $G(s)$ is given by

$$F(s) G(s) = \int_0^{\infty} e^{-sx} [f(t) * g(t)] dx$$

or

$$F(s) G(s) = L[f(t) * g(t)] \quad . \quad (585)$$

Equation (585) states that the Laplace transformation of the convolution of the two functions is equal to the product of the Laplace transforms of the functions. The convolution integral is usually expressed in terms of the inverse Laplace transform given below

$$L^{-1} [F(s) G(s)] = f(t) * g(t) \quad . \quad (586)$$

In this paragraph it was seen that the Laplace transformation converts a function of time $f(t)$ into the s -domain by means of the integral equation. It was also shown how the Laplace transform may be used to solve a differential equation by converting it into an algebraic equation resulting in an easier solution. Finally, it was shown that the convolution integral is equivalent to an inverse Laplace transformation of two functions defined in the s -domain.

3. VECTORS

A vector is an abstract quantity that has a magnitude and a direction associated with it. Suppose an n -dimensional vector space exists with a set of basis vectors $\{\vec{r}_1, \vec{r}_2, \vec{r}_3, \dots, \vec{r}_n\}$. A set of vectors such as $\{r_i\}$ is called a basis for a vector space if:

- a. These vectors are in the vector space and form a linearly independent set (linearly independent means that one basis vector is not a linear combination of the other $(n-1)$ basis vectors).
- b. Every vector in the space is a linear combination of these basis vectors.

In the special three dimensional case, the basis vectors are denoted by \vec{i} , \vec{j} , and \vec{k} where \vec{i} , \vec{j} , \vec{k} are unit vectors along the X, Y, and Z axis,

respectively. Any vector in the n-dimensional space may thus be written as

$$\vec{V} = X_1\vec{r}_1 + X_2\vec{r}_2 + X_3\vec{r}_3 + \dots + X_n\vec{r}_n \quad (587)$$

$$\vec{V} = \sum_{i=1}^n X_i \vec{r}_i$$

For the three dimensional case, a vector \vec{P} would be written as

$$\vec{P} = X\vec{i} + Y\vec{j} + Z\vec{k} \quad (588)$$

Suppose the vector \vec{V} is referred to a different set of basis vectors $\{\vec{s}_i\}$, then \vec{V} is written as

$$\vec{V} = Y_1\vec{s}_1 + Y_2\vec{s}_2 + Y_3\vec{s}_3 + \dots + Y_n\vec{s}_n$$

$$\vec{V} = \sum_{i=1}^n Y_i \vec{s}_i \quad (589)$$

A vector is usually represented by a set of scalar functions which are the components of the vector. Thus, in the first reference frame utilizing the set of basic vectors $\{\vec{r}_i\}$, \vec{V} could be represented as

$$V \rightarrow \begin{bmatrix} X_1 \\ X_2 \\ \cdot \\ \cdot \\ \cdot \\ X_n \end{bmatrix} \quad (590)$$

Written in this form, \vec{V} is called a column vector. In the second reference frame using the set of basic vectors $\{\vec{s}_i\}$, \vec{V} may be represented by

$$V \rightarrow \begin{bmatrix} Y_1 \\ Y_2 \\ \vdots \\ Y_n \end{bmatrix} \quad (591)$$

The following problem arises. One set of components $\{X_i\}$ is given and it is desired to obtain the other set of components $\{Y_i\}$. This is interpreted in one sense as changing coordinate systems. Some type of operator is defined to change the set $\{X_i\}$ into the set $\{Y_i\}$. Written in an operator form, the transformation is given by

$$T \{X_i\} = \{Y_i\} \quad (592)$$

This equation may be thought of as representing a transformation of the vector \vec{V} from one coordinate system to another and is accomplished by the transformation of its coordinates. Therefore, the concept of a vector or any abstract object is important from the standpoint of how its components change by a transformation from one coordinate system to another.

A quantity that is a function of several variables is called a functional. The vector \vec{V} in the preceding paragraphs is a function of several quantities $X_1, X_2, X_3, \dots, X_n$ in the first coordinate system and is a functional. Thus, the transformation of the vector \vec{V} is a transformation of one functional space onto another functional space.

a. Basic Operations

The operations performed with vectors will be described in this paragraph. The addition and subtraction of vectors poses no problem. Two vectors \vec{V}_1 and \vec{V}_2 may be added to give a new vector \vec{V}_3 if \vec{V}_1 and \vec{V}_2 are defined on the same vector space. That is

$$\vec{V}_1 + \vec{V}_2 = \vec{V}_3 \quad (593)$$

$$\vec{V}_1 = a_1 \vec{r}_1 + a_2 \vec{r}_2 + \dots + a_n \vec{r}_n$$

and

$$\vec{V}_2 = b_1 \vec{r}_1 + b_2 \vec{r}_2 + \dots + b_n \vec{r}_n$$

then

$$\vec{V}_3 = (a_1 + b_1) \vec{r}_1 + (a_2 + b_2) \vec{r}_2 + \dots + (a_n + b_n) \vec{r}_n \quad (594)$$

$$\vec{V}_3 = \sum_{i=1}^n (a_i + b_i) \vec{r}_i \quad .$$

Two types of vector multiplication that will be discussed are the scalar or inner product and the vector or cross product.

The scalar product of two vectors is a scalar quantity that is equal to the product of the magnitude of the two vectors times the cosine of the angle between the two vectors.

$$\vec{V}_1 \cdot \vec{V}_2 = \vec{V}_2 \cdot \vec{V}_1 = |\vec{V}_1| |\vec{V}_2| \cos \theta \quad (595)$$

where θ is the angle between the vectors. An alternate form is usually seen.

Assume that \vec{V}_1 and \vec{V}_2 have the form that \vec{V}_1 and \vec{V}_2 have in the paragraph on the addition of vectors. Then, by definition,

$$\vec{V}_1 \cdot \vec{V}_2 = a_1 b_1 + a_2 b_2 + a_3 b_3 + \dots + a_n b_n \quad (596)$$

$$\vec{V}_1 \cdot \vec{V}_2 = \sum_{i=1}^n a_i b_i \quad .$$

A common example of the use of the scalar product is in the calculation of the work expended by a force \vec{F} acting over a displacement $d\vec{x}$. Then

$$W = \int \vec{F} \cdot d\vec{x} \quad . \quad (597)$$

The vector product is more difficult to define because the vector product is also a vector; that is

$$\vec{V}_m \times \vec{V}_n = \vec{V}_R \quad . \quad (598)$$

Note that the symbols \cdot and \times are not interchangeable in vector terminology.

Also, the operation is not commutative; i.e., $\vec{V}_m \times \vec{V}_n \neq \vec{V}_n \times \vec{V}_m$. Only the magnitude of the vector obtained by the cross product of two vectors \vec{V}_m and \vec{V}_n is given by

$$|\vec{V}_m \times \vec{V}_n| = |\vec{V}_m| |\vec{V}_n| \sin \theta \quad (599)$$

where θ is the angle between the vectors. The direction of the vector product is conserved by using a determinant form to calculate the cross product. The determinant of a three dimensional case is

$$\vec{A} \times \vec{B} = \begin{vmatrix} \vec{i} & \vec{j} & \vec{k} \\ A_x & A_y & A_z \\ B_x & B_y & B_z \end{vmatrix} \quad . \quad (600)$$

This is the most useable form, generally. From this form it is seen that $\vec{A} \times \vec{B} = -(\vec{B} \times \vec{A})$.

Three additional operation vectors are the gradient, divergence, and curl. These operations are defined in terms of the vector differential operator "del" given by

$$\nabla = \vec{i} \frac{\partial}{\partial x} + \vec{j} \frac{\partial}{\partial y} + \vec{k} \frac{\partial}{\partial z} \quad (601)$$

for a three dimensional system using an x - y - z coordinate system.

Consider some scalar function R . The gradient is defined to be

$$\nabla R = \vec{i} \frac{\partial R}{\partial x} + \vec{j} \frac{\partial R}{\partial y} + \vec{k} \frac{\partial R}{\partial z} . \quad (602)$$

The gradient is the sum of the rates of change of the scalar functions in the respective directions; that is, $\partial R / \partial x$ gives the rate of change of R in the x direction, etc.

The divergence is a scalar quantity representing the rate of change of a vector field. Consider a vector field \vec{S} . Then the divergence is given by

$$\nabla \cdot \vec{S} = \frac{\partial S_x}{\partial x} + \frac{\partial S_y}{\partial y} + \frac{\partial S_z}{\partial z} . \quad (603)$$

The curl of the vector field is sometimes described as being the rate of "Swirl" of the vector field at a particular point. In a determinant form, the curl is given by

$$\text{Curl } \vec{S} = \nabla \times \vec{S} = \begin{vmatrix} \vec{i} & \vec{j} & \vec{k} \\ \frac{\partial}{\partial x} & \frac{\partial}{\partial y} & \frac{\partial}{\partial z} \\ S_x & S_y & S_z \end{vmatrix} \quad (604)$$

where $\nabla \times \vec{S}$ is the vector product and $\vec{S} \times \nabla$ is not defined.

4. MATRICES

In ordinary arithmetic, single numbers along with the operations of addition, etc., are considered. In more sophisticated mathematics, collections or arrays of numbers or functions are considered. The collections or arrays of numbers or functions are considered. The collections or arrays may be simple or complex and the ordering of the terms in the collection may not be important as in the representation of a vector by its components. The arrays have meaning only after a rule is determined to combine the array with other arrays.

It is from the idea of a collection along with the combining laws for collections that determinants and matrices are formulated. A determinant is always a square array of quantities and has a particular value. The rule for

determining its value is given in Reference 57. A matrix is also an array of quantities but the array does not have to be square. Also, the matrix may not have a specific value as the determinant does. Therefore, it is seen that although a matrix and determinant are both arrays of quantities, they do not have the same meaning.

A matrix is, in general, a $m \times n$ array of quantities a_{ij} , called elements, arranged in m rows and n columns as given below

$$M = \begin{pmatrix} a_{11} & a_{12} & \cdots & a_{1n} \\ a_{21} & a_{22} & \cdots & a_{2n} \\ \vdots & \vdots & \ddots & \vdots \\ a_{m1} & a_{m2} & \cdots & a_{mn} \end{pmatrix}$$

Smaller matrices may be formed from any matrix by striking out some of the rows and columns. If the smaller matrices are square then their determinants are called determinants of the matrix. If a matrix M contains at least one determinant of r rows that is not zero and all determinants of M with order greater than r are zero or nonexistent, then the matrix M is said to be of rank r . The number of rows and columns making up the matrix is called the order. Thus, a matrix having two rows and three columns would have the order stated two by three. A row matrix or row vector is a matrix consisting of only one row. Similarly, a matrix consisting of a single column is called a column matrix or column vector.

A matrix is said to be singular if the determinant of the matrix is zero or does not exist. Thus, if $m \neq n$, the matrix is singular since the determinant does not exist for an array that is not square.

a. Addition and Subtraction

Two matrices can be added if they are of the same order. Matrices A and B can be added to obtain the matrix C by adding the respective elements of A and B to obtain the corresponding elements of C

$$\begin{matrix} C & = & A & + & B \\ (m \times n) & & (m \times n) & & (m \times n) \end{matrix} \quad (605)$$

where each element of C is

$$c_{ij} = a_{ij} + b_{ij} \quad . \quad (606)$$

Since subtraction is a special case of addition, a matrix D can be obtained by subtracting B from A,

$$\begin{matrix} D & = & A & - & B \\ (mxn) & & (mxn) & & (mxn) \end{matrix} \quad (607)$$

where each element of D is

$$d_{ij} = a_{ij} - b_{ij} \quad . \quad (608)$$

It follows that

$$A + B = B + A$$

$$(A + B) + C = A + (B + C) \quad .$$

b. Multiplication

The product of matrices is more difficult than addition since the matrix can represent a transformation. Multiplication can be defined as the termwise product of the rows of the first matrix times the columns of the second matrix. This imposes the restriction that if $AB = C$, then B must have the same number of rows as A has columns. In general terms, the matrix C resulting from the product of two matrices A and B has its elements determined from this expression;

$$c_{ij} = \sum_{k=1}^n a_{ik} b_{kj} \quad . \quad (609)$$

The product of two matrices A and B is not, in general, commutative.

$$AB \neq BA \quad .$$

In fact, unless both A and B are square and of the same order one of the two products AB or BA is not defined.

In practical structural analysis, the order of matrices encountered becomes quite large and multiplication of these large order matrices becomes a problem in itself. Various reduction techniques and shortcuts are available to circumvent this problem. Some of these methods are discussed in References 57, 59, 60, and 61.

c. General Operation Definitions

In the theory of matrices there are several operational terms essential to understanding the manipulation techniques. The more commonly used terms will be discussed here.

1. Transpose - The transpose of a matrix A, denoted as A^T , is the matrix resulting from the interchange of the rows and columns of A, i.e., a_{ij} becomes a_{ji} . The transpose may be used to test the symmetry of the matrix since a matrix is symmetric if $a_{ij} = a_{ji}$ or $A = A^T$.

2. Scalar Matrix - A scalar matrix is a diagonal matrix with the diagonal elements as a single scalar n; i.e.,

$$S = \begin{bmatrix} n & 0 & 0 \\ 0 & n & 0 \\ 0 & 0 & n \end{bmatrix} = \begin{bmatrix} \diagup & & \\ & n & \\ & & \diagdown \end{bmatrix} .$$

A unity or identity matrix, I, is a special scalar matrix with the diagonal element equal to one.

3. Inverse - The inverse of a matrix A is denoted A^{-1} and is defined by this relation

$$A^{-1}A = AA^{-1} = I \quad . \quad (610)$$

The elements of the inverse matrix A^{-1} can be found by any of several methods presented in References 57 and 59. The inverse can be found for any matrix that is nonsingular. This property is especially useful for linear transformations.

4. Orthogonality - For a transformation to be orthogonal, the vector that is transformed must have the same length in the new reference frame as in the old reference frame. This condition is satisfied if

$$A^T = A^{-1} \quad .$$

Thus, in an orthogonal transformation, the inverse matrix A^{-1} is equal to the transpose A^T of the matrix A .

d. Reduction Techniques

When the number of variables in a matrix becomes large, the solution to the system of equations requires special techniques. Efficient methods depend on reducing the matrix to an equivalent system in which the matrix is sufficiently simple to solve without a great deal of effort. A system of equations can be written as

$$A x = f \quad (611)$$

where

$$A = (a_{ij}), x = \{X_i\}, f = \{f_i\} \quad . \quad (611)$$

If the matrix A is nonsingular

$$x = A^{-1} f \quad . \quad (612)$$

Now the determination of the unknowns, X_i , is contingent of developing the inverse matrix, A^{-1} . This is a major problem in numerical analysis and can be approached several ways. One such method is the Gauss reduction method discussed in Reference 59. Other methods such as orthogonalization, diagonalization and variations on the Gauss technique; i.e., Crout and Gauss-Jordan are discussed in References 57, 59, 61, and 62.

The Gauss reduction method reduces the system of equation (611) to an equivalent form

$$B x = d \quad (613)$$

where

$$B = \begin{bmatrix} 1 & b_{12} & b_{13} & \dots & b_{1n} \\ 0 & 1 & b_{23} & \dots & b_{2n} \\ . & . & & & . \\ . & . & & & . \\ . & . & . & . & . \\ 0 & 0 & 0 & . & . & 1 \end{bmatrix} \quad . \quad (614)$$

and all elements below the main diagonal are zero. It can be seen that the solution for the values of x are easily found from equation (614).

e. Eigenvalues

An eigenvalue equation is of the form $H\psi_n = E_n \psi_n$ where E_n is the eigenvalue, ψ_n is the eigenfunction, and H is the operator. If H is the Hamiltonian operator as used in mechanics, the E_n is the energy. A set of eigenfunctions is needed to describe a system. The eigenvalue equation says, "operate on the n^{th} eigenfunction with H and the n^{th} eigenvalue will be generated."

It was seen in Paragraph 3. of this subsection that a transformation of a vector from one coordinate system to another was performed by transforming the components. Thus, there exists the transformation

$$X_i' = \sum_{j=1}^n a_{ij} X_j, (i, j, = 1, 2, \dots, n) \quad (615)$$

where the set $\{X'\}$ represents the components of the vector referenced to a different coordinate system than the set $\{X_i\}$. The above vector transformation may be expressed in matrix form as

$$\vec{X}' = A \vec{X} \quad (615a)$$

If the determinant of A is not zero and is defined (A is nonsingular), the inverse transformation is given by

$$A^{-1} \vec{X}' = \vec{X} \quad (616)$$

The problem reduces to the following question. Is it possible to find another matrix C such that the matrix CAC^{-1} has the diagonal form

$$CAC^{-1} = \begin{bmatrix} \lambda_1 & 0 & . & . & . & 0 \\ 0 & \lambda_2 & . & . & . & . \\ . & . & . & . & . & . \\ 0 & . & . & . & . & \lambda_n \end{bmatrix} ?$$

This transformation is called a similarity transformation. This means that relative to some suitable coordinate system the so-called deformation of space characterized by equation (615a) assumes the form

$$\beta_1' = \lambda_1 \beta_1, \beta_2' = \lambda_2 \beta_2, \dots, \beta_n' = \lambda_n \beta_n$$

where the $\{\beta'\}$ are components of \vec{X}' and $\{\beta\}$ are the components of X in the denoted suitable coordinate system. The diagonal form remains

$$\theta = CAC^{-1} \quad . \quad (617)$$

A matrix S is defined such that $S \equiv C^{-1}$. Then equation (617) becomes

$$\theta = S^{-1}AS \quad . \quad (618)$$

Using the relation $SS^{-1} = I$, equation (618) becomes

$$S\theta = AS \quad . \quad (619)$$

The matrix equation (619) is equivalent to the system of linear equations given below

$$a_{ij} S_{jk} = S_{ik} \lambda_k; (i, j, k = 1, 2, \dots, n) \quad . \quad (620)$$

(No sum on k but j is summed). Equation (620) is usually written in the equivalent form

$$(a_{ij} - \delta_{ij} \lambda_k) S_{jk} = 0 \quad .$$

(k is not summed.) For this system of equations to have a non-trivial solution ($S_{jk} \neq 0$) the determinant of the other term has to be zero; that is,

$$|a_{ij} - \delta_{ij} \lambda_k| = 0 \quad . \quad (621)$$

Writing the determinant in a long form yields

$$\begin{vmatrix} a_{11}^{-\lambda} & a_{12} & \dots & a_{1n} \\ a_{21} & a_{22}^{-\lambda} & \dots & a_{2n} \\ \vdots & \vdots & \ddots & \vdots \\ a_{n1} & \dots & \dots & a_{nn}^{-\lambda} \end{vmatrix} = 0 \quad .$$

In the diagonalization of the matrix A, equation (619), a transformation of both \vec{X}^1 and \vec{X} was made by means of the similarity transformation $S^{-1}AS$. The purpose of the transformation was to get the eigenvalues along the diagonal of the matrix. If the roots $\lambda_1, \lambda_2, \lambda_3, \dots, \lambda_k$ are all distinct it can be proven that the matrix C will be nonsingular. If the roots of λ_k are not distinct it may not be possible to reduce A by the similitude transformation $S^{-1}AS$ to the diagonal form since S may be singular. An important exception occurs when A is a real and symmetric matrix. Then a matrix S may be found to convert $S^{-1}AS$ to a diagonal form even though the roots λ_k are not distinct.

The quantities S_{ik} that appear in equation (620) are the components of the eigenvectors obtained by transforming \vec{X}^1 and \vec{X} by means of the similitude transformation.

5. ORTHOGONALITY PRINCIPLE

Two vectors \vec{A} and \vec{B} are said to be orthogonal if their dot product is zero, that is, if

$$\vec{A} \cdot \vec{B} = 0 = A_x B_x + A_y B_y + A_z B_z = \sum_{i=1}^3 A_i B_i \quad . \quad (622)$$

Similarly, two vectors in an N dimension space having components A_i, B_i ($i = 1, 2, \dots, N$) are said to be orthogonal if

$$\sum_{i=1}^n A_i B_i = 0 \quad . \quad (623)$$

Next, imagine a vector space of an infinite number of dimensions, in which A_i and B_i become continuously distributed and everywhere dense. The index i is no longer a denumerable index but is a continuous variable. Therefore, the scalar product $A_i B_i$ turns into $\int A(X) B(X) dx$. If this integral is zero, then the functions A and B are orthogonal. The above integral is meaningless as far as a scalar product is concerned unless a specific range of integration is considered. Thus, the principle of orthogonality for real functions is given by

$$\int_R A_m(X) A_n(X) dx = a^2 \delta_{mn} \quad (624)$$

where

$$\delta_{mn} = \begin{cases} 0 & \text{if } m \neq n \\ 1 & \text{if } m = n \end{cases}$$

where R signifies a range and a^2 is a normalizing term.

A simple modification is required when complex functions are considered. The scalar product for complex functions is defined in the following way.

$$\int_R B_m^*(X) B_n(X) dX = b_n^2 \delta_{mn} \quad (625)$$

where B_m^* is the complex conjugate of B_m . This is the general form of the orthogonality principle. This principle would be used to test the orthogonality of the eigenvectors discussed in Paragraph 4. of this subsection.

6. TENSORS

In Paragraph 3. of this subsection, a brief description of vectors was presented. A vector is a special tensor of rank one (only one direction associated with each term in the vector). A tensor, which is more general than a vector, can have any rank and is therefore considered an abstract quantity. Tensor analysis is a systematic representation of these abstract quantities.

A tensor is represented in a particular reference frame by a set of functions that are similar to the representation of vectors in a reference frame by its components. Like the vector, the properties of a tensor are independent of the choice of the reference frame and is therefore a very convenient tool for representing physical laws. Since the tensor is a general representation, the transformation from one reference frame to another represents the center of any discussion on tensors.

Consider a function and an admissible transformation. The definition of an admissible transformation is provided in some detail in Reference 63, but for the purposes of this discussion, an admissible transformation can be considered reversible. This states that the transformation from one reference frame to another can be reversed back to the original reference frame. Let $\{X_i\}$ be the original set of coordinates and $\{Y_i\}$ be a new set. Then

$$Y_i \xrightarrow{T} Y_i(X_1, X_2, \dots, X_n) \quad (i = 1, 2, \dots, n) \quad (626)$$

where T represents the transformation of the coordinates. The transformation of a function of the coordinates may transform differently from the transformation of the coordinates. The transformation T of the set of coordinates $\{X_i\}$ induces a transformation law for the set of functions $\{f_j\}$. That is, for each $f_j(X_i)$, $(i = 1, \dots, n, j = 1 \dots m)$

$$f_j(X_1, X_2, \dots, X_n) \xrightarrow{G} g_j(Y_1, Y_2, \dots, Y_n) \quad . \quad (627)$$

Whatever the nature of the transformation G , it will be a function of the transformation T ; that is,

$$G_\mu = G_\mu(T) \quad . \quad (628)$$

Consider the simple case when T is an identity transformation. Then G is also an identity transformation. This means that if $X_i = Y_i$, then $f_i(X_1, X_2, \dots, X_n) = f_i(Y_1, Y_2, \dots, Y_n)$. If there exists a sequence of identity transformations T_1, T_2 and T_3 and the induced transformations G_1, G_2 and G_3 and furthermore if $T_3 = T_2 T_1$ implying $G_3 = G_2 G_1$, then T and G are said to be isomorphic. If the given set of functions $f_j(X_i)$ satisfies the preceding conditions, $f_j(X_i)$ represents the components of a tensor in the X -coordinate

system, the tensor itself being the complete set of functions $f_j (X_i)$, $g_j (Y_i)$, etc.

Within the class of tensor component transformations, three subtypes exist:

- a. Invariance.
- b. Contravariance.
- c. Covariance.

The transformation by invariance leaves the quantity unaltered by transformation although it may change form. A scalar point function would be left invariant with a transformation by invariance.

If there exists a set of functions $A_\alpha (X)$ ($\alpha = 1, \dots n$) in the X-coordinate system such that $B_i (Y)$ is given by

$$B_i (Y) = \frac{\partial X_\alpha}{\partial Y_i} A_\alpha (X) \quad , \quad (629)$$

then $A_\alpha (X)$ is transformed by the covariant law. Here $A_\alpha (X)$ is the component of a covariant vector.

If there exists a set of functions $A_\theta (X)$ ($\theta = 1, \dots s$) such that $B_j (Y)$ is given by

$$B_j (Y) = \frac{\partial Y_i}{\partial X_\theta} A_\theta (X) \quad , \quad (630)$$

then $A_\theta (X)$ is transformed by the contravariant law. $A_\theta (X)$ is the component of a contravariant vector.

For a more general tensor, the rank may be covariant of rank s and contravariant of rank r . For this case both a subscript and superscript are used to represent the tensor and the transformation is understandably more complex [63].

SECTION XIV. DESIGNING FOR VIBRATION

The vibration and acoustic environments associated with launch and space vehicles generate significant component and structural loads. These loads must be considered in the vehicle design. This section presents procedures for calculating vibration loads and discusses the use of the loads in strength analyses.

A. Vibration Load Analysis Procedure

The vibration load analysis of a dynamic system such as a component or structure is inherently difficult in that the desired loads are dependent on the dynamic characteristics of a system whose design is partially dictated by those loads. The loads are based on a dynamic analysis of a mathematical model which represents the component or structure. A modal analysis is usually done since vibration damage is assumed to occur in one or more of the system vibration modes (resonant frequencies). The following paragraphs present basic considerations for constructing mathematical models, some basic mathematical damping representations and methods of estimating damping in structures, methods of selecting input vibration environments, and examples of vibration load analyses.

1. MATHEMATICAL MODELS

The vibration load analysis must include a number of assumptions at first, which must be later proven or improved. Thus, any design development must include an iterative procedure whereby more accurate vibration loads and improved designs are produced with each iteration until a final design is produced. Throughout this iteration process, the mathematical model of the system will become more and more sophisticated and complex and will represent design conditions closer with each step.

a. Preliminary Design Models

The mathematical model of a system in preliminary design should be a simple one or two-degree-of-freedom system adaptable to simple and fast analysis methods. Examples 1, 3, and 4 of Paragraph 4 of this subsection are examples of preliminary analysis models.

b. Model Improvement

Preliminary design analysis may show the component or structure is not able to carry the calculated vibration load; therefore, a better load calculation may be needed to avoid unnecessary redesign. Or, further design work may have taken place, and the dynamics engineer can have a better description of the design. In any case, an improved mathematical model of the component or structure may be necessary.

Improved models should not be simple one or two-degree-of-freedom systems, or simple uniform beams. Multi-degree-of-freedom systems of many lumped parameters or continuous systems with changes in sections should be used. End conditions and supports should be represented by springs and should not be described as merely fully fixed or pinned. Examples 2 and 5 of Paragraph 4 of this subsection show improvements of preliminary analysis models.

If the input acceleration spectrum is accurately known, special effort should be given to obtaining loads from modes in the frequency range where the input levels are especially severe. If the preliminary analysis showed problem areas or weak components on the analyzed structure, the reanalysis should give these areas special attention by using more lumped masses and more accurate mathematical representation. All available information from drawings, specifications, etc., should be included if possible.

Information from a vibration test of a prototype component or structure should be used if available to verify natural frequencies, mode shapes, and damping characteristics of the mathematical model.

c. Final Design Models

Mathematical models of final designs should be constructed using the recommendations in Paragraph 1.b above. The final design analysis will probably utilize one or more of the various computer programs conceived for structural analysis. The complexity of the analysis should be limited only by the time allowed for design finalization and by the computer capability.

Example 6 of Paragraph 4 of this subsection is a lumped parameter representation of the final design configuration of a Saturn S-IC component.

2. DAMPING

The damping in a dynamic system is one of the most important unknown quantities to contend with in an analysis. Damping alone restricts the amplitude of response of a structure at resonance. In an analysis, the damping must be assumed, using past experience and test data (if available) as the basis for the assumption.

Damping forces are quite complex and most damping representations are approximations of actual phenomenon. The following paragraphs illustrate mathematical representations of some common types of damping.

a. Equivalent Viscous Damping and Magnification Factor

The type of damping representation usually used in vibration loads analyses is equivalent viscous damping, because other forms of damping are difficult to handle analytically. This damping representation is based on true viscous damping which is discussed in Paragraph b below. The damping of a system is approximated by viscous damping. The approximation is satisfactory for small damping, $\zeta \leq 0.1$ [64].

Equivalent viscous damping is usually expressed as percent or fraction of critical damping; i.e., 4 percent or 0.04. The symbol ζ is used for the fraction of critical damping. The most likely values for the fraction of critical damping are between 0.01 and 0.05; however, much smaller values may occur if the vibrating structure is devoid of joints and the vibration occurs in a vacuum [65].

As can be seen in the examples in Paragraph 4 of this subsection, equivalent viscous damping is usually used in the form of a magnification factor Q , where

$$Q = \frac{1}{2\zeta} = \frac{\text{Magnitude of Response}}{\text{Magnitude of Input}} \quad (\text{at resonance only})$$

and

$$\zeta = \frac{c}{c_c} \quad \text{or fraction of critical damping}$$

where c is the equivalent viscous damping coefficient, and c_c is the critical damping coefficient. The above relationships actually apply only to single-degree-of-freedom system; but in a modal analysis, each mode is considered independently and as a single-degree-of-freedom system. Therefore, the concept of Q can be used.

Figure 124 shows a curve which may be used to estimate damping of a flat panel. The data were gathered from tests of panels excited by turbulent boundary layers. The abscissa is the natural frequency of the panel and the ordinate is the fraction of critical damping ζ [66].

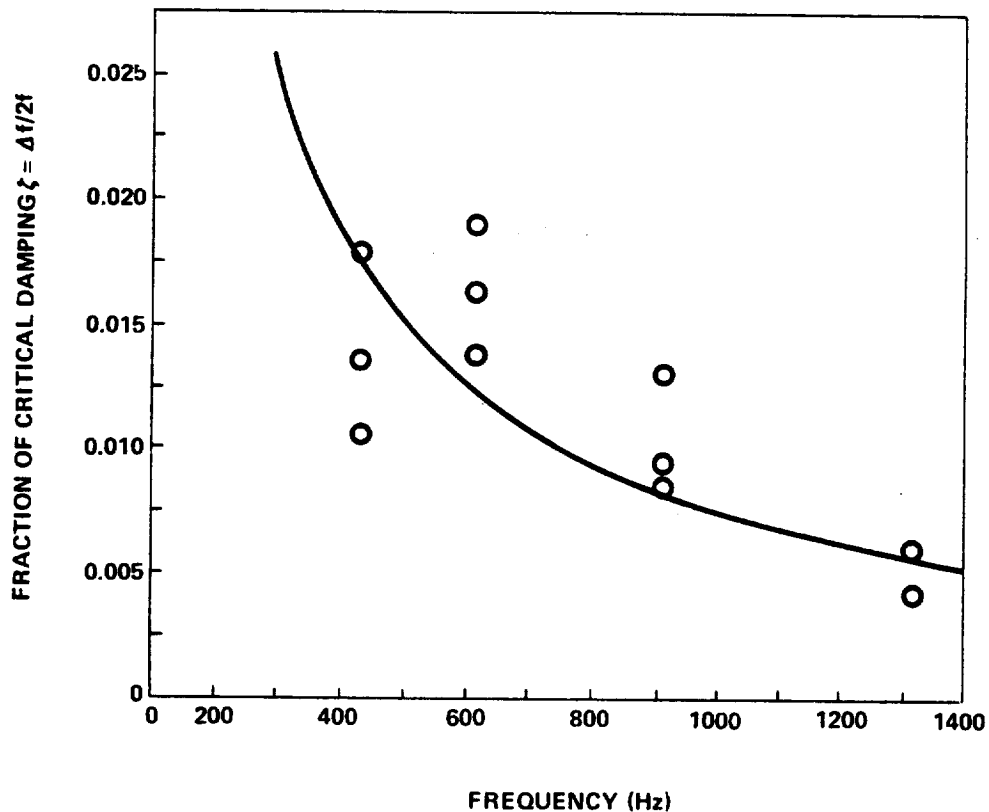


Figure 124. Panel damping [66].

For an example of the magnitude of Q , consider the first mode response of the LOX loading probe in qualification testing. The probe is a tube of about 15.24 (6 in.) O.D., length about 304.8 cm (120 in.), and of thin wall construction. The probe is shown in the weight attenuation example in Paragraph D of this section. The test set-up approximately fixed one end and hinged the

other. The first mode frequency was about 150 Hz. The input level was ± 15 g peak or about 0.033 cm (0.013 in.) D.A. The response at the center of the probe was greater than 3.81 cm (1.5 in.) D.A. Therefore, the magnification factor, $Q = 1.5/0.013$, was greater than 115; or the fraction of equivalent viscous damping would be about $\zeta = 1/2Q = 0.0043$.

b. Other Types of Damping

Other types of damping are shown below:²

1. Viscous Damping

$$m\ddot{x} + \underline{c\dot{x}} + kx = F(x)$$

where c is the coefficient of damping. The damping force is proportional to velocity and is in a direction opposing velocity.

2. Hydraulic Damping

$$m\ddot{x} + \underline{c|\dot{x}| \dot{x}} + kx = F(x)$$

where c is the coefficient of damping. The damping force is proportional to velocity squared and opposes velocity. An example of this type of damping arises when metering a liquid through a small orifice.

3. Structural Damping

$$m\ddot{x} + k(1 + \underline{ig})x = F(x)$$

where g is the coefficient of structural damping, and i is $\sqrt{-1}$. The damping force is proportional to displacement but in phase with velocity. This representation is primarily used in flutter problems where the motion is nearly sinusoidal.

2. Bohne, Q., Selected Notes on Structural Dynamics. Unpublished, Seattle, Washington: The Boeing Company, September 1961.

4. Coulomb Damping

$$m\ddot{x} + F_f \frac{\dot{x}}{|\dot{x}|} + kx = F(x) \quad .$$

The damping force F_f is "dry friction" and is constant in a direction opposing velocity.

3. ENVIRONMENT SELECTION

To complete a vibration loads analysis on a component or structure, the input vibration or forcing function must be known, given or estimated. The input levels could come from a number of different sources, such as actual data measured at the component location, specifications, or predictions. MSFC environment specifications [67, 68] and a prediction method document [69] are discussed in Paragraph 4 of this subsection. The Kennedy Space Center environment specifications are in Reference 70.

The component or structure must withstand a number of different vibration environments such as those encountered during ground transportation, qualification and acceptance testing, static firing, vehicle launch, and flight. The environment(s) which will most likely damage the component must be determined. The vibration loads resulting from the environment(s) are then calculated. Usually, the two most severe environments will be vibration qualification testing and actual service during launch and flight. The MSFC practice is to use the steady state levels simulating actual service or qualification testing as design load environments. Short duration, transient levels are not used to calculate the MSFC design vibration loads.

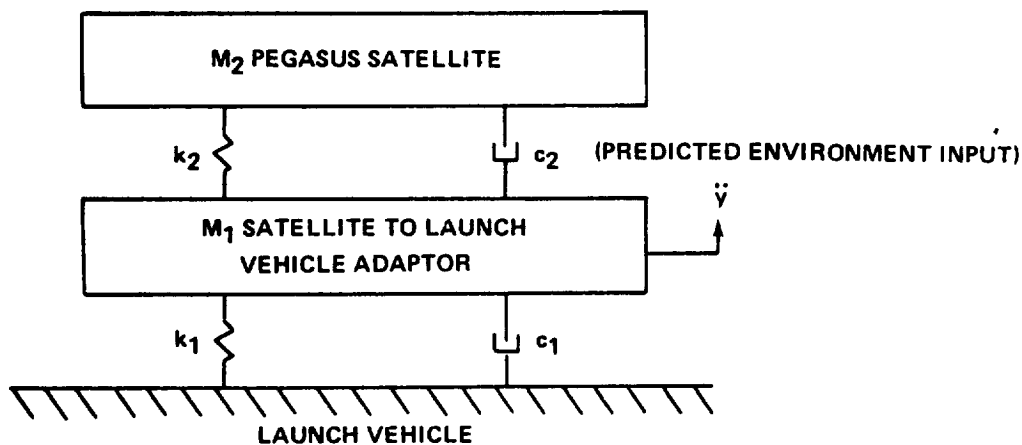
If the component or structure being analyzed has more than one input point, the input vibration environment is usually assumed to be applied to all input points simultaneously and all are assumed in phase. If the input vibration environment at each input point is not the same, then the maximum environment could be applied to all points; or all the environments could be averaged together and the average applied to all input points. Examples 3, 4, and 5 of Paragraph 4 below illustrate how the input vibration environment is used in an analysis.

4. VIBRATION LOAD ANALYSIS EXAMPLES

The following paragraphs are examples of mathematical models and modal analyses for various dynamic systems. The examples are presented to illustrate the procedures discussed in the previous paragraphs.

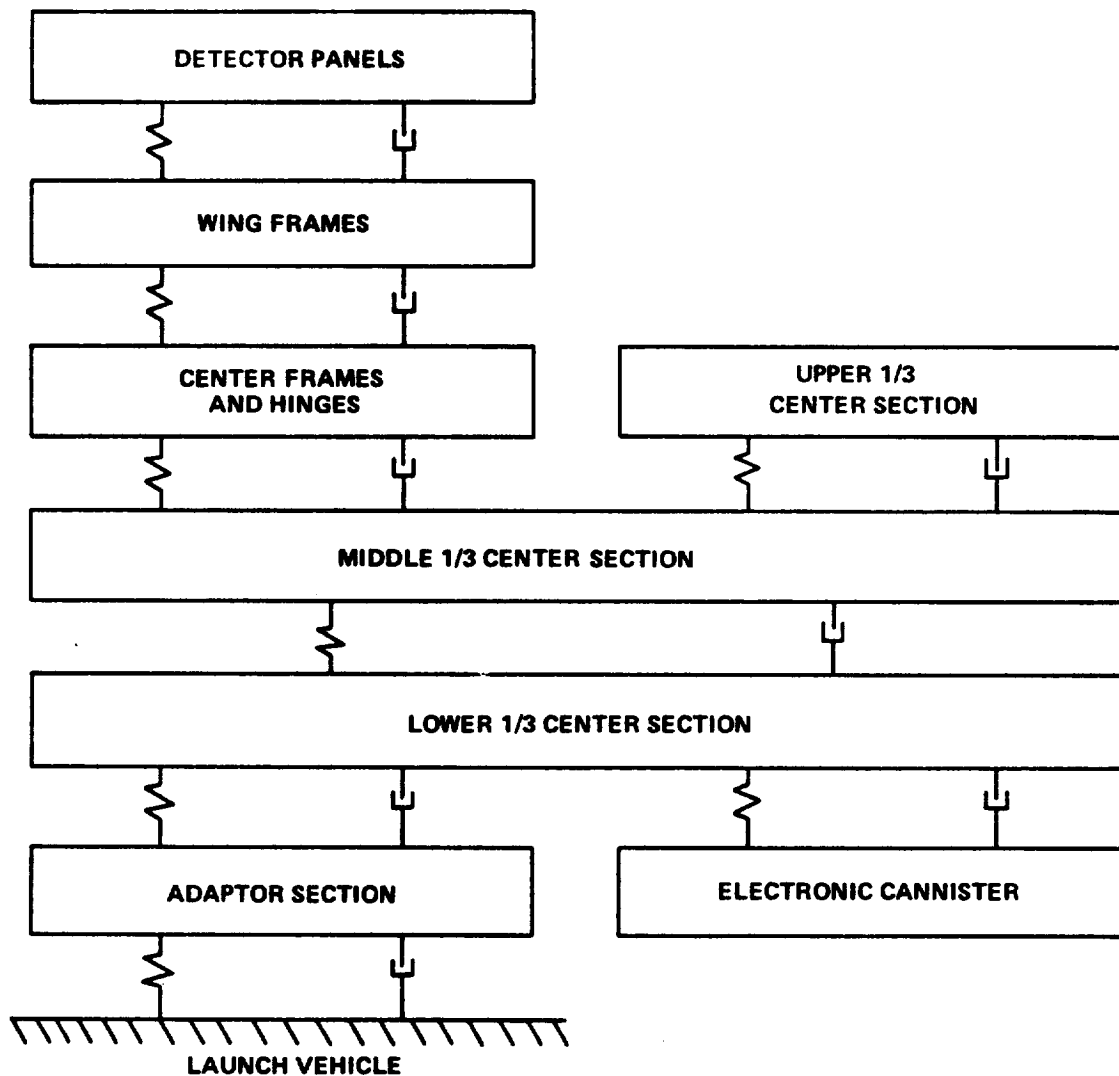
a. Example 1

An example of preliminary design analysis is presented in Reference 71. The reference describes the vibration analysis of the Pegasus Micrometeroid Measuring Satellite. The satellite is a complex structure consisting chiefly of two folding wings containing many micrometeroid detection panels. The total span of the extended wings is about 29.26 m (96 feet). These wings are folded into a compact capsule for launch. During preliminary analysis, no stiffness information or design details were known except the satellite was to weigh about 16.329 kg (3400 pounds). For purposes of calculating the vibration loads during launch on the structure attaching the satellite to the launch vehicle, the system was represented in the longitudinal direction by the following mathematical model.



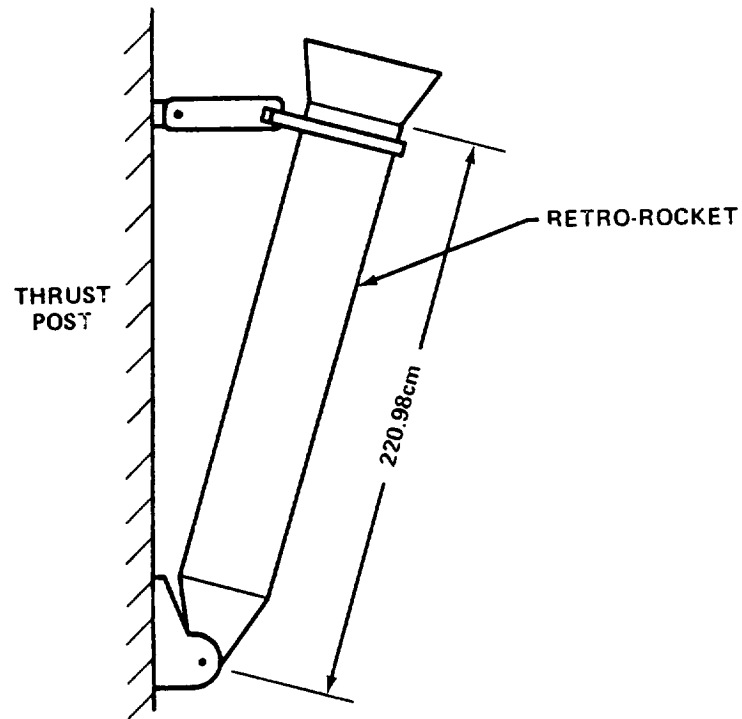
b. Example 2

Considering the Pegasus satellite discussed in Example 1, preliminary analysis showed the support structure could not carry some of the vibration loads. Before redesign was undertaken, better models of the total system were desired. The improved mathematical model shown below was then constructed in the longitudinal direction to better define the loads [71].

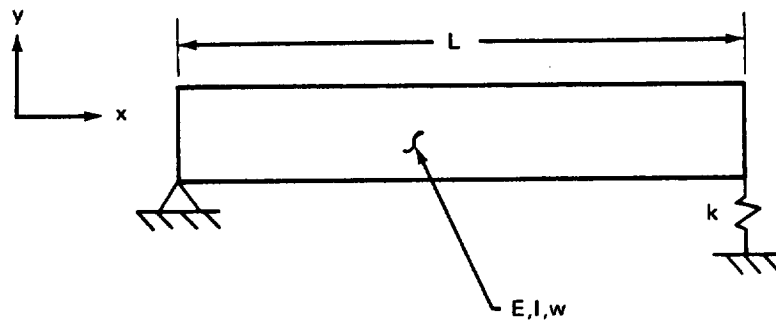


c. Example 3

Another example of a preliminary analysis shows the work done on the S-IC retro-rockets. The retro-rockets are mounted on the thrust posts as shown in the sketch:



The mathematical model idealized the component as a simple, uniform beam with one end simply supported and the other end supported on a spring:



From Reference 72, the general solution of the equation of motion of a uniform beam with end supports is:

$$y = A \sin nx + B \cos nx + C \sinh nx + D \cosh nx .$$

Differentiating,

$$y' = n(A \cos nx - B \sin nx + C \cosh nx + D \sinh nx) .$$

Differentiating three times and multiplying by EI,

$$M = (EI) y'' = n^2 (-A \sin nx - B \cos nx + C \sinh nx + D \cosh nx) (EI)$$

$$V = (EI) y''' = n^3 (-A \cos nx + B \sin nx + C \cosh nx + D \sinh nx) (EI)$$

$$q = (EI) y'''' = n^4 (A \sin nx + B \cos nx + C \sinh nx + D \cosh nx) (EI)$$

where

y = deflection, m

x = length, m

M = bending moment, N/m

V = shear force, N

q = loading, N/m

E = Modulus of elasticity, N/m

I = moment of enertia, m⁴

k = spring constant, N/m

A, B, C, D, n = constants.

The end conditions were then substituted into the foregoing equations: When

$$x = 0, y = 0$$

and

$$y'' = 0$$

$$\therefore B = D = 0$$

when

$$x = L, y'' = 0$$

$$\therefore C = \frac{A \sin nx}{\sinh nx}$$

when

$$x = L, y = \frac{EI}{k} y'''$$

or

$$A \sin nL + \left(\frac{A \sin nL}{\sinh nL} \right) \sinh nL = \frac{EI}{k} n^3 \left[-A \cos nL + \left(\frac{A \sin nL}{\sinh nL} \right) \cosh nL \right] ; \quad (631)$$

therefore,

$$n^3 = \frac{2k}{(EI) (\coth nL - \cot nL)} .$$

Also,

$$q = \frac{w}{g} \omega^2 y$$

where

g = acceleration of gravity, m/sec^2

ω = frequency rad/sec

$$n^4 = \frac{w}{g} \frac{\omega^2}{EI} . \quad (632)$$

The structural properties of the retro-rockets are given below:

$$E = 30 \times 10^6, \quad I = 13.97 \text{ m}^4 (550 \text{ in.}^4), \quad w = 1339.5 \text{ g/cm} \\ (7.5 \text{ lb/in.})$$

$$k = 750.12 \times 10^5 \text{ g/cm} (4.2 \times 10^5 \text{ lb/in.}) \text{ and } L = 2.2098 \text{ m} \\ (87 \text{ in.}) .$$

Therefore, from equation (631),

$$n = 1.114/m (0.0283/\text{in.})$$

and from equation (632),

$$f = \frac{\omega}{2\pi} = 123 \text{ Hz} .$$

The mode shape is calculated next. This is a preliminary analysis so only the first mode is calculated.

$$y = A \sin nx + \left(\frac{A \sin Lx}{\sinh Lx} \right) \sinh nx$$

at

$$x = 0, y = 0$$

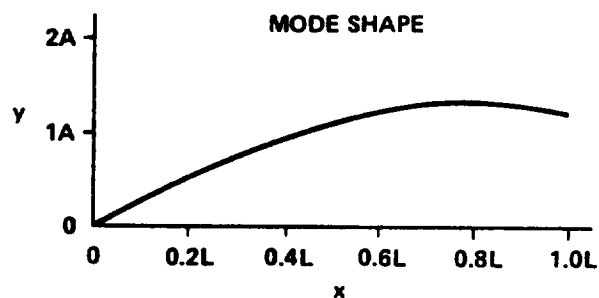
$$x = 0.2L, y = 0.527A$$

$$x = 0.4L, y = 0.958A$$

$$x = 0.6L, y = 1.218A$$

$$x = 0.8L, y = 1.301A$$

$$x = 1.0L, y = 1.258A$$



Use the environment in Sub-Zone 2-5-2-A of Reference 68 as input to the component. The input is applied at both support points in phase. At 123 Hz the vibration environments are .06 g²/Hz random and ±3.2 g steady state sinusoidal. If the damping is assumed to be 4 percent of critical, the magnification is

$$Q = \frac{1}{2(0.04)} = 12.5$$

Assume the maximum response is at $0.8L$, and the vibration load is calculated as follows:

$$\text{Random dynamic load} = (\sigma) \sqrt{\pi/2} (Q) (f) (\text{PSD}) \quad (633)$$

where

σ = confidence level described in Paragraph 2.A.4 of this section.

Q = magnification factor

f = frequency of resonance

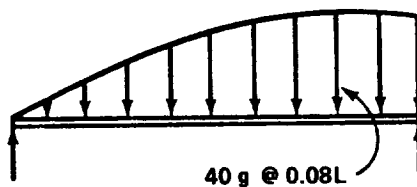
PSD = random vibration input environment at f .

This random dynamic load is the response of a single-degree-of-freedom system to a random input [73]. Because this is a modal analysis, each mode can be considered as a single-degree-of-freedom system and the above load equation applies.

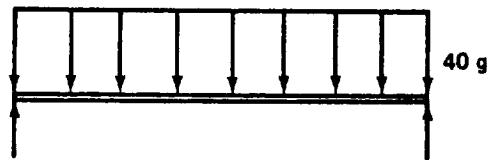
$$\text{Random dynamic load} = (2.2) \sqrt{(\pi/2) (12.5) (123) (0.06)} = 26.4g$$

$$\begin{aligned} \text{Sine dynamic load} &= (Q) (\text{steady state sine environment at } f) \\ &= (12.5) (3.2) = 40g . \end{aligned}$$

The sine load is the highest; therefore, it is used for the load calculations. Using the dynamic load and the mode shape, bending moments and shear loads can be calculated.

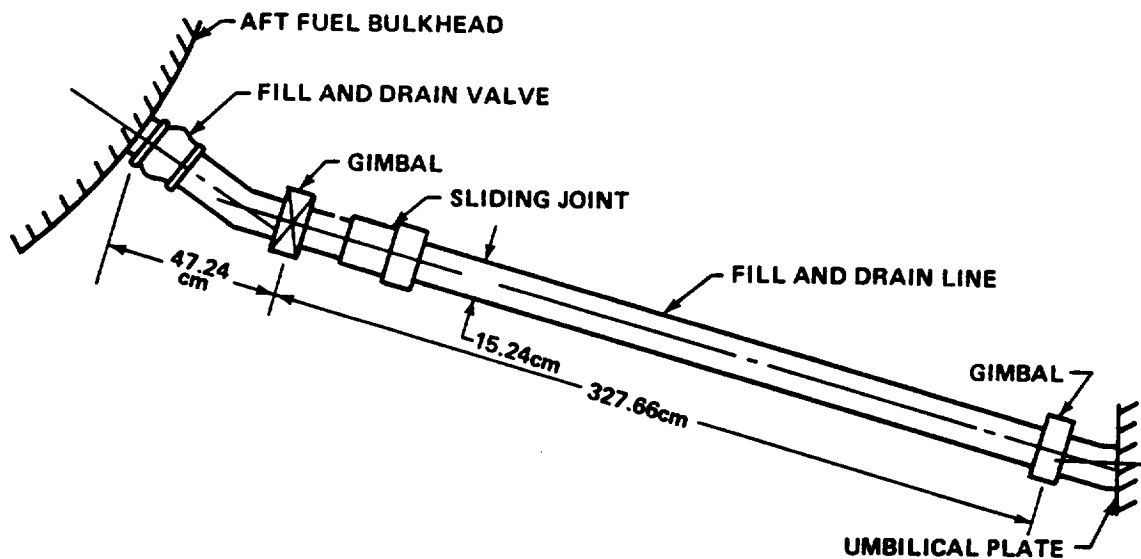


Or, for a quick analysis, the 40 g could be spread uniformly and the loads calculated.

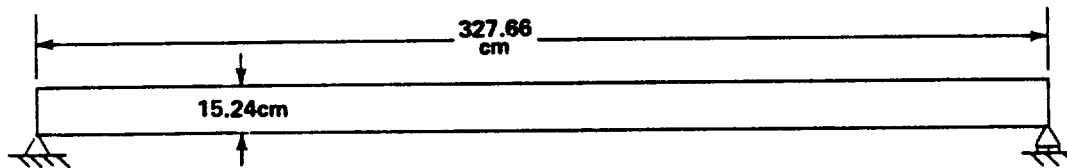


d. Example 4

The following is another example of a preliminary design analysis model. The fuel fill and drain line located in the thrust structure of the Saturn V S-IC stage is the component. The installation is shown in the following sketch:



The preliminary mathematical model is constructed as shown below. Assume the effect of the concentrated mass (sliding joint) cancels the moment carrying capability of the gimbal joints. Assume pinned-pinned end conditions.



$$f = 1.57 \sqrt{\frac{EI}{L^4 w}} = 1.57 \sqrt{\frac{(148) (10)^6 (386)}{(129)^4 (0.328)}}$$

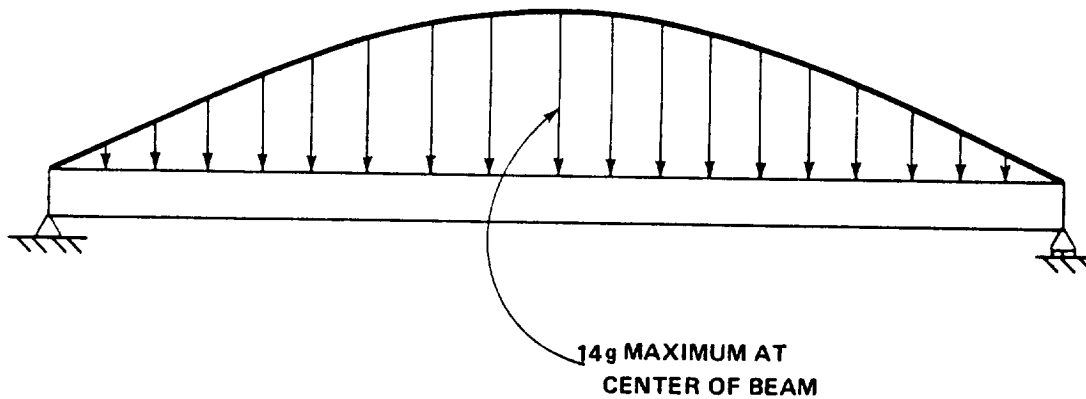
$$f = 39.4 \text{ Hz .}$$

From Reference 68, the input levels at 39.4 Hz are obtained. Use either aft skirt umbilicals (sub-zone 2-1-1-A) or aft fuel bulkhead (sub-zone 2-6), whichever is higher. At 39.4 Hz, the environments are .1 g²/Hz random for sub-zone 2-1-1-A and ±2.75 g steady state sinusoidal for sub-zone 2-6. The damping is assumed to be fairly high due to the friction in the sliding joint and the gimbals. Therefore, assume $Q = 1/2\zeta = 5$.

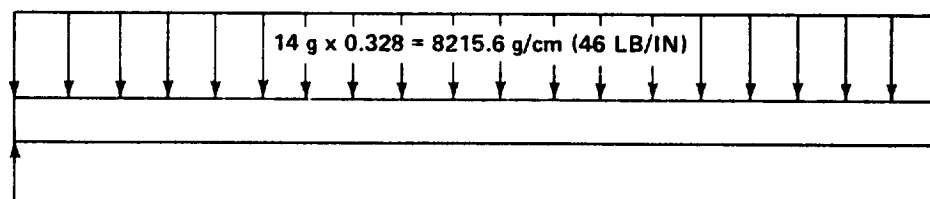
$$\begin{aligned} \text{Random dynamic load} &= (\sigma) \sqrt{(\pi/2) (Q) (f) (\text{PSD})} \\ &= (2.2) \sqrt{(\pi/2) (5) (39.4) (0.1)} = 12.2g \end{aligned}$$

$$\begin{aligned} \text{Sine dynamic load} &= (Q) (\pm G \text{ pk}) \\ &= (5) (2.75) = 14 g . \end{aligned}$$

The sinusoidal load is the highest, so it should be used. The load distribution for the calculated mode would be as shown in the following diagram:



For preliminary analysis the load was spread uniformly along beam length:

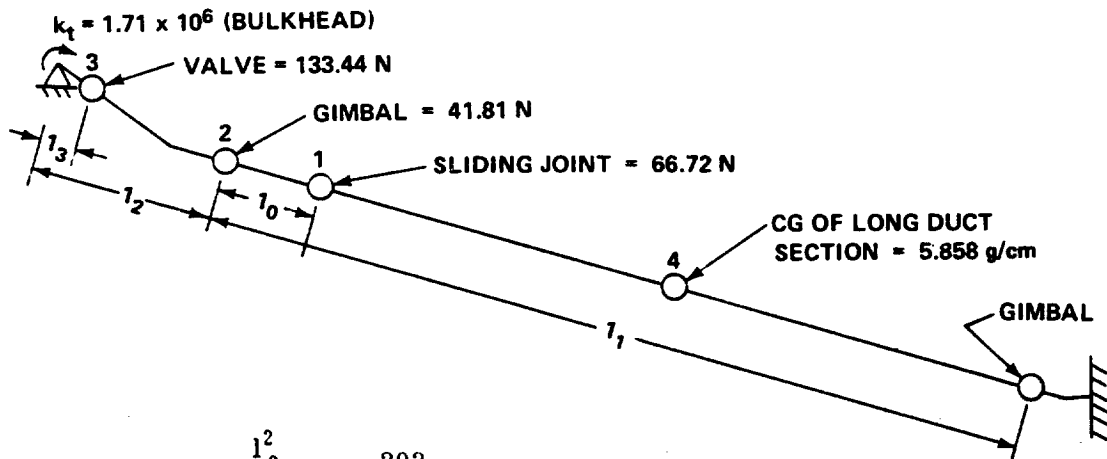


Now, bending moments and shear loads can be calculated.

e. Example 5

Referring back to Example 4, more information was available for a second iteration of the vibration loads analysis of the fuel fill and drain duct. The stiffness (k_t) of the bulkhead was estimated to be about $2.83 \times 10^6 \text{ m-kg/rad}$ ($1.71 \times 10^6 \text{ in.-lb/rad}$). Closer estimates of the weights of the gimbals and the sliding joint were available. An improved mathematical model was then constructed as shown in the following sketch. The duct was assumed straight from bulkhead to umbilical plate for response analysis purposes. The weights of the short sections of the ducts were lumped at the bulkhead and the gimbal, 2. Some of the long duct weight was lumped at the right gimbal. Therefore, $W_1 = 6804 \text{ gm (15 lb)}$, $W_2 = 9072 \text{ g (20 lb)}$, $W_3 = 13608 \text{ g (30 lb)}$, and $W_4 = 9616.3 \text{ g (21.2 lb)}$. The long duct EI is still $433 \times 10^6 \text{ kg - cm}^2$ ($148 \times 10^6 \text{ lb - in.}^2$). The duct lengths are $l_0 = 40.6 \text{ cm (16 in.)}$, $l_1 = 327.6 \text{ cm (129 in.)}$, $l_2 = 47.2 \text{ cm (18.6 in.)}$, and $l_3 = 15.36 \text{ cm (6.05 in.)}$.

The following calculations illustrate one method of estimating force influence coefficients. The equations for the influence coefficients are only estimates. Influence coefficient a_{22} is estimated by assuming the ducts and valve that make up length l_2 are infinitely stiff. Therefore, all motion is due to bulkhead flexibility. This can be assumed because the bulkhead is much less stiff.



$$a_{22} = \frac{l_2^2}{k_t} = \frac{203}{10^6} .$$

Influence coefficient a_{11} is estimated making the same assumption as in a_{22} . Also, assume duct l_1 is a simply supported beam between the gimbals. The short duct attached to the umbilical plate (at right) is assumed infinitely stiff.

$$a_{11} = a_{22} \left(\frac{l_1 - l_0}{l_1} \right)^2 + \frac{(l_1 - l_0)^2 l_0^2}{(3) (EI) (l_1)} = 213 \times 10^{-6} .$$

The other influence coefficients can be estimated in the same manner using similar assumptions.

$$a_{13} = a_{31} = a_{22} \frac{(l_1 - l_0)}{l_1} \cdot \frac{l_3}{l_2} = 58 \times 10^{-6}$$

$$a_{14} = a_{41} = \frac{l_0 (3/4 l_1^2 - l_0^2)}{12 EI} + \frac{a_{22}}{2} \cdot \frac{l_1 - l_0}{l_1} = 199 \times 10^{-6}$$

$$a_{12} = a_{21} = a_{22} \frac{l_1 - l_0}{l_1} = 178 \times 10^{-6}$$

$$a_{23} = a_{32} = a_{22} \frac{l_3}{l_2} = 66 \times 10^{-6}$$

$$a_{24} = a_{42} = \frac{a_{22}}{2} = 102 \times 10^{-6}$$

$$a_{33} = \frac{l_2^2}{k_t} = 21.4 \times 10^{-6}$$

$$a_{34} = a_{43} = \frac{a_{22}}{2} \cdot \frac{l_1}{l_2} = 33 \times 10^{-6}$$

$$a_{44} = \frac{l_1}{48EI} + \frac{a_{22}}{4} = 353 \times 10^{-6} .$$

From the above force influence coefficients, the inverse of the stiffness matrix $[K]^{-1}$ can be written, and from the weights given previously, a mass matrix $l/g[W]$ can be written. Therefore, the eigenvector equation is:

$$-(\omega_n^2/g) [K]^{-1} [W] \{x\} = 0 .$$

The derivation of the above equation can be seen in Section XIII. B. 4. and is analogous to

$$-\omega^2 \frac{m}{k} x + x = 0$$

in the single-degree-of-freedom case. The eigenvector equation becomes:

$$(\omega_n^2/g) [D] \{x\} = \{x\}$$

where $[D] = [K]^{-1} [W]$ is the dynamic matrix or

$$\begin{pmatrix} x_1 \\ x_2 \\ x_3 \\ x_4 \end{pmatrix} = \frac{\omega_n^2}{10^6 g} \begin{bmatrix} 3200 & 3560 & 1740 & 4220 \\ 2670 & 4060 & 1980 & 2160 \\ 870 & 1320 & 641 & 700 \\ 2980 & 2040 & 990 & 7490 \end{bmatrix} \begin{pmatrix} x_1 \\ x_2 \\ x_3 \\ x_4 \end{pmatrix} .$$

Solving for the eigenvalues and eigenvectors, the frequency and shape of first mode are obtained. The solution may be obtained by using any of a number of iteration techniques such as shown in Section XIII.B.5. or using a computer.

$$\omega_1 = 183 \quad f_1 = 29.2 \text{ Hz}$$

$$\begin{pmatrix} x_1 \\ x_2 \\ x_3 \\ x_4 \end{pmatrix} = \begin{pmatrix} +0.830 \\ +0.645 \\ +0.210 \\ +1.000 \end{pmatrix}$$

Then the second mode is obtained

$$\omega_2 = 322 \quad f_2 = 51.3 \text{ Hz}$$

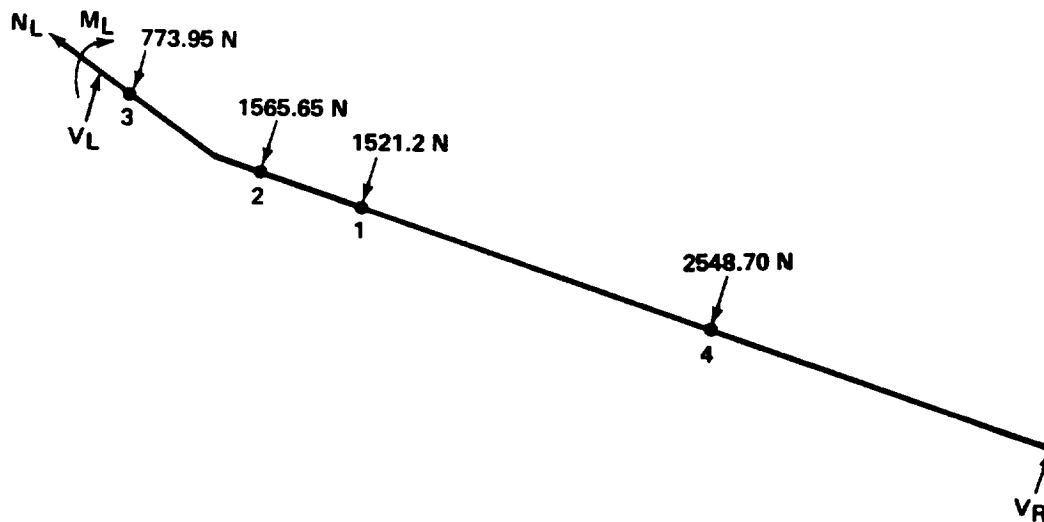
$$\begin{pmatrix} x_1 \\ x_2 \\ x_3 \\ x_4 \end{pmatrix} = \begin{pmatrix} -0.385 \\ -1.000 \\ -0.326 \\ +0.937 \end{pmatrix}$$

Since this is not a final analysis, only two modes were calculated to save time. From Reference 68, the input environments are :

<u>Zone</u>	<u>Random</u>	<u>Steady State Sine</u>	<u>Frequency</u>
2-1-1-A	0.1 g ² /Hz	±1.8 g	29.2 Hz
2-6	0.02 g ² /Hz	±2.75 g	29.2 Hz
2-1-1-A	0.1 g ² /Hz	±2 g	51.3 Hz
2-6	0.065 g ² /Hz	±2.75 g	51.3 Hz

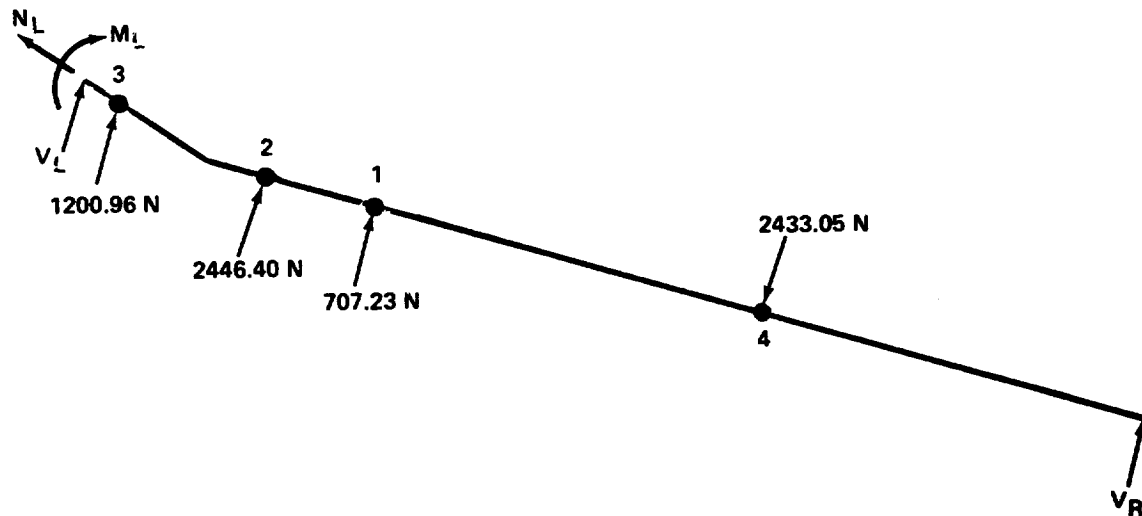
Assuming $Q = 10$, the steady state sinusoidal loads are calculated using the highest environment as the input at 29.2 Hz

$$\begin{aligned}
 \text{Dynamic load} &= (Q) (x_n) (\pm G \text{ pk}) (\text{weight}) \\
 &= (10) (0.83) (2.75) (15) = 521.21 \text{ N (342 lb) at 1} \\
 &= 1565.65 \text{ N (354 lb) at 2} \\
 &= 773.95 \text{ N (174 lb) at 3} \\
 &= 2548.70 \text{ N (573 lb) at 4}
 \end{aligned}$$



at 51.3 Hz

$$\begin{aligned}
 \text{Dynamic load} &= -707.23 \text{ N (-159 lb) at 1} \\
 &= -2446.4 \text{ N (-550 lb) at 2} \\
 &= -1200.96 \text{ N (-270 lb) at 3} \\
 &= 2433.05 \text{ N (547 lb) at 4}
 \end{aligned}$$



The random vibration loads are calculated using the highest environment as input at 29.2 Hz.

$$\text{Dynamic load} = (x_n) (\sigma) \sqrt{(\pi/2) (Q) (f) (\text{PSD}) (\text{weight})}$$

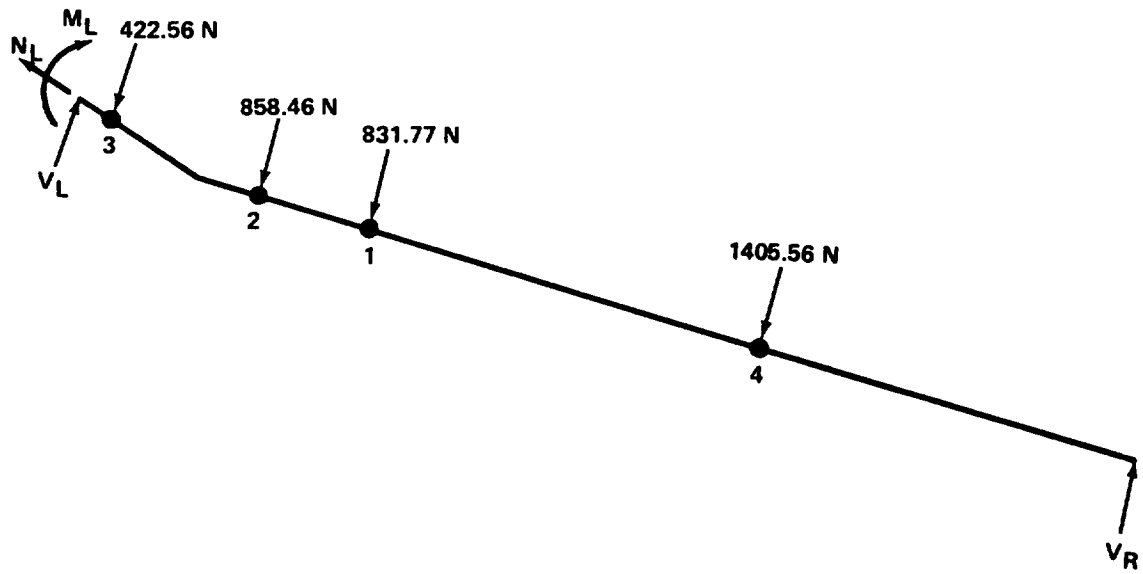
where

x_n = mode shape

(weight) = weight of lumped mass n

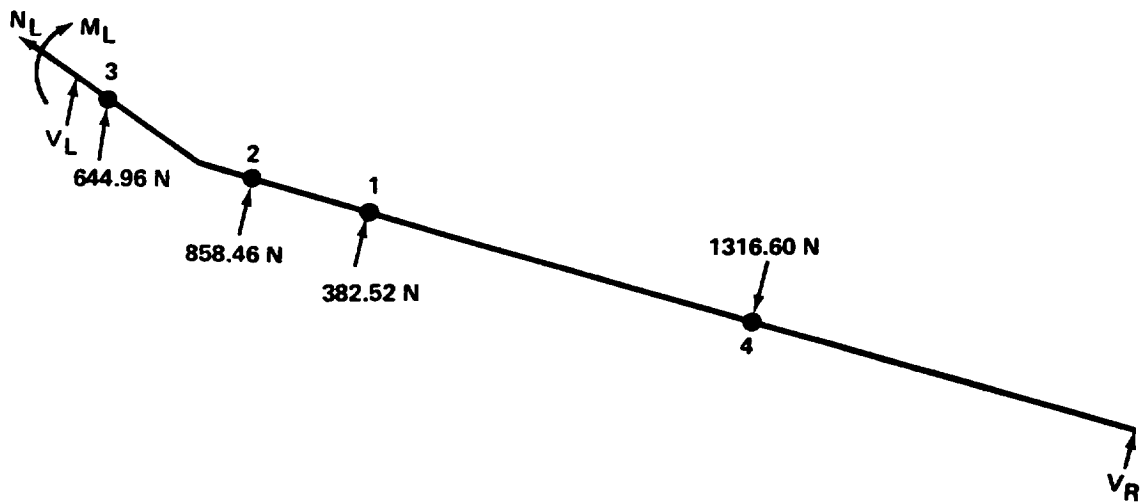
σ , Q , f , PSI are defined in equation (634).

$$\begin{aligned} \text{Dynamic load} &= (0.83) (2.2) \sqrt{(\pi/2) (10) (29.2) (0.1) (15)} \\ &= 831.77 \text{ N (187 lb) at 1} \\ &= 858.46 \text{ N (193 lb) at 2} \\ &= 422.56 \text{ N (95 lb) at 3} \\ &= 1405.56 \text{ N (316 lb) at 4} \end{aligned}$$



at 51.3 Hz

Dynamic load = -382.52 N (-86 lb) at 1
 = -858.46 N (-193 lb) at 2
 = -644.96 N (-145 lb) at 3
 = 1316.60 N (296 lb) at 4



With the above loads, the forces and moment at the bulkhead, at the right gimbal, and along the duct can be calculated.

f. Example 6

The following figures show the model used for the final design analysis of the cold helium feeder duct in the thrust structure of the Saturn V S-IC. The duct is installed as shown in Figure 125.

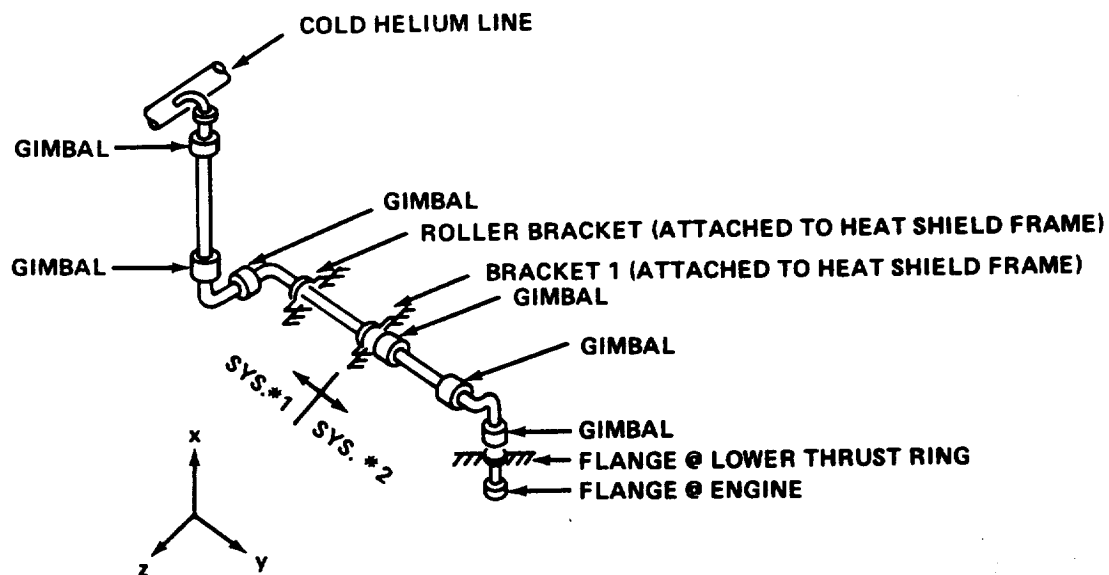
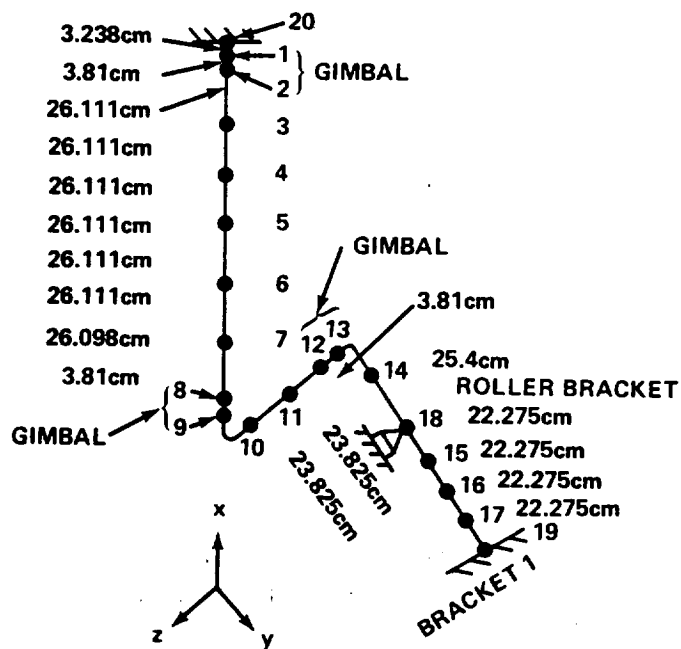


Figure 125. Cold helium feeder duct installation.

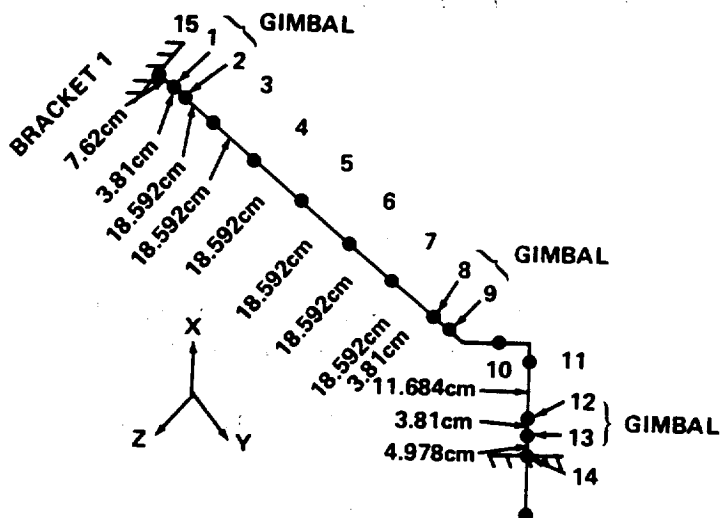
For the analysis, the duct was broken into two systems at bracket 1. The duct was analyzed in two parts because it was qualification tested that way.

The gimbals were taken as short beams [3.81 cm (1.5 inches long)] with a flexural rigidity equal to the spring rate of the gimbal. The ducts were assumed to have no rotational inertia. The ends of the ducts were fixed in all directions simulating the qualification test set-up.

SYSTEM ONE



SYSTEM TWO



B. Use of Vibration Loads in Strength Analyses

The vibration loads calculated by the methods of Paragraph 1 below are to be used by the designer and stress analyst; therefore, these people must be told the meaning of the loads and how the loads are applied. The following paragraphs describe relationships between vibration loads and design loads. The statistical confidence levels associated with vibration loads are also described.

1. DESIGN LOADS AND CONFIDENCE LEVELS

a. Limit Load

The limit load is defined to be the maximum expected steady state load that a particular component or structure will see in service. Vibration loads calculated as shown in the previous paragraphs are considered to be limit loads.

b. Yield Load

The yield load is the maximum load that a component can carry without the weakest part of the component or structure yielding (stressed beyond the defined elastic limit). For MSFC applications, the yield load should be 1.1 times the total limit load.

c. Ultimate Load

The ultimate load is the maximum load that a component can carry without the weakest part of the component or structure rupturing. The ultimate load is usually 1.4 times the total limit load.

d. Confidence Levels

In calculating a response vibration load, a statistical confidence level should be specified. All vibration loads will have an applicable confidence level unless the input levels are known exactly. For example, one can state that the shear load at a point on a structure will not exceed X newtons with a 97.5 percent confidence level, meaning that 97.5 percent of the time the structure is in use the shear load at the point will be less than X newtons.

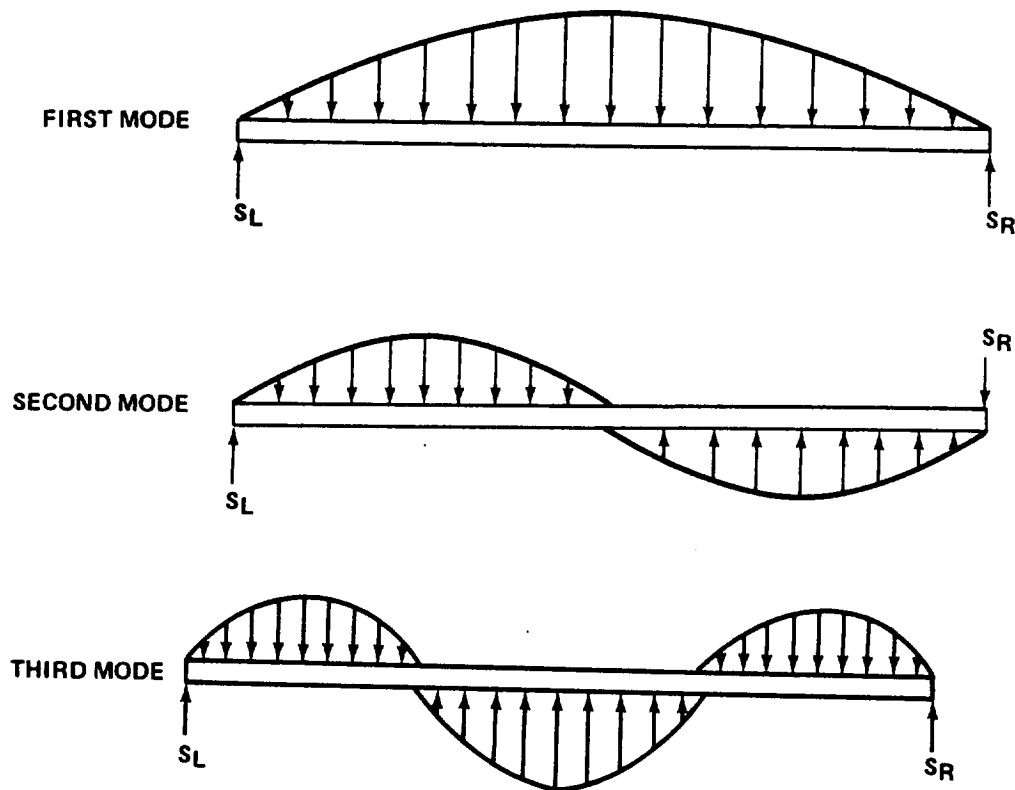
For the random vibration environment, the associated level states the confidence that the environment is the root mean square (rms) or 1 sigma acceleration level. The associated confidence level for the MSFC environments

is 97.5 percent. Therefore, the random response vibration load calculated is the rms or 1 sigma load with 97 percent confidence. MSFC requires that the design random vibration loads shall be 2.2 times the rms load. Therefore, the calculated random vibration loads (limit loads) are 2.2 sigma loads with 97.5 percent confidence.

The steady state sinusoidal loads also have a 97.5 confidence level due to the input environment. The sinusoidal loads are deterministic and do not have an associated probability occurrence. Therefore, they are not multiplied by any sigma value.

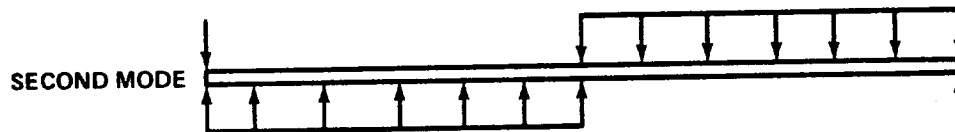
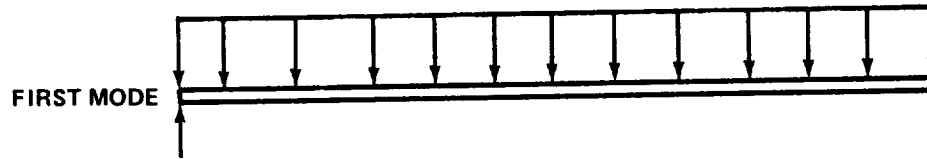
2. EQUIVALENT STATIC LOADS

Vibration response loads are usually applied as static loads in a strength analysis. For example, consider the first three modes of a pinned-pinned beam. The vibration load would be applied as a static load as shown below:

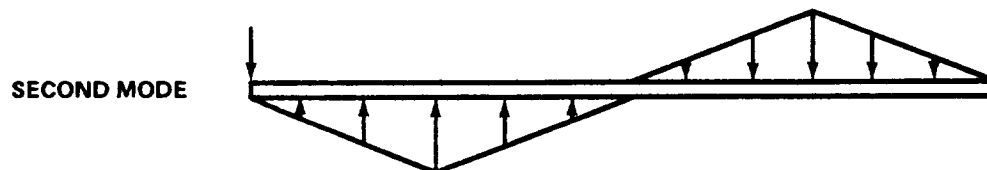
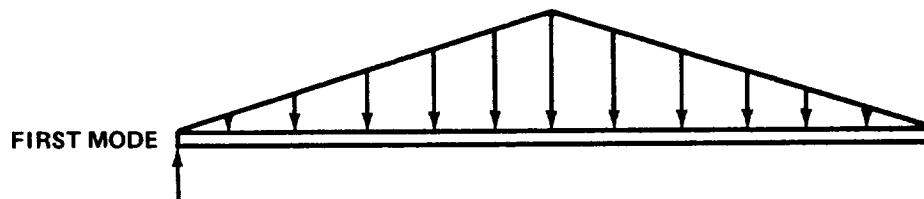


The strength analysis could then be accomplished using the above loading conditions. The loading conditions should then be reversed and the analysis re-done because the vibration load is plus and minus.

For quick analyses, the actual load diagrams, shown above, can be simplified. The curved load profile could be replaced with a rectangular load profile with either equal area under the load curves or the maximum load of the actual profile spread uniformly.



Another assumed load profile shape could be triangular. The area of the actual profile and the triangular profile could be equated, or the maximum of the actual load could be equated to the maximum of the assumed triangular profile.



3. COMBINING LOADS

a. Time Correlation of Loads

Vibration loads should be combined with all other applicable loads when conducting a strength analysis of a component or structure. Time correlation

is one method of determining whether load combination is applicable. Loads from various sources should not be combined if they do not occur at the same time. For example, transient loads which occur at stage separation or engine cutoff do not occur during periods of high steady state vibration loads; whereas other transient loads, such as hold down release, do occur during periods of high steady state vibration loads. Therefore, the former loads would not be combined with vibration loads and the latter would be combined.

The following is a list of types of loads which can and cannot be expected to combine with high, steady state vibration loads.

Loads Likely to Combine
With Vibration Loads

Pressurization
Venting
Lift-off (Hold down Release)
Vehicle Bending
Vehicle Torsion
Vehicle Acceleration
POGO
Thrust Vectoring (Gimballing)
Aerodynamic
Fluid Flow in Ducts
Slosh
Valve Opening or Closing

Loads Not Likely to Combine
With Vibration Loads

Ignition Transients
Cutoff Transients
Separation of Stages
Rebound
Propellant Loading
Pre-ignition Pressurization

b. Combining Static and Vibration Loads

Static loads and vibration loads are added directly. The vibration load should be taken as an equivalent static load, keeping in mind that the vibration load is two directional; i. e., plus and minus. Therefore, the vibration load will add to the static load in one direction and subtract in the other.

c. Combining Normal Mode Loads

Depending on circumstances, modal loads may or may not be combined. If a modal analysis is done simulating a sinusoidal qualification test, the modes are not combined since only one mode at a time is usually excited. If the analysis is simulating actual service or random testing, the modes should be added because random vibration can excite all modes simultaneously.

Loads from each of the modes in any one axis are combined by the square-root-of-the-sum-of-the-squares method. Stated in equation form, the modal loads are combined as follows:

$$\text{Dynamic Load} = \sqrt{(\text{Load of 1st mode})^2 + (\text{Load of 2nd mode})^2 + \dots}$$

d. Combining Multiple Axes Loads

Loads from different axes are usually specified separately but can be combined if desired. This type of load combination may be necessary if a single resultant vibration load is desired instead of orthogonal axes vibration loads. Another case when multiple axes loads may be combined is the addition of vehicle bending or torsion loads to component vibration loads when the vehicle axes do not correspond to the component axes.

In order to combine multiple axes loads into a resultant load in a particular direction, the component of each individual load in the desired direction must be found. The uniaxial components of all loads are then combined by the square-root-of-the-sum-of-the-squares method as shown in Paragraph c. above.

e. Combining Shock and Vibration Loads

An input shock load is assumed to excite all modes in the direction of the load. The response shock load is therefore a short duration vibration load and can be combined with steady state vibration loads. If phasing is known, then the shock and vibration loads can be added exactly; otherwise the square-root-of-the-sum-of-the-squares method applies as shown in Paragraph c. above.

C. Vibration Damage

Damage due to vibration is fatigue damage rather than any type of overload failure. Vibration fatigue damage can happen in rather short periods of time; i.e., 10^4 cycles at 100 Hz = 1.7 minutes. Therefore, methods of determining the extent of fatigue damage sustained by a component or structure may be necessary in designing for vibration.

Mechanisms of fatigue damage are complex and depend on material, notch sensitivity, stress level, time variation of loading, orientation of

the crystalline structure, flaws, etc. [74]. Due to these complexities, the cumulative fatigue damage theories now in existence are not very accurate, but lacking any simple, improved methods, the existing theories are used. The listing of fatigue damage theories could be very long if all were included; however, the following three should give the reader a general idea of fatigue damage estimation.

1. CUMULATIVE DAMAGE THEORIES

a. Miner's Linear Damage Criteria

Miner's rule [75, 76] theorizes that a structure or component will fail when a unique amount of energy has been absorbed by the structure at the point of failure. This energy absorbed is proportional to the damage inflicted. Fatigue damage due to a given load is assumed proportional to the ratio of the number of cycles at the given load to the number of cycles required to cause failure at that load. This is called the cycle ratio. If a number of different loads are applied in succession, failure will occur when the sum of the cycle ratios of the loads equals one, or

$$\frac{n_1}{N_1} + \frac{n_2}{N_2} + \frac{n_3}{N_3} + \dots + \frac{n_k}{N_k} = 1$$

where

n_k = number of cycles of applied load k

N_k = number of cycles at load k which would cause failure.

This cumulative damage theory does not account for the beneficial or detrimental effects of different levels of loading in sequence. Many investigators have found that if low load amplitudes are followed by higher load amplitudes, the cycle ratios sum will be greater than one, and high load followed by low load will result in a cycle ratios, sum less than one.

b. Non-Linear Damage Theory of Marco and Starkey

Marco and Starkey [75] explain the variation of the cycle ratios sum by assuming that damage accumulates slowly at first and then rapidly as failure approaches. The initial damage rate is higher for higher applied loads. In equation form

$$D_i = (n_j/N_j)^{X_j}$$

where

D_i = damage after the i^{th} cycle of load j

n_j/N_j = cycle ratio of load j

$X_j = f(\sigma)$, the exponent is a function of the stress level σ_j of load j for any given material.

The above equation is used in the following manner, assuming X_j is known for all the applied loads.

From cycle ratio n_1/N_1 of load 1, calculate the resultant damage D_1 :

$$D_1 = (n_1/N_1)^{X_1} .$$

Then calculate an equivalent cycle ratio for load 2 which would give damage D_1 :

$$D_1 = (n_{2e}/N_{2e})^{X_2} .$$

Add the actual cycle ratio n_2/N_2 of load 2:

$$(n_{2e}/N_{2e}) + (n_2/N_2) = (n_{1+2}/N_{1+2}) .$$

Then calculate the total damage the component has sustained after application of load 1 and load 2:

$$D_{1+2} = (n_{1+2}/N_{1+2})^{X_2} .$$

Using this method, the damage due to any number of successive loads could be calculated. The component will fail when $D_{1+2} + \dots + k = 1$. The order of succession of loads must be known when using this method.

c. Non-Linear Damage Theory of Henry

Henry [75] proposed another method of predicting fatigue damage from non-constant loading.

$$D_i = \frac{\beta_j}{1 + (1 - \beta_j) \gamma_j^{-1}}$$

where

D_i = damage after the i^{th} cycle of load j

β_j = cycle ratio of load j

γ_j = "overstress ratio" = $\frac{\sigma_j - F}{F}$ of load j with F being the material fatigue limit.

The damage due to the various loads are calculated and summed similarly to the method in Paragraph b. above. This method also requires knowledge of the order of load application.

2. APPLICATION OF DAMAGE THEORIES

a. Damage Due to Sinusoidal Loading

Sinusoidal loading would be either a constant level load or loading with a known variation. Either way, the cumulative fatigue damage can be estimated by one of the methods of Paragraph 1. above using known material fatigue strength values and measuring or calculating the stress level of the component.

For constant level loading, Miner's rule is a valid criterion. Material fatigue strengths are determined by constant level testing. It must be kept in mind that the normal S-N fatigue life curve is an average or mean curve, half of the specimens tested failed before the curve indicates and half lasted longer than the curve indicates.

For sinusoidal loading with a known load variation, non-linear fatigue damage criteria, such as Henry's theory (Paragraph 1.c above), have been shown to be more accurate [75]. Non-constant level sinusoidal loading can arise under circumstances such as sinusoidal sweep testing when passing through resonances of the test specimen.

Referring to Paragraph 1.c above, it can be seen that the cycle ratio of each loading level must be calculated. For the case of sinusoidal sweep testing, the cycle ratios of the various loading levels could be calculated as follows, knowing the response versus frequency characteristics from accelerometers or strain gages mounted on the test specimen and knowing the test frequency sweep rate. The response stress levels can be classed into amplitude steps (8 or 10 steps from minimum to maximum level). The time in each amplitude step is known; therefore, the cycle ratio of each step can be calculated, knowing the average frequency of each step. Then the accumulated damage can be estimated.

b. Damage Due to Random Loading

Random loading is more complex than constant level loading, because it is difficult to calculate cycle ratios of the various levels of loads and the sequence of loading cannot be determined. Usually some sort of damage estimate is made based on assuming a loading distribution and linear cumulative damage. Random S-N curves of the materials used would be helpful in estimating fatigue damage [77].

The fatigue damage sustained by a component could be estimated in the following manner. First the rms acceleration levels and the time at each level must be found. The time and level the component experienced during lab tests can be found from lab and test reports. The time that the component experienced actual service environments can be found from service test records. The levels during the service test must be estimated if transducers were not mounted on the component. The service level estimates can be based on predicted environments such as listed in Reference 68, or can be based on data taken near the component during a service test. The service levels must be the response, not the input levels of the component. All the loads that the component experienced must be used to get the stress history at the critical location on the component where failure will occur first.

Next, the stress history must be classed into amplitude steps (8 or 10 steps from minimum to maximum). Assuming some distribution of stress cycle levels, such as the Rayleigh distribution which has been found to fit the distribution of peaks of a random process very well, the number of cycles in each amplitude step can be estimated.

D. The MSFC Environment Documents

MSFC has published documents specifying the vibration, shock, and acoustic environments for the Saturn vehicles [67, 68, 78]. MSFC has also published a document [69] which describes a method by which an environment may be predicted if certain information is known. These documents and their use are described in the following paragraphs.

1. SELECTING THE PROPER ENVIRONMENT

In order to specify a representative environment for the various types of structure and the many components in the Saturn vehicles, they were divided into zones and subzones. For instance, the Saturn V first stage (the S-IC) is broken down into seven major zones such as the engine area, the thrust structure, the aerodynamic fins, etc. Each of these major zones is then broken into subzones corresponding to particular types of structure or even particular components. For example, in the thrust structure (Zone 2) there is a subzone for the skin stiffeners of ring frames, another subzone for the center engine support beams, etc.

In order to find the applicable subzone environment for use in a loads analysis of a particular component, one must know the exact location of the component. If the exact location is in doubt, the more severe environment of the major zone should be selected. Each of the MSFC environment documents describes the procedure for selecting the proper zone or subzone.

2. VIBRATION AND SHOCK ENVIRONMENTS

The zone or subzone vibration environment is made up of two parts; the random vibration environment and the sinusoidal sweep environment. These two environments represent the steady state level and any short duration high levels that may occur during static firing and flight.

The random vibration environment represents, with a 97.5 percent confidence level, an envelope of the steady state random vibration that will occur in the particular zone or subzone during static firing and flight. These random levels were derived from statistical analyses of data from previous vehicles and adjusted to account for significant differences in vehicles. For more information on derivation of the random vibration levels, the reader is referred to Reference 69 in conjunction with Reference 79.

The sinusoidal sweep vibration level is used to account for any short duration, high level vibration which may occur that is higher than the steady state level. One half the sinusoidal sweep level is an envelope of the steady state rms acceleration levels which will occur, with a 97.5 percent confidence level, during static firing and flight. In a dynamic loads analysis, one half the sinusoidal sweep level should be used as the input vibration level. Again, the reader is referred to References 69 and 79 for a more complete derivation.

The shock environments can be found on the same page as the vibration environments.

3. ACOUSTIC ENVIRONMENTS

The acoustic environments are divided into major zones and designated internal or external within a zone. Internal or external merely means that the environment is either within the vehicle or outside the vehicle.

4. WEIGHT ATTENUATION

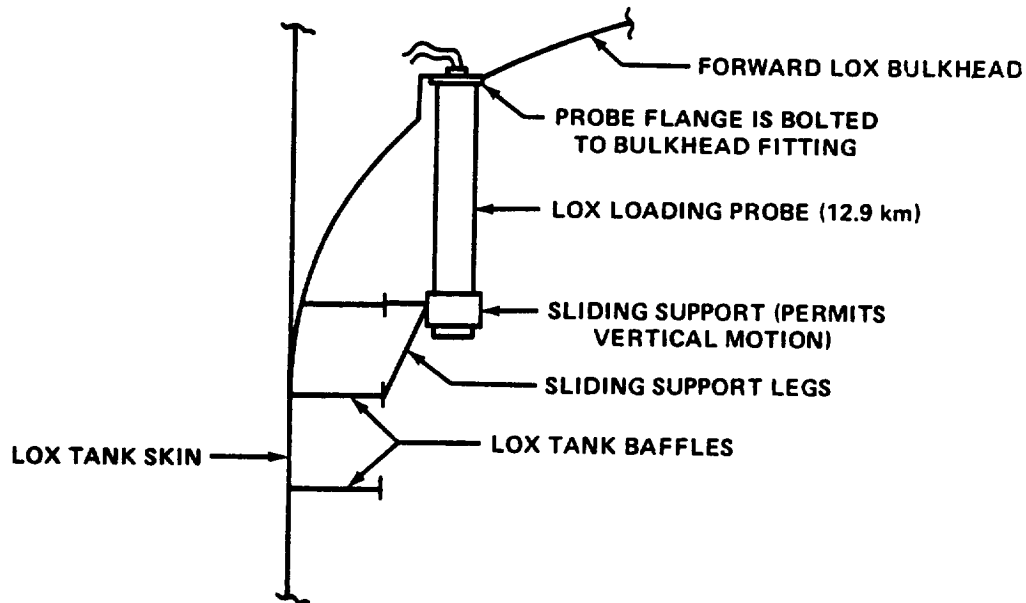
If the vibration environment specified in the environment documents [67, 68, 78] are used without modification as inputs to components, the driving structure is assumed to have an infinite impedance. That is, anything attached to the driving structure will have no effect on the motion of the driving structure. In many instances this is obviously not true, and the effect is recognized by a method of environment attenuation known as "weight attenuation." This method attempts to account for the mass impedance of the component by attenuating the driving structure environment. The attenuation factor is shown below:

$$\text{Weight Attenuation Factor} = F = \frac{\text{Weight of Structure}}{\text{Weight of Structure} + \text{Weight of Component}}$$

The weight attenuation factor F is applied to reduce the random environment. The square root of $F = \sqrt{F}$ is applied to reduce the sinusoidal environment. The square root of $F = \sqrt{F}$ is also used to lower the frequencies of both the random and the sinusoidal environment.

This method must be used with great care and judgement and approved by the Vibration and Acoustics Branch of MSFC's Propulsion and Vehicle Engineering Laboratory.

The following is an example of the weight attenuation technique used for a component mounted on the forward LOX bulkhead of the S-IC. The component is the LOX loading probe with a weight of about 12.9 kg (28.5 pounds). It extends through the bulkhead in the manner shown in the sketch below:



For this problem, the probe was assumed to be perpendicular to the bulkhead because the environment is specified in that direction. Therefore, the attenuated environment in the perpendicular direction is calculated as follows:

Weight of component = weight of probe [12.9 kg (28.5)] plus weight of bulkhead fitting [4.0 kg (8.9)]

$$W_C = 12.9 + 4.0 \text{ (28.5 + 8.9) = 16.9 kg = (37.4 pounds).}$$

An area of the bulkhead of about 2-1/2 times the fitting was assumed to be the effective structure size. The average thickness of the bulkhead was assumed to be 0.381 cm (0.15 inch).

$$\begin{aligned}\text{Weight of structure} &= (\pi) (R)^2 (t) (\rho) \\ &= (\pi) (20)^2 (0.15) (0.1) = \text{about } 9.07 \text{ kg (20 lb)}.\end{aligned}$$

Therefore, the attenuation factor is

$$F = \frac{20}{20 + 37.4} = 0.35$$

and

$$\sqrt{F} = \sqrt{0.35} = 0.59 \quad .$$

The environment to be attenuated is the forward LOX bulkhead environment, subzone 7-1 in Reference 68.

Subzone 7-1 Random Environment (perpendicular to bulkhead)

20-55 Hz at $0.1 \text{ g}^2/\text{Hz}$

55-160 Hz at +9 dB/oct

160-630 Hz at $2.5 \text{ g}^2/\text{Hz}$

630-2000 Hz at -9 dB/oct

Subzone Sinusoidal Sweep Environment (perpendicular to bulkhead)

5-36 Hz at 1.016 cm (0.4 in.) D.A.

36-450 Hz at $\pm 26.0 \text{ g pk}$

450-550 Hz at 0.00635 cm (0.0025 in.) D.A.

550-2000 Hz at $\pm 38.0 \text{ g pk}$

The attenuation factors are now used to modify the above environments. It must be kept in mind that both the acceleration levels of the environment and the frequencies of the environment are lowered by this technique.

The random environment is attenuated as shown below:

$$(G) (F) = (G \text{ attenuated})$$

$$(0.1) (0.35) = 0.035 \text{ g}^2/\text{Hz}$$

and

$$(2.5) (0.35) = 0.87 \text{ g}^2/\text{Hz} .$$

Lower frequencies

$$(f) (\sqrt{F}) = (f \text{ attenuated})$$

$$(20) (0.59) = 12 \text{ Hz}$$

and

$$(12) + (55-20) = 47 \text{ Hz}$$

$$\text{antilog} \left(\frac{3.01}{+9} \log \frac{0.87}{0.035} + \log 47 \right) = 138 \text{ Hz}$$

$$(138) + (630-160) = 608 \text{ Hz} .$$

Therefore, attenuated random environment is

12-47 Hz at $0.035 \text{ g}^2/\text{Hz}$

47-138 Hz at $+9 \text{ dB/oct}$

138-608 Hz at $0.87 \text{ g}^2/\text{Hz}$

608-2000 Hz at $-9 \text{ dB/oct} .$

The random environments in Reference 68 do not extend below 20 Hz; so the first frequency of 12 Hz could be made 20 Hz, thus slightly decreasing the width of the lower constant level bandwidth.

The sinusoidal environment is attenuated as shown below

$$(\pm G) (\sqrt{F}) = (\pm G \text{ attenuated})$$

$$(26) (0.59) = \pm 15 \text{ g pk}$$

and

$$(38) (0.59) = \pm 22 \text{ g pk} .$$

Lower frequencies

$$(f) (\sqrt{F}) = (f \text{ attenuated})$$

$$(36) (0.59) = 21 \text{ Hz}$$

and

$$(450) (0.59) = 265 \text{ Hz}$$

$$\text{D.A. displacement (at 265 Hz)} = \frac{15}{(0.051) (265)^2} = 0.01066 \text{ cm}$$

$$(0.0042 \text{ in.}) \text{ D.A.}$$

$$\text{next frequency} = \sqrt{\frac{22}{(0.051) (0.0042)}} = 320 \text{ Hz} .$$

Therefore, the attenuated sinusoidal environment is

21-265 Hz at ± 15 g pk

265-320 Hz at 0.01066 cm (0.0042 in.) D.A.

320-2000 Hz at ± 22 g pk .

The environment is complete except for less than 21 Hz so the displacement below 21 Hz must be found

$$\text{inches D.A.} = \frac{15}{(0.051)(21)^2} = 1.691 \text{ cm (0.666 in.) D.A.}$$

Therefore, the attenuated sinusoidal environment less than 21 Hz is

5-21 Hz at 1.691 cm (0.666 in.) D.A.

It was assumed that in the direction tangential to the bulkhead that little or no attenuation would occur because less of the probe weight would be effective and more of the bulkhead would probably be effective.

5. PREDICTING ENVIRONMENTS

NASA Technical Note D-1836 [69] presents a technique for predicting environments on rocket vehicles. The technique is based on certain assumptions.

a. Similar types of structure possess essentially similar dynamic characteristics.

b. There are only two sources of vibration energy, mechanically induced vibration from the rocket engines or other machinery in motion and fluctuating pressure excitation from engine noise and boundary layer noise.

c. All vibration sources have wideband random frequency content similar to spectra used as references.

The method is empirical and the inaccuracies must be recognized.

The example shown in Reference 69 illustrates the calculations necessary in applying the method.

E. Useful Relationships

This paragraph presents techniques for environment spectrum shaping, conversion of environmental quantities to other quantities, and calculation of spectrum composites. These techniques are primarily connected with vibration testing but are useful in loads calculations.

1. VIBRATION ENVIRONMENT SPECTRUM SHAPE

The shape of the spectrum of a vibration environment is influenced by the capabilities of vibration testing equipment. Even if an environment may never be used as an actual test input, it is usually shaped with test equipment in mind.

a. Sinusoidal Environments

Sinusoidal sweep environments are usually shaped such that the amplitude levels are either constant displacement or constant acceleration as frequency increases. Most modern sweep test equipment has an automatic sweep speed drive that varies the test frequency logarithmically. The equipment also has an automatic gain control which varies the power to the vibrator so the displacement or the acceleration to the test specimen can be kept constant. Therefore, the MSFC sinusoidal sweep specifications are shaped with constant levels and logarithmic frequency sweep rates.

Constant levels mean that as frequency increases the acceleration level must either increase or be constant. If one decides that the acceleration level of an environment at the higher frequencies is not realistic, a square step down can be specified, such as

XXX-500 Hz at ± 20 g pk

500-2000 Hz at ± 10 g pk .

This means that at 500 Hz, the test operator must manually turn down the gain on the test equipment. The down step is a manual operation and there may be

overshoot or the frequency may not be quite correct. This manual operation does not affect loads calculations except when the loads are supposed to represent test conditions and one of the modes is near the step-down frequency.

b. Random Vibration Environments

Random vibration environment spectrums are specified with constant power spectral density levels over rather wide frequency bandwidths. This is because random vibration test equipment cannot follow many sharp, narrow amplitude level changes in the spectrum. Modern automatic random equipment usually has filter bandwidths of about 25 or 50 Hz in the control feedback loop, which limits the bandwidths of the input spectrum. Sloping portions of a random test spectrum are approximated by the test equipment as 25 or 50 Hz wide steps.

2. USEFUL ENVIRONMENTAL RELATIONSHIPS

a. Vibration Environment Quantities

Sinusoidal Vibration Relationship

$$\pm G_{pk} = (0.0051) (D.A.) (f)^2$$

where

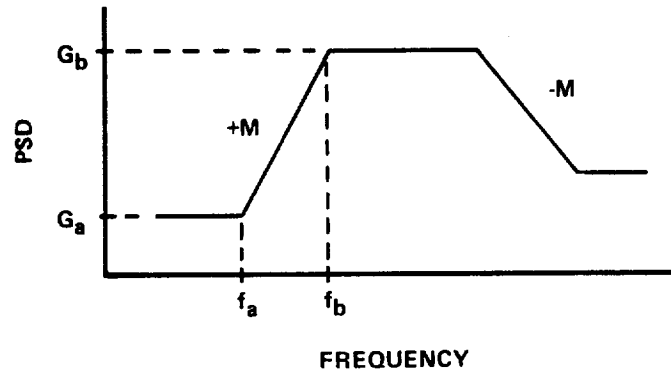
$\pm G_{pk}$ = peak acceleration

D.A. = double amplitude inches displacement

f = frequency .

Random Vibration Relationship

The relationship between the sloping and constant level portions of the PSD spectrum are as shown below:



$$\frac{M}{10 \log^2} = \frac{\log G_b/G_a}{\log f_b/f_a}$$

where

M = slope of curve in dB/oct

f_a = frequency at low frequency end of sloping PSD curve

f_b = frequency at high frequency end of sloping PSD curve

G_a = PSD level at f_a

G_b = PSD level at f_b .

Relationship between PSD and G in a frequency band

$$\text{PSD} = \frac{(\text{rms } G \text{ in bandwidth})^2}{\text{Bandwidth}}$$

The composite of a random vibration spectrum is computed as follows:
The spectrum is divided into bandwidths of the sloping and horizontal portions of the curve.

$$\begin{aligned}
 \text{Mean Square Acceleration} &= \frac{3.01 G_1}{3.01 + M} \left[(f_2) \left(\frac{f_2}{f_1} \right)^{M/3.01} - f_1 \right] \\
 \text{in bandwidth } f_1 \text{ to } f_2 &= \frac{3.01 G_2}{3.01 + M} \left[f_2 - (f_1) \left(\frac{f_1}{f_2} \right)^{M/3.01} \right] .
 \end{aligned}$$

For $M = -3.0$ to -3.02 use:

$$\begin{aligned}
 \text{Mean Square Acceleration} &= G_1 f_1 (\ln f_2 - \ln f_1) . \\
 \text{in bandwidth } f_1 \text{ to } f_2 &
 \end{aligned}$$

Then, the composite equals square root of sum of mean square values of each bandwidth.

$$\text{rms } G = \sqrt{G_{1-2}^2 + G_{2-3}^2 + \dots} .$$

If the random spectrum contains superimposed sinusoids, the total rms value of the spectrum plus the sinusoids is the square root of the sum of the square of the spectrum rms G plus the square of the rms of each of the sinusoids.

$$\text{TOT rms } G = \sqrt{G_{\text{random}}^2 + G_{\text{sine 1}}^2 + G_{\text{sine 2}}^2 + \dots} .$$

During testing, each sinusoid is rejected from the random vibration control loop by rejecting a bandwidth of random including the sinusoid; so that bandwidth does not have the correct test level.

b. Acoustic Environment Quantities

Conversion from one third octave band to spectrum level:

$$\text{PSDL} = (\text{SPL})_{1/3 \text{ O.B.}} - 10 \log_{10} \Delta f_{1/3 \text{ O.B.}}$$

where

PSDL = Pressure spectral density level (dB)

$(SPL)_{1/3 \text{ O.B.}}$ = Sound pressure level in 1/3 octave band (dB)

$\Delta f_{1/3 \text{ O.B.}}$ = Frequency bandwidth of 1/3 octave band (Hz).

Conversion from effective (rms) pressure to sound pressure level:

$$SPL = 10 \log_{10} \frac{p^2}{p_0^2}$$

where

SPL = Sound pressure level (dB)

p = Effective pressure (rms psi)

p_0 = Reference pressure (2.9×10^{-9} psi)

APPENDIX. DEFINITION OF TERMS

Acceleration - $\frac{d^2x}{dt^2}$: A vector that specifies the time rate of change of velocity.

Note: Acceleration may be (a) oscillatory, in which case it may be defined by the acceleration amplitude (if simple harmonic) or the rms acceleration (if random), or (b) nonoscillatory, in which case it is designated "sustained" or "transient acceleration."

Amplitude Distribution Analysis: The process of performing various analyses of the statistical properties of values of a wave. See Probability Density Function, and Probability Distribution.

Bandwidth: The difference in cps between the highest and lowest frequency in a band, usually taken to be the half-power points. See Half-Power Points and Bandwidth, Effective.

Bandwidth, Effective (ebw): The bandwidth of an ideal system which (a) has uniform transmission in its pass band equal to the maximum transmission of the specified system and (b) transmits the same power as the specified system when the two systems are receiving equal input signals having a uniform distribution of energy at all frequencies.

$$ebw = \int_0^{\infty} G df$$

where f is frequency in Hz and G is the ratio of the power at frequency f to the power at the frequency of maximum power. (The International Dictionary of Physics and Electronics, Van Nostrand, 1956.)

Channel, Telemeter: Designates the complete transmission route of a telemetered function including transducer, signal conditioner, multiplexer transmitter, receiver, tape recorder or other storage device if used, demultiplexer, and readout device.

Commutation: Commutation is a type of time division multiplexing transmission. See also time sharing.

Constant Bandwidth Analysis: In vibration, the analysis by means of either (a) constant bandwidth contiguous filters, or (b) sweeping through the spectrum

with a narrow-band filter. In "a" the output is displayed as a time history, showing the variation of the data within the bandpass of each filter as a function of time. In "b" the output is displayed as amplitude versus frequency; "b" may be obtained by use of a heterodyne analyzer.

Continuous Spectrum: The spectrum of a wave with its energy continuously distributed over a prescribed frequency region. A continuous spectrum has no discrete components.

Crosstalk, Electronic: The interference between circuits wherein signals in one circuit are undesirably reproduced in other circuits.

Cutoff Frequency, Filter: Represents a frequency limit beyond which the filter begins to cut off or suppress signals.

Damped Natural Frequency: The natural frequency of a damped system. The addition of a damping resistance to a single degree of freedom system decreases the natural frequency.

$$W_D = W_o \sqrt{1 - \left(\frac{C}{C_o}\right)^2} .$$

Damping: The dissipation of energy with time in a system; especially, the diminishing of amplitude of an oscillation.

Damping, Critical: That value of damping which allows the most rapid return of a system to its neutral position, without overshoot. In a simple harmonic system, which follows the equation

$$a x'' + b x' + c x = 0,$$

the condition for critical damping is that $b = 2 \sqrt{ac}$.

Damping Factor: In a simple oscillating system, in logarithmic damping this factor constant e^{-dt} , the ratio of one amplitude peak to that next succeeding it in the same direction.

Decibel: A unit for the expression of power, voltage, current, or vibration in logarithmic form.

Power: $10 \log_{10} (P_1/P_2)$ where P_1 and P_2 are two powers or intensities to be compared.

Voltage: $20 \log_{10} (E_1/E_2)$ where E_1 and E_2 are the rms voltages to be compared. In rigorous use, it must be assumed that both E_1 and E_2 are measured across the same value of resistance.

Current: $20 \log_{10} (I_1/I_2)$ where I_1 and I_2 are two currents to be compared.

Vibration: $20 \log_{10} (A_1/A_2)$ where A_1 and A_2 are two acceleration levels to be compared.

Degrees of Freedom: The number of independent generalized displacements that are possible.

Discriminator: A device the voltage output of which is proportioned to the frequency excursion of the input signal. It is used to convert an FM signal into an AM signal.

Displacement: The instantaneous distance of a vibrating particle from its position of equilibrium.

Double Amplitude Displacement: Twice the peak displacement or amplitude of a sine wave; that is, peak-to-peak displacement.

Dynamic Pressure: The kinetic energy per unit area of the air stream relative to the vehicle.

Equalizer: A network inserted in a system to modify the frequency response in a desired manner.

Excitation: (a) Addition of energy to a system, whereby it is transferred from a state of equilibrium to a state of higher energy called an "excited state," and (b) an external force or other input applied to a system that causes the system to respond in some way.

Flutter: Resonant vibration of any part of a vehicle or of any structural element in a fluid stream, maintained by oscillatory aerodynamic forces induced by deflection of the structure.

Forced Oscillation: The oscillation of a system forced by the excitation.

Forcing Function: A mathematical expression describing the relationship between the force and a time variable.

Free-Free: A term indicating the vibration of a beam-like structure unsupported at all points by structural members. A space vehicle, after liftoff, is in the free-free condition.

Free Vibration: Oscillations that continue in a system after the applied force has been removed.

Fundamental Mode of Vibration: The mode having the lowest natural frequency.

Gaussian or Normal Distribution: The Gaussian distribution is often called normal distribution and is expressed by:

$$P(X) = \frac{e^{\frac{-X^2}{\delta^2}}}{\sqrt{2\pi}} \quad .$$

The area under the curve from x_1 to x_2 represents the probability of obtaining a value of x between x_1 and x_2 .

Ground Noise: The residual system noise in the absence of the signal.

Half-Power Points (Vibration): The frequency points in a plot of a spectrum, or a filter transmission, where the rms amplitude falls to 70.7 percent of the maximum of the curve.

High Pass Filter: A filter designed to pass all the frequencies above a critical or cutoff frequency while attenuating all frequencies below this critical frequency.

Impedance: The complex ratio of a force-like quantity (force, pressure, voltage) to a related velocity-like quantity (velocity, volume, current).

Impulse: The product of a force and the time during which the force is applied;

more specifically the impulse is $\int_{t_2}^{t_1} f dt$ where the force is time dependent and equal to zero before time t_1 and after time t_2 .

Isolator: A device (such as springs, rubber pads, or mechanical linkages) which reduces the transmission of vibration in a certain frequency range.

Jerk: The change of acceleration with respect to time: $\frac{d^3x}{dt^3}$.

Linear Average Analysis: An analysis which is obtained through the use of an averaging circuit. Output may be expressed as average, or presented as average adjusted to rms (stated) for random noise.

Linear System: A system is linear if the response is linearly proportional to excitation for every element in the system.

Logarithmic Decrement: The natural logarithm of the ratio of any two successive amplitudes of like sign, in the decay of a single-frequency oscillation.

Logarithmic Sweep: A manner of varying frequency during a test wherein the common logarithm of the frequency is a linear function of time.

Longitudinal Vibration: Vibration in a direction parallel to the longitudinal axis. The positive direction is forward or in the direction of flight. Polarity should be omitted when discussing wideband vibration measurements. It should be used only with bending modes, linear acceleration, etc.

Mach Number: The ratio of any velocity to the velocity of sound in the same medium at that temperature and pressure.

Mechanical System: An aggregate of matter comprising a defined configuration of mass, mechanical stiffness, and mechanical resistance.

Mixer: A device which adds to a more input signals linearly producing a complex output with controlled percentages of each input signal.

Mode of Vibration: A characteristic motion pattern assumed by a system and dictated by the geometry of the system.

Modulation (Van Nostrand): The process or result of the process whereby some characteristics of one signal are varied in accordance with another signal. In common usage the modulated signal is called the carrier and the other signal is called the modulating signal.

Multiple-Degree-of-Freedom System: A system for which two or more coordinates are required to define completely the position of the system at any instant.

Multiplex Transmission: A technique for the simultaneous, or apparently simultaneous, transmission of two or more intelligence signals on a single carrier by frequency division, time division, or phase division.

Natural Frequency: The frequency of free oscillation of a system.

Noise: Any undesired sound, to be more exact, any unwanted disturbance such as undesired electrical signals.

Non-Stationary Random Noise: A process or noise which does not meet the requirements of a stationary random process.

Octave: An interval between two signals having a basic frequency ratio of 2.0.

Octave Analysis: An analysis made with an array of filters the center frequencies of which are separated by one octave and the effective bandwidth of which is one octave.

Octave Sweep Test: See Logarithmic Sweep, above.

One-Half Octave: An interval between two signals having a basic frequency ratio of 1.414 ($\sqrt{2}$).

One-Half Octave Analysis: Same as one octave analysis except center frequencies of filters are 1/2 octave apart, and the ebw is 1/2 octave.

One-Third Octave: An interval between two signals having a basic frequency ratio of 1.26 ($\sqrt[3]{2}$).

One-Third Octave Analysis: Same as one octave analysis except center frequencies are 1/3 octave apart, and the ebw is 1/3 octave.

Oscillograph: A device which produces a visual representation of an electrical signal.

Peak-to-Peak: The algebraic difference between the extremes of a wave, twice the peak value of a pure sine wave.

Peak Level: The maximum instantaneous level that occurs during a specified time interval.

Periodic: The recurrence of an oscillation at equal increments of the independent variable.

Piezoelectric (Crystal) Transducer: A transducer that depends for its operation on the interaction between the electric charge and the deformation of certain asymmetric crystals having piezoelectric properties.

Piezoelectric: The property of certain crystals in developing electrical charge or potential difference across certain crystals faces when subjected to a strain by mechanical forces, or conversely to produce a mechanical force when a voltage is applied across the material; that is, quartz, tourmaline, Rochelle salts, and certain ceramics.

Pitch Plane: The plane parallel with the longitudinal axis in which pitching takes place.

Pitch Vibration: Vibration in a direction parallel to the pitch plane and perpendicular to the longitudinal axis. The positive direction is toward position III.

Power Spectral Density (PSD): A measure of the power distribution as a function of frequency, in a complex wave. It is expressed by the following relationships: Where PSD is the intensity for one cycle of bandwidth, g is the root-mean-square value of the acceleration.

$$\text{PSD} = g^2 / \Delta F \text{ where } g = \sqrt{\frac{1}{T} \int_0^T A^2 dt} .$$

"A" is the instantaneous amplitude of acceleration and "T" is the analyzer time constant.

Probability Density Function: Generally, gives the probability of obtaining a value "near" any continuous variable.

$$p(x) = dF(x)/dx .$$

Sometimes called frequency function. The first differential of the probability distribution function, or simple, the ratio of instantaneous amplitude to rms amplitudes.

Probability Distribution: A plot of the probability of occurrence of the magnitude of a signal or noise. See Amplitude Distribution Analysis, above.

PSD - See Power Spectral Density, above.

Q (Quality Factor) PSD: Q is a measure of the sharpness of resonance of frequency selectivity of a resonant vibratory system having a single degree of freedom, either mechanical or electrical.

NOTE: In a mechanical system, this quantity is equal to one-half reciprocal of the damping ratio. It is commonly used only with reference to a lightly damped system, and is then approximately equal to the following: (a) Transmissibility at resonance, (b) $\pi \delta$ where δ is the logarithmic decrement, (c) $2\pi \omega / \Delta \omega$, where w is the stored energy and $\Delta \omega$ is the energy dissipation per cycle, and (d) $f_r / \Delta f$ where f_r is the resonance frequency and Δf is the bandwidth between the half-power points.

This is true only for what is termed in electrical circuits a single-tuned filter. In the case of multiple-tuned filters, although theoretically Q can be calculated, it is simpler to measure it. Nearly rectangular bandpass filters, whether obtained by cascading, paralleling, or ladder networks, commonly have a Q five times as great as that computed by the given formula. Q may be computed from a measurement of time constant by the following equation.

$$Q = \pi f_r T_c$$

where T_c is the dynamic time constant. (See Time Constant Definition.)

Random Noise: An oscillation of which instantaneous magnitude is not specified for any given instant of time. Instantaneous magnitudes of a random noise are specified only by probability distribution functions giving the fraction of the total time that the magnitude, or some sequence of magnitudes, lies within a specified range.

Random Wave Analyzer: A device, used to analyze random vibration data and which produces power spectral density (PSD), linear average, peak, and integrated amplitudes as a function of frequency.

Range Zero: First discrete second timing mark before the vehicle leaves the launching pad.

Resonance: Resonance of a system in forced oscillation exists when any change, however small, in the frequency of excitation causes a decrease in the response of the system.

Reverberation Chamber: An enclosure in which all of the inner surfaces have been made as sound-reflective as possible.

Rise Time: (a) (Shock pulse) The time required for a shock pulse to reach its maximum value. (b) Definition for electrical pulses in time of rise between 10 percent and 90 percent of maximum amplitude (see ASA 3.49 Acoustics Terminology).

Roll Plane: The plane that is perpendicular to the longitudinal axis (roll axis) in which rolling takes place.

Sensitive Axis: The axis of maximum sensitivity of an accelerometer.

Shock Spectrum: (a) A plot of the maximum acceleration experienced by a single-degree-of-freedom system as a function of its own natural frequency in response to an applied shock, and (b) frequency spectrum of a shock resulting from analysis by any method.

Signal to Noise Ratio: The ratio of the signal magnitude to the magnitude of the noise received along with the signal.

Single-Degree-of-Freedom System: A system for which one coordinate is required to define completely the configuration of the system at any instant.

Sound Pressure Level (SPL): Twenty time the common logarithm of the ratio of the pressure of the sound to the reference pressure.

Sound Pressure Level, Overall: Twenty time the logarithm (base 10) of the ratio of the dynamic (sound) pressure in rms units to a reference dynamic pressure of 0.0002 dynes/cm². The term overall indicates that the entire equipment transmission spectrum of frequencies is utilized, no additional filtering being accomplished. Bandpass bandwidth limits of equipment must be stated; e.g., 20 to 20 000 Hz.

Spectrum: A continuous range of frequencies.

Spectrum Density (Power Spectrum): The mean-square amplitude of the output of an ideal filter with unity gain responding to the oscillation, per unit bandwidth; i.e., the limit for vanishingly small bandwidth of the quotient of the mean-square amplitude divided by the bandwidth. For the practicing engineer, this is usually the spectrum amplitude reported as if measured in 1 Hz bandwidths.

Note (a): In mathematical terms, the spectrum density function of $y(t)$ is the ensemble average of $G(f)$ where (when a limit exists)

$$G(f) = \lim_{T \rightarrow \infty} \frac{1}{T} \int_{-T}^T y(t) e^{-2\pi i f t} dt$$

f being frequency (positive only).

Note (b): The mean-square output of an ideal filter with unity gain in a finite band is given by the integral of $G(f)$ with respect to frequency over the band.

Spectrum Envelope: The vibration level, or levels, which enclose the peaks on a vibration spectrum plot.

Spring Constant: The ratio of the force acting upon an elastic member to the resulting displacement of the point at which the force acts.

SS/FM (Single Sideband/Frequency Modulation): A form of frequency division multiplexing. A number of intelligence signals are each subjected to a linear frequency transformation to a different frequency. The resultant signals, each at a different frequency, are combined in a linear adder and the composite is used to frequency modulate a carrier signal.

Stationary Random Process: (a) A process which has the joint probability density dependent upon only the time differences and not upon the actual time instants. (b) A process in which the equivalent G rms of the random vibration does not vary with time. (c) A process of which all of the statistical properties depend only on the time differences and not on the actual time instants.

Steady State: (a) A condition of dynamic balance, as in an equilibrium reaction, where at equilibrium the concentration of each of the reactants remain constant. (b) A relatively unchanging dynamic condition. (c) The condition in a system when the rate of dissipation of energy is constant with respect to time.

Steady State Vibration: See Steady State, above.

Strain Bridge Accelerometer: A device composed of a mass supported by very fine strain wire or thin foil which exhibits a change in resistance with applied acceleration.

Strouhal Number: (a) The dimensionless parameter, S:

$$S = fD/V$$

where f is frequency, D is the exit diameter of a noise producing nozzle, and V is the velocity of the gases at the nozzle exit, and (b) relates frequency of shedding of vortices to the wind velocity and a characteristic dimension, where

$$S = fd/V$$

where

f = frequency of vortex shedding.

d = diameter of structure in feet.

V = velocity of air in feet/second.

Subcarrier: An intermediate frequency that is modulated by intelligence signals, and in turn is used to modulate the radio carrier.

Subcarrier Frequency Modulation: A frequency modulation technique employing a subcarrier oscillator to derive a frequency modulated subcarrier.

Telemeter System: See Chapter V.

Time Constant: In electronics, the time required for the voltage or current in a circuit to rise to 63 percent of its final value, or fall to 37 percent of its initial value, as a result of a step input.

Time Constant, Dynamic (of a resonant system): The time required for the amplitudes of decaying oscillation in a system to fall to 37 percent of the initial value.

$$T_c = 1/\pi B = Q/\pi f_r$$

for a single-degree-of-freedom system.

Time Sharing: The sharing of a telemetry channel between several vibration measurements by transmission of a short sample of each in turn. In time division multiplexing, samples are taken with a very high sampling rate with respect to signal variations so that no information is lost; while in time sharing, sampling occurs at very low rates which permits a representative measurement or analysis during each sampling period. Typically, four measurements are transmitted over one channel, each being sent for 4 seconds per sample.

Transducer: (a) A device capable of converting one form of energy to another, and (b) the sensing element of a measuring channel. It transducers a mechanical or physical quantity or movement into an analog signal which can be transmitted to a remotely located recorder.

Transfer Function: A complex ratio of a response at one place in response to an excitation to another place in a linear system. The transfer function, a complex quantity, is the cross-spectral density between response and excitation. Its absolute value is transmissibility.

Transient Vibration: A temporary vibration of a mechanical system, caused by an impulse.

Transmissibility: The ratio of the response amplitude of a system to the excitation amplitude. The ratio may be between forces, displacements, velocities, or accelerations. (Glossary of Terms Frequently used in Acoustics, AIP, October, 1960.) A plot of transmissibility versus frequency is usually made. See Transfer Function, Q, and Cross Spectral Density.

Vibration: The oscillation of a body or particle about a point of equilibrium. A parameter that defines the motion of mechanical system.

Yaw Plane: The plane parallel with the longitudinal axis in which yawing takes place. The pitch plane is perpendicular to the yaw plane.

Yaw Vibration: Vibration in a direction parallel to the yaw plane and a perpendicular to the longitudinal axis. The positive direction is toward the right hand of an observer looking forward along the longitudinal axis.

REFERENCES

1. Barrett, Robert E.: Techniques for Predicting Localized Vibratory Environments of Rocket Vehicles. NASA Technical Note D-1836. October 1963.
2. Eldred, Roberts, and White, R.: Structural Vibrations in Space Vehicles. WADD Technical Report 61-62, December 1961.
3. Bendat, Enochson, Klein and Pierson, Allan G.: The Application of Statistics to the Flight Vibration Problem. ASD Technical Report 61-123, December 1961.
4. Accelerometer Fundamentals - Part I and Part II. Bulletin, Systron-Donner Corporation, Concord, Calif.:
5. Calibration of Vibration Transducers. Tustin Institute of Technology, Santa Barbara, Calif., 1965.
6. Endevco 2200 Accelerometer Manual. Endevco Corporation, Pasadena, Calif.
7. Endevco Product Development News. Endevco Corporation, Pasadena, California; Vol. 5, No. 1, April 1967.
8. Piezoelectric Accelerometer User's Handbook. Bulletin 4200-96, C Consolidated Electronics (CEC), Pasadena, Calif.
9. Shock and Vibration Handbook, Vol. 1, New York, McGraw-Hill Book Co. Inc., 1961.
10. Shock and Vibration Handbook. Vol. 1, New York, McGraw-Hill Book Co., Inc., 1961.
11. Mangolds, B.: Effect of Mounting-Variables on Accelerometer Performance. Princeton, New Jersey, Radio Corporation of America, 1963.
12. Calibration of Vibration Transducers. Tustin Institute of Technology, Santa Barbara, California, 1965.

REFERENCES (Continued)

13. Beranek, L. L.: Acoustic Measurements. New York, John Wiley & Sons, 1962, p. 440.
14. Calibration of Vibration Transducers. Tustin Institute of Technology, Santa Barbara, Calif., 1965.
15. Shock and Vibration Handbook. Vol 1, New York, McGraw-Hill Book Co. Inc., 1961.
16. Javid, M., and Brenner, E.: Analysis, Transmission, and Filtering of Signals. New York, McGraw-Hill Book Co., 1963, pp. 204-6.
17. Telemetry Standards. IRIG Document 106-66, Inter-Range Instrumentation Group, White Sands Missile Range, April 1966.
18. Saturn S-IC-501 Static Test Vibration and Acoustic Data. Document D5-13644-1, The Boeing Company, October 1966.
19. Stiltz, Harry L. et al.: Aerospace Telemetry. Englewood Cliffs, N. J., Prentice Hall, Inc., 1964.
20. Bendat, J. S., Enochson, L. D., Klein, G. H., and Piersol, A. G.: The Application of Statistics to the Flight Vehicle Vibration Problem. ASD TR-61-123, Aeronautical Systems Division, AFSC, USAF, WPAFB, Ohio, ASTIA AD 271 913, 1961.
21. Bendat, J. S., Enochson, L. D., Klein, G. H., and Piersol, A. G.: Advanced Concepts of Stochastic Processes and Statistics for Flight Vehicle Vibration Estimation and Measurement. ASD TDR 62-973, Aeronautical Systems Division, AFSC, USAF, WPAFB, Ohio, 1962.
22. Piersol, A. G.: Nonparametric Tests for Equivalence of Vibration Data. SAE National Aeronautic and Space Engineering Meeting, Los Angeles, Calif., September 1963.
23. Crandall, S. H.: Zero-Crossings, Peaks, and Other Statistical Measures of Random Responses. Proceedings, Acoustical Society of American Meeting, Seattle, Wash., 1962.

REFERENCES (Continued)

24. Bendat, J. S.: Principles and Applications of Random Noise Theory. John Wiley and Sons, Inc., New York, 1958.
25. Goodman, N. R.: On the Joint Estimation of Spectra, Co-Spectrum and Quadrature Spectrum of a Two Dimensional Stationary Gaussian Process. Scientific Paper No. 10, Engineering Statistics Laboratory, New York University, 1957.
26. Barrett, R. E.: Techniques for Predicting Localized Vibratory Environments of Rocket Vehicles. NASA TN D-1836, October 1963.
27. Duncan, A. J.: Quality Control and Industrial Statistics, Richard D. Irwin, Inc., Homewood, Ill., Rev. Ed., 1959, p. 876.
28. Sokolnikoff, I. S., and Redheffer, R. M.: Mathematics of Physics and Modern Engineering. McGraw-Hill Book Company, Inc., New York, 1958.
29. Everitt, W. L.: Communications Engineering. McGraw-Hill, pp. 36, 94-178, 1937.
30. Blackman, R. B., and Tukey, J. W.: The Measurement of Power Spectra Dover Publications, Inc., New York, 1958, p. 30.
31. Mathematical Methods for Digital Computers, John Wiley and Sons, Inc., New York, 1960.
32. Simpson, S. M., Jr.: Time Series Techniques Applied to Underground Nuclear Detection and Further Digitized Seismic Data. MIT Scientific Report No. 2 (Contract AF19(604)-7378, ARPA Order No. 180-61), December 8, 1961.
33. Webster, A. G.: The Dynamics of Particles. New York, Dover Publications, Inc., 1959, pp. 63-70.
34. Churchill, R. V.: Fourier Series and Boundary Value Problems. New York, McGraw-Hill Book Co., Inc., 1941.

REFERENCES (Continued)

35. Setterlund, G. G., and Skoog, J. A.: Space Requirements for Equipment Items Subjected to Random Vibration. *Journal of the Acoustical Society of America*, February 1959.
36. Wyle, C. R., Jr.: *Advanced Engineering Mathematics*. New York, McGraw-Hill Book Co., Inc., 1960.
37. Tse, F. S., Morse, I. E., and Hinkle, R. T.: *Mathematical Vibrations*. Boston, Allyn and Bacon, Inc., 1964.
38. Bishop, R. E. D., and Johnson, D. C.: *The Mechanics of Vibrations*. New York, Cambridge University Press, 1960.
39. Timoshenko, S., and Woinowsky-Krieger, S.: *Theory of Plates and Shells*. New York, McGraw-Hill Book Co., Inc. 1959.
40. Levy, R. S., Ham, E. H., and Newman, M.: Experimental Determination of System Parameters for Thin-Walled Cylinders. Republic Aviation Corp. Report No. RAC 1117-6, NAS8-11514, June 29, 1964.
41. Levy, R. S., Ham, E. H., and Newman, M.: Experimental Determination of System Parameters for Thin-Walled Cylinders. Republic Aviation Corp. Report No. RAC 1117-14, NAS8-11514, June 29, 1965.
42. User's Manual for Free Vibration Analysis of Stiffened Cylinders with an Attached Weight. Republic Aviation Corp. Report No. RAC 1117-11, April 15, 1965.
43. Levy, R. S., and Forray, M. J.: Experimental Determination of System Parameters for Thin-Walled Cylinders. Fairchild Hiller - Republic Aviation Report No. FHR 1117-20, August 1966.
44. User's Manual for Natural Frequencies and Mode Shapes of Ring Stiffened Cylinders with an Attached Weight. Fairchild Hiller - Republic Aviation Report No. FHR 1117-19, Revision A, December 1966.

REFERENCES (Continued)

45. Hwang, C., and Brass, J.: Analytical and Experimental Determination of Localized Structure to Be Used in Laboratory Vibration Testing of Shell Structure - Mounted Components, Saturn V. Northrop Corp. Report NOR 66-201, Vol. I, May 1966.
46. Hwang, C., Pi, W. S., and Bhatia, N. M.: Analytical and Experimental Determination of Localized Structure to Be Used in Laboratory Vibration Testing of Shell Structure-Mounted Components, Saturn V. Northrop Corp. Report NOR 67-127, July 1967.
47. Yamane, J. R.: Analytical and Experimental Determination of Localized Structure to Be Used in Laboratory Vibration Testing of Shell Structure-Mounted Components, Saturn V. Northrop Corp. Report NOR 66-201, Vol. II, May 1966.
48. Hwang, C., and Pi, W. S.: Analytical and Experimental Determination of Localized Structure to Be Used in Laboratory Vibration Testing of Shell Structure-Mounted Components, Saturn V. Northrop Corp. Report NOR 67-19, January 1967.
49. Seto, W. W.: Schaum's Outline of Theory and Problems of Mechanical Vibrations. New York, Schuam Publishing Co., 1964.
50. Andronow, A. A., and Chaikin, C. E.: Theory of Oscillations. Princeton, New Jersey, Princeton University Press, 1949.
51. Contributions to the Theory of Nonlinear Oscillations. Vols. I-V, Princeton, New Jersey, Princeton University Press.
52. Ku, Y. H.: Analysis and Control of Nonlinear Systems. New York, The Ronald Press Company, 1958.
53. Levinson, N., and Smith, O. K.: A General Equation for Relaxation Oscillations. Duke Mathematical Journal, 9, 1942.
54. Stoker, J. J.: Nonlinear Vibrations in Mechanical and Electrical Systems. New York, New York, Interscience Publishers, Inc., 1950.

REFERENCES (Continued)

55. Minorsky, N.: Introduction to Nonlinear Mechanics. Ann Arbor, Michigan, J. W. Edwards, 1947.
56. Minorsky, N.: Nonlinear Oscillations. Princeton, New Jersey, D. Van Nostrand Company, Inc., 1962.
57. Margenau, H., and Murphy, G. M.: The Mathematics of Physics and Chemistry. Princeton, D. Van Nostrand Co., Inc., 1947.
58. Franklin, P.: An Introduction to Fourier Methods and the LaPlace Transformation. New York, Dover Publications, Inc., 1958.
59. Sokolmikov, I. S., and Redheffer, R. H.: Mathematics of Physics and Modern Engineering. New York, McGraw-Hill Book Co., Inc., 1958.
60. Milne, W. E.: Numerical Calculus. Princeton, Princeton University Press, 1959.
61. Pipes, L. A.: Matrix Methods for Engineering. Englewood Cliffs, N. J., Prentice-Hall, Inc.
62. Hildebrand, F. B.: Introduction to Numerical Analysis. New York, McGraw-Hill Book Co., Inc., 1956.
63. Sokolnikoff, I. S.: Tensor Analysis. New York, John Wiley and Sons, Inc., 1964.
64. Shock and Vibration Handbook, New York, McGraw-Hill Book Company, 1961, pp. 36-16.
65. Crede, C. E.: Shock and Vibration Concepts in Engineering Design. Englewood Cliffs, Prentice-Hall, Inc., 1965, p. 135.
66. A Finite Element Analysis of Simple Panel Response to Turbulent Boundary Layers. Renton, Washington, The Boeing Company Document D6-19392, July 1967, p. 25.

REFERENCES (Continued)

67. Preliminary Vibration, Acoustic and Shock Specifications for Components on Saturn IB Vehicle. Huntsville, Marshall Space Flight Center Document IN-P&VE-S-63-1, September 1964.
68. Preliminary Vibration, Acoustic and Shock Specifications for Components on Saturn V Vehicle. Huntsville, Marshall Space Flight Center Document IN-P&VE-S-63-2, September 1964.
69. Techniques for Predicting Localized Vibratory Environments of Rocket Vehicles. Huntsville, Marshall Space Flight Center Document NASA TN D-1836.
70. Shock and Vibration Environments and Test Specification Levels, Ground Support Equipment, Launch Complex 39. Huntsville, Kennedy Space Center Document SP-4-38-D.
71. The Shock and Vibration Bulletin. Bulletin 34, Parts 2 of 5, U. S. Naval Research Laboratory, Washington, D. C., December 1964.
72. Thomson, W. T.: Mechanical Vibrations. 2nd Ed., Englewood Cliffs, Prentice-Hall, Inc., 1953, p. 214.
73. Random Vibration. New York, Technology Press of Massachusetts Institute of Technology and John Wiley and Sons, Inc., September 1959, paragraph 4.2.
74. Aspects of Cumulative Damage in Fatigue Design. Air Force Materials Laboratory Report AFML-TR-67-112, Wright-Patterson Air Force Base, Ohio, August 1967.
75. Fatigue Damage During Two-Level Biaxial-Stress Tests. Air Force Materials Laboratory Report, AFML-TR-66-355, Wright-Patterson Air Force Base, Ohio, February 1967.
76. Miner, M. A.: Cumulative Damage in Fatigue. Journal of Applied Mechanics Vol. 12, pp. A-159 through A-164, September 1945.
77. Fuller, J. R.: Research on Technique of Establishing Random Type Fatigue Curves for Broad Band Sonic Loading. Air Force Flight Dynamics Laboratory Report ASD-TDR-62-501, Wright-Patterson Air Force Base, Ohio, October 1962.

REFERENCES (Concluded)

78. Preliminary Vibration, Acoustic and Shock Specifications for Components on Saturn I Vehicle. Huntsville, Marshall Space Flight Center Document IN-P&VE-S-62-7, 1962.
79. Statistical Techniques for Describing Localized Vibratory Environments of Rocket Vehicles. Huntsville, Marshall Space Flight Center Document NASA TN D-2158.

BIBLIOGRAPHY

Anand, G. V.: Resonance in Strings with Viscous Damping. J.A.S., 40, 1517, 1966.

Banerji, D.: On the Theory and Some Applications of Sub-Synchronous Pendulums. Proceedings of the Indian Association for the Cultivation of Science, 7, 145-158, 1921-1922.

Bendat, J.S.: Principles and Applications of Random Noise Theory. New York, John Wiley and Sons, Inc., 1958.

Beranek, L. L.: Acoustic Measurements. John Wiley and Sons, New York, 1956, p. 433.

Bradford, H. K.: High Speed Analysis of Electronic Circuits by Geometry. Electronic Buyers Guide, McGraw-Hill, 1961, pp. R50-64.

Braunbeck, W., and Lauter, E.: Forced Oscillations of a Simple Nonlinear System.

I. The Differential Equations and Their Stationary Solution.
Z. Physik, 147, 297-306, 195, 1957.

II. Non-Stationary Motion. Zeit. für Physik, 147, 507, 1957.

Chobotov, V. A., and Binder, R. C.: Nonlinear Response of a Circular Membrane to Sinusoidal Acoustic Excitation. J.A.S., 36, 59, 1964.

Church, A. H.: Mechanical Vibrations. New York, John Wiley and Sons, Inc., 1964.

Cocking, W. T.: Cathode Follower Dangers. Wireless World, Vol. 52, March 1946, pp. 79-82.

Crandall, S. H., Khabaz, G. R., and Manning, J. E.: J.A.S., 36, 1330, 1964.

Crede, C. E.: Shock and Vibration Concepts in Engineering Design. Englewood Cliffs, Prentice-Hall, Inc., 1965.

BIBLIOGRAPHY (Continued)

Determination of Structural Transfer Functions by Statistical Correlation
The Boeing Company Document LDRM 40.

Dey, A., and Raman, C. V.: On the Maintenance of Vibrations by a Periodic Field of Force. Proceedings of the Indian Association for the Cultivation of Science, 2, 1-15, 1917.

Firestone, F. A.: The Mobility Method of Computing the Vibration of Linear Mechanical and Acoustical Systems: Mechanical-Electrical Analogies. Journal of Applied Physics, Vol. 9, June 1938.

Goldberg, H.: Internal Impedance of Cathode Followers. Proc. IRE, Vol. 33, November 1945, pp. 778-782.

Hale, J.: Oscillations in Nonlinear Systems. New York, McGraw-Hill Book Co., Inc., 1963.

Hayashi, C.: Forced Oscillations In Nonlinear Systems. First Edition, Osaka, Japan, Nippon Printing and Publishing Col, Ltd., 1953.

Heckl, M.: Nonlinear Flexural Vibrations of Sandwich Plates. J.A.S., 34, 803, 1962.

Herbert, R. E.: Random Vibrations of a Nonlinear Elastic Beam. J.A.S., 36, 2090, 1960.

Kerchner, R.M., and Corcoran, G. F.: Alternating-Current Circuits. New York, John Wiley and Sons, Inc., 1962.

Kirchman, E. J., and Greenspon, J.E.: Nonlinear Response of Aircraft Panels in Acoustic Noise. J.A.S., 29, 854, 1957.

Klein, G. H.: Random Excitation of Nonlinear System with Tangent Elasticity Characteristics. J.A.S., 36, 2095, 1964.

Langford-Smith, F.: Radiotron Designers Handbook. Wireless Press for Amalgamated Wireless Valve Co. Pty. Ltd., Sidney, Australia, reproduced and distributed by RCA Victor Div., Harrison, N. J.

BIBLIOGRAPHY (Continued)

Lindsay, R. B.: Mechanical Radiation. New York, McGraw-Hill Book Co., Inc., 1960.

Miles, J. W.: Stability of Forced Oscillations of a Vibrating String. J.A.S., 38, 855, 1965.

Morse, P. M.: Vibration and Sound. New York, McGraw-Hill Book Co., Inc., 1948.

Olsen, H. F.: Dynamical Analogies. Princeton, D. Van Nostrand Co., Inc., 1958.

On the Maintenance of Combinatorial Vibrations by Two Simple Harmonic Forces. No. 11, Indian Association for the Cultivation of Science, 1-24, 1914.

Pliss, V. A.: Nonlocal Problems of the Theory of Oscillations. New York, Academic Press, 1966.

Ranman, C. V.: On Motion in a Periodic Field of Force, Bulletin, No. 11, Indian Association for the Cultivation of Science, 25-42, 1914.

Raman, C. V.: The Small Motion at the Modes of a Vibrating String. Physical Review, 32, 309-315, 1911.

Results of An Experimental Program to Determine the Response of Unstiffened Cylindrical Steel Shells to Free Field, Reverberant and Progressive Wave Acoustic Excitations. Boeing Company Document D2-24122-1, November 1966.

Rideout, V. C.: Active Networks. Prentice-Hall, Inc., New York, N. Y., 1954, p. 82.

Savant, C. J.: Control Systems Engineering. New York, McGraw-Hill Book Co., Inc., 1958.

Scanlon, R. H., and Rosenbaum, R.: Aircraft Vibration and Flutter. New York, The MacMillan Co., 1960.

BIBLIOGRAPHY (Concluded)

- Smith D. A., and Lambert, R. F.: Effects of Dynamical Nonlinearity on External Statistics. J.A.S., 32, 1700, 1960.
- Smith, P. W., Jr.: Response of Nonlinear Structures to Random Excitation. J.A.S., 34, 827, 1962.
- Smith, P. W., Jr., Malme, C. I., and Goga, C. M.: Nonlinear Response of a Simple Clamped Panel. J. A. S., 33, 1476, 1961.
- Sneddon, I. N.: Elements of Partial Differential Equations. New York, McGraw-Hill Book Co., Inc., 1957.
- Snowden, J. C. Representation of the Mechanical Damping Possessed by Rubber like Material and Structures. J.A.S., 35, 821, 1963.
- Snowden, J. C.: Transient Response of Nonlinear Isolation Mountings to Pulselike Displacements. J.A.S., 35, 389, 1963.
- Srinwasa Murphy, G. S., and Ramakrishna, B. S.: Nonlinear Character of Resonance in Stretched Strings. J.A.S., 38, 46, 1965.
- Symon, K. R.: Mechanics. Reading, Pa., Addison-Wesley Publishing Co., Inc., 1964.
- Thompson, W. T.: Mechanical Vibrations. Englewood Cliffs, Prentice-Hall, Inc. 1962.
- von Ardenne, M.: On the Theory of Power Amplification, Proc. IRE, vol. 16, February 1928, pp. 193-207.
- Wadd Technical Report 61-62, p. 133.